Aqueous solid-phase peptide synthesis (ASPPS): A novel concept of peptide synthesis

TECHNISCHE UNIVERSITÄT DARMSTADT

Vom Fachbereich Chemie
der Technischen Universität Darmstadt

zur Erlangung des Grades

Doktor-Ingenieur

(Dr.-Ing.)

Dissertation
von Dipl.-Ing. Sascha Knauer

Referent:	Prof. Dr. Harald Kolmar
Korreferentin:	Prof. Dr. Katja Schmitz
Korreferent:	Prof. Dr. Oliver Seitz (Humboldt-Universität zu Berlin)

Darmstadt 2020

Tag der Einreichung: 18. November 2019

Tag der mündlichen Prüfung: 11. Februar 2020

Knauer, Sascha: Aqueous solid-phase peptide synthesis (ASPPS): A novel concept of peptide synthesis
Darmstadt, Technische Universität Darmstadt,
Jahr der Veröffentlichung der Dissertation auf TUprints: 2020
URN: urn:nbn:de:tuda-tuprints-90665

Die vorliegende Arbeit wurde unter der Leitung von Herrn Prof. Dr. Harald Kolmar am Clemens-Schöpf-Institut für Organische Chemie und Biochemie der Technischen Universität Darmstadt sowie in der Sulfotools GmbH von September 2013 bis Juni 2019 angefertigt.

"*We cannot solve our problems with the same level of thinking that created them.*"
*(Albert Einstein, *1879 †1955)*

"I am among those who think that science has great beauty. A scientist in his laboratory is not only a technician: he is also a child placed before natural phenomena which impress him like a fairy tale."
*(Maria Skłodowska-Curie, *1867 †1934)*

The following publications and patents based on the results of the present work were submitted or published in the following places:

- **Knauer, Sascha**;[‡*] Koch, Niklas;[‡] Uth, Christina;[‡] Meusinger, Reinhard; Avrutina, Olga and Kolmar, Harald[*] How a Transient Protecting Group Enables a Sustainable Peptide Synthesis; Paper submitted in Oct. 2019 ([‡] Authors contributed equally, [*]Corresponding Authors)

- **Knauer, Sascha;** Roese, Tobias Michael Louis; Avrutina, Olga; Kolmar, Harald; Uth, Christina; 2016, Method for peptide synthesis and apparatus for carrying out a method for solid phase synthesis of peptides, Technische Universität Darmstadt, Sulfotools GmbH, WO 2016 050764.
    - EU 14186879.4
    - US 20170218010
    - RU 1017113219
    - ISR 251438
    - KOR 10-2017-7011833
    - AUS 2015326947
    - CAN 2962704
    - ZAF 2017/01887
    - CN 201580063451.2
    - IND 201747014578,
    - JAP 2017-516513

- **Knauer, Sascha**; 2017, Improved method for preparing peptides, Sulfotools GmbH, WO 2019 101939.

- **Knauer, Sascha**; 2017, Method for preparing peptides, Sulfotools GmbH, WO 2019 101940.

- S. Hörner,[‡] **S. Knauer**,[‡] C. Uth,[‡] Marina Jöst, Volker Schmidts, Holm Frauendorf, Christina Marie Thiele, Olga Avrutina, and Harald Kolmar, Ultrasmall biodegradable organic-inorganic hybrids for efficient cell penetration and drug delivery., Angew. Chem. Int. Ed. 2016, 55, 14842. (‡ Authors contributed equally)

- S. Hörner, [‡] **S. Knauer**, [‡] C. Uth, [‡] Marina Jöst, Volker Schmidts, Holm Frauendorf, Christina Marie Thiele, Olga Avrutina, and Harald Kolmar, Nanoskalige, biologisch abbaubare organisch-anorganische Hybride für effiziente Zellaufnahme und Wirkstofftransport, Angew. Chem. 2016, 128, 15063. (‡ Authors contributed equally)

- **Knauer, Sascha**; Kolmar, Harald; Hörner, Sebastian; Uth, Christina; Avrutina, Olga; 2016, *Silsesquioxane Transportverbindung*, Technische Universität Darmstadt, Sulfotools GmbH, WO 2017 186866.

Conference contributions

- 12th German Peptide Symposium, Darmstadt, March 20th 2015 (talk)
- 12th German Peptide Symposium, Darmstadt, March 18th - 21th 2015 (poster)
- 25th Dutch Peptide Symposium, Eindhoven, June 8th 2017 (talk)

Table of Contents

1. Introduction

Part of my work was carried out in the field of cell-penetrating, cube-octameric silsesquioxane (COSS) nanoparticles and the results of the respective investigation were summarized in my Diploma Thesis and the publication in *Angewandte Chemie International Edition*.[1] The topic is not further illustrated in this work. Nevertheless, the research on the modified COSS structures gave a good overview of the properties and effects of ionic groups on the solubility of organic compounds as well as the behaviour of certain functional groups in chemical reactions.

This was a helpful preliminary work to optimize the peptide synthesis in view of a sustainable process. In order to give an overview of the problems of peptide synthesis and its consequences, especially in industrial applications, the following gives an in-depth look at peptide synthesis and the achievements in the field of sustainable peptide synthesis.

1.1. Peptides

Being elementary components in all living systems, peptides are active biomolecules comprising a chain of up to 100 covalently linked amino acids (aa). Their biological properties depend on the number of residues and their specific sequence. Natural, endogenous peptides regulate many biological processes such as blood sugar levels, hunger, blood coagulation, and pain. Peptides are currently produced on industrial scale for the treatment of cancer, diabetes, cardiovascular and neurodegenerative diseases.[2-4] In addition, synthetic peptides are also used in cosmetics[5-6], diagnostic and medical technology products, as well as in veterinary medicine, agrochemistry or dietary supplements.[2, 7] Thus, peptide synthesis continues to be an important and growing area of research.

Peptide synthesis is the way to form an amide bond between amino acid building blocks. Interestingly, there is no precise definition of a peptide; it usually refers to a macromolecular chain of up to 100 amino acids. Chemists are able to link amino acids with peptide bonds since the beginning of the 20th century, but it took another 50-60 years until complex peptides like oxytocin and insulin have been chemically synthesized.[8] This demonstrates that peptide synthesis is a rather difficult chemical goal. In the last 120 years, advances in peptide chemistry in view of methods and instruments have developed to the point where the synthesis of peptides is a rank-and-file task for chemists. A very brief overview of the milestones of peptide synthesis is given in the following introduction, a graphical overview in **Figure 1**.

The first chemical synthesis of an *N*-terminally masked dipeptide glycylglycine was performed by Theodor Curtius in 1882 by reacting the silver salt of glycine with benzoylchloride.[9] Nineteen years later, in 1901, Emil Fischer and Ernest Fourneau published their variant of its synthesis by a partial HCl hydrolysis of glycine diketopiperazine. About 100 peptides consisting of up to 17 amino acid residues were synthesized by Emil Fischer and his co-workers using the methods developed in his laboratory.[10-11] In 1932, Bergmann and Zervas introduced the first removable N_{α}-protecting group, the carboxybenzoxy (CBz, also referred to as Z) one.[12] About 20 years later, in 1953, du Vigneaud synthesized the peptide hormone oxytocin[8] comprising nine amino acids and a disulfide-bridged backbone, using the actual synthetic methods. For this work he was awarded the Nobel Prize in Chemistry in 1955 and initiated the development of peptides as pharmaceuticals.

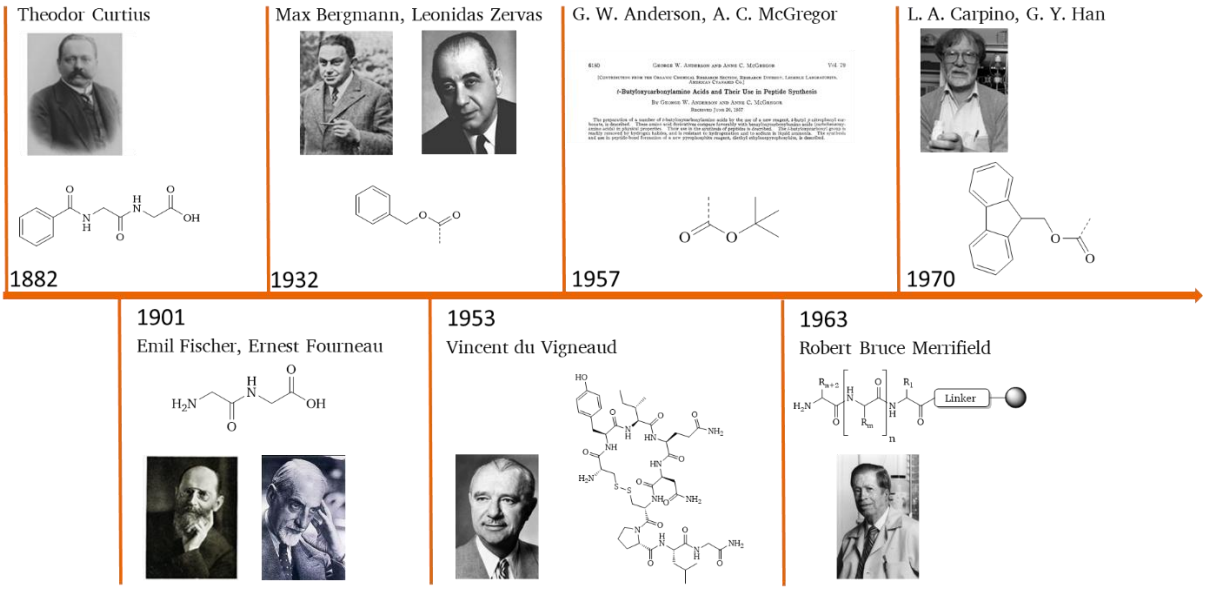

Figure 1: Graphical summary of the peptide synthesis milestones.

In 1957, Anderson and McGegor introduced the *tert*-butyloxycarbonyl (Boc) group to protect an alpha-amine. This was a significant step forward. Indeed, besides the urethane protection against racemization, the mild acidic cleavage of the Boc protecting group provides obvious advantage compared to the Cbz one.[13]

In the early 1960s, Bruce Merrifield pioneered the solid-phase peptide synthesis having suggested a completely novel strategy based on a polystyrene-based solid support to grow a peptide chain.

In his concept, the peptides were synthesized in a stepwise manner from *C*- to *N*-terminus applying N_α-protected and C_α-activated amino acids; polymeric support played a role of a constant *C*-terminal protection. The tetrapeptide LAGV was synthesized using Cbz to protect an alpha amine, and *N,N'*-dicyclohexylcarbodiimide (DCC) to activate an alpha carboxylic group; the method was called solid-phase peptide synthesis (SPPS).[14] After the chain assembly, the peptide was cleaved form solid support by saponification or HBr.[14] Later, Merrifield modified SPPS protocol to use the Boc N_α-protecting group.[15] In 1967, Sakakibara *et al.* reported hydrogen fluoride (HF) to cleave peptides from solid support[16] and the first common SPPS protocol had acquired its modern shape. Now it combined the Boc protection labile in the presence of TFA (trifluoroacetic acid) for the *N*-terminus with benzyl-based groups for the side chains. Obviously, the side chain protecting moieties and the cleavable linker between solid support and the growing peptide chain needed to be stable in the presence of moderate acids like TFA and labile in the presence of strong acids like HF. During the period from the 1960s through the 1980s Merrifield fine-tuned his Boc-SPPS protocol,[17] which resulted in the successful synthesis of several functional polypeptides, among them a protein interleukin-3[18] and enzymes ribonuclease A and HIV-1 aspartyl protease.[19]

In 1970, the 9-fluorenylmethoxycarbonyl (Fmoc) group was introduced by Carpino and Han for the N_α-protection.[20] A moderate base is required for its cleavage, thus providing a chemically milder alternative to the acid-labile Boc. Initially, this new group was applied to protect suitable amines in solution-based chemistry[20-21] and was proven unsuitable for this application. 9-Methylene-fluorene, the initial deprotection product, is reactive and able to reattach to the free amines.[22] However, during the screening process for the application of

base-labile protecting groups in solid-phase synthesis, the Fmoc group showed its advantages.[23-24] Indeed, the conditions of SPPS imply the possibility for all the undesired, potentially harmful products to be washed away, thus avoiding possible side reactions. Moreover, the 9-methylene-fluorene intermediate emerging in course of deprotection turns yellow and allows therefore to monitor this process by UV-VIS.[25]

The Fmoc group was adopted for solid-phase peptide synthesis in the late 1970s. The respective Fmoc-SPPS uses *tert*-butyl based side-chain protecting groups and in the majority of cases hydroxymethylphenoxy-based resin linkers.[23] The mild N_{α}-deprotection conditions as well as the relatively soft global cleavage are doubtlessly beneficial for peptide assembly. However, synthesis of Fmoc-protected amino acids using 9-fluorenylmethoxycarbonyl chloride (Fmoc-Cl) or 9-fluorenylmethyl *N*-hydroxy-succinimidyl carbonate (Fmoc-NHS) is associated with several side reactions. Regarding the use of Fmoc-NHS, the most frequently encountered one is a Lossen-type rearrangement resulting in the formation of Fmoc-β-Ala-OH and Fmoc-β-Ala-aa-OH.[26-27] An unwanted carboxyl activation of the amino acids was observed by using Fmoc-Cl, resulting in the formation of the Fmoc-aa-aa-OH dipeptides.[28-29] During the peptide assembly, these impurities can be incorporated into the growing peptide if they are not removed prior to the synthesis process.

The advantages given by Fmoc-SSPS and the improvements in the related chemistry led to new dimensions in peptide synthesis. To date, SPPS has been continuously improved in terms of efficacy, reaction rate (e.g. acceleration by temperature increase, including microwave-assisted synthesis) and reduction of solvent consumption. The most common methods of obtaining peptides today are shown in **Figure 2**.

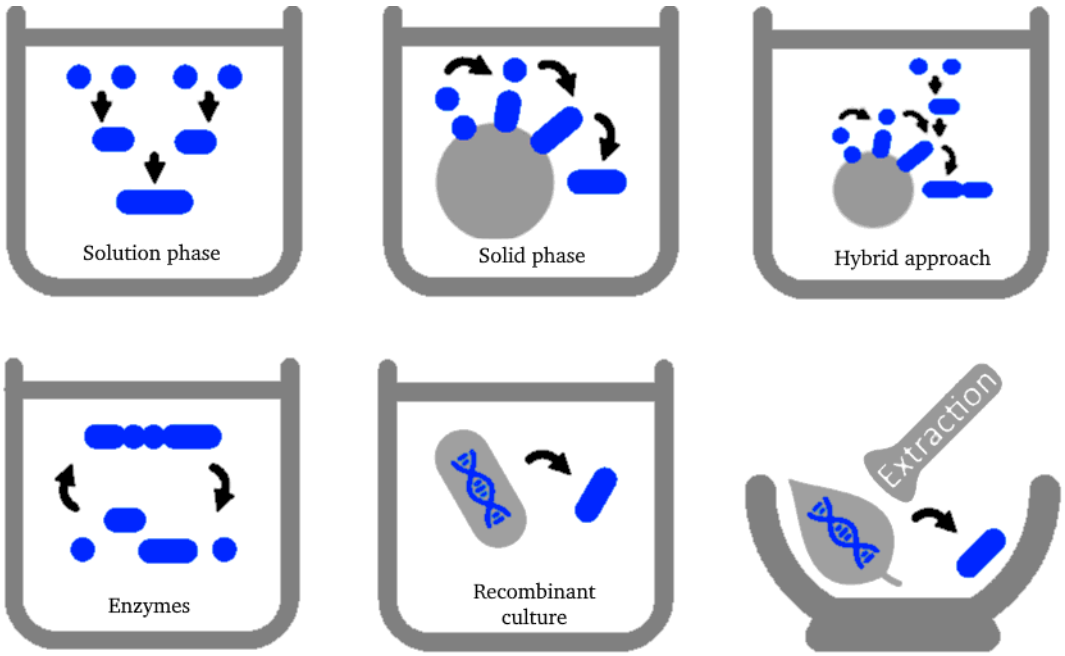

Figure 2: Approaches to peptide production. Peptides can be assembled by chemical synthesis either in solution (liquid phase synthesis) (top left), solid phase synthesis (top middle) or by a hybrid approach (top right) with fragment condensations of smaller peptide fragments or a combination of the other methods. Alternative methods for peptide production are enzyme-based coupling or cleavage methods (bottom left) recombinant synthesis pathways by microorganisms (bottom middle) or extraction methods from natural sources (bottom right). (Modified figure by Uhlig *et al.*[3], distributed under the terms of the Creative Commons Attribution-NonCommercial-ShareAlike, Licence: CCBY-NC-SA 3.0 (https://creativecommons.org/licenses/by-nc-sa/3.0/))

Methods relying on extraction from natural sources as well as recombinant synthesis of peptides using microorganisms are however limited in terms of using unnatural amino acids, post synthetic modifications on *C*- and/or *N*-Terminus or selective-side chain modifications. This work focuses on the chemical synthesis of peptides.

1.2. Liquid-phase peptide synthesis (LPPS)

Peptide synthesis in solution is called LPPS. Depending on the used technique, LPPS is divided into two classes: step-by-step peptide synthesis from the *C*- to the *N*-terminus by subsequent adding of protected amino acids[30] and convergent or semi-convergent block synthesis, with coupling of smaller polypeptide fragments.[31] A big disadvantage of LPPS is the necessary purification after each coupling step with unpredicted solubility issues. By-products from incomplete transformations, side reactions that may occur, or reagent impurities will accumulate over time and reduce the purity of the synthesized peptide. With growing length of the peptide chain, the purification gets more and more complicated, and each isolation step is accompanied by physical loss of material. Nevertheless, LPPS is still in use for industrial-scale production of short, up to fifteen amino acids, peptide sequences.

1.3. Solid-phase chemistry

The concept of solid-phase peptide synthesis was developed by Bruce Merrifield in 1963.[14] His idea was to find a fast, simple and effective way for peptide assembly. Merrifield showed 1964 that his new method of synthesis[32] had many advantages compared to the classical solution-phase approach to bradykinin reported by Guttman *et al.*[33-34] and Nicolaides *et al.*[35] In 1972, in his article in Nature, Mutter *et al.* addressed the problems of early SPPS, among them accumulation of erroneous sequences due to incomplete coupling steps, lack of isolation/purification methods, and restricted repertoire of solvents and coupling methods.[30] In general, the solubility issue was recognised as cause of synthetic problems during the SPPS process.[36]

The maturation of high performance liquid chromatography (HPLC) for peptide purification was a major boost for the SPPS method as it made possible removal of by-products associated with chain assembly and cleavage from the polymeric support.[37-39] Following HPLC

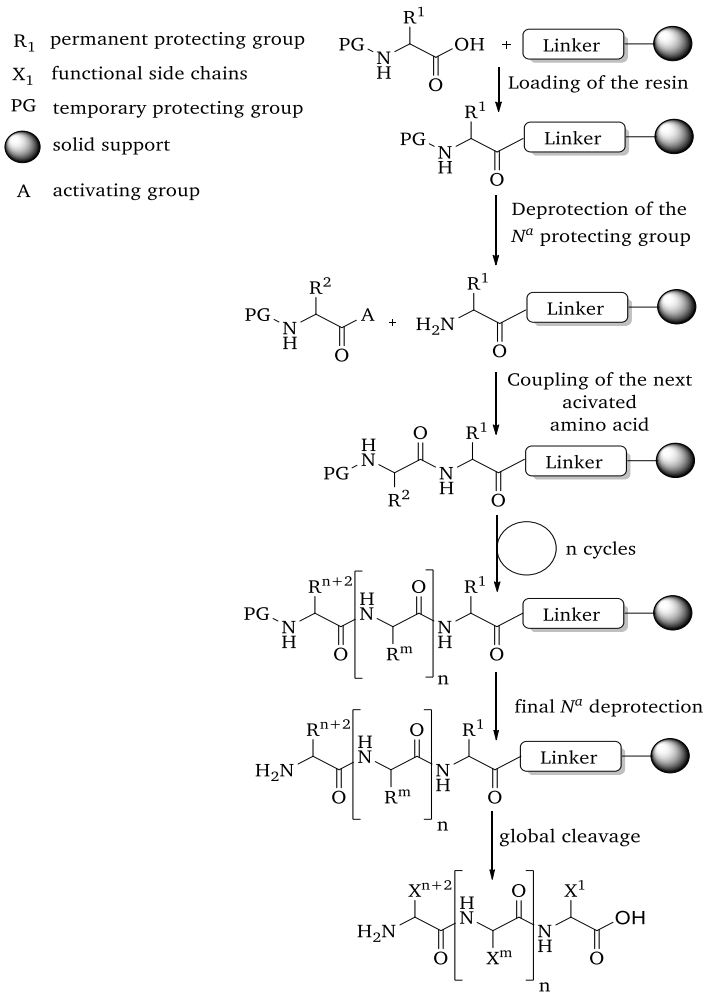

Scheme 1: Schematic representation of the SPPS cycle.[14]

advancement, SPPS has become the standard method in peptide synthesis, and Bruce Merrifield was awarded the Nobel Prize in Chemistry (1982).[40-41]

The SPPS strategy (**Scheme 1**) is as follows: The first amino acid is attached to a polymer (solid support) by a covalent bond *via* a cleavable linker. Then coupling and Fmoc deprotecting steps of the ongoing amino acids are repeated until the sequence is complete. The final step is the cleavage from solid support, very often with simultaneous liberation of the side-chain functionalities, the so-called global cleavage. The *N*-terminus of the coupled amino acid has to be masked by a protecting group, as otherwise the newly added amino acid could couple with itself which would result in by-products.[12],[13],[20]

The enormous advantage of this method is that the purification after each reaction step is simply performed by washing/filtration, and the peptide intermediates remain on the solid support located inside the reaction vessel. This allows to add the amino acids during the coupling steps in a significant excess compared to the loaded resin, which leads to higher yields.[14]

1.4. Hybrid approach (Fragment condensation)

Hybrid approaches combining solid- and solution-phase steps to synthesize peptide sequences (fragments) that are coupled to make longer peptides (>50 aa), difficult sequences or proteins[42] are getting more popular.[43-45] Two main elaborated strategies based on fragment condensation approaches are available to date, the solid phase fragment condensation (SPFC)[46] and fragment condensation in solution. The fragment condensation itself can be performed applying a variety of methods, e.g. amide bond formation, native chemical ligation[47-50] or enzymatic reactions[51-53], a schematic overview is shown in **Scheme 2**. Depending on the used strategy, fully protected peptide fragments are required, or the orthogonal approach relying on fully deprotected blocks under aqueous conditions is needed.

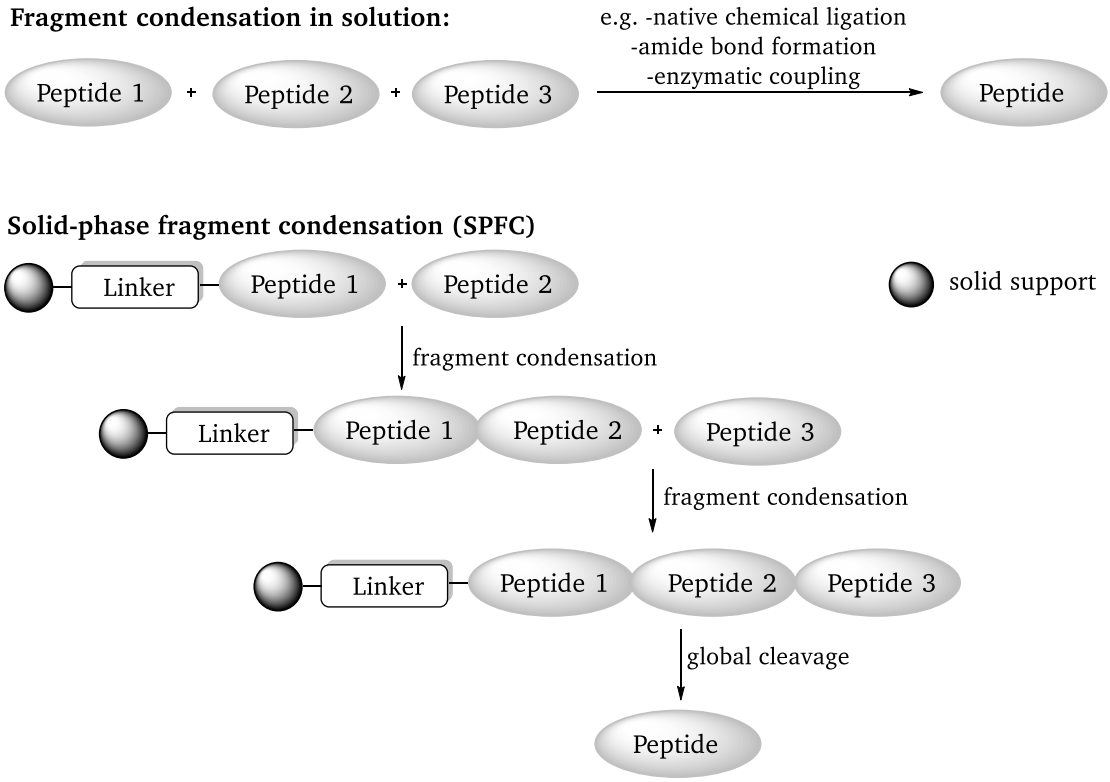

Scheme 2: Schematic representation of the two fragment condensation routes.

1.5. SPPS: Synthetic strategies

There are two strategies of masking the *N*-terminus, the acid-labile Boc group (Boc-SPPS)[15] and the base-labile Fmoc one (Fmoc-SPPS).[14, 20] During chain assembly, Boc is removed with 25% TFA, and cleavage from the solid support is performed with HF.[16] **Scheme 3** shows the Boc-SPPS strategy.

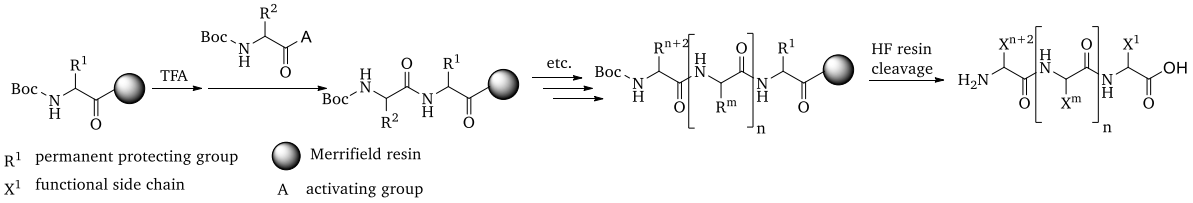

Scheme 3: Boc-SPPS strategy (Merrifield SPPS).[15-16]

The usage of highly toxic hydrofluoric acid is quite unpopular, so the number of users of this method decreases; however it is still used for special applications.[54] The main disadvantage of the Boc SPPS has always been the lack of orthogonality regarding the temporary (Boc) and the constant (side chains and *C*-terminus) protecting groups. The repeated TFA treatment bears the risk of cleaving some portion of the side-chain protecting groups as well as the resin linker during the peptide assembly.[54] The repetitive acidolysis was also shown to result in acid-catalyzed side reactions, e.g. a modification of the Trp (Tryptophan) indole ring.[55] This particular problem during Boc-based SPPS is easily solved upon switching to Fmoc chemistry as demonstrated by Fields *et al*. for gramicidin A (containing four Trp residues).[56]

The Fmoc method makes use of the base-labile Fmoc group to protect an amino terminus and an orthogonal scheme for the functional side chains. The temporary Fmoc protecting group can be cleaved with liquid ammonia, 20% piperidine or other moderate bases.[20] **Scheme 4** shows the Fmoc-strategy.

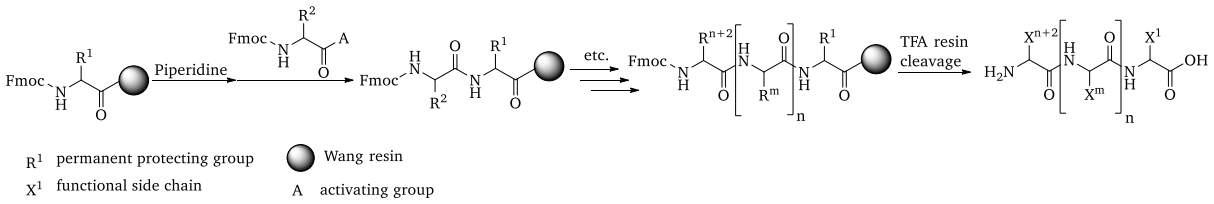

Scheme 4: Fmoc-SPPS strategy (Wang resin).[20]

The coupling reaction takes place in DMF with pre-formed or *in situ* produced active species, often in form of active esters. Excess reagents are removed by washing the resin with DMF. Following deprotection in 20% piperidine, the next activated Fmoc-amino acid is coupled to the growing sequence. Global cleavage occurs in 95% TFA.[57] Fmoc-SPPS method is very popular because of its orthogonality, adaptability to multiple peptide synthesis, and the easy removal of the Fmoc protecting group under mild conditions, which makes it compatible with a wide variety of modified peptides, among them phosphorylated, PEGylated, glycosylated or biotinylated ones.[54, 58] A number of studies carried out by Angeletti *et al.* for the Peptide Synthesis Research Committee (PSRC) illustrate this trend. Over a period of six years (1991-1996) the PSRC performed studies on the synthetic methods and analytical techniques for peptide synthesis.[59] At the beginning of the study in 1991, around 50% of the participating member labs used Fmoc-based peptide chemistry, and 50% were still using Boc-based peptide synthesis. By 1994, already 98% of participating laboratories switched to Fmoc-based approach.

One of the reasons for this development is the wide availability of Fmoc amino acids in high purity (>99%) and falling prices for the building blocks.

Besides the amino group of the coupling amino acid, all side chains in the growing peptide sequence need to be protected to prevent side reactions. These side chains are usually masked with acid-labile moieties.

1.5.1. Side-chain protecting groups

Synthetic organic chemistry is aimed on the formation of new covalent bonds by using specific reagents or catalysts. If several functional groups in the molecule are reactive under the desired conditions, suitable protective groups are required to prevent the formation of by-products during the synthesis.[60-61] If the protective groups used are not selected correctly regarding the chosen reaction pathway, the synthesis strategy may be endangered.

The ideal protecting group should match the following criteria:
1) be easily introducible at the desired site;
2) tolerate wide range of reaction conditions (even more important for multiple reaction steps);
3) be easily removable after the synthesis.

It is important to mention that the second and third criteria are often in an obvious conflict. Indeed, the repeated Boc deprotection with TFA could also result in the cleavage of small amounts of the side-chain protecting groups as a side reaction. Addressing this issue, the concept of orthogonal protecting groups by Barany *et al.*[62-63] became the next synthetic milestone. In this concept, at least two functional groups are masked by protecting groups that are removable by different deprotection mechanisms. The protecting groups can be cleaved stepwise and in the presence of each other, and often under milder conditions, compared to reaction rate-based mechanisms.

Since the introduction of the CBz protecting group by Zervas and Bergmann,[12] peptide chemistry has facilitated the development of new protective groups.[13, 20, 64] Generally, among the natural amino acids a number of functional groups need protection, among them hydroxy, carboxy, amino, thiol, amide, and guanidine groups as well as sometimes indole and imidazole rings. The following two tables give a short insight into the protecting group strategies for Boc- (**Table 1**) and Fmoc-(**Table 2**) based peptide synthesis. The table contains the most frequently used protecting groups for the Boc/Fmoc strategy, their chemical structure and deprotection conditions. This is only a small selection from the available repertoire. Comprehensive description of the protecting group possibilities is given in the literature[60-61], in particular the application possibilities in peptide synthesis.[57, 64]

Table 1: Side-chain protection for amino acids in Boc-based SPPS. [57, 60-61, 64]

Amino acids (Abbreviations)	Protecting group	Name (Abbreviation)	Cleavage conditions
Arginine (Arg)	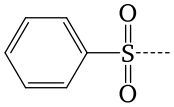	toluolsulfonyl[65] (Tos)	HF/scavengers
	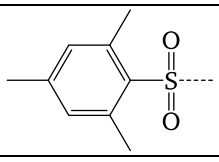	mesitylen-2-sulfonyl[66] (Mts)	CF_3SO_3H/TFA

Aspartic acid (Asp) Glutamic acid (Glu)	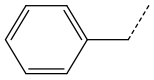	benzyl[67] (Bzl)	1)HF/scavenger 2)H_2 cat.
Serine (Ser) Threonine (Thr) Tyrosine (Tyr)	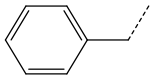	benzyl[67] (Bzl)	1)HF/scavenger 2)H_2 cat.
Asparagine (Asn) Glutamine (Gln)	Asn and Gln can be used without side-chain protection. The unprotected aa show poor solubility in organic solvents resulting in slow coupling rates.		
	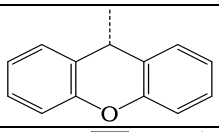	9-xanthenyl[68] (Xan)	90% TFA and scavengers[1,69-70]
Cysteine (Cys)	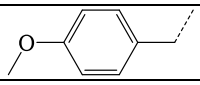	4-methoxybenzyl[71] (MeOBzl)-	HF
	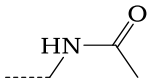	acetamidomethyl[72] (Acm)	Hg(II), Ag(I), I_2, Tl(III), RSCL, $Ph(SO)Ph\text{-}CH_3SiCl_3$
Histidine (His)	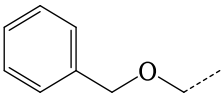	benzyloxymethyl[73-74] (Bom)	1)HF/scavengers 2) TFMSA/TFA
	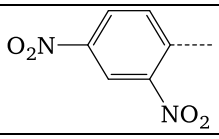	dinitrophenyl[75] (DNP)	1)HF 2)Thiolysis
	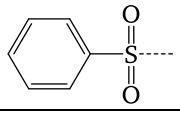	toluolsulfonyl[65] (TOS)	HF/scavengers
Lysine (Lys)	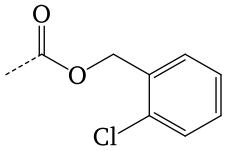	2-chlorobenzyloxycarbonyl[76] (2-Cl-Z)	HF/scavenger
	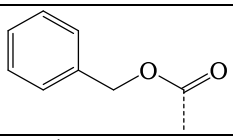	benzyloxycarbonyl[12] (CbZ)	HF [2]
	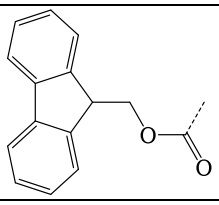	9-fluorenylmethoxycarbony[20-21] (Fmoc)	Piperidine
Tryptophan (Trp)	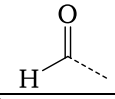	formyl[77] (For)	1)HF/scavengers 2)Piperidine/water
	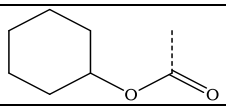	cyclohexyloxycarbonyl[78] (Hoc)	HF, scavengers

The side chains are usually masked with an acid-labile protecting group during an orthogonal Fmoc-based SPPS scheme. This allows performing simultaneous side-chain deprotection and cleavage from the solid support in 95% TFA. For every amino acid orthogonal side chain

[1] The Xan protecting group is concurrently removed during Boc deprotection by TFA treatment; Dehydration side reaction of Asn or Gln residues is only possible during the coupling step, therefore Xan elimination after coupling is only a minor problem.[42-43]

[2] acid-labile, does not withstand repetitive treatments with TFA

protecting groups are possible, that allows to solely liberate a single side chain moiety if a specific post-synthetic modification is necessary.[57, 64]

Table 2: Side-chain protection for amino acids in Fmoc-based SPPS [57, 60-61, 64]

Amino acids (Abbreviations)	Protection groups	Name (Abbreviation)	Cleavage conditions
Arginine (Arg)	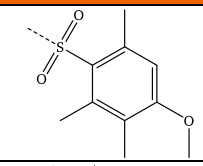	4-methoxy-2,3,6-trimethyl-benzenesulphonyl[79] (Mtr)	1)90-95% TFA, 4-6h 2)TFA-anisole (9:1), 1h
	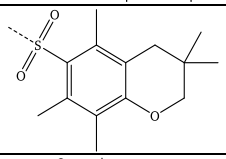	2,2,5,7,8-pentamethyl-chroman-6-sulfonyl[80] (Pmc)	1)50% TFA v/v in DCM, 3h 2)TFA-scavanger
	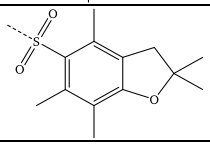	2,2,4,6,7-pentamethyl-dihydro-benzofuran-5-sulfony[81] (Pbf)	95% v/v TFA in DCM, 0,5h
Aspartic acid (Asp) Glutamic acid (Glu)	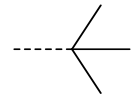	*tert*-butyl[82-83] (*t*Bu)	90% v/v TFA, 0.5h
	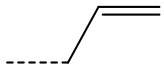	allyl[84] (Al)	1)$Pd(Ph_3P)_4$-AcOH-NMM 2)$Pd(Ph_3P)_4$ (0.02 eq.) in DCM
	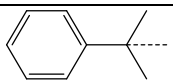	2-phenylisopropyl[85] (2-PhiPr)	4% TFA in DCM, 15min
Asparagine (Asn) Glutamine (Gln)	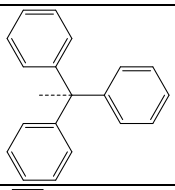	trityl[86-88] (Trt)	90% v/v TFA, 30min
	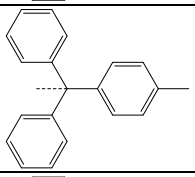	4-methyltrityl[89] (Mtt)	95% v/v TFA, 30min
Cysteine (Cys)	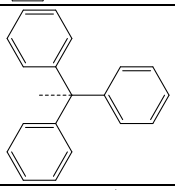	trityl[86-88] (Trt)	90% v/v TFA, 30min
	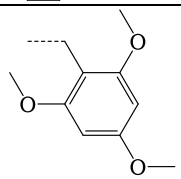	2,4,6-trimethoxybenzyl[90] (Tmob)	90% v/v TFA, 1h
	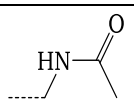	acetamidomethyl[72] (Acm)	Hg(II), Ag(I), I_2, Tl(III), RSCL, Ph(SO)Ph-CH_3SiCl_3
	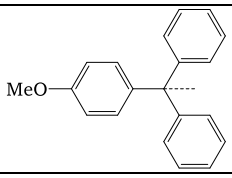	monomethoxytrityl[91] (MMT)	2% TFA in DCM

	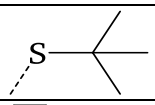	*tert*-butylsulfenyl[92] (StBu)	RSH R_3P
Histidine (His)	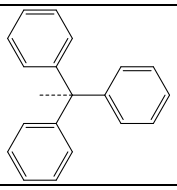	trityl[86-88] (Trt)	90% v/v TFA, 30min
	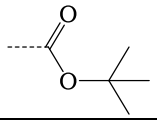	*tert*-butyloxycarbonyl[13, 93] (Boc)	90% v/v TFA, 30 min
	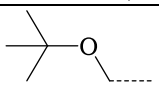	*tert*-butoxymethyl[94] (Bum)	95% v/v TFA, 1-2 h
Lysine (Lys)	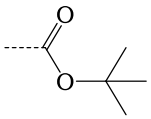	*tert*-butyloxycarbonyl[13, 93] (Boc)	90% v/v TFA, 30 min
	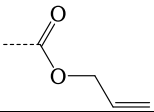	allyloxycarbonyl[84] (Alloc)	1)Pd($Ph_3P)_4$ (0.1 eq.) 2)$PdSiH_3$ (24 eq.) in DCM, 10min
	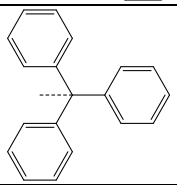	trityl[86-88] (Trt)	90% v/v TFA, 30min
	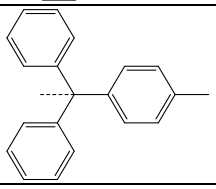	4-methyltrityl[89] (Mtt)	95% v/v TFA, 30min
Serine (Ser) Threonine (Thr) Tyrosine (Tyr)	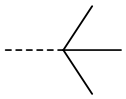	*tert*-butyl[95] (*t*Bu)	90% v/v TFA, 0,5 h
	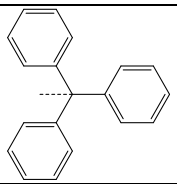	trityl[86-88, 96] (Trt)	90% v/v TFA, 30min
	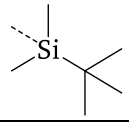	*tert*-butyldimethylsilyl[97-98] (Tbdms)	0.1M TBAF-DMF, 15min (Tyr) TFA, 15min (Ser/Thr)
Tryptophan (Trp)	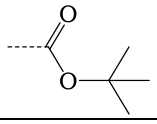	*tert*-butyloxycarbonyl[13, 93, 99] (Boc)	90% v/v TFA, 30 min

1.5.2. Solid support

The success of a peptide synthesis by SPPS strongly depends on the solid support and its performance during the synthesis. These supports, referred to as resins, usually comprise a rather chemically inert polymeric bead decorated with a functional linker. In 1963, Merrifield defined the solid support as an insoluble, in all utilized solvents stable physical form which permits filtration and a functional group to which a linker or an amino acid are bound by a

covalent bond.[14] The optimal properties of the solid support have been further expanded by van den Nest and Albericio:[100] "1) mechanically and physically stable beads; 2) stability in variation of temperature; 3) mobile, well-solvated and reagent-accessible sites; 4) acceptable loadings; 5) good swelling in a broad range of solvents; 6) functionalized beads permitting covalent coupling of the first compound; 7) the resin should be chemically stable under most reaction conditions."[100] But as van den Nest and Albericio stated, it is unrealistic to expect a solid support to have all these characteristics, therefore the resin that is best suited for the planned task should be chosen.[100]

Most resins are based on polystyrenes (PS) with different functional groups, but cross-linked polyamides (PA), composite PS-polyethylene glycols (PEG) or totally PEG-based resins are also available.[100-101] The polymeric network of the resin can be modelled in two ways: 1) the rigid carrier model, where the resin is considered as a compact sphere and 2) the co-solvent model, where the effect of the resin is accounted in reactions. Several direct and indirect studies have been carried out to determine which is the most appropriate model to describe the solid support role. Regen *et al*. investigated PS-and PEG-PS based solid supports and concluded that both resins showed significant mobility and the co-solvent model would fit best.[102-104] His findings were validated by Czarnik and Meldal.[100, 105-106]

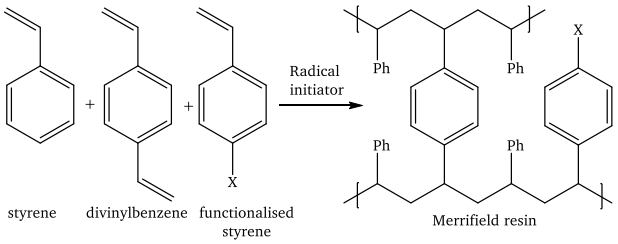

Scheme 5: Synthesis of a Merrifield resin. Cross-linking and functionalization depend on ratio of the starting materials.

The resin Merrifield used for his SPPS was a styrene-divinylbenzene co-polymer functionalized by chloromethylation.[14] The first amino acid was bound to the resin *via* an ester linkage. The synthesis of a Merrifield resin is shown in **Scheme 5**. The cross-linkage extent affects the solvation and swelling properties of the resin. Standard crosslinking is performed with 1-2% DVB (divinylbenzene) which leads to a resin with a strong hydrophobic character. PS-DVB resins are widely used in the solid-phase organic chemistry.[107-108] Merrifield and others observed that reaction rates were slower than in solution and the incorporation of amino acids decreases with increasing peptide length on solid support.

To address these intrinsic problems a PEG moiety was incorporated into the resin to enhance flexibility and solvation. The effect of resins with incorporated PEG units on the amide bond formation was investigated by Czarnik *et al*.[105] and others.[106, 109] Under similar reaction conditions, faster kinetics have been observed on PEG-PS resins. Increasing the amount of PEG units in the resin resulted in faster reaction kinetics.[109] It is assumed that PEG chains influence solvation behaviour, dielectric properties and hydrogen bond pattern. Known representatives of this resin group are POE-PS[110] (Tentagel®); PEGA[111] (glycol polyacrylamide copolymers with a high content of PEG); TTEGDA-PS[112] (PS resin with tetra(ethylene glycol) diacrylate (TTEGDA) as crosslinker); Clear®[113] (cross-linked ethoxylate acrylate resin).

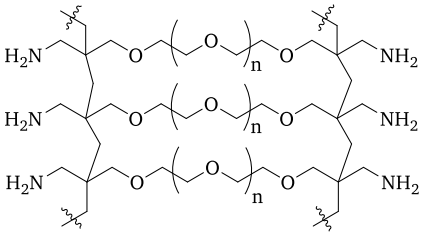

Figure 3: Structure of ChemMatrix® resin.

Development of fully PEG-based resins followed, resulting in more hydrophilic polymeric supports with excellent swelling properties in a wide range of solvents (water, alcohols and many organic solvents). This allowed using the resins for multiple applications. The amphiphilic nature of the

resins was reported to increase reactivity during the coupling and deprotection steps. These swelling properties arise from the stretched helical superstructure of PEG in aqueous solutions.[114] Known representatives of PEG-based resins are SPOCC[115] (polyoxyethylene/polyoxy-propylene) and ChemMatrix® (CM, **Figure 3**).[116]

As the ChemMatrix® resin was frequently used for the present work, the properties of this resin are briefly discussed. The resin is totally PEG-based, linked by primary ether bonds, and is highly cross-linked. The improved polarity of the CM resin allows to use polar solvents like water, acetonitrile, methanol and other alcohols in addition to classic hydrophobic solvents without the loss of swelling properties (shown in **Figure 4**). The high efficiency of this solid support was demonstrated by the synthesis of complex peptides like HIV protease (99aa)[117], Rantes (1-68)[118] and β-amyloid (1-42).[116]

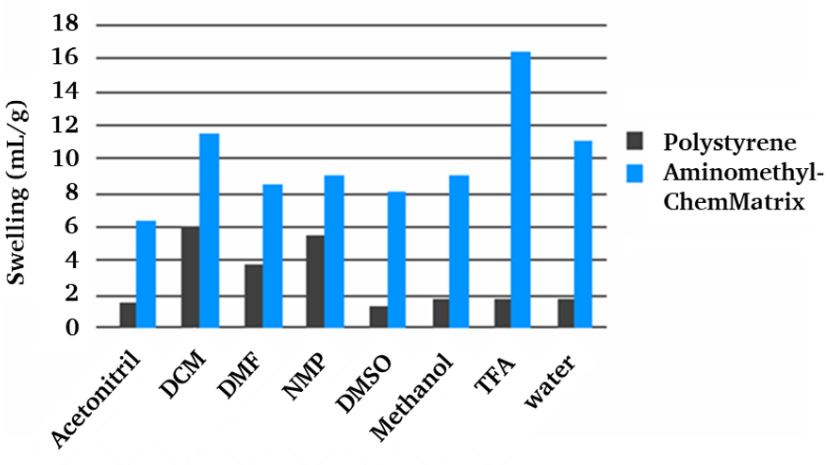

Figure 4: Comparison of the swelling properties of polystyrene and CM resins in different solvents. (Adapted with permission from García-Martín *et al.*, *J. Comb. Chem.* **2006**, 8, (2), 213-220).[116] Copyright 2006 American Chemical Society).

1.5.3. Linkers

The reversible connection between the peptide and the resin is provided by the linker molecule. This is the unit that stipulates the choice of chemistry used both for the assembly and the global cleavage. A wide variety of SPPS linkers has been developed to date, allowing to obtain acids, amides, esters, thioesters, hydrazides, alcohols or aldehydes after the cleavage from the solid support (examples shown in **Scheme 6**).

A broad range of resins decorated with linker molecules of different nature is currently available as commercial products. **Table 3** shows some of the most common SPPS linkers, their specific cleavage conditions and the resulted *C*-terminal functionalisation. Many linkers form carboxylic acids or carboxylic amides upon acidic cleavage. Sulfonamide and hydrazide linkers allow

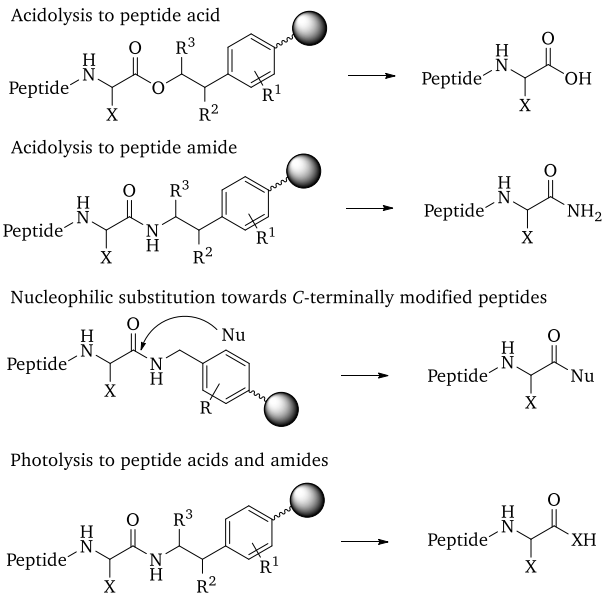

Scheme 6: Examples of different linker types and cleavage reactions for SPPS. R^1, R^2, R^3: rests depending on linker; X: aa side chain).

releasing of the peptide from solid support with different functional groups, depending on the conditions.

Table 3: SPPS linkers and their cleavage conditions

Linker	Resin-bound structure	Cleavage conditions	C-terminus
Wang	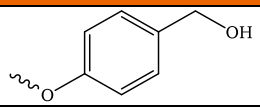	90–95% TFA, 1–2h	Acid
Rink acid[119]	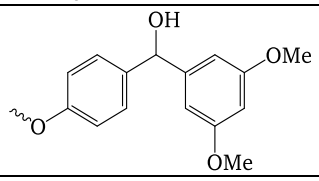	1)1–5% TFA, 5–15min 2)10% AcOH, 2h	Acid
4-(4-hydroxymethyl-3-methoxyphenoxy)butyric acid (HMPB)[120]	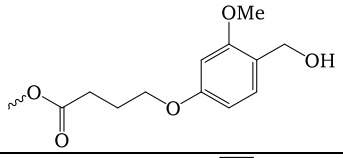	1% TFA, 2–5min	Acid
2-chlorotrityl chloride (2-CTC)[121]	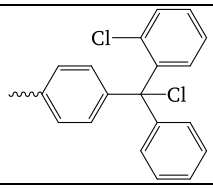	1–5% TFA, 1min	Acid
SASRIN (super acid-sensitive resin)[122]	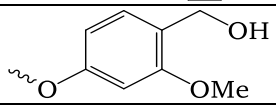	1% TFA, 5–10min	Acid
Rink amide[119]	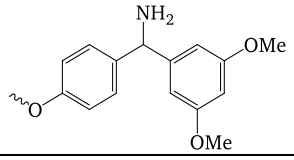	50% TFA, 1h	Amide
4-methylbenzhydrylamine (MBHA)[123]	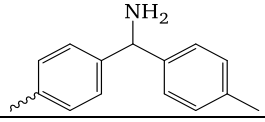	HF 0°C, 1h	Amide
Hydrazine[124]	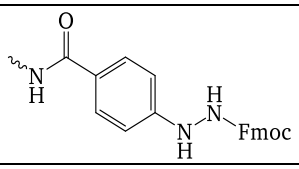	Cu(OAc)2, pyridine, acetic acid, nucleophile	Acid, ester, amide
Sulfonamide[125]	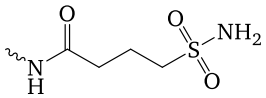	1) Iodoacetonitrile/ DIPEA/NMP, 24h 2) Nucleophile, DMAP, 24h	Acid, ester, thioester, amide, etc.
4-hydroxymethylbenzoic acid (HMBA)[126]	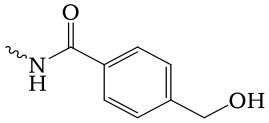	NaOH N_2H_4 NH_3 ROH $LiBH_4$	Acid Hydrazide Amide Ester Alcohol
Backbone amide linker (BAL)[127]	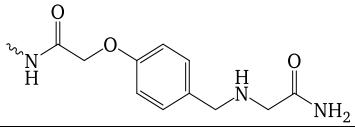	TFA/trifluoromethane-sulfonic acid (TFMSA) (19 :1)	Acid

1.5.4. Coupling methods

Along with the development of novel protecting groups, the optimisation of coupling reagents and conditions became an important research direction. Amide (peptide) bonds are typically formed between carboxylic acids and amines under elimination of water. However, the amide bond formation does not occur spontaneously at RT (room temperature) and requires heating above 200°C.[128] Jursic *et al.* restricted this reaction to compounds matching the following terms: The ideal reactants should have melting points below 200°C, be non-volatile and thermally stable at this temperature for 30 minutes.[128] This is definitely not the case for most amino acids, at least the natural ones.

Therefore, the α-carboxy group of the incoming amino acid has to be activated for an effective coupling. This usually means converting the OH group of the carboxylic acid into a good leaving group (increasing the electrophilicity of the carboxy group) to allow amide bond formation with amines under mild conditions. **Scheme 7** shows the reactivity of the different carboxylic acid derivatives.

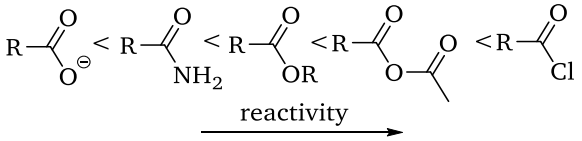

Scheme 7: Activity of the carboxy derivatives.

The introduction of carbodiimides by Sheehan *et al.* in 1955 became a real feat in peptide synthesis.[129] Symmetrical carbodiimides, like *N,N'*-dicyclohexylcarbodiimide (DCC) and *N,N'*-diisopropylcarbodiimide (DIC) activate the carboxy group by forming an O-acylurea derivative that serves as a leaving group upon coupling (**Figure 5**).

In his SPPS, Merrifield used DCC as coupling reagent in DCM (dichloromethane) or DMF (*N,N*-dimethylformamide) although dicyclohexylurea, a byproduct formed from DCC, is nearly insoluble in most organic solvents.[14] DIC is often used instead of DCC in SPPS because the urea byproduct remains in solution.

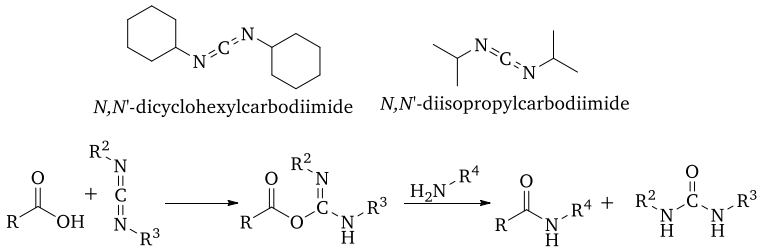

Figure 5: Top: Structure of DIC and DCC. Bottom: carbodiimide-based activation of a carboxylic acid.

However, the carbodiimide activation method has been reported to cause racemization at the C_α-atom of certain amino acids due to the high reactivity of the O-acyl isourea. In solution-phase chemistry an oxazolone intermediate could be formed upon an intramolecular cyclisation, resulting in the potential loss of chiral integrity of the amino acid as shown in **Scheme 8.**[130] In SPPS reactions this mechanism is prevented by growing peptides from *C*- to *N*-Terminus and using urethane (carbamate) protecting groups for the amine. Racemization might also occur at the C_α-position under basic conditions resulting in the formation of a carbanion, especially with cysteine[131-132] and histidine.[133] Protonation of the carbanion might also lead to a racemic mixture similar to the oxazolone mechanism.[134]

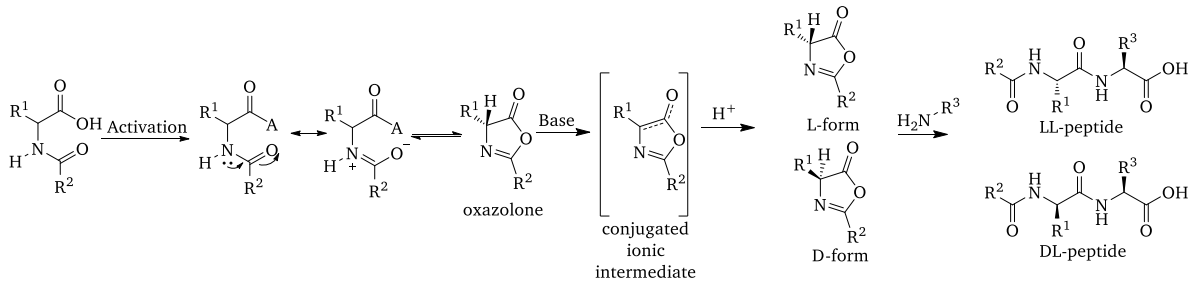

Scheme 8: Racemization following an oxazolone mechanism. R_1, R_2, R_3: side chain residues, A: leaving group

To address this issue, König and Geiger developed 1-hydroxy-1H-benzotriazole (HOBt)[135] as an additive when using carbodiimides to reduce the racemization level by formation of a less reactive HOBt ester.[136] The usage of HOBt and carbodiimides can lead to the formation of diazetidine, which is catalyzed by HOBt.[137] Carpino *et al.* reported the usage of 1-hydroxy-7-azabenzotriazole (HOAt)[138], which was reported to be more efficient than HOBt in terms of yield, kinetics and racemization levels.[139] In recent years, a highly efficient leaving group has been introduced, called Oxyma (ethyl-2-cyano-2-(hydroxyimino)acetate). It has coupling efficiency and racemization suppression rates like HOAt but is less hazardous than HOBt and HOAt.[140] Structures of the compounds are shown in **Figure 6**.

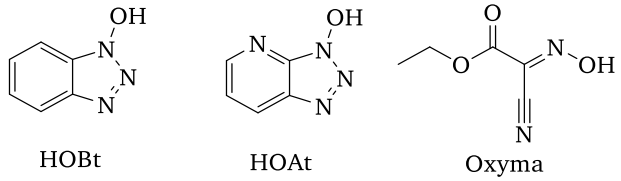

Figure 6: Coupling additives upon ester formation.

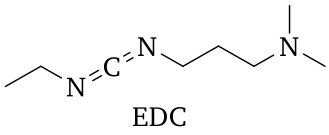

Figure 7: EDC.

To date, a vast number of carbodiimides has been reported. Several water-soluble derivatives like 1-ethyl-3-(3-dimethylaminopropyl)-carbodiimide (EDC, **Figure 7**) were investigated by Sheehan *et al.*[141-142] He concluded that coupling was more efficient when using tertiary amine carbodiimides rather than quaternary derivatives. The main advantage of the water–soluble carbodiimides was the easy remove of urea byproducts, as the ureas formed when using DCC or DIC are sometimes difficult to remove. Today, water-soluble carbodiimides are widely used in protein chemistry.

Carpino compared DIC, EDC and other carbodiimide analogues. The combination of DIC and HOAt as an active ester showed the best results upon coupling.[139]

Over the years, new-generation coupling reagents have been developed. Modern activation methods prefer esters as leaving group. This can be achieved by pre-formation or by *in situ* generation.

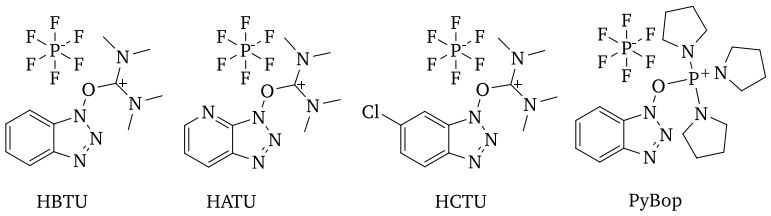

Figure 8: Phosphonium- and uronium-based *in situ* activators.

Most of the modern *in situ* activators are based on benzotriazole alcohols, phosphonium or uronium salts. The most widely used coupling reagents for *in situ* activation are 2-(1H-benzotriazol-1-yl)-1,1,3,3-tetramethyluronium hexafluorophosphate (HBTU)[143], benzotriazole-1-yl-oxy-tris-pyrrolidinophosphonium hexafluorophosphat (PyBOP)[144], 1-[bis(dimethylamino)-methylene]-1H-1,2,3-triazolo[4,5-b]pyridinium-3-oxid hexafluorophosphate (HATU)[138] and

O-(1H-6-chlorobenzotriazole-1-yl)-1,1,3,3-tetramethyl-uronium hexafluorophosphate (HCTU)[145]; structures are shown in **Figure 8**.

HATU and HCTU are similar to HBTU but react faster with less epimerization during the coupling step.[145-146] The reactive species of all these activators are benzotriazole esters or derivatives thereof. The coupling step is often performed with an excess of about 2 to 8 equivalents in the presence of a base like *N,N*-diisopropyl-ethylamine (DIPEA) to effectively complete the desired reaction. DIPEA (Hünig base) deprotonates the α-carboxy group, see **Scheme 9**.

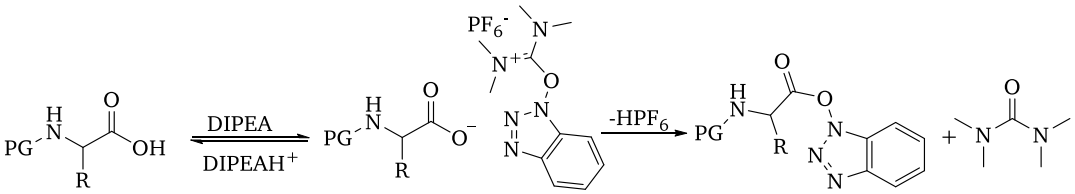

Scheme 9: Amino acid deprotonation with DIPEA and active ester formation with HBTU. HATU and HCTU follow a similar mechanism. R: side-chain residue, PG: protecting group.

The efficacy of the coupling reagents can be ordered in the following way:

OPfp esters/HOBt < DIC/HOBt < HBTU ≈ PyBOP < HATU ≈ HCTU[146]

In 2002, Carpino *et al.* showed that the common coupling reagents HBTU, HATU and HCTU have been identified to exist in two forms, as a uronium salt (O form) and as a guanidinium salt (also referred to as an aminium salt) (N Form) (**Figure 9**).[147] They have been originally classified as O-uronium salts and later the structure was revised to guanidinium salts by Carpino *et al*. The formation of a particular form is influenced by the following factors: solvent, isolation method, counter anion, etc. This area is of interest considering the fact that the new uronium coupling reagents seem to be more efficient than the corresponding guanidinium coupling reagents.[147]

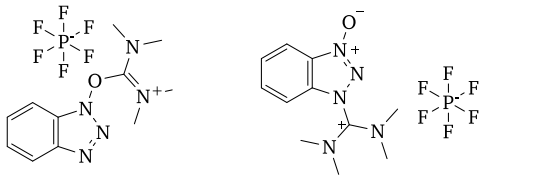

HBTU uronium salt (O form) HBTU guanidinium salt (N form)

Figure 9: HBTU O- and N-form.[146]

In addition, HBTU, HATU and HCTU can often cause a capping side reaction, which leads to *N*-terminal guanylated peptides shown in **Scheme 10**.[148-149] Especially the aminium salts (guanidinium salts) are prone to cap the free *N*-terminus.[148-149] This side reaction leads to reduced yield or even terminates the chain growth. In order to prevent this side reaction, HBTU, HATU and HCTU need to be kept in a small stoichiometrically deficient amount to the coupled amino acids.[148]

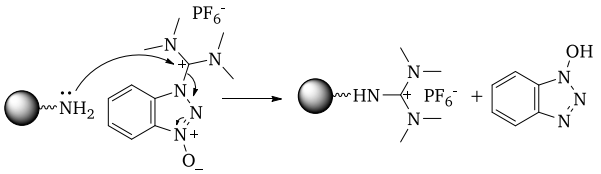

Scheme 10: Side reaction with HBTU yields an *N*-terminal guadinylated peptide.

In 1995, Carpino and El-Faham introduced tetramethylfluoroformamidinium hexafluorophosphate (TFFH) as coupling reagent. Generating acid fluorides *in situ,* TFFH was reported to be beneficial for the incorporation of hindered amino acids.[150]

A series of new Oxyma-based coupling reagents such as (1-cyano-2-ethoxy-2-oxoethylidenaminooxy)dimethylaminomorpholinocarbenium hexafluorophosphate (COMU)[151], Oxyma-B-based reagents like *N*-((1,3-dimethyl-2,4,6-trioxotetrahydropyrimidin-5(6H)-ylidene-amino-

oxy)(dimethylamino)methylene)-*N*-methylmethanaminiumhexafluorophosphate (TOMBU)[152] or 4-((1,3-dimethyl-2,4,6-trioxotetrahydro-pyrimidin-5(6H)ylidene-aminooxy)(dimethyl-amino)methylene)morpholin-4-ium hexafluorophosphate (COMBU)[152] have been recently developed (shown in **Figure 10**). These reagents have been reported to be advantageous over classic benzotriazole-based reagents in certain applications.[151-152]

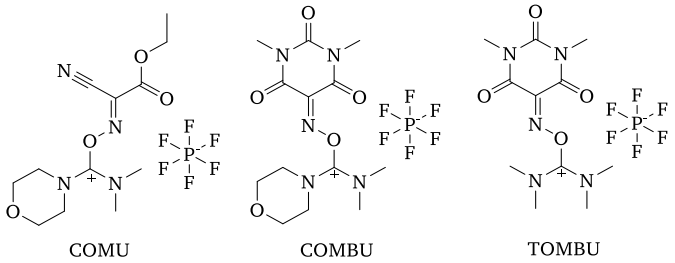

Figure 10: Structures of Oxyma/Oxyma-B based coupling reagents.[151-152]

1.5.5. Automated SPPS

The basic idea of Merrifield's SPPS was to develop a faster, simpler and automatable approach to the chemical peptide synthesis.[14, 153-154] In 1965, he presented his vision of an automated device in Science magazine.[153] The device should have a single reaction vessel that is placed in a special reactor block. The device should be equipped with separate reservoirs for all necessary amino acids, organic solvents as well as activation and deprotection reagents. The device should be able to add the solutions required for each reaction step and afterwards remove the solvents and wash the vessel.[153] The first instrument for automated Boc-SPPS was built by Merrifield *et al.* in 1965, shown in **Figure 11**.[153-154] The introduction of the Fmoc-group[20] and its reduction to SPPS practice in the late 1970s made automatization even easier because there was no more need to use corrosive substances like TFA during the repetitive deprotection cycles. Moreover, automated peptide synthesis could also be performed in a parallel mode to synthesize different peptides simultaneously in different reaction vessels. To that end, the deprotection and washing steps are performed simultaneously, and the coupling step is individual for each peptide sequence.

To date automated peptide synthesizers for small-scale assembly are well established for Fmoc-SPPS (single or parallel mode) and can be purchased in various sizes, with different acceleration (microwave irradiation, infrared heating, etc.) and monitoring mechanism (e.g. UV, conductivity).[155]

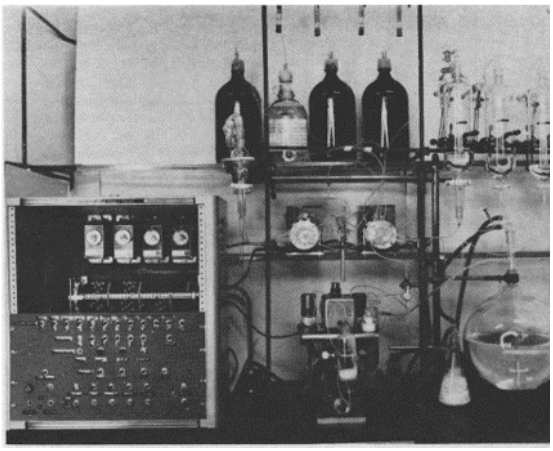

Figure 11: The instrument designed for automation of peptide synthesis by Merrifield.[153] [From R. B. Merrifield, Science 1965, 150, 178-185. Reprinted with permission from AAAS (American Association for the Advancement of Science)].

Today continuous-flow peptide synthesis is getting more and more popular and the respective devices are commercially available. Since the introduction of a continuous-flow SPPS system in the early 1980s,[156-157] the interest in this technology has been diminished. However, recently it has got into the research focus again[54, 158-160] as it allows reducing the excess of reagents for the coupling und the solvents necessary for the SPPS synthesis.[159] Additionally, compared to a standard SPPS synthesis the washing and the reaction steps are inherently more rapid and efficient.[160]

1.5.6. Microwave-assisted SPPS

In 1945, having noticed that a chocolate bar had melted in his pocket in close proximity to a magnetron, Percy Spencer discovered the ability of microwaves (MW) to heat food. Nine years later commercial MW devices appeared on the market, and in 1986 initial reports on the MW acceleration of organic synthesis were published.[161]

To date, three main approaches to thermal activation are generally applied: Conventional heating like oil baths, microwave-accelerated heating, and infrared heating. Conventional heating activates the reactants slowly using an external source. Heat needs to pass the walls of the vessel to reach the solvents and the reactants in it. This is a rather slow and energy inefficient method to transfer energy into a reaction system. In the second way, the energy of the microwaves is applied directly to molecules of the reaction system, rising the temperature of the reaction fluid.

Microwave heating has two fundamental requirements for energy transfer, dipole rotation or ionic conduction. If one of these criteria is fulfilled, it allows instantaneous superheating of the substance(s).[162] **Figure 12** shows the difference between microwave and conventional heating.

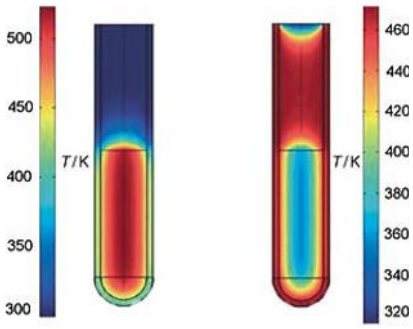

Figure 12: Inverse temperature gradient after microwave heating (left) and conventional heating in oil bath (right) after one minute. Figure by C. O. Kappe[162], Reproduced with kind permission of John Wiley & Sons.

The effect of temperature on velocity of a chemical reaction is described by the Arrhenius equation (**Equation 1**). Arrhenius equation gives the dependence of the rate constant (k) of a chemical reaction on the absolute temperature, a pre-exponential factor (A) and other constants of the reaction, where E_a is the activation energy for the reaction, R is the universal gas constant and T is the absolute temperature that controls the kinetics of the reaction.

Equation 1: $$k = A \times e^{-E_a/RT}$$

Numerous publications have shown that microwave assistance accelerates the reaction rate by a factor of 1000 compared to conventional heating.[162] Microwaves were found advantageous not only for conventional organic chemistry, but for SPPS as well. In 1991 Chen *et al.* reported the use of microwave irradiation to increase coupling efficiency and reduce reaction times in SPPS and monitored racemization of amino acids under microwave heating.[163] Several publications speculate that microwaves interact to a considerable extent directly with amide dipoles in peptides. According to these publications, microwave heating in SPPS is often not only faster but also offers higher purities compared to conventional SPPS at ambient temperature.[164-165] Thus, Bacsa *et al.* compared SPPS with microwave heating and conventional heating.[166] They synthesized three peptides with a length from 9 to 24 amino acids by microwave and oil-bath heating at 86 °C. The results showed similar crude purities, racemization levels, and identical impurity profiles of the peptides. They concluded that the main effect of microwave irradiation applied on SPPS appears to be a thermal one (Arrhenius equation; temperature increase of ~60° results in an estimated 50-fold reaction rate acceleration) and is not related to the electromagnetic field.[166] In 2009 Obermayer *et al.* showed that no observable athermic effects like electromagnetic field influence in microwave

chemistry exists at all.[167] In general, microwave-assisted solid-phase peptide chemistry reduces reaction times accompanied by an increase in the crude peptide purity. [155, 168] However the use of elevated temperatures is known to compromise the stereo integrity of sensitive amino acids.[163, 166] Racemization is discussed in detail in the following chapter.

1.5.7. Side reactions in SPPS

Racemization during the activation process is a problem that often occurs in SPPS. Natural amino acids, except glycine, have a chiral center with L-configuration at its α-carbon. In all these 19 optically active amino acids one of the substituents at the α-carbon is a potentially acidic hydrogen atom. Removal and subsequent reattachment of this hydrogen bears a risk of racemization (**Scheme 11**). The acidity of the hydrogen at the α-carbon is increased upon activation of the carboxyl group. An increased rate of racemization is also pronounced at elevated temperatures, e.g. upon microwave heating.[163, 166] Histidine and cysteine are known as extremely racemization-prone amino acids.

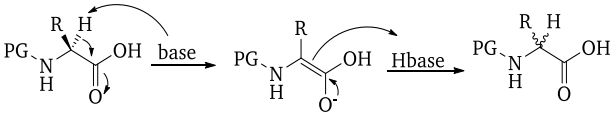

Scheme 11: Base-catalyzed racemization of an amino acid.

Histidine

Histidine may undergo significant racemization during base-mediated activation methods (e.g. phosphonium or uronium reagents with DIPEA) or if the coupling takes a significant amount of time.[73-74, 94, 169] The imidazole π-nitrogen electrons affect the enol formation of histidine active esters, resulting in increased racemization.[170] To avoid this side-reaction, Jones *et al.* established the imidazole π-nitrogen protecting group Bom, which is employed in Boc-chemistry.[74] Later, they introduced the TFA-labile Bum group to be used in Fmoc-SPPS.[94] The 4-methoxy-benzyloxymethyl (MBom) introduced by Hibino and Nishiuchi proved to be very effective to supress epimerisation.[171-172] Unfortunately, the production of Fmoc-His(MBom)-OH is expensive; moreover, in course of cleavage a number of unwanted side reactions was observed. A methoxybenzyl cation (electrophilic alkylating species) is formed during the cleavage process that was reported to induce alkylation of side chain residues.[171, 173] Structures of the protected histidine derivatives are shown in **Figure 13**.

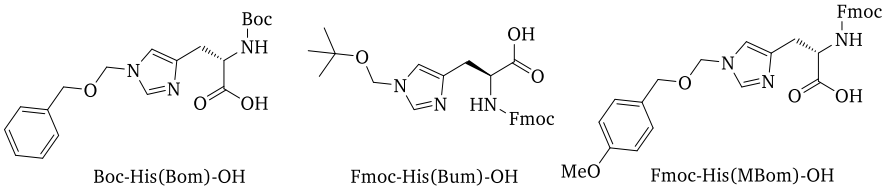

Figure 13: Boc-His(Bom)-OH, Fmoc-His(Bum)-OH and Fmoc-His(MBom)-OH

Therefore, Fmoc-His(Trt)-OH is still in use, even if there is a certain risk of histidine racemization, which becomes only minor if the coupling is performed under slightly acidic conditions (e.g. DIC, HOBt) at ambient temperature.[174]

Cysteine

Using base-mediated activation methods (e.g. phosphonium or uronium reagents with DIPEA) may result in cysteine racemization.[132, 175] Preactivation and microwave heating increase racemization rate,[164] but this can be reduced by using base-free carbodiimide activation methods.[132, 174] Different protecting groups have been examined on the potential reduction of cysteine racemization during the synthesis process, compared to the standard trityl protection. MBom was shown to reduce the D-Cys formation to 0.4%.[71, 176] Unfortunately, the MBom group is linked to the alkylation of side chain residues during the cleavage process (similar to

histidine). A complete suppression however was not possible with the tested protecting groups.[176]

In addition, cysteine racemization often takes place during coupling and Fmoc deprotection with piperidine if the cysteine residue is linked *C*-terminally to the resin by an ester bond.[54] Another enantiomerization mechanism involves the deprotonation and ring opening of an oxazolone intermediate. This intermediate is obtained by a nucleophilic attack on the activated carboxy group from the neighbouring amide bond (see chapter **1.5.4**,**Scheme 8**).

Aspartimide formation

Aspartimide formation is the most harmful side reaction in Fmoc-based SPPS of peptide sequences containing aspartic acid. [54, 177-184] It is caused by both acids and bases,[183] being extremely pronounced in the case of strong bases. Therefore, it has been frequently observed in Fmoc-SPPS (see **Scheme 12**). If a peptide contains several aspartic acid residues, the formation of aspartimide is a serious problem resulting in a number of side products, depending on the reaction conditions.

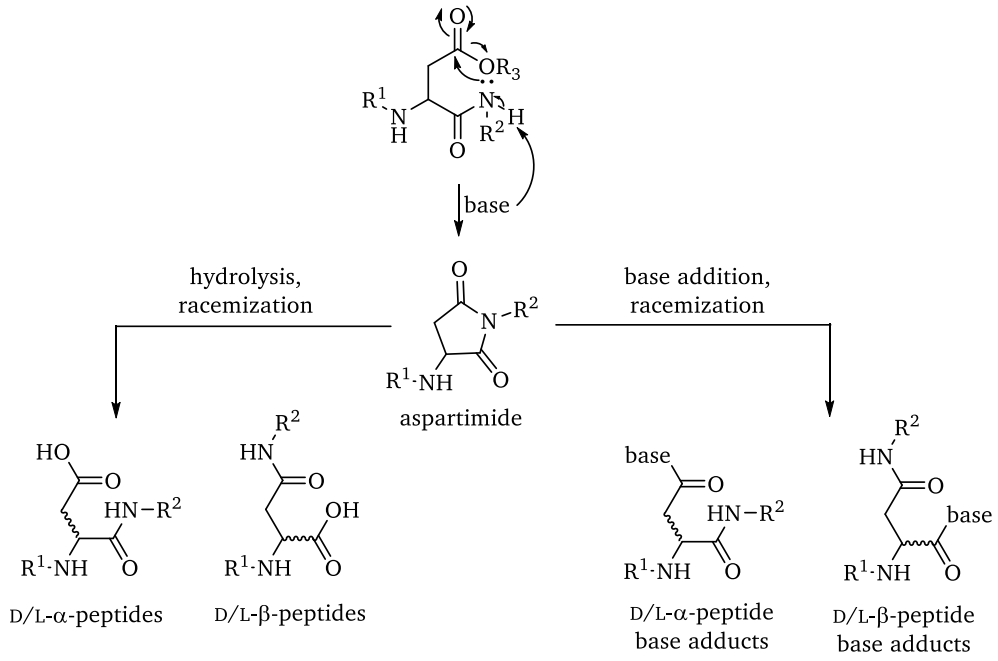

Scheme 12: Aspartimide formation (R^1,R^2,R^3: residues).

First the D/L aspartimide intermediate is formed, followed by the nucleophilic attack of water leading to the formation of the D/L-β-peptides and the D/L-α-peptide in a ratio between 3:1 (observed in amyloid β-protein)[185] and 2:1.[186] The attack of piperidine on the D/L aspartimide ring results in a mixture of D/L-α-piperidides and D/L-β-piperidides.[179-181] If the nucleophilic attack on the aspartimide intermediate is exercised by an amine group, the formation of dipeptides, cyclic peptides or piperidine adducts is observed.[187] The resulting α-piperidides and β-piperidides can be easily removed from the crude peptide by HPLC, the HPLC separation of the D/L-α-aspartyl peptides is however quite difficult.[188] Reduction of aspartimide formation is possible by the addition of acidic modifiers in Fmoc-SPPS.[189-190]

Thus, Subirós-Funosas *et al.* showed that the addition of 1M Oxyma[140] in 20% piperidine during Fmoc deprotection resulted in a significant reduction of aspartimide side products.[190] Backbone protection of the aspartyl α-carboxyamide bond is currently the only strategy to prevent aspartimide formation completely.[191-193] This is usually applied for peptides containing

Asp-Gly, because the coupling of the amino acid following the 2-hydroxyl-4-methoxybenzyl (Hmb)[194] residue can be extremely difficult.[195]

Another method for aspartimide reduction are Mutter's pseudoproline (ψPro) dipeptides. Pseudoprolines are oxazolidine- or thiazolidine-based derivatives of serine, threonine and cysteine residues. The corresponding derivative is formed by a cyclocondensation with an aldehyde or ketone.[196-198] Usage of pseudoproline dipeptide building blocks allow for the incorporation of two amino acid residues at once; the native sequence is regenerated upon global cleavage, as shown in **Scheme 13.**[198-199]

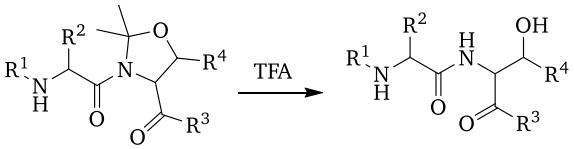

Scheme 13: Peptide sequence with incorporated pseudoproline and deprotection with TFA (ψPro) (R^1,R^2,R^3: residues, R^4=H, Me).

These commercially available surrogates improve cyclisation, aspartimide suppression and epimerization-free segment coupling during peptide synthesis.[200] However, they are limited to sequences containing serine, threonine or cysteine at convenient positions.

1.6. Peptide purification

Merrifield's breakthrough in peptide chemistry proved viable only after the introduction of efficient HPLC purification. An isolation/purification, which is necessary to achieve a peptide purity of >95%, is one of the bottlenecks of peptide production even now.

Over the past 40 years the purification of peptides by HPLC has been significantly improved. Today it is the state-of-the-art process for the isolation and purification of peptides of different nature, structure, and complexity grade.[37-39, 201] In most cases, the purification of peptides is performed *via* reversed phase high-performance liquid chromatography (RP-HPLC). Due to the high resolution of modern RP-HPLC purification, peptides with nearly identical sequences can be separated. In reversed-phase mode, a hydrophobic molecule is captured by the stationary phase comprising C_4, C_8 or C_{18} alkyl ligands. The retention time depends on the hydrophobicity of the molecule and of the used mobile phase. RP-HPLC for peptide purification is performed in the presence of an organic modifier and an ion-pairing reagent, with acetonitrile and TFA being the compounds of choice for standard operating procedures. Purification by RP-HPLC has limitations regarding highly polar/unpolar peptides. The first ones bind only weakly or not at all to the stationary phase. The second ones do not elute from the column. The limiting factors for peptide purification by HPLC are usually solvent consumption and/or the time effort for the purification process.

Alternative techniques mainly used for protein purification such as size-exclusion chromatography (SEC), ion-exchange chromatography (IEC)[202-206] or hydrophobic interaction chromatography (HIC)[207] can be applied to peptide purification as well.

Ion-exchange chromatography has been used as separation method for charged biological molecules such as proteins, peptides, amino acids, or nucleotides for around 70 years.[202-206] Amino acids are amphoteric; that means they are zwitterionic compounds that contain both positively and negatively charged functional groups. Depending on the pH of their environment, amino acids (and therefore peptides and proteins as well) may carry a net charge. The isoelectric point is the pH value where the molecules has no net charge. The ion-exchange material is based on spherical particles substituted with ionic groups that are negatively or positively charged. The material is usually porous to increase the surface area.

Ion-exchange chromatography (IEC) has large capacity, the material is available at moderate costs, scale-up is easy to perform and automation is possible. IEC process comprises the following steps: Equilibration of the column, adding the sample, gradient elution of the loaded sample, regeneration of the column material.[208] High-performance ion-exchange chromatography is also available.[209-210] In addition to the amphoteric character of the amino acids, functional groups may be introduced chemically to allow an easy ion-exchange process. In 1978, Merrifield and Bach introduced a monosulfonated Fmoc to allow peptide purification after SPPS cleavage on a ion-exchange column (**Figure 14**).[206] This method offered the possibility of a simple purification of the crude peptide. However, due to the complicated handling and the special protection for the *N*-terminus, the technique has not found practical application.

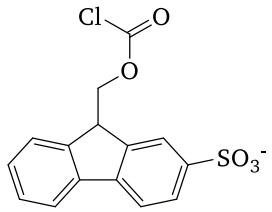

Figure 14: 9-(2-Sulfo)fluorenyl-methyloxycarbonyl chloride.[205]

In recent years different affinity-based approaches have been reported for peptide isolation.[211-213] Affinity chromatography, widely used for the purification of recombinantly expressed proteins, is based on specific binding interactions between molecules. To that end, a particular ligand is chemically bound to a solid support; if a crude mixture passes over the column all molecules with specific binding affinity to the ligand remain on the column. After all impurities are washed away, the bound molecule is stripped from the solid support resulting in a purified peptide or protein. One or more of these techniques can be used in combination to improve the peptide purity.

1.7. Towards sustainable peptide synthesis

For decades, peptides have been in the research focus in view of their pharmaceutical and cosmetic applications. Obviously, chemical peptide synthesis is very inefficient in terms of solvent and reagent consumption. Indeed, the reagents are used in high excess, solvents are expensive and hazardous thus posing a threat to the environment and human health. Additionally, the European REACH[3] Regulation classifies commonly used DMF and NMP (*N*-methylpyrrolidone) as substances of very high concern due to their CMR (carcinogenic, mutagenic or toxic for reproduction) properties. In recent years, different approaches to improve peptide synthesis in terms of green chemistry or sustainable engineering have been reported.[214-224] In an article entitled "The ideal peptide plant", Dr. Olivier Ludemann-Hombourger, PolyPeptide Group, discusses aspects of the synthesis process that industry considers to be in urgent need of improvement: „Let us dream of the future steps: A process with no waste of organic solvent; a fully automated process with online monitoring of the progress of reactions; the addition of reagents and amino acid derivatives to reduce the consumption of all chemicals; a reduced process time for each amino acid derivative incorporation; an automated purification process with quantitative yield without compromising productivity.“[225]

Many organic solvents are harmful, toxic and poisonous to the environment. Their use therefore poses a risk to human health and surrounding milieu. As understanding solvent properties is an obligatory part of sustainable development, the majority of them have been classified according to their environmental, safety and health (ESH) issues.[226] These rankings are the core principle of the guidelines on solvent selection used by pharmaceutical companies (GSK, AstraZeneca,

[3] Regulation (EC) No. 1907/2006 of the European Parliament and of the Council of 18 December 2006 concerning the Registration, Evaluation, Authorisation and Restriction of Chemicals (“REACH”)

Pfizer and Sanofi) and by professional groups such as the ACS Green Chemistry Institute Pharmaceutical Roundtable (GCI-PR).[227-230] Byrne *et al.* have drawn an overall conclusion from the Sanofi, Pfizer and GSK solvent selection guide shown in **Table 4**.

Table 4: Summary of solvent selection tables by Byrne *et al.* (Adapted table by Byrne *et al.*[227] distributed under the terms of the Creative Commons Attribution 4.0, Licence: CC BY 4.0. (https://creativecommons.org/licenses/by/4.0/).

Class	Solvent	Conclusion (Pfizer)	Conclusion (GSK)	Conclusion (Sanofi)
Alcohols	Methanol	Preferred	Some issues	Recommended
	Ethanol	Preferred	Some issues	Recommended
	1-propanol	Preferred	Some issues	Recommended
	i-propanol	Preferred	Some issues	Recommended
	1-Butanol	Preferred	Few issues	Recommended
	2-Butanol		Few issues	Substitution advisable
	t-butanol	Preferred	Some issues	Substitution advisable
	Ethylene glycol	Usable		Substitution advisable
	2-methoxyethanol		Major issues	Substitution requested
Hydro-carbons	n-pentane	Undesirable		Banned
	Hexane(s)	Undesirable	Major issues	Substitution requested
	Cyclohexane	Usable	Some issues	Substitution advisable
	Methylcyclohexane	Usable		Substitution advisable
	Heptane	Usable	Some issues	Substitution advisable
	Isooctane	Usable	Some issues	
	Benzene	Undesirable	Major issues	
	Toluene	Usable	Some issues	Substitution advisable
	Xylene(s)	Usable	Some issues	Substitution advisable
Dipolar aprotic	DMSO	Usable	Some issues	Substitution advisable
	Acetonitrile	Usable	Major issues	Recommended
	DMF	Undesirable	Major issues	Substitution requested
	DMAc	Undesirable	Major issues	Substitution requested
	NMP	Undesirable	Major issues	Substitution requested
Esters	Methyl acetate		Some issues	Substitution advisable
	Ethyl acetate	Preferred	Some issues	Recommended
	n-propyl acetate		Few issues	Recommended
	i-propyl acetate	Preferred	Few issues	Recommended
Ethers	THF	Usable	Major issues	Substitution advisable
	2-MeTHF	Usable	Some issues	Recommended
	TBME	Usable	Some issues	Substitution advisable
	CPME		Some issues	Substitution requested
	Diethyl ether	Undesirable	Major issues	
	Diisopropyl ether	Undesirable	Major issues	Substitution advisable
	1,2-DME	Undesirable	Major issues	Substitution requested
	1,4-dioxane	Undesirable	Major issues	Substitution requested
Ketones	Acetone	Preferred	Some issues	Recommended
	Methylethyl keton	Preferred	Major issues	Recommended
	MIBK		Some issues	Recommended
Halo-genated	Dichloromethane	Undesirable	Major issues	Substitution advisable
	1,2-dichloethane	Undesirable	Major issues	
	Chloroform	Undesirable	Major issues	
	CCl_4	Undesirable	Major issues	
Miscellan-eous	Water	Preferred	Few issues	Recommended
	Acetic acid	Usable		Substitution advisable
	Pyridine	Undesirable		Substitution advisable

The data collected by Pfizer, GSK and Sanofi show that the greenest solvents are water, propyl acetate, *i*-propylacetate, 1-butanol, and 2-butanol. This selection is very limited, as only alcohols and esters, in addition to water, are recognized as green solvents. Acetonitrile achieves a

different result in each of the solvent selection aids, Pfizer recommends MeCN as a substitute for DMF and NMP. 2-MeTHF and DMSO are also considered possible as substitutes for DMF.[228-229]

A recent publication of the American Chemical Society (ACS) Green Chemistry Institute Pharmaceutical Roundtable summarizes the current situation as follows: "… the current state of the art in peptide synthesis involves primarily legacy technologies with use of large amounts of highly hazardous reagents and solvents and little focus on green chemistry and engineering."[231] The authors call to innovation and the problems in the currently used peptide synthesis they identified are shown in **Figure 15**.

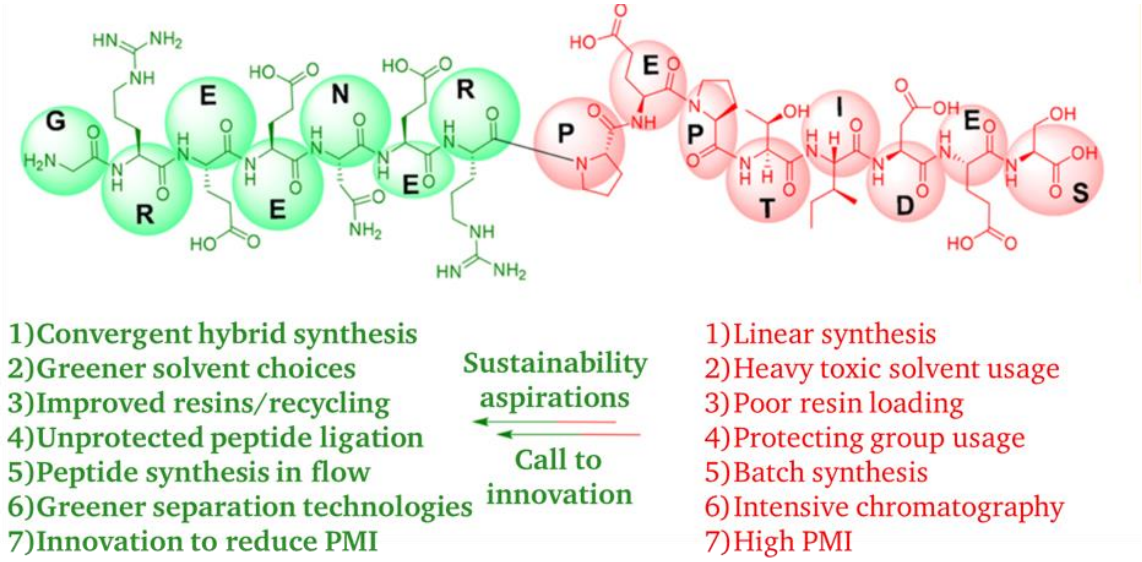

Figure 15: A call to innovation to develop a sustainable peptide synthesis by ACS Green Chemistry Institute Pharmaceutical Roundtable (Adapted with permission from Isidro-Llobet *et al.*, The Journal of Organic Chemistry **2019**, 84, (8), 4615-4628).[231] Copyright 2019 American Chemical Society).

Some preliminary work has already been done in this direction, but so far, no industrial solution has been found. Two general trends can be observed, change to alternative solvents or reduction of reagent excesses.

1.7.1. Peptide synthesis in alternative organic solvents

McMillan *et al*. screened different organic solvents like *tert*-butyl methyl ether, cyclopentyl-methyl ether, dimethyl carbonate, ethyl acetate, *iso*-propyl alcohol, as well as 2-methyl tetrahydrofuran (2-MeTHF) for their effect on the formation of amide bonds. Their studies showed that dimethyl carbonate, ethyl acetate, and 2-MeTHF are comparable to DMF and DCM.[232] Jad *et al.* performed peptide synthesis with THF and MeCN as DMF replacement and achieved comparable results, even with a minor improvement in some cases.[233] Later Jad *et al.* used 2-methyltetrahydrofuran and cyclopentyl methyl ether for green SPPS.[214] They concluded that the use of 2-MeTHF in combination with DIC/Oxyma Pure gives the lowest degree of racemization in the case of short peptides, up to five amino acids in length. However, as the selection of building blocks was limited to only five amino acids, it could obviously indicate that the others suffer from insufficient solubility in the given solvent. Jad *et al.* showed an improvement of their method by introducing a protocol for the use of 2-MeTHF for Fmoc deprotection, however additional washing steps with EtOAc were required.[215] Even with these steps the Fmoc deprotection was still not optimal[217], the solvent system was further changed to γ-valerolactone (GVL) and *N*-formylmorpholine (NFM) as a "greener" alternative to DMF.

[218] Having determined the solubility of different Fmoc-aa-OH compounds and Oxyma Pure in GVL or NFM and compared the data with those for DMF, it was found that Fmoc-Leu-OH, Fmoc-Aib-OH, Fmoc-Tyr(tBu)-OH) were well soluble (>0.2 M) in GVL and NFM, and Fmoc-Phe-OH had a solubility of 0.16 M in GVL.[218]

Lawrenson *et al.* have shown recently that propylene carbonate (PC) can replace DMF in solution- and solid-phase peptide synthesis by using either the Fmoc or Boc strategy for the synthesis of the nonapeptide bradykinin.[219]

Many of the recent publications indicate that a conversion to green solvents is often limited by the currently used Fmoc amino acid building blocks and their low solubility in alternative organic solvents. This represents a major obstacle that often prevents the use of greener solvents in peptide chemistry.

1.7.2. Solvent-free peptide synthesis

Different synthesis protocols for solvent-free peptide synthesis have been published to date. Declerck *et al.* synthesized di- and tripeptides by using the ball-milling (see **Figure 16** for schematic drawing[234]) method with urethane-protected α-amino acid *N*-carboxy-anhydrides.[235] This method was later optimized by Bonnamour *et al.* for the synthesis of a pentapeptide Leu-enkephalin by adding small amounts of ethyl acetate with an overall yield of 46%. Boc deprotection was performed with gaseous HCl.[236]

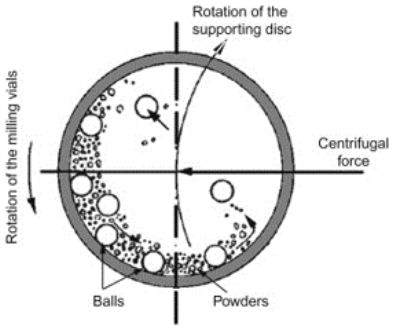

Figure 16: Schematic representation of a high-energy planetary ball mill. [Reprinted from El-Eskandarany, Mechanical Alloying (Second Edition), William Andrew Publishing, Oxford, 2015, pp. 13-47.[233] With permission from Elsevier].

Another group synthesized dipeptides by using 2,4,6-trichloro-1,3,5-triazine and triphenylphosphine upon ball-grinding with solvent drops.[237] Konnert *et al.* published the solvent-free synthesis of Fmoc-, Boc- and Z-protected amino acids by ball grinding.[238] Although the use of ball-milling is an interesting approach to achieve a greener peptide synthesis protocol, at the moment the method is limited to rather short peptides.

1.7.3. Peptide synthesis in water

Hojo *et al*. reported the preparation of different water-soluble *N*-protected amino acids with the 2-[phenyl(methyl)sulfonio]ethyloxycarbonyl (Pms)[239-240] group, the ethanesulfonyl-ethoxycarbonyl (Esc)[241] group and the 2-(4-sulfophenylsulfonyl)ethoxy-carbonyl (Sps)[242] group and their application to solid-phase peptide synthesis (structures are shown in **Figure 17**).[239-242]

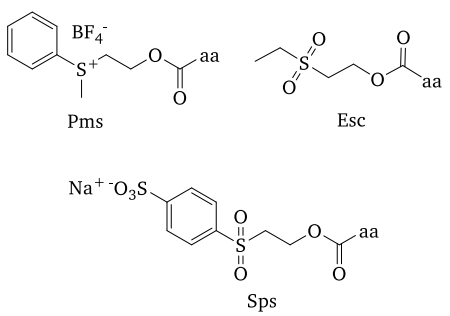

Figure 17: Structures of Pms, Esc and Sps protecting groups by Hojo *et al.*

However, Pms-amino acids were rather unstable due to their onium form and Esc-amino acids (except Esc aromatic amino acids) were not detectable by measurement of optical absorption and showed only moderate solubility in water. In addition, the starting materials for the Esc group are relatively expensive. Usage of Sps protecting groups resulted in autooxidation of cysteine and methionine. Hojo *et al.* were able to

synthesize only one short peptide in water and due to the intrinsic problems of their protecting groups switched to another concept. They stated: „Peptide synthesis can be carried out in water via chemical conversion of protected amino acids to water-soluble forms. However, additional conversion steps are required in total synthetic process, and it is not desirable in terms of preparation costs, resource saving, and energy conservation. Thus, development of simplified techniques other than chemical conversion is urgently needed for environmentally friendly peptide synthesis."[243]

As a solution for this, Hojo *et al.* described a technology using water-dispersible nanoparticulate Fmoc-amino acids.[243-247] This concept however was successful only in the case of amide bond formation. Indeed, only amino acid coupling was conducted in water; deprotection and washing steps had to be performed in DMF due to the intrinsic hydrophobic properties of fluorenylmethyl moiety, which result in water-incompatibility. Hojo *et al.* also showed a strategy for Boc-amino acid nanoparticles.[243, 248-249] However, all of these approaches required long coupling times, some reaction steps had to be performed in organic solvents and upscaling was quite limited. Microwaves were proposed as an energy source to accelerate the coupling step in water or in the absence of solvents,[250] although the use of elevated temperatures is known to compromise the stereo integrity of sensitive amino acids.[163, 166]

Hojo *et al.* concluded: "In general, many organic compounds of synthetic intermediates for industrial use are poorly soluble in water, and therefore inadequate for reactions in water."[243] This is confirmed by Cortes-Clerget *et al.*: "Nonetheless, in most of these reports the scope of the reaction is limited and large amounts of co-solvents are often needed to prevent aggregation."[220]

Cortes-Clerget *et al*. introduced a method using aqueous micellar medium. The reaction takes place within the core of nanomicelles, formed by a 2 wt% aqueous solution of TPGS-750-M to overcome insolubility of protected amino acids in water.[220, 223] However, the synthesis procedure seems to be limited to di- or tripeptides.[220, 223]

In 2012, John Collins introduced a series of water-compatible *N*-terminal protecting groups in a patent application.[251] However, all of them possessed a hydrophobic character leading to low water solubility of the protected amino acids. The 1,1-dioxonaptho[1,2-b]-thiophene-2-methyloxy-carbonyl group (Nsmoc), shown in **Figure 18**, seemed to be the most promising structure, but the synthesis of the compound is sophisticated and the protected amino acids had only a moderate water solubility, so scale-up seemed to be quite limited as well.

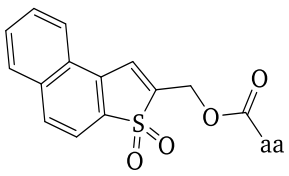

Figure 18: Structure of the Nsmoc group.

A recent publication by Přibylka *et al.* suggests using sodium hydroxide in a 2-MeTHF/MeOH mixture for Fmoc deprotection.[224] The authors state, that their protocol is only incompatible with Wang linker molecules.[224] Our own work (see results) however showed, that NaOH is capable of cleaving all ester molecules during the deprotection step (linker molecules and side chain protecting groups), so use of this method is quite limited to peptide amides without Asp and Glu side chain residues.

2. Objective

The present work is aimed at the development of a water-based peptide synthesis as a sustainable alternative to the state-of-the-art process.

To achieve this goal, a lot of of synthetic and technical challenges should be addressed.

To get access to water-compatible SPPS/LPPS building blocks, polar N_α-protecting groups are required which should ensure solubility of particular amino acids in water or aqueous solution. At the same time these groups must meet the requirements of peptide assembly in terms of stability, liability, and usability. This issue includes design and synthesis of the respective protecting groups and their installation in amino acids of choice with subsequent approbation in peptide synthesis.

Following elaboration of an N_α protection, a reliable water-compatible convergent protecting group strategy for the functional side chain should be developed. The required moieties must demonstrate orthogonality to the aminoterminal counterpart, being at the same time easily removable upon global cleavage. Within the coded amino acids 12 side chains require protection upon peptide assembly. As my previous research on cell-penetrating COSS derivatives[1] has revealed that the introduction of solitair or multiple ionic pendants wielded major influence on the polarity/solubility of the resulting compounds, the focus was set on equipping commercially available protecting groups with ionic moieties.

To allow for a real-time monitoring of peptide assembly, especially on solid support, a protecting group with UV/Vis or fluorescent properties is highly desirable. Therefore, the starting point for the design and synthesis was set at the fluorene molecular framework known for its fluorescent properties.

The success of the chosen protecting group strategy should be verified by assembling several model peptides under aqueous conditions.

In addition, the basic bottlenecks of peptide synthesis in the context of coupling/deprotection efficiency, enantiomeric purity, side reactions, and postsynthetic isolation/purification should be comprehensively studied.

3. Results and discussion

3.1 Design of water-compatible protecting groups

Protecting groups that can be used for peptide assembly in polar solvents like alcohols or water must possess hydrophilic properties. However, most of the currently used protecting groups are strongly hydrophobic, because they must be soluble in organic solvents. To change this behaviour, either modifications of the existing protective groups are necessary to increase their solubility in polar solvents, or the development of novel, alternative groups for polar solvents is required. In this thesis, the focus was set on the modification of available protecting blocks. Upon preliminary work with highly polar COSS compounds, basic knowledge about the influence of functional groups on solubility and the chemical behaviour was already obtained.

The initial idea was to decorate existing protecting groups by additional polar moieties and to assess their usability in peptide synthesis.

To that end, the following functional groups were taken into consideration: sulfo-, phospho-, cyano-, guanidino-, as well as quaternary ammonium bases and some other candidates. The sulfonated protecting groups proved to be easily accessible with no side reactions under the conditions of peptide synthesis. Therefore, first experiments were performed with sulfonated protecting groups. An overview of the modified protecting blocks is given in **Figure 19**.

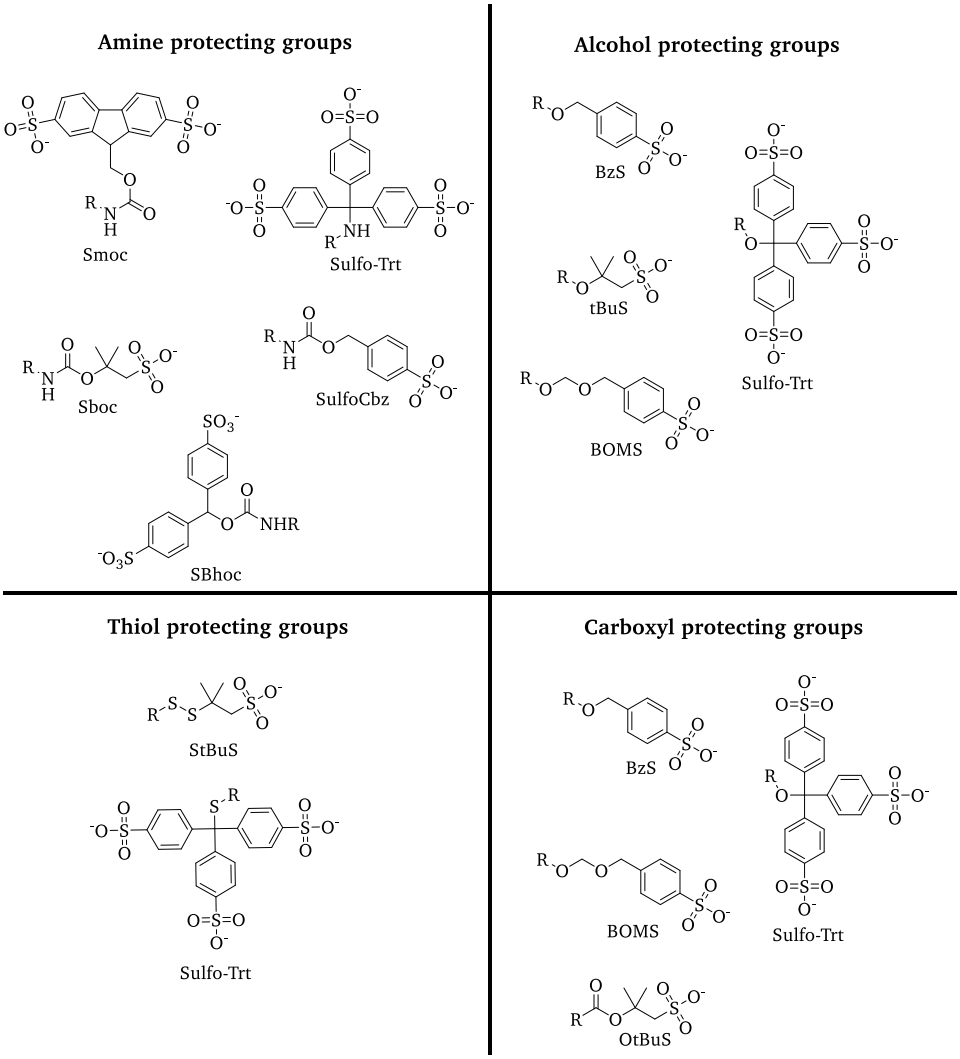

Figure 19: Overview of the sulfonated protecting-group candidates.

All of the shown protecting groups demonstrated high water solubility, and some of them, e.g. 2,7-disulfo-9-fluorenylmethoxycarbonyl chloride possessed additional benefits as intrinsic fluorescent properties and possibility to be cleaved under milder reaction conditions. Some examined groups revealed increased stability, resulting in harsh cleavage conditions and were found therefore inapplicable (data not shown). As a result, the Smoc protecting group was selected as the most promising candidate for the further work.

The jump-start for the present investigation was given accidentally. Thus, during the synthesis of a novel protecting group for peptide backbone an N_{α}-Fmoc protected amino acid was treated with sulfuric acid giving an unexpected water soluble, fluorescent product in preference to the desired compound. Thorough analysis of this molecule and the horizons that its application could open gave rise to the novel field of peptides synthesis.

3.1. Synthesis of 2,7-disulfo-9-fluorenylmethoxycarbonyl chloride (Smoc-Cl) 2

The synthesis of the Smoc protecting group **2** started from commercially available Fmoc chloride **1**, shown in **Scheme 14**.

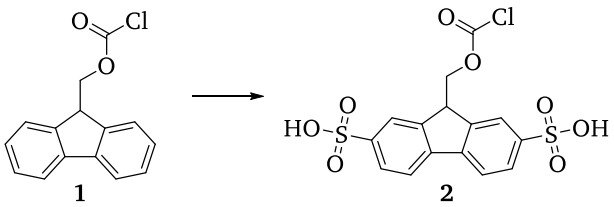

Scheme 14: Synthesis of Smoc-Cl **2**.

In order to introduce two sulfo groups, different sulfonation regents were examined, among them sulfuric acid, oleum, chlorosulfonic acid, as well as sulphur trioxide complexes with pyridine, trimethylamine, DMF, and dioxane. Although application of most of the sulfonation reagents yielded mixtures of mono- and disulfonated products, sulfuric acid and oleum gave exclusively the desired 2,7-disulfo-9-fluorenylmethoxycarbonyl chloride **2**.

However, the lability of the Smoc chloride **2** in the presence of bases did not allow to remove the excess of acids by simple neutralization. Therefore, the surplus of oleum/sulfuric acid needs to be purged by other methods. The best results were achieved by using dioxane for complexation of SO_3 excess followed by washing with 1,2-dichloroethane to obtain a pure product. Our work showed that the synthesis of Smoc-NHS is possible by the same reaction pathway, the product purification is however more complicated and therefore Smoc-Cl was used for the following work.

Further optimisation resulted in an easily scalable, sustainable reaction for the synthesis of Smoc-Cl **2** (not part of this work) without the need to use critical solvents like dioxane and 1,2-dichloroethane.

3.2. Synthesis of N_{α}-Smoc amino acids

Introduction of an Smoc group at the α-amine of amino acids is possible by two different reaction pathways, shown in **Scheme 15**.

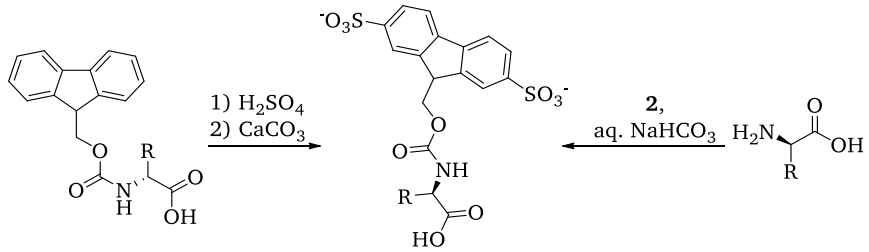

Scheme 15: Synthesis of N_α-Smoc amino acids by direct sulfonation of an N_α-Fmoc amino acids or upon condensation with Smoc-Cl **2**.

A direct conversion of Fmoc-bearing amino acids lacking functional side chains to the respective Smoc derivatives (**3**, **4**, **7**, **12**, **16**, **21**, **30**, **31**) was performed successfully applying sulfuric acid with subsequent neutralisation of its excess by calcium carbonate. The resulting calcium sulfate was removed by filtration, and the respective Smoc amino acids were isolated from aqueous solution by freeze-drying.

The second route relied on the usage of Smoc-Cl **2** to synthesize the corresponding Smoc amino (**3**-**32**). This method was successfully applied to all canonic amino acids as well as to a number of non-natural building blocks, giving desired Smoc products in high yields. Moderate yield obtained in reaction of Smoc chloride **2** with 2-aminoisobutyric acid (AiB) **107** was attributed to its obvious steric hindrance. Interestingly, it was noticed that addition of minimal amounts of MeCN during the reaction process reduced Smoc cleavage to a minimum, thus leading to increased product formation. To remove excess of amino acids, HPLC purification was applied.

All Smoc-protected amino acids used in this work were synthesized *via* the second route. The respective derivatives, their structures and the synthesis yields are summarized in **Table 5**. Amino acids with functional side chains either combined N_α-Smoc protection with the standard side chain protecting groups (**6**, **8**, **9**, **11**, **14**, **18**, **23**, **25**, **27**, **29**) or possessed unprotected side chains (**5**, **7**, **10**, **13**, **22**, **24**, **26**, **28**) to validate if a side chain protection is necessary under aqueous peptide synthesis conditions. Within the natural amino acid repertoire, Lys, Glu, Asp and Cys required side chain protection under aqueous conditions.

Table 5: Synthesized N_α-Smoc amino acids, their structure and yields.

Compound	Structure	Abbreviation	Yield [%]
3	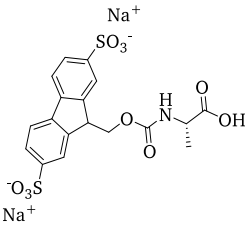	Smoc-L-Ala-OH	87.2
4	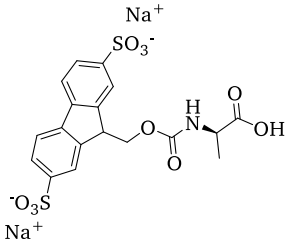	Smoc-D-Ala-OH	86.9

5	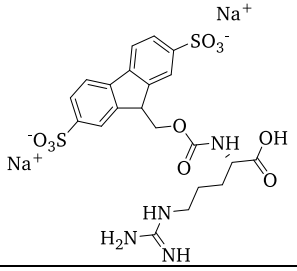	Smoc-L-Arg-OH	85.7
6	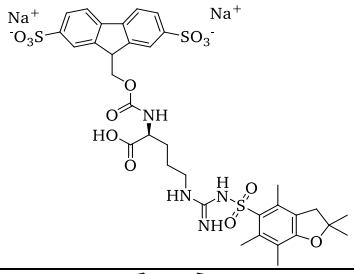	Smoc-L-Arg(Pbf)-OH	85.1
7	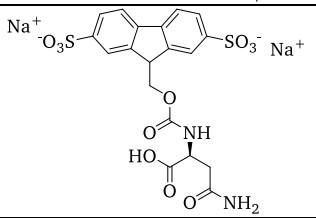	Smoc-L-Asn-OH	90.4
8	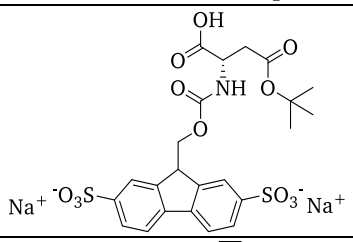	Smoc-L-Asp(OtBu)-OH	86.7
9	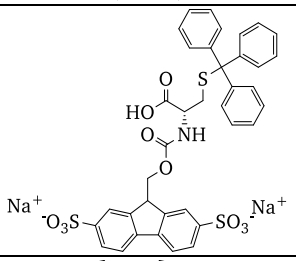	Smoc-L-Cys(Trt)-OH	85.1
10	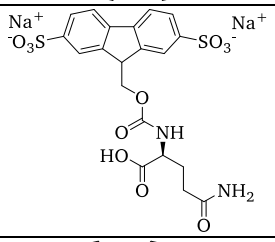	Smoc-L-Gln-OH	90.8
11	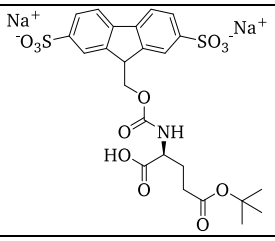	Smoc-L-Glu(OtBu)-OH	88.2

12	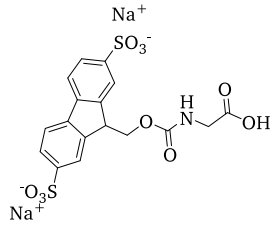	Smoc-Gly-OH	93.7
13	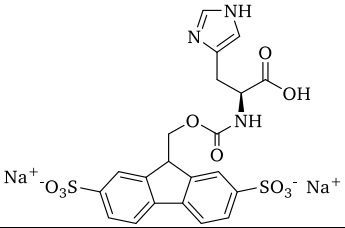	Smoc-L-His-OH	92.4
14	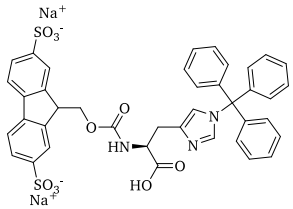	Smoc-L-His(Trt)-OH	86.6
15	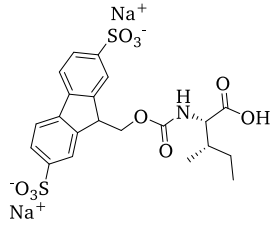	Smoc-L-Ile-OH	88.9
16	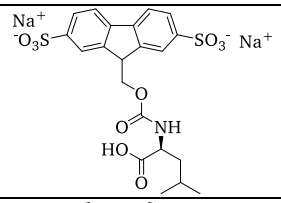	Smoc-L-Leu-OH	90.6
17	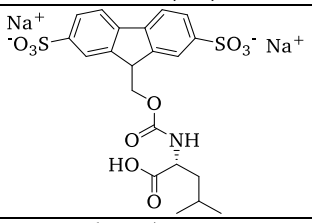	Smoc-D-Leu-OH	88.7
18	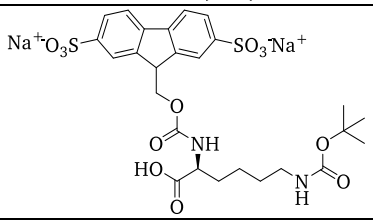	Smoc-L-Lys(Boc)-OH	87.4
19	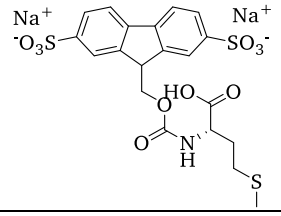	Smoc-L-Met-OH	95.1

20	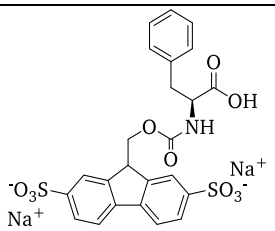	Smoc-L-Phe-OH	93.7
21	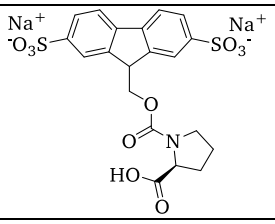	Smoc-L-Pro-OH	85.8
22	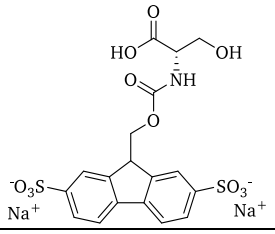	Smoc-L-Ser-OH	90.0
23	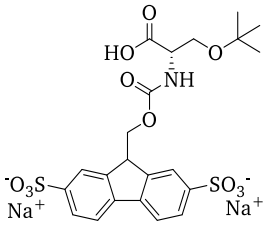	Smoc-L-Ser(tBu)-OH	87.9
24	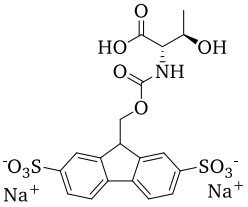	Smoc-L-Thr-OH	92.2
25	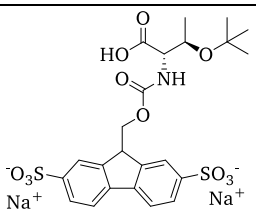	Smoc-L-Thr(tBu)-OH	89.2
26	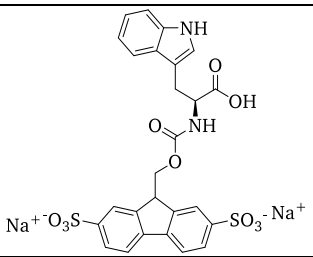	Smoc-L-Trp-OH	90.7
27	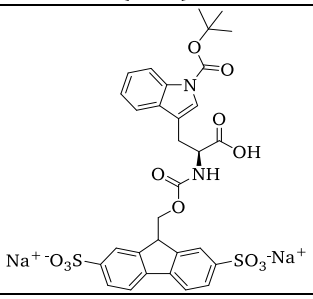	Smoc-L-Trp(Boc)-OH	86.9

28	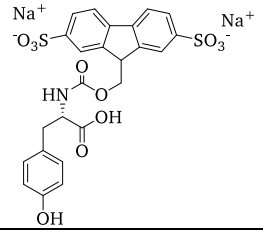	Smoc-L-Tyr-OH	89.7
29	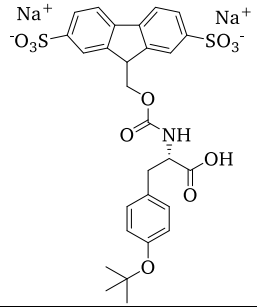	Smoc-L-Tyr(tBu)-OH	91.4
30	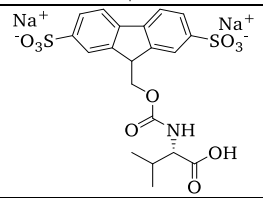	Smoc-L-Val-OH	87.2
31	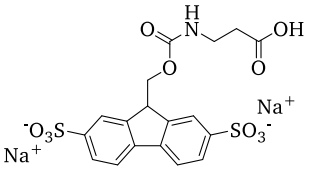	Smoc-β-Ala-OH	92.5
32	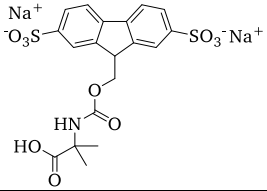	Smoc-Aib-OH	57.8

3.3. N_α-Smoc deprotection

During the solid-phase peptide synthesis, the N_α-protecting group needs to be cleavable under mild conditions to prevent side chain deprotection, thus retaining the orthogonality. Smoc cleavage conditions were examined applying different aqueous bases or their solutions in polar solvents and the grade of deprotection after five minutes is summarized in **Table 6**.

Table 6: Summary of deprotection experiments.

Deprotection agent	Concentration	Solvent	Extent of deprotection after 5 min
NaOH	0.2 M	water	100%
NaOH	1 M	water ethanol	100% 100%
Ethanolamine	10% (v/v)	water ethanol	95% 75%
Ethylenediamine	10% (v/v)	water	100%
Piperazine	5% (w/v)	water	100%
Ammonia	10% (v/v)	water	100%
Piperidine	20% (v/v)	water	100%

After 5 min, the deprotection progress was monitored by HPLC. In general, two cleavage products (**33**, **34**) were observed for all used bases; in some cases, Smoc-base adducts were detected as well. The deprotection process is shown in **Scheme 16**.

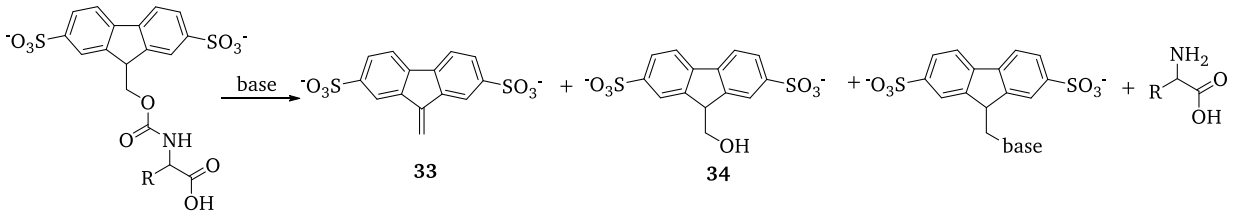

Scheme 16: Deprotection of the Smoc protecting group leads to the products **33**, **34** as well as the possible base adduct.

Deprotection was performed with different N_{α}-Smoc amino acids. Here, cleavage of Smoc is exemplarily shown for Smoc-Arg-OH **5**, Smoc-Leu-OH **16** and Smoc-Tyr-OH **28**.

Deprotection of Smoc-Arg-OH **5** resulted mainly in the formation of cleavage product **33**; cleavage product **34** was detected in higher yields after 10 minutes. Piperidine and piperazine led to the formation of the corresponding base adducts. Except for the deprotection experiment in suspension using ethanolamine in ethanol, in all base systems 95%, of the Smoc protecting group were cleaved within 5 minutes. Surprisingly, the suspension experiment with NaOH in ethanol was as efficient as the solution-based deprotection in NaOH.

Figure 20 shows the relevant sections of all HPLC runs for easier comparability. The complete data can be seen in section **8.3.1**.

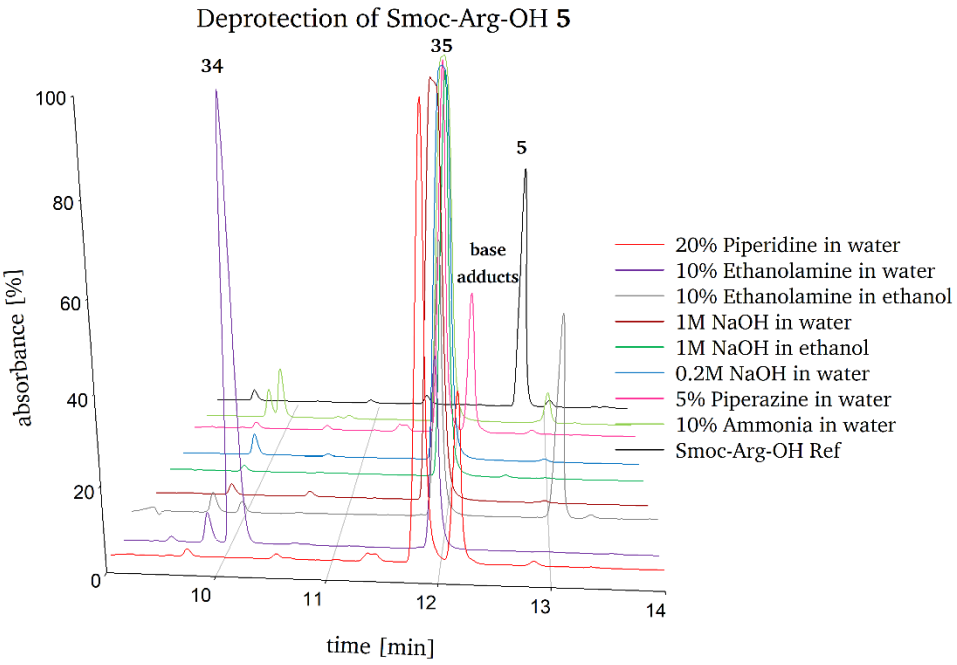

Figure 20: Deprotection of Smoc-Arg-OH **5** applying different bases. The shown area is reduced to the relevant range of the HPLC runs. Absorption values were normalized from 0 to 100%. HPLC traces were monitored at λ=220 nm with a gradient of 0 to 40% MeCN, see section **7.2.3** for details.

The deprotection studies of Smoc-Leu-OH **16** led to similar results. **33** was the main cleavage product, and **34** appeared as the major one in this experiment with piperazine and ethanolamine. Piperidine and piperazine also led to the formation of the corresponding base

adducts. In this case, the deprotection using the suspension systems (ethanolamine or NaOH in ethanol) led to similar results as the solution-based deprotection in water. This could be due to the slightly better solubility of Smoc-Leu-OH **16**, compared to Smoc-Arg-OH **5**, under these reaction conditions. In all base systems except for piperazine and ethanolamine, the Smoc protecting group was removed quantitatively. **Figure 21** shows the relevant sections of all HPLC runs for easier comparability. The complete data can be seen in section **8.3.2**.

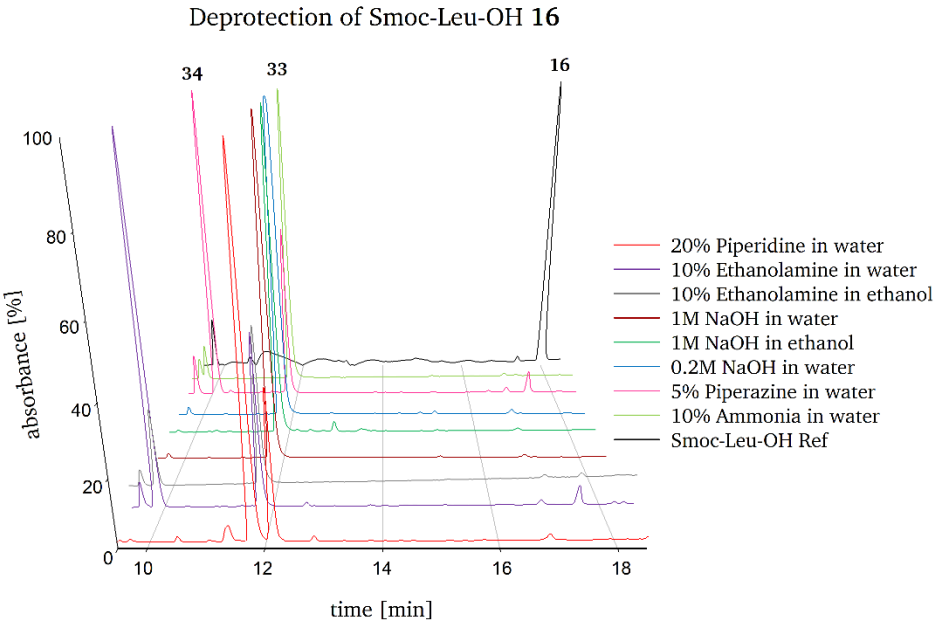

Figure 21: Deprotection of Smoc-Leu-OH **16** with different bases. The shown area is reduced to the relevant range of the HPLC runs. Absorption values were normalized from 0 to 100%. HPLC traces were monitored at λ=220 nm with a gradient of 0 to 40% MeCN, see section **7.2.3** for details.

Similar results were obtained in deprotection studies of Smoc-Tyr-OH **28**. **33** was the major cleavage product, however **34** was formed in higher amounts in comparison to the two other experiments. Piperidine and piperazine formed the corresponding base adducts as well. In all base systems, the N_{α}-Smoc protecting group was cleaved nearly quantitatively. **Figure 22** shows the relevant sections of all HPLC runs for easier comparability. The complete data can be seen in section **8.3.3**.

In addition to the standard bases used in Fmoc-SPPS, deprotection was found possible applying water-soluble bases such as ammonia or sodium hydroxide. This provides an access to significantly cheaper and easier procedures compared to the piperidine-based deprotection. In general, the performed deprotection experiments showed an increased base lability of the Smoc group, compared to that of the Fmoc one in view of deprotection duration and chosen base.[252] All water-soluble bases could be applied, with aqueous sodium carbonate and ethylenediamine demonstrating similar behavior to the shown bases outcomes.

However, the deprotection experiments and the application of the results to solid-phase peptide synthesis have revealed some limitations concerning the choice of the base. The use of sodium hydroxide-based systems led to the cleavage of all ester bonds during peptide synthesis. The quantitative cleavage of the *tert*-butyl esters from the side chains of Glu and Asp was observed as well as the cleavage of the peptide from solid support if the first amino acid was anchored by an ester bond. This effect however could be useful if cleavage from the support upon preservation of certain side chain protecting groups is required.

Although the usage of NaOH in methanol for Fmoc deprotection has been recently published[224], we also examined the ester bond cleavage in alcohol-based systems. Our results clearly showed that application of bases other than NaOH, both in water and alcohol, should be omitted in the case of ester side chain protection or ester-based solid-phase linkers. Thus, 5% aq. piperazine has proven to be rather efficient.

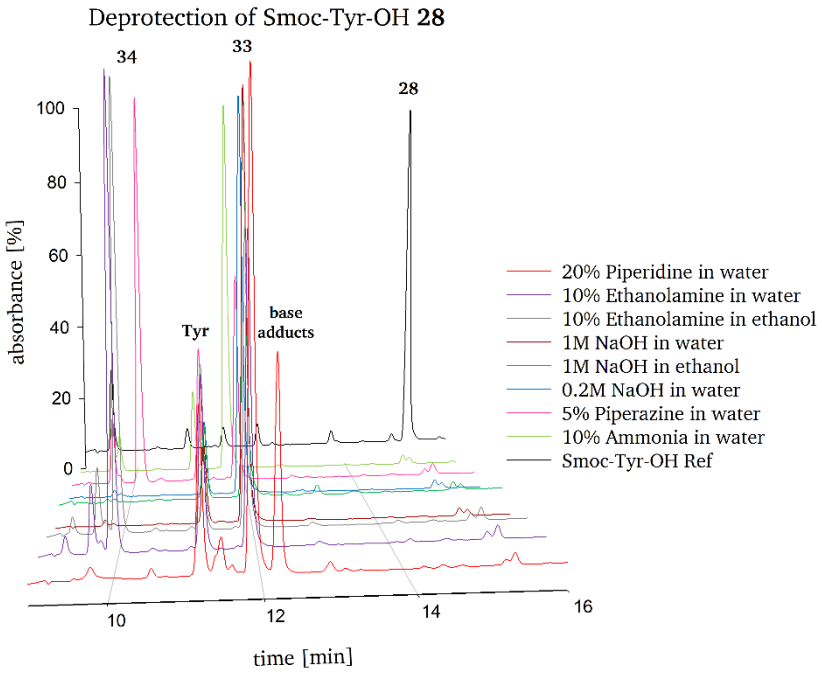

Figure 22: Deprotection of Smoc-Tyr-OH **28** with different bases. The shown area is reduced to the relevant range of the HPLC runs. Absorption values were normalized from 0 to 100%. HPLC traces were monitored at λ=220 nm with a gradient of 0 to 40% MeCN, see section **7.2.3** for details.

However, if the linker molecule is stable to NaOH and no Glu/Asp are present in the peptide sequence, the usage of NaOH-based systems is a rapid and highly efficient method for Smoc deprotection on-support.

3.4. Stability of Smoc-protected amino acids

After the conditions for the Smoc group deprotection had been thoroughly examined, the stability of N_α-Smoc amino acids during aqueous peptide synthesis was studied. Only with this knowledge Smoc could be considered as an N_α-protecting group. To that end, Smoc-Arg-OH **5**, Smoc-Ile-OH **15**, Smoc-Phe-OH **20**, Smoc-Pro-OH **21** and Smoc-Ser-OH **22** were dissolved in water with 3eq. $NaHCO_3$ and the resulting solutions were subjected to HPLC analysis after 7, 14 and 21 days; results are shown in **Figure 23**.

Interestingly, some of the impurities reduced over time, but the N_α-Smoc amino acids were stable under reaction conditions for 21 days, which is a sufficient time window. Stability might even be longer, but monitoring was stopped after 21 days.

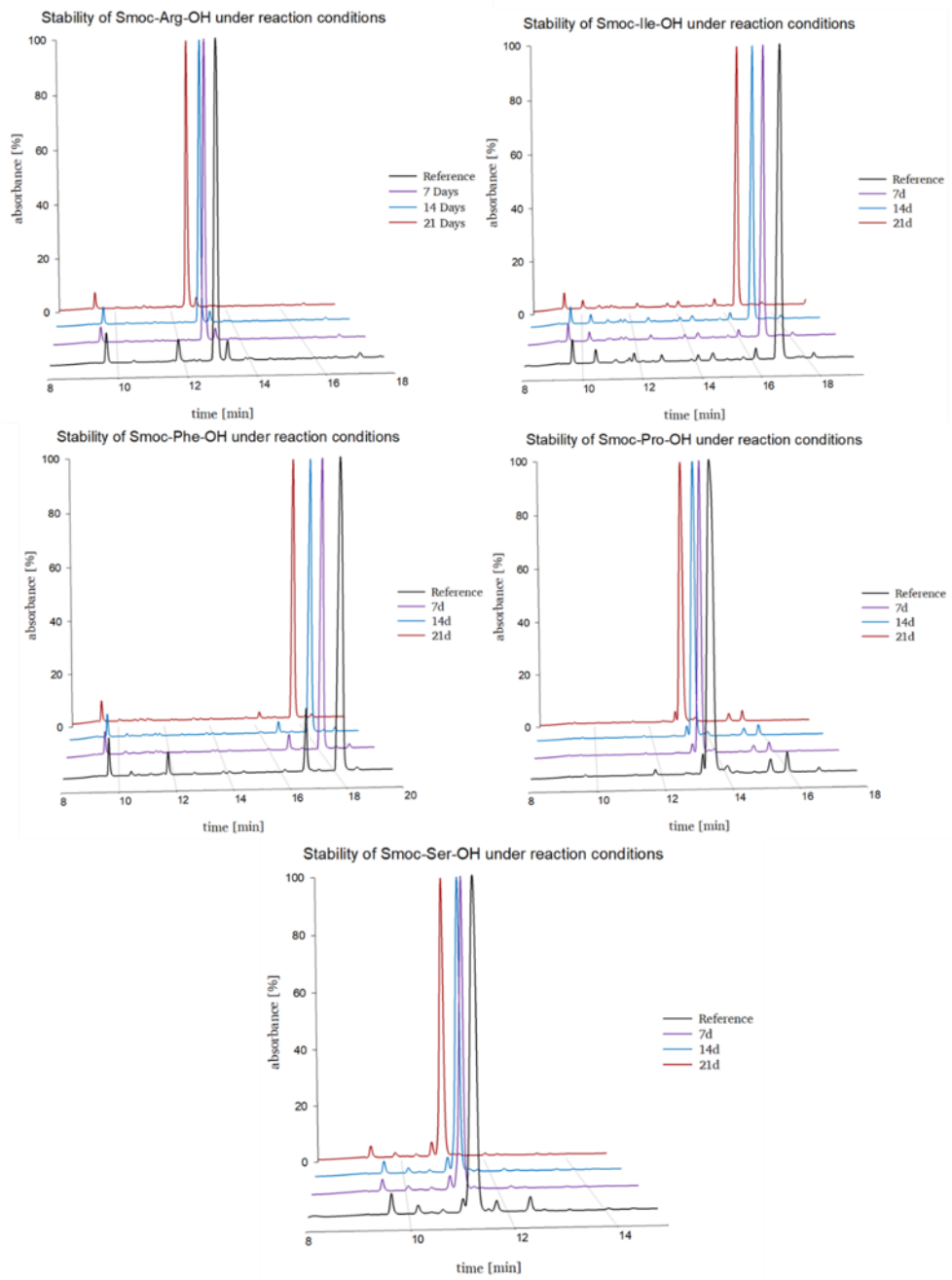

Figure 23: Stability studies of Smoc-Arg-OH **5** (top left), Smoc-Ile-OH **15** (top right), Smoc-Phe-OH **20** (middle left), Smoc-Pro-OH **21** (middle right) and Smoc-Ser-OH **22** (bottom). Reference is shown in black, 7 days in purple , 14 days in blue and 21 day in red. The shown area is reduced to the relevant range of the HPLC runs. Absorption values were normalized from 0 to 100%. HPLC traces were monitored at λ=220 nm with a gradient of 0 to 40% MeCN, see section **7.2.3** for details.

3.5. Synthetic concept of aqueous SPPS (ASPPS)

After all natural and some non-canonic amino acids appeared accessible as Nα-protected Smoc building blocks possessing significant stability in basic aqueous solutions, but easily losing their aminoterminal protection upon mild treatment with particular water-soluble bases, a protocol for aqueous solid-phase peptide synthesis (ASPPS) was developed based on Merrifield's solid-phase peptide synthesis.[14]

To that end, a water-compatible resin (e.g. Tentagel, ChemMatrix, PEGA, etc.) was required. The first amino acid was loaded under aqueous conditions or a commercially available preloaded resin was used. Loading of the first amino acid was followed by the Smoc

deprotection with either aqueous NaOH, NH_3, piperazine or ethanolamine. Then, coupling of the next activated amino acid was performed followed if required by capping of unconverted amines with sulfoacetic acid or similar compounds. Interestingly, this ensures labelling of all remaining free amines with a sulfonated tag that allows for an easy purification after global cleavage. This cycle was repeated until the desired length of a peptide had been reached. After global cleavage, the target peptide, all labelled side products and the free side chain protecting groups appeared in solution. This mixture was loaded onto an ion-exchange column, (IE column) and only the target peptide was able to pass through as all impurities had been negatively charged upon labelling and stayed on the column. This is indeed a fast, sustainable and cheap purification option. Of course, if the highest purity grade is required, ion-exchange chromatography could serve as a prepurification step to remove most of the side products, thus making subsequent HPLC separation much easier. The ASSPS scheme is shown in **Scheme 17**.

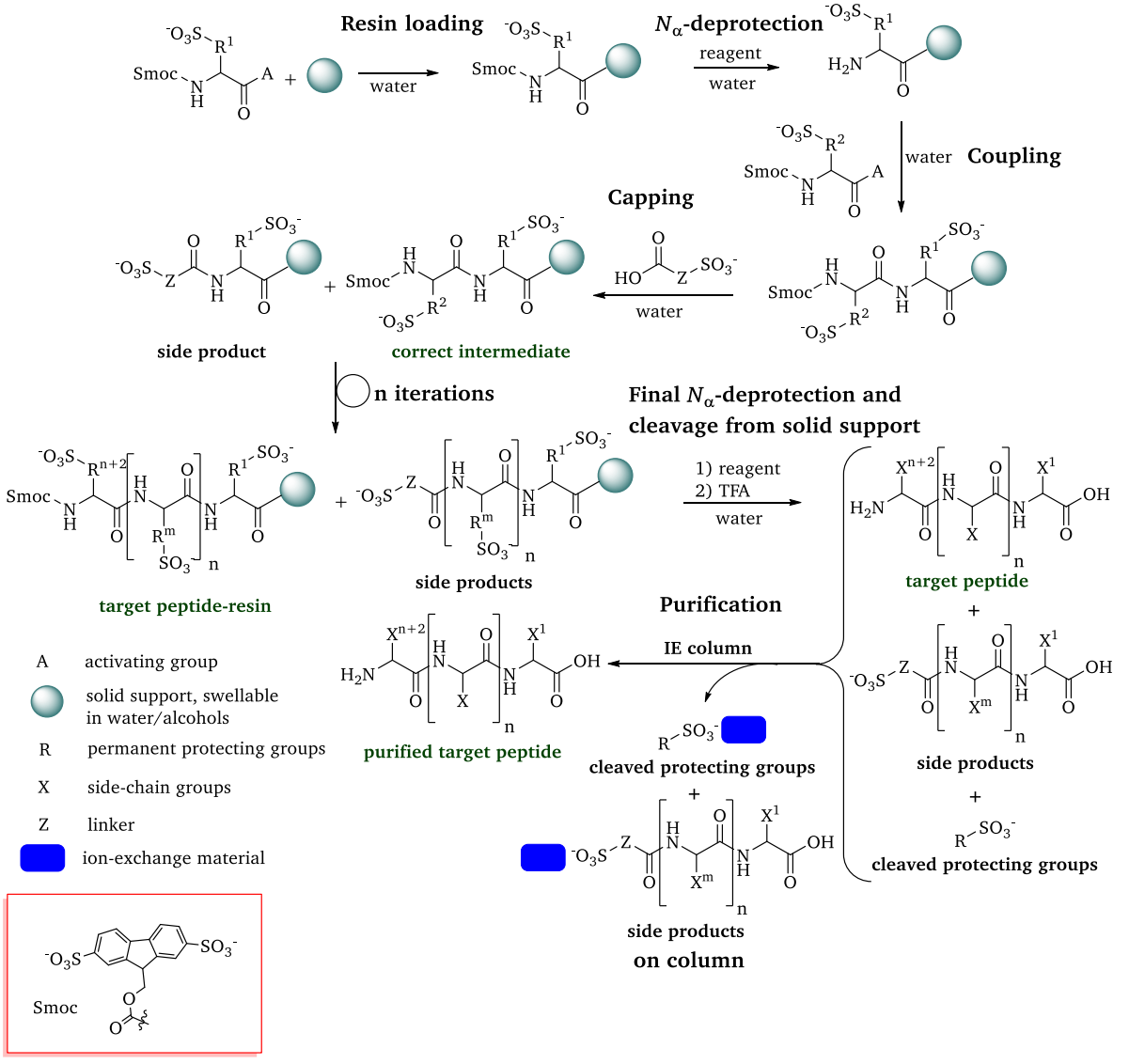

Scheme 17: ASPPS scheme.

Initially, an orthogonal protecting group strategy was considered based on sulfonated N_α and side-chain protection. The Smoc-group was used as N_α-protecting block, side chain protection was performed with Sboc for amines, tBuS for alcohols, OtBuS for carboxyl groups and StBuS for thiols, as shown at **Figure 24**.

However, already the preliminary experiments showed that presence of an aminoterminal Smoc ensures sufficient water solubility of amino acids bearing classic tBu, OtBu and Boc protecting groups at their side chains. Therefore, elaboration of sulfonated side-chain protection was postponed within this work in order to generate resilient results more rapidly. Interestingly, certain side chains which are usually protected in course of classic SPPS, e.g. amides of Asn and Gln, guanidine of Arg, and hydroxyl of Tyr, do not require masking upon ASPPS. This is without any doubt a significant advantage as no time-consuming deprotection (especially in the case of Arg and Tyr) is required any more (see **Table 7**). To validate the ASPPS method, additional experiments were necessary. First, the coupling efficiency in water-based systems had to be assessed and optimized. Subsequently, peptides had to be synthesized under ASPPS conditions with subsequent investigation of common SPPS side reactions like racemization and aspartimide formation. Finally, a proof-of-concept scheme for purification and fluorescence monitoring had to be provided.

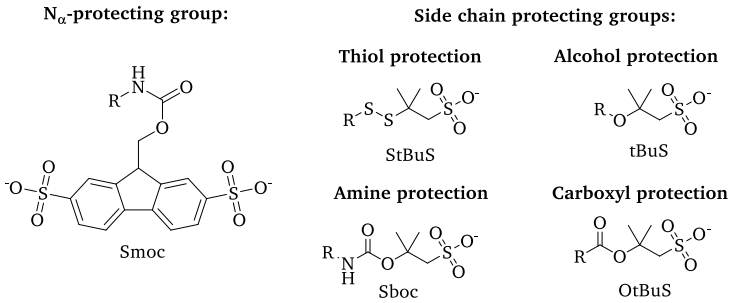

Figure 24: Initial ASPPS orthogonal protecting group strategy.

Table 7: Comparison of Boc- and Fmoc-SPPS and the used ASPPS protection group schemes in this work.

Protecting group scheme for		
Boc-SPPS	**Fmoc-SPPS**	**ASPPS**
Boc-Arg(Tos)-OH	Fmoc-Arg(Pbf)-OH	Smoc-Arg-OH
Boc-Asn(Trt)-OH	Fmoc-Asn(Trt)-OH	Smoc-Asn-OH
Boc-Asp(OBzl)-OH	Fmoc-Asp(OtBu)-OH	Smoc-Asp(OtBu)-OH
Boc-Cys(Acm)-OH	Fmoc-Cys(Trt)-OH	Smoc-Cys(Trt)-OH
Boc-Gln(Trt)-OH	Fmoc-Gln(Trt)-OH	Smoc-Gln-OH
Boc-Glu(OBzl)-OH	Fmoc-Glu(OtBu)-OH	Smoc-Glu(OtBu)-OH
Boc-His(Dnp)-OH	Fmoc-His(Trt)-OH	Smoc-His(Trt)-OH/Smoc-His-OH
Boc-Lys(2-Cl-Z)-OH	Fmoc-Lys(Boc)-OH	Smoc-Lys(Boc)-OH
Boc-Ser(Bzl)-OH	Fmoc-Ser(tBu)-OH	Smoc-Ser(tBu)-OH
Boc-Thr(Bzl)-OH	Fmoc-Thr(tBu)-OH	Smoc-Thr(tBu)-OH
Boc-Trp(For)-OH	Fmoc-Trp(Boc)-OH	Smoc-Trp(Boc)-OH/Smoc-Trp-OH
Boc-Tyr(Bzl)-OH	Fmoc-Tyr(tBu)-OH	Smoc-Tyr-OH

3.6. Coupling efficiency in water-based systems

Being one of the most fundamental chemical bonds in nature, an amide bond is the major constituent of protein backbone and a dominant motif in many natural products, biopolymers, and pharmaceuticals. To date, a vast repertoire of synthetic approaches towards amide bonds has been developed (see section **1.5.4** for details).

From the early years of peptide synthesis, it has been generally accepted that the formation of amide/peptide bonds implies anhydrous coupling conditions. Indeed, in the presence of water, the condensation equilibrium is shifted towards the starting reagents and the active esters are hydrolysed (**Scheme 18**). However, the acidity of carboxylic acids in water is increased compared to the polar aprotic solvents commonly applied in peptide synthesis.[253] Therefore, the acidic proton of the carboxylic group is transferred to a water molecule, resulting in an increased reactivity of the carboxylate ion towards carbodiimides.[221]

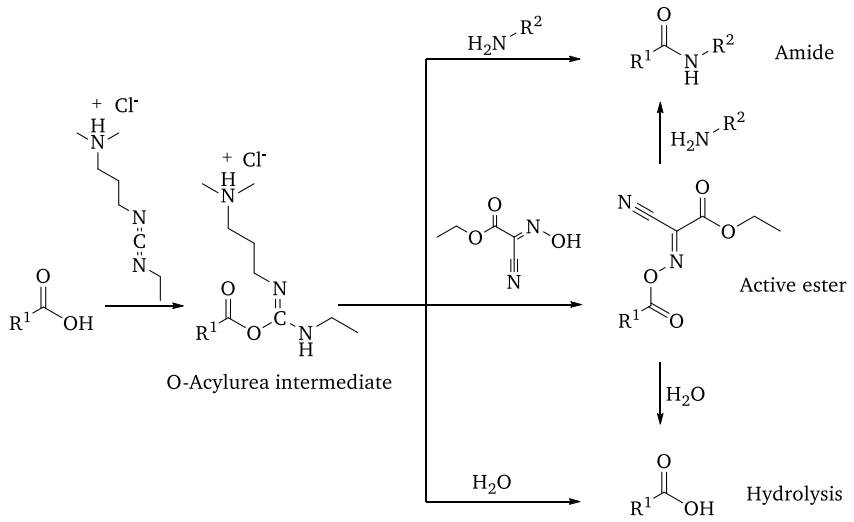

Scheme 18: EDC-HCl **37** based activation of a carboxylic acid, followed by direct amide bond formation (top), formation of an Oxyma **39** active ester (middle) or hydrolysis of the activated species (bottom). (R^1, R^2: residues).

In order to investigate how active esters are formed under aqueous conditions and how these activated species participate in the amide bond formation, series of experiments with N_α-Smoc amino acids were performed.

Initially, different coupling reagents or active ester-forming compounds were evaluated in the synthesis of a dipeptide **36** at room temperature; the synthesis scheme is shown in **Scheme 19**.

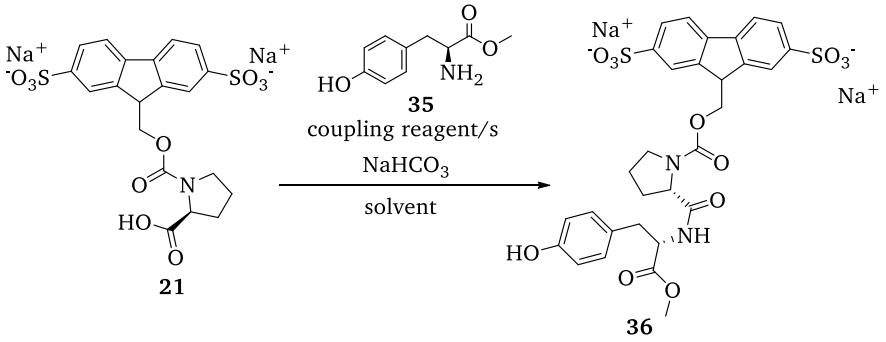

Scheme 19: Synthesis of Smoc-L-Pro-L-Tyr-OMe **36**.

This experiment was performed using 1 eq. Smoc-Pro-OH **21**, 1.2 eq. H-Tyr-OMe **35**, 1 eq. $NaHCO_3$ as base and 1.5 eq. of the coupling reagents **37**, **42**, **43** or **44** (**Table 8**).Coupling reagent **37** was used with either **38**, **39**, **40** or **41** as an active ester-forming reagent. After 25 minutes, the formation of **36** was monitored by HPLC.

Table 8: Summary of the used coupling additives and active ester-forming compounds.

Compound	Coupling reagents	Structure
37	1-ethyl-3-(3-dimethylaminopropyl)carbodiimide hydrochloride (EDC-HCl)	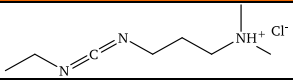
38	*N*-hydroxysuccinimide (NHS)	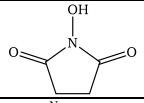
39	Oxyma	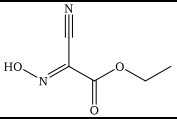
40	1-hydroxy-2-pyridone (HOPO)	

41	*N*-hydroxybicyclo[2.2.1]hept-5-ene-2,3-dicarboximide (HONB)	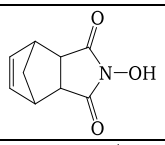
42	*N*-ethoxycarbonyl-2-ethoxy-1,2-dihydroquinoline(EEDQ)	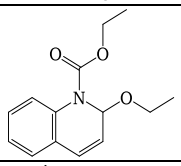
43	4-(4,6-dimethoxy-1,3,5-triazin-2-yl)-4-methyl-morpholinium chloride (DMT-MM)	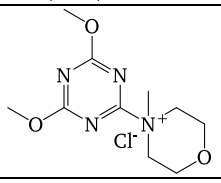
44	(1-Cyano-2-ethoxy-2-oxoethylidenaminooxy)-dimethylamino-morpholino-carbenium hexafluoro-phosphate (COMU)	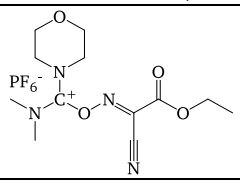

The HPLC analysis of aqueous reaction mixtures with the respective coupling reagents is shown in **Figure 25**.

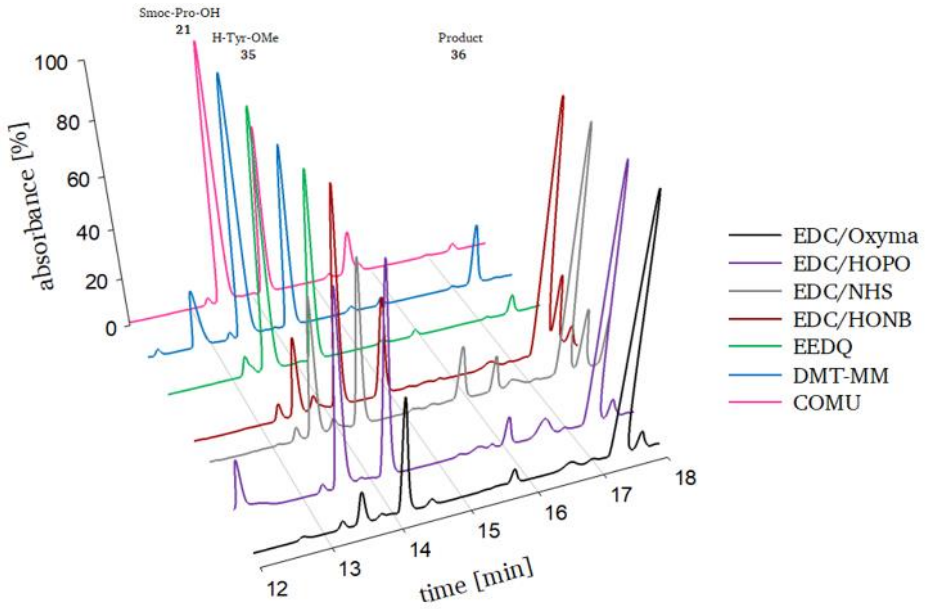

Figure 25: Synthesis of Smoc-L-Pro-L-Tyr-OMe **36** in water. The shown area is reduced to the relevant range of the HPLC runs. Absorption values were normalized from 0 to 100%. A direct comparison between the HPLC runs in terms of product formation is not possible. HPLC traces were monitored at λ=220 nm with a gradient of 0 to 40% MeCN, see section **7.2.3** for details.

The HPLC section shown is selected in such a way, that the resulting product and the starting reagents are visible. The graphs were normalized to 0-100%. A direct graphical comparison of the product peaks is not possible, since no additional normalization on the respective maxima was carried out. The product Smoc-L-Pro-L-Tyr-OMe **36** has a retention time of ~17.2 minutes, the educt Smoc-Pro-OH **21** - 13.5, and H-Tyr-OMe **35** - 14.2 minutes. The complete HPLC data is shown in section **8.5.3**; the reference data of the educts **21** and **35**, coupling reagents **37-44** and product **36** is shown in section **8.5.1**.

The obtained data showed that the product formation in water was most efficient using EDC-HCl **37** activation with active ester reagents. Usage of EEDQ **42**, DMT-MM **43** and COMU **44** resulted only in a minor product formation after 25 minutes. Product formation *via* activation with DMT-MM and EEDQ increased with longer reaction times, but these are not suitable for peptide synthesis with repetitive coupling steps. In addition, EEDQ has a low solubility in water, which further reduces its efficacy. To summarize, Oxyma **39** appeared the most efficient additive, followed by HOPO **40**. HONB **41** is less active, this may be caused by its poorer solubility compared to the other additives. HPLC studies showed the formation of Smoc-Pro-NHS **45** and Smoc-Pro-HONB **46**. These esters are quite stable under the reaction conditions, both of them could be isolated by HPLC, structures are shown in **Figure 26**.

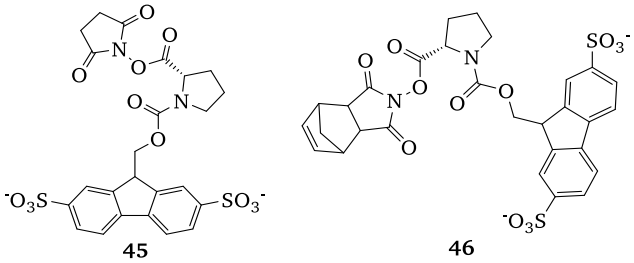

Figure 26: Structures of the isolated Smoc-Pro-NHS **45** and Smoc-Pro-HONB **46** ester.

NHS activation was found to be quite fast, but the formed NHS ester appeared rather stable and less reactive under aqueous conditions, which resulted in diminished product formation. Interestingly, NHS ester activation was associated with a number of side products, which were not formed with the other additives. The following **Table 9** summarizes the efficiency of the used coupling reagents in water after 25 minutes. In general, the coupling efficiency increased along with reaction time (up to 45 minutes).

Table 9: Summary of coupling efficiency of the different reagents in water after 25 minutes.

Coupling reagent	Coupling efficiency*	Active ester side products
EDC-HCl **37**/Oxyma **39**	90.7%	Not observed
EDC-HCl **37**/HOPO **40**	58.3%	Not observed
EDC-HCl **37**/NHS **38**	54%	5.7% NHS ester
EDC-HCl **37**/HONB **41**	57.8%	28.9% HONB ester
EEDQ **42**	6.7%	not applicable
DMT-MM **43**	17.3%	not applicable
COMU **44**	3.2%	Not observed

* The coupling efficiency was calculated based on the area under the HPLC curve of the product, the starting materials and detected active ester derivatives.

The same experiment was performed in 30% aq. acetonitrile, to examine if the addition of small amounts of an organic solvent can influence amide bond formation. The obtained HPLC data for different coupling reagents after 25 minutes coupling in water are shown in **Figure 27**. The complete HPLC data are shown in section **8.5.4**; the reference data of the educts **21** and **35**, coupling reagents **37-44** and product **36** - in section **8.5.1**.

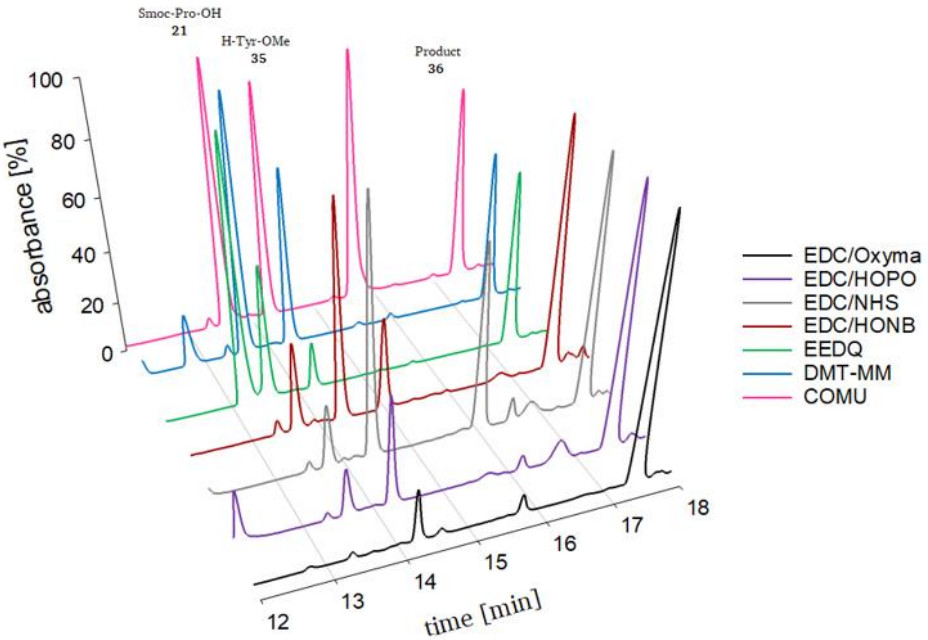

Figure 27: Synthesis of Smoc-L-Pro-L-Tyr-OMe **36** in 30% aq. MeCN. The shown area is reduced to the relevant range of the HPLC runs. Absorption values were normalized from 0 to 100%. A direct comparison between the HPLC runs in terms of product formation is not possible. HPLC traces were monitored at λ=220 nm with a gradient of 0 to 40% MeCN, see section **7.2.3** for details.

Generally, the efficiency of all used coupling reagents significantly increased in 30% aq. MeCN. As expected, the general tendency was maintained, but a clear increase in the performance of HONB **40** and EEDQ **42** possessing low solubility in pure water was observed. The following **Table 10** summarizes the coupling efficiency of the employed reagents in 30% aq. MeCN within 25 minutes. It is interesting to note that combination of EDC-HCl **37**/Oxyma **39** under these conditions allows an almost quantitative conversion. Starting Smoc-Pro-OH **21** was not observed in HPLC and LC-MS.

Table 10: Summary of coupling efficiency of the different reagents in 30% aq. MeCN after 25 minutes.

Coupling reagents	Coupling efficiency*	Active ester side products
EDC-HCl **37**/Oxyma **39**	99.8%	Not observed
EDC-HCl **37**/HOPO **40**	84.2%	Not observed
EDC-HCl **37**/NHS **38**	48.8%	38.9% NHS ester
EDC-HCl **37**/HONB **41**	47.6%	37.09% HONB ester
EEDQ **42**	40.5%	not applicable
DMT-MM **43**	37.3%	not applicable
COMU **44**	41.9%	Not observed

* The coupling efficiency was calculated based on the area under the HPLC curve of the product, the starting materials and detected active ester derivatives.

The same experimental setup was applied to other organic solvents. Results for 30% aq. ethanol are shown **Figure 28**. The complete HPLC data shown in section **8.5.6**; the reference data of the educts **21** and **35**, coupling reagents **37-44** and product **36** - in section **8.5.1**.

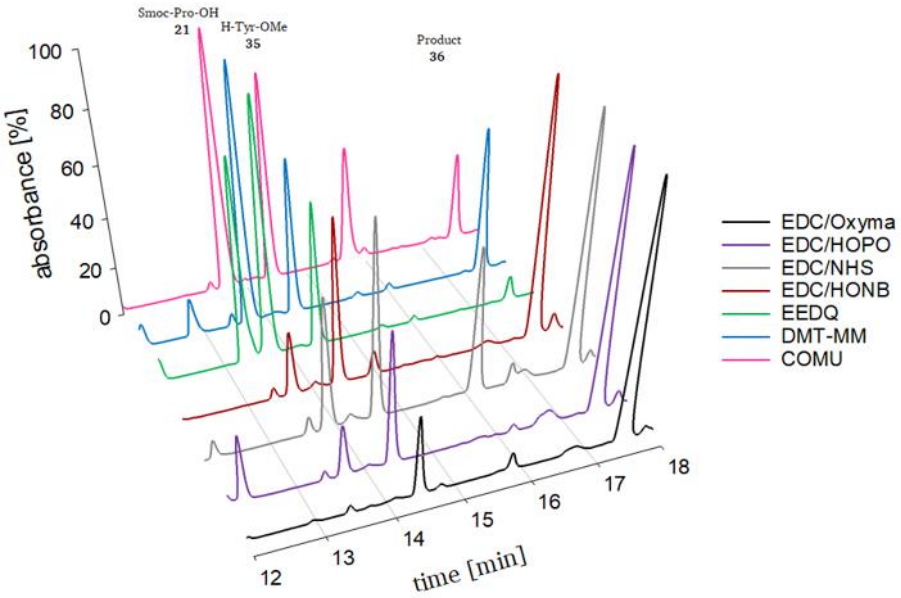

Figure 28: Synthesis of Smoc-L-Pro-L-Tyr-OMe **36** in 30% aq. ethanol. The shown area is reduced to the relevant range of the HPLC runs. Absorption values were normalized from 0 to 100%. A direct comparison between the HPLC runs in terms of product formation is not possible. HPLC traces were monitored at λ=220 nm with a gradient of 0to40 MeCN, see section **7.2.3** for details.

The direct comparison of ethanol and MeCN shows similar results in terms of EDC-HCl **37** and active ester-forming additives **38-41**, but a significant reduction in efficiency for the coupling reagents **42-44**. Compared to water, an increase in efficiency can be observed for all compounds. The following **Table 11** summarizes the coupling efficiency of the used reagents in 30% aq. ethanol after 25 minutes.

Table 11: Summary of coupling efficiency of the different reagents in 30% aq. ethanol after 25 minutes.

Coupling reagents	Coupling efficiency*	Active ester side products
EDC-HCl **37**/Oxyma **39**	99.0%	Not observed
EDC-HCl **37**/HOPO **40**	83.6%	Not observed
EDC-HCl **37**/NHS **38**	46.7%	28.9% NHS ester
EDC-HCl **37**/HONB **41**	50.5%	37.2% HONB ester
EEDQ **42**	8%	not applicable
DMT-MM **43**	36.5%	not applicable
COMU **44**	24.3%	Not observed

* The coupling efficiency was calculated based on the area under the HPLC curve of the product, the starting materials and detected active ester derivatives.

The formation of ethanol esters as side products was observed in LC-MS, but it was significantly reduced compared to pure alcohols. By extending the reaction time, the amount of ethanol ester increased, but was still less than 4% in our experiments and therefore in an acceptable range for the application in SPPS.

Similar experiments were performed with 30% aq. isopropanol; the results are presented in **Figure 29**. The complete HPLC data are shown in section **8.5.7**; the reference data of the educts **21** and **35**, coupling reagents **37-44** and product **36** shown in section **8.5.1**.

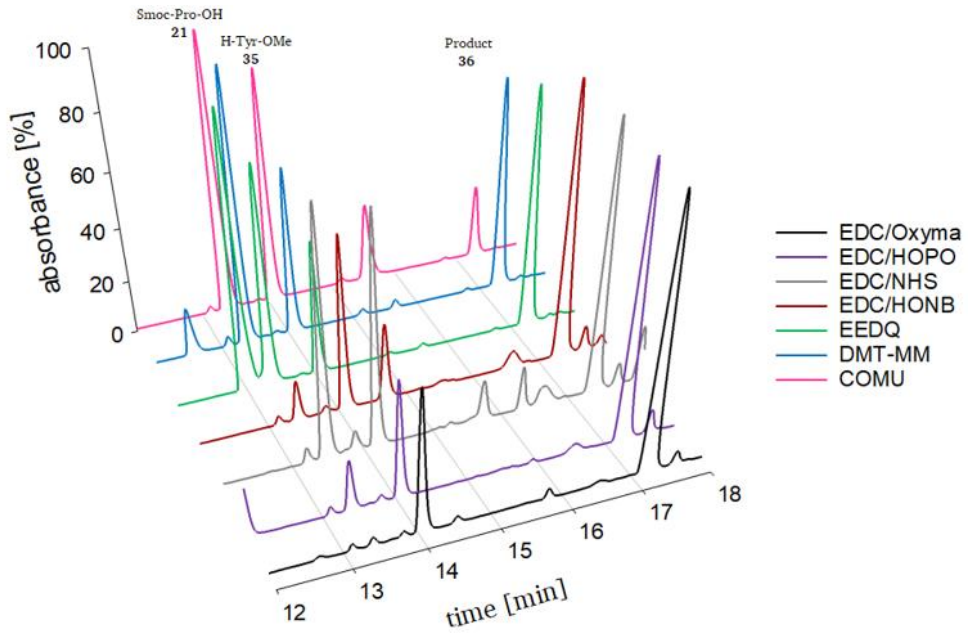

Figure 29: Synthesis of Smoc-L-Pro-L-Tyr-OMe **36** in 30% aq. isopropanol. The shown area is reduced to the relevant range of the HPLC runs. Absorption values were normalized from 0 to 100%. A direct comparison between the HPLC runs in terms of product formation is not possible. HPLC traces were monitored at λ=220 nm with a gradient of 0 to 40% MeCN, see section **7.2.3** for details.

Using 30% aq. isopropanol delivered similar results as for the ethanol-based system, with EEDQ coupling efficiency clearly improved due to the better solubility. The following **Table 12** summarizes the coupling efficiency of the used coupling reagents in 30% isopropanol after 25 minutes.

Table 12: Summary of coupling efficiency of the different reagents in 30% aq. isopropanol after 25 minutes.

Coupling reagents	Coupling efficiency*	Active ester side products
EDC-HCl **37**/Oxyma **39**	98.8%	Not observed
EDC-HCl **37**/HOPO **40**	83.6%	Not observed
EDC-HCl **37**/NHS **38**	47.8%	8.8% NHS ester
EDC-HCl **37**/HONB **41**	62.2%	30.4% HONB ester
EEDQ **42**	53.2%	not applicable
DMT-MM **43**	45.1%	not applicable
COMU **44**	25.6%	Not observed

* The coupling efficiency was calculated based on the area under the HPLC curve of the product, the starting materials and detected active ester derivatives.

An additional experiment was performed with 10% 2-methyltetrahydrofuran (Me-THF) as an additive using the same reaction setting as before. The obtained HPLC data are shown in **Figure 30**. The complete HPLC data shown in section **8.5.9**; the reference data of the educts **21** and **35**, coupling reagents **37-44** and product **36** - in section **8.5.1**.

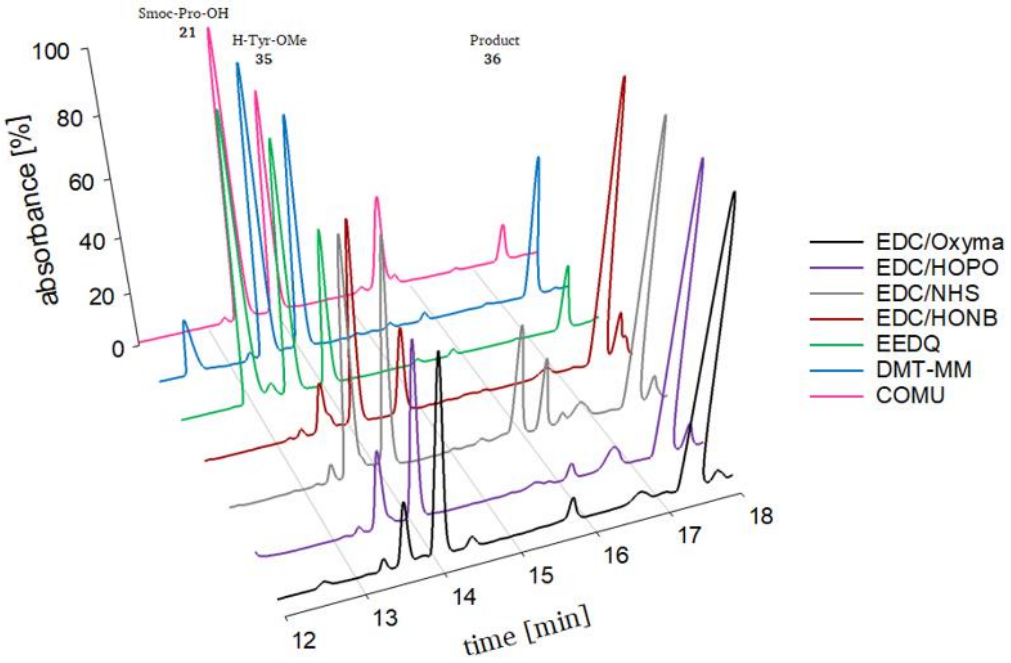

Figure 30: Synthesis of Smoc-L-Pro-L-Tyr-OMe **36** in 10% aq. Me-THF. The shown area is reduced to the relevant range of the HPLC runs. Absorption values were normalized from 0 to 100%. A direct comparison between the HPLC runs in terms of product formation is not possible. HPLC traces were monitored at λ=220 nm with a gradient of 0 to 40% MeCN, see section **7.2.3** for details.

Coupling efficiency in 10% aq. Me-THF was even lower than in pure water. Therefore, the usage of 10%-MeTHF was excluded from SPPS experiments. The following **Table 13** summarizes the coupling efficiency of the used coupling reagents in 10% Me-THF after 25 minutes.

Table 13: Summary of coupling efficiency of the different reagents in 10% aq. Me-THF after 25 minutes.

Coupling reagents	Coupling efficiency*	Active ester side products
EDC-HCl **37**/Oxyma **39**	88.7%	Not observed
EDC-HCl **37**/HOPO **40**	79.4%	Not observed
EDC-HCl **37**/NHS **38**	44.6%	17.4% NHS ester
EDC-HCl **37**/HONB **41**	61.5%	26.2% HONB ester
EEDQ **42**	34.9%	not applicable
DMT-MM **43**	39.9%	not applicable
COMU **44**	11.2%	Not observed

* The coupling efficiency was calculated based on the area under the HPLC curve of the product, the starting materials and detected active ester derivatives.

The same experiment was repeated with 30% aq. Me-THF. However, at this concentration phase separation occurred and the reaction was carried out in an emulsion. The obtained HPLC data are shown in **Figure 31**. The complete HPLC data shown in section **8.5.8**; the reference data of the educts **21** and **35**, coupling reagents **37-44** and product **36** - in section **8.5.1**.

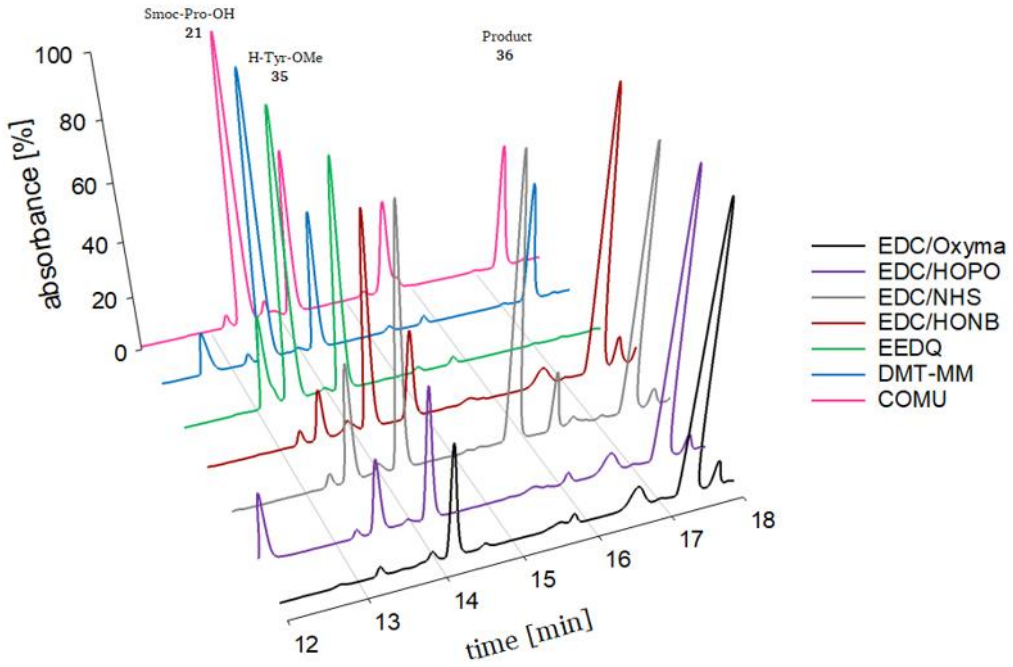

Figure 31: Synthesis of Smoc-L-Pro-L-Tyr-OMe **36** in 30% Me-THF in water (biphasic). The shown area is reduced to the relevant range of the HPLC runs. Absorption values were normalized from 0 to 100%. A direct comparison between the HPLC runs in terms of product formation is not possible. HPLC traces were monitored at λ=220 nm with a gradient of 0 to 40% MeCN, see section **7.2.3** for details.

Interestingly, in a biphasic system higher coupling yields were observed compared to those for the 10% aq. Me-THF. Although most of the coupling systems demonstrated increased efficiency, EDC-HCl **37**/HONB **41** and DMT-MM **43** showed decreased coupling yields, and EEDQ **42** did not lead to detectable product formation at all. Due to their hydrophobic properties, these reagents seem to be located exclusively in the organic layer, and a phase-transfer catalyst is presumably required to make this system viable. The following **Table 14** summarizes the coupling efficiency of the used reagents in 30% aq. Me-THF after 25 minutes.

Table 14: Summary of coupling efficiency of the different reagents in 30% Me-THF/water (biphasic) after 25 minutes.

Coupling reagents	Coupling efficiency*	Active ester side products
EDC-HCl **37**/Oxyma **39**	99.8%	Not observed
EDC-HCl **37**/HOPO **40**	81.5%	Not observed
EDC-HCl **37**/NHS **38**	66.6%	23.3% NHS ester
EDC-HCl **37**/HONB **41**	57.4%	35.2% HONB ester
EEDQ **42**	0%	not applicable
DMT-MM **43**	28.6%	not applicable
COMU **44**	29.8%	Not observed

* The coupling efficiency was calculated based on the area under the HPLC curve of the product, the starting materials and detected active ester derivatives.

Based on the results of the biphasic Me-THF-water system, a similar experiment was performed with 30% ethyl acetate in water. As before, a phase separation was observed and the reaction was performed in an emulsion. The obtained HPLC data are shown in **Figure 32**. The complete HPLC data shown in section **8.5.5**; the reference data of the educts **21** and **35**, coupling reagents **37-44** and product **36** - in section **8.5.1**.

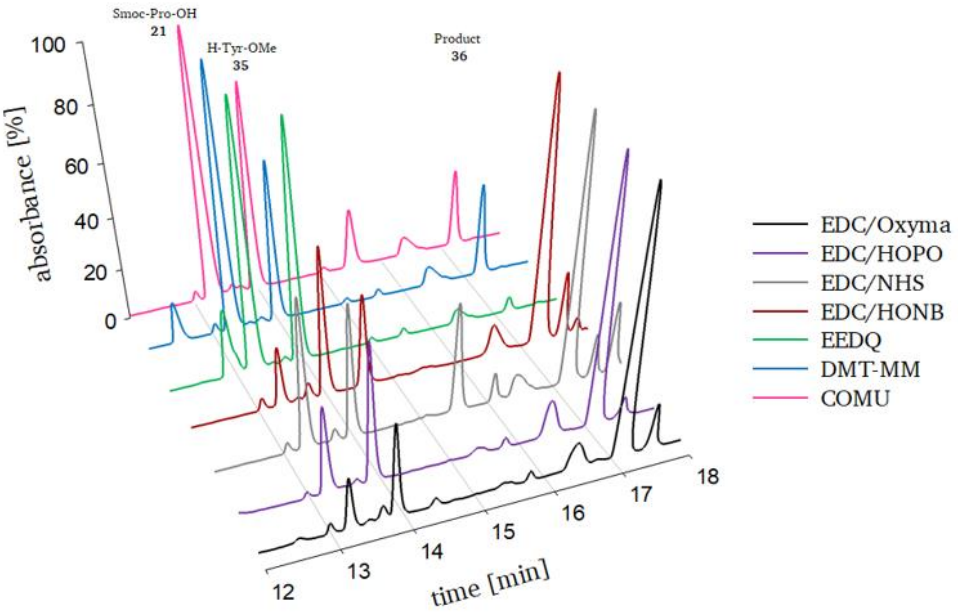

Figure 32: Synthesis of Smoc-L-Pro-L-Tyr-OMe **36** in 30% EtOAc in water (biphasic). The shown area is reduced to the relevant range of the HPLC runs. Absorption values were normalized from 0 to 100%. A direct comparison between the HPLC runs in terms of product formation is not possible. HPLC traces were monitored at λ=220 nm with a gradient of 0 to 40% MeCN, see section **7.2.3** for details.

The results are similar to those observed for 30% MeTHF in water, the product formation rates are slightly lower. Due to the difficult handling and the low efficiency of the biphasic systems in comparison to MeCN or alcohol-water mixtures, no SPPS reaction was carried out under these conditions. The following **Table 15** summarizes the efficiency of the used coupling reagents in 30% EtOAc after 25 minutes.

Table 15: Summary of coupling efficiency of the different reagents in 30% EtOAc/water (biphasic) after 25 minutes.

Coupling reagents	Coupling efficiency*	Active ester side products
EDC-HCl **37**/Oxyma **39**	87.3%	Not observed
EDC-HCl **37**/HOPO **40**	76.9%	Not observed
EDC-HCl **37**/NHS **38**	53%	21.5% NHS ester
EDC-HCl **37**/HONB **41**	64.9%	24.5% HONB ester
EEDQ **42**	4.4%	not applicable
DMT-MM **43**	29.9%	not applicable
COMU **44**	21.1%	Not observed

* The coupling efficiency was calculated based on the area under the HPLC curve of the product, the starting materials and detected active ester derivatives.

The coupling efficiency of the used coupling systems are summarized for easy comparability in the following **Table 16**. In summary, the EDC-HCl **37**/Oxyma **39** and EDC-HCl **37**/HOPO **40** mixtures have proven to be the most suitable candidates for water-based peptide synthesis applying sodium bicarbonate as a general base. Therefore, these reagents were used for SPPS test reactions with a short test peptide.

Table 16: Summary of coupling efficiency of the different reagents after 25 minutes.

Coupling reagents	Coupling efficiency*						
	water	30% MeCN	30% EtOH	30% *i*PrOH	10% Me-THF	30% Me-THF**	30% EtOAc**
EDC-HCl **37**/Oxyma **39**	90.7%	99.8%	99.0%	98.8%	88.7%	99.8%	87.3%
EDC-HCl **37**/HOPO **40**	58.3%	84.2%	83.6%	83.6%	79.4%	81.5%	76.9%
EDC-HCl **37**/NHS **38**	54%	48.8%	46.7%	47.8%	44.6%	66.6%	53%
EDC-HCl **37**/HONB **41**	57.8%	47.6%	50.5%	62.2%	61.5%	57.4%	64.9%
EEDQ **42**	6.7%	40.5%	8%	53.2%	34.9%	0%	4.4%
DMT-MM **43**	17.3%	37.3%	36.5%	45.1%	39.9%	28.6%	29.9%
COMU **44**	3.2%	41.9%	24.3%	25.6%	11.2%	29.8%	21.1%

* The coupling efficiency was calculated based on the area under the HPLC curve of the product, the starting materials and detected active ester derivatives.
** Biphasic

3.7. EDC-HCl mediated on-support coupling with Oxyma/HOPO as additives

Following the previous experiments in solution, coupling experiments were carried out on solid phase. The two most promising candidates, EDC-HCl **37**/Oxyma **39** and EDC-HCl **37**/HOPO **40**, were used for the synthesis of the tetrapeptide Smoc-**LAGV**-NH_2 **47**. The synthesis was performed in water and 30% aq. MeCN, respectively.

The experimental setup and the molar excess are aligned to a standard Fmoc-SPPS approach. Thus, 3 eq. of the respective N_α-Smoc amino acid, 5.5 eq. EDC-HCl **37** and either 3 eq. of Oxyma **40** or HOPO **41** with 3 eq. $NaHCO_3$ have been used for the coupling steps. An optimization with regard to peptide yield was not carried out. The peptides were synthesized on solid phase (see section **7.8** for experimental details). After cleavage from solid support, the crude peptides **47** were analysed by HPLC and ESI-MS. The following **Table 17** summarizes the synthetic yields.

Table 17: Summary of the SPPS yields for Oxyma **39** and HOPO **40** based peptide synthesis in water or 30% aq. MeCN.

Coupling reagents	Solvent	Yield (calculated from average loading)
EDC-HCl **37**/Oxyma **39**	water	19mg (51%)
EDC-HCl **37**/Oxyma **39**	30% $MeCN_{(aq)}$	24mg (65%)
EDC-HCl **37**/HOPO **40**	water	18mg (49%)
EDC-HCl **37**/HOPO **40**	30% $MeCN_{(aq)}$	17mg (46%)

The yields of the synthesized peptides showed that the syntheses with EDC-HCl **37**/Oxyma **39** is resulting in slightly higher yields compared to EDC-HCl **37**/HOPO **40**. This corresponds to the results obtained for solution-based peptide synthesis before. The usage of 30% organic solvents such as MeCN or alcohols showed a significant increase of the yield. Therefore, I assume that the addition of organic solvents seems to slow down the hydrolysis of the activated species and leads to a higher product formation. The low performance of EDC-HCl **37**/HOPO **40** in 30% MeCN seems to be caused by a mistake during the synthesis or precipitation problem.

The synthesis for all subsequent peptides was thus performed with EDC-HCl **37**/Oxyma **39** as standard coupling mixture.

3.8. Aqueous SPPS (ASPPS) of model peptides

In order to demonstrate that water-based peptide synthesis with N_α-Smoc amino acids and the previously determined coupling conditions is possible, a series of prominent peptides was synthesized to validate the method. All peptides have been assembled manually on either a commercially available ChemMatrix H-Rink amide resin (loading capacity 0.4-0-6 mmol/g) or on a preloaded HMPB-ChemMatrix resin (loading capacity 0.3-0.65 mmol/g). Other water-compatible resins could be used as well, some tests with TentaGel™ showed good results, too. The ChemMatrix H-Rink amide resin was loaded in a double coupling (2×25min) with a solution of N_α-Smoc amino acid (3 eq.), EDC-HCl **37** (5.5 eq.), Oxyma **39** (3 eq.) and $NaHCO_3$ (3 eq.). Smoc deprotection was carried out in dependency of the used resin with either 1M NaOH, 25% ethanolamine$_{(aq)}$ or 5-10% piperazine$_{(aq)}$ for 5 and 10 minutes. Coupling of the amino acids was performed with 3 eq. N_α-Smoc amino acid, 5.5 eq. EDC-HCl **37**, 3 eq. Oxyma **39** and 3 eq. $NaHCO_3$. For the details of the synthetic approach see section **7.9**. Peptides of different lengths and complexity were chosen, most of them being bioactive molecules used in cosmetic or pharmaceutical applications. The peptides H-CYEIS-NH_2 **61**, H-ANKPG-NH_2 **62** are model peptides that were used to determine racemization levels of the respective amino acids during peptide assembly. The sequence Smoc-E(OtBu)K(Boc)R(Pbf)S(tBu)C(Trt)-OH **60** was synthesized as a model for a fully protected peptide that could be used in a fragment condensation approach.

All peptides were synthesized as proof-of-concept; no optimization of the specific peptide synthesis process was performed regarding purity or yield. Therefore, there are still possibilities to optimize the synthesis of the specific peptides in case of a possible upscaling of the target peptides. The following **Table 18** summarizes the synthesized peptides, the used solvents and the obtained yields.

Table 18: Summary of the synthesized peptides, the used solvent and obtained yields.

Entry	Peptide sequence	Solvent	Yield (calculated from average loading)
1	H-AGELS-NH_2 (Pentapeptide-31) **48**	water	13.7 mg (57.7%)
2	H-GPQGPQ-OH (Hexapeptide-9) **49**	water	9.2 mg (38.7%)
3	H-EEMQRR-NH_2 (Hexapeptide 3) **50**	water	21.7 mg (51.3%)
4	Ac-EEMQRR-NH_2 (Acetyl-Hexapeptide 3) **51**	water	18.7 mg (42.2%)
5	Leu-Enkephalin amide H-YGGFM-NH_2 **52**	water	19.6 mg (70.9%)
6	Met-Enkephalin H-YGGFM-OH **53**	30% MeCN$_{(aq)}$	9 mg (63%)
7	Leu-Enkephalin H-YGGFL-OH **54**	30% MeCN$_{(aq)}$	10.3 mg (71.8%)
8	(ACP) 65-74 H-VQAAIDYING-OH **55**	50% MeCN$_{(aq)}$	18 mg (36%)
9	(ACP) 65-74 H-VQAAIDYING-NH_2 **56**	50% MeCN$_{(aq)}$	23 mg (46%)
10	H-GPRP-OH **57**	water	8 mg (38%)
11	Smoc-VVIA-NH_2 **58**	water	26 mg (67%)
12	Smoc-DIIW-OH **59**	water	22 mg (50%)
13	Smoc-E(OtBu)K(Boc)R(Pbf)S(tBu)C(Trt)-OH **60**	50% MeCN$_{(aq)}$	18 mg (44%)
14	H-CYEIS-NH_2 **61**	30% MeCN$_{(aq)}$	15mg (49%)
15	H-ANKPG-NH_2 **62**	30% MeCN$_{(aq)}$	13mg (53.7%)
16	Pal-GHK-OH **63***	20% ethanol$_{(aq)}$	14.1 mg (54.2%)

17	Pal-GQPR-OH **64***	20% ethanol$_{(aq)}$	18.7 mg (59.7%)
18	H-GPRPA-NH_2 Vialox **65**	30% MeCN$_{(aq)}$	12 mg (48.4%)
19	Oxytocin **66**	30% MeCN$_{(aq)}$	18 mg (35.8%)
20	Vasopressin **67**	30% MeCN$_{(aq)}$	20 mg (39.7%)
21	Heptaarginine **68**	30% MeCN$_{(aq)}$	23 mg (41.4%)
22	Leuphasyl **69**	20% MeCN$_{(aq)}$	17.3 mg (57.9%)

*Pal=Palmitic acid

The results show that a water-based SPPS is possible. The yields of the synthesized peptides are within an acceptable range for a non-optimized synthesis process. It was concluded that ASPPS could be used as a replacement for Fmoc-based peptide synthesis in DMF.

3.9. Racemization studies

Two model peptides were synthesized by ASPPS to investigate potential racemization behaviour during the synthesis. The two peptide sequences are shown in the following **Figure 33**.

H—C-Y-E-I-S—NH_2 Chemical Formula: $C_{26}H_{40}N_6O_9S$

H—A-N-K-P-G—NH_2 Chemical Formula: $C_{20}H_{36}N_8O_6$

Figure 33: Model peptides H-CYEIS-NH_2 **61** and H-ANKPG-NH_2 **62** for racemization tests.

The synthesis of both peptides was performed on ChemMatrix H-Rink amide resins that was loaded in double coupling (2×25min) with a solution of N_α-Smoc amino acids (3 eq.), EDC-HCl **37** (5.5 eq.), Oxyma **39** (3 eq.) and $NaHCO_3$ (3 eq.). Smoc deprotection was carried out with 1M NaOH for 5 and 10 minutes. NaOH was used as base, as this is the strongest base used in the ASPPS process. If there are base catalyzed side-reactions during the synthesis process, it should increase the amount of side products. Coupling of the following amino acids was performed with 3 eq. N_α-Smoc amino acids, 5.5 eq. EDC-HCl **37**, 3 eq. Oxyma **39** and 3 eq. $NaHCO_3$ as base. Smoc-Asn-OH **7** and Smoc-Tyr-OH **29** were used without side-chain protecting groups. Peptide samples of **61** and **62** were sent to *C.A.T. GmbH & Co Chromatographie und Analysentechnik KG (Tübingen, Germany)* for the analysis of enantiomeric purity. The obtained results are shown in **Table 19**. Since the measured racemization for Asn appeared to be quite high, an additional sample Smoc-Asn-OH **7** was send to *C.A.T. GmbH & Co Chromatographie und Analysentechnik KG (Tübingen, Germany)* for analysis.

Table 19: Determined racemization levels of the amino acids in both test peptides

Amino acid	Enantiomeric composition
Isoleucine	>99.7% L-Isoleucine
	<0.10% D-Isoleucine
	<0.10% L-*allo*-Isoleucine
	<0.10% D-*allo*-Isoleucine
Serine	<0.10% D-Enantiomer
Cysteine	<0.10% D-Enantiomer
Glutamine/Glutamic acid	<0.10% D-Enantiomer
Tyrosine	0.25% D-Enantiomer
Alanine	0.50% D-Enantiomer
Proline	0.43% D-Enantiomer
Asparagine/Aspartic acid	2.04% D-Enantiomer
Lysine	0.11% D-Enantiomer
Smoc-Asn-OH **7**	0.30% D-Enantiomer

The racemization of the amino acids during the ASPPS corresponds to those expected within the context of a Fmoc-based SPPS in DMF. The slightly increased values for proline and alanine can be attributed to the synthesis process of amino acids, which was therefore easily adapted for future syntheses. The elevated level of racemization in the case of Asn cannot be explained by the used N_{α}-Smoc amino acid, which contains 0.30% D-enantiomer. This indicates a base-catalyzed side reaction during the synthesis process. As the other amino acids showed no anomalies, and the used base concentration of $NaHCO_3$ during the coupling process is too low to cause racemization it can only be a result of Smoc deprotection with NaOH. Therefore, additional aspartimide formation studies have been performed as this was suspected to be the source of racemization of Asn during the synthesis process.

3.10. Aspartimide formation studies

Aspartimide formation in Fmoc-SPPS is a well-documented side reaction occurring frequently at Asn-R or Asp-R where R is an amino acid such as Gly, Ala or Ser.[164, 177-181, 188, 191-193, 195, 254-255]

The treatment of the peptides containing Asp/Asn with bases such as piperidine results in the formation of the cyclic D/L aspartimide intermediate. Depending on the following reaction, multiple possible side products are formed. Hydrolysis of the D/L aspartimide intermediate could result in the formation of the D/L-α- or the D/L-β-peptides. Nucleophilic attack of the base or other amines could result in the corresponding D/L-α- or the D/L-β-peptide adducts (shown in **Scheme 20**).[179-181, 187]

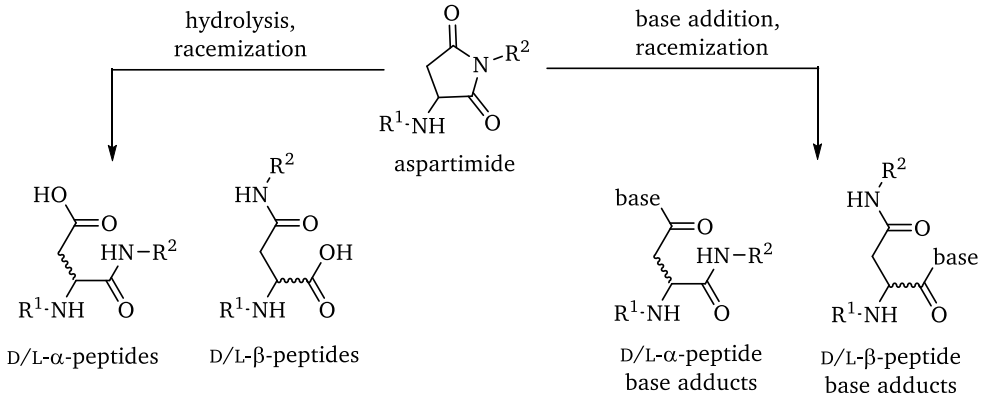

Scheme 20: Aspartimide formation under basic conditions and the possible side products. (R^1, R^2: residues).

To clarify whether aspartimide formation during ASPPS is a frequent side reaction, four model peptides derived from peptide scorpion toxin II (H-VKDGYI-NH_2 **70**, H-VK(D-D)GYI-NH_2 **71**, H-VKNGYI-NH_2 **72** and H-VK(β-D)GYI-NH_2 **73**) were synthesized. Afterwards the peptide-resins **70-73** were split into 15 equal parts and incubated for 3h and 16h with the following bases: 1M $NaOH_{(aq)}$, 1M NaOH in EtOH, 5% piperazine in DMF, 5% $piperazine_{(aq)}$, 20% piperidine in DMF and 10% $ethanolamine_{(aq)}$. As a reference, a non-incubated resin was subjected to global cleavage. After the respective incubation time, the samples were cleaved from the resin and analyzed by RP-HPLC and LC-MS. The results of the 3h and 16h incubation of H-VKDGYI-NH_2 **70** are shown in **Figure 34**. As expected and described in detail in the literature, aspartimide formation depends on the used bases and the incubation time. Using 20% piperidine in DMF results in several side products after 16 hours. The main observed side products are the corresponding base adducts. Using 5% piperazine in DMF results in less side products after 16 hours, as previously described by Wade *et al.*[182]

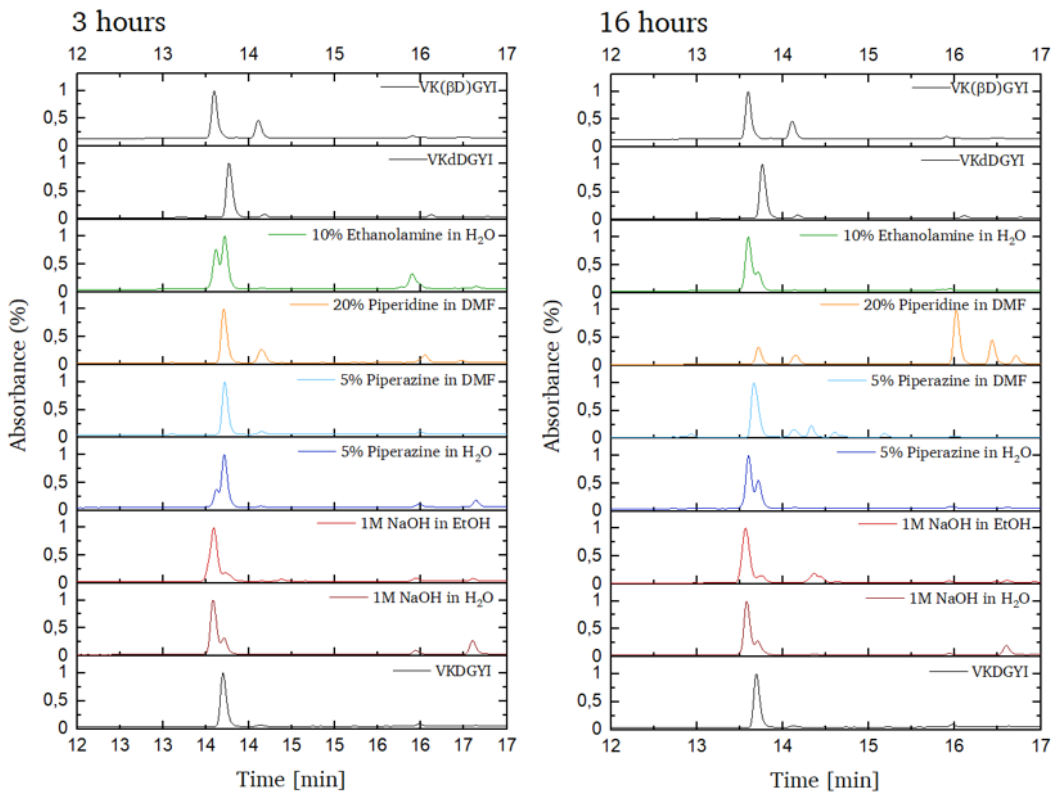

Figure 34: Summary of HPLC data of the incubation of H-VKDGYI-NH_2 **70** with different bases for 3h (left) and for 16h (right) and the resulting aspartimide side product formation caused by the used bases. Retention times were calibrated using ascorbic acid as internal standard; absorbance was normalized between 0 and 1. HPLC traces were monitored at λ=220 nm with a gradient of 0 to 40% MeCN, see section 7.2.3 for details.

The formation of the D-product and the β–product was not observed in organic solvents. Interestingly, using NaOH in either water or alcohol mainly resulted in the formation of the β-product, the D-product was not observed. Using ethanolamine in water results mainly in the formation of the β–product. The usage of 5% piperazine in water results in the formation of the β–product in a ratio of 1:3 (β–product:α-product) after 3h, after 16h incubation time the ratio is switched to 3:2 (β–product: α-product). In summary, in organic solvents the observed side products are mainly the corresponding L/D-α-base adducts or L/D-β-base adducts, the formation of the β–product was not observed. In water-based synthesis mainly the β–product is formed as side product. The ratio of the β-product formation corresponds to the D/L-β-peptides and the D/L-α-peptide ratio described in the literature for the aspartimide formation of proteins under *in vivo* conditions (3:1 ,observed in amyloid β-protein,[185] and 2:1[186]). Using stronger bases like NaOH in water results in an inreased amount of β–product formation. This could depend on the base strength but is more likely based on the nearly instantaneous cleavage of the *tert*-butyl ester side chain of Asp, resulting in a high amount of reactive species. Therefore, NaOH could not be used in ASPPS if esters are applied as linkers or side chain protecting groups.

The results of the 3h and 16h incubation of H-VK(D-D)GYI-NH_2 **71** are shown in **Figure 35**. As expected, the incubation of H-VK(D-D)GYI-NH_2 **71** for 3h and 16h yielded the same results as the incubation of H-VKDGYI-NH_2 **70**. Main side products in organic solvents are the corresponding L/D-α-base or L/D-β-base adducts, the formation of the β–product was not observed as well. In water-based synthesis mainly the β–product is formed as side product in the same ratio as observed during the H-VKDGYI-NH_2 **71** incubation. Interestingly, the incubation with 10% ethanolamine in water also results in the formation of L-product; this was

the only time when racemization was observed. After 16h, a ratio of 2.3:1:1 (β-peptide: D-peptide:L-peptide) was observed.

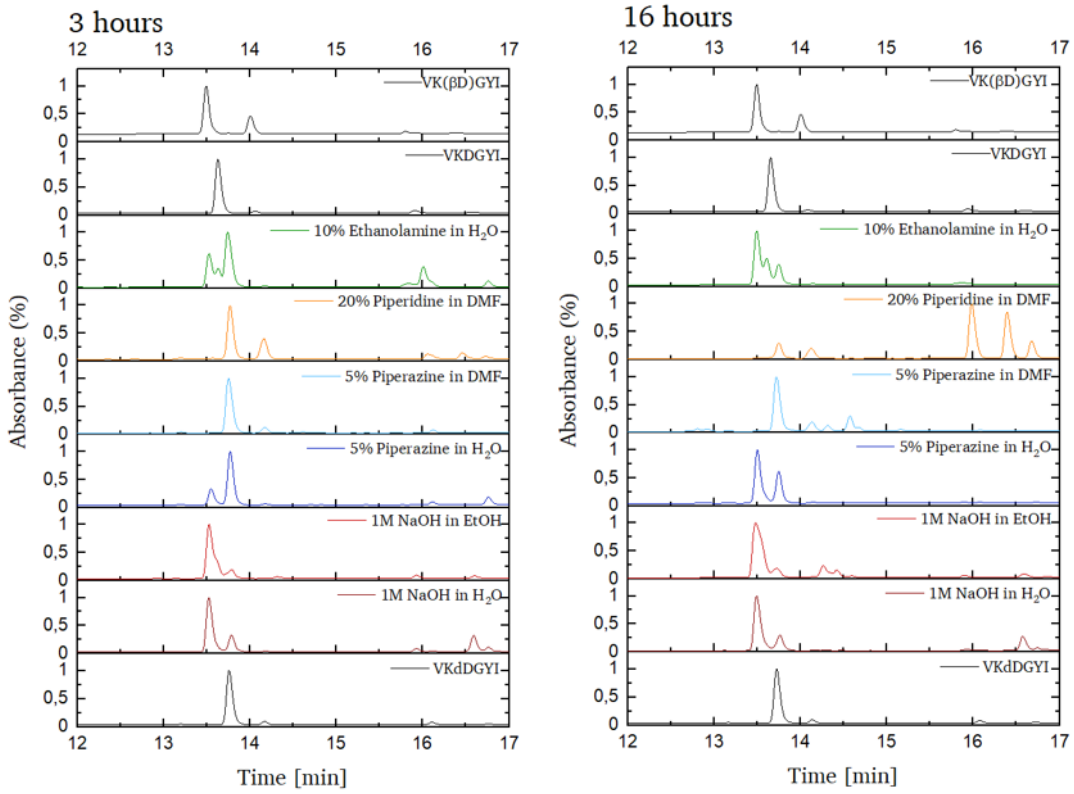

Figure 35: Summary of HPLC data of the incubation of H-VK(D-D)GYI-NH_2 **71** with different bases for 3h (left) and for 16h (right) and the resulting aspartimide side product formation caused by the used bases. Retention times were calibrated using ascorbic acid as internal standard; absorbance was normalized between 0 and 1. HPLC traces were monitored at λ=220 nm with a gradient of 0 to 40% MeCN, see section 7.2.3 for details.

As Asn is prone to aspartimide formation as well, the same experiments were performed with H-VKNGYI-NH_2 **72**, the results of the 3h and 16h incubation are shown in **Figure 36**. Using 20% piperidine and 5% piperazine in DMF results in a minimal amount of side products after 16h of incubation. 5% piperazine in water delivers results similar to those obtained for the DMF-based incubation after 16h, after 3h there seemed to be a side product formation that was not observed after 16h. The usage of 10% ethanolamine results in the formation of minor side products after 3h and 16h. Usage of NaOH in water or ethanol results in the formation of side products. With increasing time, the incubation with NaOH in ethanol seems to increase a possible deamination of Asn. Interestingly, this was not observed with other bases in water or DMF. The formation of a side product observed upon NaOH incubation is not time-dependent, but its isolation and LC-MS identification was not possible. In summary, using 5% piperazine for Smoc deprotection of aspartimide-prone sequences is advised. In comparison with 20% piperidine in DMF, less side product formation is observed, but compared to 5% piperazine in DMF there is a significant increase of side product formation. This β-peptide side product seems to be caused less by the base itself but by the aspartimide formation in water itself, as observed by proteins degradation under *in vivo* conditions.

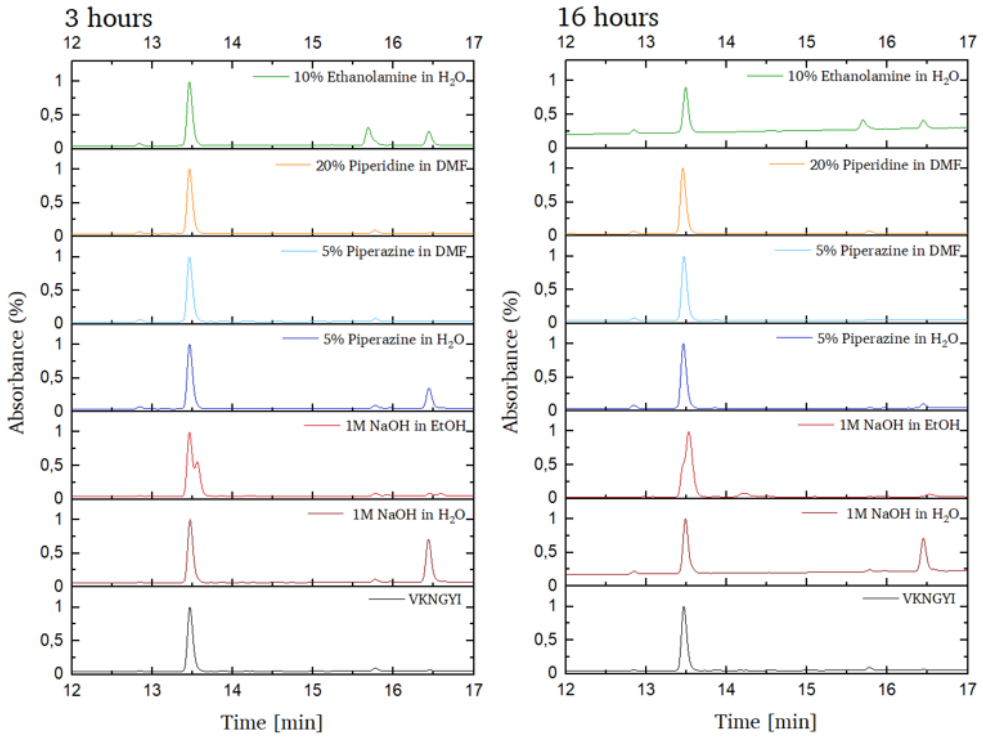

Figure 36: Summary of HPLC data of the incubation of H-VKNGYI-NH_2 **72** with different bases for 3h (left) and for 16h (right) and the resulting aspartimide side product formation caused by the used bases. Retention times were calibrated using ascorbic acid as internal standard; absorbance was normalized between 0 and 1. HPLC traces were monitored at λ=220 nm with a gradient of 0 to 40% MeCN, see section 7.2.3 for details.

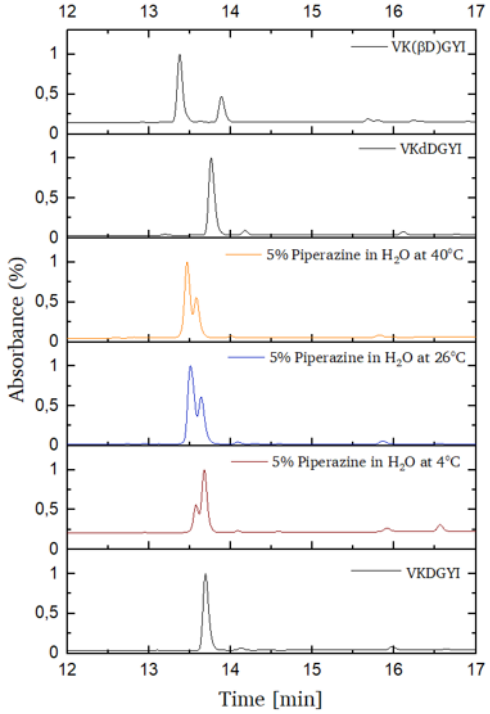

Figure 37: Summary of HPLC data of the incubation of the temperature dependent formation of H-VK(β-D)GYI-NH_2 **73** with 5% Piperazine in water after 16 h. Retention times were calibrated using ascorbic acid as internal standard; absorbance was normalized between 0 and 1. HPLC traces were monitored at λ=220 nm with a gradient of 0 to 40% MeCN, see section 7.2.3 for details.

Based on the literature[256], the protein degradation should increase at higher temperatures and decrease at the lower ones. Therefore, an additional incubation of H-VKDGYI-NH_2 **70** with 5% piperazine in water was performed at 4°C, RT and 40°C respectively. The temperature-

dependent formation of H-VK(β-D)GYI-NH_2 **73** with 5% piperazine in water after 16h is shown in the following **Figure 37**.

The obtained results show that the aspartimide formation in water is temperature dependent. At 4°C the (β–product:α-product) ratio is 1:3 and with increasing temperature shifted at 40°C to a ratio of 2.5:1. Therefore, deprotection of aspartimide-prone sequences in water should be performed at 4°C or below this temperature to reduce the amount of aspartimide side products.

3.11. Fluorescent properties of the Smoc group

Figure 38: A sample of Smoc-Cl **2** in water illuminated at 254nm.

Due to its particular electronic structure, the Smoc group absorbs in the UV/Vis spectral area and possesses fluorescent properties, being therefore detectable by respective analytical methods as shown in **Figure 38**. It is spectroscopically active and fluorescent both in N_{α}-Smoc amino acids and in its cleaved form. This is a significant advantage over the classical Fmoc group, which can only be observed after deprotection,[257] and allows to establish a real-time monitoring of the synthesis process. **Figure 39** shows a direct comparison of Smoc-Gly-OH **12** with Fmoc-Gly-OH upon UV irradiation.

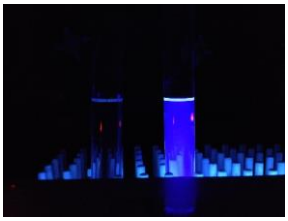

Figure 39: A sample of Smoc-Gly-OH **12** (right) and Fmoc-Gly-OH (left) as a reference, illuminated at 254nm.

It is necessary to determine the fluorescent properties of the N_{α}-Smoc amino acids to establish a real-time monitoring. For this purpose, the fluorescence spectra of a 100 nM solution of all amino acids were recorded between 300 nm and 400 nm. As an example, the absorption spectra and the fluorescence spectra of a 100 nM solution of Smoc-Ala-OH were recorded between 300 nm and 400 nm, results are shown in **Figure 40**. The experimental data shows excitation maxima of 281 nm and emission maxima of 338 nm, resulting in a Stokes shift of 57 nm.

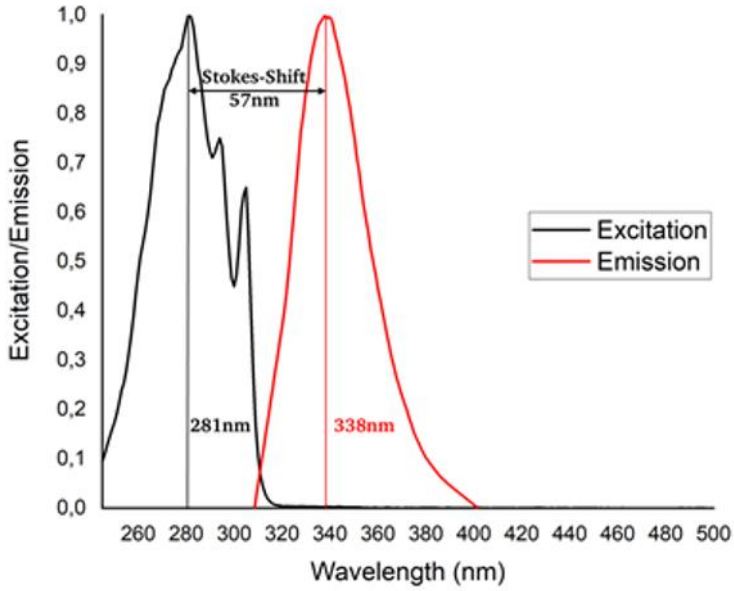

Figure 40: Emission and excitation spectra of Smoc-Ala-OH **3**. Excitation and emission have been normalized.

The determined spectral data of all synthesized N_{α}-Smoc amino acids are listed in **Table 20**. Excitation spectra of all N_{α}-Smoc amino acids were measured between 220 nm and 700 nm. All

N_α-Smoc amino acids show absorbance between 200nm and 220 nm (due to technical limitations of the used equipment this is not shown here) but only the range of 245-310 nm was identified as excitation area.

Table 20: Excitation and emission maxima of all synthesized N_α-Smoc amino acids and their Stokes shift in water.

N_α-Smoc amino acid	Excitation maxima	Emission maxima	Stokes shift
Smoc-L-Ala-OH **3**	281 nm	338 nm	57 nm
Smoc-D-Ala-OH **4**	281 nm	340 nm	59 nm
Smoc-L-Arg-OH **5**	282 nm	340 nm	58 nm
Smoc-L-Arg(Pbf)-OH **6**	282 nm (Abs max. 220nm)	338 nm	56 nm
Smoc-L-Asn-OH 7	281 nm	340 nm	59 nm
Smoc-L-Asp(OtBu)-OH **8**	282 nm	340 nm	58 nm
Smoc-L-Cys(Trt)-OH **9**	282 nm (Abs max. 220nm)	340 nm	58 nm
Smoc-L-Gln-OH **10**	281 nm	338 nm	57 nm
Smoc-L-Glu(OtBu)-OH **11**	282 nm	340 nm	58 nm
Smoc-Gly-OH **12**	281 nm	338 nm	57 nm
Smoc-L-His-OH **13**	281 nm	338 nm	57 nm
Smoc-L-His(Trt)-OH **14**	282 nm (Abs max. 220nm)	338 nm	57 nm
Smoc-L-Ile-OH **15**	282 nm	340 nm	58 nm
Smoc-L-Leu-OH **16**	281 nm	340 nm	59 nm
Smoc-D-Leu-OH **17**	282 nm	340 nm	58 nm
Smoc-L-Lys(Boc)-OH **18**	281 nm	338 nm	57 nm
Smoc-L-Met-OH **19**	281 nm	340 nm	59 nm
Smoc-L-Phe-OH **20**	281 nm	338 nm	57 nm
Smoc-L-Pro-OH **21**	281 nm	340 nm	59 nm
Smoc-L-Ser-OH **22**	281 nm	340 nm	59 nm
Smoc-L-Ser(tBu)-OH **23**	281 nm	340 nm	59 nm
Smoc-L-Thr-OH **24**	281 nm	340 nm	59 nm
Smoc-L-Thr(tBu)-OH **25**	281 nm	340 nm	59 nm
Smoc-L-Trp-OH **26**	281 nm (Abs max. 220, 225nm)	341 nm	60 nm
Smoc-L-Trp(Boc)-OH **27**	281 nm (Abs max. 220nm)	340 nm	59 nm
Smoc-L-Tyr-OH **28**	282 nm	341 nm	59 nm
Smoc-L-Tyr(tBu)-OH **29**	281 nm	340 nm	59 nm
Smoc-L-Val-OH **30**	281 nm	340 nm	59 nm
Smoc-β-Ala-OH **31**	281 nm	340 nm	59 nm
Smoc-Aib-OH **32**	281 nm	338 nm	57 nm

Fluorescence was measured between 300 nm and 500 nm. As the results show, excitation maxima for Smoc was around 280 nm and the emission maxima - around 340 nm. The minor differences between the N_α-Smoc amino acids seem to be caused by the limited measuring accuracy of the used device.

Quantum efficiency is critical for fluorescence measurements, however in this work the quantum efficiency of all N_{α}-Smoc amino acids could not be determined due to a lack of required equipment. Generally, a decreased fluorescence was observed with aromatic amino acids tyrosine and tryptophan as well as with aromatic side chain protecting groups like trityl (Cys, His) or Pbf (Arg). This might be caused by an inter- or intramolecular quenching effect. An example for an overlap is shown in **Figure 41**.

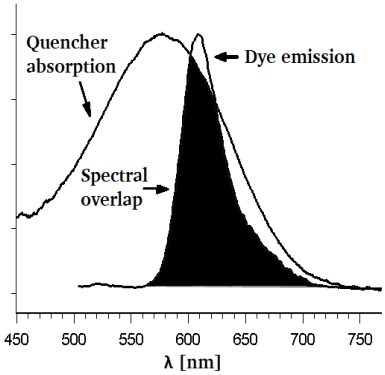

Figure 41: Donor emission and quencher absorption spectral overlap. Adapted figure by MkJohansson, distributed under the terms of the Attribution 3.0 Unported license (CC BY 3.0). https://creativecommons.org/licenses/by/3.0/

In case of Cys the problem of decreased fluorescence can be avoided by using different side chain protecting groups, Arg does not need side-chain protection at all. As proof-of-concept, the loading of a resin and the synthesis of a model peptide were monitored by fluorescence measurements.

3.12. Fluorescence monitoring of resin loading and coupling status during ASPPS

Monitoring of the reaction progress during SPPS requires the usage of additional markers and detection reactions or it is only possible after the Fmoc group has been cleaved off as only the formed dibenzofulvene product is spectrally active.[258-262] The Smoc protecting group allows for detection either by UV/Vis measurements using a photometer (this generally known method is therefore not explicitly discussed here) or by fluorescence monitoring. The fluorescence properties of the Smoc group allow the detection in solution or even if bound to the solid support, thus enabling a real-time monitoring of the coupling and deprotection process for the first time in the history of solid-phase peptide synthesis.

As a proof-of-concept study, Smoc-Gly-OH **12** in two different concentrations was loaded onto a water-compatible 2-CTC resin with DMSO as solvent. The choice of a solvent for this step was stipulated by the fact that the loading of this resin is hydrolysis-prone under aqueous conditions. The fluorescence was measured at the excitation maxima of 280 nm and emission maxima of 340 nm. The obtained data (shown in **Table 21**) clearly show a dependence between the amounts of coupled amino acid and fluorescence measured.

Table 21: Fluorescence intensity of different on-resin concentrations of Smoc-Gly-OH **12** measured on resin.

Experiment	DMSO	2-CTC resin	Smoc-Gly-resin 0.08mM loading	Smoc-Gly-resin 0.04mM loading
1	8	255	6493	2742
2	13	235	6363	3212
3	6	249	6923	3540
4	7	222	6240	3471
mean value	8.5	240.25	6504.75	3241.25
standard deviation	3.10	14.77	297.35	361.54

To show the real-time monitoring of fluorescence is possible during the ASPPS process, a model peptide with the sequence H-L-V-A-I-G-NH_2 **74** was synthesised on a Rink amide PEGA resin in

water. After each synthesis step, the fluorescence of the peptide-resin was measured. The results are shown in **Figure 42**.

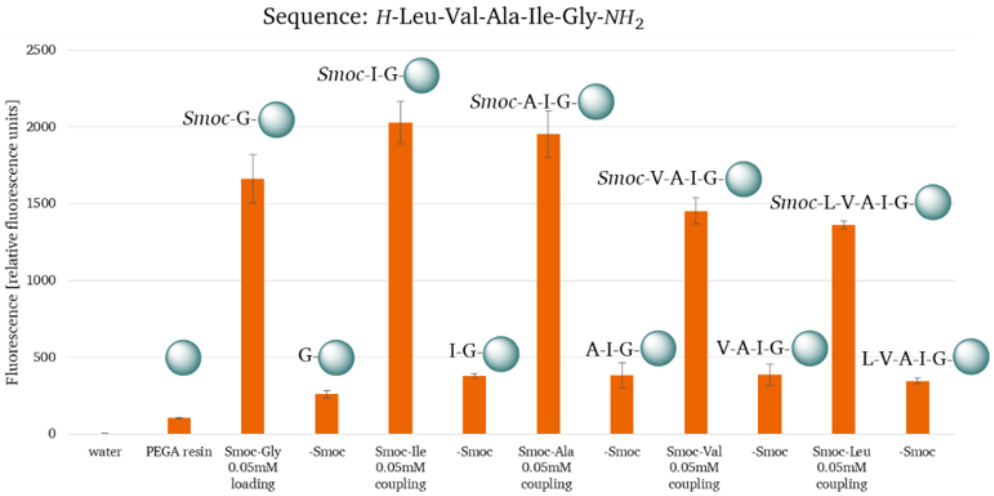

Figure 42: Synthesis of H-LVAIG-NH_2 **74** in water. Fluorescence was measured on solid support after each coupling and deprotection step.

The fluorescence measurement was performed by excitation at 280 nm and emission at 340 nm. The fluorescence allows distinguishing between the reaction steps. After Smoc deprotection, the fluorescence adjusts itself to a baseline value with a specific auto-fluorescence. After coupling of an N_α-Smoc amino acid, the fluorescence increases. The amino acids show intrinsically different fluorescence properties. This could be compensated by a normalisation that takes the quantum yield of each amino acid into account. The experiment shows that measuring the fluorescence on the solid phase to monitor the course of the reaction is basically possible. However, since it is easier to apply, fluorescence detection in solution of the coupling and deprotection mixture is more likely to be used.

Although the fluorescence measurements are possible, the absorption measurements with the Smoc group are probably the easiest way to monitor the reaction in real time.

3.13. Purification by affinity chromatography

Preparative RP-HPLC is currently the industrial state-of-the-art method for peptide purification allowing one to remove impurities in the crude product. Productivity, yield, and solvent consumption have to be considered for each purification process. Unfortunately, these three factors influence each other, as shown in **Figure 43**.[225] A general trend in peptide synthesis is to optimize the chemical synthesis (upstream process) and then accept up to 50% loss during the HPLC isolation (downstream) due to severe purification problems and in order to keep solvent consumption in acceptable ranges.[225]

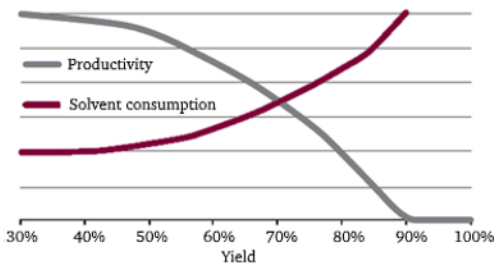

Figure 43: Productivity & solvent consumption of preparative HPLC depending on yield. (Modified picture by Ludemann-Hombourger[225]).

The purification system proposed by Merrifield and Bach and their 2-sulfo-Fmoc derivate[206] for product purification could of course be applied to the Smoc derivatives (**Scheme 21**).

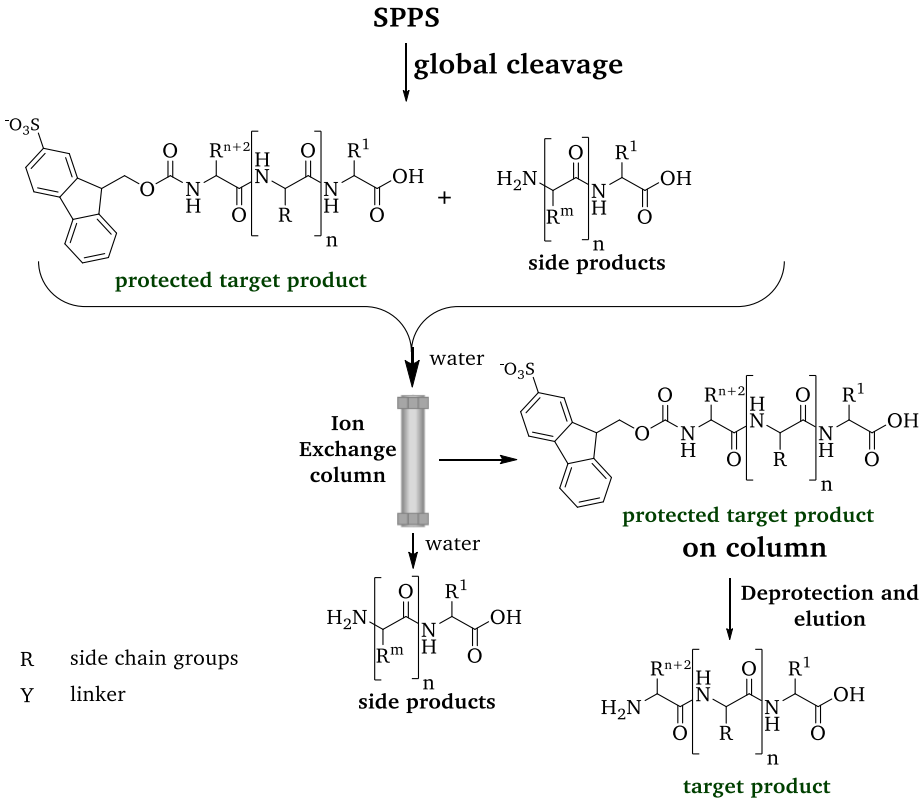

Scheme 21: Purification method by Merrifield and Bach.[206] After global cleavage, mixture is put on an ion-exchange column and the protected target peptide stays on the column. This is followed by an on-column deprotection of the respective 2-sulfo-Fmoc derivate and the elution of the target peptide in the deprotection cocktail.

However, this strategy is quite labor intensive as an additional deprotection step after the purification is necessary. As a consequence, we aimed at modifying the purification concept for the ASPPS strategy. In order to simplify the peptide isolation/purification process, we developed the capping strategy based on *Sulfo-tags*. This allows a large number of by-products to be removed using IEC. The advantages of the IEC method are high capacity, low time effort, application of water as solvent and easy automation. Moreover, compared to HPLC purification, the IEC is quite inexpensive.

The capping method is based on Sulfo-carboxylic compounds, e.g. 4-sulfobenzoic acid **75** or sulfoacetic acid **76**. Structures are shown in **Figure 44**. After each coupling step, capping with **75**, **76** or similar compounds is performed to label all free amine residues. After cleavage from solid support, the target peptide, all labelled side products and the cleaved side chain protecting groups are in solution. This mixture is subjected to IEC. Only the target peptide is able to pass, all labelled impurities stay on the column. The strategy is shown in **Scheme 22**

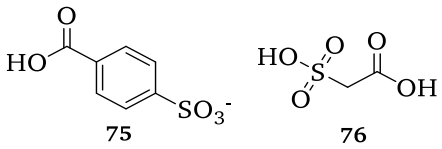

Figure 44: Structures of 4-sulfobenzoic acid **75** and sulfoacetic acid **76** as examples for capping reagents.

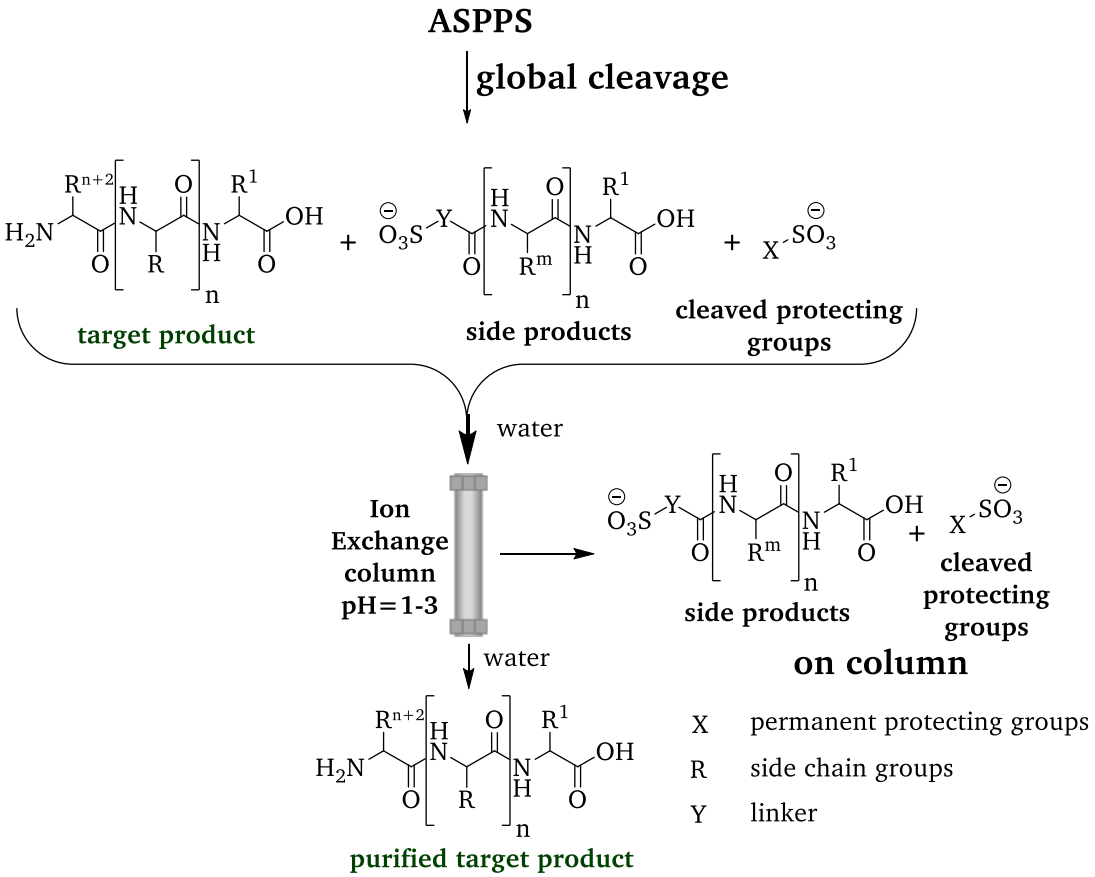

Scheme 22: Purification of peptide by IEC using the *Sulfo-tag* method.

As proof-of-concept, two peptides were synthesized applying amino acid building blocks in deficiency to increase side-product formation for purification tests. Hexapeptide-9 **49** has been synthesized in water with 0.95 eq. of N_α-Smoc amino acids, compared to prior coupling, in order to maximize by-product formation. Capping was performed with sulfoacetic acid **76** in water. After cleavage from solid support, an HPLC of the crude peptide was performed. Afterwards the pH of the solution was adjusted to pH=2 and the solution was transferred to a DEAE Sephadex A-25 ion-exchange column. After washing the column with additional water, a HPLC of the elution was performed. The results are shown in **Scheme 23**.

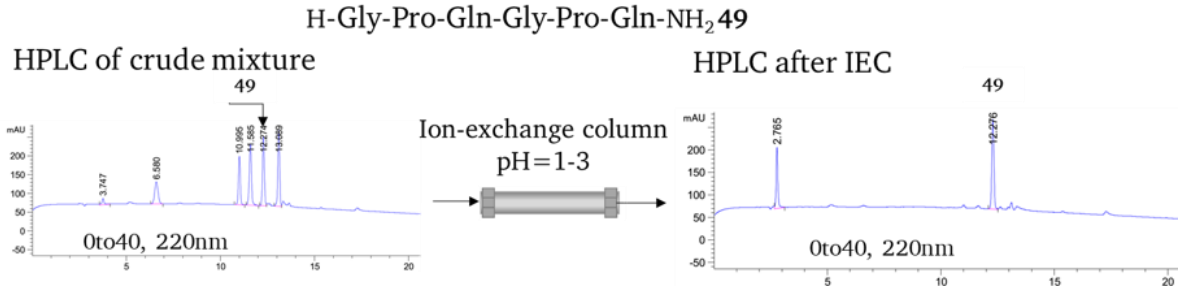

Scheme 23: Synthesis of H-GPQGPQ-OH hexapeptide 9 **49** in water using 0.95 eq. of an N_α-Smoc amino acid compared to prior coupling in order to maximize by-product formation; capping was performed with sulfoacetic acid **76**. HPLC chromatogram on the left shows crude peptide with labelled impurities after cleavage from solid support, HPLC chromatogram on the right shows purified product after IEC. HPLC traces were monitored at λ=220 nm with a gradient of 0 to 40% MeCN, see section 7.2.3 for details.

The second peptide was synthesized in a similar way. Adrenorphin **77** was synthesized in DMF with 0.95 eq. of an N_α-Fmoc-amino acid compared to prior coupling in order to maximize by-product formation. Capping was performed with a 4-sulfobenzoic acid **75** salt in DMF. After

cleavage from solid support, an HPLC of the crude peptide was performed. Afterwards the pH of the solution was adjusted to pH=1 and the solution was applied to a DEAE Sephadex A-25 ion-exchange column. After washing the column with additional water, a HPLC of the eluatewas performed. The results are shown in **Scheme 24**.

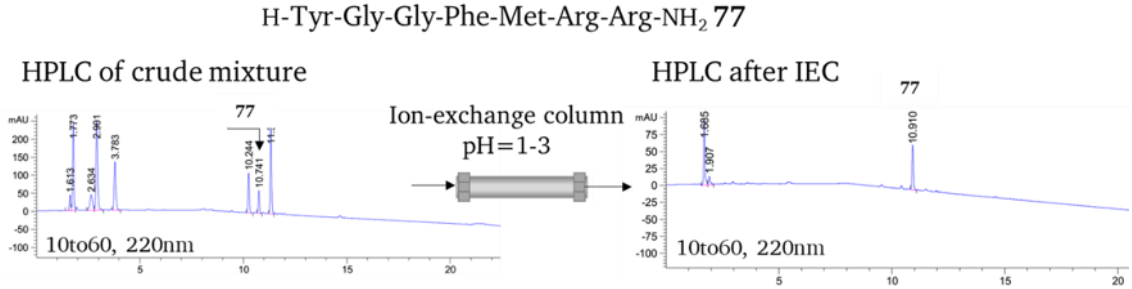

Scheme 24: Synthesis of H-YGGFMRRV-NH_2 **77** in DMF using 0.95 eq. of Fmoc-amino acid compared to prior coupling in order to maximize by-product formation, capping was performed with 4-sulfobenzoic acid **75**. HPLC chromatogram on the left shows crude peptide with labelled impurities after cleavage from solid support, HPLC chromatogram on the right shows purified product after IEC. HPLC traces were monitored at λ=220 nm with a gradient of 10 to 60% MeCN, see section 7.2.3 for details.

Both proof-of-concept experiments showed good results for the peptide purification process. Most of the side products were removed by IEC in around 1 minute. Interestingly, this method could be used for ASPPS as well as for classic DMF-based SPPS processes.

Purification by IEC could be used as only purification step if a certain level of purity is required. For pharmaceutical peptides, an additional HPLC step would be necessary of course, but as most of the side-products are removed prior to the HPLC purification, the separation should be more efficient and reduced amounts of organic solvents should be assumed. This method is also applicable as pre-purification system or as part of multicolumn chromatography (MCC) systems.

The same concept could be used in another way. As proof-of-concept an excess of Smoc-Gly-OH **12** was applied to a DEAE Sephadex A-25 ion-exchange column. After the ion-exchange chromatography, the HPLC chromatogram showed no detectable amounts of Smoc-Gly-OH **12** in the solution. After elution from the column, the excess of Smoc-Gly-OH **12** was detected in HPLC again. This could be used to remove all Sulfo-tagged impurities from the wastewater or for a possible regeneration of N_α-Smoc amino acids, used in excess, after coupling steps. Results are shown in **Scheme 25**.

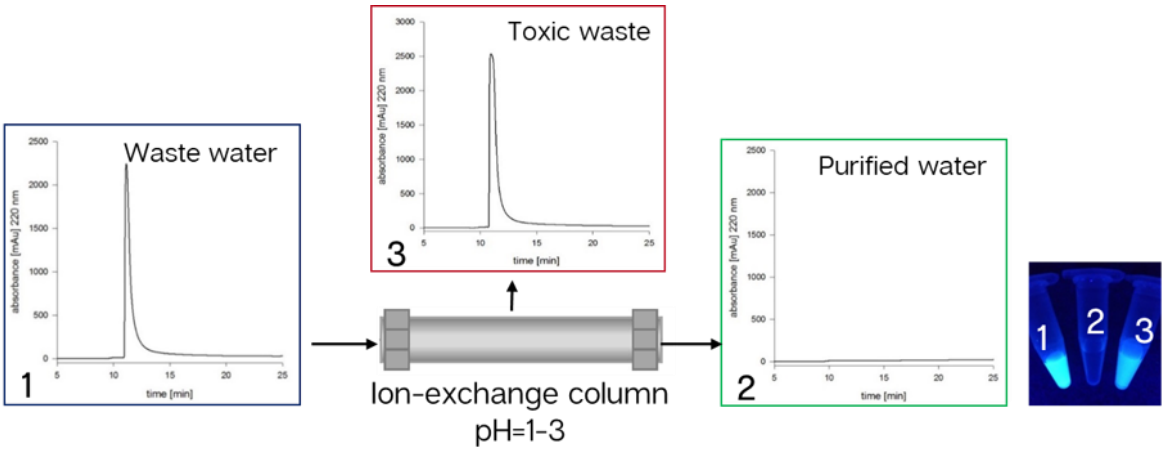

Scheme 25: Removal of N_α-Smoc amino acid excess from wastewater by IEC. 1 shows the analytical HPLC of the wastewater, 2 the HPLC after the IEC, 3 shows the elution from the IEC. The picture on the right shows the fluorescence of 1-3 upon UV-irradiation as additional analytical method. HPLC traces were monitored at λ=220 nm with a gradient of 0 to 40% MeCN, see section 7.2.3 for details.

3.14. NMR studies

All NMR spectra were measured on a Bruker DRX 500 MHz spectrometer equipped with a room temperature 5 mm ATMA BBFO probe (Bruker Biospin, Karlsruhe, Germany) at 303 K. All samples were dissolved in deuterated DMSO purchased from Sigma Aldrich (Merck KGaA, Darmstadt, Germany) or deuterated CH_3CN purchased from Eurisotop (Gif-Sur-Yvette, France). The concentrations of the samples were ~10^{-2}mol/l. The solvent signals were used for referencing the ^{1}H- and ^{13}C-NMR spectra at 2.5 ppm and 39.5 ppm respectively. Chemical shift assignment was achieved with ^{1}H-, ^{13}C- and ^{13}C-DEPT-135 1D spectra, 2D ^{1}H-^{1}H COSY (correlated spectroscopy), NOESY (nuclear overhauser enhancement spectroscopy), 2D ^{1}H-^{13}C HSQC (heteronuclear single quantum correlation) and 2D ^{1}H-^{13}C HMBC (heteronuclear multiple-bond correlation), using the Bruker pulse sequences zg30, zgpg30, dept135, cosygpmfqf, noesygptp, invietgpsi and inv4gplrl2ndqf, respectively. 1D spectra were recorded using an excitation pulse of 30° and a repetition time of 4.5 s (^{1}H) and 1.5 s (^{13}C). 32 scans (^{1}H) and 2.000 scans (^{13}C) were added and Fourier transformed with a final digital resolution of 0.08 Hz (1H, 0.26 Hz ^{13}C). The hetero-nuclear long-range correlation spectrum (HMBC) was recorded by a matrix of 1 k data points (f2, ^{1}H dimension) and 256 increments (data points in f1 ^{13}C dimension). The spectrum has been optimized for a heteronuclear coupling constant of 9 Hz. Raw data were processed with Topspin (Bruker Biospin, Karlsruhe, Germany) and 2D data were analyzed using MestReNova 11.0.3 (Mestrelab Research S.L., Spain). Assessment of NMR results is shown in **Table 22**-**Table 52**.

Table 22: Smoc-Cl **2** in MeCN-d_3 (^{1}H-NMR at 500 MHz, ^{13}C-NMR at 126 MHz).

Position	^{1}H	#H	Multi-plicity	Coupling constant	^{13}C	
1 and 8	8.18	2	s	-	124.48	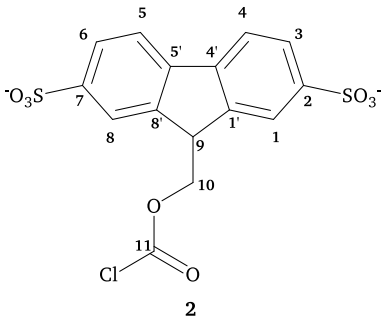
2 and 7	-	-	-	-	140.82	
3 and 6	8.0	2	d	8.1	128.13	
4 and 5	8.08	2	d	8.1	122.98	
4' and 5'	-	-	-	-	144.97	
1' and 8'	-	-	-	-	145.68	
9	4.55	1	t	5.7	47.8	
10	4.9	2	d	5.7	72.67	
11	-	-	-	-	151.05	

2

Table 23: Smoc-L-Ala-OH **3** in DMSO-d_6 (^{1}H-NMR at 500 MHz, ^{13}C-NMR at 126 MHz).

Position	^{1}H	#H	Multi-plicity	Coupling constant	^{13}C	
1 and 8	7.91; 7.89	2	s	-	121.97; 122.01	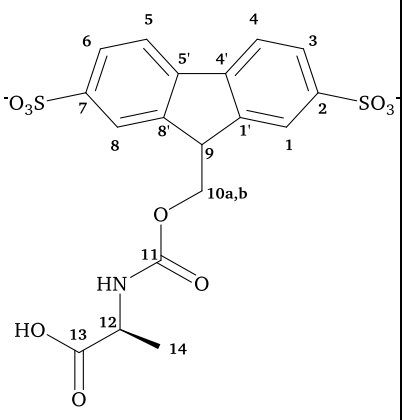
2 and 7	-	-	-	-	147.16	
3 and 6	7.68	2	d	7.9	125.31	
4 and 5	7.83	2	d	7.9	119.47	
4' and 5'	-	-	-	-	140.52	
1' and 8'	-	-	-	-	143.99; 144.17	
9	4.23	1	t	5.5	47.02	
10a	4.38	1	dd	10.9; 5.7	65.14	
10b	4.49	1	dd	10.9; 5.4		
11	-	-	-	-	155.93	
NH	7.52	1	br	-	-	
12	3.95	1	q	7.3	49.27	
13	-	-	-	-	174.27	
14	1.22	3	d	7.4	16.83	

3

Table 24: Smoc-D-Ala-OH **4** in DMSO-d_6 (^{1}H-NMR at 500 MHz, ^{13}C-NMR at 126 MHz).

Position	^{1}H	#H	Multi-plicity	Coupling constant	^{13}C	
1 and 8	7.89; 7.91	2	s	-	121.94	
2 and 7	-	-	-	-	147.19	
3 and 6	7.68	2	d	8.2	125.28	
4 and 5	7.83	2	d	7.9	119.43	
4' and 5'	-	-	-	-	140.49	
1' and 8'	-	-	-	-	143.97; 144.15	
9	4.23	1	t	5.5	47.01	
10a	4.37	1	dd	11.0; 5.7	65.11	
10b	4.38	1	dd	10.9; 5.5		
11	-	-	-	-	155.91	
NH	7.5	1	br	-	-	
12	3.95	1	q	7.3	49.26	
13	-	-	-	-	174.22	
14	1.22	3	d	7.4	16.82	

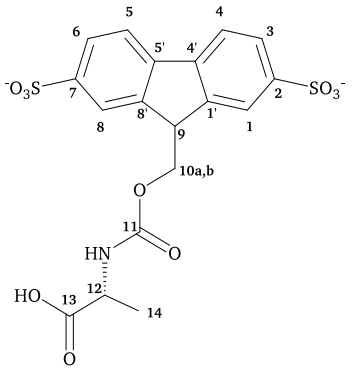

4

Table 25: Smoc-L-Arg-OH **5** in DMSO-d_6 (^{1}H-NMR at 500 MHz, ^{13}C-NMR at 126 MHz).

Position	^{1}H	#H	Multi-plicity	Coupling constant	^{13}C	
1 and 8	7.88; 7.93	2	s	-	122.01	
2 and 7	-	-	-	-	146.76	
3 and 6	7.7	2	d	7.7	125.3	
4 and 5	7.85; 7.86	2	d	7.9	119.6	
4' and 5'	-	-	-	-	140.61	
1' and 8'	-	-	-	-	143.51; 144.50	
9	4.32	1	t	5.5	46.91	
10a	4.33	1	dd	10.0; 6.3	64.85	
10b	4.54	1	dd	10.0; 6.3		
11	-	-	-	-	155.93	
NH	7.52	1	d	8.5	-	
12	3.96	1	dt	9.2; 4.3	52.91	
13	-	-	-	-	173.3	
14	1.56; 1.72	2	m	-	27.87	
15	1.47	2	m	-	24.93	
16a	3.02	1	dq	13.0; 6.5	40.0	
16b	3.1	1	dq	13.0; 6.5		
NH	7.74	1	t	5.6	-	
17	-	-	-	-	156.63	

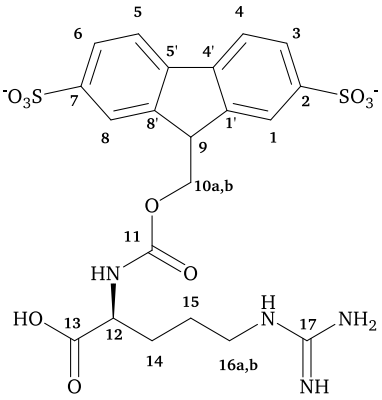

5

Table 26: Smoc-L-Arg(Pbf)-OH **6** in DMSO-d_6 (^{1}H-NMR at 500 MHz, ^{13}C-NMR at 126 MHz).

Position	^{1}H	#H	Multi-plicity	Coupling constant	^{13}C	
1 and 8	7.88; 7.91	2	d	1.4	122.03	
2 and 7	-	-	-	-	146.91	
3 and 6	7.68	2	dd	7.8; 1.4	125.28	
4 and 5	7.84	2	d	7.9	119.54	
4' and 5'	-	-	-	-	140.55	
1' and 8'	-	-	-	-	143.58; 144.39	
9	4.3	1	t	5.5	46.92	
10a	4.32	1	m	-	64.98	
10b	4.51	1	m	-		
11	-	-	-	-	155.96	
NH	7.52	1	br	-	-	
12	3.9	1	dt	9.1; 4.7	53.17	
13	-	-	-	-	173.35	
14	1.50; 1.63	2	m	-	27.8	
15	1.37	2	m	-	25.1	
16	3.07	2	q	7.3	39.71	
NH	7.74	1	t	5.6	-	
17	-	-	-	-	166.74	
18	-	-	-	-	133.9	
19	-	-	-	-	131.42	
20	-	-	-	-	124.33	
21	-	-	-	-	157.57	
22	-	-	-	-	116.34	
23	-	-	-	-	137.32	
24	2.97	2	s	-	42.35	
25	-	-	-	-	86.32	
26	1.41	6	s	-	28.25	
27	2.43	3	s	-	18.91	
28	2.48	3	s	-	17.51	
29	2.01	3	s	-	12.22	

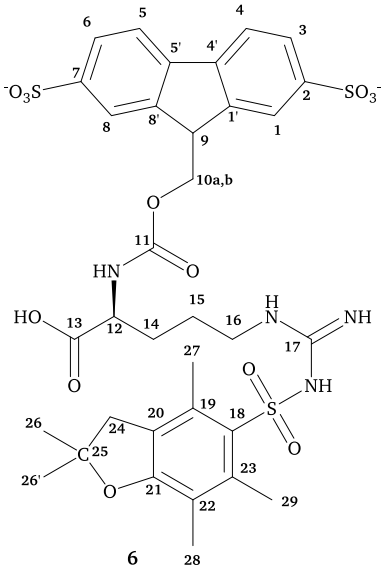

Table 27: Smoc-L-Asn-OH **7** in DMSO-d_6 (^{1}H-NMR at 500 MHz, ^{13}C-NMR at 126 MHz).

Position	^{1}H	#H	Multi-plicity	Coupling constant	^{13}C	
1 and 8	7.90; 7.91	2	s	-	122.11	
2 and 7	-	-	-	-	146.99	
3 and 6	7.69	2	d	7.5	125.37	
4 and 5	7.84	2	d	7.9	119.57	
4' and 5'	-	-	-	-	140.59	
1' and 8'	-	-	-	-	144.03; 144.14	
9	4.26	1	t	-	46.06	
10	4.42	2	m	-	65.25	
11	-	-	-	-	155.83	
NH	7.4	1	d	8.2	-	
12	4.27	1	m	-	50.71	
13	-	-	-	-	172.83	
14	2.43	1	dd	15.2; 7.5	36.78	
14b	2.54	1	dd	15.2; 5.8		
15	-	-	-	-	171.56	
NH_2	5.6	2	br	-	-	

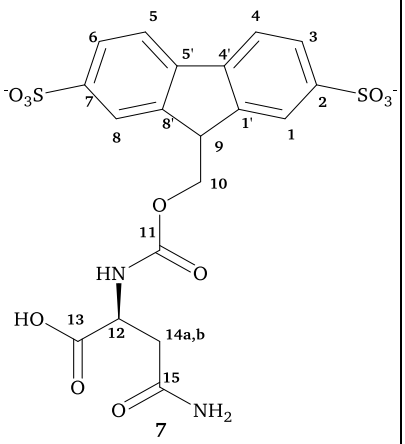

Table 28: Smoc-L-Asp(OtBu)-OH **8** in DMSO-d_6 (^{1}H-NMR at 500 MHz, ^{13}C-NMR at 126 MHz).

Position	^{1}H	#H	Multi-plicity	Coupling constant	^{13}C	
1 and 8	7.89; 7.94	2	s	-	122.31; 122.45	
2 and 7	-	-	-	-	147.26	
3 and 6	7.69	2	d	7.7	125.25	
4 and 5	7.83	2	d	7.9	119.35	
4' and 5'	-	-	-	-	140.31	
1' and 8'	-	-	-	-	143.78; 144.15	
9	4.23	1	m	-	46.62	
10	4.22	2	m	-	65.47	
11	-	-	-	-	155.36	
NH	6.8	1	d	7.5	-	
12	3.97	1	dt	7.5; 5.3	52.92	
13	-	-	-	-	170.72	
14	2.4	1	dd	14.7; 7.8	39.54	
14b	2.59	1	dd	14.7; 5.4		
15	-	-	-	-	172.58	
16	-	-	-	-	79.1	
17	1.38	9	s	-	27.78	

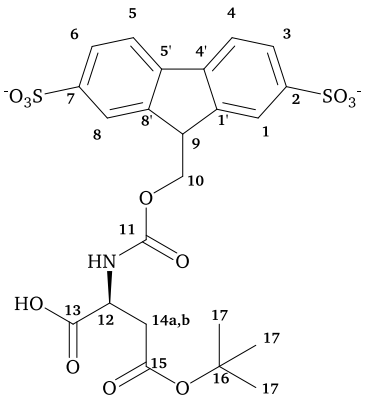

8

Table 29: Smoc-L-Cys(Trt)-OH **9** in DMSO-d_6 (^{1}H-NMR at 500 MHz, ^{13}C-NMR at 126 MHz).

Position	^{1}H	#H	Multi-plicity	Coupling constant	^{13}C	
1 and 8	7.90; 7.91	2	s	-	122.0	
2 and 7	-	-	-	-	147.4	
3 and 6	7.68	2	d	7.9	125.3	
4 and 5	7.82	2	d	7.8	119.35	
4' and 5'	-	-	-	-	140.36	
1' and 8'	-	-	-	-	143.97	
9	4.2	1	t	5.6	47.0	
10a	4.37	1	dd	11.1; 5.8	65.57	
10b	4.41	1	dd	11.5; 6.5		
11	-	-	-	-	155.94	
NH	6.6	1	d	8.4		
12	3.77	1	m	-	53.58	
13	-	-	-	-	171.63	
14	2.38	1	dd	12.4; 5.0	32.52	
14b	2.56	1	dd	12.6; 9.4		
15	-	-	-	-	66.28	
16	-	-	-	-	144.21	
17	7.3	6	m	-	129.0	
18	7.3	6	m	-	128.0	
19	7.24	3	t	6.9	126.67	

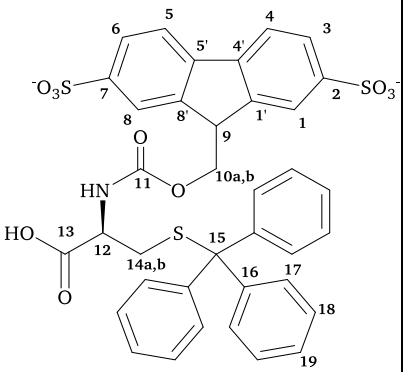

9

Table 30: Smoc-L-Gln-OH **10** in DMSO-d_6 (^{1}H NMR at 500 MHz, ^{13}C-NMR at 126 MHz).

Position	^{1}H	#H	Multi-plicity	Coupling constant	^{13}C	
1 and 8	7.90; 7.93	2	s	-	122.15	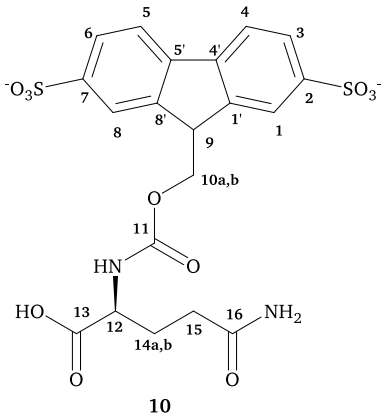
2 and 7	-	-	-	-	147.12	
3 and 6	7.69	2	d	7.8	125.32	
4 and 5	7.84	2	d	7.8	119.48	
4' and 5'	-	-	-	-	140.45; 140.50	
1' and 8'	-	-	-	-	143.67; 144.32	
9	4.27	1	t	6	46.86	
10a	4.32	1	dd	10.7; 5.7	65.18	
10b	4.45	1	dd	10.7; 6.8		
11	-	-	-	-	156.12	
NH	7.54	1	d	7.7	-	
12	3.88	1	dt	10.4; 5.0	53.47	
13	-	-	-	-	173.68	
14a	1.68	1	m	-	26.16	
14b	1.99	1	m	-		
15	2.16	2	ddd	9.5; 6.8; 3.2	31.23	
16	-	-	-	-	173.58	

10

Table 31: Smoc-L-Glu(OtBu)-OH **11** in DMSO-d_6 (^{1}H-NMR at 500 MHz, ^{13}C-NMR at 126 MHz).

Position	^{1}H	#H	Multi-plicity	Coupling constant	^{13}C	
1 and 8	7.89; 7.94	2	s	-	122.3	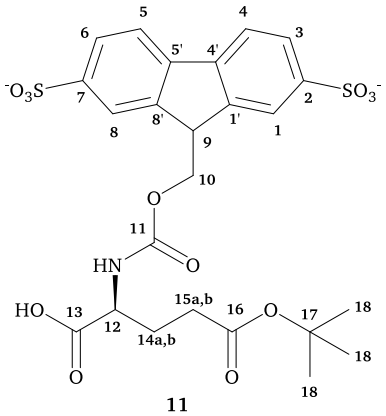
2 and 7	-	-	-	-	147.2	
3 and 6	7.69	2	d	8.0	125.0	
4 and 5	7.83	2	d	8.0	119.3	
4' and 5'	-	-	-	-	140.31	
1' and 8'	-	-	-	-	143.95	
9	4.23	1	m	-	46.2	
10	4.23	2	m	-	65.2	
11	-	-	-	-	155.5	
NH	6.63	1	d	6.7	-	
12	3.65	1	q	6.0	54.8	
13	-	-	-	-	172.4	
14	1.78	1	tt	12.1; 5.6	27.96	
14b	1.9	1	tt	10.7; 5.2		
15a	2.12	1	ddd	16.0; 10.8; 5.3	30.73	
15b	2.23	1	ddd	16.1; 10.9; 5.5		
16	-	-	-	-	173.5	
17	-	-	-	-	79.13	
18	1.38	9	s	-	27.73	

11

Table 32: Smoc-Gly-OH **12** in DMSO-d_6 (^{1}H-NMR at 500 MHz, ^{13}C-NMR at 126 MHz).

Position	^{1}H	#H	Multi-plicity	Coupling constant	^{13}C	
1 and 8	7.91	2	s	-	122.05	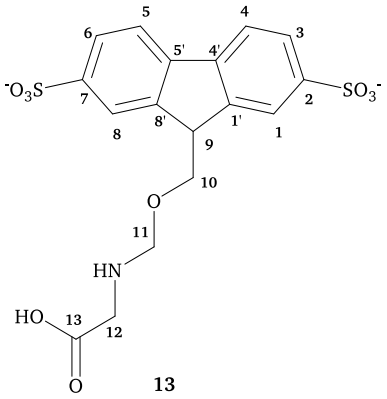
2 and 7	-	-	-	-	147.04	
3 and 6	7.69	2	d	7.9	125.36	
4 and 5	7.85	2	d	7.9	119.56	
4' and 5'	-	-	-	-	140.59	
1' and 8'	-	-	-	-	144.11	
9	4.25	1	t	5.7	46.97	
10	4.43	2	d	5.8	65.37	
11	-	-	-	-	156.52	
NH	7.49	1	br	-	-	
12	3.61	2	s	-	42.15	
13	-	-	-	-	171.39	

Table 33: Smoc-L-His-OH **13** in DMSO-d_6 (^{1}H-NMR at 500 MHz, ^{13}C-NMR at 126 MHz).

Position	^{1}H	#H	Multi-plicity	Coupling constant	^{13}C	
1 and 8	7.84; 7.92	2	s	-	121.9; 122.0	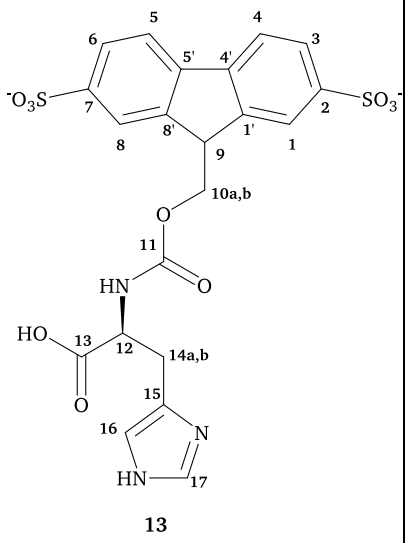
2 and 7	-	-	-	-	146.86	
3 and 6	7.71	2	d	7.9	125.36	
4 and 5	7.85	2	d	7.9	119.65	
4' and 5'	-	-	-	-	140.57; 140.66	
1' and 8'	-	-	-	-	143.60; 144.34	
9	4.23	1	m	-	46.69	
10a	4.33	1	dd	10.8; 5.3	65.12	
10b	4.41	1	dd	10.8; 6.8		
11	-	-	-	-	155.78	
NH	7.66	1	d	8.8	-	
12	4.23	1	m	-	52.73	
13	-	-	-	-	171.97	
14	2.94	1	dd	15.0; 7.9	26.03	
14b	3.13	1	dd	15.0; 4.4		
15	-	-	-	-	129.28	
16	7.27	1	s	-	117.38	
17	8.92	1	s	-	133.71	

Table 34: Smoc-L-His(Trt)-OH **14** in DMSO-d_6 (^{1}H-NMR at 500 MHz, ^{13}C-NMR at 126 MHz).

Position	^{1}H	#H	Multi-plicity	Coupling constant	^{13}C	
1 and 8	7.89; 7.99	2	s	-	122.3	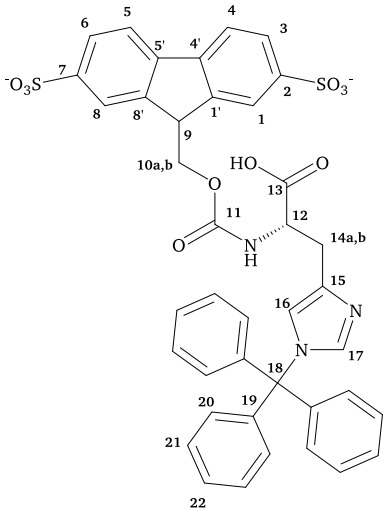
2 and 7	-	-	-	-	147.65	
3 and 6	7.69	2	d	7.7	125.6	
4 and 5	7.84	2	d	7.7	119.1	
4' and 5'	-	-	-	-	140.8	
1' and 8'	-	-	-	-	143.76; 144.0	
9	4.19	1	t	6.3	46.9	
10a	3.94	1	m	-	65.23	
10b	4.13	1	m	-		
11	-	-	-	-	156.0	
NH	6.97	1	br	-	-	
12	3.96	1	m	-	55.81	
13	-	-	-	-	171.29	
14	2.65	1	dd	14.9; 8.6	31.95	
14b	2.99	1	dd	14.8; 4.6		
15	-	-	-	-	138.3	
16	?*	-	-	-	118.8	
17	7.22	-	br	-	137.5	
18	-	-	-	-	74.38	
19	-	-	-	-	142.4	
20	7.06	6	m	-	128.9	
21	7.37	6	m	-	128.5	
22	7.06	3	m	-	127.5	

14

*: Signals have not been detected under the used conditions

Table 35: Smoc-L-Ile-OH **15** in DMSO-d_6 (^{1}H-NMR at 500 MHz, ^{13}C-NMR at 126 MHz).

Position	^{1}H	#H	Multi-plicity	Coupling constant	^{13}C	
1 and 8	7.92	2	s	-	122.09	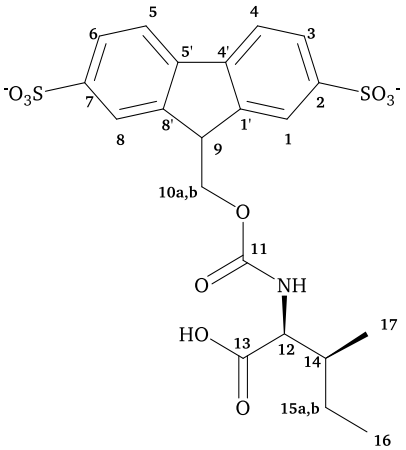
2 and 7	-	-	-	-	147.15; 147.17	
3 and 6	7.68	2	dd	7.9; 1.2	125.31	
4 and 5	7.83	2	d	7.9	119.44	
4' and 5'	-	-	-	-	140.48	
1' and 8'	-	-	-	-	144.03; 144.16	
9	4.23	1	t	5.8	47.11	
10a	4.37	1	dd	10.9; 5.7	65.46	
10b	4.86	1	dd	10.9; 5.9		
11	-	-	-	-	156.44	
NH	7.46	1	d	8.1	-	
12	3.87	1	t	6.5	58.68	
13	-	-	-	-	173.06	
14	1.75	1	m	-	35.72	
15a	1.17	1	ddq	13.6; 8.9; 7.3	24.88	
15b	1.39	1	ddq	13.6; 7.4; 4.5		
16	0.81	3	t	7.4	11.22	
17	0.84	3	d	6.9	15.48	

15

Table 36: Smoc-L-Leu-OH **16** in DMSO-d_6 (^{1}H-NMR at 500 MHz, ^{13}C-NMR at 126 MHz).

Position	^{1}H	#H	Multi-plicity	Coupling constant	^{13}C	
1 and 8	7.90; 7.91	2	s	-	122.0	
2 and 7	-	-	-	-	147.29	
3 and 6	7.68	2	d	8	125.27	
4 and 5	7.83	2	d	8	119.37	
4' and 5'	-	-	-	-	140.42	
1' and 8'	-	-	-	-	144.01; 144.09	
9	4.22	1	t	5.6	47.06	
10a	4.38	1	dd	11.0; 5.6	65.35	
10b	4.46	1	dd	11.0; 5.6		
11	-	-	-	-	156.29	
NH	7.51	1	d	7.9	-	
12	3.93	1	dt	10.7; 5.4	52.28	
13	-	-	-	-	174.17	
14a	1.53	1	ddd	13.4; 10.2; 5.1	39.5	
14b	1.41	1	ddd	13.5; 9.0; 4.9		
15	1.61	1	m	-	24.17	
16	0.83	3	d	6.5	21.28	
17	0.85	3	d	6.6	22.78	

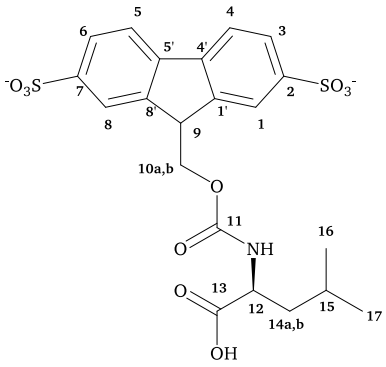

16

Table 37: Smoc-D-Leu-OH **17** in DMSO-d_6 (^{1}H-NMR at 500 MHz, ^{13}C-NMR at 126 MHz).

Position	^{1}H	#H	Multi-plicity	Coupling constant	^{13}C	
1 and 8	7.92; 7.93	2	s	-	122.07	
2 and 7	-	-	-	-	146.96; 146.99	
3 and 6	7.69	2	dd	8; 1.5	125.36	
4 and 5	7.85	2	d	8.0	119.56	
4' and 5'	-	-	-	-	140.61	
1' and 8'	-	-	-	-	144.14; 144.23	
9	4.23	1	t	5.6	47.12	
10a	4.39	1	dd	11.0; 5.6	65.35	
10b	4.47	1	dd	11.0; 5.7		
11	-	-	-	-	156.33	
NH	7.51	1	br	-	-	
12	3.92	1	dd	9.7; 4.8	52.32	
13	-	-	-	-	174.23	
14a	1.52	1	ddd	13.7; 10.1; 5.1	39.56	
14b	1.41	1	ddd	13.7; 9.0; 4.9		
15	1.61	1	m	-	24.23	
16	0.82	3	d	6.6	21.33	
17	0.85	3	d	6.6	22.83	

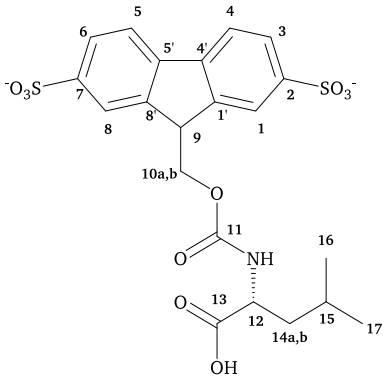

17

Table 38: Smoc-L-Lys(Boc)-OH **18** in DMSO-d_6 (^{1}H-NMR at 500 MHz, ^{13}C-NMR at 126 MHz).

Position	^{1}H	#H	Multi-plicity	Coupling constant	^{13}C	
1 and 8	7.88; 7.93	2	s	-	122.26; 122.38	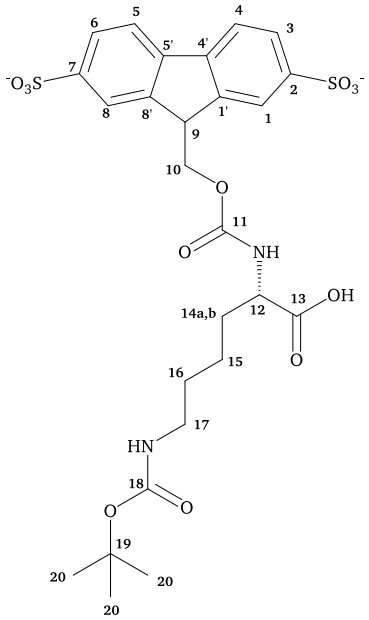
2 and 7	-	-	-	-	147.24; 147.31	
3 and 6	7.68	2	dd	7.9; 1.4	125.22	
4 and 5	7.82	2	d	7.9	119.33	
4' and 5'	-	-	-	-	140.3	
1' and 8'	-	-	-	-	143.92; 144.08	
9	4.24	1	t	-	46.75	
10	4.23	2	m	-	65.3	
11	-		-	-	155.45	
NH	6.56	1	br	-	-	
12	3.61	1	q	6.1	55.58	
13	-	-	-	-	173.58	
14a	1.54	1	m	-	32.44	
14b	1.64	1	dq	10.3; 5.4		
15	1.22	2	m	-	22.53	
16	1.33	2	m	-	29.6	
17	2.86	2	dt	7.4; 6.9	40.03	
NH	6.69	1	br	-	-	
18	-	-	-	-	155.24	
19	-	-	-	-	77.14	
20	1.33	9	s	-	28.24	

18

Table 39: Smoc-L-Met-OH **19** in DMSO-d_6 (^{1}H-NMR at 500 MHz, ^{13}C-NMR at 126 MHz).

Position	^{1}H	#H	Multi-plicity	Coupling constant	^{13}C	
1 and 8	7.91; 7.92	2	s	-	122.1	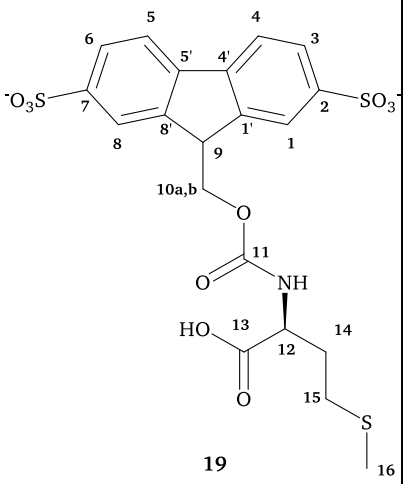
2 and 7	-	-	-	-	147.08	
3 and 6	7.69	2	dd	7.9; 1.2	125.36	
4 and 5	7.84	2	d	7.9	119.53	
4' and 5'	-	-	-	-	140.56	
1' and 8'	-	-	-	-	144.02; 144.18	
9	4.24	1	t	5.7	47.06	
10a	4.38	1	dd	10.9; 5.6	65.33	
10b	4.47	1	dd	10.9; 5.9		
11	-	-	-	-	156.33	
NH	7.6	1	d	7.6	-	
12	4.03	1	dt	7.7; 5.6	52.93	
13	-	-	-	-	173.5	
14	1.87	2	m	-	30.31	
15	2.47	2	m	-	29.83	
16	2.01	3	s	-	14.53	

19

Table 40: Smoc-L-Phe-OH **20** in DMSO-d_6 (^{1}H-NMR at 500 MHz, ^{13}C-NMR at 126 MHz).

Position	^{1}H	#H	Multi-plicity	Coupling constant	^{13}C	
1 and 8	7.9	2	s	-	122.02; 122.08	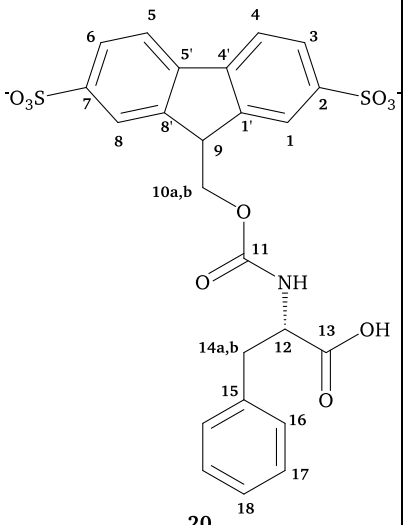
2 and 7	-	-	-	-	147.2	
3 and 6	7.69	2	dd	7.9; 1.2	125.31	
4 and 5	7.83	2	d	7.9	119.43	
4' and 5'	-	-	-	-	140.44	
1' and 8'	-	-	-	-	143.99; 144.05	
9	4.16	1	t	5.5	47.05	
10a	4.33	1	dd	11.0; 5.8	65.37	
10b	4.38	1	dd	11.0; 5.7		
11	-	-	-	-	156.05	
NH	7.61	1	d	8.1	-	
12	4.12	1	m	-	55.65	
13	-	-	-	-	173.02	
14a	2.88	1	dd	13.8; 9.5	36.43	
14b	2.99	1	dd	13.8; 5.3		
15	-	-	-	-	137.81	
16	7.22	2	d	7.4	129.06	
17	7.26	2	t	7.5	128.19	
18	7.15	1	t	7.2	126.22	

Table 41: Smoc-L-Pro-OH **21** in DMSO-d_6 (^{1}H-NMR at 500 MHz, ^{13}C-NMR at 126 MHz).

Position	^{1}H	#H	Multi-plicity	Coupling constant	^{13}C	
1 and 8	7.91; 7.92	2	d	1.4	122.42	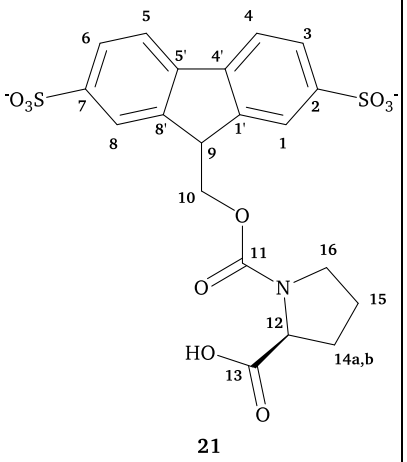
2 and 7	-	-	-	-	147.17	
3 and 6	7.68	2	dd	7.9; 1.4	125.3	
4 and 5	7.84	2	d	7.9	119.49	
4' and 5'	-	-	-	-	140.43	
1' and 8'	-	-	-	-	143.66; 143.90	
9	4.29	1	t	5.6	46.47	
10	4.2-4.3	2	m	-	66.28	
11	-	-	-	-	153.84	
12	4.17	1	dd	8.6; 3.2	58.85	
13	-	-	-	-	173.5	
14a	1.85	1	m	-	29.34	
14b	2.21	1	m	-		
15	1.85	2	m	-	23.9	
16	3.41	2	m	-	46.01	

Table 42: Smoc-L-Ser-OH **22** in DMSO-d_6 (^{1}H-NMR at 500 MHz, ^{13}C-NMR at 126 MHz).

Position	^{1}H	#H	Multi-plicity	Coupling constant	^{13}C	
1 and 8	7.90; 7.92	2	s	-	122.0; 122.07	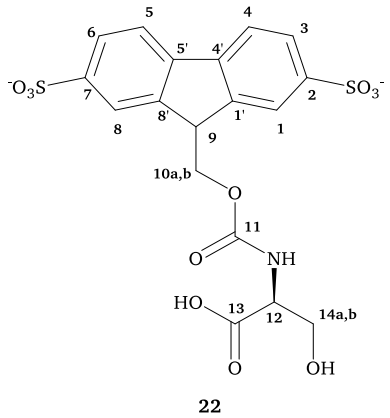
2 and 7	-	-	-	-	147.1	
3 and 6	7.69	2	dd	7.9; 1.5	125.32	
4 and 5	7.84	2	d	7.9	119.53	
4' and 5'	-	-	-	-	140.54	
1' and 8'	-	-	-	-	143.92; 144.20	
9	4.25	1	t	5.7	46.96	
10a	4.41	1	dd	11.0; 5.6	65.29	
10b	4.47	1	dd	11.0; 6.0		
11	-	-	-	-	156.01	
NH	7.14	1	br	-	-	
12	4.0	1	t	5.2	56.72	
13	-	-	-	-	171.94	
14a	3.62	1	dd	11.3; 5.3	61.27	
14b	3.65	1	dd	11.3; 4.2		
OH	4.01	1	br	-	-	

22

Table 43: Smoc-L-Ser(tBu)-OH **23** in DMSO-d_6 (^{1}H-NMR at 500 MHz, ^{13}C-NMR at 126 MHz).

Position	^{1}H	#H	Multi-plicity	Coupling constant	^{13}C	
1 and 8	7.92	2	s	-	122.08	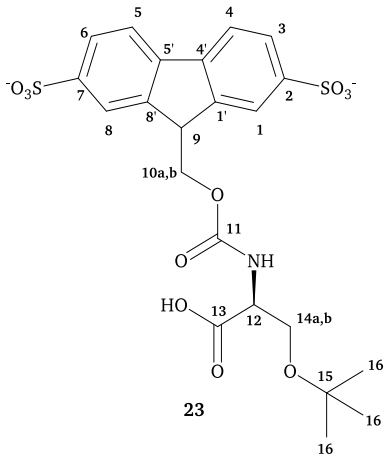
2 and 7	-	-	-	-	147.43	
3 and 6	7.69	2	d	7.9	125.29	
4 and 5	7.82	2	d	7.9	119.32	
4' and 5'	-	-	-	-	140.33	
1' and 8'	-	-	-	-	143.87; 144.94	
9	4.23	1	t	5.9	46.94	
10a	4.37	1	dd	10.9; 5.9	65.6	
10b	4.42	1	dd	10.9; 6.0		
11	-	-	-	-	156.01	
NH	7.17	1	d	8.1	-	
12	4.08	1	dt	8.0; 5.2	54.9	
13	-	-	-	-	171.79	
14a	3.54	1	dd	9.5; 4.9	61.23	
14b	3.57	1	dd	9.5; 5.5		
15	-	-	-	-	72.78	
16	1.1	9	s	-	27.14	

23

Table 44: Smoc-L-Thr-OH **24** in DMSO-d_6 (^{1}H-NMR at 500 MHz, ^{13}C-NMR at 126 MHz).

Position	^{1}H	#H	Multi-plicity	Coupling constant	^{13}C	
1 and 8	7.91; 7.92	2	s	-	122.07	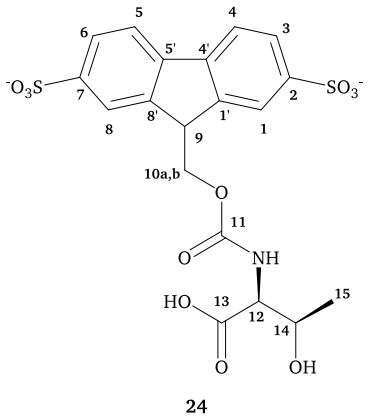
2 and 7	-	-	-	-	147.22	
3 and 6	7.69	2	d	7.9	125.3	
4 and 5	7.83	2	d	7.9	119.43	
4' and 5'	-	-	-	-	140.44	
1' and 8'	-	-	-	-	143.86; 144.07	
9	4.25	1	t	6.0	46.95	
10a	4.39	1	dd	10.9; 5.7	65.52	
10b	4.46	1	dd	10.9; 6.1		
11	-	-	-	-	156.38	
NH	6.83	1	d	8.7	-	
12	3.92	1	dd	8.1. 3;8	60.18	
13	-	-	-	-	172.09	
14	4.02	1	dq	6.5; 3.7	66.44	
15	1.07	3	d	6.5	20.32	

24

Table 45: Smoc-L-Thr(tBu)-OH **25** in DMSO-d_6 (^{1}H-NMR at 500 MHz, ^{13}C-NMR at 126 MHz).

Position	^{1}H	#H	Multi-plicity	Coupling constant	^{13}C	
1 and 8	7.90. 7.96	2	s	-	122.6. 122.7	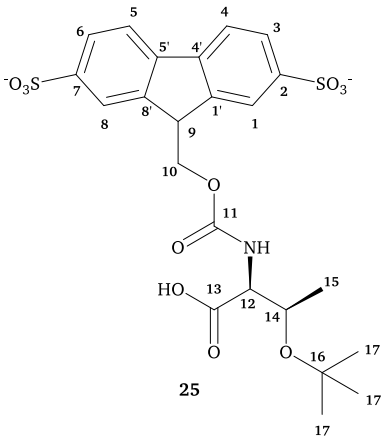
2 and 7	-	-	-	-	147.19	
3 and 6	7.69	2	dd	7.9; 15	125.55	
4 and 5	7.83	2	d	7.9	119.56	
4' and 5'	-	-	-	-	140.28	
1' and 8'	-	-	-	-	143.95	
9	4.23	1	m	-	46.54	
10	4.23	2	m	-	65.58	
11	-	-	-	-	156.1	
NH	6.18	1	d	8.7	-	
12	3.59	1	dd	8.7; 3.3	61.82	
13	-	-	-	-	173	
14	3.96	1	dq	6.2; 3.4	68.37	
15	1.05	3	d	6.2	21.08	
16	-	-	-	-	72.43	
17	1.1	9	s	-	28.56	

25

Table 46: Smoc-L-Trp-OH **26** in DMSO-d_6 (^{1}H-NMR at 500 MHz, ^{13}C-NMR at 126 MHz).

Position	^{1}H	#H	Multi-plicity	Coupling constant	^{13}C	
1 and 8	7.90; 7.93	2	s	-	122.02	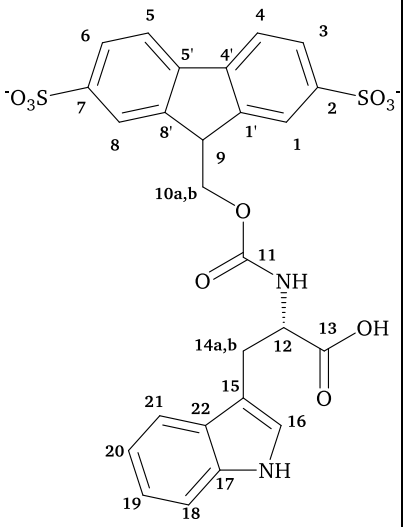
2 and 7	-	-	-	-	147.00; 147.07	
3 and 6	7.69; 7.70	2	dd	7.9. 1.5	125.32; 125.35	
4 and 5	7.82; 7.83	2	d	7.9	119.54	
4' and 5'	-	-	-	-	140.54; 140.57	
1' and 8'	-	-	-	-	143.96; 144.25	
9	4.21	1	t	5.8	46.9	
10a	4.29	1	dd	10.8; 5.5	65.28	
10b	4.4	1	dd	10.8; 6.1		
11	-	-	-	-	155.96	
NH	7.53	1	d	8.2	-	
12	4.12	1	dt	9; 4.5	45.18	
13	-	-	-	-	173.47	
14a	2.95	1	dd	14.6; 9.9	26.53	
14b	3.16	1	dd	14.6; 4.5		
15	-	-	-	-	109.67	
16	7.14	1	s	-	124.31	
NH	10.87	1	s	-	-	
17	-	-	-	-	135.84	
18	7.29	1	d	7.5	111.33	
19	7.03	1	t	7.5	120.64	
20	6.96	1	t	7.4	118.18	
21	7.48	1	d	7.8	117.81	
22	-	-	-	-	127.04	

26

Table 47: Smoc-L-Trp(Boc)-OH **27** in DMSO-d_6 (^{1}H-NMR at 500 MHz, ^{13}C-NMR at 126 MHz).

Position	^{1}H	#H	Multi-plicity	Coupling constant	^{13}C	
1 and 8	7.87; 7.94	2	s	-	122.3; 122.5	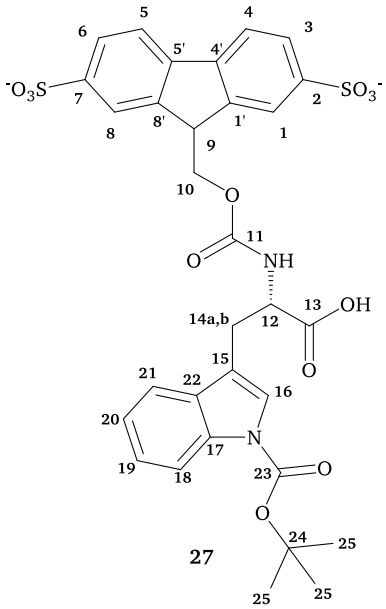
2 and 7	-	-	-	-	147.77	
3 and 6	7.69	2	d	7.9	125.2	
4 and 5	7.82	2	d	7.9	119.3	
4' and 5'	-	-	-	-	?*	
1' and 8'	-	-	-	-	?*	
9	4.18	1	m	-	46.27	
10	4.18	2	m	-	65.18	
11	-	-	-	-	?*	
NH	6.72	1	d	6.8	-	
12	3.93	1	q	6.1	55.19	
13	-	-	-	-	173.45	
14a	2.97	1	dd	14.6; 6.3	27.4	
14b	3.16	1	dd	14.6; 5.4		
15	-	-	-	-	?*	
16	7.43	1	s	-	?*	
17	-	-	-	-	?*	
18	8.0	1	d	8.2	114.3	
19	7.26	1	t	7.7	123.9	
20	7.21	1	t	7.4	122.2	
21	7.64	1	d	7.7	119.3	
22	-	-	-	-	?*	

27

23	-	-	-	-	?*	
24	-	-	-	-	83.24	
25	1.61	9	s	-	27.69	

*: Signals have not been detected under the used conditions or assignment was not possible.

Table 48: Smoc-L-Tyr-OH **28** in DMSO-d_6 (^{1}H-NMR at 500 MHz, ^{13}C-NMR at 126 MHz).

Position	^{1}H	#H	Multi-plicity	Coupling constant	^{13}C	
1 and 8	7.9	2	s	-	122.05	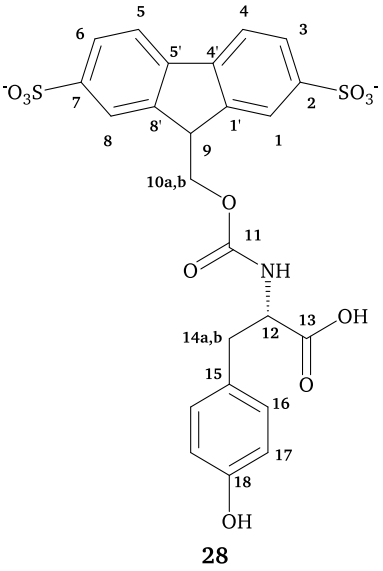
2 and 7	-	-	-	-	147.06; 147.13	
3 and 6	7.69	2	d	8.0	125.34	
4 and 5	7.84	2	d	8.0	119.5	
4' and 5'	-	-	-	-	140.52	
1' and 8'	-	-	-	-	144.1	
9	4.18	1	t	5.7	47.06	
10a	4.33	1	dd	11.0; 5.8	65.33	
10b	4.39	1	dd	11.0; 5.7		
11	-	-	-	-	156.05	
NH	7.5	1	d	8.0	-	
12	4.03	1	q	7.1	56.0	
13	-	-	-	-	173.19	
14a	2.74	1	dd	13.9; 9.3	35.74	
14b	2.86	1	dd	13.9; 5.4		
15	-	-	-	-	127.8	
16	6.98	2	d	8.1	129.97	
17	6.64	2	d	8.1	115.05	
18	-	-	-	-	155.77	
OH	8.15	1	s	-	-	

28

Table 49: Smoc-L-Tyr(tBu)-OH **29** in DMSO-d_6 (^{1}H-NMR at 500 MHz, ^{13}C-NMR at 126 MHz).

Position	^{1}H	#H	Multi-plicity	Coupling constant	^{13}C	
1 and 8	7.86; 7.92	2	s	-	122.71	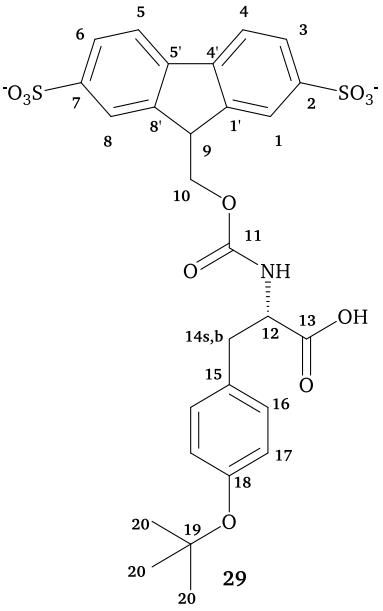
2 and 7	-	-	-	-	147.78	
3 and 6	7.67; 7.68	2	d	8.0	125.5	
4 and 5	7.81	2	d	8.0	119.48	
4' and 5'	-	-	-	-	140.24	
1' and 8'	-	-	-	-	143.89	
9	4.14	1	m	-	46.53	
10	4.15	2	m	-	65.34	
11	-	-	-	-	155.31	
NH	6.51	1	d	7.2	-	
12	3.83	1	q	6.6	57.47	
13	-	-	-	-	173.08	
14a	2.79	1	dd	13.6; 7.1	37.56	
14b	3.0	1	dd	13.6; 4.9		
15	-	-	-	-	134.06	
16	7.07	2	d	8.1	129.71	
17	6.78	2	d	8.1	123.09	
18	-	-	-	-	152.97	
19	-	-	-	-	77.37	
20	1.21	9	s	-	28.54	

29

Table 50: Smoc-L-Val-OH **30** in DMSO-d_6 (^{1}H-NMR at 500 MHz, ^{13}C-NMR at 126 MHz).

Position	^{1}H	#H	Multi-plicity	Coupling constant	^{13}C	
1 and 8	7.92; 7.93	2	s	-	122.1	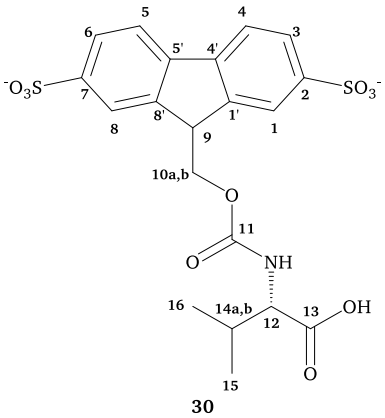
2 and 7	-	-	-	-	147.13	
3 and 6	7.68	2	dd	8.0; 1.3	125.31	
4 and 5	7.83	2	d	8.0	119.45	
4' and 5'	-	-	-	-	140.48	
1' and 8'	-	-	-	-	144.02; 144.18	
9	4.23	1	t	5.7	47.13	
10a	4.38	1	dd	11.0; 5.7	65.45	
10b	4.46	1	dd	11.0; 5.9		
11	-	-	-	-	156.53	
NH	7.46	1	d	8.3	-	
12	3.81	1	t	6.7	59.82	
13	-	-	-	-	173.07	
14a	2	1	oct	6.7	29.41	
14b	2.86	1	dd	13.9; 5.4		
15	0.87	3	d	6.8	18.4	
16	0.87	3	d	6.8	19.08	

30

Table 51: Smoc-β-Ala-OH **31** in DMSO-d_6 (^{1}H-NMR at 500 MHz, ^{13}C-NMR at 126 MHz).

Position	^{1}H	#H	Multi-plicity	Coupling constant	^{13}C	
1 and 8	7.87	2	s	-	121.92	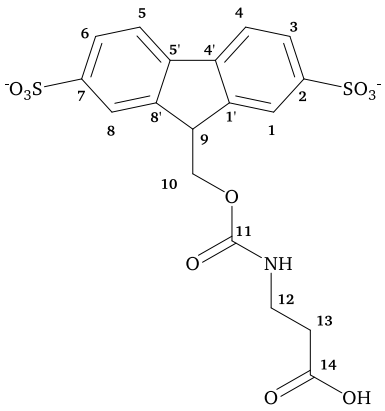
2 and 7	-	-	-	-	147.28	
3 and 6	7.67	2	d	8	125.21	
4 and 5	7.81	2	d	7.9	119.34	
4' and 5'	-	-	-	-	140.39	
1' and 8'	-	-	-	-	144.01	
9	4.22	1	t	5.7	47.0	
10	4.42	2	d	5.7	64.86	
11	-	-	-	-	155.99	
NH	7.19	1	br	-	-	
12	3.14	2	t	7.4	36.84	
13	2.36	2	t	7.3	34.01	
14	-	-	-	-	173.58	

31

Table 52: Smoc-Aib-OH **32** in DMSO-d_6 (^{1}H-NMR at 500 MHz, ^{13}C-NMR at 126 MHz).

Position	^{1}H	# H	Multi-plicity	Coupling constant	^{13}C	
1 and 8	7.89	2	s	-	121.97	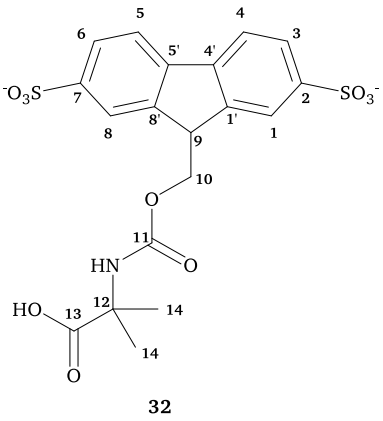
2 and 7	-	-	-	-	147.23	
3 and 6	7.67	2	d	7.8	125.23	
4 and 5	7.82	2	d	7.8	119.35	
4' and 5'	-	-	-	-	140.43	
1' and 8'	-	-	-	-	144.04	
9	4.21	1	t	5.5	47.05	
10	4.41	2	d	5.3	64.8	
11	-	-	-	-	155.06	
NH	7.44	1	br	-	-	
12	-	-	-	-	55.2	
13	-	-	-		175.6	
14	1.29	6	s	-	24.97	

32

1. Synthesis of Smoc-Cl and respective N_α-Smoc amino acids

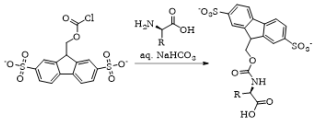

Compound	Abbreviation	Yield [%]
3	Smoc-L-Ala-OH	87.2
4	Smoc-D-Ala-OH	86.9
5	Smoc-L-Arg-OH	85.7
6	Smoc-L-Arg(Pbf)-OH	85.1
7	Smoc-L-Asn-OH	90.4
8	Smoc-L-Asp(OtBu)-OH	86.7
9	Smoc-L-Cys(Trt)-OH	85.1
10	Smoc-L-Gln-OH	90.8
11	Smoc-L-Glu(OtBu)-OH	88.2
12	Smoc-Gly-OH	93.7
13	Smoc-L-Ile-OH	92.4
14	Smoc-L-His(Trt)-OH	86.6
15	Smoc-L-Ile-OH	88.9
16	Smoc-L-Leu-OH	90.6
17	Smoc-D-Leu-OH	88.7
18	Smoc-L-Lys(Boc)-OH	87.4
19	Smoc-L-Met-OH	95.1
20	Smoc-L-Phe-OH	93.7
21	Smoc-L-Pro-OH	85.8
22	Smoc-L-Ser-OH	90.0
23	Smoc-L-Ser(tBu)-OH	87.9
24	Smoc-L-Thr-OH	92.2
25	Smoc-L-Thr(tBu)-OH	89.2
26	Smoc-L-Trp-OH	90.7
27	Smoc-L-Trp(Boc)-OH	86.9
28	Smoc-L-Tyr-OH	89.7
29	Smoc-L-Tyr(tBu)-OH	91.4
30	Smoc-L-Val-OH	87.2
31	Smoc-β-Ala-OH	92.5
32	Smoc-Ab-OH	57.8

2. Synthetic concept of aqueous SPPS (ASPPS)

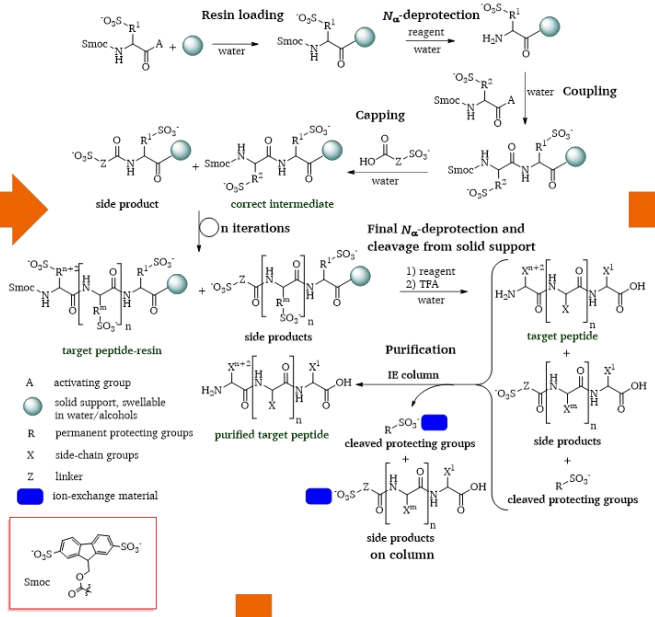

3. Peptide synthesis

Entry	Peptide sequence	Solvent	Yield (calculated from average loading)
1	H-AGELS-NH_2 (Pentapeptide-31) 48	water	13.72 mg (57.71%)
2	H-GPQGPQ-OH (Hexapeptide-9) 49	water	9.22 mg (30.7%)
3	H-EEMQRR-NH_2 (Hexapeptide 3) 50	water	21.73 mg (51.31%)
4	Ac-EEMQRR-NH_2 (Acetyl-Hexapeptide 3) 51	water	10.74 mg (4.216%)
5	Leu-Enkephalin amide H-YGGFM-NH_2 52	water	19.65 mg (70.06%)
6	Met-Enkephalin H-YGGFM-OH 53	30% MeCN$_{(aq)}$	9 mg (63%)
7	Leu-Enkephalin H-YGGFL-OH 54	30% MeCN$_{(aq)}$	10.3 mg (71.02%)
8	(ACP) 65-74 H-VQAADYING-OH 55	50% MeCN$_{(aq)}$	10 mg (36%)
9	(ACP) 65-74 H-VQAADYING-NH_2 56	50% MeCN$_{(aq)}$	23 mg (46%)
10	H-GPRP-OH 57	water	8 mg (30%)
11	Smoc-VWIA-NH_2 58	water	26 mg (67%)
12	Smoc-DIIW-OH 59	water	22 mg (50%)
13	Smoc-E(OtBu)K(Boc)R(Pbf)S(tBu)C(Trt)-OH 60	50% MeCN$_{(aq)}$	16 mg (44%)
14	H-CYEIS-NH_2 61	30% MeCN$_{(aq)}$	15mg (40.99%)
15	H-ANKPG-NH_2 62	30% MeCN$_{(aq)}$	13mg (53.66%)
16	Pal-GHK-OH 63*	20% ethanol$_{(aq)}$	14.12 mg (54.23%)
17	Pal-GQPR-OH 64*	20% Ethanol$_{(aq)}$	13.60 mg (59.74%)
18	H-GPRPA-NH_2 Vialox 65	30% MeCN$_{(aq)}$	12 mg (40.43%)
19	Oxytocin 66	30% MeCN$_{(aq)}$	16 mg (35.75%)
20	Vasopressin 67	30% MeCN$_{(aq)}$	20 mg (39.71%)
21	Heptaarginine 68	30% MeCN$_{(aq)}$	23 mg (41.43%)
22	Leuphasyl 69	20% MeCN$_{(aq)}$	17.30 mg (57.06%)

4. Fluorescent properties of N_α-Smoc amino acids

5. Capping strategy and purification by IEC

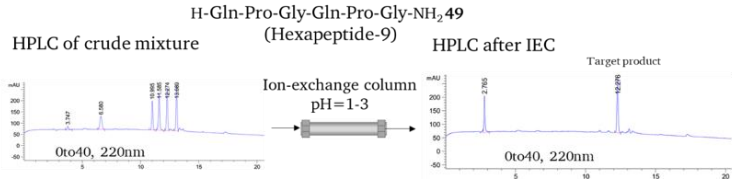

6. Wastewater purification

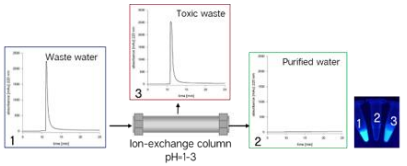

Figure 45: Graphical abstract of the present work

5. Summary & Outlook

During the time elapsed since the first oligopeptide has been assembled by chemical means, scientists constantly improve the methods of peptide synthesis in view of optimized reaction conditions, protecting schemes, tailor-made coupling agents, and solvent systems. The introduction of Merrifield's solid-phase approach in early 1960s became a major breakthrough that has designated the vector of peptide synthesis for the following decades. To date, production of peptides has gained almost optimal efficiency in terms of coupling yield and reaction times. However, solvent consumption, that has been recognized as an economic and environmental issue since a decade, makes solid-phase peptide synthesis one of the most inefficient synthetic approaches known. Indeed, DMF and NMP which are currently the solvents of choice in SPPS, are classified by the European REACH Regulation as substances of very high concern due to their carcinogenic, mutagenic or toxic for reproduction (CMR) properties. Therefore, sustainable, green peptide synthesis that does not require or minimizes application of highly hazardous solvents is currently in research focus.

In the frame of the present work, a water-based solid-phase peptide synthesis (ASPPS) was developed, which relies on an original water-compatible protecting group strategy. The cornerstone of this concept, an Smoc protecting group, combines the fluorenyl system with charged sulfonic pendants and therefore possesses high water solubility and intrinsic fluorescent properties. This moiety was efficiently introduced at the aminoterminus in all the natural amino acids using the corresponding Smoc-Cl **2.** Reliable synthesis routes were developed that provided synthetic access to the respective N_{α}-Smoc amino acids in good to excellent yields (derivatives **3**-**31**, **Table 53**). Non-natural Smoc-Aib-OH **32** was obtained in moderate yield due to the obvious steric hindrance.

Table 53: Summary of the N_{α}-Smoc amino acid yields.

Compound	3	4	5	6	7	8	9	10	11	12
Yield [%]	87.2	86.9	85.7	85.1	90.4	86.7	85.1	90.8	88.2	93.7
Compound	**13**	**14**	**15**	**16**	**17**	**18**	**19**	**20**	**21**	**22**
Yield [%]	92.4	86.6	88.9	90.6	88.7	87.4	95.1	93.7	85.8	90.0
Compound	**23**	**24**	**25**	**26**	**27**	**28**	**29**	**30**	**31**	**32**
Yield [%]	87.9	92.2	89.2	90.7	86.9	89.7	91.4	87.2	92.5	57.8

Stability of N_{α}-Smoc amino acids under reaction conditions and liability of Smoc in the presence of deprotection bases was thoroughly investigated. It was found that all N_{α}-Smoc amino were stable within days in aqueous solutions of sodium bicarbonate. The Smoc protection was easily cleaved with aqueous sodium hydroxide or ammonia as well as under milder conditions by ethanolamine or piperazine. Our studies showed the slightly higher base-lability of an Smoc- compared to the Fmoc-protecting group.

Generation of a peptide bond in aqueous environment is a synthetic challenge *per se*. Throughout the whole story of peptide synthesis water was assigned as the major handicap for successful amide coupling, and water-free peptide synthesis grade chemicals were obligatory. To provide access to aqueous peptide synthesis, coupling efficacy was assessed in water-based systems applying respective N_{α}-Smoc amino acids and using different activation approaches. In our hands, several water-compatible activating additives were found appropriate, with EDC-HCl **37**, Oxima **39** and HOPO **40** being the most efficient.

The experiments showed that although coupling of amino acids in pure water gave reasonable yields and purity of peptides, the addition of organic co-solvents enhanced coupling performance significantly (**Table 54**).

Table 54: Summary of coupling efficiency of EDC-HCl **37**, Oxima **39** and HOPO **40** after 25 minutes.

Coupling reagents	Coupling efficiency				
	water	30% MeCN	30% EtOH	30% *i*PrOH	10% Me-THF
EDC-HCl **37**/Oxyma **39**	90.7%	99.8%	99.0%	98.8%	88.7%
EDC-HCl **37**/HOPO **40**	58.3%	84.2%	83.6%	83.6%	79.4%

Indeed, in 20-30% aqueous acetonitrile or alcohols amide coupling was as efficient as in water-free organic solvents, presumably due to stabilization of intermediate active esters.

The concept of aqueous SPPS (ASPPS) was further validated by assembling certain prominent peptides in water or water-based systems. Thus, we established a reliable synthesis of peptides **47**-**69** in good yields and purity (**Table 55**). To the best of our knowledge, to date our ASPPS approach is the most efficient water-based peptide synthesis process known.

Table 55: Summary of the peptide yields.

Compound	48	49	50	51	52	53	54	55	56	57	58
Yield [%]	57.7	38.7	51.3	42.2	70.9	63	71.8	36	46	38	67
Compound	**59**	**60**	**61**	**62**	**63**	**64**	**65**	**66**	**67**	**68**	**69**
Yield [%]	50	44	49	53.7	54.2	59.7	48.4	35.8	39.7	41.4	57.9

Additional studies on enantiomeric composition showed no increased racemization levels during the ASPPS process. Studies on the aspartimide formation showed that usage of 5% piperazine at 4°C is advised for Smoc deprotection of aspartimide-prone sequences resulting in the formation of around 15-25% of the corresponding β-peptide while the deprotection in 20% piperidine in DMF resulted in 83% aspartimide by-products.

Special attention was given to spectral properties of Smoc-bearing molecular constructs. Additional studies aimed at investigating the absorbance and fluorescent characteristics of the N_α-Smoc amino acids showed that both in resin-bound and in-solution state this moiety could be used for the real-time monitoring of the reaction progress upon both the coupling and the deprotection steps as well as to determine the concentration of loaded on-support N_α-Smoc amino acids.

An elegant approach towards a reliable purification of synthetic peptides has been proposed based on the ionic properties of the Smoc protecting group. Already Merrifield showed that mono-sulfonated Fmoc derivative could be applied to peptide isolation with ion-exchange chromatography.[206] This method was further optimized and integrated as capping strategy into the ASPPS-based peptide assembly. To that end, all the by-products originating from incomplete couplings are labelled with charged *Sulfo-tags* and can be easily removed upon successive IEC after cleavage from solid support. Our studies showed that this method could also be applied to Fmoc-based peptide synthesis. This method allows tailoring of purification strategy depending on required peptide purity grade. It can be applied solely or serve as a pre-purification system to simplify and optimize the following HPLC separation. In addition, the same method could be used to refine the wastewater.

It is important to mention that development of specific, water-optimized resins and respective linker systems still remains the challenge that must be addressed. However, this issue was beyond the scope of the present work. The next goal in the frame of this study would be to synthesize longer, more complex peptides and develop automated protocols for ASPPS.

6. Zusammenfassung und Ausblick

Seit der ersten chemischen Herstellung eines Oligopeptids verbesserten Wissenschaftler die Methoden der Peptidsynthese im Hinblick auf optimierte Reaktionsbedingungen, Schutzgruppenstrategien, maßgeschneiderte Kupplungsreagenzien und Lösungsmittelsysteme ständig weiter. Die Einführung des Festphasenansatzes von Merrifield Anfang der 1960er Jahre hat die Peptidsynthese revolutioniert und die Peptidsynthese für Jahrzehnte geprägt. Mittlerweile hat die Synthese von Peptiden eine nahezu optimale Effizienz in Bezug auf Kupplungsausbeute und Reaktionszeiten erreicht. Der Verbrauch an organischen Lösungsmitteln, der seit einem Jahrzehnt als ökonomisches und ökologisches Problem erkannt ist, macht die Festphasen-Peptidsynthese jedoch zu einem der ineffizientesten bekannten synthetischen Ansätze. Tatsächlich werden DMF und NMP, derzeit die Lösungsmittel der Wahl in der SPPS, nach der europäischen Reach-Verordnung aufgrund ihrer krebserzeugenden, erbgutverändernden oder fortpflanzungsgefährdenden (CMR) Eigenschaften als besonders besorgniserregend eingestuft. Daher steht derzeit die nachhaltige, grüne Peptidsynthese im Fokus, die den Einsatz hochgefährlicher Lösungsmittel nicht erfordert oder minimiert.

Im Rahmen der vorliegenden Arbeit wurde eine wasserbasierte Festphasen-Peptidsynthese (ASPPS) entwickelt, die auf einer originären wasserverträglichen Schutzgruppenstrategie basiert. Die in dieser Arbeit entwickelte Smoc-Schutzgruppe, kombiniert das Fluorenylsystem mit geladenen Sulfonsäuregruppen und verfügt somit über eine hohe Wasserlöslichkeit und intrinsische Fluoreszenzeigenschaften. Diese Gruppe wurde mit dem entsprechenden Smoc-Cl **2** effizient am Aminoterminus von allen natürlichen Aminosäuren angebracht. Es wurden zuverlässige Synthesewege entwickelt, die einen synthetischen Zugang zu den entsprechenden N_α-Smoc-Aminosäuren in guten bis sehr guten Ausbeuten ermöglichten (Derivate **3**-**31**, **Tabelle 53**). Nicht-natürliches Smoc-Aib-OH **32** wurde aufgrund der offensichtlichen sterischen Hinderung nur in moderater Ausbeute hergestellt.

Tabelle 53: Zusammenfassung der N_α-Smoc Aminosäure Ausbeuten.

Verbindung	3	4	5	6	7	8	9	10	11	12
Ausbeute [%]	87.2	86.9	85.7	85.1	90.4	86.7	85.1	90.8	88.2	93.7
Verbindung	**13**	**14**	**15**	**16**	**17**	**18**	**19**	**20**	**21**	**22**
Ausbeute [%]	92.4	86.6	88.9	90.6	88.7	87.4	95.1	93.7	85.8	90.0
Verbindung	**23**	**24**	**25**	**26**	**27**	**28**	**29**	**30**	**31**	**32**
Ausbeute [%]	87.9	92.2	89.2	90.7	86.9	89.7	91.4	87.2	92.5	57.8

Die Stabilität von N_α-Smoc-Aminosäuren unter Reaktionsbedingungen und die Abspaltbarkeit von Smoc in Gegenwart von Entschützungsbasen wurde untersucht. Es wurde festgestellt, dass alle N_α-Smoc Aminosäuren stabil für mehrere Tage in wässrigen Natriumhydrogencarbot Lösungen waren. Die Smoc-Schutzgruppe konnte leicht mit wässrigem Natriumhydroxid oder Ammoniak sowie unter milderen Bedingungen mit Ethanolamin oder Piperazin abgespalten werden. Unsere Studien zeigten eine etwas erhöhte Basen-Labilität der Smoc-Gruppe im Vergleich zur Fmoc-Schutzgruppe.

Die Erzeugung einer Peptidbindung in wässriger Umgebung ist *per se* eine synthetische Herausforderung. Während der gesamten Geschichte der Peptidsynthese wurde Wasser als Haupthindernis für eine erfolgreiche Amidkopplung genannt, und wasserfreie Chemikalien waren obligatorisch. Um Zugang zur wässrigen Peptidsynthese zu erhalten, wurde die Kopplungseffizienz in wässrigen Systemen mit entsprechenden N_α-Smoc-Aminosäuren und mit verschiedenen Aktivierungsreagenzien untersucht. Es wurden mehrere wasserverträgliche

Aktivierungsreagenzien identifiziert, wobei EDC-HCl **37**, Oxima **39** und HOPO **40** die effizientesten waren.

Die Experimente zeigten, dass, obwohl die Kopplung von Aminosäuren in reinem Wasser eine angemessene Ausbeute und Reinheit der Peptide ergab, die Zugabe von organischen Co-Lösungsmitteln die Kopplungseffizienz signifikant verbesserte. (**Tabelle 54**).

Tabelle 54: Zusammenfassung der Kopplungseffizienz von EDC-HCl **37**, Oxima **39** und HOPO **40** nach 25 Minuten.

Kopplungsreagenzien	Kopplungseffizienz				
	Wasser	30% MeCN	30% EtOH	30% *i*PrOH	10% Me-THF
EDC-HCl **37**/Oxyma **39**	90.7%	99.8%	99.0%	98.8%	88.7%
EDC-HCl **37**/HOPO **40**	58.3%	84.2%	83.6%	83.6%	79.4%

Tatsächlich war die Kopplung in 20-30% wässrigem Acetonitril oder Alkoholen genauso effizient wie in wasserfreien organischen Lösungsmitteln, vermutlich aufgrund der Stabilisierung der intermediären Aktivester.

Das Konzept des wässrigen SPPS (ASPPS) wurde weiter validiert, indem ausgewählte bekannte Peptide in wässrigen oder wasserbasierten Systemen synthetisiert wurden. So haben wir eine zuverlässige Synthese der Peptide **47**-**69** in guter Ausbeute und Reinheit etabliert (**Tabelle 55**). Nach bestem Wissen ist der hier beschriebene ASPPS-Ansatz der effizienteste bisher bekannte wasserbasierte Peptidsyntheseprozess.

Tabelle 55: Zusammenfassung der Peptid-Ausbeuten.

Verbindung	48	49	50	51	52	53	54	55	56	57	58
Ausbeute [%]	57.7	38.7	51.3	42.2	70.9	63	71.8	36	46	38	67
Verbindung	**59**	**60**	**61**	**62**	**63**	**64**	**65**	**66**	**67**	**68**	**69**
Ausbeute [%]	50	44	49	53.7	54.2	59.7	48.4	35.8	39.7	41.4	57.9

Zusätzliche Studien zur enantiomere Zusammensetzung zeigten keine erhöhte Racemisierung während des ASPPS-Prozesses. Studien zur Aspartimidbildung zeigten, dass die Verwendung von 5% Piperazin bei 4°C für die Smoc-Entschützung von Aspartimid-gefährdeten Sequenzen vorteilhaft ist. Dies führt zur Bildung von etwa 15-25% des entsprechenden β-Peptids, die Entschützung in 20% Piperidin in DMF führte dagegen zu 83% Aspartimid Nebenprodukten.

Besonderes Augenmerk wurde auf die spektralen Eigenschaften von Smoc-tragenden Verbindungen gelegt. Studien zur Absorption und Fluoreszenz der N_{α}-Smoc-Aminosäuren zeigten, dass dieser Teil sowohl im harzgebundenen als auch in Lösung zur Echtzeitüberwachung des Reaktionsfortschritts sowohl beim Kupplungs- als auch beim Entschützungsschritt sowie zur Bestimmung der N_{α}-Smoc-Aminosäurebeladung auf der festen Phase verwendet werden kann.

Ein eleganter Ansatz für eine einfache und kostengünstige Reinigung synthetischer Peptide wurde auf der Grundlage der ionischen Eigenschaften der Smoc-Schutzgruppe in dieser Arbeit etabliert. Merrifield zeigte bereits, dass monosulfoniertes Fmoc-Derivat zur Peptidisolierung mit IEC eingesetzt werden kann.[206] Diese Methode wurde weiter optimiert und als Capping-Strategie in die ASPPS-basierte Peptidsynthese integriert. Zu diesem Zweck sind alle Nebenprodukte, die bei unvollständigen Kupplungen entstehen, mit geladenen *Sulfotags* markiert und können durch IEC nach der Abspaltung von der festen Phase leicht entfernt werden. Unsere Studien zeigten, dass diese Methode auch auf die Fmoc-basierte Peptidsynthese angewendet werden kann. Diese Methode ermöglicht die Anpassung der Aufreinigungsstrategie an den gewünschten Peptidreinheitsgrad. Sie kann allein angewendet werden oder als Vorreinigungsstrategie zur Vereinfachung und Optimierung der anschließenden HPLC-

Trennung dienen. Darüber hinaus kann das gleiche Verfahren zur Reinigung des bei der ASPPS anfallenden wässrigen Lösungsmittels eingesetzt werden.

Die Entwicklung spezifischer, für den Einsatz in wässrigen Lösungsmitteln optimierte Harze und entsprechender Linkersysteme bleibt nach wie vor die Herausforderung und wird Gegenstand von künftigen Arbeiten zur Verbesserung der hier vorgeschlagenen Synthesestrategie sein. Auch steht noch an, längere und komplexere Peptide zu synthetisieren und automatisierte Protokolle für die ASPPS zu entwickeln.

7. Experimental

7.1. General

7.1.1. Solvents

Solvents were obtained *from Carl Roth GmbH + Co. KG* (Karlsruhe, Germany), *Fisher Scientific GmbH* (Schwerte, Germany) or *Merck KGaA* (Darmstadt, Germany) and used without further purification except when mentioned specifically.

7.1.2. Reagents

All reagents, amino acids and reagents were used as supplied by *Carl Roth GmbH + Co. KG* (Karlsruhe, Germany), *Fisher Scientific GmbH* (Schwerte, Germany), *Merck KGaA* (Darmstadt, Germany), *Iris Biotech GmbH* (Marktredwitz, Germany) or *Carbolution Chemicals GmbH* (St. Ingbert, Germany).

7.1.3. Freeze-drying

Removal of the solvents was performed with a Beta 2-8 LDplus freeze-dryer (*Martin Christ Gefriertrocknungsanlagen GmbH,* Osterode, Germany) equipped with a high vacuum pump, Vacuubrand chemistry hybrid pump RC6 (*Vacuubrand GmbH+Co*. KG, Wertheim, Germany).

7.1.4. Centrifugation

The phase separation and the washing of peptides were done in a Multifuge 3 L-R centrifuge (*Thermo Fisher Scientific*, Schwerte, Germany).

7.1.5. Storage

All Fmoc-protected amino acids and activation reagents were stored at 4°C. All other substances were stored as recommended by the supplier.

7.1.6. Removal of organic solvents

Organic solvents were evaporated under reduced pressure using a rotary evaporator.

7.2. Analytics

7.2.1. Mass spectrometry

Electrospray ionization mass spectroscopy (ESI-MS) spectra were obtained by using a Shimadzu LCMS-2020 mass spectrometer equipped with a *Phenomenex* Synergi™ Hydro-RP LC Column (4 u, 80 Å, 100 x 3 mm). Eluent system consisted of 0.1% aq. formic acid, LC-MS grade (eluent A) and 100% acetonitrile containing 0.1% formic acid, LC-MS grade (eluent B).

7.2.2. HR-MS

HR-MS electron ionization were obtained by using a Bruker Impact II using electrospray ionization mass spectroscopy (ESI-MS).

7.2.3. Liquid chromatography

Analytical reversed-phase high performance liquid chromatography (RP-HPLC) was performed on a Agilent 1100 series HPLC equipped with a Interchim US5C18HQ-250/046 (5u, 250×4.6mm) at a flow rate of 1 mL/min. Eluent A: 0.1% aq. trifluoroacetic acid (TFA), eluent B: MeCN with 0.1% TFA. 4 min of isocratic flow (starting concentration of eluent B) was followed by 20 min of gradient flow. Absorption was measured by UV/VIS detector at 220 nm and 280 nm.

For isolation of peptides or N_{α}-Smoc amino acids on a semi-preparative *Interchim* PuriFlash 4250 equipped with a preparative C_{18} column (*Interchim* US5C18HQ-250/212 (5u, 250×21.2mm) was used at a flow rate of 18 mL/min. Eluent A: 0.1% aq. trifluoroacetic acid (TFA), eluent B: MeCN with 0.1% TFA. 5 min of isocratic flow (starting concentration of eluent B) was followed by 20 min of gradient flow. Absorption was measured by UV/VIS detector at 220 nm and 280 nm.

7.2.4. NMR

^{1}H, ^{13}C, ^{13}C DEPT and the 2D NMR spectra ^{1}H-^{13}C HMBC, ^{1}H-^{1}H NOESY, ^{1}H-^{1}H COSY were recorded with a 500 MHz NMR Spectrometer DRX 500 (Bruker BioSpin GmbH, Karlsruhe) equipped with a 5mm ATMA BBFO probe . All Samples were dissolved in deuterated DMSO d6 purchased from *Sigma Aldrich* (*Merck KGaA*, Darmstadt, Germany) or deuterated MeCN purchased from *Euriso Top* (Gif-Sur-Yvette, France).

7.3. Synthesis of Smoc-Cl 2

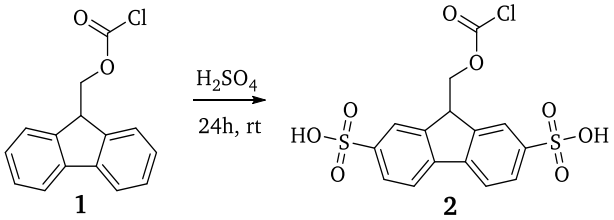

Scheme 26: Synthesis of Smoc-Cl **2**.

60g Fmoc chloride **1** were dissolved in 250 ml dichloromethane (DCM). 62 ml of 20% oleum were slowly dropped into the solution under stirring. After precipitation of a white-grey solid, the solution was drained and 20 ml of 1,4-dioxane were added under ice-cooling and stirring until the SO_3-dioxane complex was formed (approx. 10-15 min). To dissolve this rubber-like compound, 150 ml of 1,2-dichloroethane were added and stirred. SO_3-dioxane complex remained in solution, Smoc-Cl **2** precipitated as solid. The crude product was filtered, washed twice with DCM, and dried in vacuo and the used 1,2-dichlorethane was regenerated. Smoc-Cl **2** was obtained as a slightly yellow powder (yield ~75%).

HR-MS calc. for $C_{15}H_{11}ClO_8S_2$ m/z: 416.95111, meas. 416.95146 $[M-H]^{-}$.

^{1}H NMR (500 MHz, CD_3CN) δ: 4.55 (t, J = 5.7 Hz, 1H), 4.90 (d, J = 5.7 Hz, 2H), 8.00 (d, J = 8.1 Hz, 2H), 8.08 (d, J = 8.1 Hz, 2H), 8.18 (s, 2H).

^{13}C NMR (126 MHz, CD_3CN): δ 47.80, 72.67, 122.98, 124.48, 128.13, 140.82, 144.97, 145.68, 151.05.

7.4. Synthesis of N_α-Smoc amino acids

7.4.1. General procedure

Typically, 1 eq. of the corresponding amino acid was dissolved in water and 1 eq. Smoc-Cl **2** was added to the solution. The pH of the solution was adjusted to 8.5 to allow the formation of the N_α-Smoc amino acid. After 30 minutes, the reaction mixture was frozen and lyophilized, with subsequent isolation by preparative HPLC, giving the respective Smoc-protected amino acid as a white or slightly white powder after freeze-drying (yields > 85%).

7.4.2. Synthesis of Smoc-L-Ala-OH 3

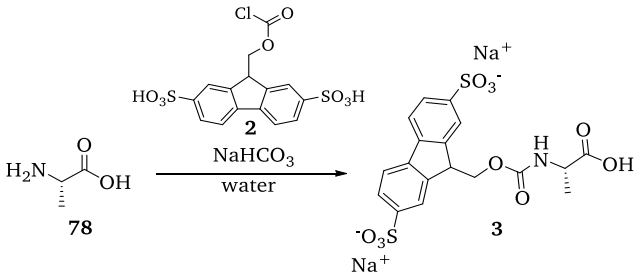

Scheme 27: Synthesis of Smoc-L-Ala-OH **3**.

According to the general procedure, 2.00g (22.45 mmol, 1 eq.) L-alanine **78** and 9.36g (22.45 mmol, 1 eq.) Smoc-Cl **2** were dissolved in 30ml water and sodium hydrogen carbonate was added to adjust the pH to 8.5. The reaction mixture was stirred at ambient temperature and the solvent was removed by lyophilization. The product was isolated by preparative RP-HPLC (gradient normalized B). After work up, 10.72g (87.2%) of Smoc-L-alanine **3** were obtained as a white powder.

RP-HPLC (gradient normalized B): t_R = 12.54 min.

ESI-MS calc. for $C_{18}H_{17}NO_{10}S_2$ m/z: 471.45, meas. 470.17 $[M+H]^-$; calc. 235.73, meas. 234.84 $[M+H]^{2-}$.

HR-MS calc. for $C_{18}H_{17}NO_{10}S_2$ m/z: 472.03666, meas. 472.03698 $[M+H]^+$.

^{1}H NMR (500 MHz, DMSO-d_6) δ: 1.22 (d, J = 7.4 Hz, 3H), 3.95 (q, J = 7.3 Hz, 1H), 4.23 (t, J = 5.5 Hz, 1H), 4.38 (dd, J = 10.9, 5.7 Hz, 1H), 4.49 (dd, J = 10.9, 5.4 Hz, 1H), 7.52 (br, NH), 7.68 (d, J = 7.9 Hz, 2H), 7.83 (d, J = 7.9 Hz, 2H), 7.89 (s, 1H), 7.91 (s, 1H).

^{13}C NMR (126 MHz, DMSO) δ: 16.83, 47.02, 49.27, 65.14, 119.47, 121.97, 122.01, 125.31, 140.52, 143.99, 144.17, 147.16, 155.93, 174.24.

7.4.3. Synthesis of Smoc-D-Ala-OH 4

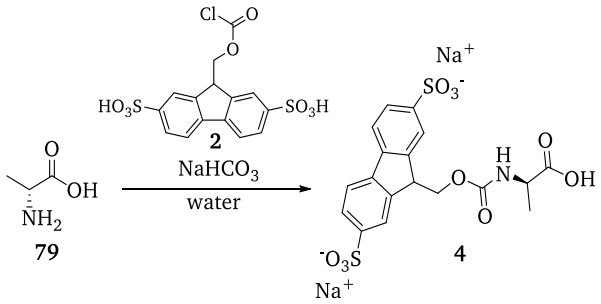

Scheme 28: Synthesis of Smoc-D-Ala-OH **4**.

According to the general procedure, 2.00g (22.45 mmol, 1 eq.) D-alanine **79** and 9.36g (22.45 mmol, 1 eq.) Smoc-Cl **2** were dissolved in 30ml water and sodium hydrogen carbonate was added to adjust the pH to 8.5. The reaction mixture was stirred at ambient temperature and the solvent was removed by lyophilization. The product was isolated by preparative RP-HPLC (gradient normalized B). After work up, 10.58g (86.9%) of Smoc-D-alanine **4** were obtained as a white powder.

RP-HPLC (normalized B): t_R = 12.29 min.

ESI-MS calc. for $C_{18}H_{17}NO_{10}S_2$ m/z: 471.45, meas. 470.05 $[M+H]^-$; calc. 235.73, meas. 234.92 $[M+H]^{2-}$.

HR-MS calc. for $C_{15}H_{11}ClO_8S_2$ m/z: 470.0221, meas. 470.02370 $[M-H]^-$.

^{1}H NMR (500 MHz, DMSO-d_6) δ: 1.22 (d, J = 7.3 Hz, 3H), 3.95 (q, J = 7.3 Hz, 1H), 4.23 (t, J = 5.5 Hz, 1H), 4.37 (dd, J = 11.0, 5.7 Hz, 1H), 4.38 (dd, J = 10.9, 5.5 Hz, 1H), 7.5 (br, NH), 7.68 (d, J = 8.2 Hz, 2H), 7.83 (d, J = 7.9 Hz, 2H), 7.89 (s, 1H), 7.91 (s, 1H).

^{13}C NMR (126 MHz, DMSO) δ: 16.82, 47.01, 49.26, 65.11, 119.43, 121.94, 125.28, 140.49, 143.97, 144.15, 147.19, 155.91, 174.22.

7.4.4. Synthesis of Smoc-L-Arg-OH 5

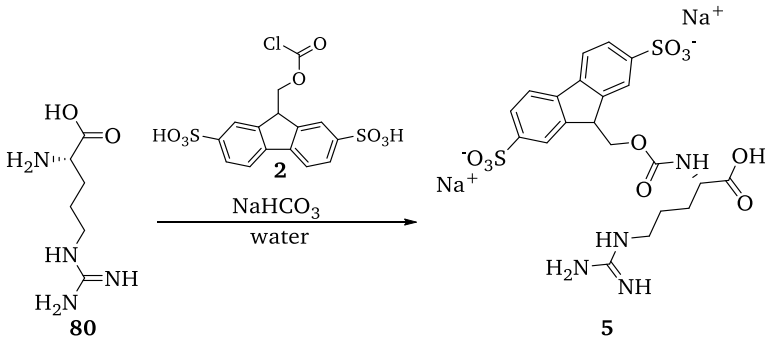

Scheme 29: Synthesis of Smoc-L-Arg-OH 5.

According to the general procedure, 3.91g (22.45 mmol, 1 eq.) L-arginine **80** and 9.36g (22.45 mmol, 1 eq.) Smoc-Cl **2** were dissolved in 30ml water and sodium hydrogen carbonate was added to adjust the pH to 8.5. The reaction mixture was stirred at ambient temperature and the solvent was removed by lyophilization. The product was isolated by preparative RP-HPLC (gradient normalized B). After work up, 11.55g (85.7%) of Smoc-L-arginine-OH **5** were obtained as a white powder.

RP-HPLC (normalized B): t_R = 12.88 min.

ESI-MS calc. for $C_{21}H_{24}N_4O_{10}S_2$ m/z: 556.56, meas. 555.4 $[M-H]^-$; calc. 278.28, meas. 277.3 $[M-H]^{2-}$.

HR-MS calc. for $C_{21}H_{24}N_4O_{10}S_2$ m/z: 557.10066, meas. 557.10069 $[M+H]^+$.

^{1}H NMR (500 MHz, DMSO-d_6) δ: 1.47 (m, 2H), 1.56, 1.72 (m, 2H), 3.02 (dq, J = 13.0, 6.5 Hz, 1H), 3.10 (dq, J = 13.0, 6.5 Hz, 1H), 3.96 (dt, J = 9.2, 4.3 Hz, 1H), 4.32 (t, J = 5.5, 21), 4.33 (dd, J = 10.0, 6.3 Hz, 1H), 4.54 (dd, J = 10.0, 6.3 Hz, 1H), 7.52 (d, J = 8.5 Hz, NH), 7.70 (d, J = 7.7, 2H), 7.74 (t, J = 5.6 Hz, NH), 7.85, 7.86 (d, J = 7.9, 2H), 7.88 (s, 1H), 7.93 (s, 1H).

^{13}C NMR (126 MHz, DMSO) δ: 24.93, 27.87, 40.00, 46.91, 52.91, 64.85, 119.60, 125.30, 140.61, 143.51, 144.50, 146.76, 155.93, 156.63, 173.30.

7.4.5. Synthesis of Smoc-L-Arg(Pbf)-OH 6

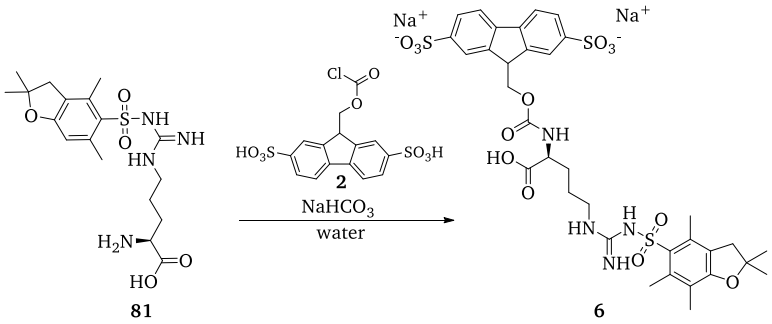

Scheme 30: Synthesis of Smoc-L-Arg(Pbf)-OH **6**.

According to the general procedure, 3.00g (7.27 mmol, 1 eq.) L-Arg(Pbf)-OH **81** and 3.03g (7.27 mmol, 1 eq.) Smoc-Cl **2** were dissolved in 30ml water acetonitrile mixture (2:1) and sodium hydrogen carbonate was added to adjust the pH to 8.5. The reaction mixture was stirred at ambient temperature and the solvent was removed by lyophilization. The product was isolated by preparative RP-HPLC (gradient 10 to 100% B). After work up, 5.19g (85.1%) of Smoc-L-Arg(Pbf)-OH **6** were obtained as a slightly yellow powder.

RP-HPLC (10 to 100% B): t_R = 14.70 min.

ESI-MS calc. for $C_{33}H_{38}N_4O_{13}S_3$ m/z: 808.89, meas. 807.19 $[M-H]^-$; calc. 404.45, meas. 403.46 $[M-2H]^{2-}$.

HR-MS calc. for $C_{33}H_{38}N_4O_{13}S_3$ m/z: 809.18268, meas. 809.18227 $[M+H]^+$.

^{1}H NMR (500 MHz, DMSO-d_6) δ: 1,41 (s, 6H), 1.47 (m, 2H), 1.56 – 1.64 (m, 2H), 2.01 (s, 6H), 2.43 (s, 6H), 2.48 (s, 6H), 3.07 (q, J = 7.3 Hz, 2H), 2.97 (s, 2H), 3.96 (td, J = 9.1, 4.7 Hz, 1H), 4.3 (t, J = 5.5 Hz, 1H), 4.32 (m, 1H), 4.51 (m, 1H), 7.68 (d,d J = 7.8, 1.4 Hz, 2H), 7.52 (br, NH), 7.74 (t, J = 5.6 Hz, NH), 7.84 (d, J = 7.9, 2H), 7.88 (s, 1H), 7.91 (s, 1H).

^{13}C NMR (126 MHz, DMSO) δ: 12.22, 17.51, 18.91, 25.10, 27.80, 28.25, 39.71, 42.35; 46.92, 53.17, 64.98, 86.32, 116.34, 119.54, 122.03, 124.33, 125.28, 131.42, 133.90, 137.32, 140.55, 143.58, 144.39, 146.91, 155.96, 157.57, 166.74, 173.35.

7.4.6. Synthesis of Smoc-L-Asn-OH 7

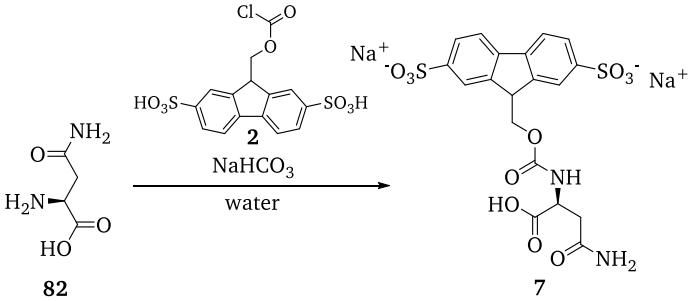

Scheme 31: Synthesis of Smoc-L-Asn-OH **7**.

According to the general procedure, 3.37g (22.45 mmol, 1 eq.) L-asparagine **82** (mono hydrate) and 9.36g (22.45 mmol, 1 eq.) Smoc-Cl **2** were dissolved in 30ml water and sodium hydrogen carbonate was added to adjust the pH to 8.5. The reaction mixture was stirred at ambient temperature and the solvent was removed by lyophilization. The product was isolated by

preparative RP-HPLC (gradient normalized B). After work up, 12.03g (90.4%) of Smoc-L-asparagine-OH **7** were obtained as a white powder.

RP-HPLC (normalized B): t_R = 10.76 min.

ESI-MS calc. for $C_{19}H_{18}N_2O_{11}S_2$ m/z: 514.48, meas. 513.20 $[M-H]^-$; calc. 257.24, meas. 256.30 $[M-2H]^{2-}$.

HR-MS calc. for $C_{19}H_{18}N_2O_{11}S_2$ m/z: 515.04248, meas. 515.04298 $[M+H]^+$.

^{1}H NMR (500 MHz, DMSO-d_6) δ: 2.43 (dd, J = 15.2, 7.5 Hz, 1H), 2.54 (dd, J = 15.2, 5.8 Hz, 1H), 4.26 (t, 1H), 4.27 (m, 1H), 4.42 (m, 2H), 5.6 (br, NH), 7.40 (d, J = 8.2 Hz, 1H), 7.69 (d, J = 7.5 Hz, 2H), 7.84 (d, J = 7.9 Hz, 1H), 7.90 (s, 1H), 7.91 (s, 1H).

^{13}C NMR (126 MHz, DMSO) δ: 36.78, 46.06, 50.71, 65.25, 119.57, 122.11, 125.37, 140.59, 144.03, 144.14, 146.99, 155.83, 171.56, 172.83.

7.4.7. Synthesis of Smoc-L-Asp(OtBu)-OH 8

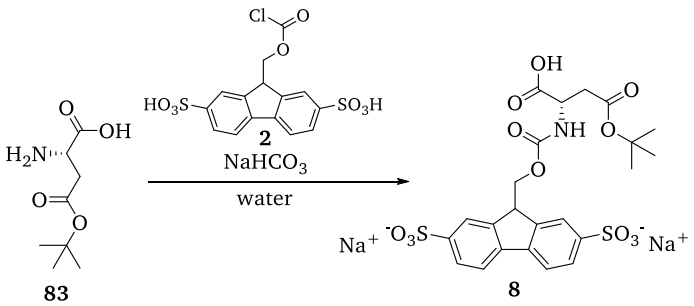

Scheme 32: Synthesis of Smoc-L-Asp(OtBu)-OH **8**.

According to the general procedure, 4.00g (21.14 mmol, 1 eq.) L-Asp(OtBu)-OH **83** and 8.81g (21.14 mmol, 1 eq.) Smoc-Cl **2** were dissolved in 40ml water and sodium hydrogen carbonate was added to adjust the pH to 8.5. The reaction mixture was stirred at ambient temperature and the solvent was removed by lyophilization. The product was isolated by preparative RP-HPLC (gradient 0 to 60% B). After work up, 11.32g (86.7%) of Smoc- L-Asp(OtBu)-OH **8** were obtained as a white powder.

RP-HPLC (0 to 60% B): t_R = 15.14 min.

ESI-MS calc. for $C_{23}H_{25}NO_{12}S_2$ m/z: 571.57, meas. 570.08 $[M-H]^-$; calc. 285.79, meas. 284.84 $[M-2H]^{2-}$.

HR-MS calc. for $C_{23}H_{25}NO_{12}S_2$ m/z: 610.04498, meas. 610.04568 $[M+H]^+$.

^{1}H NMR (500 MHz, DMSO-d_6) δ: 1.38 (s, 9H), 2.40 (dd, J = 14.7, 7.8 Hz, 1H), 2.59 (dd, J = 14.7, 5.4 Hz, 1H), 3.97 (dt, J = 7.5, 5.3 Hz, 1H), 4.22 (m, 2H), 4.23 (m, 1H), 6.80 (d, J = 7.5 Hz, NH), 7.69 (d, J = 7.7 Hz, 2H), 7.83 (d, J = 7.9 Hz, 2H),7.89 (s, 1H), 7.94 (s, 1H).

^{13}C NMR (126 MHz, DMSO) δ: 27.78, 39.54, 46.62, 52.92, 65.47, 79.10, 119.35, 122.31, 122.45, 125.25, 140.31, 143.78, 144.15, 147.26, 155.36, 170.72, 172.58.

7.4.8. Synthesis of Smoc-L-Cys(Trt)-OH 9

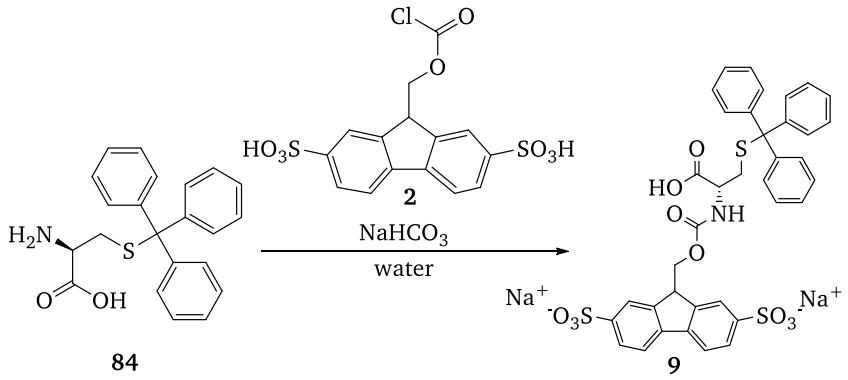

Scheme 33: Synthesis of Smoc-L-Cys(Trt)-OH **9**.

According to the general procedure, 4.00g (11.00 mmol, 1 eq.) L-Cys(Trt)-OH **84** and 4.59g (11.00 mmol, 1 eq.) Smoc-Cl **2** were dissolved in 40ml water acetonitrile mixture (1:1) and sodium hydrogen carbonate was added to adjust the pH to 8.5. The reaction mixture was stirred at ambient temperature and the solvent was removed by lyophilization. The product was isolated by preparative RP-HPLC (30 to 100% B). After work up, 7.40g (85.1%) of Smoc-L-Cys(Trt)-OH **9** were obtained as a white powder.

RP-HPLC (10 to 100% B): t_R = 16.94 min.

ESI-MS calc. for $C_{37}H_{31}NO_{10}S_3$ m/z: 745.83, meas. 744.18 $[M-H]^-$; calc. 372.92, meas. 371.96 $[M-2H]^{2-}$.

HR-MS calc. for $C_{37}H_{31}NO_{10}S$ m/z: 744.10373, meas. 744.10393 $[M-H]^-$.

^{1}H NMR (500 MHz, DMSO-d_6) δ: 2.38 (dd, J = 12.4, 5.0 Hz, 1H), 2.56 (dd, J = 12.6, 9.6 Hz, 1H), 3.77 (m, 1H), 4.37 (dd, J = 11.1; 5.8 Hz, 1H), 4.20 (t, J = 5.6 Hz, 1H), 4.41 (dd, J = 11.5, 6.5 Hz, 1H), 6.6 (d, J = 8.4 Hz, NH), 7.24 (t, J = 6.9 Hz, 3H), 7.3 (m, 12H), 7.68 (d, J = 7.9 Hz, 2H), 7.82 (d, J = 7.8 Hz, 2H), 7.90 (s, 1H), 7.91 (s, 1H).

^{13}C NMR (126 MHz, DMSO) δ: 32.52, 47.0, 53.58, 65.57, 66.28, 119.35, 122.0, 125.30, 126.67, 128.0, 129.0, 140.36, 143.97, 144.21, 147.4, 155.94, 171.63.

7.4.9. Synthesis of Smoc-L-Gln-OH 10

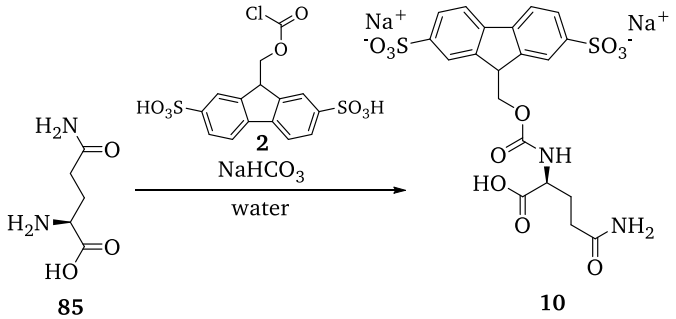

Scheme 34: Synthesis of Smoc-L-Gln-OH **10**.

According to the general procedure, 3.28g (22.45 mmol, 1 eq.) L-glutamine **85** and 9.36g (22.45 mmol, 1 eq.) Smoc-Cl **2** were dissolved in 30ml water and sodium hydrogen carbonate was added to adjust the pH to 8.5. The reaction mixture was stirred at ambient temperature and the solvent was removed by lyophilization. The product was isolated by preparative RP-

HPLC (gradient normalized B). After work up, 12.24g (90.8%) of Smoc-L-Gln-OH **10** were obtained as a white powder.

RP-HPLC (normalized B): t_R = 11.38 min.

ESI-MS calc. for $C_{20}H_{20}N_2O_{11}S_2$ m/z: 528.50, meas. 527.20 $[M-H]^-$; calc. 264.25, meas. 263.30 $[M-2H]^{2-}$.

HR-MS calc. for $C_{20}H_{20}N_2O_{11}S_2$ m/z: 529.05813, meas. 529.05847 $[M+H]^+$.

^{1}H NMR (500 MHz, DMSO-d_6) δ: 1.68 (m, 1H), 1.99 (m, 1H), 2.16 (ddd, J = 9.5, 6.8, 3.2 Hz, 2H), 3.88 (dt, J = 10.4, 5.0 Hz, 1H), 4.27 (t, J = 6.0 Hz, 1H), 4.32 (dd, J = 10.7, 5.7 Hz, 1H), 4.45 (dd, J = 10.7, 6.8 Hz, 1H), 7.54 (d, J = 7.7 Hz, NH), 7.69 (d, J = 7.8 Hz, 2H), 7.84 (d, J = 7.9 Hz, 2H), 7.90 (s, 1H), 7.93 (s, 1H).

^{13}C NMR (126 MHz, DMSO) δ: 26.16, 31.23, 46.86, 53.47, 65.18, 119.48, 122.15, 125.32, 140.45, 140.50, 143.67, 144.32, 147.12, 156.12, 173.58, 173.68.

7.4.10.Synthesis of Smoc-L-Glu(OtBu)-OH 11

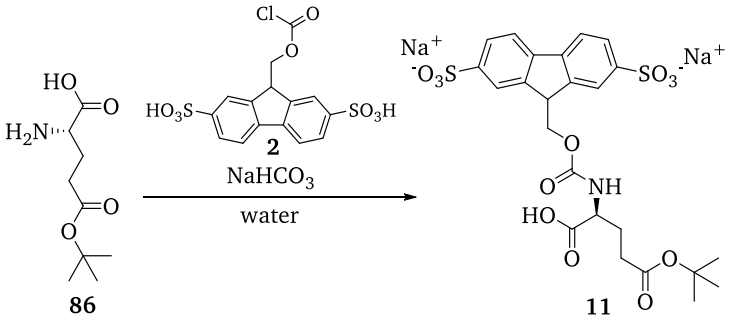

Scheme 35: Synthesis of Smoc-L-Glu(OtBu)-OH **11**.

According to the general procedure, 4.50g (22.14 mmol, 1 eq.) L-Glu(OtBu)-OH **86** and 9.23g (22.14 mmol, 1 eq.) Smoc-Cl **2** were dissolved in 30ml water and sodium hydrogen carbonate was added to adjust the pH to 8.5. The reaction mixture was stirred at ambient temperature and the solvent was removed by lyophilization. The product was isolated by preparative RP-HPLC (gradient 0 to 60% B). After work up, 12.29g (88.2%) of Smoc-L-Glu(OtBu)-OH **11** were obtained as a white powder.

RP-HPLC (0 to 60% B): t_R = 16.31 min.

ESI-MS calc. for $C_{24}H_{27}NO_{12}S_2$ m/z: 585.60, meas. 584.08 $[M-H]^-$; calc. 292.80, meas. 291.85 $[M-2H]^{2-}$.

HR-MS calc. for $C_{24}H_{27}NO_{12}S_2$ m/z: 608.08669, meas. 608.08709 $[M+H]^+$; calc. 624.06063 meas. 624.06093 $[M+K]^+$.

^{1}H NMR (500 MHz, DMSO-d_6) δ: 1.38 (s, 9H), 1.78 (tt, J = 12.1, 5.6, 1H), 1.90 (tt, J = 10.7, 5.2, 1H), 2.12 (ddd, J = 16.0, 10.8, 5.3 Hz, 1H), 2.23 (ddd, J = 16.1, 10.9, 5.5 Hz, 1H), 3.65 (q, J = 6.0 Hz, 1H), 4.23 (m, 3H), 6.63 (d, J = 6.7 Hz, NH), 7.69 (d, J = 8.0 Hz, 2H), 7.83 (d, J = 8.0 Hz, 2H), 7.89 (s, 1H), 7.94 (s, 1H).

^{13}C NMR (126 MHz, DMSO) δ: 27.73, 27.96, 30.73, 46.20, 54.80, 65.20, 79.13; 119.30, 122.30, 125.00, 140.31, 143.95, 147.20, 155.50, 172.40, 173.50.

7.4.11.Synthesis of Smoc-Gly-OH 12

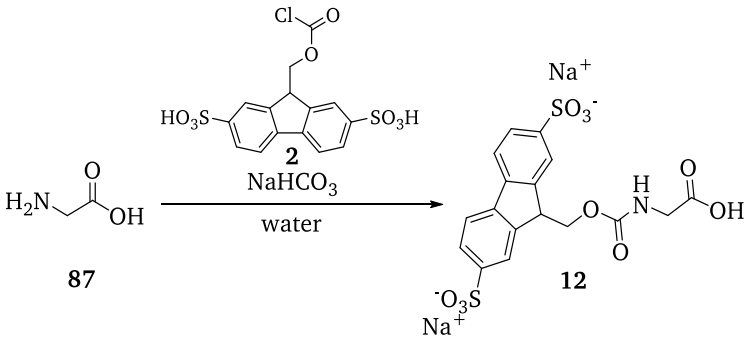

Scheme 36: Synthesis of Smoc-Gly-OH **12**.

According to the general procedure, 1.69g (22.45 mmol, 1 eq.) glycine **87** and 9.36g (22.45 mmol, 1 eq.) Smoc-Cl **2** were dissolved in 30ml water and sodium hydrogen carbonate was added to adjust the pH to 8.5. The reaction mixture was stirred at ambient temperature and the solvent was removed by lyophilization. The product was isolated by preparative RP-HPLC (gradient normalized B). After work up, 10.55g (93.7%) of Smoc-Gly-OH **12** were obtained as a white powder.

RP-HPLC (normalized B): t_R = 11.48 min.

ESI-MS calc. for $C_{17}H_{15}NO_{10}S_2$ m/z: 457.42, meas. 456.17 $[M-H]^-$; calc. 228.71, meas. 227.84 $[M-2H]^{2-}$.

HR-MS calc. for $C_{17}H_{15}NO_{10}S_2$ m/z: 458.02101, meas. 458.02086 $[M+H]^+$.

^{1}H NMR (500 MHz, DMSO-d_6) δ: 3.61 (s, 2H), 4.25 (t, J = 5.7 Hz, 1H), 4.43 (d, J = 5.8 Hz, 2H), 7.49 (br, NH), 7.69 (d, J = 7.9, 2H), 7.85 (d, J = 7.9 Hz, 2H), 7.91 (s, 2H).

^{13}C NMR (126 MHz, DMSO) δ: 42.15, 46.97, 65.37, 119.56, 122.05, 125.36, 140.59, 144.11, 147.04, 156.52, 171.39.

7.4.12.Synthesis of Smoc-L-His-OH 13

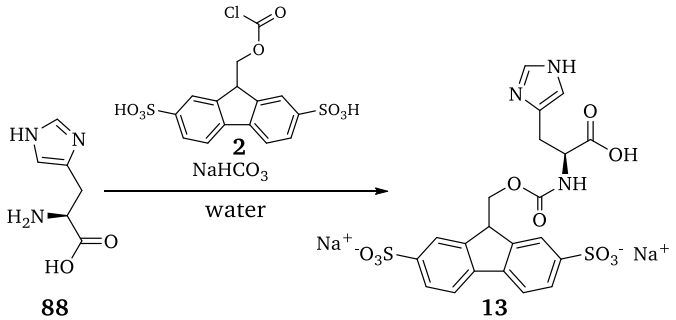

Scheme 37: Synthesis of Smoc-L-His-OH **13**.

According to the general procedure, 3.48g (22.45 mmol, 1 eq.) L-histidine **88** and 9.36g (22.45 mmol, 1 eq.) Smoc-Cl **2** were dissolved in 30ml water and sodium hydrogen carbonate was added to adjust the pH to 8.5. The reaction mixture was stirred at ambient temperature and the solvent was removed by lyophilization. The product was isolated by preparative RP-HPLC (gradient normalized B). After work up, 12.06g (92.4%) of Smoc-L-His-OH **13** were obtained as a white powder.

RP-HPLC (normalized B): t_R = 11.90 min.

ESI-MS calc. for $C_{21}H_{19}N_3O_{10}S_2$ m/z: 537.51, meas. 536.40 $[M-H]^-$; calc. 268.76, meas. 267.80 $[M-2H]^{2-}$.

HR-MS calc. for $C_{21}H_{19}N_3O_{10}S_2$ m/z: 538.05846, meas. 538.05888 $[M+H]^+$.

^{1}H NMR (500 MHz, DMSO-d_6) δ: 2.94 (dd, J = 15.0, 7.9 Hz, 1H), 3.13 (dd, J = 15.0, 4.4 Hz, 1H), 4.23 (m, 1H), 4.33 (dd, J = 10.8, 5.3 Hz, 1H), 4.41 (dd, J = 10.8, 6.8 Hz, 1H), 7.27 (s, 1H), 7.66 (d, J = 8.8 Hz, NH), 7.71 (d, J = 7.9 Hz, 2H), 7.84 (s, 1H), 7.85 (d, J = 7.9 Hz, 2H), 7.92 (s, 1H), 8.92 (s, 1H).

^{13}C NMR (126 MHz, DMSO) δ 26.03, 46.69, 52.73, 65.12, 117.38, 119.65, 121.90, 122.00, 125.36, 129.28, 133.71, 140.57, 140.66, 143.60, 144.34, 146.86, 155.78, 171.97.

7.4.13.Synthesis of Smoc-L-His(Trt)-OH 14

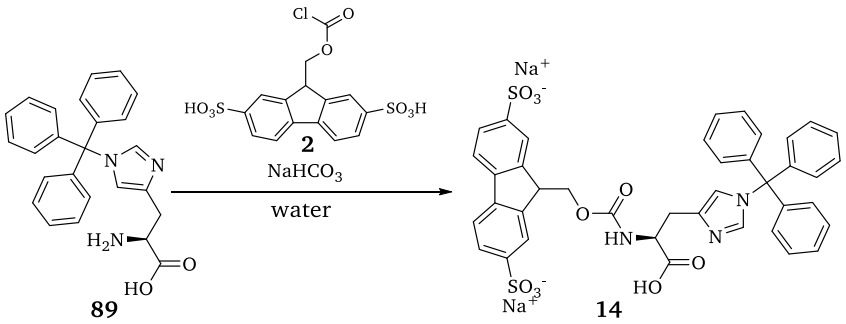

Scheme 38: Synthesis of Smoc-L-His(Trt)-OH **14**.

According to the general procedure, 2.89g (7.27 mmol, 1 eq.) L-His(Trt)-OH **89** and 3.03g (7.27 mmol, 1 eq.) Smoc-Cl **2** were dissolved in 50ml water acetonitrile mixture (1:1) and sodium hydrogen carbonate was added to adjust the pH to 8.5. The reaction mixture was stirred at ambient temperature and the solvent was removed by lyophilization. The product was isolated by preparative RP-HPLC (30 to 100% B). After work up, 5.19g (86.6%) of Smoc-L-His(Trt)-OH **14** were obtained as a white powder.

RP-HPLC (10 to 100% B): t_R = 15.28 min.

ESI-MS calc. for $C_{40}H_{33}N_3O_{10}S_2$ m/z: 779.84, meas. 778.19 $[M-H]^-$; calc. 389.92, meas. 388.86 $[M-2H]^{2-}$.

HR-MS calc. for $C_{40}H_{33}N_3O_{10}S_2$ m/z: 780.16801, meas. 780.16788 $[M+H]^+$.

^{1}H NMR (500 MHz, DMSO-d_6) δ: 2.65 (dd, J = 14.9, 8.6 Hz, 1H), 2.99 (dd, J = 14.8, 4.6 Hz, 1H), 3.94 (m, 1H), 3.96 (m, 1H), 4.13 (m, 1H), 4.19 (t, J = 6.3 Hz, 1H), 6.97 (br, NH), 7.06 (m, 9H), 7.22 (br, 1H), 7.37 (m, 6H), 7.69 (d, J = 7.7 Hz, 2H), 7.84 (d, J = 7.7 Hz, 2H), 7.89 (s, 1H), 7.99 (s, 1H).

^{13}C NMR (126 MHz, DMSO) δ: 31.95, 46.9, 55.81, 65.23, 74.38, 118.80, 119.10, 122.30, 125.60, 127.50, 128.5, 128.9, 137.50, 138.30, 140.80, 142.40, 143.76, 144.00, 147.65, 156.0, 171.29.

7.4.14.Synthesis of Smoc-L-Ile-OH 15

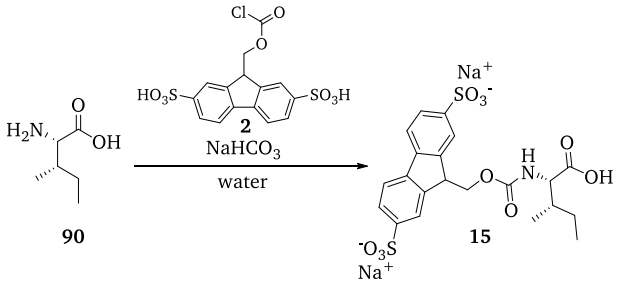

Scheme 39: Synthesis of Smoc-L-Ile-OH **15**.

According to the general procedure, 2.94g (22.45 mmol, 1 eq.) L-isoleucine **90** and 9.36g (22.45 mmol, 1 eq.) Smoc-Cl **2** were dissolved in 30ml water acetonitrile mixture (3:1) and sodium hydrogen carbonate was added to adjust the pH to 8.5. The reaction mixture was stirred at ambient temperature and the solvent was removed by lyophilization. The product was isolated by preparative RP-HPLC (gradient normalized B). After work up, 11.13g (88.9%) of Smoc-L-isoleucine **15** were obtained as a white powder.

RP-HPLC (normalized B): t_R = 17.12 min.

ESI-MS calc. for $C_{21}H_{23}NO_{10}S_2$ m/z: 513.53, meas. 512.17 $[M-H]^-$; calc. 256.77, meas. 255.84 $[M-2H]^{2-}$.

HR-MS calc. for $C_{21}H_{23}NO_{10}S_2$ m/z: 514.08361, meas. 514.08407 $[M+H]^+$.

^{1}H NMR (500 MHz, DMSO-d_6) δ: 0.81 (d, J = 7.4 Hz, 3H), 0.84 (d, J = 6.9 Hz, 3H), 1.17 (ddq, J = 13.6, 8.9, 7.3 Hz, 1H), 1.39 (ddq, J = 13.6, 7.4, 4.5 Hz, 1H), 1.75 (m, 1H), 3.87 (t, J = 6.5 Hz, 1H), 4.23 (t, J = 5.8 Hz, 1H), 4.37 (dd, J = 10.9, 5.7 Hz, 1H), 4.86 (dd, J = 10.9, 5.9 Hz, 1H), 7.46 (d, J = 8.1 Hz, NH), 7.68 (dd, J = 7.9, 1.2 Hz, 2H), 7.83 (d, J = 7.9 Hz, 2H), 7.92 (s, 2H).

^{13}C NMR (126 MHz, DMSO) δ: 11.22, 15.48, 24.88, 35.72, 47.11, 58.68, 65.46, 119.44, 122.09, 125.31, 140.48, 144.03, 144.16, 147.15, 147.17, 156.44, 173.06.

7.4.15.Synthesis of Smoc-L-Leu-OH 16

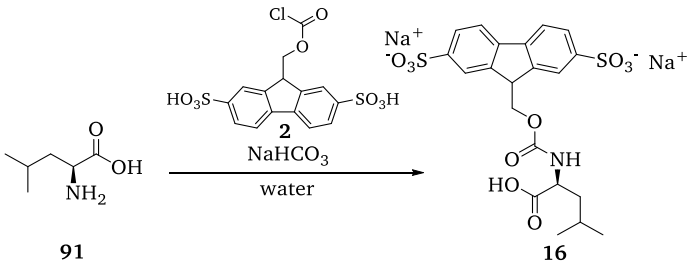

Scheme 40: Synthesis of Smoc-L-Leu-OH **16**.

According to the general procedure, 2.94g (22.45 mmol, 1 eq.) L-leucine **91** and 9.36g (22.45 mmol, 1 eq.) Smoc-Cl **2** were dissolved in 30ml water acetonitrile mixture (3:1) and sodium hydrogen carbonate was added to adjust the pH to 8.5. The reaction mixture was stirred at ambient temperature and the solvent was removed by lyophilization. The product was isolated by preparative RP-HPLC (gradient normalized B). After work up, 11.33g (90.6%) of Smoc-L-leucine **16** were obtained as a white powder.

RP-HPLC (normalized B): t_R = 17.52 min.

ESI-MS calc. for $C_{21}H_{23}NO_{10}S_2$ m/z: 513.53, meas. 512.17 $[M-H]^-$; calc. 256.77, meas. 255.84 $[M-2H]^{2-}$.

HR-MS calc. for $C_{21}H_{23}NO_{10}S_{22}$ m/z: 514.08361, meas. 514.08410 $[M+H]^+$.

^{1}H NMR (500 MHz, DMSO-d_6) δ: 0.83 (d, J = 6.5 Hz, 3H), 0.85 (d, J = 6.6 Hz, 3H), 1.41 (ddd, J = 13.5, 9.0, 4.9 Hz, 1H), 1.53 (ddd, J = 13.5, 10.2, 5.1 Hz, 1H), 1.61 (m, 1H), 3.93 (dt, J = 10.7, 5.4 Hz, 1H), 4.22 (t, J = 5.6 Hz, 1H), 4.38 (dd, J = 11.0, 5.6 Hz, 1H), 4.46 (dd, J = 11.0, 5.6 Hz, 1H), 7.51 (d, J = 7.9 Hz, NH), 7.68 (d, J = 8.0, 2H), 7.83 (d, J = 8.0 Hz, 2H), 7.90 (s, 1H), 7.91 (s, 1H).

^{13}C NMR (126 MHz, DMSO) δ: 21.28, 22.78, 24.17, 39.5, 47.06, 52.28, 65.35, 119.37, 122.00, 125.27, 140.42, 144.01, 144.09, 147.29, 156.29, 174.17.

7.4.16.Synthesis of Smoc-D-Leu-OH 17

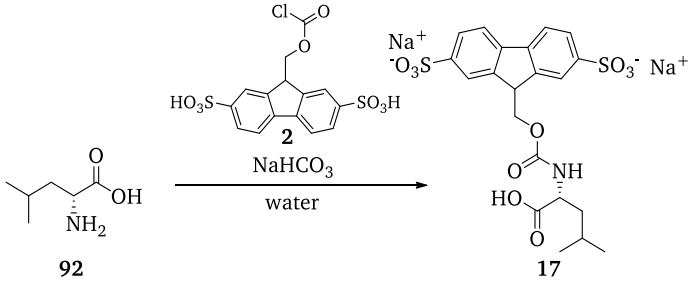

Scheme 41: Synthesis of Smoc-D-Leu-OH **17**.

According to the general procedure, 2.94g (22.45 mmol, 1 eq.) D-leucine **92** and 9.36g (22.45 mmol, 1 eq.) Smoc-Cl **2** were dissolved in 30ml water acetonitrile mixture (3:1) and sodium hydrogen carbonate was added to adjust the pH to 8.5. The reaction mixture was stirred at ambient temperature and the solvent was removed by lyophilization. The product was isolated by preparative RP-HPLC (gradient normalized B). After work up, 11.10g (88.7%) of Smoc-D-leucine **17** were obtained as a white powder.

RP-HPLC (normalized B): t_R = 17.70 min.

ESI-MS calc. for $C_{21}H_{23}NO_{10}S_2$ m/z: 513.53, meas. 512.07 $[M-H]^-$; calc. 256.77, meas. 255.84 $[M-2H]^{2-}$.

HR-MS calc. for $C_{15}H_{11}ClO_8S_2$ m/z: 512.0691, meas. 512.0739 $[M-H]^-$.

^{1}H NMR (500 MHz, DMSO-d_6) δ: 0.82 (d, J = 6.6 Hz, 3H), 0.85 (d, J = 6.6 Hz, 3H), 1.41 (ddd, J = 13.7, 9.0, 4.9 Hz, 1H), 1.52 (ddd, J = 13.7, 10.1, 5.1 Hz, 1H), 1.61 (m, 1H), 3.92 (dd, J = 9.7, 4.8 Hz, 1H), 4.23 (t, J = 5.6 Hz, 1H), 4.39 (dd, J = 11.0, 5.6 Hz, 1H), 4.47 (dd, J = 11.0, 5.7 Hz, 1H), 7.51 (br, NH), 7.69 (d, J = 8.0, 2H), 7.85 (dd, J = 8.0, 1.5 Hz, 2H), 7.92 (s, 1H), 7.93 (s, 1H).

^{13}C NMR (126 MHz, DMSO) δ: 21.33, 22.83, 24.23, 39.56, 47.12, 52.32, 65.35, 119.56, 122.07, 125.36, 140.61, 144.14, 144.23, 146.96, 146.99, 156.33, 174.23.

7.4.17.Synthesis of Smoc-L-Lys(Boc)-OH 18

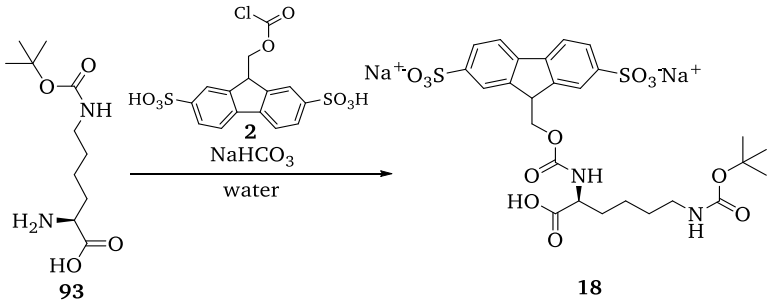

Scheme 42: Synthesis of Smoc-L-Lys(Boc)-OH **18**.

According to the general procedure, 5.53g (22.45 mmol, 1 eq.) L-Lys(Boc)-OH **93** and 9.36g (22.45 mmol, 1 eq.) Smoc-Cl **2** were dissolved in 30ml water and sodium hydrogen carbonate was added to adjust the pH to 8.5. The reaction mixture was stirred at ambient temperature and the solvent was removed by lyophilization. The product was isolated by preparative RP-HPLC (0 to 60% B). After work up, 13.20g (87.4%) of Smoc-L-Lys(Boc)-OH **18** were obtained as a white powder.

RP-HPLC (0 to 60% B): t_R = 16.96 min.

ESI-MS calc. for $C_{26}H_{32}N_2O_{12}S_2$ m/z: 628.66, meas. 627.09 $[M-H]^-$; calc. 314.33, meas. 313.35 $[M-2H]^{2-}$.

HR-MS calc. for $C_{26}H_{32}N_2O_{12}S_2$ m/z: 629.14694, meas. 629.14704 $[M+H]^+$.

^{1}H NMR (500 MHz, DMSO-d_6) δ: 1.22 (m, 2H), 1.33 (m, 11H), 1.54 (m, 1H), 1.64 (dq, J = 10.3, 5.4 Hz, 1H), 2.86 (dt, J = 7.4, 6.9 Hz, 2H), 3.61 (q, J = 6.1 Hz, 1H), 4.23 (m, 2H), 4.24 (t, 1H), 6.56 (br, NH), 6.69 (br, NH), 7.68 (dd, J = 7.9, 1.4 Hz, 2H), 7.82 (d, J = 7.9 Hz, 2H), 7.88 (s, 1H), 7.93 (s, 1H).

^{13}C NMR (126 MHz, DMSO) δ: 22.53, 28.24, 29.60, 32.44, 40.03, 46.75, 55.58, 65.30, 77.14, 119.33, 122.26, 122.38, 125.22, 140.30, 143.92, 144.08, 147.24, 147.31, 155.24, 155.45, 173.58.

7.4.18.Synthesis of Smoc-L-Met-OH 19

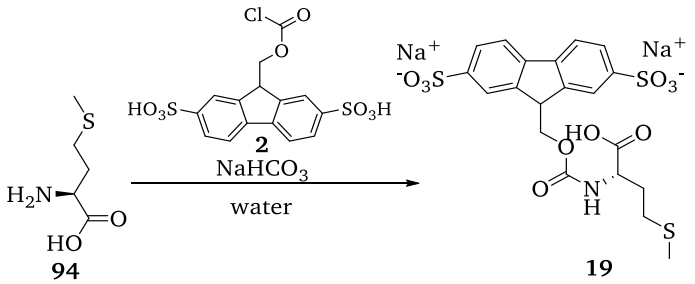

Scheme 43: Synthesis of Smoc-L-Met-OH **19**.

According to the general procedure, 3.35g (22.45 mmol, 1 eq.) L-methionine **94** and 9.36g (22.45 mmol, 1 eq.) Smoc-Cl **2** were dissolved in 30ml water and sodium hydrogen carbonate was added to adjust the pH to 8.5. The reaction mixture was stirred at ambient temperature and the solvent was removed by lyophilization. The product was isolated by preparative RP-HPLC (gradient normalized B). After work up, 12.29g (95.1%) of Smoc-L-Met-OH **19** were obtained as a white powder.

RP-HPLC (normalized B): t_R = 15.27 min.

ESI-MS calc. for $C_{20}H_{21}NO_{10}S_3$ m/z: 531.57, meas. 530.10 $[M-H]^-$; calc. 265.79, meas. 264.80 $[M-2H]^{2-}$.

HR-MS calc. for $C_{20}H_{21}NO_{10}S_3$ m/z: 432.04004, meas. 432.04046 $[M+H]^+$.

^{1}H NMR (500 MHz, DMSO-d_6) δ: 1.87 (m, 2H), 2.01 (s, 3H), 2.47 (m, 2H), 4.03 (dt, J = 7.7, 5.6 Hz, 1H), 4.24 (t, J = 5.7 Hz, 1H), 4.38 (dd, J = 10.9, 5.6 Hz, 1H), 4.47 (dd, J = 10.9, 5.9 Hz, 1H), 7.60 (d, J = 7.6 Hz, NH), 7.69 (dd, J = 7.9, 1.2 Hz, 2H), 7.84 (d, J = 7.9 Hz, 2H), 7.91 (s, 1H), 7.92 (s, 1H).

^{13}C NMR (126 MHz, DMSO) δ: 14.53, 29.83, 30.31, 47.06, 52.93, 65.33, 119.53, 122.10, 125.36, 140.56, 144.02, 144.18, 156.33, 173.50.

7.4.19.Synthesis of Smoc-L-Phe-OH 20

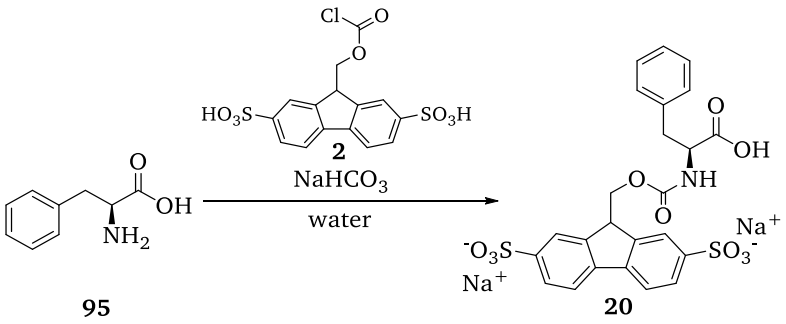

Scheme 44: Synthesis of Smoc-L-Phe-OH **20**.

According to the general procedure, 3.71g (22.45 mmol, 1 eq.) L-Phe **95** and 9.36g (22.45 mmol, 1 eq.) Smoc-Cl **2** were dissolved in 30ml water and sodium hydrogen carbonate was added to adjust the pH to 8.5. The reaction mixture was stirred at ambient temperature and the solvent was removed by lyophilization. The product was isolated by preparative RP-HPLC (gradient normalized B). After work up, 12.44g (93.7%) of Smoc-L-Phe-OH **20** were obtained as a white powder.

RP-HPLC (normalized B): t_R = 18.32 min.

ESI-MS calc. for $C_{24}H_{21}NO_{10}S_2$ m/z: 547.55, meas. 546.20 $[M-H]^-$; calc. 273.76, meas. 272.80 $[M-2H]^{2-}$.

HR-MS calc. for $C_{24}H_{21}NO_{10}S_2$ m/z: 548.06796, meas. 548.06857 $[M+H]^+$.

^{1}H NMR (500 MHz, DMSO-d_6) δ: 2.88 (dd, J = 13.8, 9.5 Hz, 1H), 2.99 (dd, J = 13.8, 5.3 Hz, 1H), 4.12 (m, 1H), 4.16 (t, J = 5.5 Hz, 1H), 4.33 (dd, J = 11.0, 5.8 Hz, 1H), 4.38 (dd, J = 11.0, 5.7 Hz, 1H), 7.15 (t, J = 7.2 Hz, 1H), 7.22 (d, J = 7.4 Hz, 2H), 7.26 (t, J = 7.5 Hz, 2H), 7.61 (d, J = 8.1 Hz, NH), 7.69 (dd, J = 7.9, 1.2 Hz, 2H), 7.83 (d, J = 7.9 Hz, 2H), 7.90 (s, 2H).

^{13}C NMR (126 MHz, DMSO) δ: 36.43, 47.05, 55.65, 65.37, 119.43, 122.02, 122.08, 125.31, 126.22, 128.19, 129.06, 137.81, 140.44, 143.99, 144.05, 147.20, 156.05, 173.02.

7.4.20.Synthesis of Smoc-L-Pro-OH 21

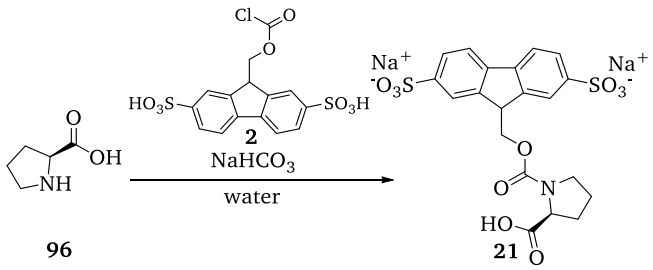

Scheme 45: Synthesis of Smoc-L-Pro-OH **21**.

According to the general procedure, 2.58g (22.45 mmol, 1 eq.) L-Pro **96** and 9.36g (22.45 mmol, 1 eq.) Smoc-Cl **2** were dissolved in 30ml water and sodium hydrogen carbonate was added to adjust the pH to 8.5. The reaction mixture was stirred at ambient temperature and the solvent was removed by lyophilization. The product was isolated by preparative RP-HPLC (gradient normalized B). After work up, 10.43g (85.8%) of Smoc-L-Pro-OH **21** were obtained as a white powder.

RP-HPLC (normalized B): t_R = 13.50 min.

ESI-MS calc. for $C_{20}H_{19}NO_{10}S_2$ m/z: 497.49, meas. 496.17 $[M-H]^-$; calc. 248.75, meas. 247.84 $[M-2H]^{2-}$.

HR-MS calc. for $C_{20}H_{19}NO_{10}S_2$ m/z: 498.05231, meas. 498.05248 $[M+H]^+$.

^{1}H NMR (500 MHz, DMSO-d_6) δ: 1.85 (m, 3H), 2.21 (m, 1H), 3.41 (m, 2H), 4.17 (dd, J = 8.6, 3.2 Hz, 1H), 4.20 – 4.30 (m, 2H), 4.29 (t, J = 5.6 Hz, 1H), 7.68 (dd, J = 7.9, 1.4 Hz, 2H), 7.84 (d, J = 7.9 Hz, 2H), 7.91 (d, J = 1.4 Hz, 1H), 7.92 (d, J = 1.4 Hz, 1H).

^{13}C NMR (126 MHz, DMSO) δ: 23.90, 29.34, 46.47, 58.85, 119.49, 122.42, 125.30, 140.43, 143.66, 143.90, 147.17, 153.84, 173.50.

7.4.21.Synthesis of Smoc-L-Ser-OH 22

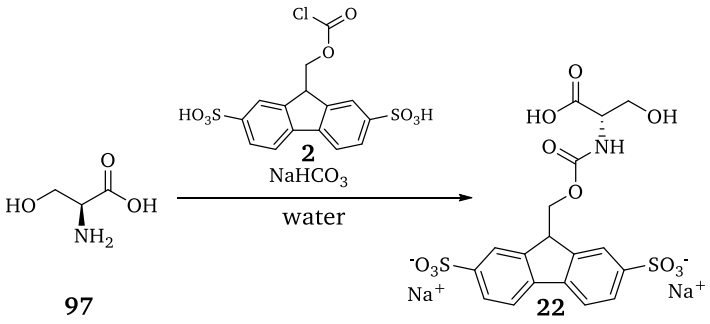

Scheme 46: Synthesis of Smoc-L-Ser-OH **22**.

According to the general procedure, 2.36g (22.45 mmol, 1 eq.) L-Ser-OH **97** and 9.36g (22.45 mmol, 1 eq.) Smoc-Cl **2** were dissolved in 30ml water and sodium hydrogen carbonate was added to adjust the pH to 8.5. The reaction mixture was stirred at ambient temperature and the solvent was removed by lyophilization. The product was isolated by preparative RP-HPLC (gradient normalized B). After work up, 10.74g (90.0%) of Smoc-L-Ser-OH **22** were obtained as a white powder.

RP-HPLC (normalized B): t_R = 11.30 min.

ESI-MS calc. for $C_{18}H_{17}NO_{11}S_2$ m/z: 487.45, meas. 486.20 $[M-H]^-$; calc. 243.73, meas. 242.80 $[M-2H]^{2-}$.

HR-MS calc. for $C_{18}H_{17}NO_{11}S_2$ m/z: 488.03158, meas. 488.03176 $[M+H]^+$.

^{1}H NMR (500 MHz, DMSO-d_6) δ: 3.62 (dd, J = 11.3, 5.3 Hz, 1H), 3.65 (dd, J = 11.3, 4.2 Hz, 1H), 4.00 (t, J = 5.2 Hz, 1H), 4.01 (br, OH), 4.25 (t, J = 5.7 Hz, 1H), 4.41 (dd, J = 11.0, 5.6 Hz, 1H), 4.47 (dd, J = 11.0, 6.0 Hz, 1H), 7.14 (br, NH), 7.69 (dd, J = 7.9, 1.5 Hz, 2H), 7.84 (d, J = 7.9 Hz, 2H), 7.90 (s, 1H), 7.92 (s, 1H).

^{13}C NMR (126 MHz, DMSO) δ: 46.96, 56.72, 61.27, 65.29, 119.53, 122.00, 122.07, 125.32, 140.54, 143.92, 144.20, 147.10, 156.01, 171.94.

7.4.22.Synthesis of Smoc-L-Ser(tBu)-OH 23

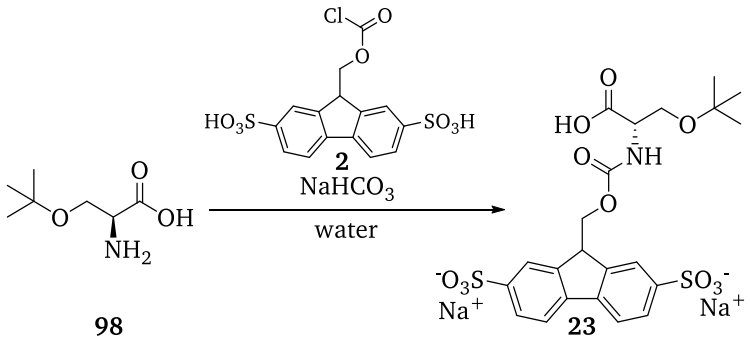

Scheme 47: Synthesis of Smoc-L-Ser(tBu)-OH **23**.

According to the general procedure, 3.62g (22.45 mmol, 1 eq.) L-Ser(tBu)-OH **98** and 9.36g (22.45 mmol, 1 eq.) Smoc-Cl **2** were dissolved in 30ml water and sodium hydrogen carbonate was added to adjust the pH to 8.5. The reaction mixture was stirred at ambient temperature and the solvent was removed by lyophilization. The product was isolated by preparative RP-HPLC (gradient 0 to 60% B). After work up, 11.59g (87.9%) of Smoc-L-Ser(tBu)-OH **23** were obtained as a white powder.

RP-HPLC (0 to 60% B): t_R = 14.36 min.

ESI-MS calc. for $C_{22}H_{25}NO_{11}S_2$ m/z: 543.56, meas. 542.08 $[M-H]^-$; calc. 271.78, meas. 270.84 $[M-2H]^{2-}$.

HR-MS calc. for $C_{22}H_{25}NO_{11}S$ m/z: 544.09418, meas. 544.09431 $[M+H]^+$.

^{1}H NMR (500 MHz, DMSO-d_6) δ: 1.10 (s, 9H), 3.54 (dd, J = 9.5, 4.9 Hz, 1H), 3.57 (dd, J = 9.5, 5.5 Hz, 1H), 4.08 (dt, J = 8.0, 5.2 Hz, 1H), 4.23 (t, J = 5.9 Hz, 1H), 4.37 (dd, J = 10.9, 5.9 Hz, 1H), 4.42 (dd, J = 10.9, 6.0 Hz, 1H), 7.17 (d, J = 8.1 Hz, NH), 7.69 (d, J = 7.9 Hz, 2H), 7.82 (d, J = 7.9 Hz, 2H), 7.92 (s, 2H).

^{13}C NMR (126 MHz, DMSO) δ: 27.14, 46.94, 54.90, 61.23, 65.60, 72.78, 119.32, 122.08, 125.29, 140.33, 143.87, 143.94, 147.43, 156.01, 171.79.

7.4.23.Synthesis of Smoc-L-Thr-OH 24

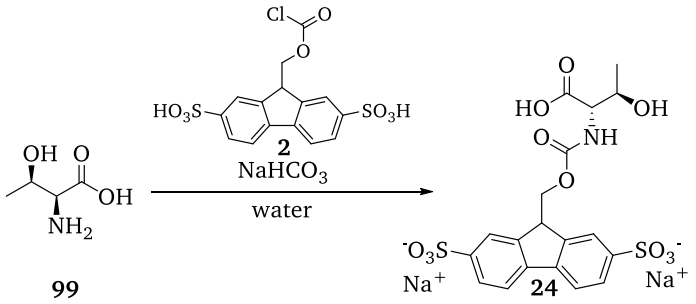

Scheme 48: Synthesis of Smoc-L-Thr-OH **24**.

According to the general procedure, 2.67g (22.45 mmol, 1 eq.) L-Thr-OH **99** and 9.36g (22.45 mmol, 1 eq.) Smoc-Cl **2** were dissolved in 30ml water and sodium hydrogen carbonate was added to adjust the pH to 8.5. The reaction mixture was stirred at ambient temperature and the solvent was removed by lyophilization. The product was isolated by preparative RP-HPLC (normalized B). After work up, 11.30 (92.2%) of Smoc-L-Thr-OH **24** were obtained as a white powder.

RP-HPLC (gradient normalized B): t_R = 12.07 min.

ESI-MS calc. for $C_{19}H_{19}NO_{11}S_2$ m/z: 501.48, meas. 500.07 $[M-H]^-$; calc. 250.74, meas. 249.84 $[M-2H]^{2-}$.

HR-MS calc. for $C_{19}H_{19}NO_{11}S_2$ m/z: 502.04723, meas. 502.04749 $[M+H]^+$.

^{1}H NMR (500 MHz, DMSO-d_6) δ: 1.07 (d, J = 6.5 Hz, 3H), 3.92 (dd, J = 8.1, 3.8 Hz, 1H), 4.02 (qd, J = 6.5, 3.7 Hz, 1H), 4.25 (t, J = 6.0 Hz, 1H), 4.39 (dd, J = 10.9, 5.7 Hz, 1H), 4.46 (dd, J = 10.9, 6.1 Hz, 1H), 6.83 (d, J = 8.7 Hz, NH), 7.69 (d, J = 7.9 Hz, 2H), 7.83 (d, J = 7.9 Hz, 2H), 7.91 (s, 1H), 7.92 (s, 1H).

^{13}C NMR (126 MHz, DMSO) δ: 20.32, 46.95, 60.18, 65.52, 66.44, 119.43, 122.07, 125.30, 140.44, 143.86, 144.07, 147.22, 156.38, 172.09.

7.4.24.Synthesis of Smoc-L-Thr(tBu)-OH 25

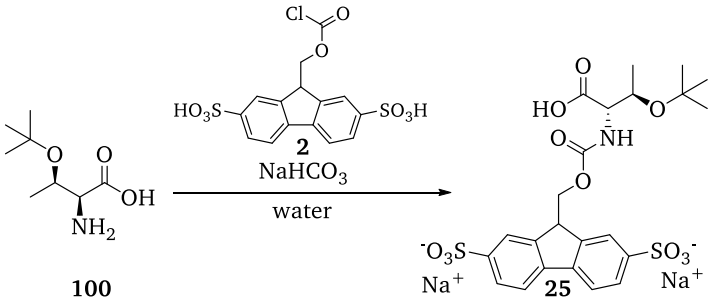

Scheme 49: Synthesis of Smoc-L-Thr(tBu)-OH **25**.

According to the general procedure, 3.93g (22.45 mmol, 1 eq.) L-Thr(tBu)-OH **100** and 9.36g (22.45 mmol, 1 eq.) Smoc-Cl **2** were dissolved in 30ml water and sodium hydrogen carbonate was added to adjust the pH to 8.5. The reaction mixture was stirred at ambient temperature and the solvent was removed by lyophilization. The product was isolated by preparative RP-HPLC (0 to 60% B). After work up, 12.05 (89.2%) of Smoc-L-Thr(tBu)-OH **25** were obtained as a white powder.

RP-HPLC (0 to 60% B): t_R = 15.14 min.

ESI-MS calc. for $C_{23}H_{27}NO_{11}S_2$ m/z: 557.59, meas. 556.08 $[M-H]^-$; calc. 278.80, meas. 277.74 $[M-2H]^{2-}$.

HR-MS calc. for $C_{23}H_{27}NO_{11}S_2$ m/z: 580.09177 meas. 580.09193 $[M+Na]^+$; m/z: calc. 596.06571 meas. 596.06589 $[M+K]^+$.

^{1}H NMR (500 MHz, DMSO-d_6) δ: 1.05 (d, J = 6.2 Hz, 3H), 1.10 (s, 9H), 3.59 (dd, J = 8.7, 3.3 Hz, 1H), 3.96 (dq, J = 6.2, 3.4 Hz, 1H), 4.23 (m, 3H), 6.18 (d, J = 8.7 Hz, NH), 7.69 (dd, J = 7.9, 1.5 Hz, 2H), 7.83 (d, J = 7.9 Hz, 2H), 7.90 (s, 1H), 7.96 (s, 1H).

^{13}C NMR (126 MHz, DMSO) δ: 21.08, 28.56, 46.54, 61.82, 65.58, 68.37, 72.43, 119.56, 122.60, 122.70, 125.55, 140.28, 143.95, 147.19, 156.10, 173.00.

7.4.25.Synthesis of Smoc-L-Trp-OH 26

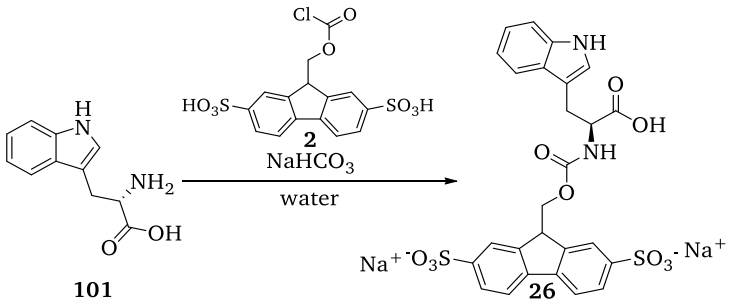

Scheme 50: Synthesis of Smoc-L-Trp-OH **26**.

According to the general procedure, 4.48g (22.45 mmol, 1 eq.) L-Trp-OH **101** and 9.36g (22.45 mmol, 1 eq.) Smoc-Cl **2** were dissolved in 30ml water and sodium hydrogen carbonate was added to adjust the pH to 8.5. The reaction mixture was stirred at ambient temperature and the solvent was removed by lyophilization. The product was isolated by preparative RP-HPLC (gradient normalized B). After work up, 12.84g (90.7%) of Smoc-Trp-OH **26** were obtained as a white powder.

RP-HPLC (normalized B): t_R = 19.55 min.

ESI-MS calc. for $C_{26}H_{22}N_2O_{10}S_2$ m/z: 586.59, meas. 585.20 $[M-H]^-$; calc. 293.30, meas. 292.30 $[M-2H]^{2-}$.

HR-MS calc. for $C_{26}H_{22}N_2O_{10}S_2$ m/z: 587.07886, meas. 587.07914 $[M+H]^+$.

^{1}H NMR (500 MHz, DMSO-d_6) δ: 2.95 (dd, J = 14.6, 9.9 Hz, 1H), 3.16 (dd, J = 14.6, 4.5 Hz, 1H), 4.12 (dt, J = 9.0, 4.5 Hz, 1H), 4.21 (t, J = 5.8 Hz, 1H), 4.29 (dd, J = 10.8, 5.5 Hz, 1H), 4.40 (dd, J = 10.8, 6.1 Hz, 1H), 6.96 (t, J = 7.4 Hz, 1H), 7.03 (t, J = 7.5 Hz, 1H), 7.14 (s, 1H), 7.29 (d, J = 7.5 Hz, 1H), 7.48 (d, J = 7.8 Hz, 1H), 7.53 (d, J = 8.2 Hz, 1H), 7.69, 7.70 (dd, J = 7.9, 2.5 Hz, 2H), 7.82, 7.83 (dd, J = 7.9, 2.5 Hz, 2H), 7.90 (s, 1H), 7.93 (s, 1H), 10.87 (s, NH).

^{13}C NMR (126 MHz, DMSO) δ: 26.53, 45.18, 46.90, 65.28, 109.67, 111.33, 117.81, 118.18, 119.54, 120.64, 122.02, 124.31, 125.32, 125.35, 127.04, 135.84, 140.54, 140.57, 143.96, 144.25, 147.00, 147.07, 155.96, 173.47.

7.4.26.Synthesis of Smoc-L-Trp(Boc)-OH 27

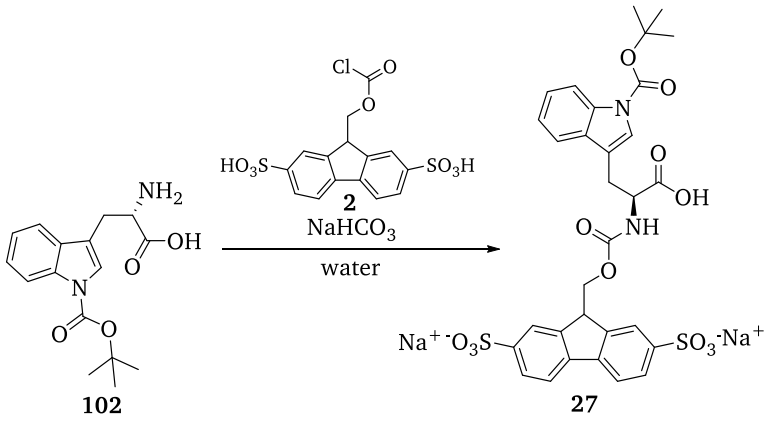

Scheme 51: Synthesis of Smoc-L-Trp(Boc)-OH **27**.

According to the general procedure, 3.00g (9.86 mmol, 1 eq.) L-Trp(Boc)-OH **102** and 4.11g (9.86 mmol, 1 eq.) Smoc-Cl **2** were dissolved in 30ml water and sodium hydrogen carbonate was added to adjust the pH to 8.5. The reaction mixture was stirred at ambient temperature and the solvent was removed by lyophilization. The product was isolated by preparative RP-HPLC (gradient 0 to 80% B). After work up, 6.26g (86.9%) of Smoc-Trp(Boc)-OH **27** were obtained as a white powder.

RP-HPLC (0 to 100% B): t_R = 15.14 min.

ESI-MS calc. for $C_{31}H_{30}N_2O_{12}S_2$ m/z: 686.70, meas. 685.08 $[M-H]^-$; calc. 343.35, meas. 342.36 $[M-2H]^{2-}$.

HR-MS calc. for $C_{31}H_{30}N_2O_{12}S_2$ m/z: 685.11679, meas. 685.11674 $[M-H]^-$.

^{1}H NMR (500 MHz, DMSO-d_6) δ: 1.61 (s, 9H), 2.97 (dd, J = 14.6, 6.3 Hz, 1H), 3.16 (dd, J = 14.6, 5.4 Hz, 1H), 3.93 (q, J = 6.1 Hz, 1H), 4.18 (s, 3H), 6.72 (d, J = 6.8 Hz, 1H), 7.21 (t, J = 7.4 Hz, 2H), 7.26 (t, J = 7.7 Hz, 1H), 7.43 (s, 1H), 7.64 (d, J = 7.7 Hz, 1H), 7.69 (d, J = 7.9 Hz, 4H), 7.82 (d, J = 7.9 Hz, 3H), 7.87 (s, 1H), 7.94 (s, 1H), 8.00 (d, J = 8.2 Hz, 1H).

^{13}C NMR (126 MHz, DMSO) δ: 27.4, 27.69, 55.99, 65.18, 83.24, 110.23, 114.30, 118.13, 118.55, 119.29, 119.37, 122.21, 122.30, 122.5, 123.48, 123.91, 125.2, 130.90, 134.56, 137.32, 138.88, 142.08, 147.77, 149.10, 173.45.

7.4.27.Synthesis of Smoc-L-Tyr-OH 28

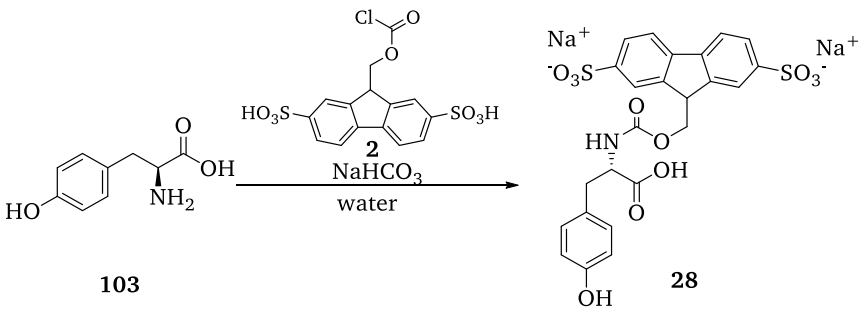

Scheme 52: Synthesis of Smoc-L-Tyr-OH **28**.

According to the general procedure, 4.07g (22.45 mmol, 1 eq.) L-Tyr-OH **103** and 9.36g (22.45 mmol, 1 eq.) Smoc-Cl **2** were dissolved in 30ml water and sodium hydrogen carbonate was added to adjust the pH to 8.5. The reaction mixture was stirred at ambient temperature and the

solvent was removed by lyophilization. The product was isolated by preparative RP-HPLC (gradient normalized B). After work up, 12.24g (89.7%) of Smoc-L-Tyr-OH **28** were obtained as a white powder.

RP-HPLC (normalized B): t_R = 15.65 min.

ESI-MS calc. for $C_{24}H_{21}NO_{11}S_2$ m/z: 563.55, meas. 562.20 $[M-H]^-$; calc. 281.77, meas. 280.80 $[M-2H]^{2-}$.

HR-MS calc. for $C_{24}H_{21}NO_{11}S_2$ m/z: 564.06288, meas. 564.06314 $[M+H]^+$; m/z: calc. 586.04482 meas. 586.04494 $[M+Na]^+$.

^{1}H NMR (500 MHz, DMSO-d_6) δ: 2.74 (dd, J = 13.9, 9.3 Hz, 1H), 2.86 (dd, J = 13.9, 5.4 Hz, 1H), 4.03 (q, J = 7.1 Hz, 1H), 4.18 (t, J = 5.7 Hz, 1H), 4.33 (dd, J = 11.0, 5.8 Hz, 1H), 4.39 (dd, J = 11.0, 5.7 Hz, 1H), 6.64 (d, J = 8.1 Hz, 2H), 6.98 (d, J = 8.0 Hz, 2H), 7.50 (d, J = 8.0 Hz, NH), 7.69 (d, J = 8.0 Hz, 2H), 7.84 (d, J = 7.9 Hz, 2H), 7.90 (s, 2H), 8.15 (s, OH).

^{13}C NMR (126 MHz, DMSO) δ: 35.74, 47.06, 56.00, 65.33, 115.05, 119.50, 122.05, 125.34, 127.80, 129.97, 140.52, 144.10, 147.06, 147.13, 155.77, 156.05, 173.19.

7.4.28.Synthesis of Smoc-L-Tyr(tBu)-OH 29

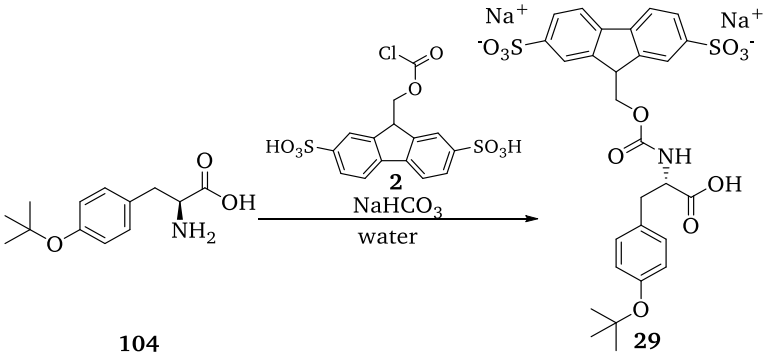

Scheme 53: Synthesis of Smoc-L-Tyr(tBu)-OH **29**.

According to the general procedure, 5.33g (22.45 mmol, 1 eq.) L-Tyr(tBu)-OH **104** and 9.36g (22.45 mmol, 1 eq.) Smoc-Cl **2** were dissolved in 30ml water and sodium hydrogen carbonate was added to adjust the pH to 8.5. The reaction mixture was stirred at ambient temperature and the solvent was removed by lyophilization. The product was isolated by preparative RP-HPLC (gradient 0 to 60% B). After work up, 13.61g (91.4%) of Smoc-L-Tyr(tBu)-OH **29** were obtained as a white powder.

RP-HPLC (0 to 60% B): t_R = 17.95 min.

ESI-MS calc. for $C_{28}H_{29}NO_{11}S_2$ m/z: 619.66, meas. 618.09 $[M-H]^-$; calc. 309.83, meas. 308.85 $[M-2H]^{2-}$.

HR-MS calc. for $C_{28}H_{29}NO_{11}S_2$ m/z: 620.12548, meas. 620.12539 $[M+H]^+$.

^{1}H NMR (500 MHz, DMSO-d_6) δ: 1.21 (s, 9H), 2.79 (dd, J = 13.6, 7.1 Hz, 1H), 3.00 (dd, J = 13.6, 4.9 Hz, 1H), 3.83 (q, J = 6.6 Hz, 1H), 4.14 (m, 3H), 6.51 (d, J = 7.2 Hz, NH), 6.78 (d, J = 8.0 Hz, 2H), 7.07 (d, J = 8.1 Hz, 2H), 7.68 (d, J = 8.0 Hz, 2H), 7.81 (d, J = 8.0 Hz, 2H), 7.86 (s, 1H), 7.92 (s, 1H).

^{13}C NMR (126 MHz, DMSO) δ: 28.54, 37.56, 46.53, 57.47, 65.34, 77.37, 119.48, 122.71, 123.09, 125.50, 129.71, 134.06, 140.24, 143.89, 147.78, 152.97, 155.31, 173.08.

7.4.29.Synthesis of Smoc-L-Val-OH 30

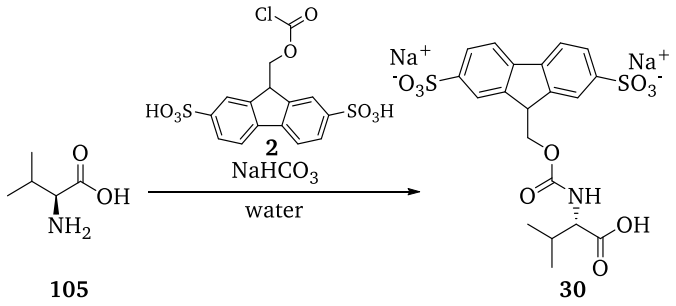

Scheme 54: Synthesis of Smoc-L-Val-OH **30**.

According to the general procedure, 2.63g (22.45 mmol, 1 eq.) L-Val-OH **105** and 9.36g (22.45 mmol, 1 eq.) Smoc-Cl **2** were dissolved in 30ml water and sodium hydrogen carbonate was added to adjust the pH to 8.5. The reaction mixture was stirred at ambient temperature and the solvent was removed by lyophilization. The product was isolated by preparative RP-HPLC (gradient normalized B). After work up, 10.64g (87.2%) of Smoc-L-Val-OH **30** were obtained as a white powder.

RP-HPLC (normalized B): t_R = 15.04 min.

ESI-MS calc. for $C_{20}H_{21}NO_{10}S_2$ m/z: 499.51, meas. 498.20 $[M-H]^-$; calc. 249.76, meas. 248.80 $[M-2H]^{2-}$.

HR-MS calc. for $C_{20}H_{21}NO_{10}S_2$ m/z: 500.06796 meas. 500.06823 $[M+H]^+$.

^{1}H NMR (500 MHz, DMSO-d_6) δ: 0.87 (d, J = 6.8 Hz, 6H), 2.00 (oct, J = 13.9 Hz, 1H), 2.86 (dd, J = 13.9, 5.4 Hz, 1H), 3.81 (t, J = 6.7 Hz, 1H), 4.23 (t, J = 5.7 Hz, 1H), 4.38 (dd, J = 11.0, 5.7 Hz, 1H), 4.46 (dd, J = 11.0, 5.9 Hz, 1H), 7.46 (d, J = 8.3 Hz, NH), 7.68 (dd, J = 8.0, 1.3 Hz, 2H), 7.83 (d, J = 8.0 Hz, 2H), 7.92 (s, 1H), 7.93 (s, 1H).

^{13}C NMR (126 MHz, DMSO) δ: 18.40, 19.08, 29.41, 47.13, 59.82, 65.45, 119.45, 122.10, 125.31, 140.48, 144.02, 144.18, 147.13, 156.53, 173.07.

7.4.30.Synthesis of Smoc-β-Ala-OH 31

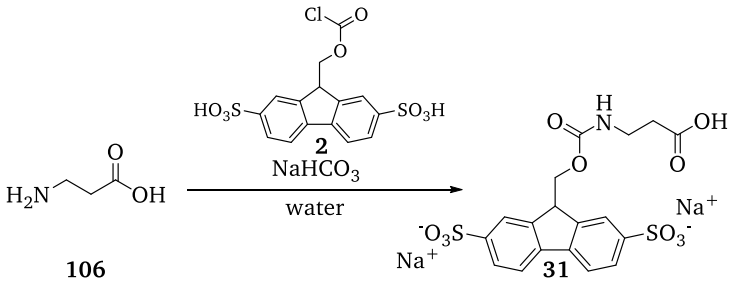

Scheme 55: Synthesis of Smoc-β-Ala-OH **31**.

According to the general procedure, 2.03g (22.45 mmol, 1 eq.) β-Ala-OH **106** and 9.36g (22.45 mmol, 1 eq.) Smoc-Cl **2** were dissolved in 30ml water and sodium hydrogen carbonate was added to adjust the pH to 8.5. The reaction mixture was stirred at ambient temperature and the solvent was removed by lyophilization. The product was isolated by preparative RP-HPLC (gradient normalized B). After work up, 10.71g (92.5%) of Smoc-β-Ala-OH **31** were obtained as a white powder.

RP-HPLC (normalized B): t_R = 12.12 min.

ESI-MS calc. for $C_{18}H_{17}NO_{10}S_2$ m/z: 471.45, meas. 470.20 $[M-H]^-$; calc. 235.73, meas. 234.80 $[M-2H]^{2-}$.

HR-MS calc. for $C_{18}H_{17}NO_{10}S_2$ m/z: 470.02211, meas. 470.02236 $[M-H]^-$.

^1H NMR (500 MHz, DMSO-d_6) δ: 2.36 (t, J = 7.3 Hz, 2H), 3.14 (t, J = 7.4 Hz, 2H), 4.22 (t, J = 5.7 Hz, 1H), 4.42 (d, J = 5.7 Hz, 2H), 7.19 (br, NH), 7.67 (d, J = 8.0 Hz, 2H), 7.81 (d, J = 7.9 Hz, 2H), 7.87 (s, 2H).

^{13}C NMR (126 MHz, DMSO) δ: 34.01, 36.48, 47.00, 64.86, 119.34, 121.92, 125.21, 140.39, 144.01, 147.28, 155.99, 173.58.

7.4.31.Synthesis of Smoc-Aib-OH 32

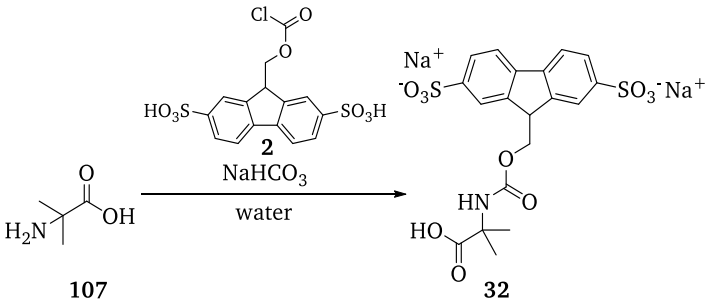

Scheme 56: Synthesis of Smoc-Aib-OH **32**.

According to the general procedure, 1.00g (9.55 mmol, 1 eq.) 2-aminoisobutyric acid **107** and 3.98g (9.55 mmol, 1 eq.) Smoc-Cl **2** were dissolved in 30ml water acetonitrile mixture (1:1) and sodium hydrogen carbonate was added to adjust the pH to 8.5. The reaction mixture was stirred at ambient temperature and the solvent was removed by lyophilization. The product was isolated by preparative RP-HPLC (50 to 100% B). After work up, 2.93g (57.8%) of Smoc-Aib-OH **32** were obtained as a white powder.

RP-HPLC (normalized B): t_R = 13.49 min.

ESI-MS calc. for $C_{19}H_{19}NO_{10}S_2$ m/z: 485.48, meas. 484.20 $[M-H]^-$; calc. 242.74, meas. 241.80 $[M-2H]^{2-}$.

HR-MS calc. for $C_{19}H_{19}NO_{10}S_2$ m/z: 484.03776, meas. 484.03817 $[M-H]^-$.

^1H NMR (500 MHz, DMSO-d_6) δ: 1.29 (s, 6H), 4.21 (t, J = 5.5 Hz, 1H), 4.41 (d, J = 5.3 Hz, 2H), 7.44 (br, NH), 7.67 (d, J = 7.8 Hz, 2H), 7.82 (d, J = 7.8 Hz, 2H), 7.89 (s, 2H).

^{13}C NMR (126 MHz, DMSO) δ: 24.97, 47.05, 55.20, 64.80, 119.35, 121.97, 125.23, 140.43, 144.04, 147.23, 155.06, 175.60.

7.5. Deprotection studies

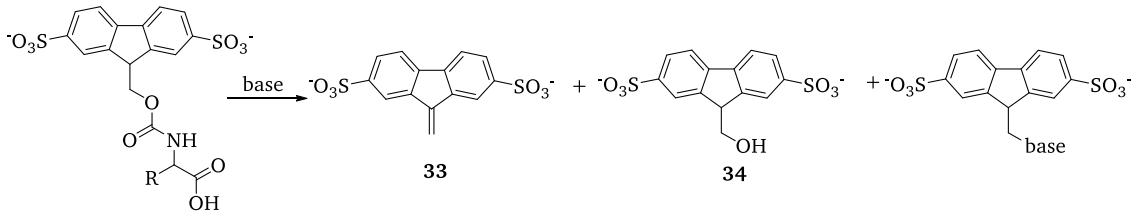

Scheme 57: Deprotection of the N_α-Smoc protecting group.

Deprotection studies were performed with 15mg of Smoc-Arg-OH **5**, Smoc-Leu-OH **16** and Smoc-Tyr-OH **28** upon the addition of 1 ml of the respective base (20% piperidine in water; 10% ethanolamine in water and ethanol; 1M NaOH in water and ethanol; 0.2M NaOH in water; 5% piperazine in water and 10% ammonia in water) to 15 mg of the respective amino acid. The resulting mixture was incubated under shaking for 5 min at ambient temperature. Mixtures of ethanol and N_α-Smoc amino acids gave a suspension due to a low solubility in pure ethanol. After 5min the deprotection progress was monitored by HPLC.

7.6. Stability of Smoc-protected amino acids

To determine the stability of N_α-Smoc protected amino acids under reaction conditions, 3mg of Smoc-Arg-OH **5**, Smoc-Ile-OH **15**, Smoc-Phe-OH **20**, Smoc-Pro-OH **21** or Smoc-Ser-OH **22** were dissolved in 0.1 ml water and 3eq. $NaHCO_3$ were added to each sample. The solutions were stored at ambient temperature and monitored by analytical RP-HPLC after 7, 14 and 21 days.

7.7. Coupling efficiency in solution and solvent influence

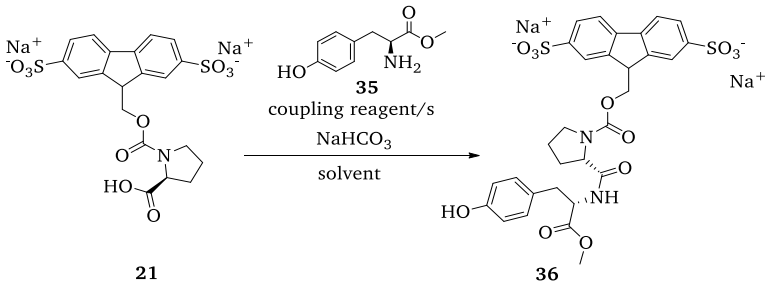

Scheme 58: Synthesis of Smoc-L-Pro-L-Tyr-OMe **36**.

For all coupling tests 1 eq. Smoc-Pro-OH **21**, 1.2 eq. H-Tyr-OMe **35**, 1 eq. $NaHCO_3$ and either 1.5 eq. EDCI-HCl **37** with 1 eq. of the following ester-forming reagents NHS **38**, Oxyma **39**, HOPO **40**, HONB **41** or 1.5 eq. of EEDQ **42**, DMT-MM **43** or COMU **44** were dissolved in 3 mL of the following solvent systems: water, 30% aq. MeCN, 30% aq. ethanol, 30% aq. isopropanol, 10% aq. Me-THF, 30% Me-THF/water (biphasic) and 30% ethyl acetate/water (biphasic). After that time, the reaction progress was monitored by RP-HPLC.

7.8. SPPS coupling efficiency: Test with Oxyma 39 and HOPO 40

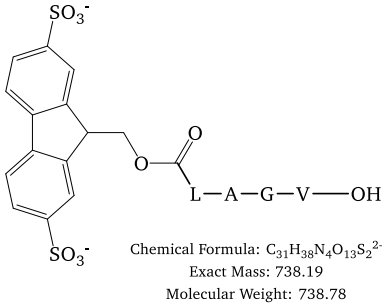

Figure 46: Smoc-LAGV-NH_2 **47** synthesis with EDC-HCl **37** and Oxyma **39**/HOPO **40**.

Peptide synthesis was carried out in a plastic syringe attached to a vacuum manifold to remove excess of reagents and solvents rapidly. The synthesis was carried out on 100 mg ChemMatrix H-Rink amide resin (loading capacity 0.4-0-6 mmol/g, 0.05 mmol; calculated on average loading). The resin was swollen for 2h in either water or 30% $MeCN_{(aq)}$ and loaded in double coupling (2×25min) using a solution of N_α-Smoc amino acid (3 eq.), EDC-HCl **37** (5.5 eq.), Oxyma **39** (3 eq.) or HOPO **40** (3 eq.) and $NaHCO_3$ (3 eq.) as base in 6 mL water or 30% $MeCN_{(aq)}$. Then the resin was washed with water twice followed by Smoc deprotection in 1M NaOH for 5 and 10 minutes with subsequent wash with water (2 times 5 mL). The coupling step of the next N_α-Smoc amino acid followed. After the chain assembly, the peptide was cleaved from the resin (without drying step) with TFA:H_2O (98:2) at ambient temperature for 2 h. The crude peptides **47** were precipitated in ice-cold diethyl ether, dried, dissolved in water and isolated by lyophilization. Analysis was performed by LC-MS and reverse-phase HPLC.

47 using EDC-HCl 37/Oxyma 39 activation:
Yield in water: 19 mg (51% calculated on average loading)
Yield in 30% $MeCN_{(aq)}$: 24 mg (65% calculated on average loading)

47 using EDC-HCl 37/HOPO 40 activation:
Yield in water: 18 mg (49% calculated on average loading)
Yield in 30% $MeCN_{(aq)}$: 17 mg (46% calculated on average loading)

RP-HPLC (normalized B): t_R = 15.3 min.
ESI-MS calc. for $C_{31}H_{40}N_4O_{13}S_2$ m/z: 740.80 meas. 738.18 $[M-2H]^-$, calc. 370.40 meas. 368.86 $[M-2H]^{2-}$.

7.9. Peptide synthesis

7.9.1. General procedure for peptide synthesis

Peptide synthesis was carried out in a plastic syringe attached to a vacuum manifold to remove excess of reagents and solvents rapidly. The synthesis was conducted either on ChemMatrix H-Rink amide resin (loading capacity 0.4-0-6 mmol/g), HMPB-ChemMatrix resin (loading capacity 0.3-0.65 mmol/g) or on a commercially available preloaded HMPB resin; all resins were swollen for 2h in water. The first amino acid was attached by double coupling (2×25min) using a solution of N_α-Smoc amino acid (3 eq.), EDC-HCl **37** (5.5 eq.), Oxyma **39** (3 eq.) and $NaHCO_3$ (3 eq.) as base in 6 mL water or its mixture with organic solvent. The resin was washed with water twice followed by Smoc deprotection with either 1M NaOH, 25% aq. ethanolamine or 5-10% aq. piperazine for 5 and 10 minutes (depending on the used resin). Afterwards the resin was washed twice with water followed by coupling of the next amino acid until the desired

peptide was completed. If not otherwise mentioned, the peptide was cleaved from the resin upon treatment with TFA:H_2O:TES (96:2:2) at RT for 1 h. The crude peptide was precipitated in ice-cold diethyl ether, dried, dissolved in water or aqueous acetonitrile and isolated by lyophilization. Analysis was performed by LC MS and reverse-phase HPLC.

7.9.2. Synthesis of H-AGELS-NH_2 (Pentapeptide-31) 48

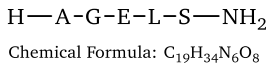

Chemical Formula: $C_{19}H_{34}N_6O_8$
Exact Mass: 474.24
Molecular Weight: 474.52

Figure 47: H-AGELS-NH_2 (Pentapeptide-31) **48**.

Peptide synthesis was carried out according to the general procedure. Synthesis was carried out on 500 mg H-Rink amide-ChemMatrix (0.40-0.60 mmol/g, 0.25 mmol; calculated on average loading) in water. Preloading and coupling were performed according to the general procedure for 45 min at ambient temperature, deprotection of the Smoc protecting group was performed with 1M $NaOH_{(aq)}$. The crude peptide **48** was precipitated in ice-cold diethyl ether, dried, dissolved in water and isolated by lyophilization. Analysis was performed by LC MS and reverse-phase HPLC.

Yield: 13.72 mg (57.71% calculated on average loading)

RP-HPLC (0 to 60% B): t_R = 11.18 min.
ESI-MS calc. for $C_{19}H_{34}N_6O_8$ m/z: 474.52 meas. 475.37 $[M+H]^+$.

7.9.3. Synthesis of H-GPQGPQ-OH (Hexapeptide-9) 49

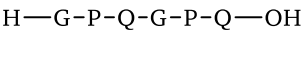

Chemical Formula: $C_{24}H_{38}N_8O_9$
Exact Mass: 582.28
Molecular Weight: 582.62

Figure 48: H-GPQGPQ-OH (Hexapeptide-9) **49**.

Peptide synthesis was carried out according to the general procedure. Synthesis was carried out on 200 mg preloaded H-Gln-HMPB-ChemMatrix resin (0.30-0.70 mmol/g, 0.09 mmol; calculated on average loading) in water. Coupling was performed according to the general procedure for 45 min at ambient temperature, deprotection of the Smoc protecting group was performed with 25% ethanolamine$_{(aq)}$. Smoc-glutamine **10** was used without side-chain protecting group. The crude peptide **49** was precipitated in ice-cold diethyl ether, dried, dissolved in water and isolated by lyophilization. Analysis was performed by LC MS and reverse-phase HPLC.

Yield: 9.22 mg (38.7% calculated on average loading)

RP-HPLC (0 to 60% B): t_R = 11.09 min.
ESI-MS calc. for $C_{24}H_{38}N_8O_9$ m/z: 582.62 meas. 581.37 $[M-H]^-$.

7.9.4. Synthesis of H-EEMQRR-NH_2 (Hexapeptide 3) 50

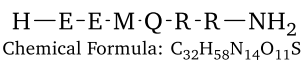

Chemical Formula: $C_{32}H_{58}N_{14}O_{11}S$
Exact Mass: 846.41
Molecular Weight: 846.96

Figure 49: H-EEMQRR-NH2 (Hexapeptide 3) **50**.

Peptide synthesis was carried out according to the general procedure. Synthesis was carried out on 100 mg H-Rink amide-ChemMatrix (0.40-0.60 mmol/g, 0.05 mmol; calculated on average loading) in water. Preloading and coupling were performed according to the general procedure for 45 min at ambient temperature, deprotection of the Smoc protecting group was performed with 1M $NaOH_{(aq)}$. Smoc-glutamine **10** and Smoc-arginine **5** were used without side-chain protecting groups. The crude peptide **50** was precipitated in ice-cold diethyl ether, dried, dissolved in water and isolated by lyophilization. Analysis was performed by LC MS and reverse-phase HPLC.

Yield: 21.73 mg (51.31% calculated on average loading).

RP-HPLC (normalized B): t_R = 9.24 min.
ESI-MS calc. for $C_{32}H_{58}N_{14}O_{11}S$ m/z: 846.96 meas. 847.60 $[M+H]^+$.

7.9.5. Synthesis of Ac-EEMQRR-NH_2 (Acetyl-Hexapeptide 3) 51

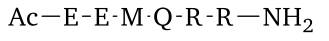

Chemical Formula: $C_{34}H_{60}N_{14}O_{12}S$
Exact Mass: 888.42
Molecular Weight: 889.00

Figure 50: Ac-EEMQRR-NH_2 (Acetyl-Hexapeptide 3) **51**.

Peptide synthesis was carried out according to the general procedure. Synthesis was carried out on 100 mg H-Rink amide-ChemMatrix (0.40-0.60 mmol/g, 0.05 mmol; calculated on average loading) in water. Preloading and coupling were performed according to the general procedure for 45 min at ambient temperature, deprotection of the Smoc protecting group was performed with 1M $NaOH_{(aq)}$. Smoc-glutamine **10** and Smoc-arginine **5** were used without side-chain protecting groups. The crude peptide **51** was precipitated in ice-cold diethyl ether, dried, dissolved in water and isolated by lyophilization. Analysis was performed by LC MS and reverse-phase HPLC.

Yield: 18.74 mg (42.16% calculated on average loading).

RP-HPLC (0 to 60% B): t_R = 9.28 min.
ESI-MS calc. for $C_{34}H_{60}N_{14}O_{12}S$ m/z: 889.00 meas. 889.70 $[M+H]^+$; calc. 444.50 meas. 445.60 $[M+2H]^{2+}$.

7.9.6. Synthesis of Leu-Enkephalin amide 52

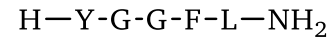

Chemical Formula: $C_{28}H_{38}N_6O_6$
Exact Mass: 554.29
Molecular Weight: 554.65

Figure 51: Leu-Enkephalin amide **52**.

Peptide synthesis was carried out according to the general procedure. Synthesis was carried out on 100 mg H-Rink amide-ChemMatrix (0.40-0.60 mmol/g, 0.05 mmol; calculated on average loading) in water. Preloading and coupling were performed according to the general procedure for 45 min at ambient temperature, deprotection of the Smoc protecting group was performed with 1M $NaOH_{(aq)}$. Smoc-tyrosine **28** was used without side-chain protecting group. The crude peptide **52** was precipitated in ice-cold diethyl ether, dried, dissolved in water and isolated by lyophilization. Analysis was performed by LC MS and reverse-phase HPLC.

Yield: 19.65mg (70.86% calculated on average loading).

RP-HPLC (normalized B): t_R = 17.98 min.
ESI-MS calc. for $C_{28}H_{38}N_6O_6$ m/z: 554.65 meas. 555.47 $[M+H]^+$.

7.9.7. Synthesis of Met-Enkephalin: H-YGGFM-OH 53

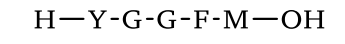

Chemical Formula: $C_{27}H_{35}N_5O_7S$
Exact Mass: 573.23
Molecular Weight: 573.67

Figure 52: Met-Enkephalin **53**.

Peptide synthesis was carried out according to the general procedure. Synthesis was carried out on 50 mg preloaded H-Met-HMPB-ChemMatrix resin (0.30-0.70 mmol/g, 0.025 mmol; calculated on average loading) in a water MeCN mixture (70:30). Coupling was performed according to the general procedure for 45 min at ambient temperature, deprotection of the Smoc protecting group was performed with 25% ethanolamine$_{(aq)}$. Peptide **53** was cleaved from solid support using 20% HFIP (in DCM)[263] to prevent oxidation of the Met-residue for 120 min, solvent was removed by rotary evaporator, dissolved in water and isolated by lyophilization. Analysis was performed by LC MS and reverse-phase HPLC.

Yield: 9 mg (63% calculated on average loading)

RP-HPLC (0 to 60% B): t_R = 17.77 min.
ESI-MS calc. for $C_{27}H_{35}N_5O_7S$ m/z: 573.67 meas. 574.18 $[M+H]^+$.

7.9.8. Synthesis of Leu-Enkephalin: H-YGGFL-OH 54

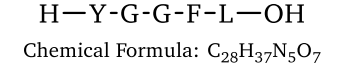

Chemical Formula: $C_{28}H_{37}N_5O_7$
Exact Mass: 555.27
Molecular Weight: 555.63

Figure 53: Leu-Enkephalin **54**.

Peptide synthesis was carried out according to the general procedure. Synthesis was carried out on 50 mg preloaded H-Leu-HMPB-ChemMatrix resin (0.30-0.70 mmol/g, 0.025 mmol; calculated on average loading) in a water MeCN mixture (70:30). Coupling was performed according to the general procedure for 45 min at ambient temperature, deprotection of the Smoc protecting group was performed with 25% ethanolamine$_{(aq)}$. Smoc-tyrosine **28** was used without side-chain protecting group. Peptide **54** was cleaved from solid support using HFIP (0.1% HCl)[264] for 120 min, solvent was removed by rotary evaporator, dissolved in water and isolated by lyophilization. Analysis was performed by LC MS and reverse-phase HPLC.

Yield: 10.3 mg (71.82% calculated on average loading)

RP-HPLC (0 to 60% B): t_R = 19.46 min.
ESI-MS calc. for $C_{28}H_{37}N_5O_7$ m/z: 555.63 meas. 556.37 $[M+H]^+$.

7.9.9. Synthesis of Acyl-Carrier-Protein (ACP) 65-74 peptide: H-VQAAIDYING-OH 55

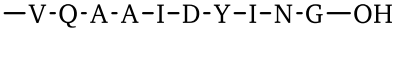

Chemical Formula: $C_{47}H_{75}N_{13}O_{15}$
Exact Mass: 1061.55
Molecular Weight: 1062.19

Figure 54: Acyl-Carrier-Protein (ACP) 65-74: H-VQAAIDYING-OH **55**.

Peptide synthesis was carried out according to the general procedure. Synthesis was carried out on 100 mg preloaded H-Gly-HMPB-ChemMatrix resin (0.30-0.65 mmol/g, 0.045 mmol; calculated on average loading) in a water MeCN mixture (50:50). Coupling was performed according to the general procedure for 25 min at ambient temperature as double coupling step, deprotection of the Smoc protecting group was performed with 5% piperazine$_{(aq)}$. Smoc-tyrosine **28**, Smoc-asparagine **7** and Smoc-glutamine **10** were used without side-chain protecting groups. Peptide **55** was cleaved from solid support using HFIP with 0.1% HCl[264] for 120 min. The crude peptide **55** was precipitated in ice-cold diethyl ether, dried, dissolved in water and isolated by lyophilization. Analysis was performed by LC MS and reverse-phase HPLC.

Yield: 18 mg (36% calculated on average loading)

RP-HPLC (10 to 100% B): t_R = 11.66 min.
ESI-MS calc. for $C_{47}H_{75}N13O_{15}$ m/z: 1062.19 meas. 1063.67 $[M+H]^+$, calc. 531.5 meas. 532.55 $[M+2H]^{2+}$.

7.9.10.Synthesis of Acyl-Carrier-Protein (ACP) 65-74: H-VQAAIDYING-NH$_2$ 56

H—V-Q-A-A-I-D-Y-I-N-G—NH_2

Chemical Formula: $C_{47}H_{74}N_{12}O_{16}$
Exact Mass: 1062.53
Molecular Weight: 1063.18

Figure 55: Acyl-Carrier-Protein (ACP) 65-74: H-VQAAIDYING-NH$_2$ **56**.

Peptide synthesis was carried out according to the general procedure. Synthesis was carried out on 100 mg H-Rink amide-ChemMatrix (0.40-0.60 mmol/g, 0.05 mmol; calculated on average loading) in a water MeCN mixture (50:50). Preloading and coupling were performed according to the general procedure for 25 min at ambient temperature as double coupling step, deprotection of the Smoc protecting group was performed with 5% piperazine$_{(aq)}$. Smoc--tyrosine **28**, Smoc-asparagine **7** and Smoc-glutamine **10** were used without side-chain protecting groups. Peptide **56** was cleaved from solid support using TFA:H_2O:TES (95:2.5:2.5) for 60 min. The crude peptide **56** was precipitated in ice-cold diethyl ether, dried, dissolved in water and isolated by lyophilization. Analysis was performed by LC MS and reverse-phase HPLC.

Yield: 23 mg (46% calculated on average loading)

RP-HPLC (10 to 100% B): t_R = 11.57 min.
ESI-MS calc. for $C_{47}H_{74}N_{12}O_{16}$ m/z: 1063.18 meas. 1062.67 $[M+H]^+$, calc. 531.59 meas. 532.05 $[M+2H]^{2+}$.

7.9.11.Synthesis of H-GPRP-OH 57

H—G-P-R-P—OH

Chemical Formula: $C_{18}H_{31}N_7O_5$
Exact Mass: 425.24
Molecular Weight: 425.49

Figure 56: H-GPRP-OH **57**.

Peptide synthesis was carried out according to the general procedure. Synthesis was carried out on 100 mg preloaded H-Gly-HMPB-ChemMatrix resin (0.30-0.65 mmol/g, 0.045 mmol;

calculated on average loading) in water. Coupling was performed according to the general procedure for 45 min at ambient temperature, deprotection of the Smoc protecting group was performed with 25% ethanolamine$_{(aq)}$. Peptide **57** was cleaved from solid support using HFIP with 0.1% HCl[264] for 120 min. The crude peptide **57** was precipitated in ice-cold diethyl ether, dried, dissolved in water or aqueous acetonitrile and isolated by lyophilization. Analysis was performed by LC MS and reverse-phase HPLC.

Yield: 8 mg (38% calculated on average loading)

RP-HPLC (normalized B): t_R = 13.29 min.
ESI-MS calc. for $C_{18}H_{31}N_7O_8$ m/z: 425.49 meas. 426.40 $[M+H]^+$, calc. 212.75 meas. 214.00 $[M+2H]^{2+}$.

7.9.12.Synthesis of Smoc-VVIA-NH$_2$ 58

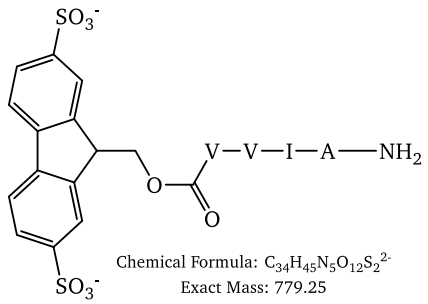

Figure 57: Smoc-VVIA amide **58**.

Peptide synthesis was carried out according to the general procedure. Synthesis was carried out on 100 mg H-Rink amide-ChemMatrix (0.40-0.60 mmol/g, 0.05 mmol; calculated on average loading) in water. Coupling was performed according to the general procedure for 45 min at ambient temperature, deprotection of the Smoc protecting group was performed with 1M NaOH$_{(aq)}$. The final N_α-Smoc protecting group was left on the peptide for an easier HPLC detection, Smoc-peptide **58** was cleaved from solid support using TFA:H_2O (95:5). The crude Smoc-peptide **58** was precipitated in ice-cold diethyl ether, dried, dissolved in water and isolated by lyophilization. Analysis was performed by LC MS and reverse-phase HPLC.

Yield: 26 mg (67% calculated on average loading)

RP-HPLC (normalized B): t_R = 16.45 min.
ESI-MS calc. for $C_{34}H_{47}N_5O_{12}S_2$ m/z: 781.89 meas. 780.40 $[M-H]^-$, calc. 390.20 meas. 390.00 $[M-2H]^{2-}$.

7.9.13.Synthesis of Smoc-DIIW-OH 59

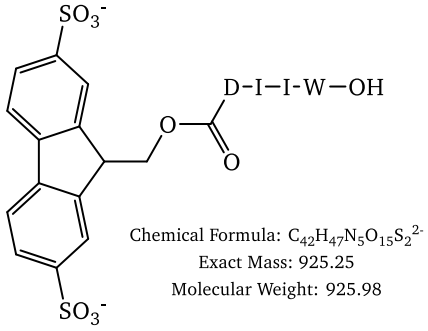

Figure 58: Smoc-DIIW-OH **59**.

Peptide synthesis was carried out according to the general procedure. Synthesis was carried out on 100 mg preloaded H-Trp-HMPB-ChemMatrix resin (0.30-0.65 mmol/g, 0.045 mmol; calculated on average loading) in water. Coupling was performed according to the general procedure for 45 min at ambient temperature, deprotection of the Smoc protecting group was performed with 1M $NaOH_{(aq)}$. The final N_{α}-Smoc protecting group was left on the peptide for an easier HPLC detection, Smoc-peptide **59** was cleaved from solid support using HFIP with 0.1% HCl[264] for 120 min. The crude Smoc-peptide **59** was precipitated in ice-cold diethyl ether, dried, dissolved in water and isolated by lyophilization. Analysis was performed by LC MS and reverse-phase HPLC.

Yield: 22 mg (50% calculated on average loading)

RP-HPLC (normalized B): t_R = 16.32 min.
ESI-MS calc. for $C_{42}H_{49}N_5O_{15}S_2$ m/z: 927.99 meas. 928.40 $[M-H]^-$, calc. 464.20 meas. 463.97 $[M-2H]^{2-}$.

7.9.14. Synthesis of Smoc-E(OtBu)K(Boc)R(Pbf)S(tBu)C(Trt)-OH 60 as model for a fully protected peptide.

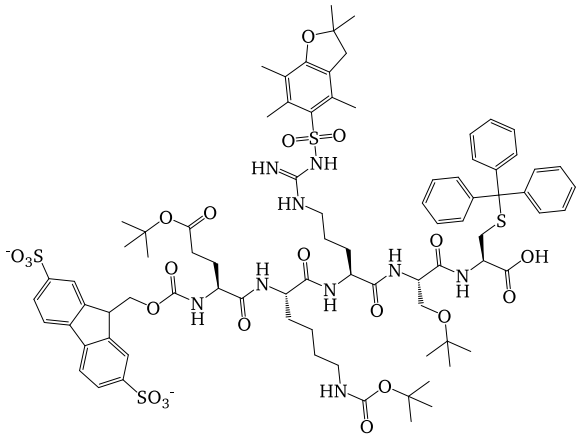

Figure 59: Structure of Smoc-E(OtBu)K(Boc)R(Pbf)S(tBu)C(Trt)-OH **60**.

Peptide synthesis was carried out according to the general procedure. Synthesis was carried out on 50 mg preloaded H-Cys(Trt)-HMPB-ChemMatrix resin (0.30-0.65 mmol/g, 0.045 mmol; calculated on average loading) in a water MeCN mixture (50:50). Preloading and coupling were performed according to the general procedure for 25 min at ambient temperature as double coupling step, deprotection of the Smoc protecting group was performed with 5% $piperazine_{(aq)}$. The fully protected Peptide **60** was cleaved from solid support using 20% HFIP (in DCM) for 120 min and solvent removed by rotary evaporator. The crude peptide **60** was dried, dissolved in aqueous acetonitrile and isolated by lyophilization. Analysis was performed by LC MS and reverse-phase HPLC.

Yield: 18 mg (44% calculated on average loading)

RP-HPLC (50 to 100% B): t_R = 18.83 min.
ESI-MS calc. for $C_{19}H_{19}NO_{10}S_2$ m/z: 855.53 meas. 854.30 $[M-2H]^{2-}$.

7.9.15.Synthesis of model peptides 61,62 for racemization tests

H—C-Y-E-I-S—NH_2

Chemical Formula: $C_{26}H_{40}N_6O_9S$
Exact Mass: 612.26
Molecular Weight: 612.70

H—A-N-K-P-G—NH_2

Chemical Formula: $C_{20}H_{36}N_8O_6$
Exact Mass: 484.28
Molecular Weight: 484.56

Figure 60: Model peptides H-CYEIS-NH_2 **61** and H-ANKPG-NH_2 **62** for racemization tests.

Peptide synthesis was carried out according to the general procedure. Synthesis was carried out on 100 mg H-Rink amide-ChemMatrix (0.40-0.60 mmol/g, 0.05 mmol; calculated on average loading) in a water MeCN mixture (70:30). Preloading and Coupling was performed according to the general procedure for 25 min at ambient temperature as double coupling step, deprotection of the Smoc protecting group was performed with 1M $NaOH_{(aq)}$. Smoc-asparagine **7** and Smoc-tyrosine **28** were used without side-chain protecting groups. Peptides **61**, **62** were cleaved from solid support using TFA:H_2O:TES (95:2.5:2.5) for 60 min. The crude peptides **61, 62** were precipitated in ice-cold diethyl ether, dried, dissolved in water or aqueous acetonitrile and isolated by lyophilization. Analysis was performed by LC MS and reverse-phase HPLC.

H-CYEIS-NH_2 61
Yield: 15mg (48.99% calculated on average loading)
RP-HPLC (50 to 100% B): t_R = 19.21 min.
ESI-MS calc. for $C_{26}H_{40}N_6O_9S$ m/z: 612.70 meas. 613.28 $[M+H]^+$.

H-ANKPG-NH_2 62
Yield: 13mg (53.66% calculated on average loading)
RP-HPLC (normalized B): t_R = 9.94 min.
ESI-MS calc. for $C_{20}H_{36}N_8O_9$ m/z: 484.56 meas. 485.37 $[M+H]^+$.

Samples **61**, **62** as well as Smoc-Asn-OH **7** were sent to *C.A.T. GmbH & Co Chromatographie und Analysentechnik KG* (Tübingen, Germany) for analysis of amino acid racemization.

7.9.16.Synthesis of Pal-GHK-OH 63

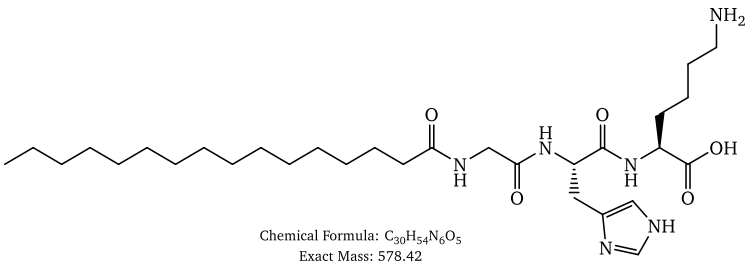

Chemical Formula: $C_{30}H_{54}N_6O_5$
Exact Mass: 578.42
Molecular Weight: 578.80

Figure 61: Structure of Pal-GHK-OH **63**.

Peptide synthesis was carried out according to the general procedure. Synthesis was carried out on 100 mg preloaded H-Lys(Boc)-HMPB-ChemMatrix resin (0.30-0.60 mmol/g, 0.045 mmol; calculated on average loading) in a water ethanol mixture (80:20). Coupling was performed according to the general procedure for 30 min at ambient temperature, deprotection of the Smoc protecting group was performed with 1M $NaOH_{(aq)}$. Palmitoylation was performed with palmitic acid (3 eq.), EDC-HCl **37** (5.5 eq.), Oxyma **39** (3 eq.) and $NaHCO_3$ (3 eq.) in ethanol water (70:30) at pH 7.2 for 45 min. Washing was performed twice with ethanol water (70:30) at pH 7.2 and twice with diethyl ether. Peptide **63** was cleaved from solid support using 95% $TFA_{(aq)}$ for 60 min, solvent was removed by lyophilisation.

Yield: 14.12 mg (54.23% calculated on average loading)

RP-HPLC (10 to 60% B): t_R = 20.34 min.
ESI-MS calc. for $C_{30}H_{54}N_6O_5$ m/z: 578.80 meas. 579.57 $[M+H]^+$.

7.9.17.Synthesis of Pal-GQPR-OH 64

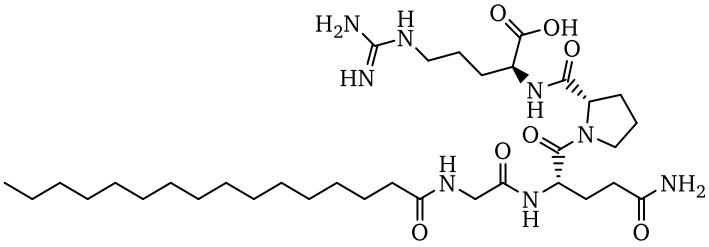

Chemical Formula: $C_{34}H_{62}N_8O_7$
Exact Mass: 694.47
Molecular Weight: 694.92

Figure 62: Structure of Pal-GQPR-OH **64**.

Peptide synthesis was carried out according to the general procedure. Synthesis was carried out on 100 mg preloaded H-Arg-HMPB-ChemMatrix resin (0.30-0.60 mmol/g, 0.045 mmol; calculated on average loading) in a water ethanol mixture (80:20). Coupling was performed according to the general procedure for 30 min at ambient temperature, deprotection of the Smoc protecting group was performed with 1M $NaOH_{(aq)}$. Smoc-Glutamine **10** was used without side-chain protecting group. Palmitoylation was performed with palmitic acid (3 eq.), EDC-HCl **37** (5.5 eq.), Oxyma **39** (3 eq.) and $NaHCO_3$ (3 eq.) in ethanol water (70:30) at pH 7.2 for 45 min. Washing was performed twice with ethanol water (70:30) at pH 7.2 and twice with diethyl ether. Peptide **64** was cleaved from solid support using 95% $TFA_{(aq)}$ for 60 min, solvent was removed by lyophilisation.

Yield: 18.68 mg (59.74% calculated on average loading)

RP-HPLC (0 to 60% B): t_R = 20.26 min.
ESI-MS calc. for $C_{34}H_{62}N_8O_7$ m/z: 694.92 meas. 695.66 $[M+H]^+$.

7.9.18.Synthesis of H-GPRPA-NH_2 Vialox (Pentapeptide-3) 65

Chemical Formula: $C_{21}H_{37}N_9O_5$
Exact Mass: 495.29
Molecular Weight: 495.59

Figure 63: H-GPRPA-NH_2 Vialox (Pentapeptide-3) **65**.

Peptide synthesis was carried out according to the general procedure. Synthesis was carried out on 100 mg H-Rink amide-ChemMatrix (0.40-0.60 mmol/g, 0.05 mmol; calculated on maximal loading) in a water MeCN mixture (70:30). Preloading and coupling were performed according to the general procedure for 25 min at ambient temperature, deprotection of the Smoc protecting group was performed with 1M $NaOH_{(aq)}$. Peptide **65** was cleaved from solid support using TFA:H_2O:TES (95:2.5:2.5) for 60 min. The crude peptide **65** was precipitated in ice-cold diethyl ether, dried, dissolved in water and isolated by lyophilization. Analysis was performed by LC MS and reverse-phase HPLC.

Yield: 12 mg (48.43% calculated on average loading)

RP-HPLC (normalized B): t_R = 11.35 min.

ESI-MS calc. for $C_{21}H_{37}N_9O_5$ m/z: 495.59 meas. 496.37 $[M+H]^+$, calc. 247.80 meas. 248.95 $[M+2H]^{2+}$.

7.9.19.Synthesis of Oxytocin 66

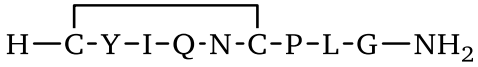

Chemical Formula: $C_{43}H_{66}N_{12}O_{12}S_2$
Exact Mass: 1006.44
Molecular Weight: 1007.19

Figure 64: Oxytocin **66**.

Peptide synthesis was carried out according to the general procedure. Synthesis was carried out on 100 mg H-Rink amide-ChemMatrix (0.40-0.60 mmol/g, 0.05 mmol; calculated on average loading) in a water MeCN mixture (70:30). Preloading and coupling were performed according to the general procedure for 25 min at ambient temperature as double coupling step, deprotection of the Smoc protecting group was performed with 1M $NaOH_{(aq)}$. Smoc-tyrosine **28**, Smoc-asparagine **7** and Smoc-glutamine **10** were used without side-chain protecting groups. Peptide **66** was cleaved from solid support using TFA:TES:H_2O:DTT (90:2.5:2.5:5) for 60 min. The crude peptide **66** was precipitated in ice-cold diethyl ether, dried, dissolved in water and isolated by lyophilization. The disulfide bond was closed in 0.1M NH_4HCO_3 buffer pH 8 in a concentration 1 mg/mL for 3 days at room temperature. Analysis was performed by LC MS and reverse-phase HPLC.

Yield: 18 mg (35.75% calculated on average loading)

RP-HPLC (10 to 100% B): t_R = 11.82 min.
ESI-MS calc. for $C_{43}H_{66}N_{12}O_{12}S_2$ m/z: 1007.19 meas. 1007.67 $[M+H]^+$, calc. 503.60 meas. 504.55 $[M+2H]^{2+}$.

7.9.20.Synthesis of Vasopressin (peptide hormone) 67

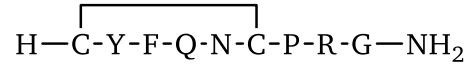

Chemical Formula: $C_{46}H_{65}N_{15}O_{12}S_2$
Exact Mass: 1083.44
Molecular Weight: 1084.24

Figure 65: Vasopressin **67**.

Peptide synthesis was carried out according to the general procedure. Synthesis was carried out on 100 mg H-Rink amide-ChemMatrix (0.40-0.60 mmol/g, 0.05 mmol; calculated on average loading) in a water MeCN mixture (70:30). Preloading and coupling were performed according to the general procedure for 25 min at ambient temperature as double coupling step, deprotection of the Smoc protecting group was performed with 1M $NaOH_{(aq)}$. Smoc-tyrosine **28**, Smoc-asparagine **7** and Smoc-glutamine **10** were used without side-chain protecting groups. Peptide **67** was cleaved from solid support using TFA:TES:H_2O:DTT (90:2.5:2.5:5) for 60 min. The crude peptide **67** was precipitated in ice-cold diethyl ether, dried, dissolved in water and isolated by lyophilization. The disulfide bond was closed in 0.1M NH_4HCO_3 buffer pH 8 in a concentration 1 mg/mL for 3 days at room temperature. Analysis was performed by LC MS and reverse-phase HPLC.

Yield: 20 mg (39.71% calculated on average loading)

RP-HPLC (10 to 100% B): t_R = 10.47 min.

ESI-MS calc. for $C_{46}H_{65}N_{15}O_{12}S_2$ m/z: 1084.24 meas. 1084.57 $[M+H]^+$, calc. 542.12 meas. 543.05 $[M+2H]^{2+}$.

7.9.21.Synthesis of heptaarginine cell-penetrating peptide 68

H—R-R-R-R-R-R-R—NH_2

Chemical Formula: $C_{42}H_{87}N_{29}O_7$

Exact Mass: 1109.73

Molecular Weight: 1110.35

Figure 66: Heptaarginine cell-penetrating peptide **68**.

Peptide synthesis was carried out according to the general procedure. Synthesis was carried out on 100 mg H-Rink amide-ChemMatrix (0.40-0.60 mmol/g, 0.05 mmol; calculated on average loading) in a water MeCN mixture (70:30). Preloading and coupling were performed according to the general procedure for 45 min at ambient temperature, deprotection of the Smoc protecting group was performed with 1M $NaOH_{(aq)}$. Smoc-arginine **5** was used without side-chain protecting groups. Peptide **68** was cleaved from solid support using TFA:H_2O: (95:5) for 60 min. The crude peptide **68** was precipitated in ice-cold diethyl ether, dried, dissolved in water or aqueous acetonitrile and isolated by lyophilization. Analysis was performed by LC MS and reverse-phase HPLC.

Yield: 23 mg (41.43% calculated on average loading)

RP-HPLC (normalized B): t_R = 13.86 min. (Smoc-heptaarginine for easier detection)
ESI-MS calc. for $C_{42}H_{87}N_{29}O_7$ m/z: 1110.35 meas. 1113.27 $[M+H]^+$, calc. 555.18 meas. 557.15 $[M+2H]^{2+}$.

7.9.22.Synthesis of H-Y(D-A)GFL-OH Leuphasyl 69

H—Y−a−G−F−L—OH

Chemical Formula: $C_{29}H_{39}N_5O_7$

Exact Mass: 569.28

Molecular Weight: 569.66

Figure 67: Leuphasyl **69.**

Peptide synthesis was carried out according to the general procedure. Synthesis was carried out on 100 mg preloaded H-Leu-HMPB-ChemMatrix resin (0.30-0.60 mmol/g, 0.045 mmol; calculated on average loading) in a water MeCN mixture (80:20). Coupling was performed according to the general procedure for 45 min at ambient temperature, deprotection of the Smoc protecting group was performed with 1M NaOH(aq). Peptide **69** was cleaved from solid support using 1% TFA for 60 min. The crude peptide **69** was precipitated in ice-cold diethyl ether, dried, dissolved in water or aqueous acetonitrile and isolated by lyophilization. Analysis was performed by LC MS and reverse-phase HPLC.

Yield: 17.3 mg (57.85% calculated on average loading)

RP-HPLC (0 to 60% B): t_R = 18.7 min.
ESI-MS calc. for $C_{29}H_{39}N_5O_7$ m/z: 569.66 meas. 570.27 $[M+H]^+$.

7.9.23.Studies on aspartimide formation

For aspartimide formation, 4 classic model peptides derived from peptide scorpion toxin II (H-VKDGYI-NH_2 **70**, H-VK(D-D)GYI-NH_2 **71**, H-VKNGYI-NH_2 **72** and H-VK(β-D)GYI-NH2 **73**) were chosen.

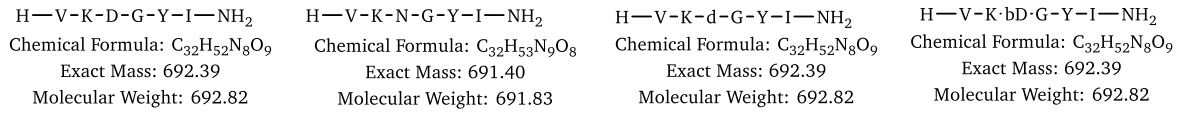

Figure **68:** Model peptides for aspartimide formation H-VKDGYI-NH_2 **70**, H-VKNGYI-NH_2 **72**, H-VK(D-D)GYI-NH_2 **71** and H-VK(β-D)GYI-NH_2 **73**.

Synthesis was performed on 200 mg ChemMatrix Rink amide resin (0.4-0.6 mmol/g, 0.23 mmol; calculated on average loading) by manual standard Fmoc-based SPPS. Afterwards the peptide-resins 70-73 were split into 15 equal parts and incubated for 3h and 16h with the following bases: 1M $NaOH_{(aq)}$, 1M NaOH in EtOH, 5% piperazine in DMF, 5% $piperazine_{(aq)}$, 20% piperidine in DMF and 10% $ethanolamine_{(aq)}$. As a reference, a non-incubated resin was subjected to global cleavage. After the respective incubation time, the samples were cleaved from the resin and analyzed by RP-HPLC and LC-MS. Aspartic acid was added as internal standard to all HPLC runs to achieve comparable HPLC retention times.

Aspartimide tests with model peptides with organic synthesis and incubation with various bases for 3h and 16h:

- Standard
- 1M NaOH in H_2O
- 1M NaOH in EtOH
- 5% piperazine in DMF
- 5% piperazine in H_2O
- 20% piperidine in DMF
- 10% ethanolamine in H_2O

7.10. Fluorescence monitoring of N_α-Smoc amino acids

A 100 nM aqueous solutions of all N_α-Smoc amino acids were prepared and transferred to a Greiner Bio-One (Kremsmünster, Austria) UV-STAR®, flat-bottom, black 96 well plate for fluorescent measurements. Absorbance and fluorescent measurements were performed with a CLARIOstar (*BMG LABTECH GmbH*, Ortenberg, Germany), absorbance was measured in the range of 220-700 nm and fluorescence was measured in the range of 300-400nm.

7.11. Fluorescence monitoring of resin loading and coupling status during ASPPS

Smoc-Gly-OH **12** was loaded in two different concentrations onto a water-compatible 2-CTC resin with DMSO as solvent. The resin was washed thrice with water, suspended in water and split into three equal portions that were transferred to a Greiner Bio-One (Kremsmünster, Austria) UV-STAR®, flat-bottom, black 96 well plate for fluorescent measurements. The fluorescence was measured at the excitation maxima of 280 nm and emission maxima of 340 nm.

Figure 69: H-LVAIG-NH_2 **74.**

H-LVAIG-NH_2 **74** was synthesized on a Rink amide PEGA resin in water according to the general procedure. After each respective coupling or deprotection step, the resin was washed thrice with water, suspended in water and split into three equal portions that were transferred to a *Greiner Bio-One (Kremsmünster, Austria)* UV-STAR®, flat-bottom, black 96 well plate for fluorescent measurements. After the measurements, the resin was reunited and the synthesis continued.

7.12. Purification by affinity column chromatography

7.12.1.Synthesis of H-GPQGPQ-OH Hexapeptide 9 49 in water

H—G-P-Q-G-P-Q—OH

Chemical Formula: $C_{24}H_{38}N_8O_9$
Exact Mass: 582.28
Molecular Weight: 582.62

Figure 70: H-GPQGPQ-OH (Hexapeptide-9) **49** for capping experiments.

Peptide synthesis was carried out according to the general procedure. Synthesis was performed on 100 mg preloaded H-Gln-HMPB-ChemMatrix resin (0.30-0.70 mmol/g, 0.05 mmol; calculated on average loading) in water. Coupling was performed with 0.95 eq. of N_α-Smoc amino acid compared to prior coupling in order to maximize by-product formation, EDC-HCl **37** (2 eq.), Oxyma **39** (1 eq.) and $NaHCO_3$ (1 eq.) as base in 6 mL water for 25 min at ambient temperature. Resin was washed thrice with water followed by capping with sulfoacetic acid **76** (50 eq.), EDC-HCl **37** (60 eq.), Oxyma **39** (50 eq.) and $NaHCO_3$ (100 eq.) as base for 15 min (capping mixture was reused). Deprotection of the Smoc protecting group was performed with 5% $piperazine_{(aq)}$. Smoc-glutamine **10** was used without sidechain protecting group. Peptide **49** was cleaved from solid support using TFA:H_2O (95:5) for 120 min. The crude mixture was analysed by analytical HPLC. Afterwards, the crude mixture was put on a DEAE Sephadex A-25 ion-exchange column for purification. The column was washed twice with water and an additional HPLC of the purified peptide was monitored.

7.12.2.Synthesis of H-YGGFMRRV-NH_2 Adrenorphin 77 in DMF

H—Y-G-G-F-M-R-R-V—NH_2
Chemical Formula: $C_{44}H_{69}N_{15}O_9S$
Exact Mass: 983.51
Molecular Weight: 984.19

Figure 71: H-YGGFMRRV-NH_2 Adrenorphin **77** for capping experiments in DMF.

Synthesis was performed on 100 mg ChemMatrix rink amide resin (0.4-0.6 mmol/g, 0.05 mmol; calculated on average loading) by manual standard Fmoc-based SPPS in DMF. Coupling was performed with 0.95 eq. of Fmoc-amino acid compared to prior coupling in order to maximize by-product formation, HBTU (0.95 eq. to the amino acid) and DIPEA (2 eq. to the amino acid) as base in 6 mL DMF for 25 min at ambient temperature. Resin was washed thrice with DMF followed by capping with an organic 4-sulfobenzoic acid **75** salt in DMF (50 eq.), HBTU (49.8 eq.) and DIPEA (100 eq.) as base for 15 min (capping mixture was reused). Deprotection of the Fmoc-protecting group was performed with 20% piperidine in DMF. Peptide **77** was cleaved from solid support using TFA:H_2O (95:5) for 120 min. The crude mixture was analysed by analytical HPLC. Afterwards, the crude mixture was put on a DEAE Sephadex A-25 ion-exchange column for purification. The column was washed twice with water and an additional HPLC of the purified peptide was monitored.

8. Supporting information

8.1. Analytical data of Smoc-Chloride 2

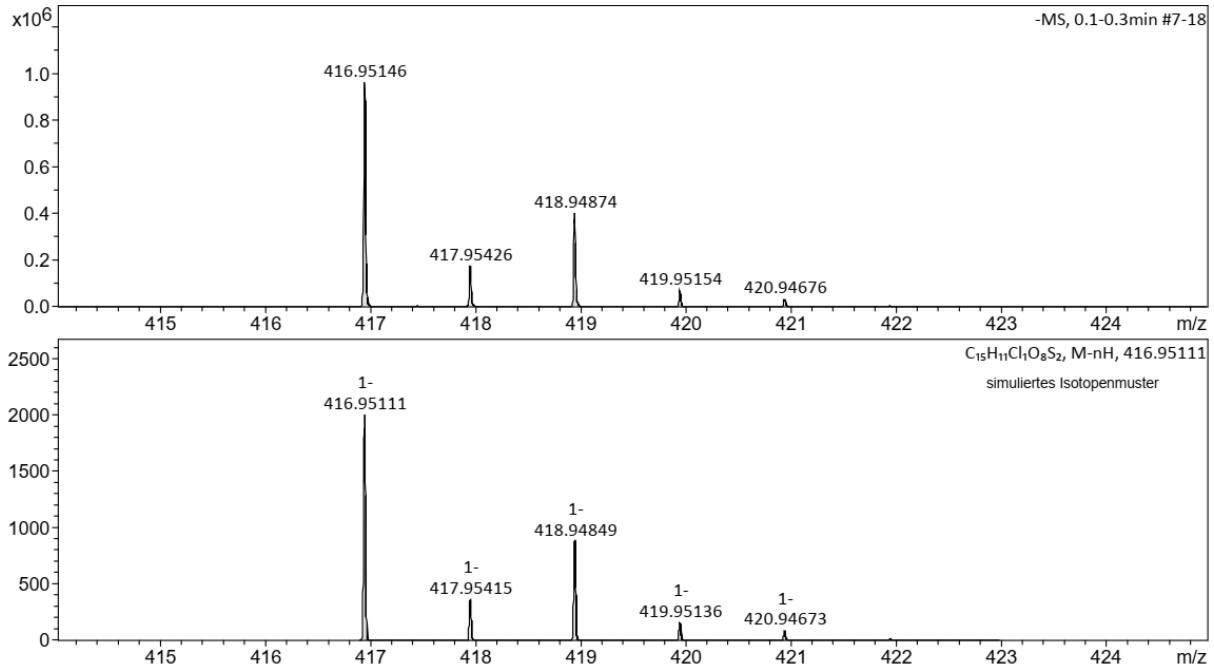

Figure 72: HR-MS of Smoc-chloride **2** (M measured=416.95146 $[M-H]^-$, M calc.=416.95111).

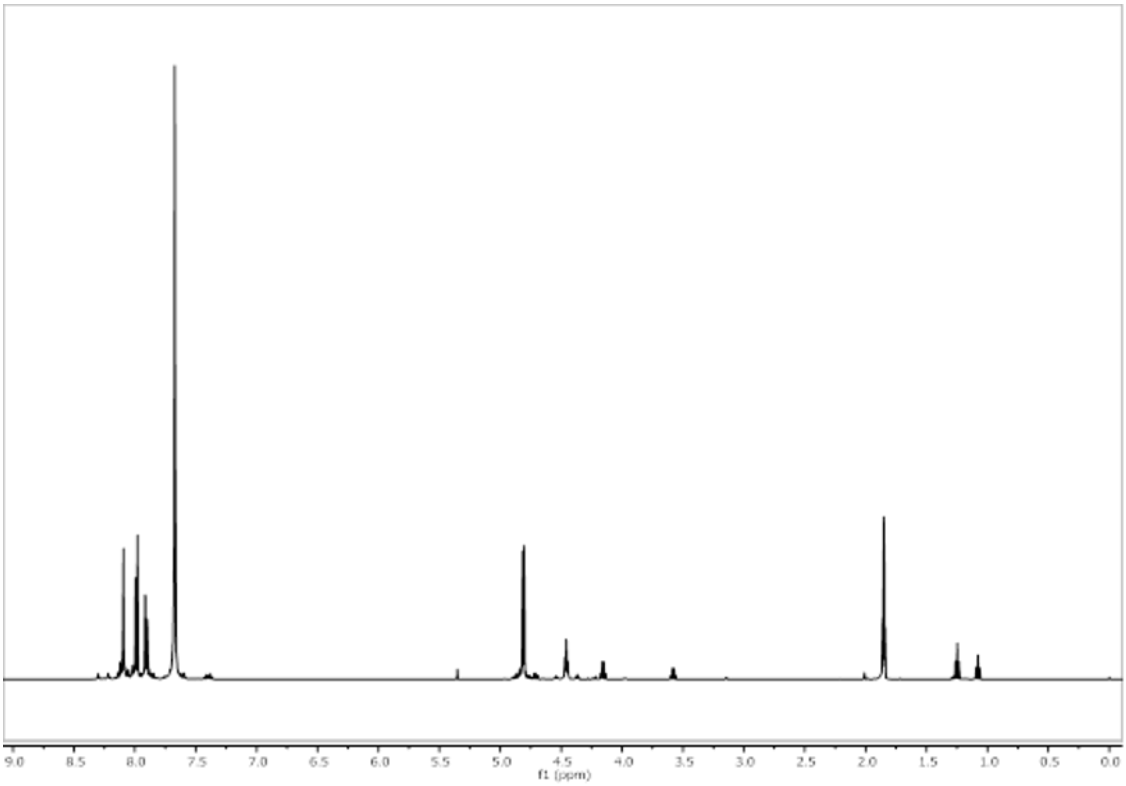

Figure 73: ^{1}H-NMR of Smoc-Cl **2.**

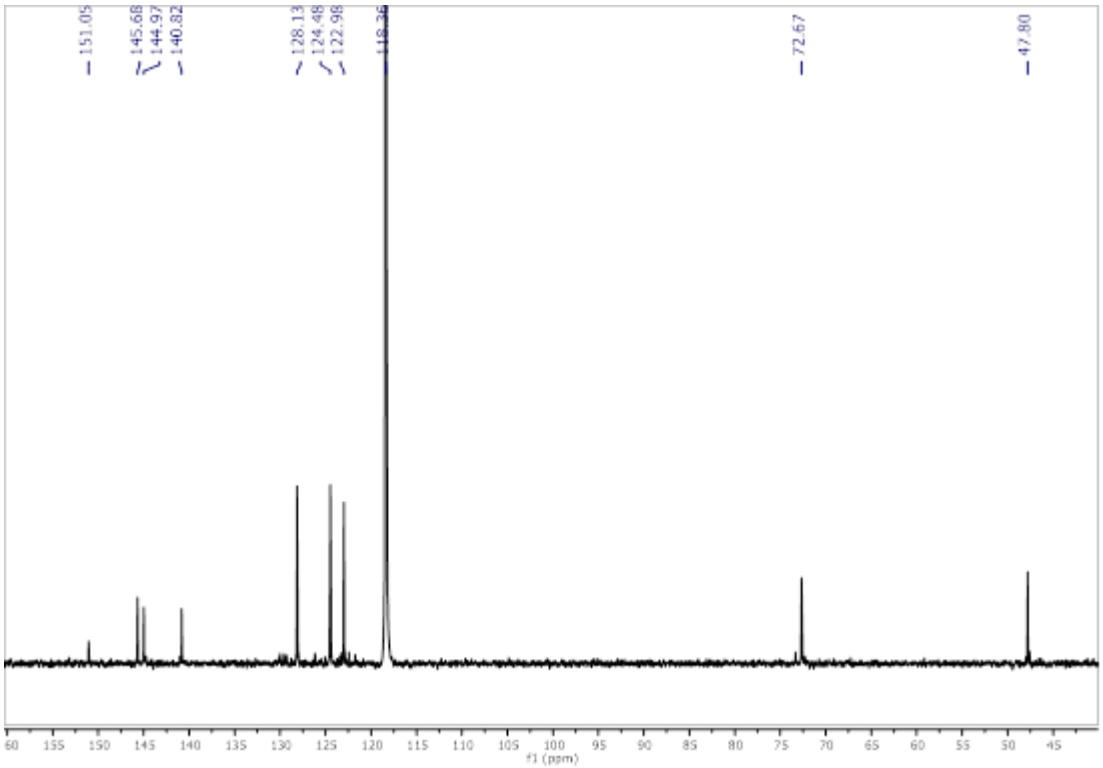

Figure 74: ^{13}C-NMR of Smoc-Cl **2.**

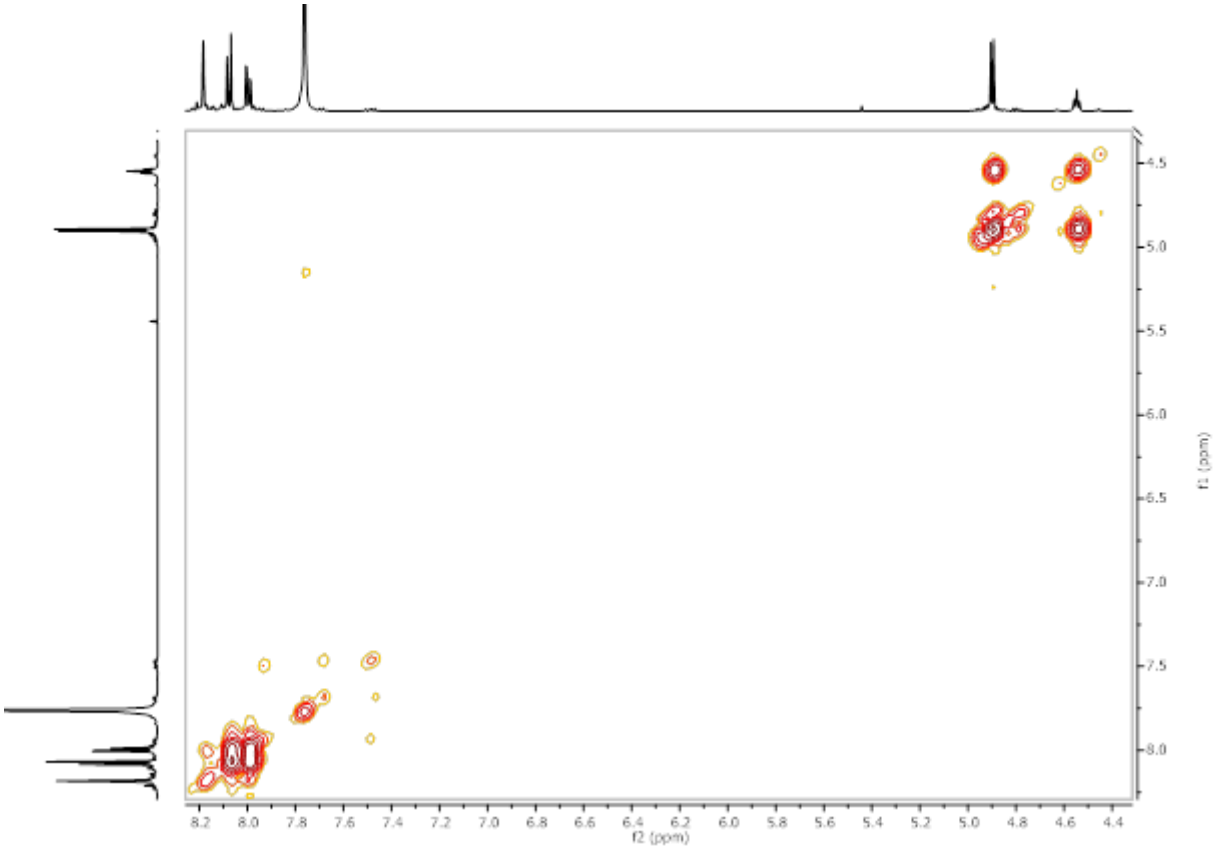

Figure 75: ^{1}H-^{1}H COSY-NMR of Smoc-Cl **2.**

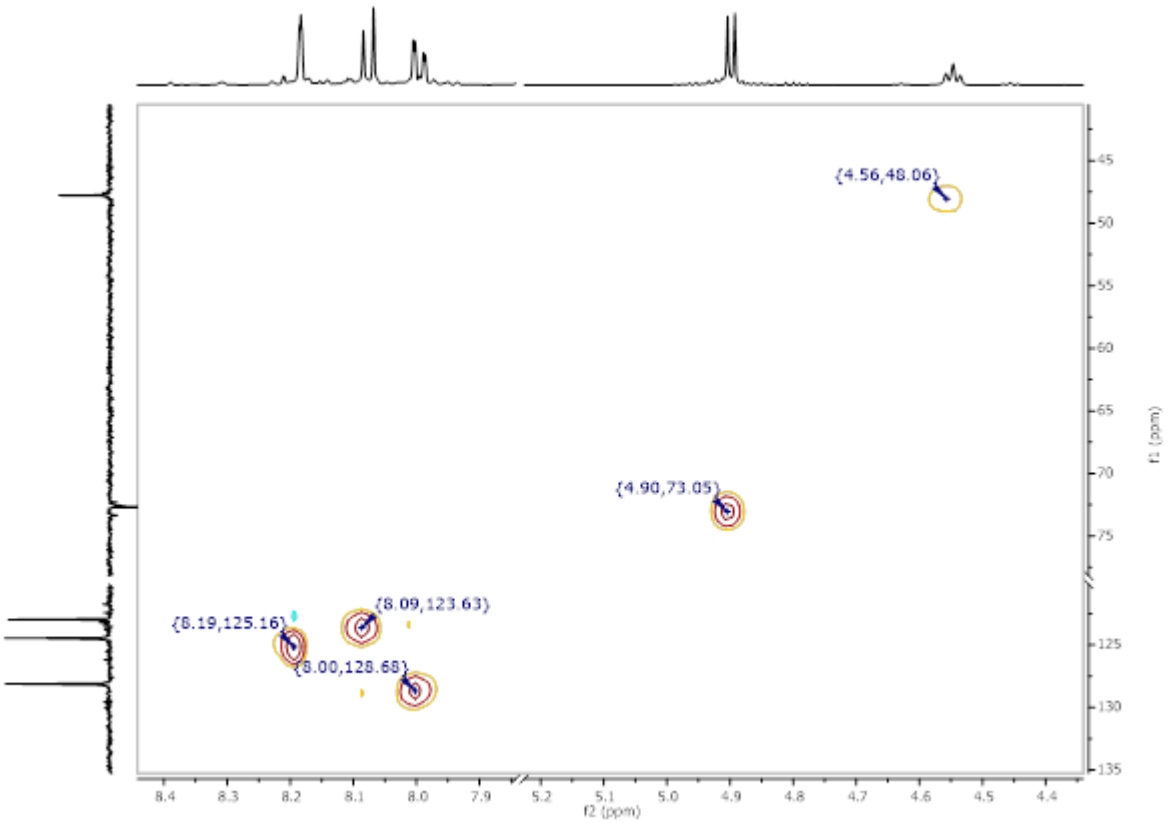

Figure 76: ^{1}H-^{13}C HSQC-NMR of Smoc-Cl **2.**

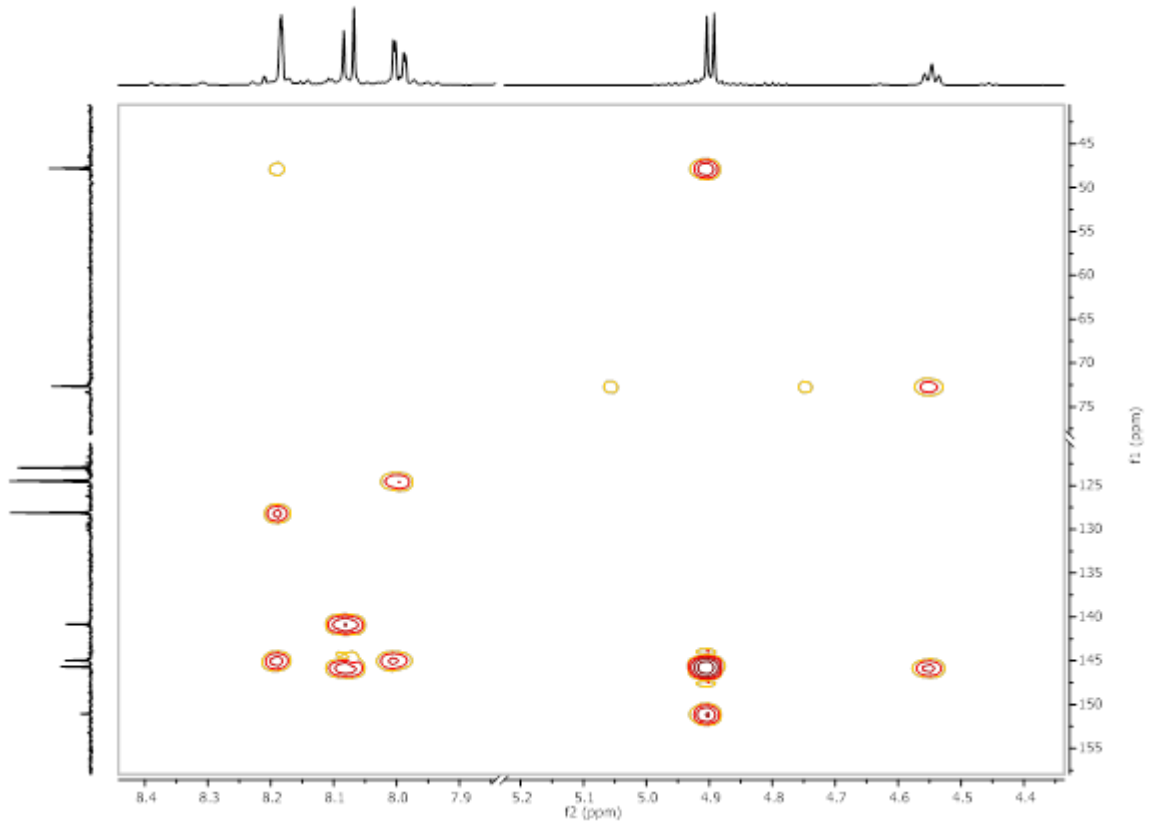

Figure 77: ^{1}H-^{13}C HMBC-NMR of Smoc-Cl **2.**

8.2. Amino Acids

8.2.1. Analytical data of Smoc-L-Ala-OH 3

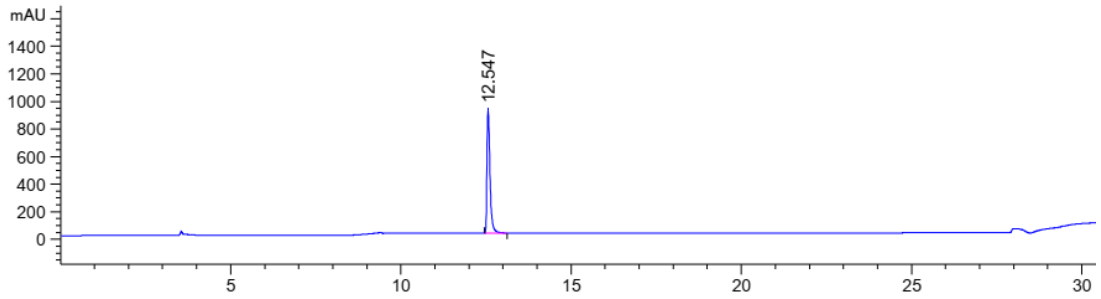

Figure 78: HPLC chromatogram of Smoc-L-Ala-OH **3** at λ=220 nm (0 to 40% MeCN).

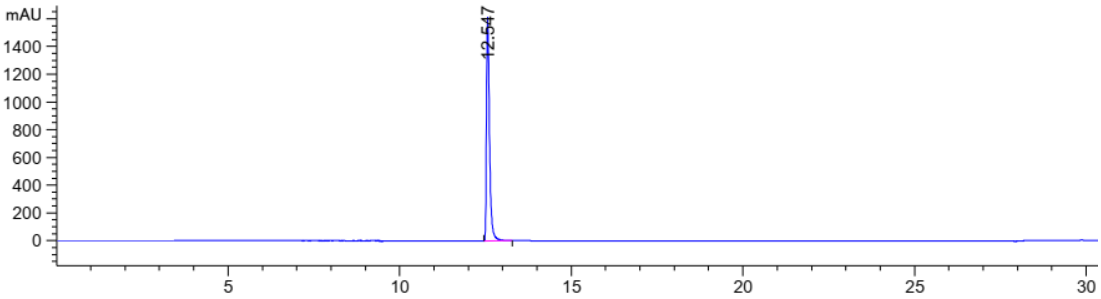

Figure 79: HPLC chromatogram of Smoc-L-Ala-OH **3** at λ=280 nm (0 to 40% MeCN).

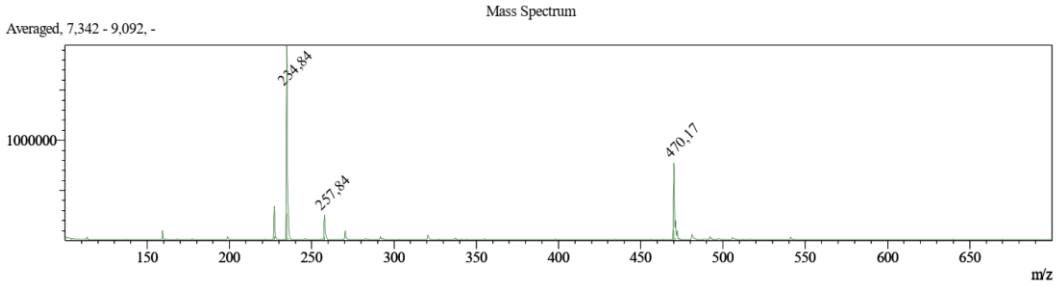

Figure 80: ESI-MS of Smoc-L-Ala-OH **3** (M measured=470.17[M-H]$^-$, M calc.=471.45).

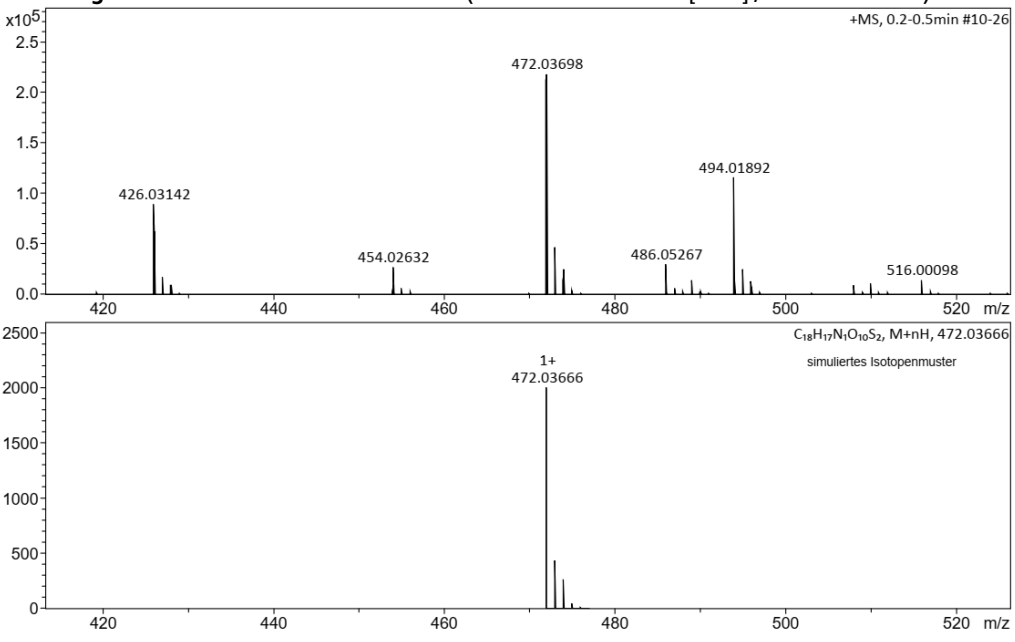

Figure 81: HR-MS of Smoc-L-Ala-OH 3 (M measured=472.03698 [M+H]$^+$, M calc.=472.03666)

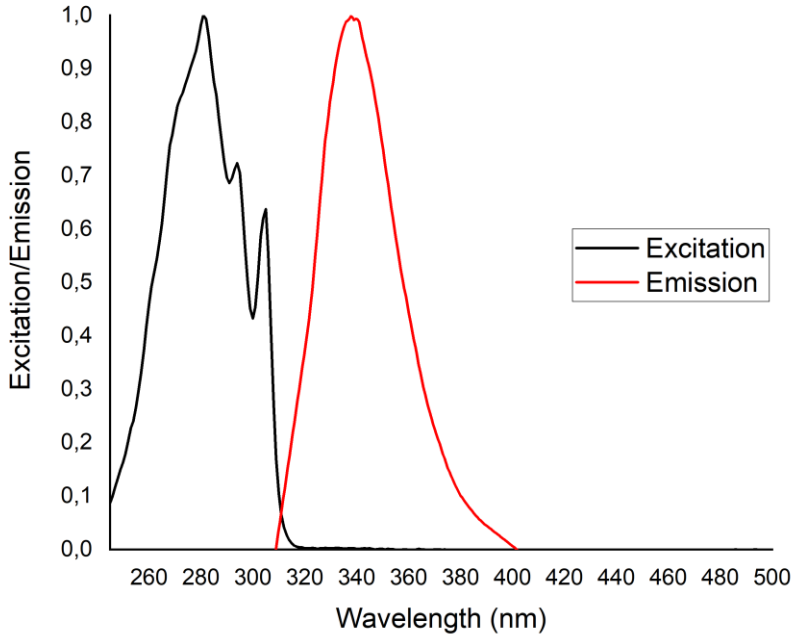

Figure 82: Excitation and emission spectra of Smoc-L-Ala-OH **3**, excitation and emission have been normalized between 0 and 1 for illustration.

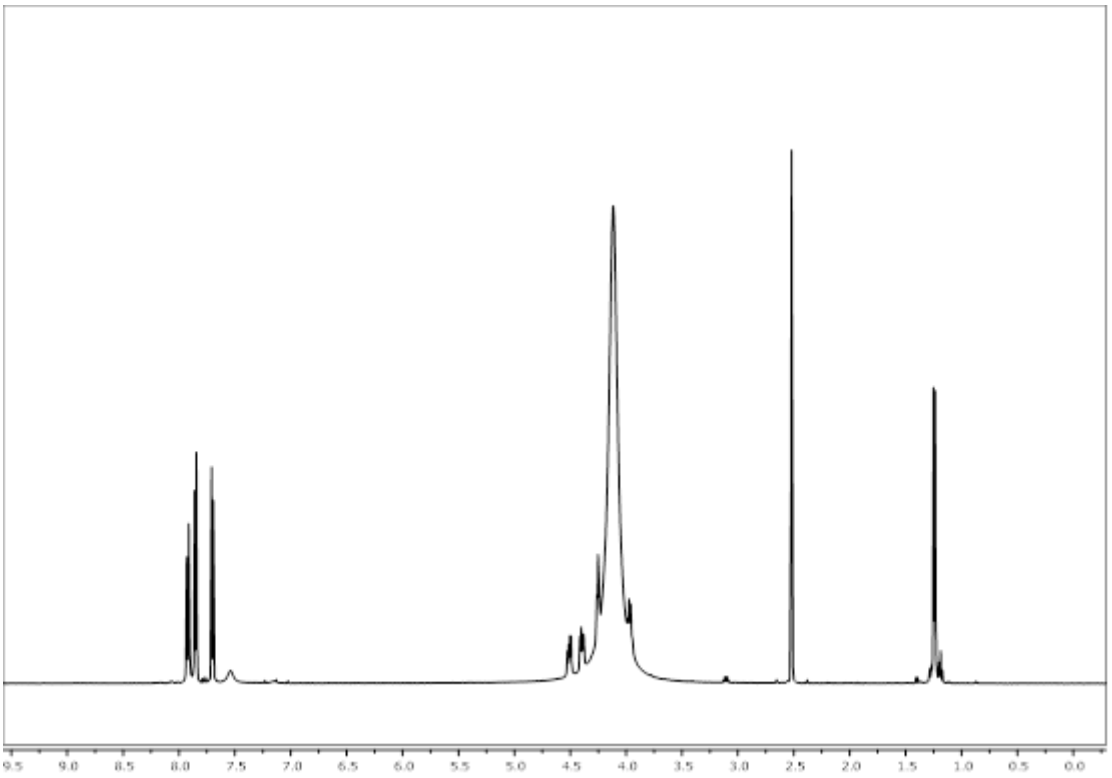

Figure 83: ^{1}H-NMR of Smoc-L-Ala-OH **3**.

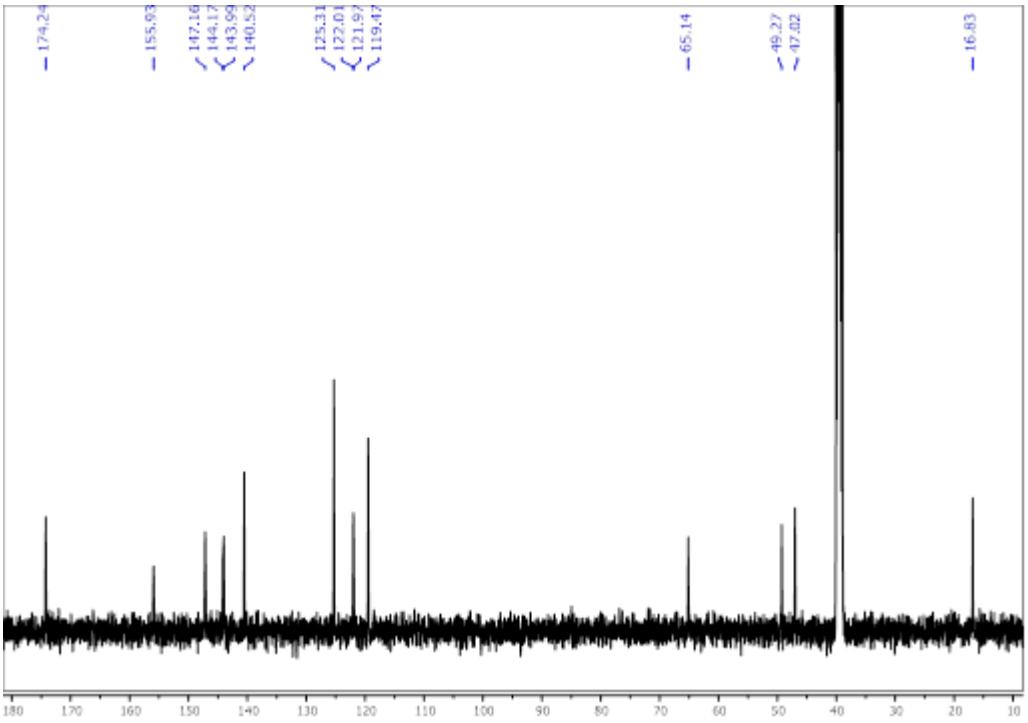

Figure 84: ^{13}C NMR of Smoc-L-Ala-OH **3**.

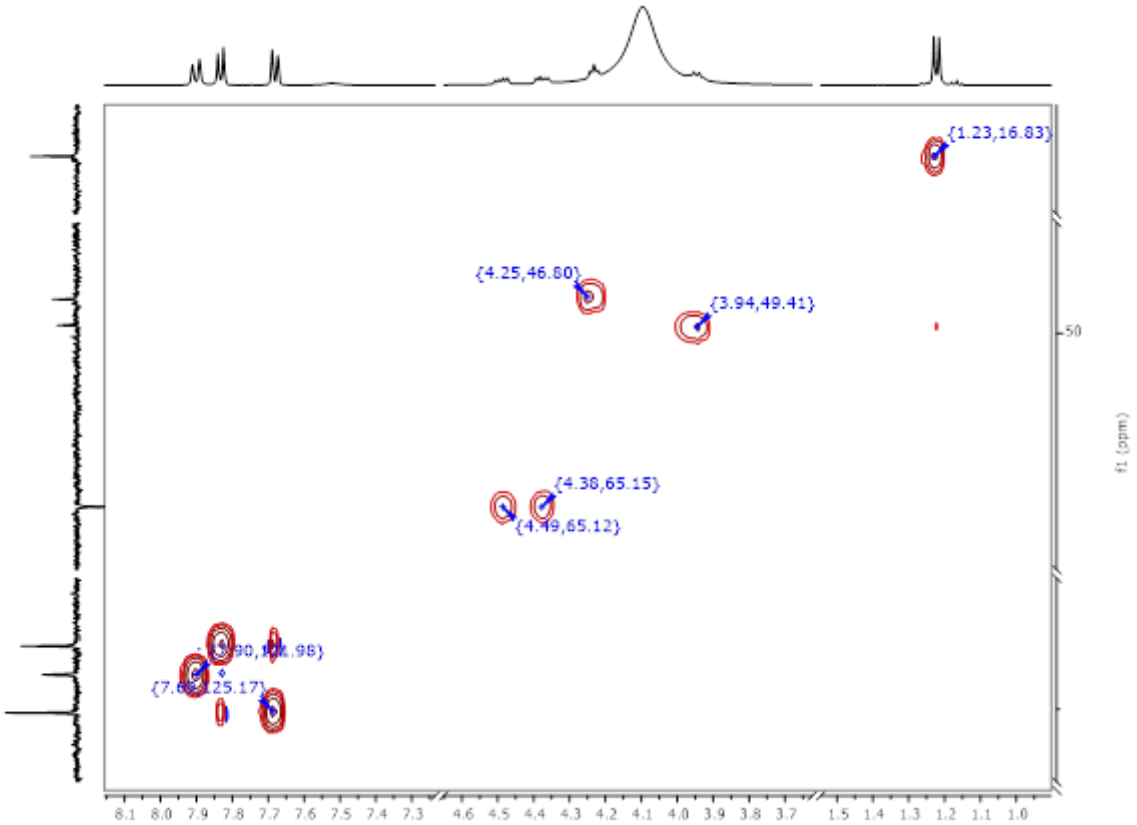

Figure 85: ^{1}H-^{13}C HSQC-NMR of Smoc-L-Ala-OH **3**.

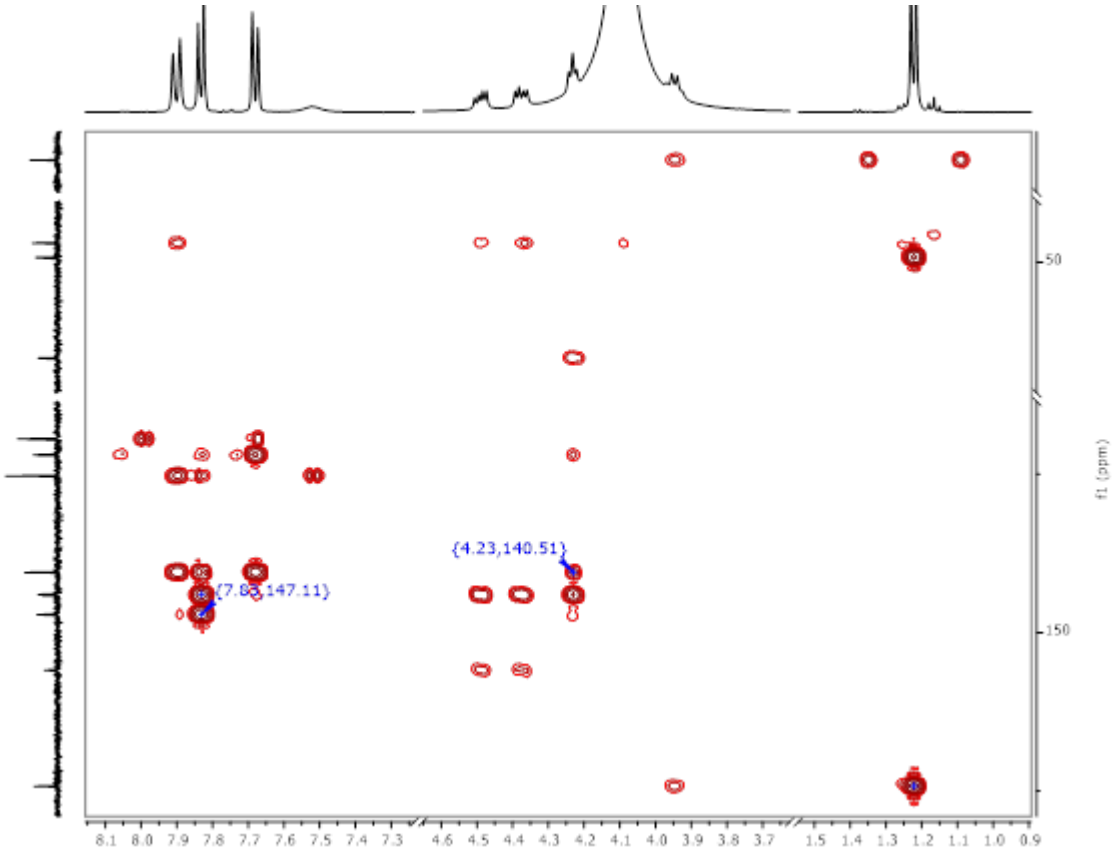

Figure 86: ^{1}H-^{13}C HMBC-NMR of Smoc-L-Ala-OH **3**.

8.2.2. Analytical data of Smoc-D-Ala-OH 4

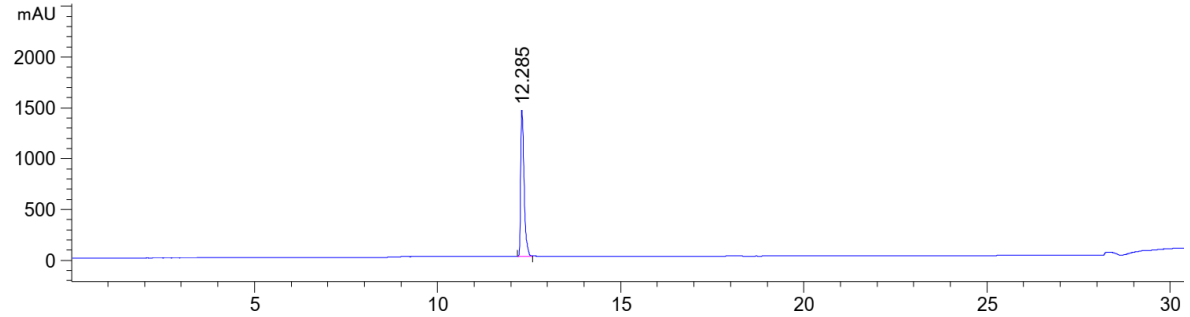

Figure 87: HPLC chromatogram of Smoc-D-Ala-OH **4** at λ=220 nm (0 to 40% MeCN).

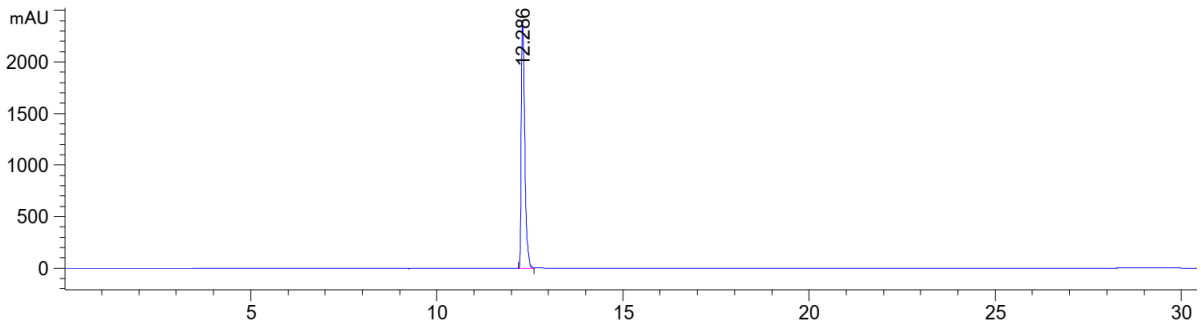

Figure 88: HPLC chromatogram of Smoc-D-Ala-OH **4** at λ=280 nm (0 to 40% MeCN).

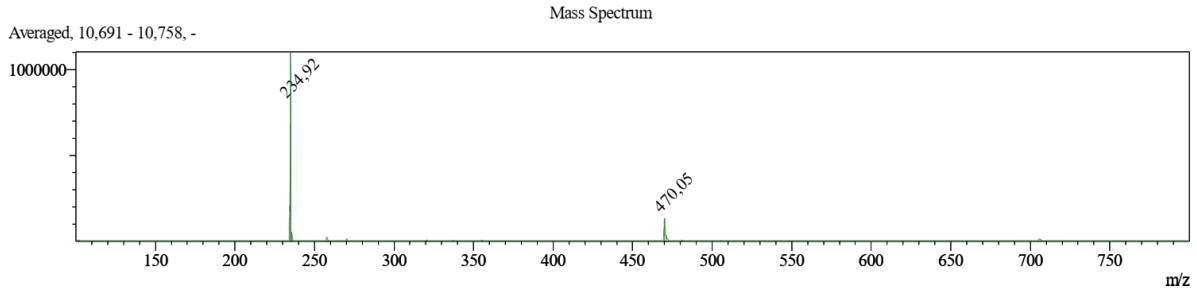

Figure 89: ESI-MS of Smoc-D-Ala-OH **4** (M measured=470.05[M-H]$^-$, M calc.=471.45).

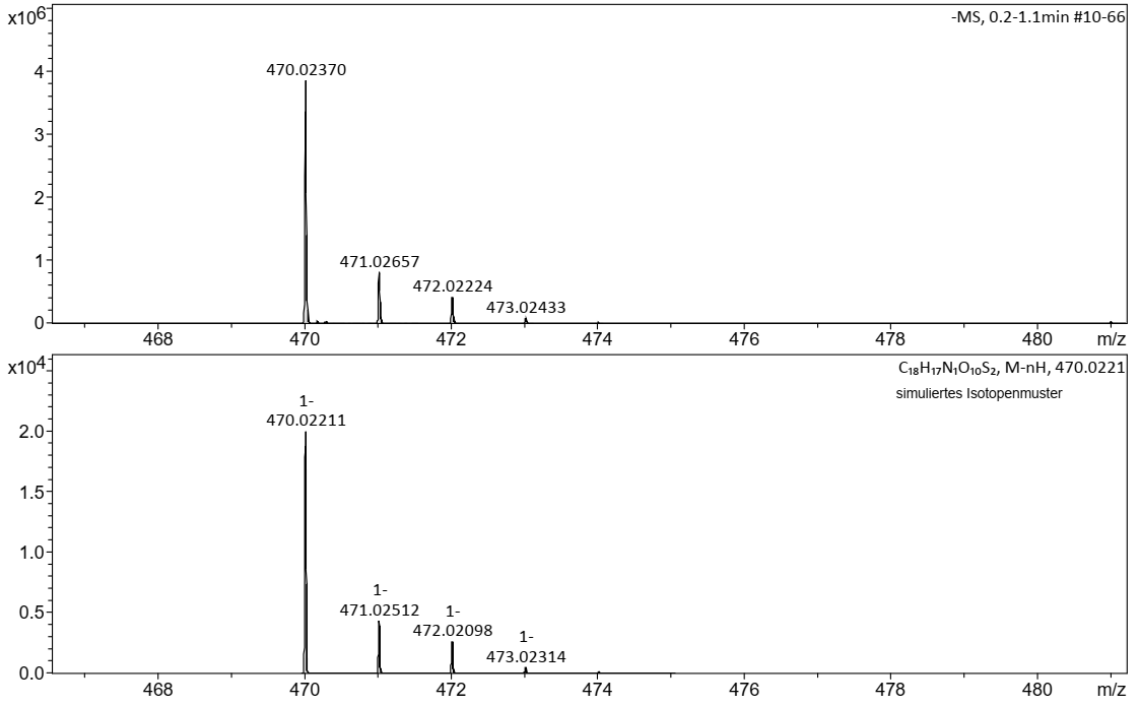

Figure 90: HR-MS of Smoc-D-Ala-OH **4** (M measured=470.02370 [M-H]$^-$, M calc.=470.02211).

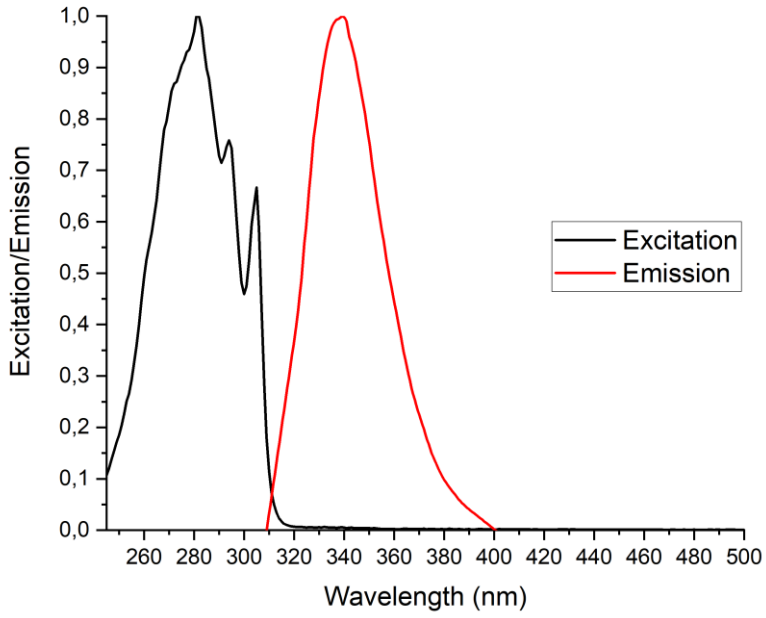

Figure 91: Excitation and emission spectra of Smoc-D-Ala-OH **4**, excitation and emission have been normalized between 0 and 1 for illustration.

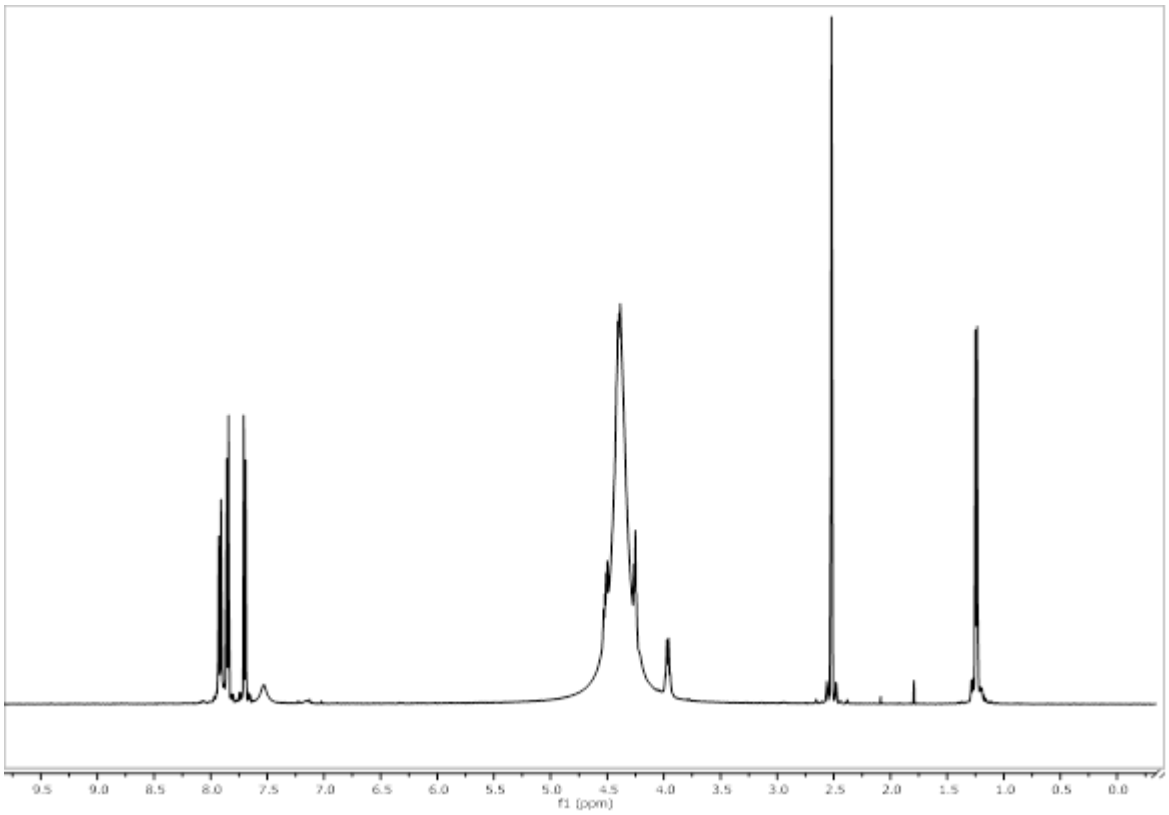

Figure 92: ^{1}H-NMR of Smoc-D-Ala-OH **4**.

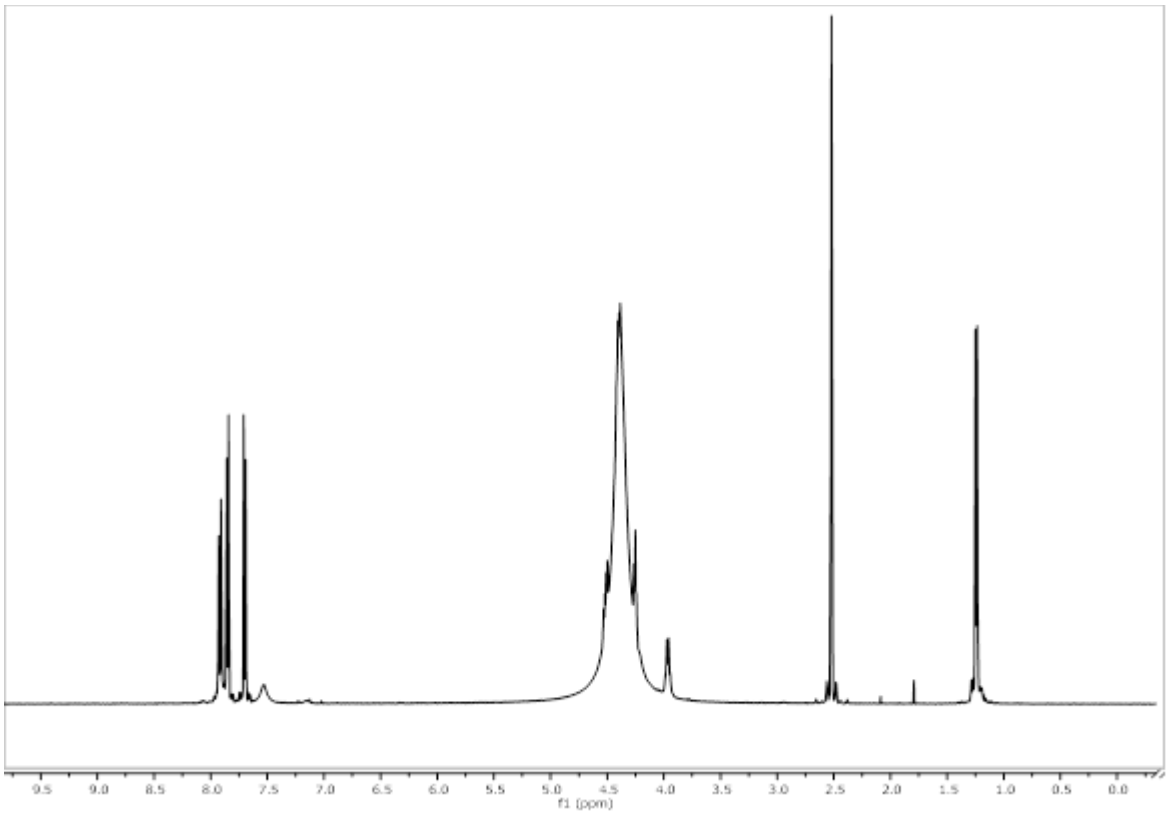

Figure 93: ^{13}C-NMR of Smoc-D-Ala-OH **4**.

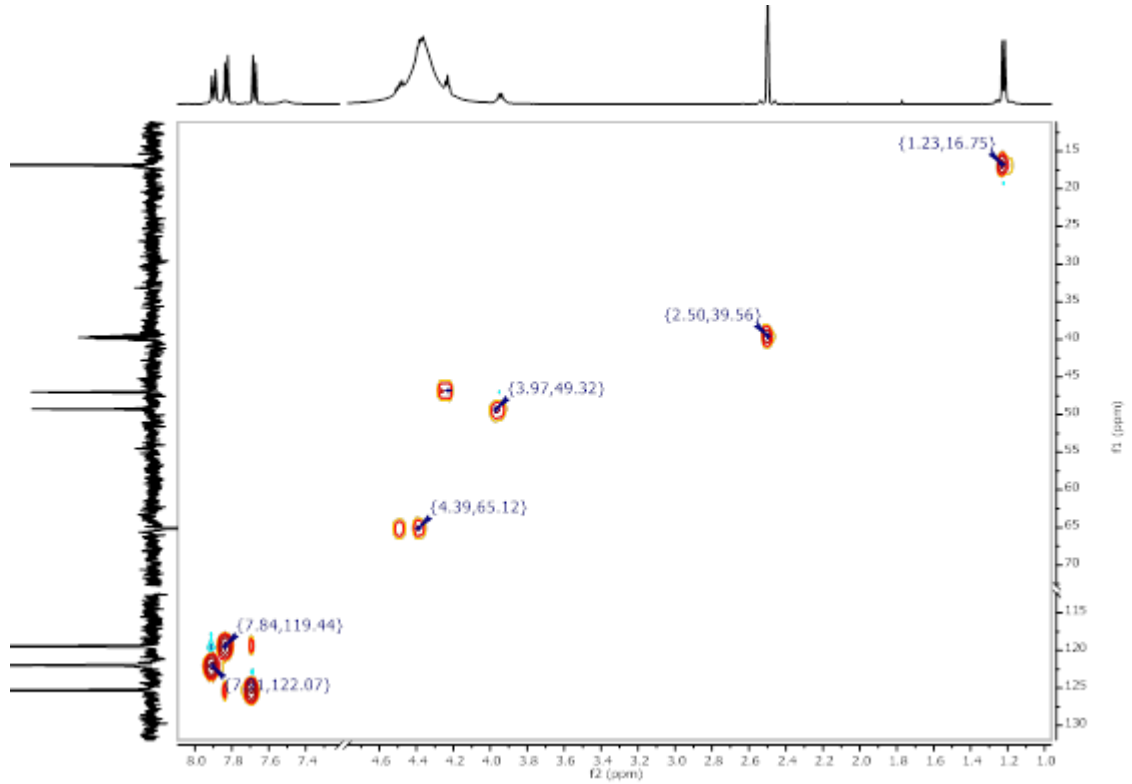

Figure 94: ^{1}H-^{13}C HSQC-NMR of Smoc-D-Ala-OH **4**.

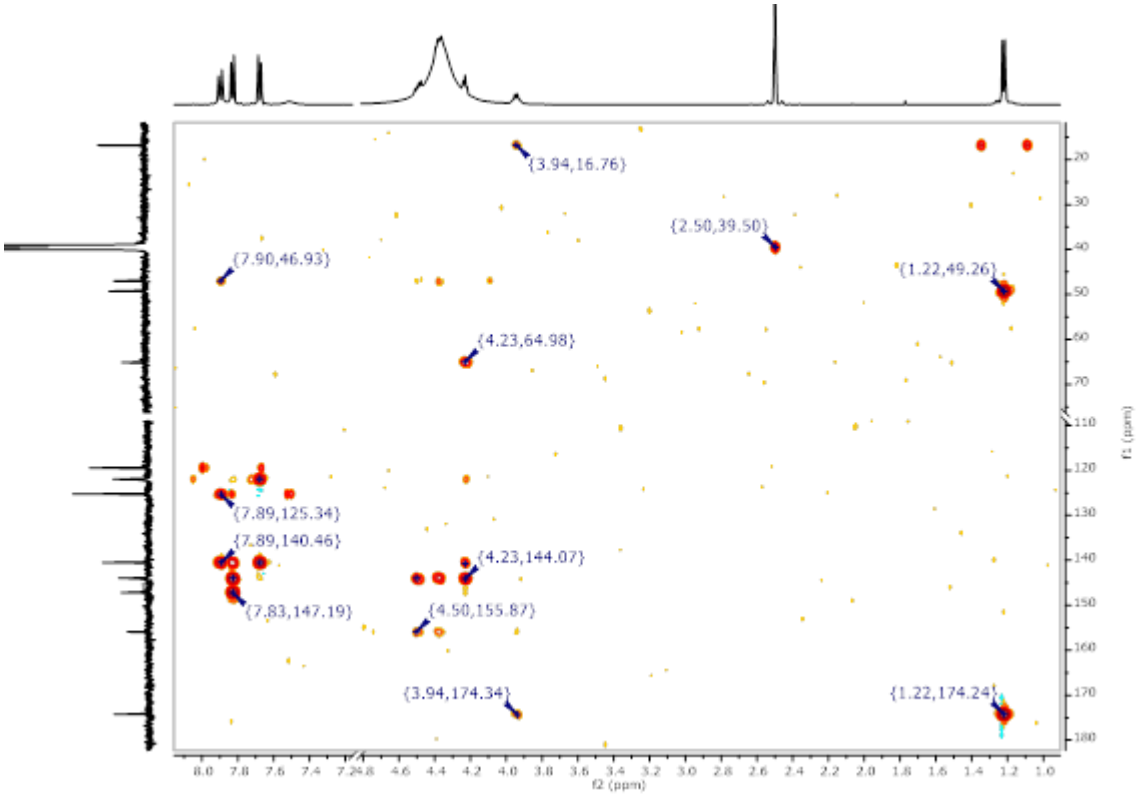

Figure 95: ^{1}H-^{13}C HMBC-NMR of Smoc-D-Ala-OH **4**.

8.2.3. Analytical data of Smoc-L-Arg-OH 5

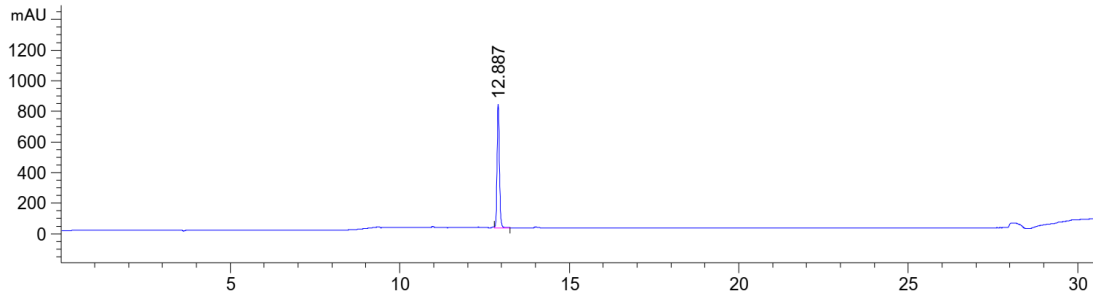

Figure 96: HPLC chromatogram of Smoc-L-Arg-OH **5** at λ=220 nm (0 to 40% MeCN).

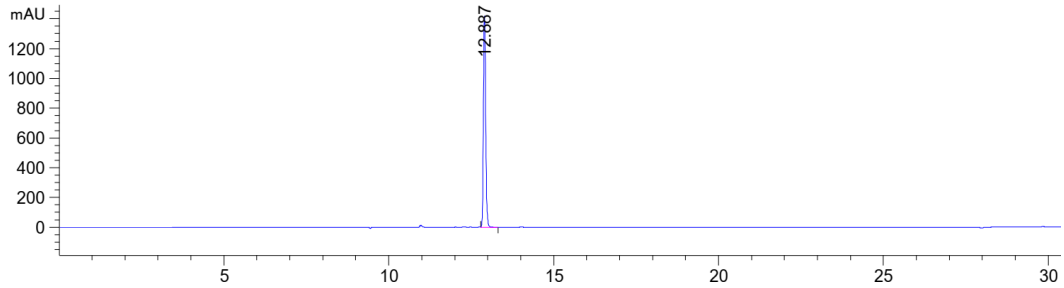

Figure 97: HPLC chromatogram of Smoc-L-Arg-OH **5** at λ=280 nm (0 to 40% MeCN).

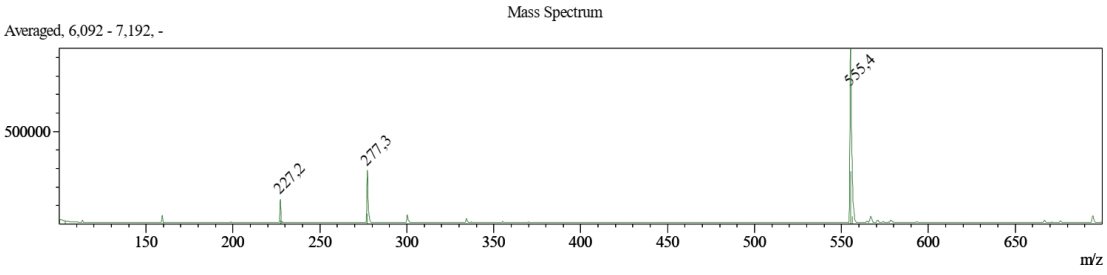

Figure **98:** ESI-MS of Smoc-L-Arg-OH **5** (M measured=555.40 $[M-H]^-$, M calc.=556.56).

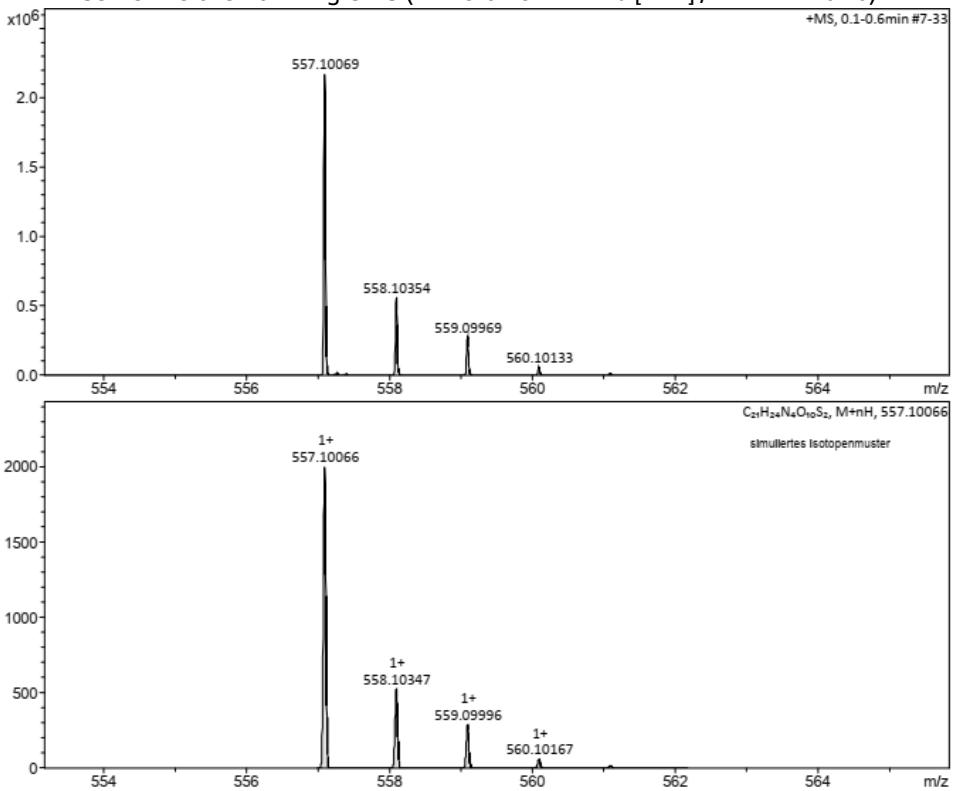

Figure 99: HR-MS of Smoc-L-Arg-OH **5** (M measured=557.10069 $[M+H]^+$, M calc.=557.010066).

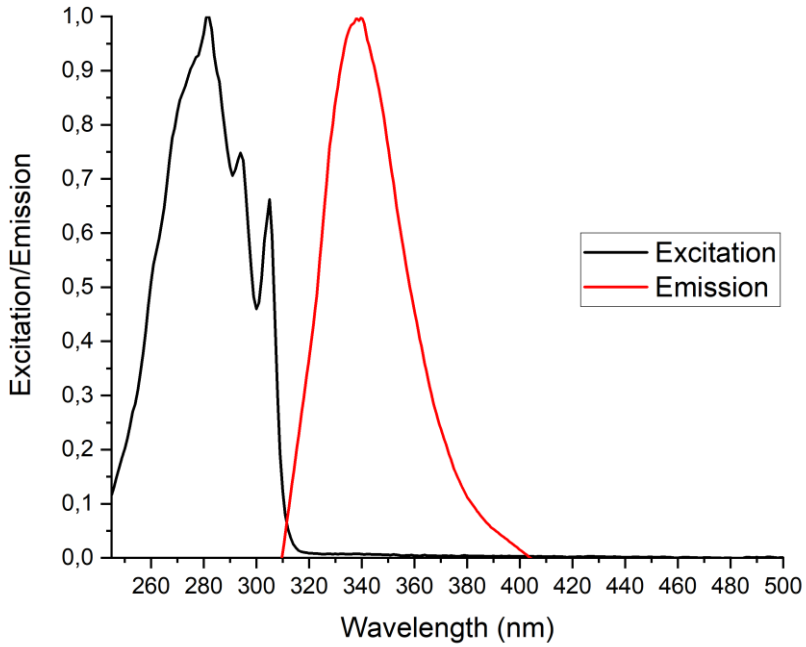

Figure 100: Excitation and emission spectra of Smoc-L-Arg-OH **5**, excitation and emission have been normalized between 0 and 1 for illustration.

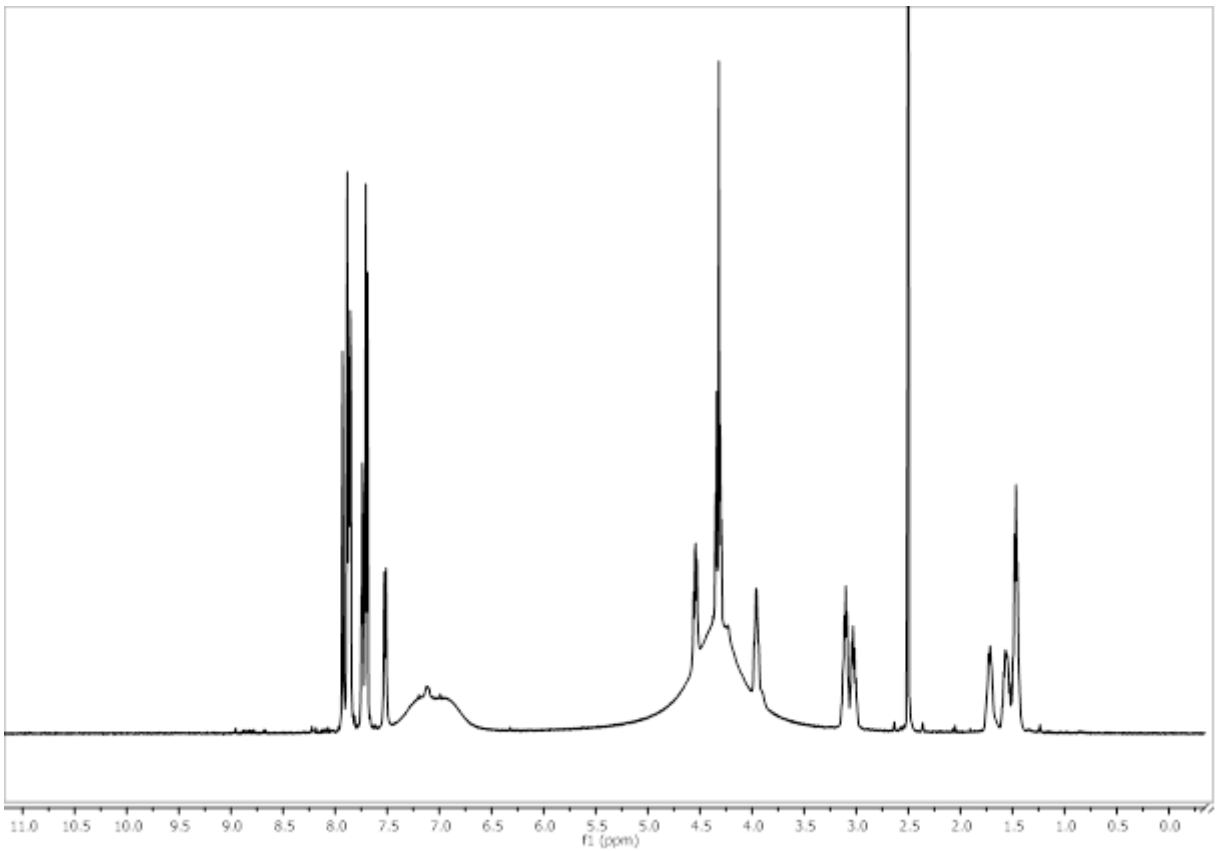

Figure 101: ^{1}H-NMR of Smoc-L-Arg-OH **5**.

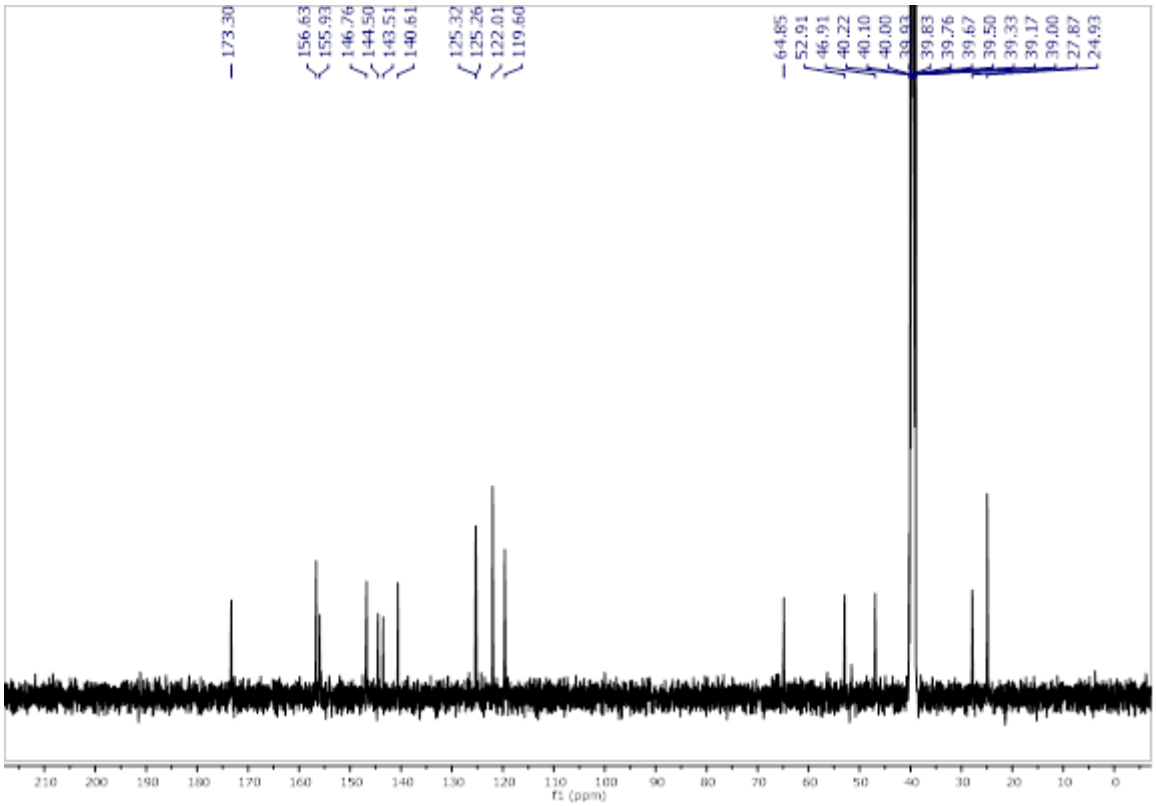

Figure 102: ^{13}C-NMR of Smoc-L-Arg-OH **5**.

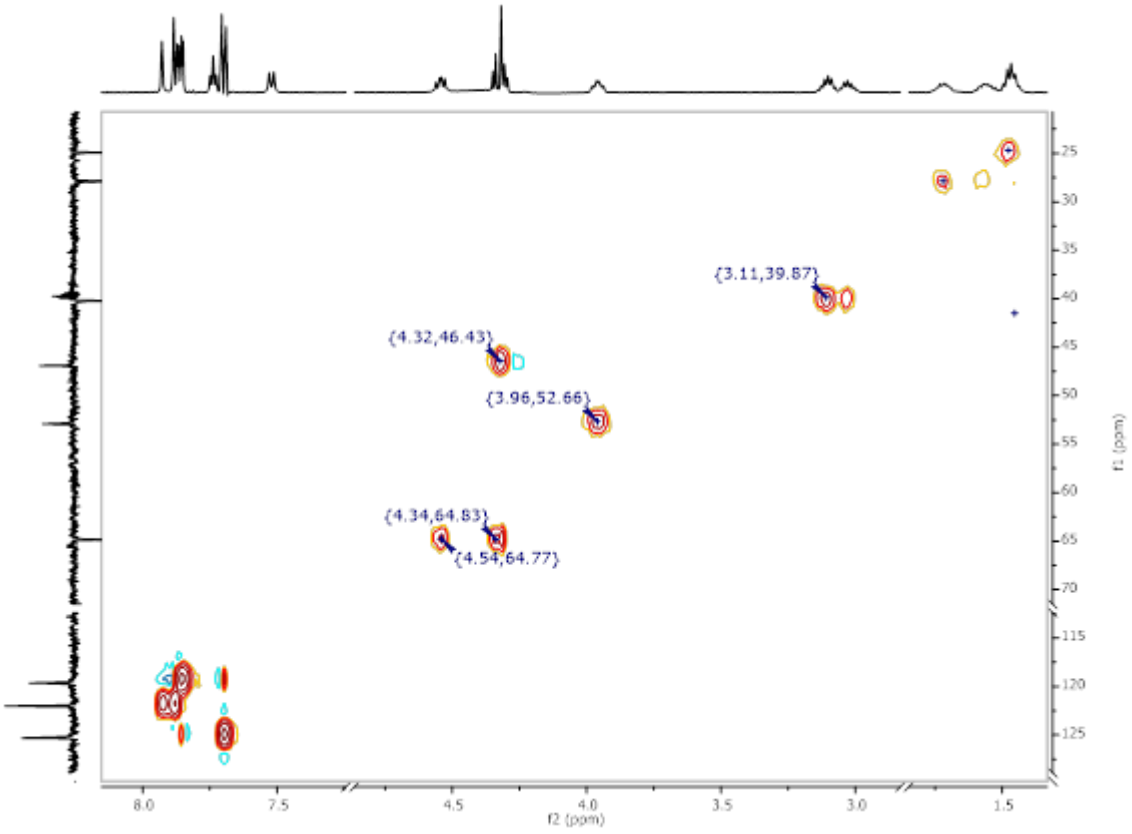

Figure 103: ^{1}H-^{13}C HSQC-NMR of Smoc-L-Arg-OH **5**.

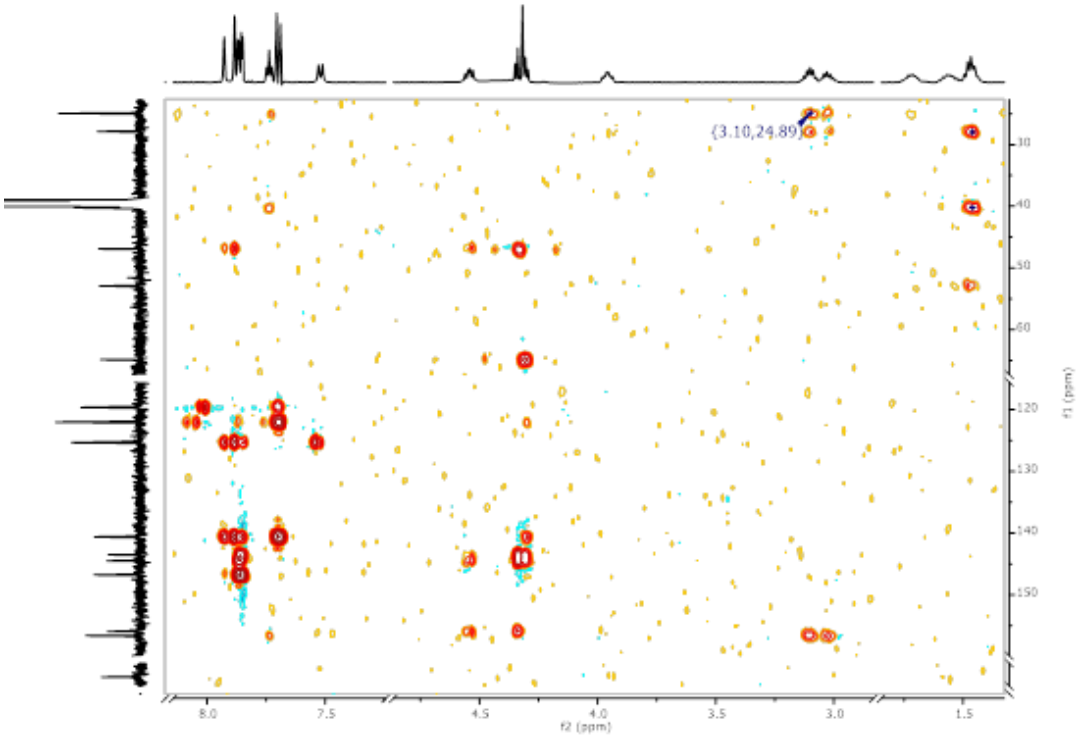

Figure 104: ^{1}H-^{13}C HMBC-NMR of Smoc-L-Arg-OH **5**.

8.2.4. Analytical data of Smoc-L-Arg(Pbf)-OH 6

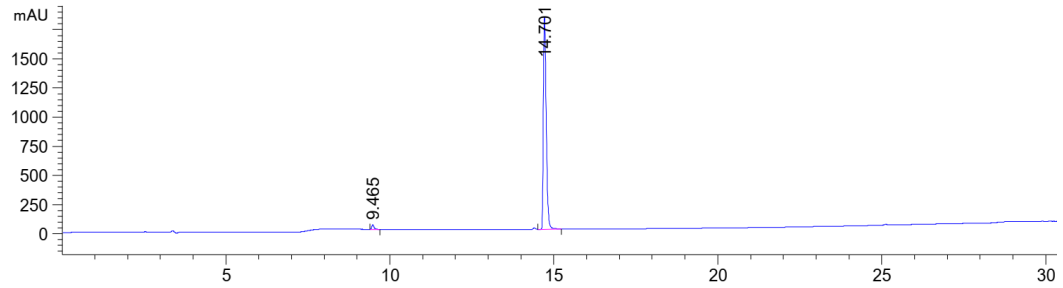

Figure 105: HPLC chromatogram of Smoc-L-Arg(Pbf)-OH **6** at λ=220 nm (10 to 100% MeCN).

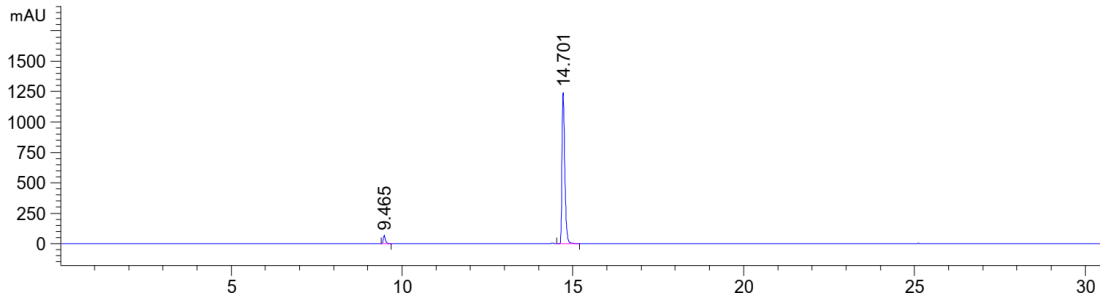

Figure 106: HPLC chromatogram of Smoc-L-Arg(Pbf)-OH **6** at λ=280 nm (10 to 100% MeCN).

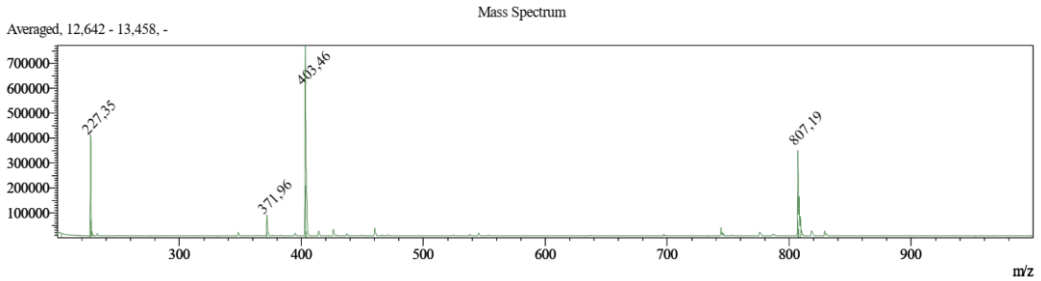

Figure 107: ESI-MS of Smoc-L-Arg(Pbf)-OH **6** (M measured=807.19 $[M-H]^{-}$, M calc.=808.89).

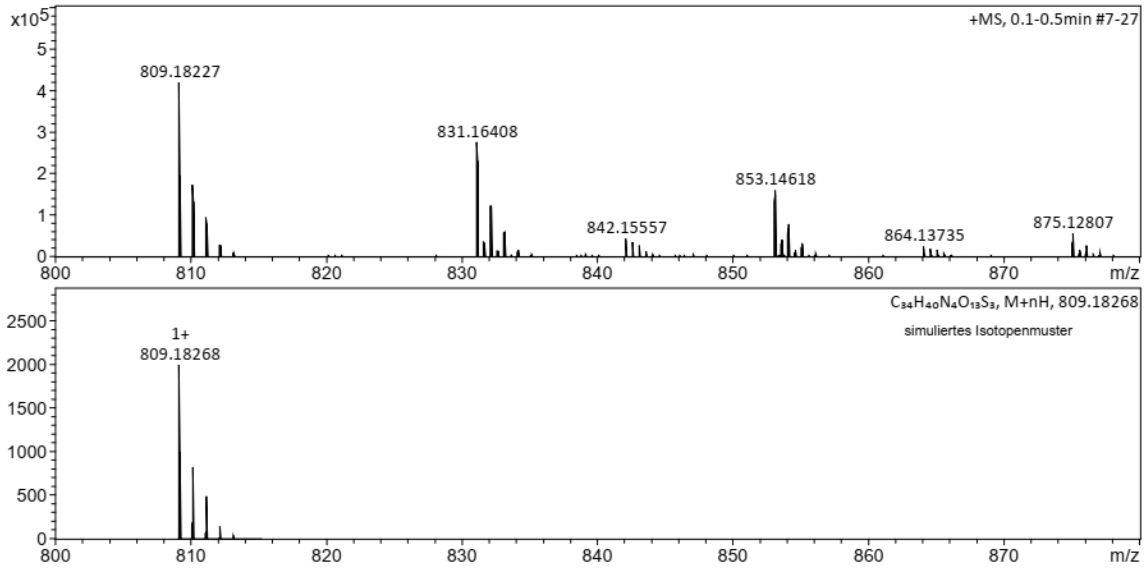

Figure 108: HR-MS of Smoc-L-Arg(Pbf)-OH **6** (M measured=809.18227 $[M+H]^+$, M calc.=809.18268).

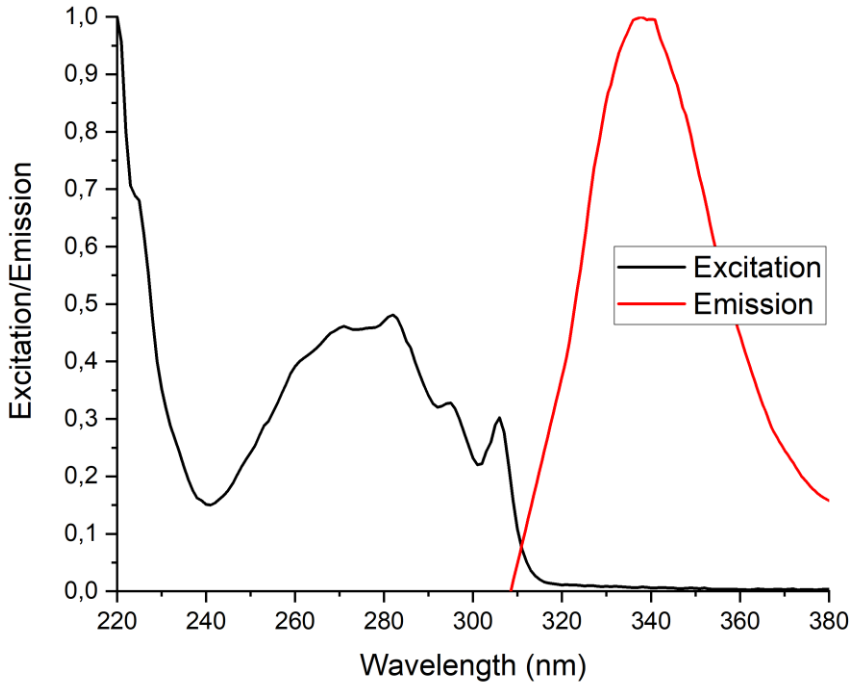

Figure 109: Excitation and emission spectra of Smoc-L-Arg(Pbf)-OH **6**, excitation and emission have been normalized between 0 and 1 for illustration.

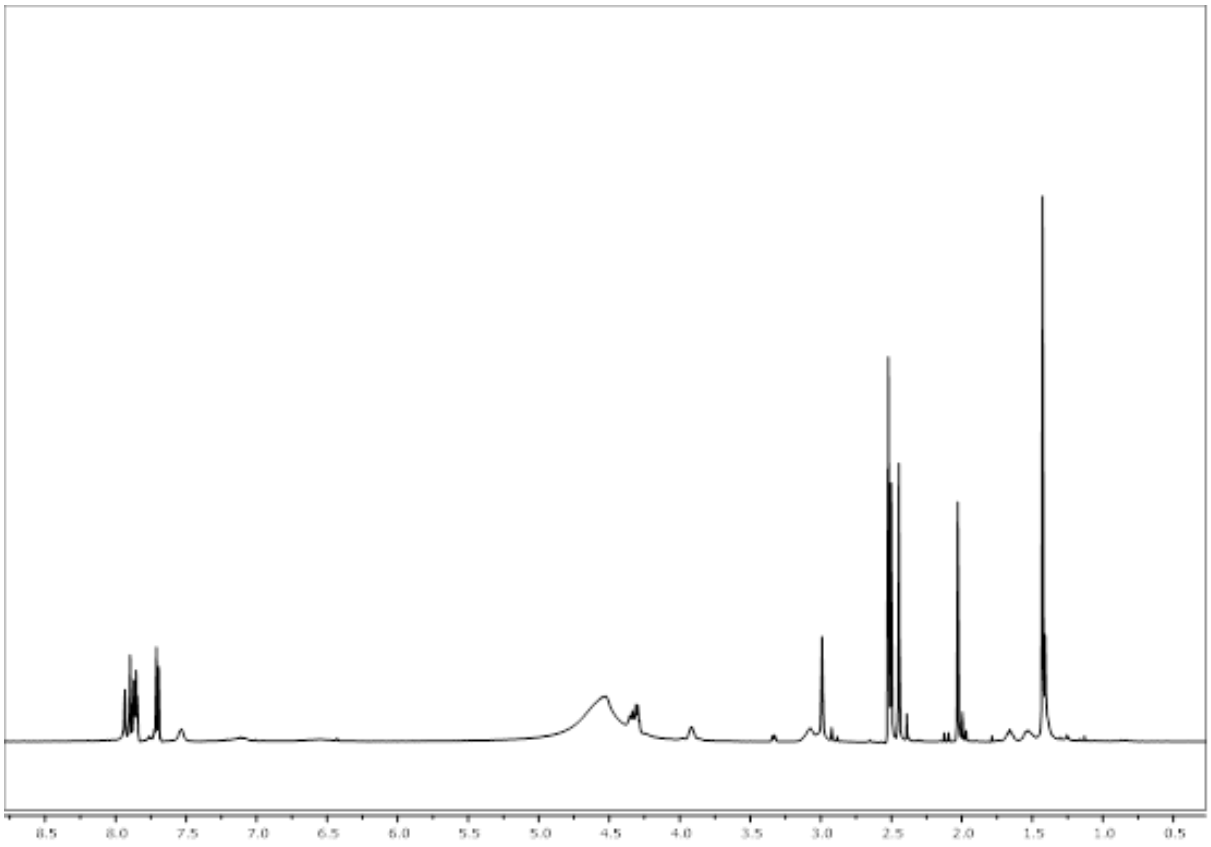

Figure 110: [1]H-NMR of Smoc-L-Arg(Pbf)-OH **6**.

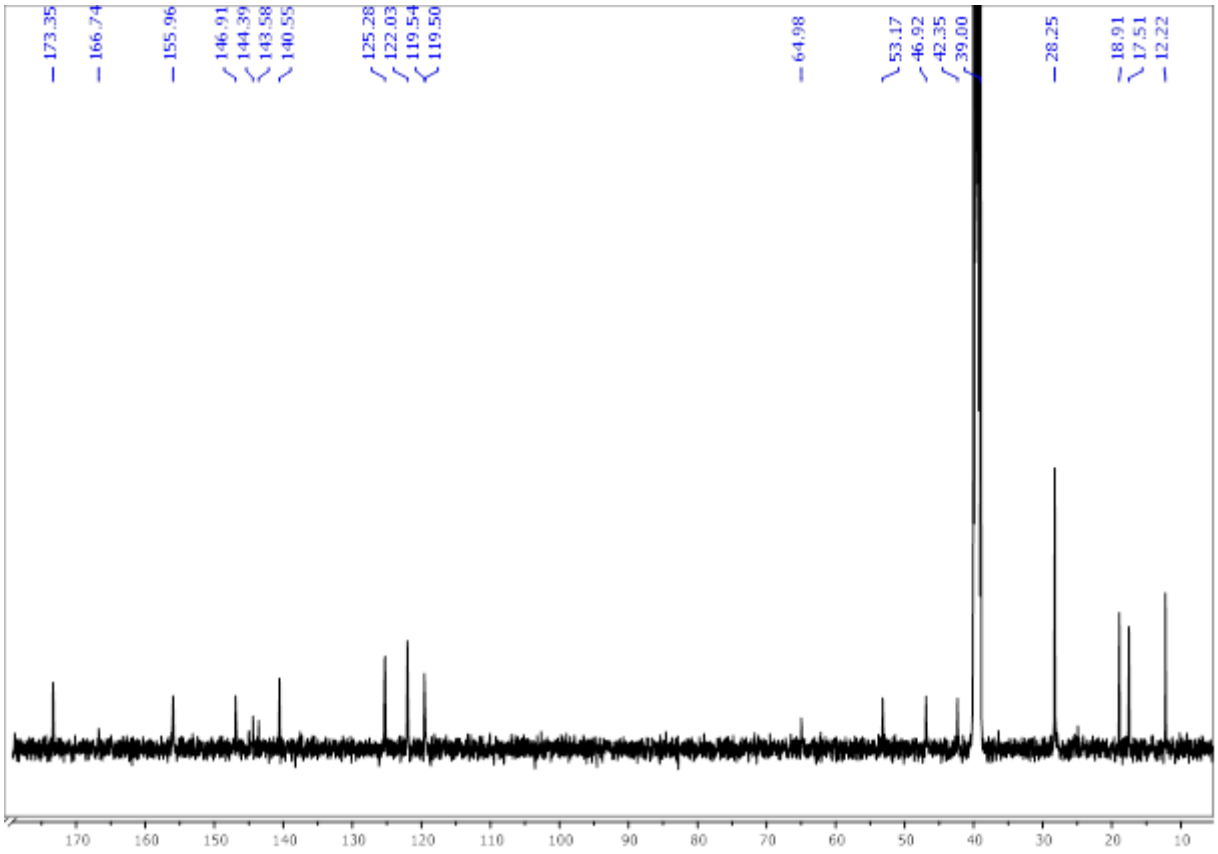

Figure 111: [13]C-NMR of Smoc-L-Arg(Pbf)-OH **6**.

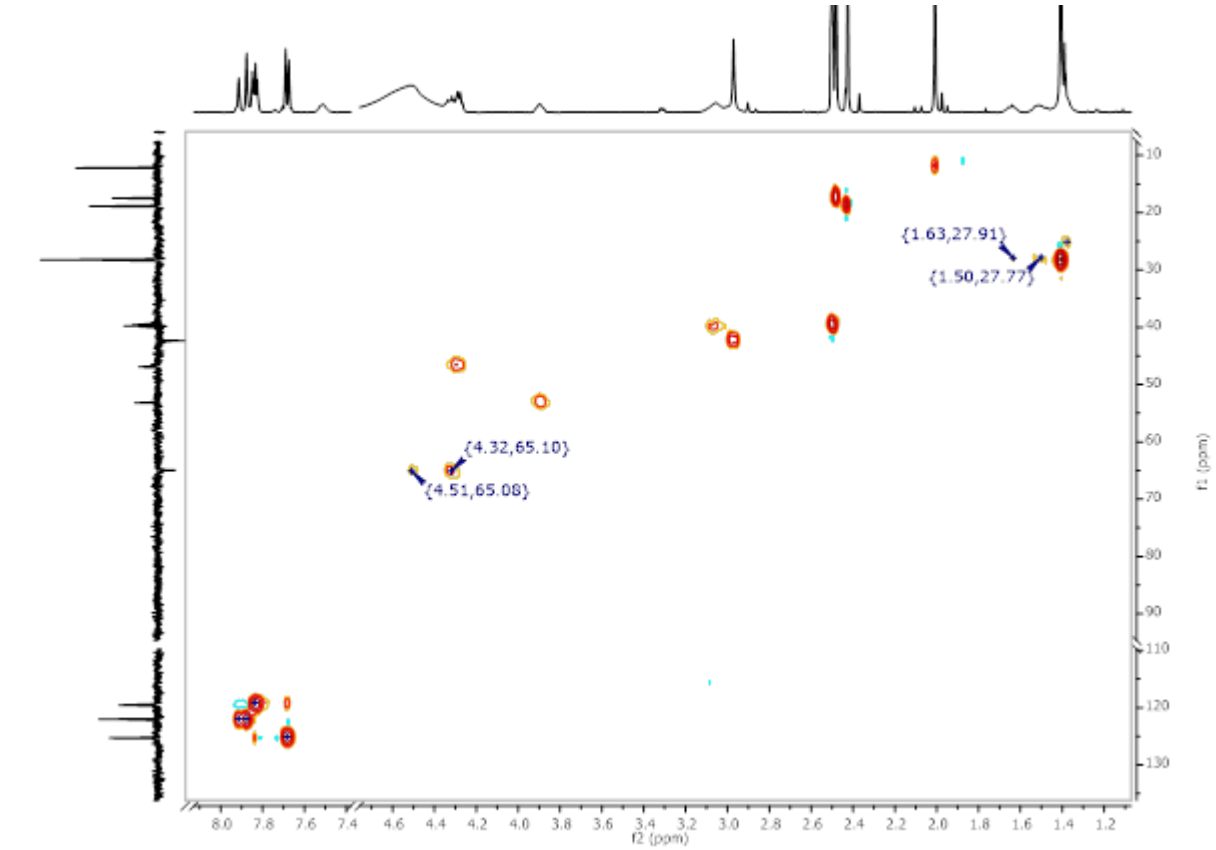

Figure 112: ^{1}H-^{13}C HSQC-NMR of Smoc-L-Arg(Pbf)-OH **6**.

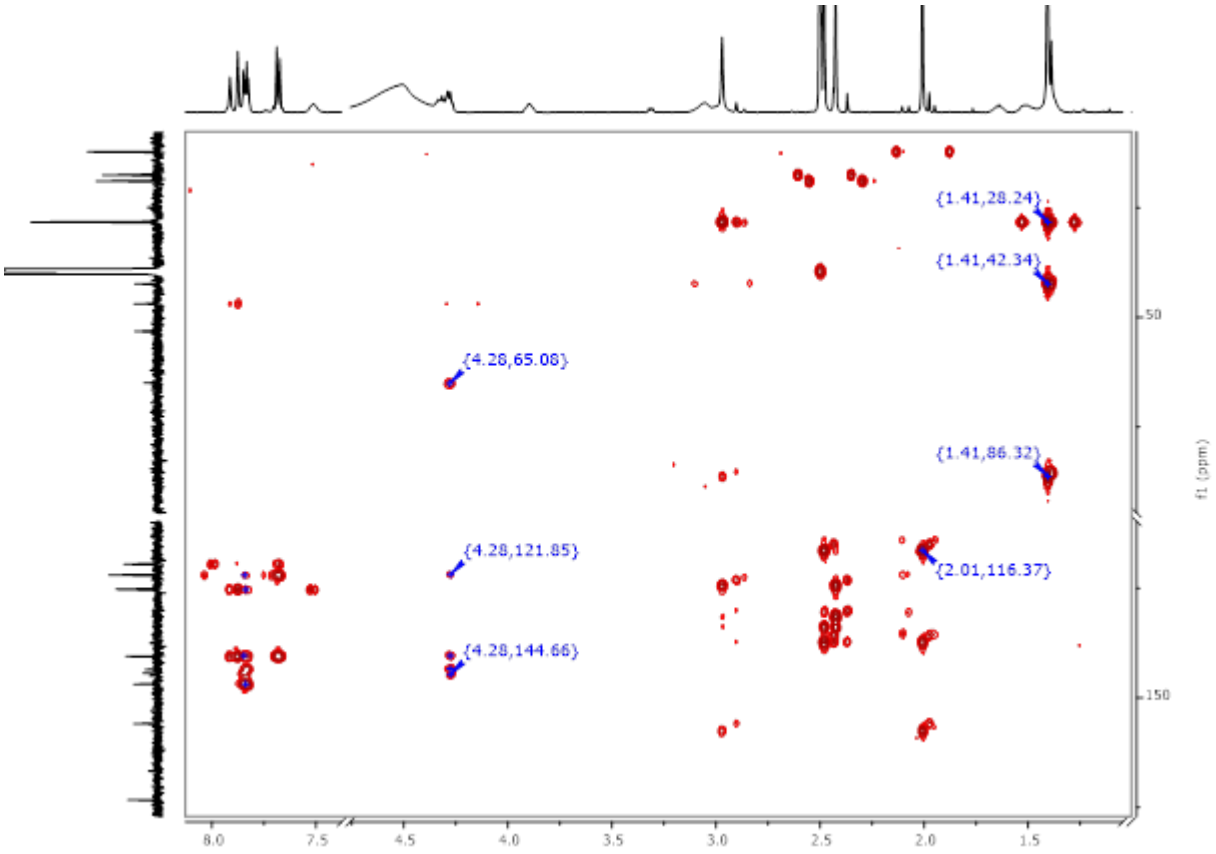

Figure 113: ^{1}H-^{13}C HMBC-NMR of Smoc-L-Arg(Pbf)-OH **6**.

8.2.5. Analytical data of Smoc-L-Asn-OH 7

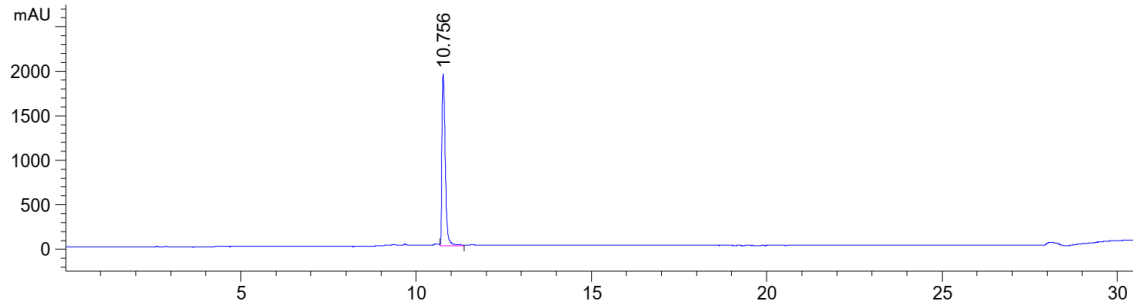

Figure 114: HPLC chromatogram of Smoc-L-Asn-OH **7** at λ=220 nm (0 to 40% MeCN).

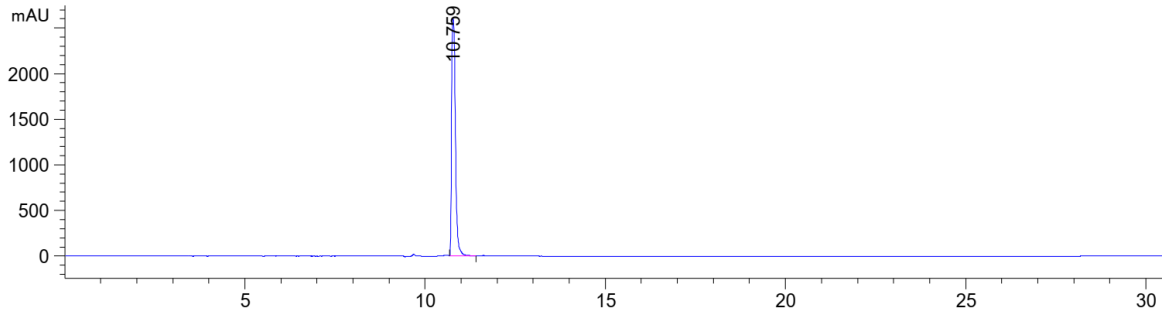

Figure 115: HPLC chromatogram of Smoc-L-Asn-OH **7** at λ=280 nm (0 to 40% MeCN).

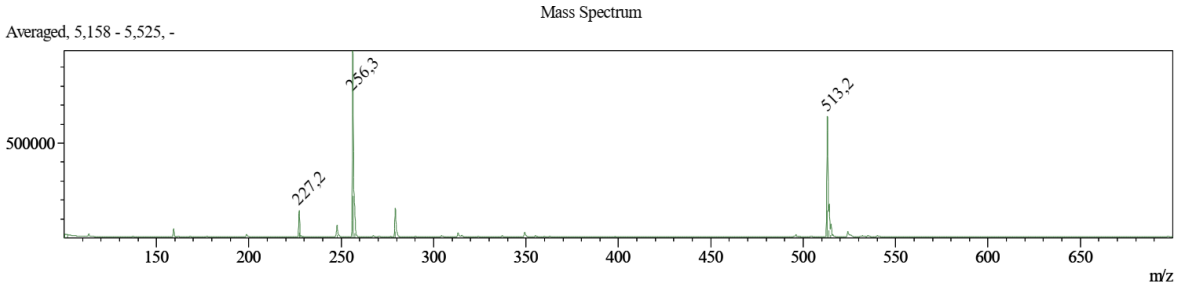

Figure 116: ESI-MS of Smoc-L-Asn-OH **7** (M measured=513.20 $[M-H]^-$, M calc.=514.48).

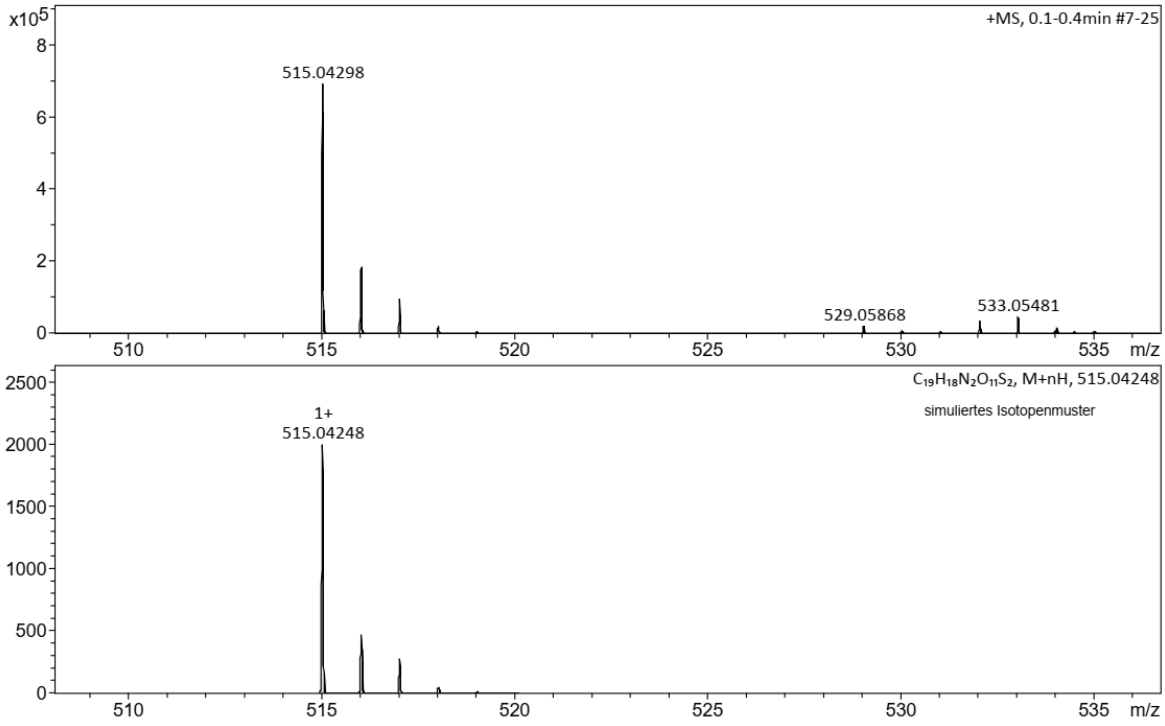

Figure 117: HR-MS of Smoc-L-Asn-OH **7** (M measured=515.04298 $[M+H]^+$, M calc.=515.04248).

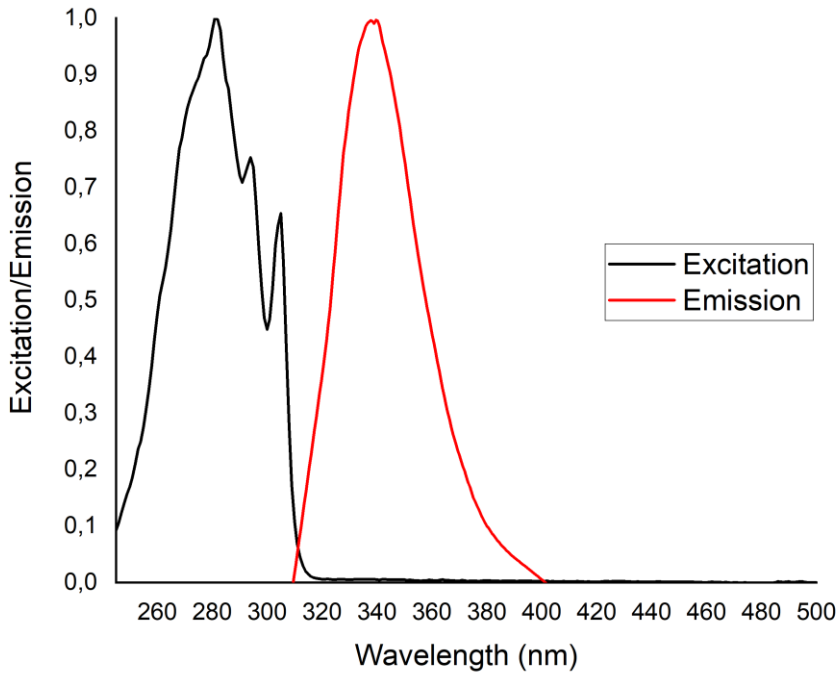

Figure 118: Excitation and emission spectra of Smoc-L-Asn-OH **7**, excitation and emission have been normalized between 0 and 1 for illustration.

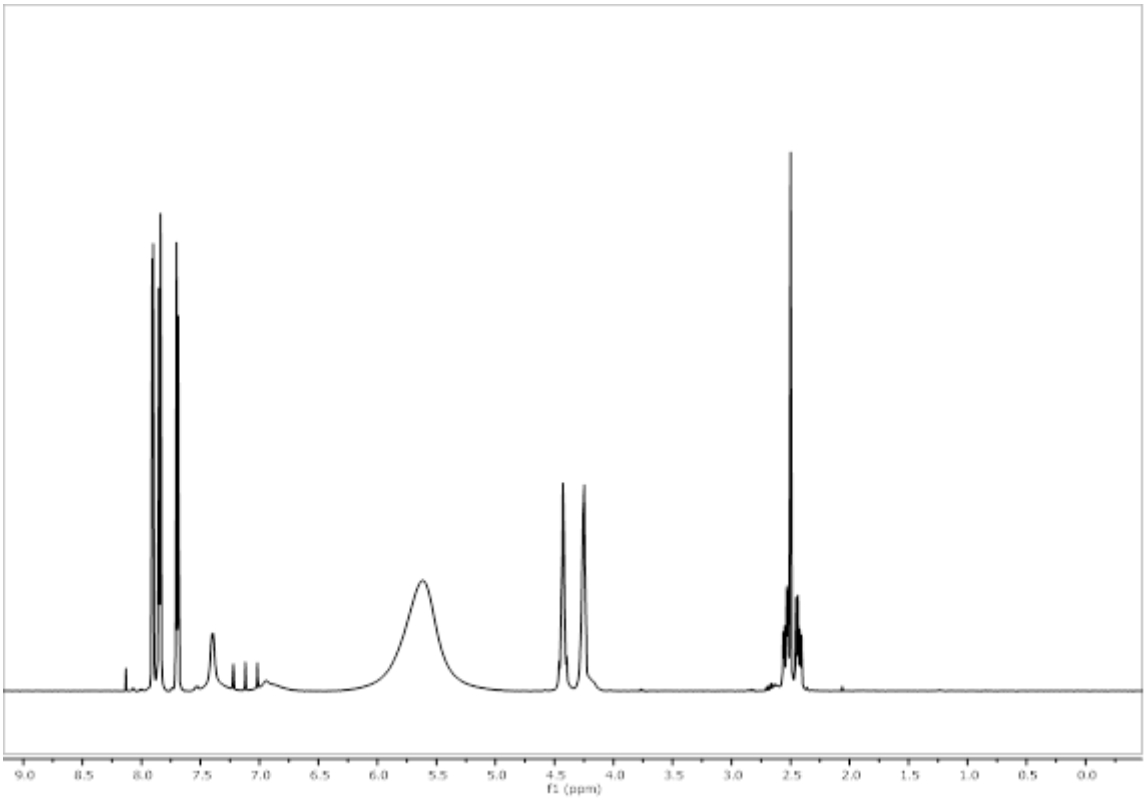

Figure 119: ^{1}H-NMR of Smoc-L-Asn-OH **7**.

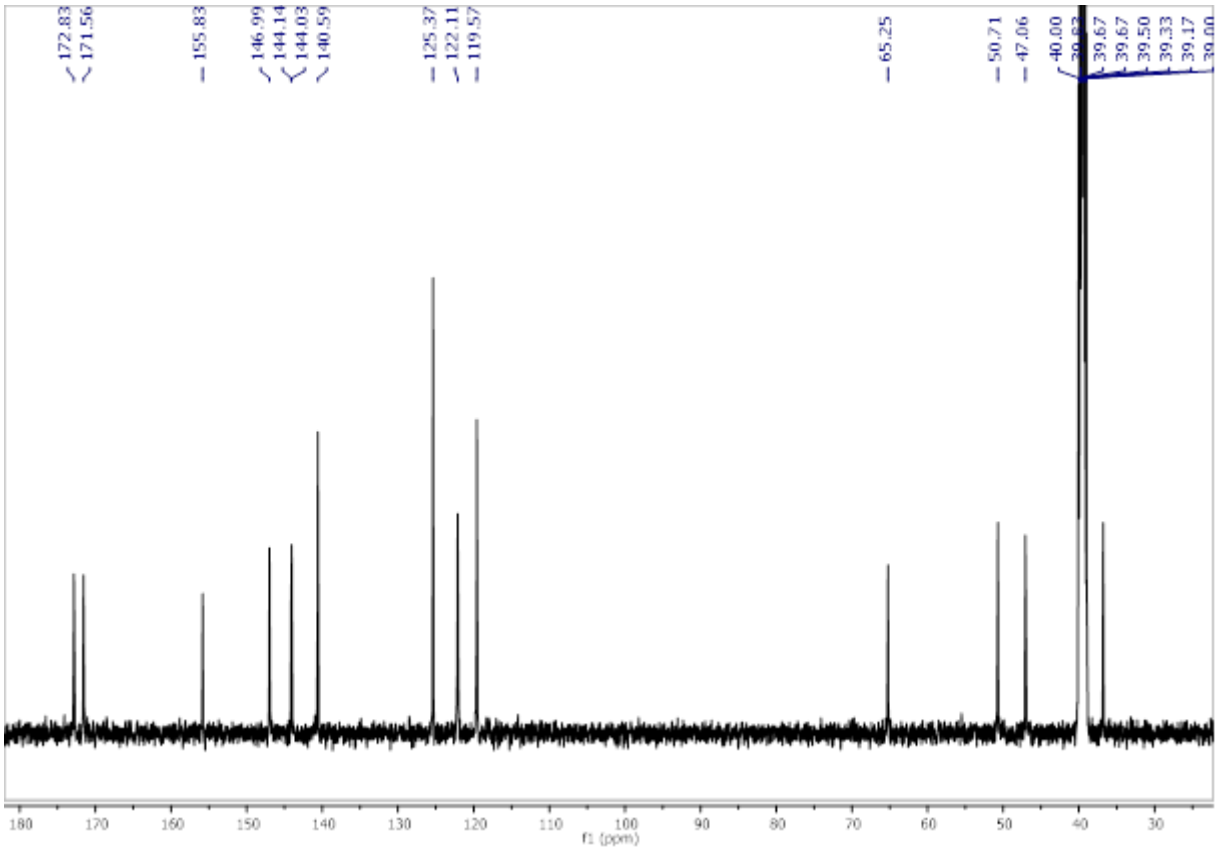

Figure 120: ^{13}C-NMR of Smoc-L-Asn-OH **7**.

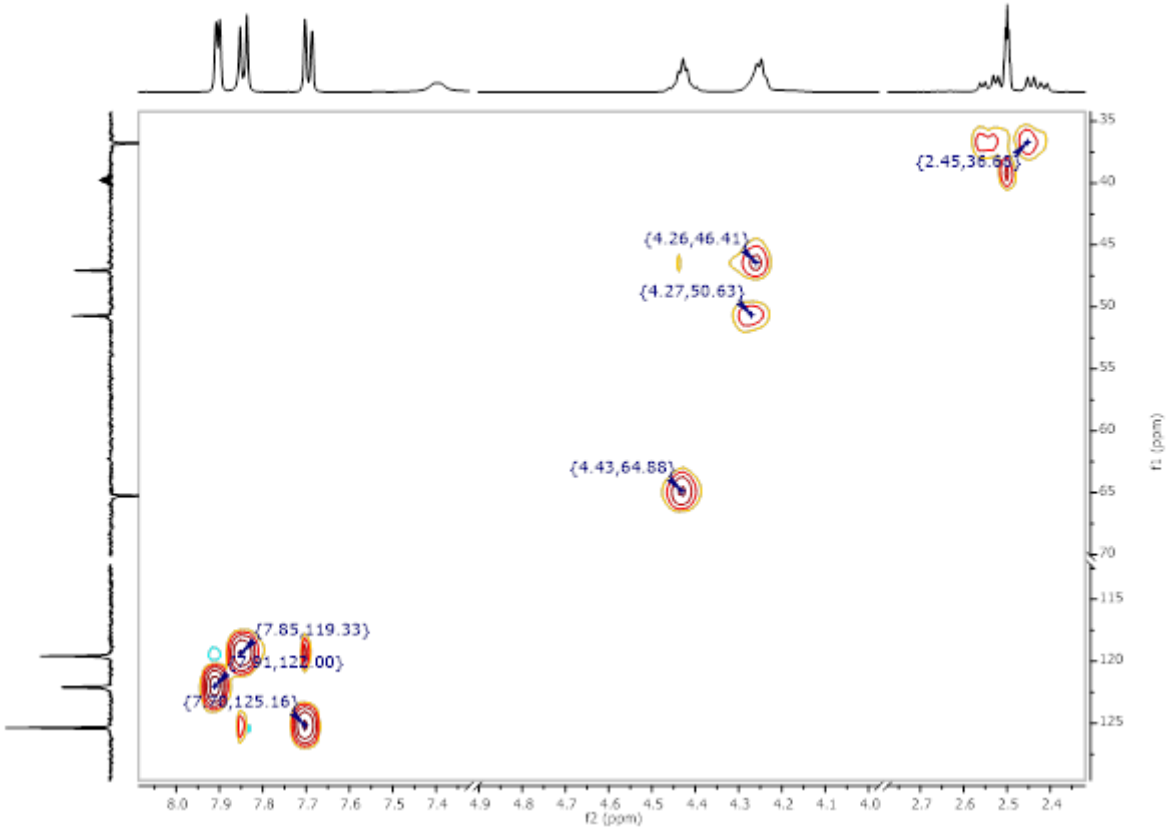

Figure 121: ^{1}H-^{13}C HSQC-NMR of Smoc-L-Asn-OH **7**.

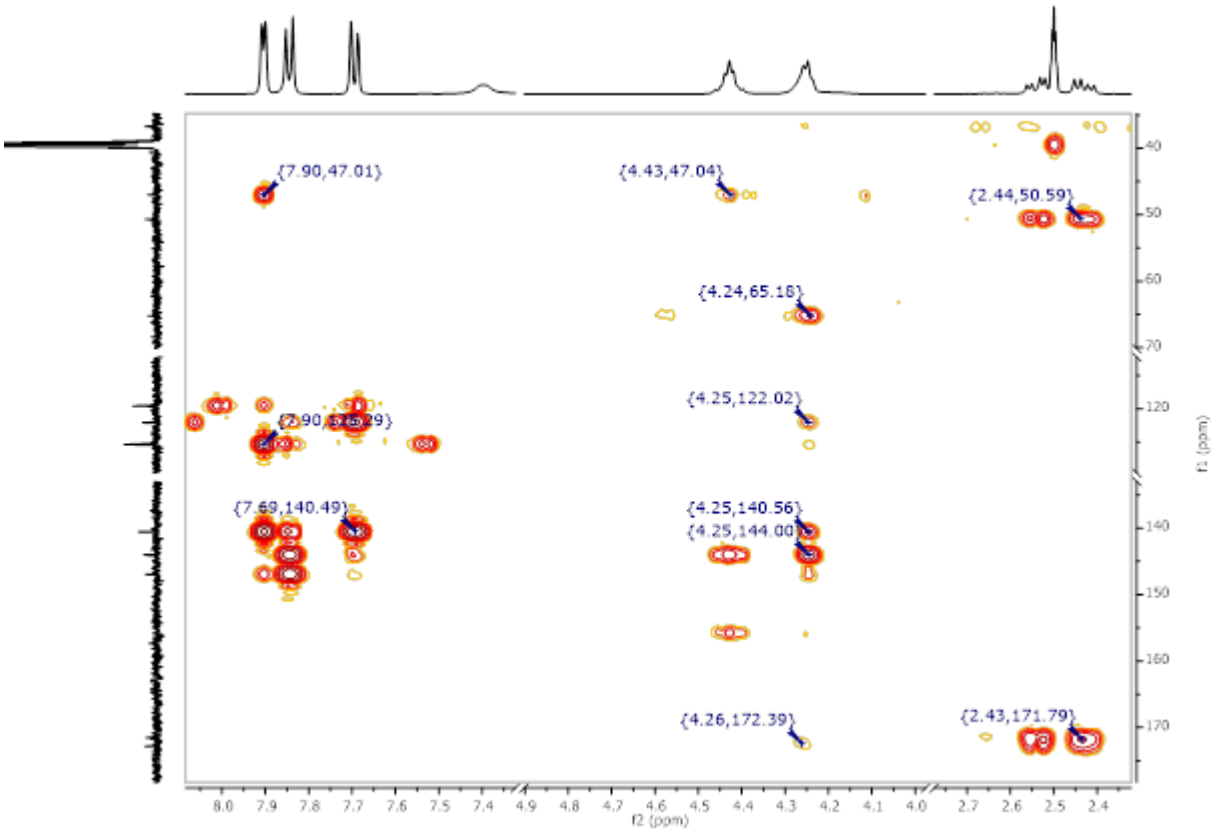

Figure 122: ^{1}H-^{13}C HMBC-NMR of Smoc-L-Asn-OH **7**.

8.2.6. Analytical data of Smoc-L-Asp(OtBu)-OH 8

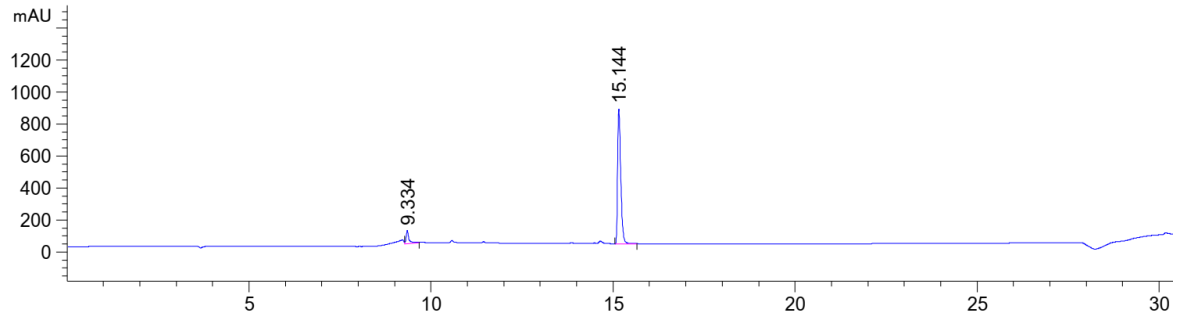

Figure 123: HPLC chromatogram of Smoc-L-Asp(OtBu)-OH **8** at λ=220 nm (0 to 60% MeCN).

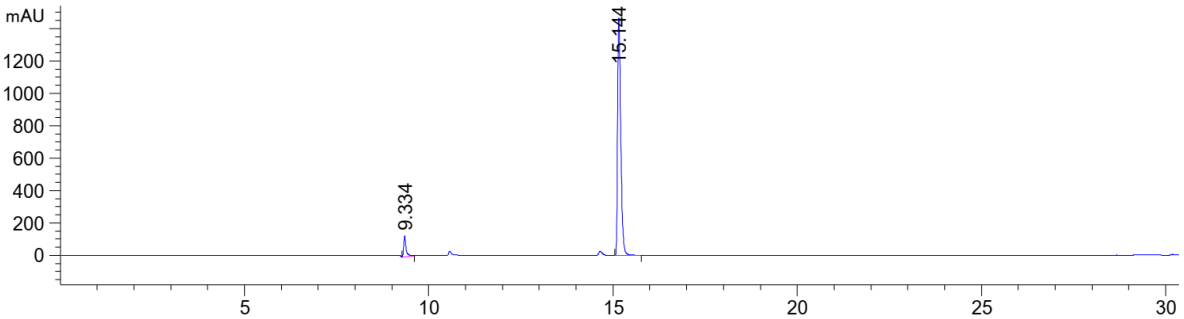

Figure 124: HPLC chromatogram of Smoc-L-Asp(OtBu)-OH **8** at λ=280 nm (0 to 60% MeCN).

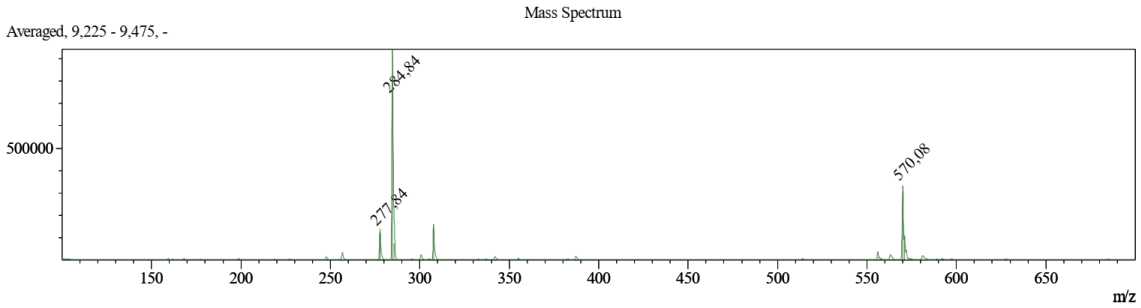

Figure 125: ESI-MS of Smoc-L-Asp(OtBu)-OH **8** (M measured=570.08 $[M-H]^-$, M calc.= 571.57).

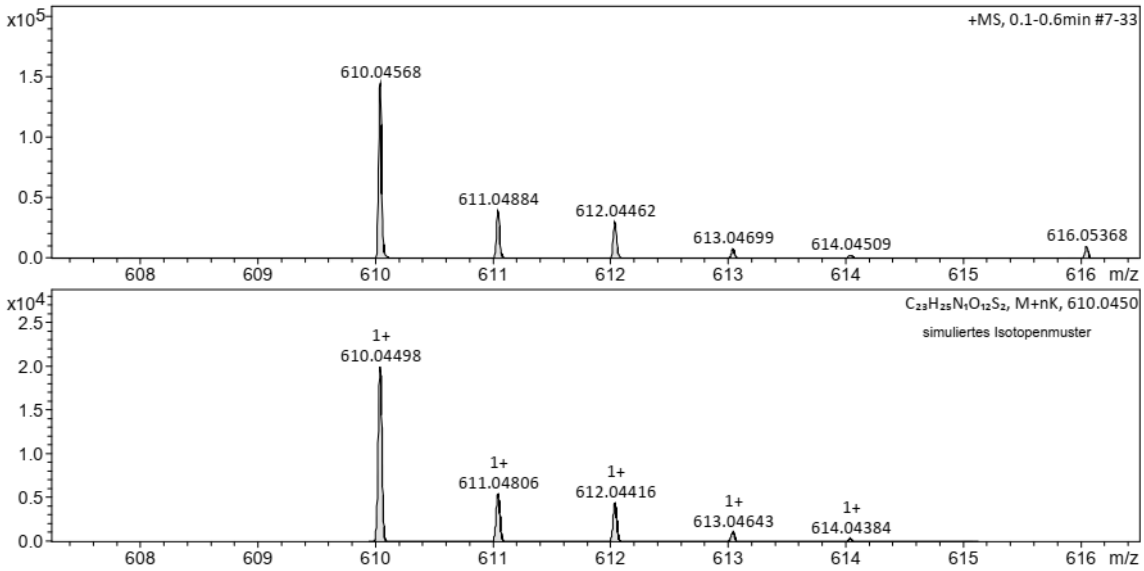

Figure **126:** HR-MS of Smoc-L-Asp(OtBu)-OH **8** (M measured=610.04568 $[M+H]^+$, M calc.=610.04498).

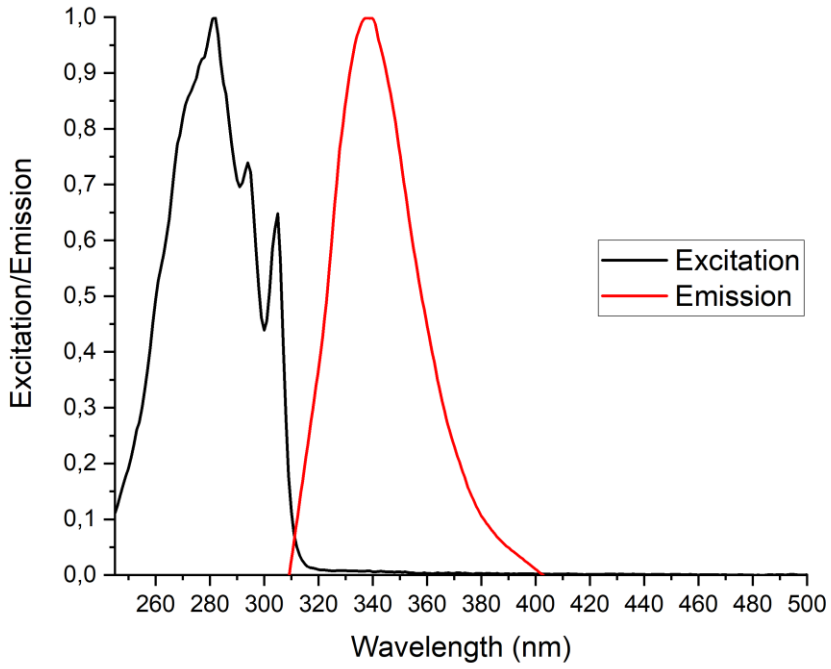

Figure 127: Excitation and emission spectra of Smoc-L-Asp(OtBu)-OH **8**, excitation and emission have been normalized between 0 and 1 for illustration.

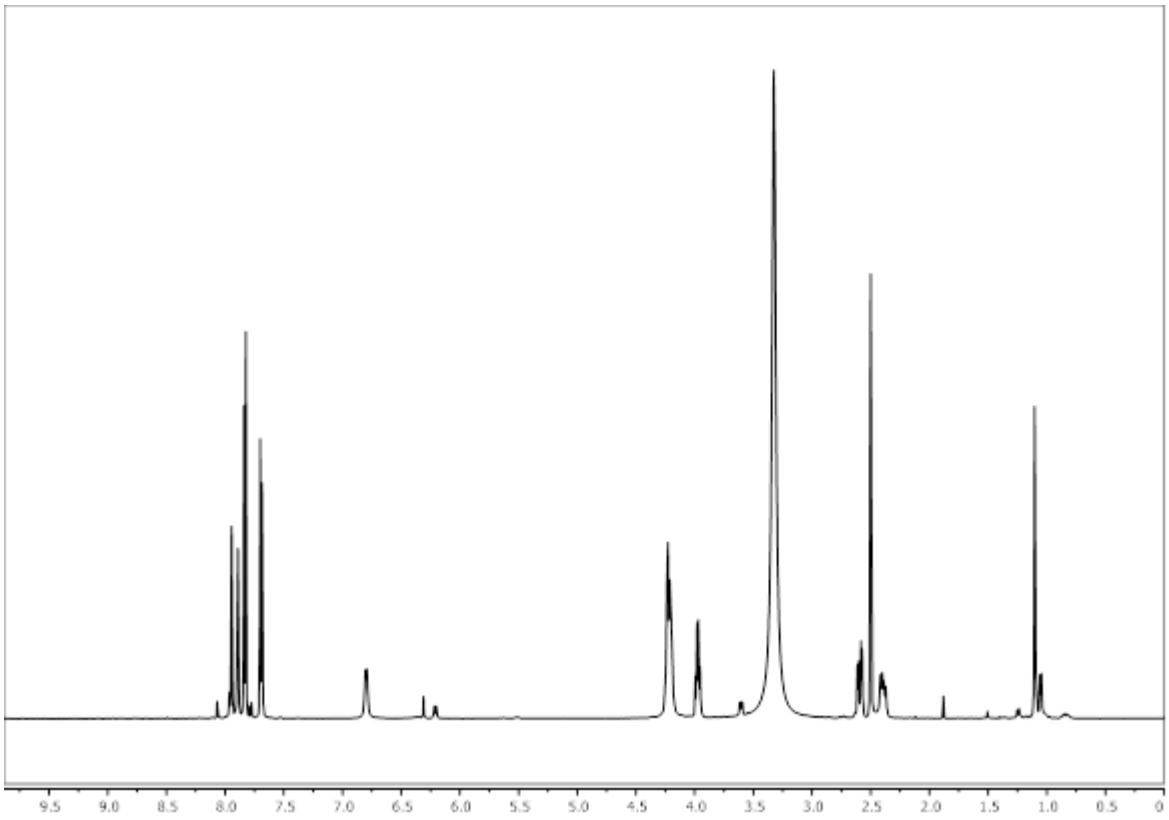

Figure 128: ^{1}H-NMR of Smoc-L-Asp(OtBu)-OH **8**.

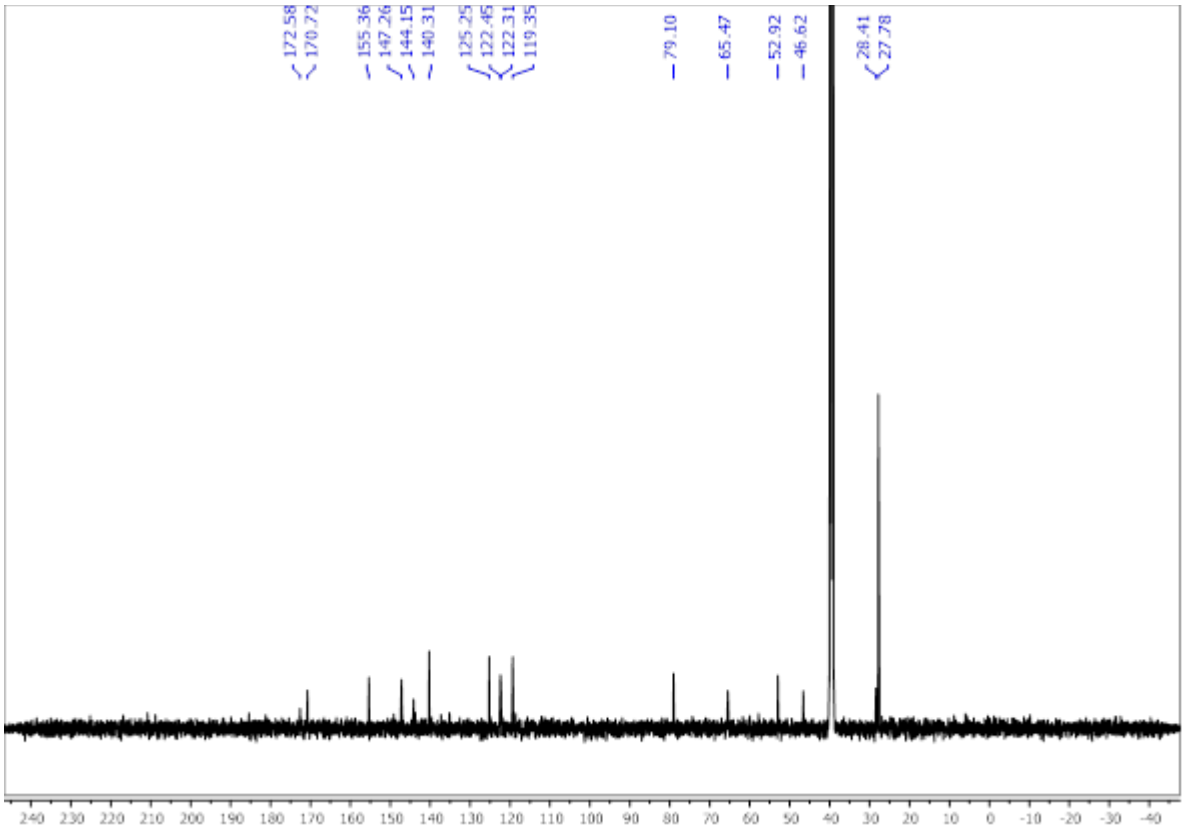

Figure 129: ^{13}C-NMR of Smoc-L-Asp(OtBu)-OH **8**.

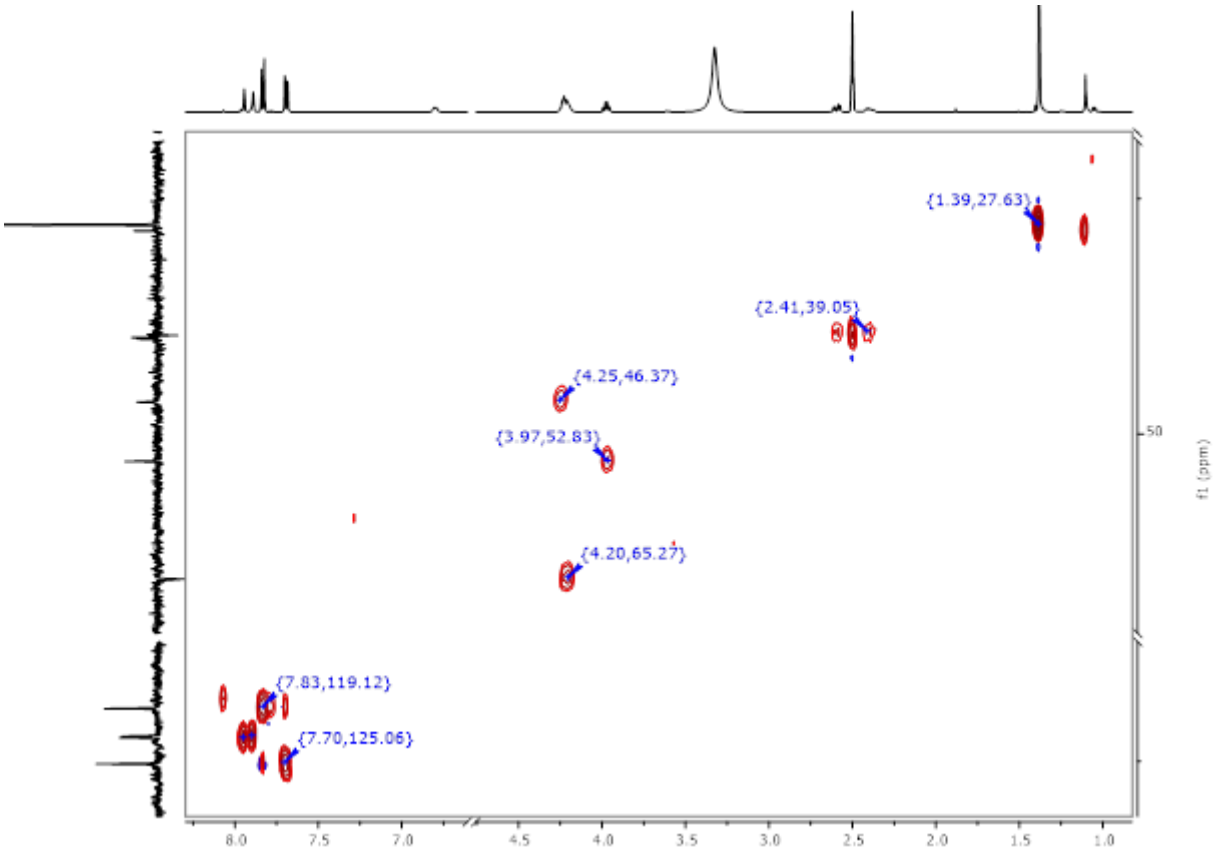

Figure 130: ^{1}H-^{13}C HSQC-NMR of Smoc-L-Asp(OtBu)-OH **8**.

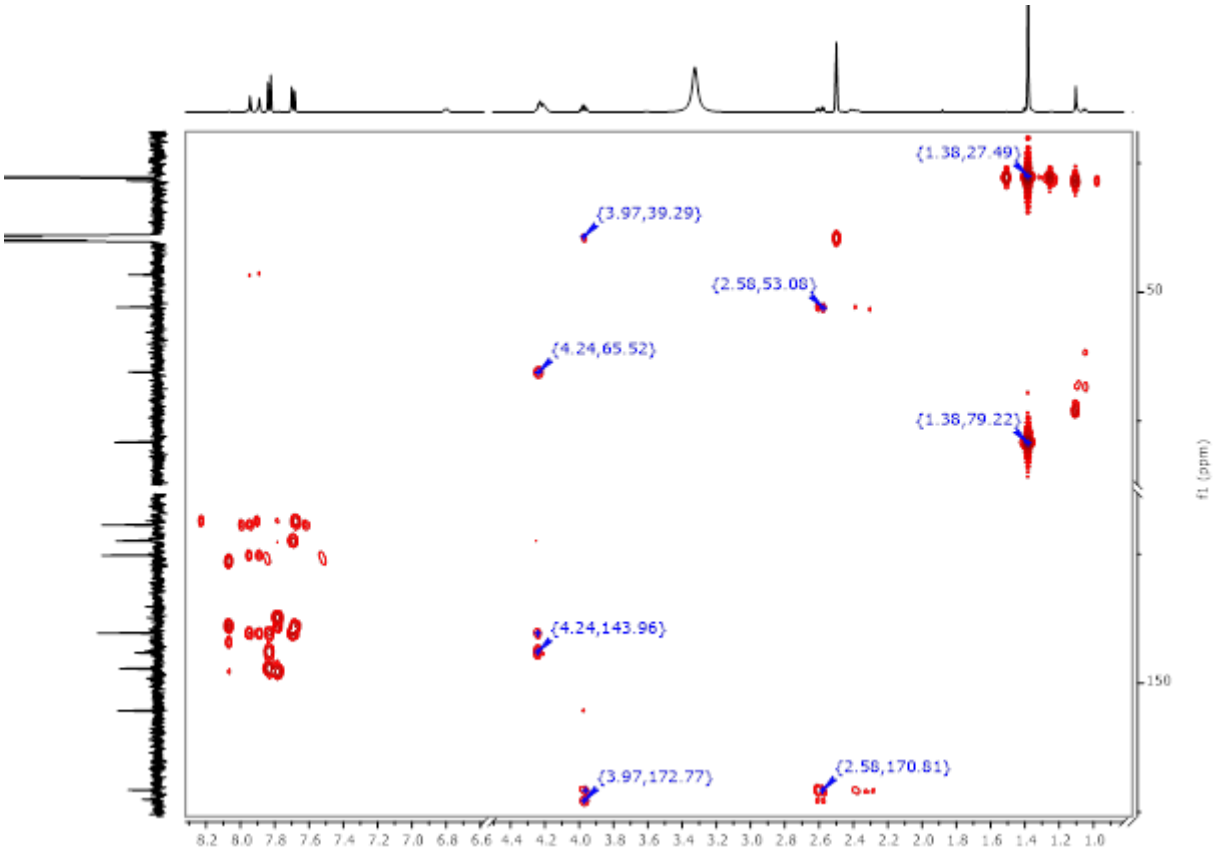

Figure 131: ^{1}H-^{13}C HMBC-NMR of Smoc-L-Asp(OtBu)-OH **8**.

8.2.7. Analytical data of Smoc-L-Cys(Trt)-OH 9

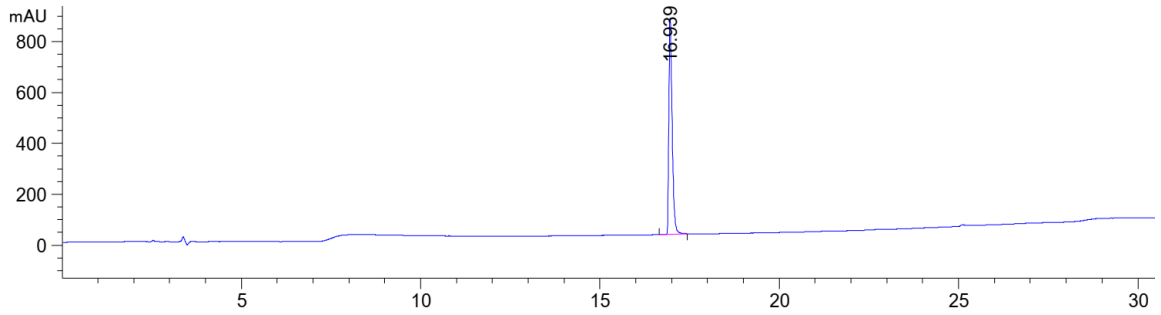

Figure 132: HPLC chromatogram of Smoc-L-Cys(Trt)-OH **9** at λ=220 nm (10 to 100% MeCN).

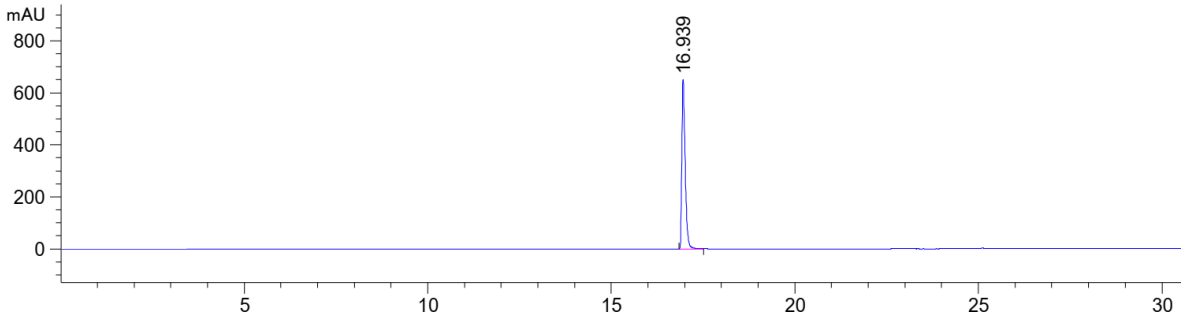

Figure 133: HPLC chromatogram of Smoc-L- Cys(Trt)-OH **9** at λ=280 nm (10 to 100% MeCN).

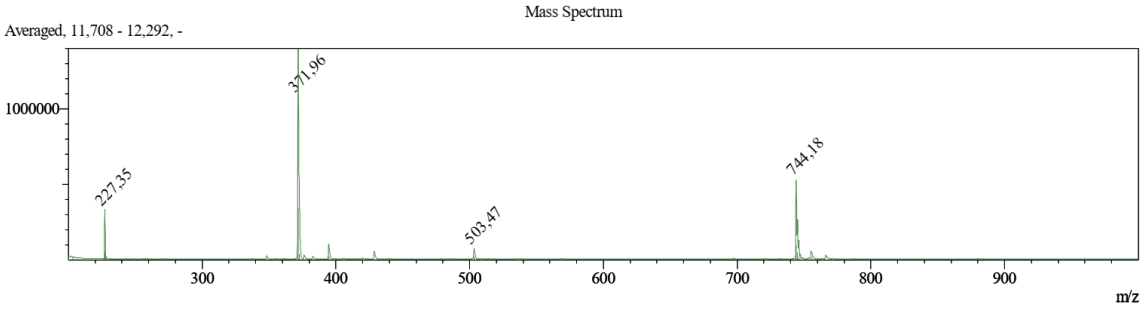

Figure 134: ESI-MS of Smoc-L- Cys(Trt)-OH **9** (M measured=744.18 [M-H]$^-$, M calc.=745.83).

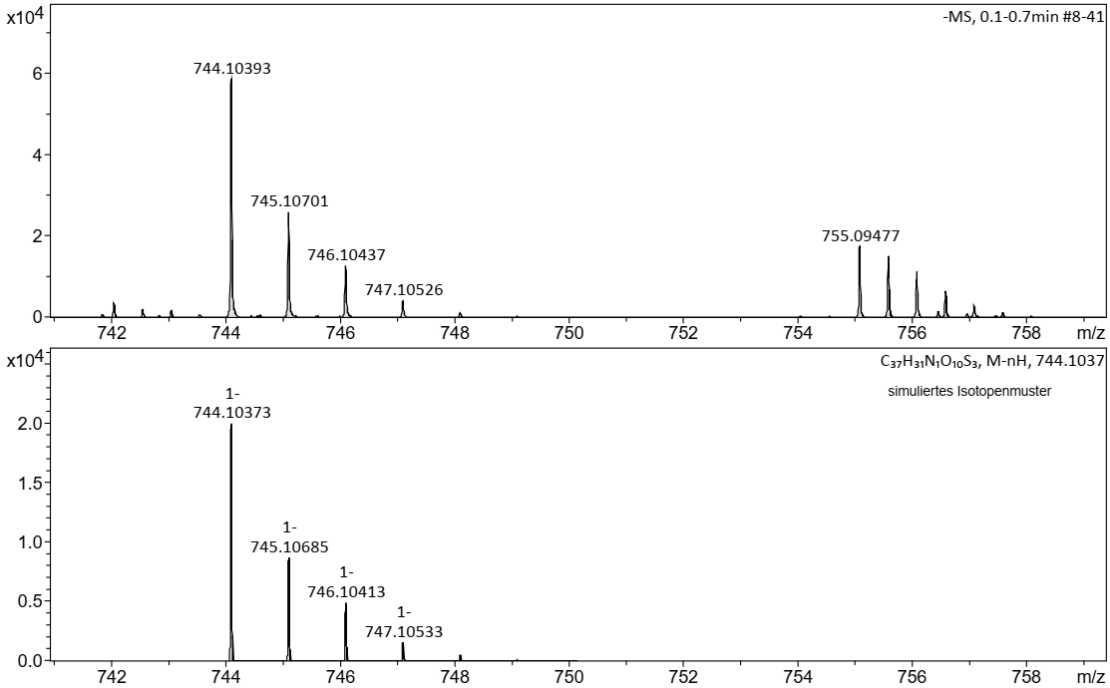

Figure 135: HR-MS of Smoc-L-Cys(Trt)-OH **9** (M measured=744.10393 [M-H]$^-$, M calc.=744.10373).

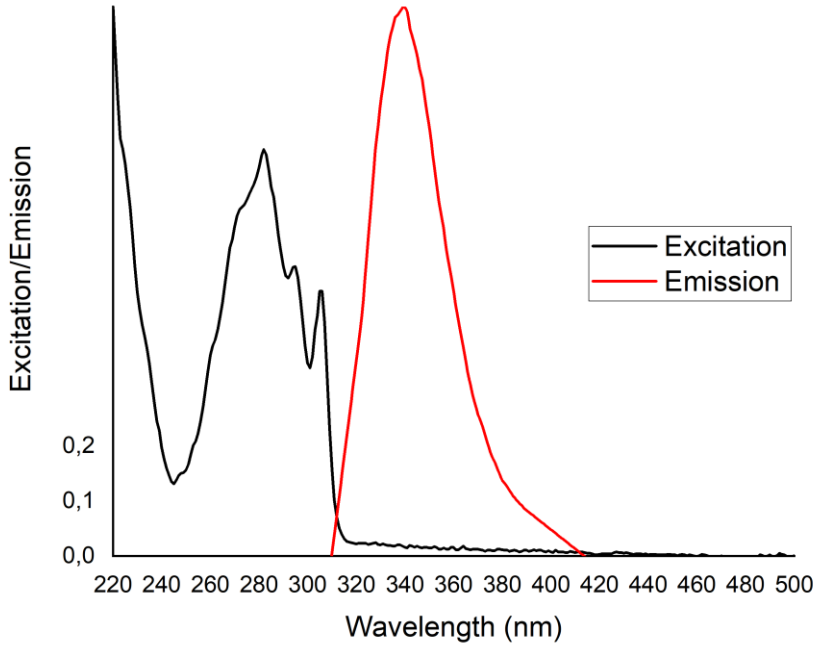

Figure 136: Excitation and emission spectra of Smoc-L-Cys(Trt)-OH **9**, excitation and emission have been normalized between 0 and 1 for illustration.

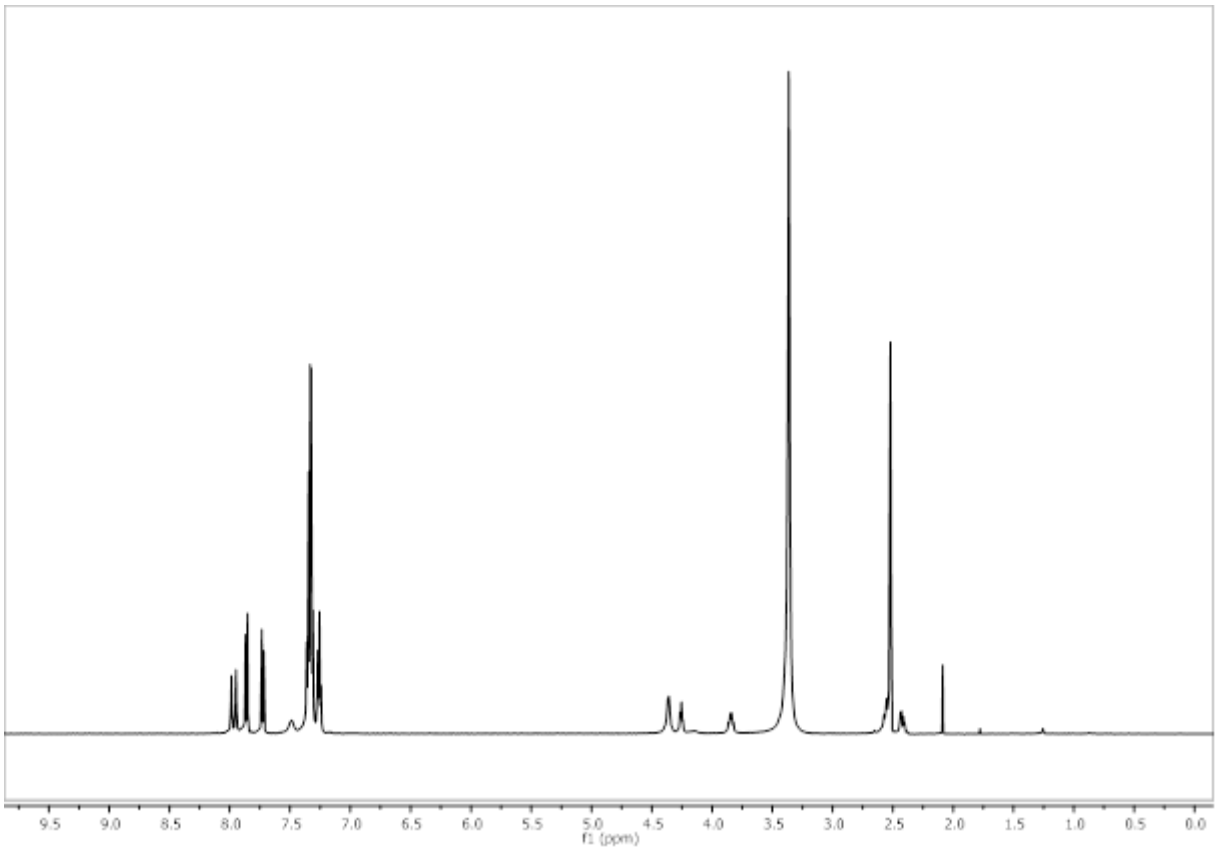

Figure 137: ^{1}H-NMR of Smoc-L-Cys(Trt)-OH **9**.

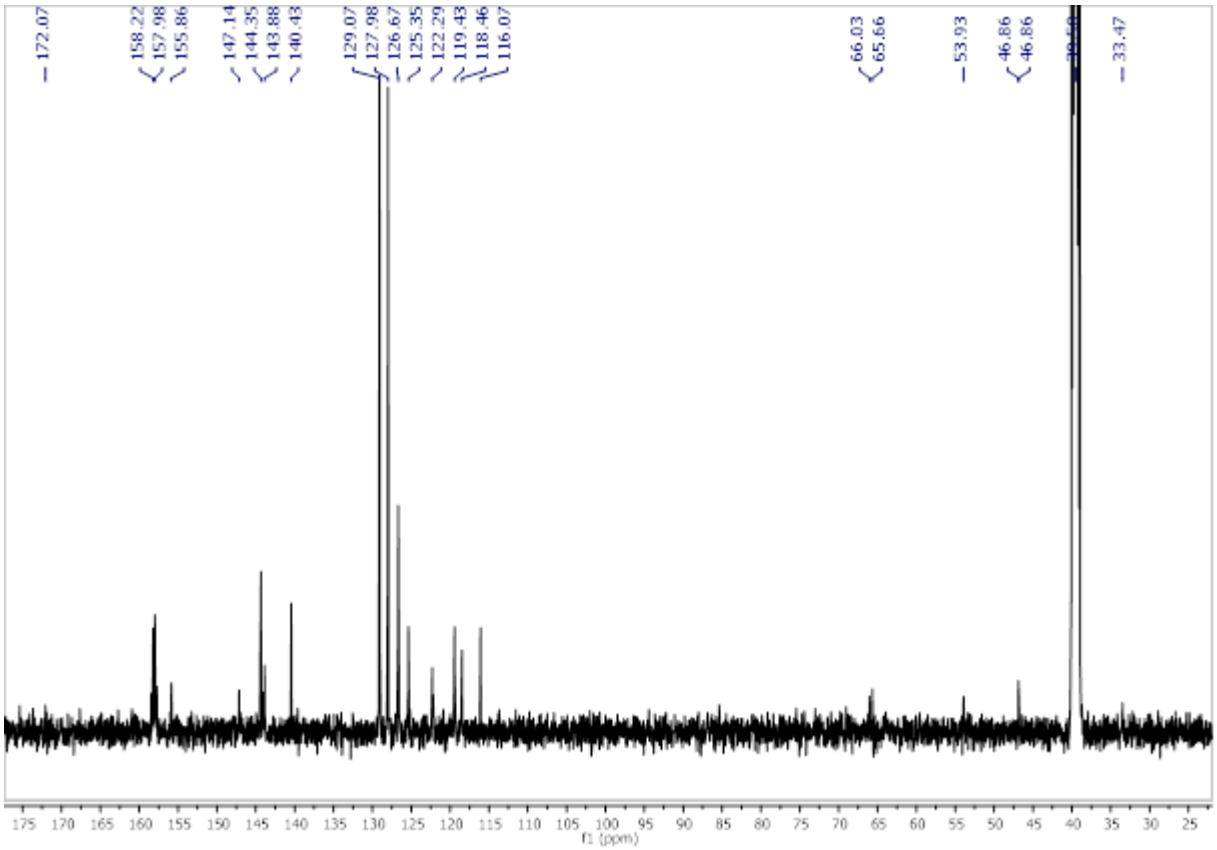

Figure 138: ^{13}C-NMR of Smoc-L-Cys(Trt)-OH **9**.

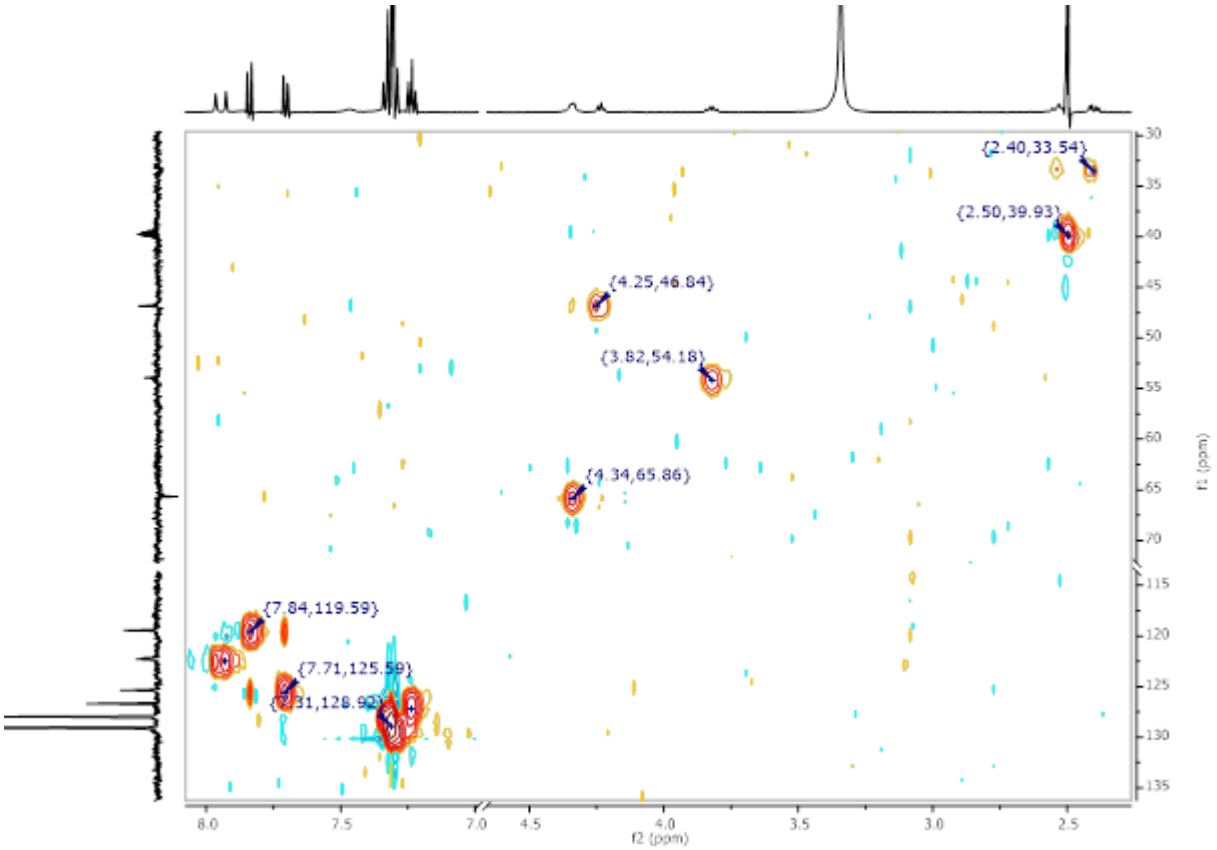

Figure 139: ^{1}H-^{13}C HSQC-NMR of Smoc-L-Cys(Trt)-OH **9**.

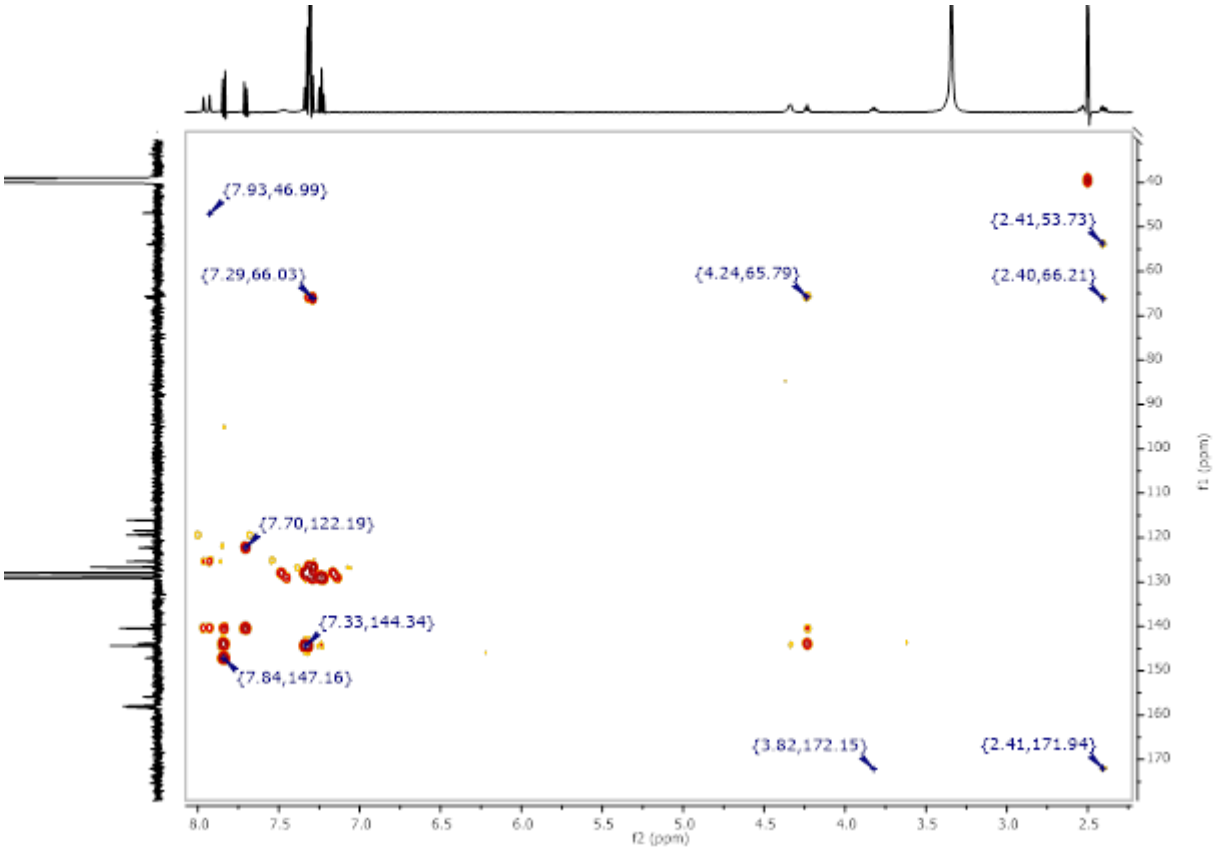

Figure 140: ^{1}H-^{13}C HMBC-NMR of Smoc-L-Cys(Trt)-OH **9**.

8.2.8. Analytical data of Smoc-L-Gln-OH 10

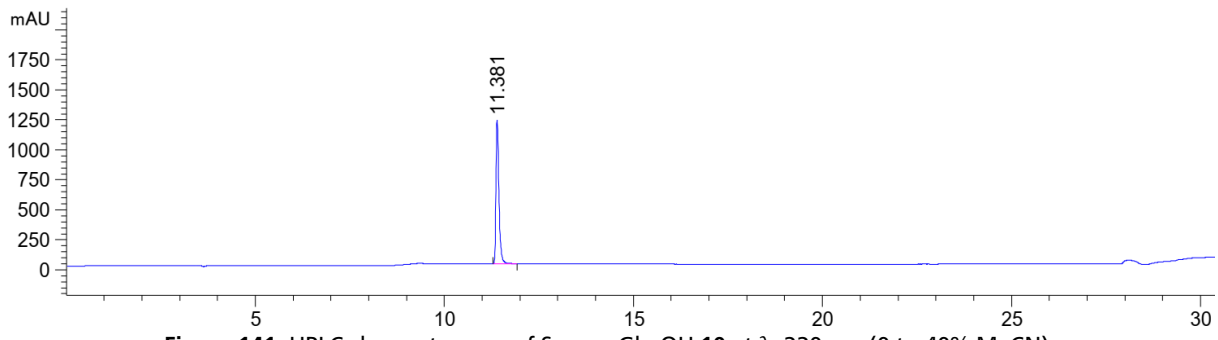

Figure 141: HPLC chromatogram of Smoc-L-Gln-OH **10** at λ=220 nm (0 to 40% MeCN).

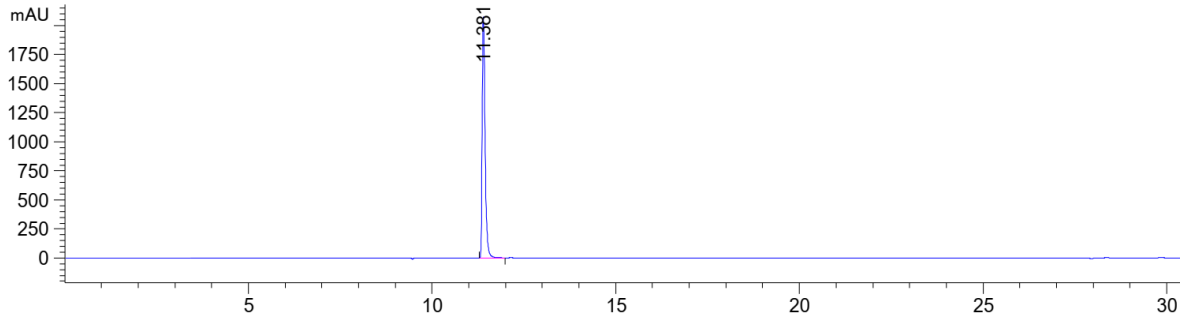

Figure 142: HPLC chromatogram of Smoc-L- Gln-OH **10** at λ=280 nm (0 to 40% MeCN).

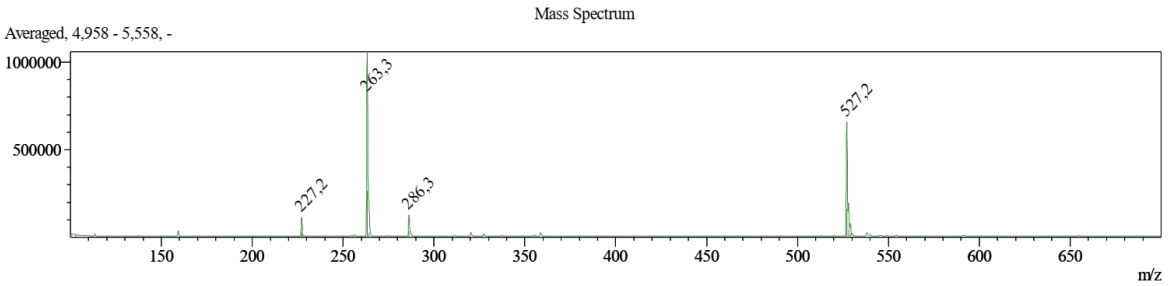

Figure 143: ESI-MS of Smoc-L- Gln-OH **10** (M measured=527.20 $[M-H]^-$, M calc.=528.50).

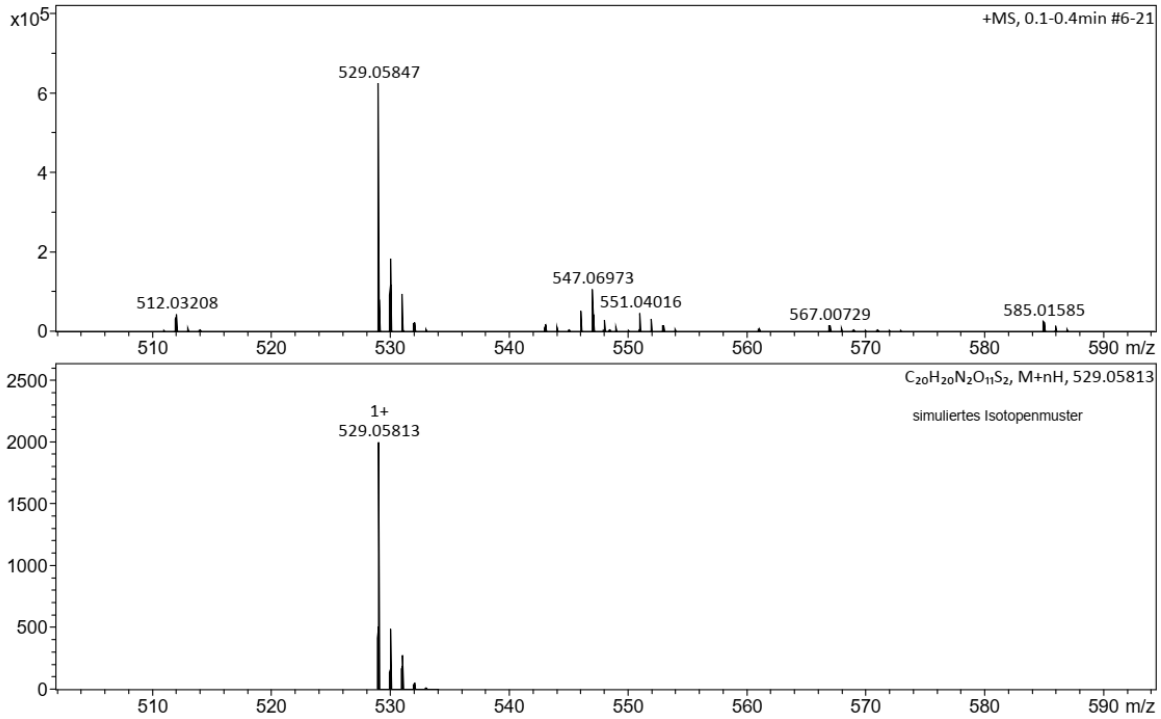

Figure 144: HR-MS of Smoc-L-Gln-OH **10** (M measured=529.05847 $[M+H]^+$, M calc.=529.05813).

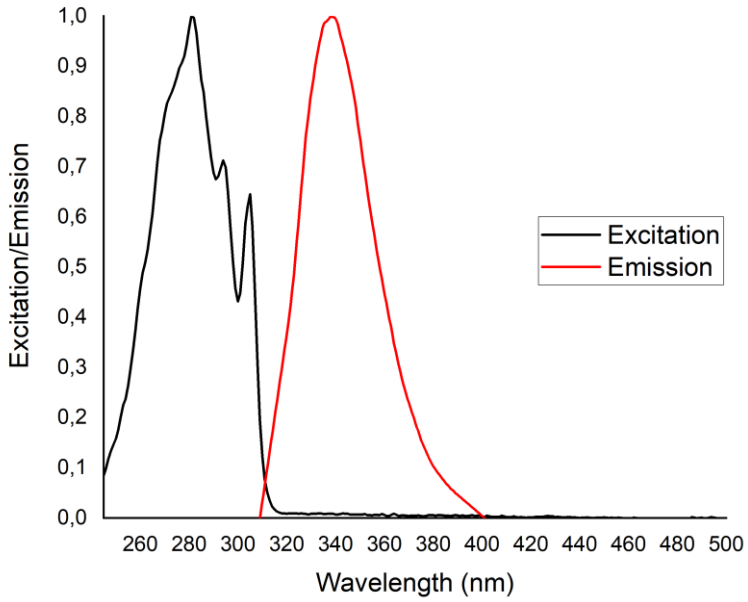

Figure 145: Excitation and emission spectra of Smoc-L-Gln-OH **10**, excitation and emission have been normalized between 0 and 1 for illustration.

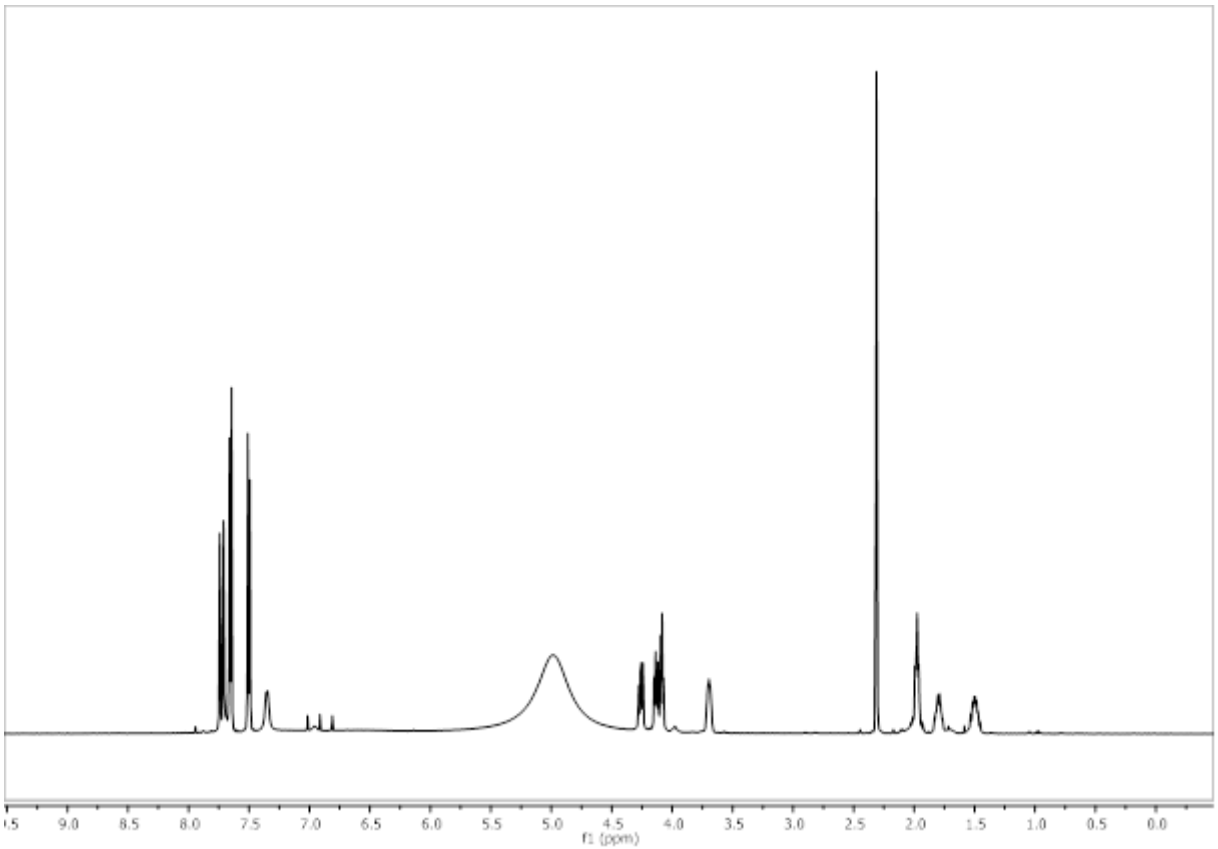

Figure 146: ^{1}H-NMR of Smoc-L- Gln-OH **10**.

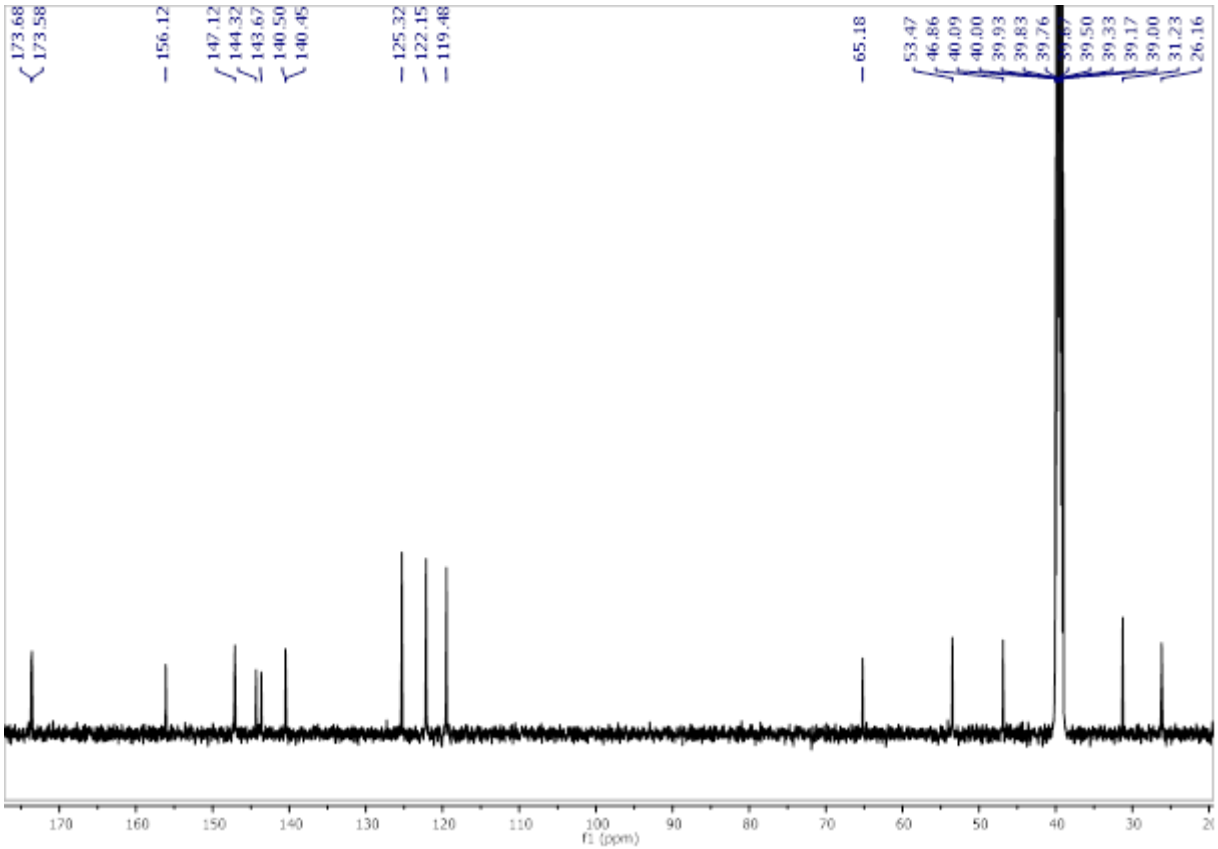

Figure 147: ^{13}C-NMR of Smoc-L- Gln-OH **10**.

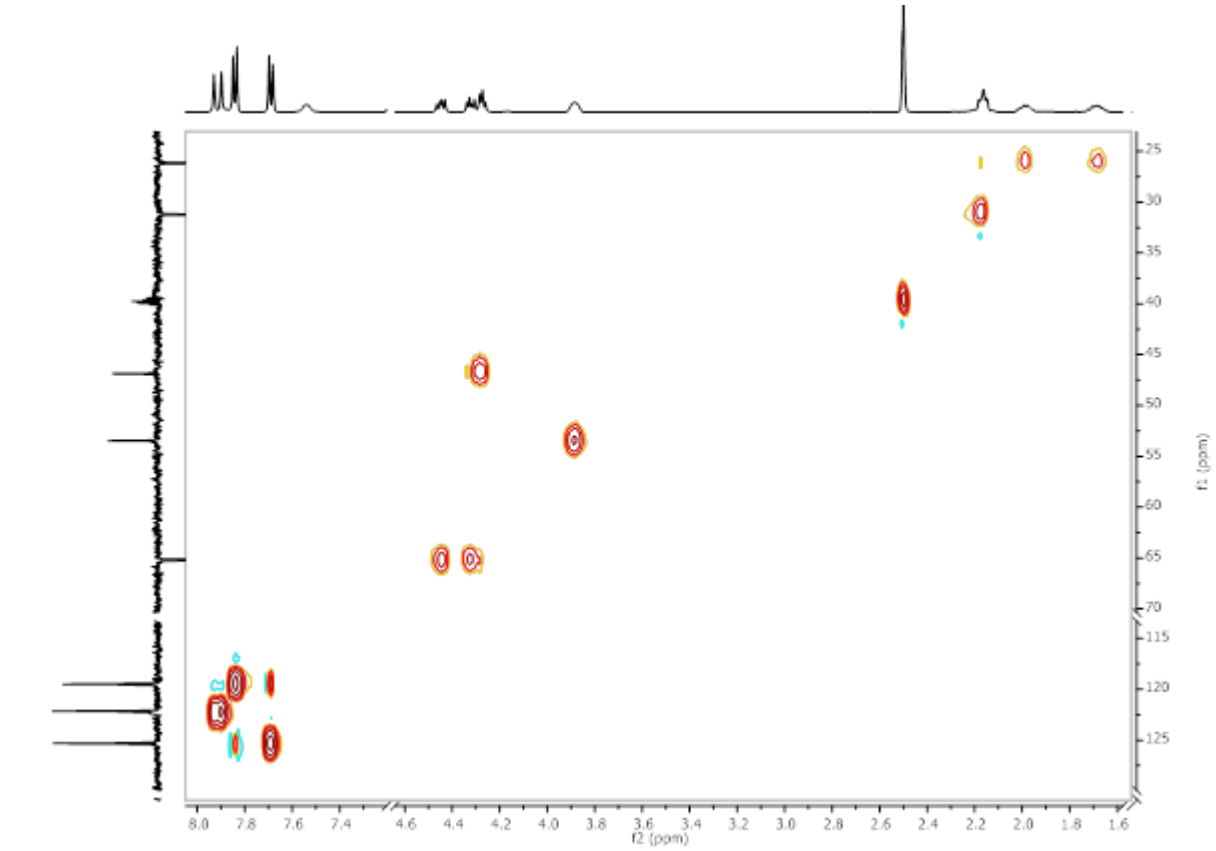

Figure 148: ^{1}H-^{13}C HSQC-NMR of Smoc-L- Gln-OH **10**.

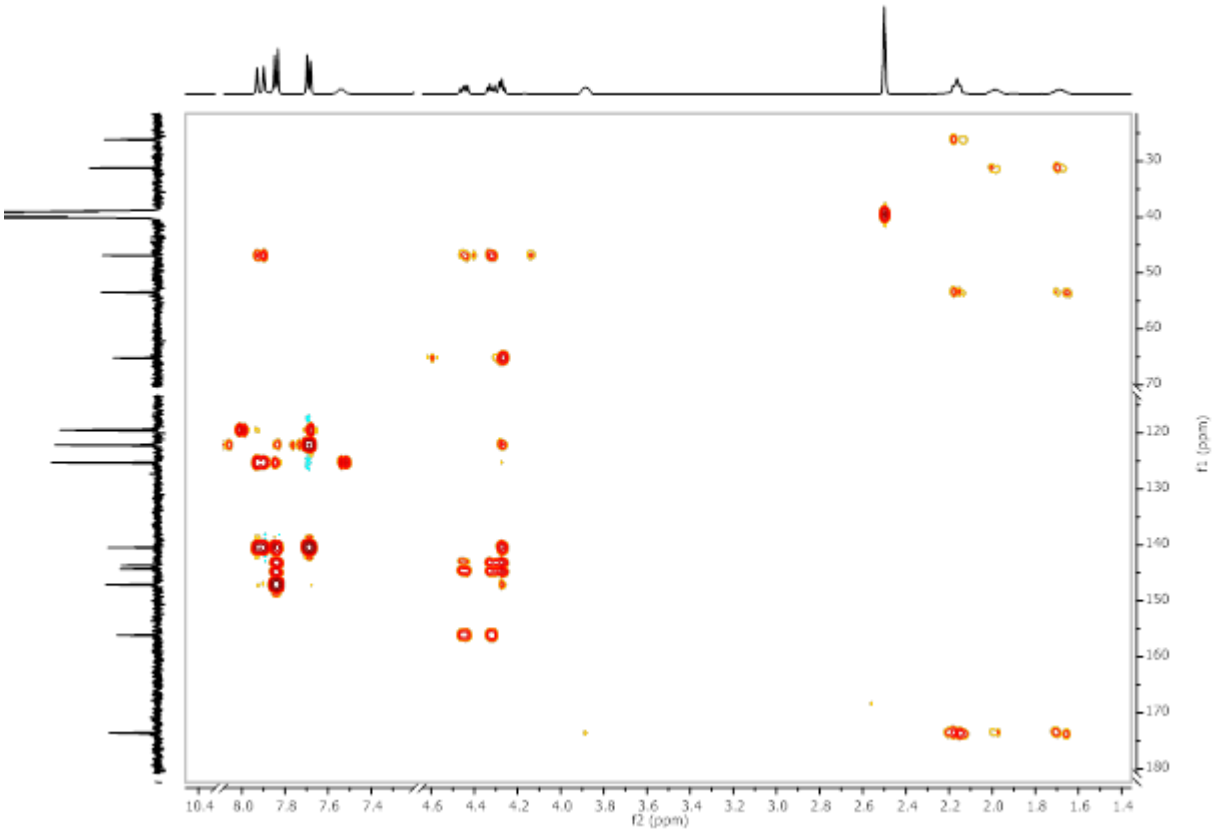

Figure 149: ^{1}H-^{13}C HMBC-NMR of Smoc-L- Gln-OH **10**.

8.2.9. Analytical data of Smoc-L-Glu(OtBu)-OH 11

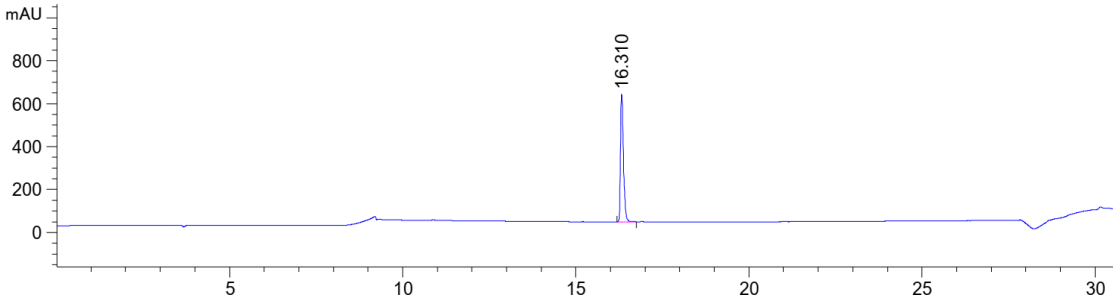

Figure 150: HPLC chromatogram of Smoc-L-Glu(OtBu)-OH **11** at λ=220 nm (0 to 60% MeCN).

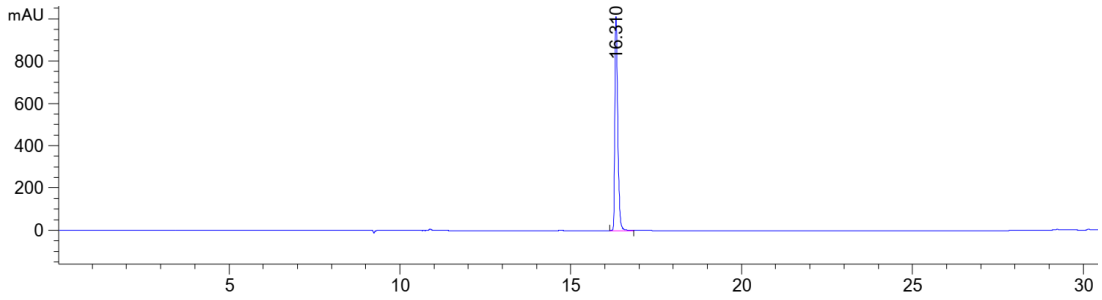

Figure 151: HPLC chromatogram of Smoc-L-Glu(OtBu)-OH **11** at λ=280 nm (0 to 60% MeCN).

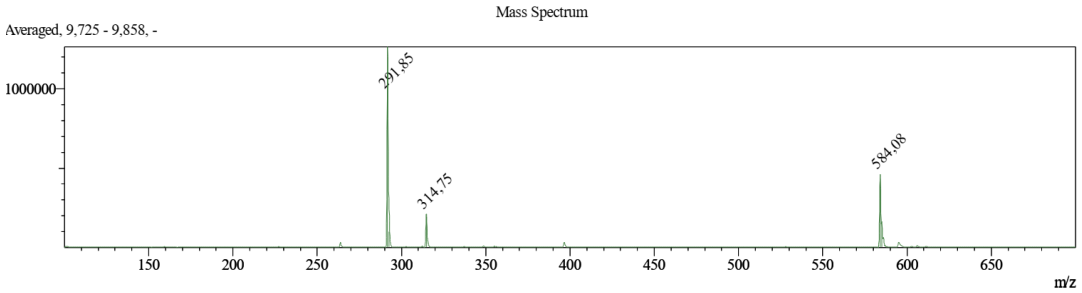

Figure 152: ESI-MS of Smoc-L-Glu(OtBu)-OH **11** (M measured=584.08 $[M-H]^-$, M calc.=585.60).

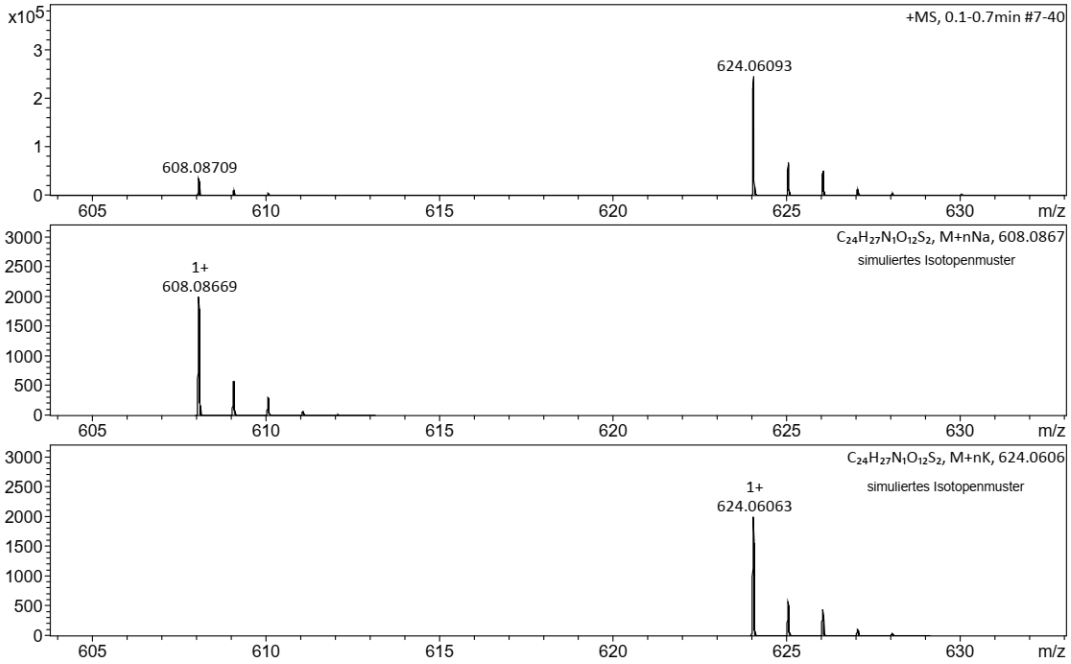

Figure 153: HR-MS of Smoc-L-Glu(OtBu)-OH **11** (M measured=608.08669 $[M+H]^+$, M calc.=608.08709).

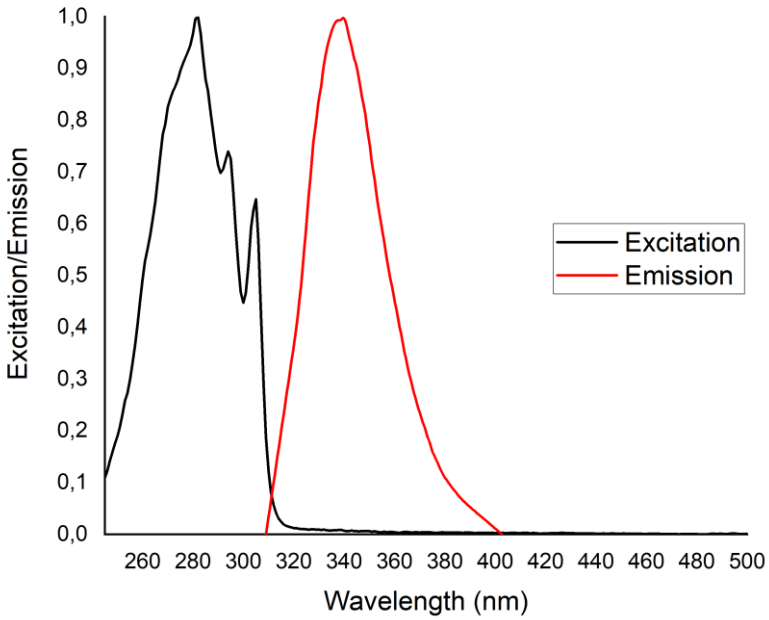

Figure 154: Excitation and emission spectra of Smoc-L-Glu(OtBu)-OH **11**, excitation and emission have been normalized between 0 and 1 for illustration.

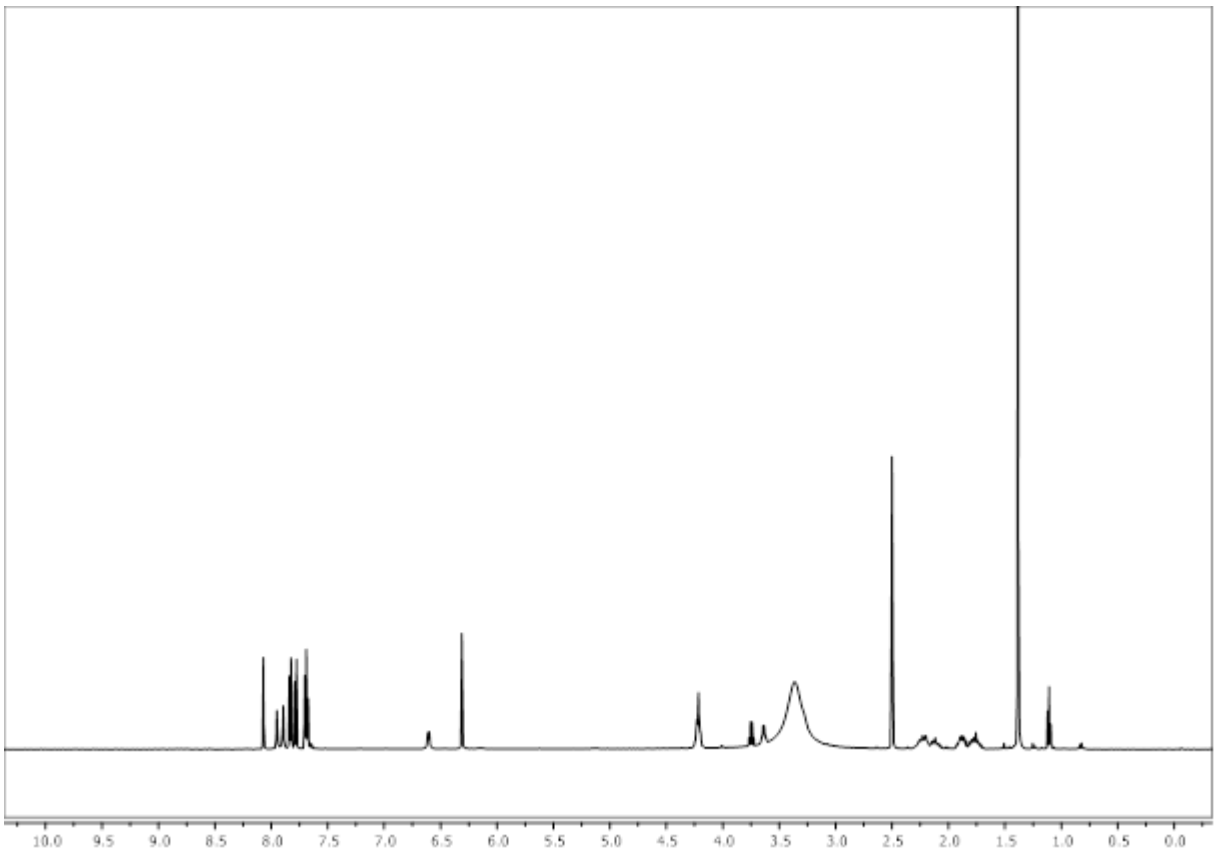

Figure 155: ^{1}H-NMR of Smoc-L-Glu(OtBu)-OH **11**.

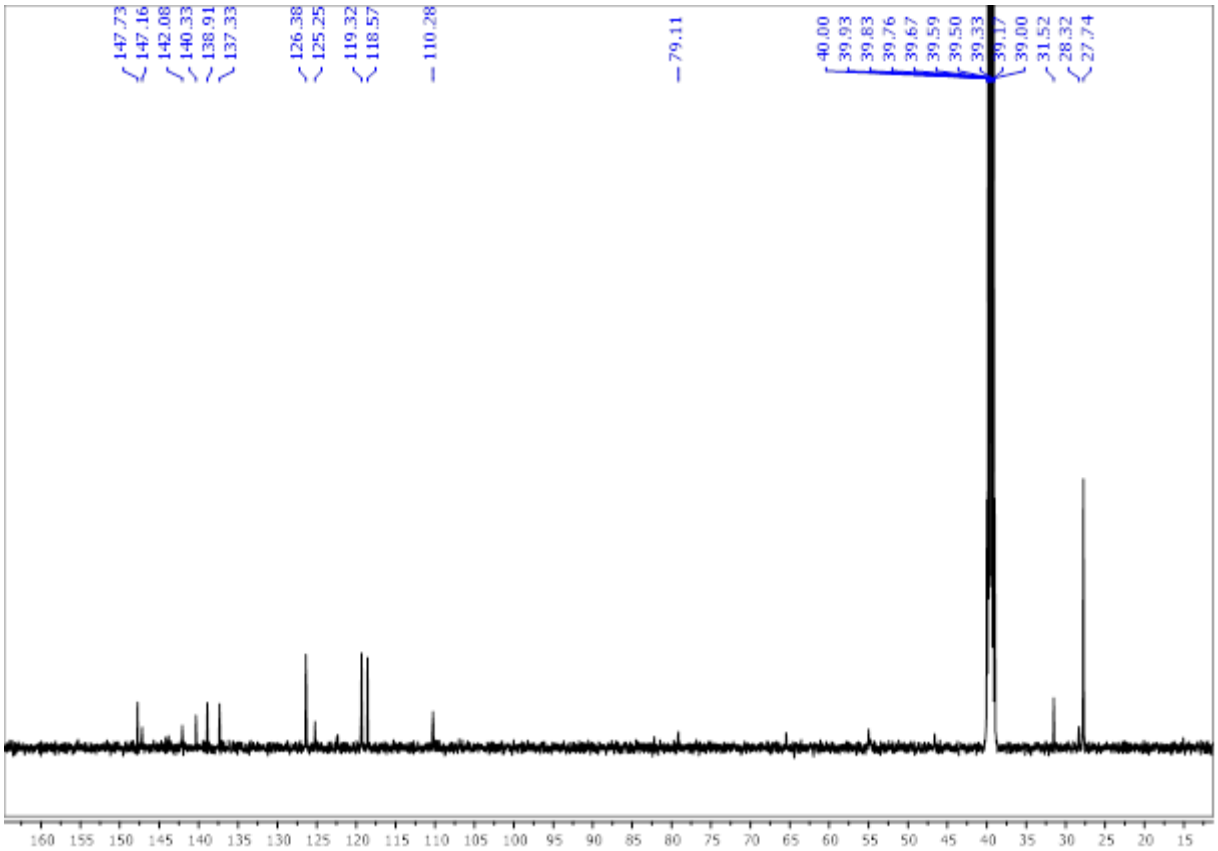

Figure 156: ^{13}C-NMR of Smoc-L-Glu(OtBu)-OH **11**.

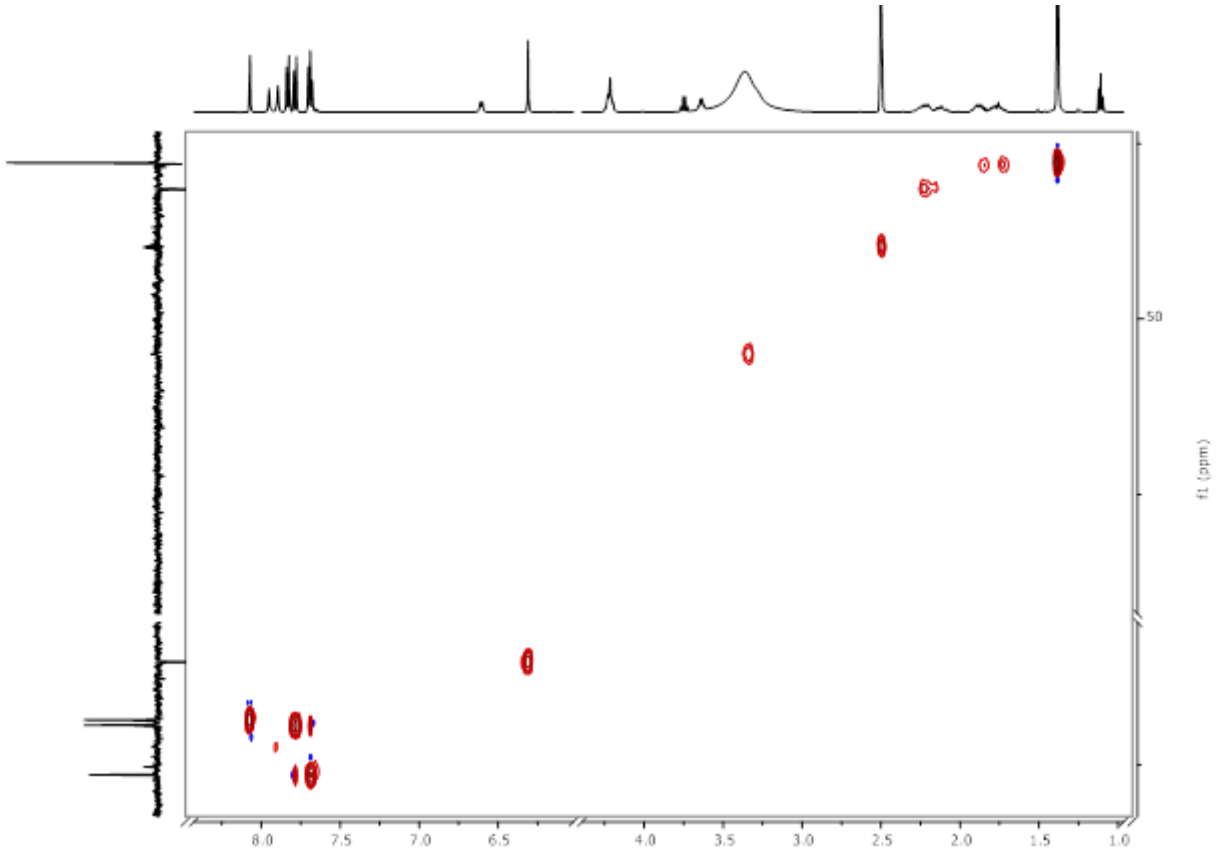

Figure 157: ^{1}H-^{13}C HSQC-NMR of Smoc-L-Glu(OtBu)-OH **11**.

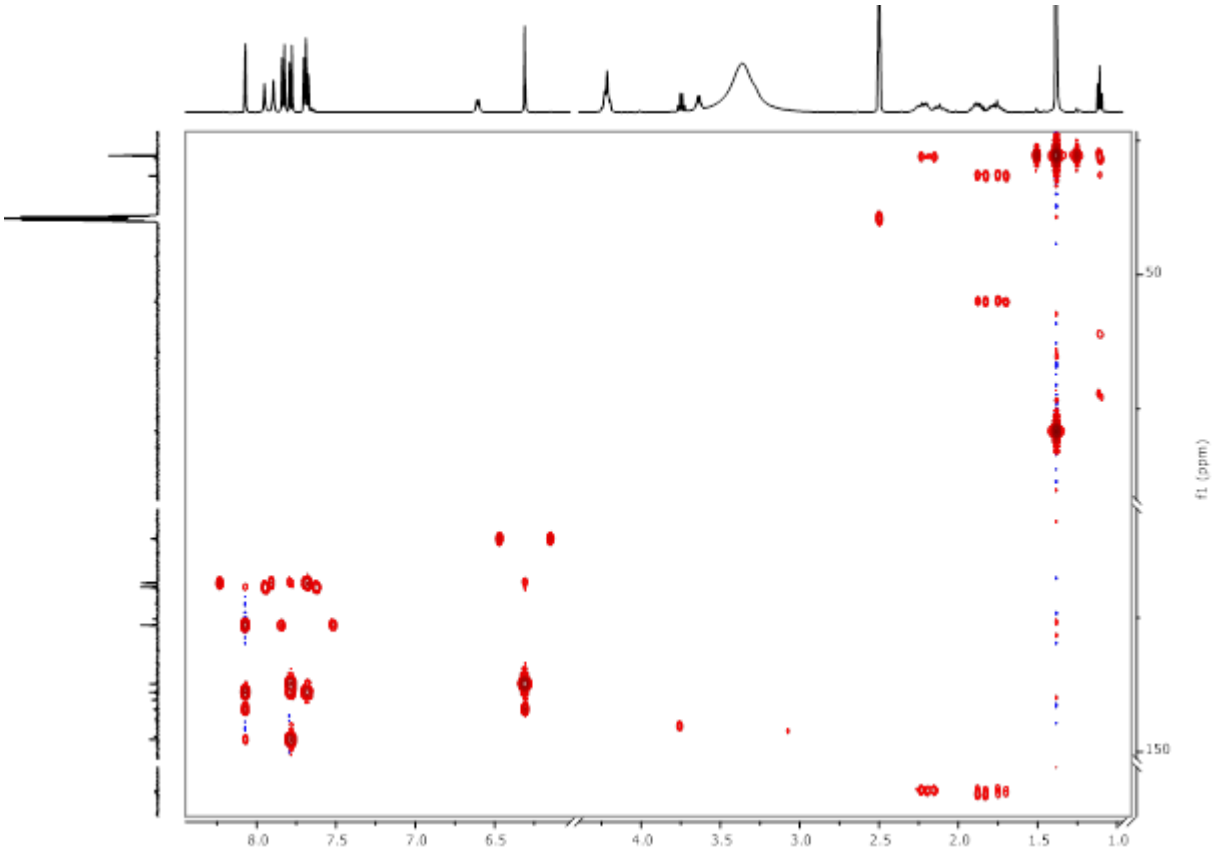

Figure 158: ^{1}H-^{13}C HMBC-NMR of Smoc-L-Glu(OtBu)-OH **11**.

8.2.10.Analytical data of Smoc-Gly-OH 12

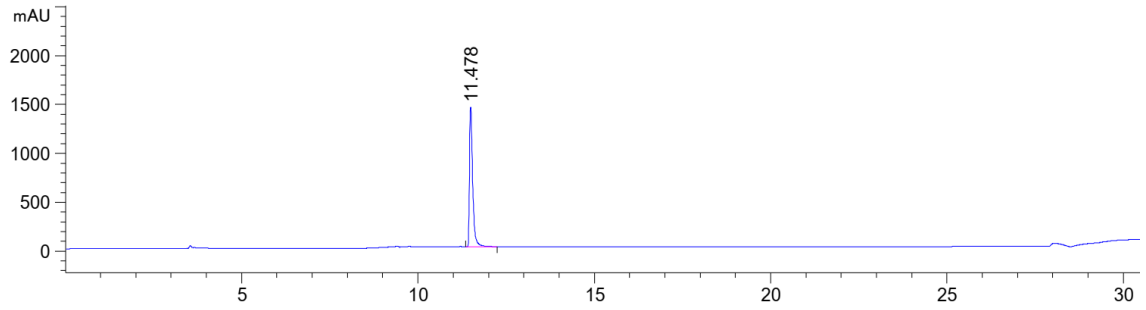

Figure 159: HPLC chromatogram of Smoc-Gly-OH **12** at λ=220 nm (0 to 40% MeCN).

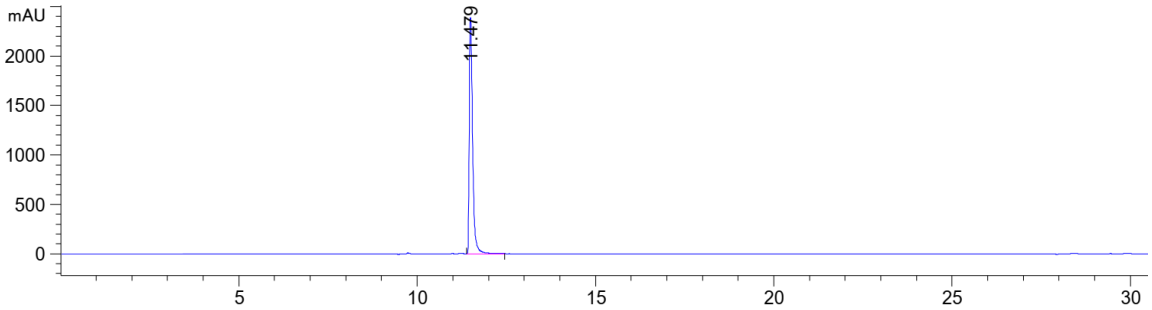

Figure 160: HPLC chromatogram of Smoc-Gly-OH **12** at λ=280 nm (0 to 40% MeCN).

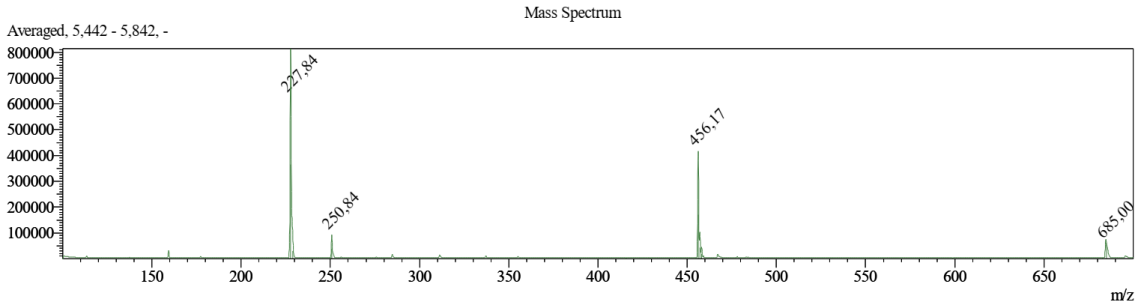

Figure 161: ESI-MS of Smoc-Gly-OH **12** (M measured=456.17 $[M-H]^-$, M calc.=457.42).

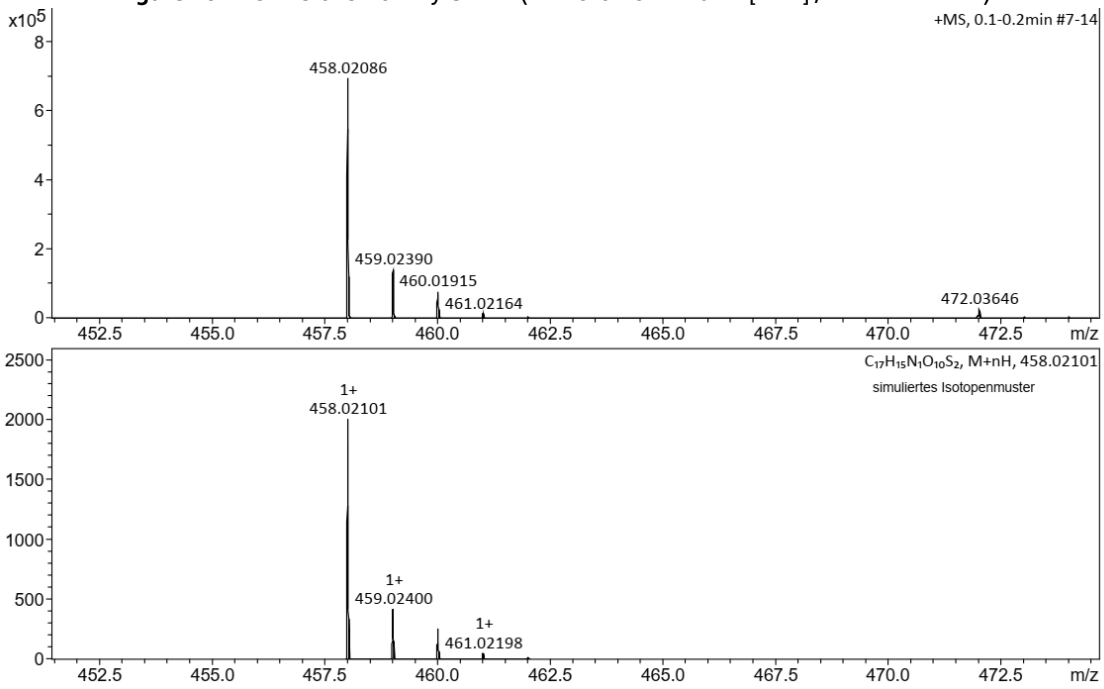

Figure 162: HR-MS of Smoc-Gly-OH **12** (M measured=458.02086 $[M+H]^+$, M calc.=458.02101).

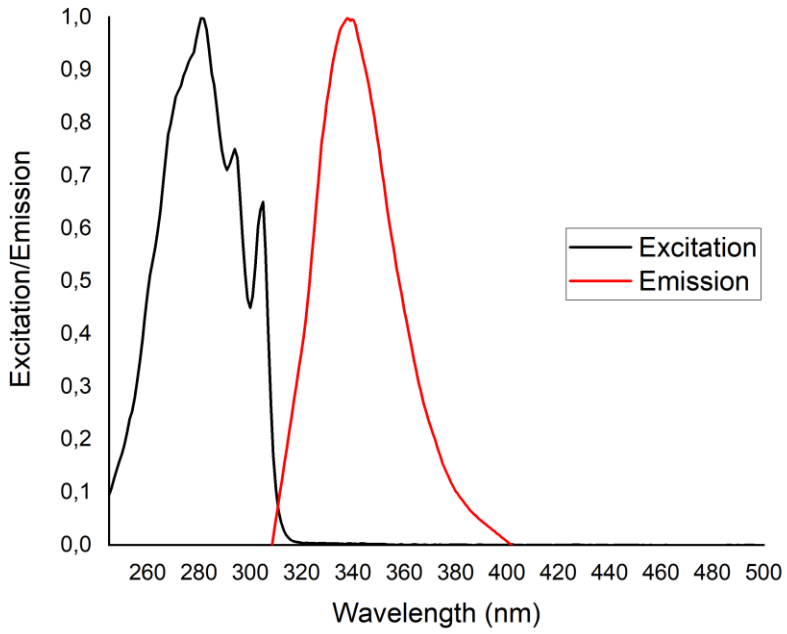

Figure 163: Excitation and emission spectra of Smoc-Gly-OH **12**, excitation and emission have been normalized between 0 and 1 for illustration.

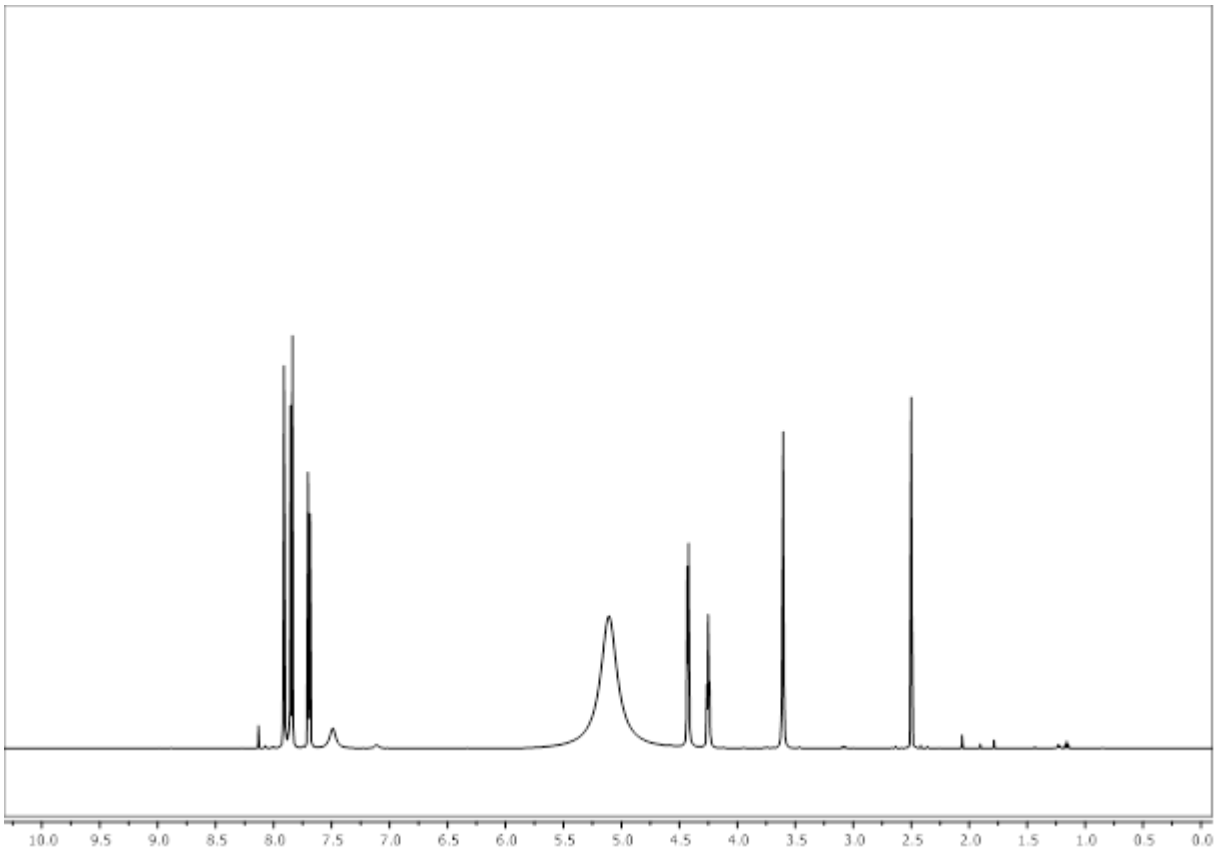

Figure 164: ^{1}H-NMR of Smoc-Gly-OH **12**.

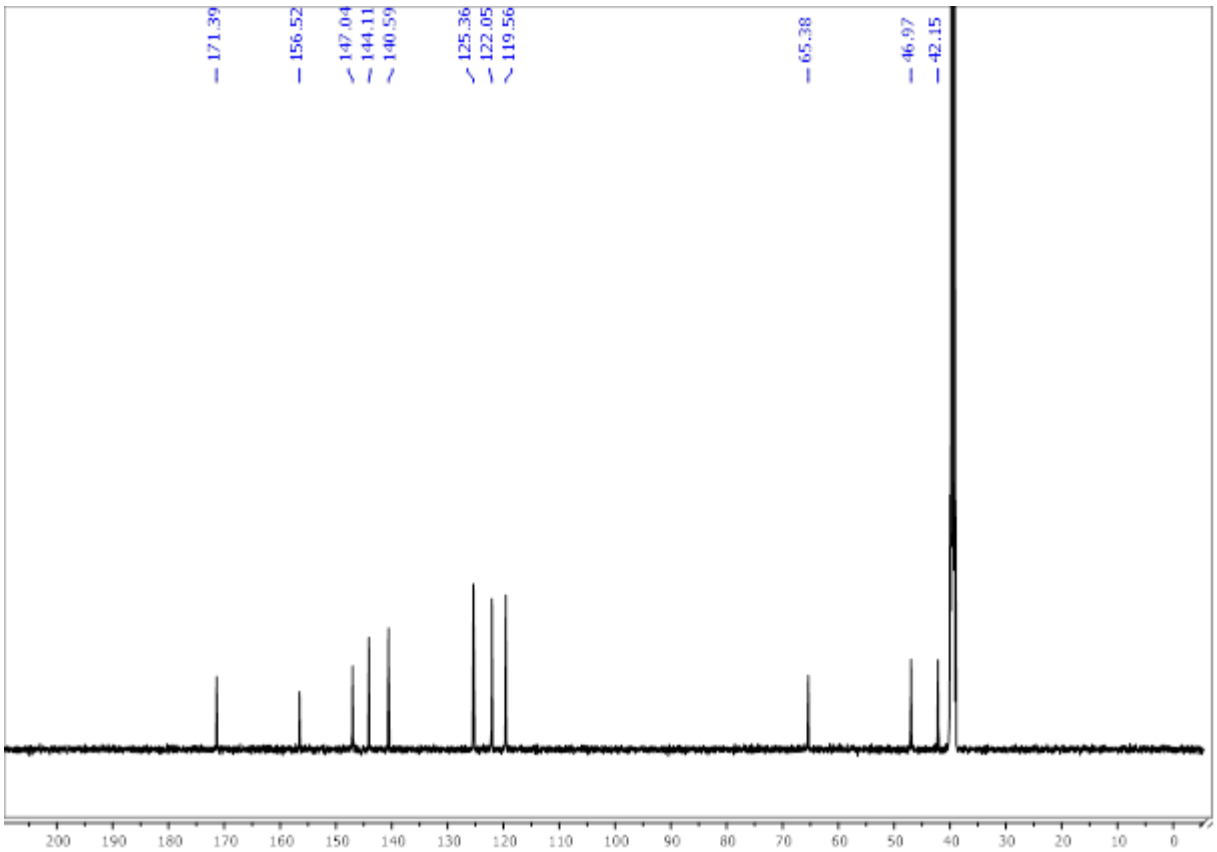

Figure 165: ^{13}C-NMR of Smoc-Gly-OH **12**.

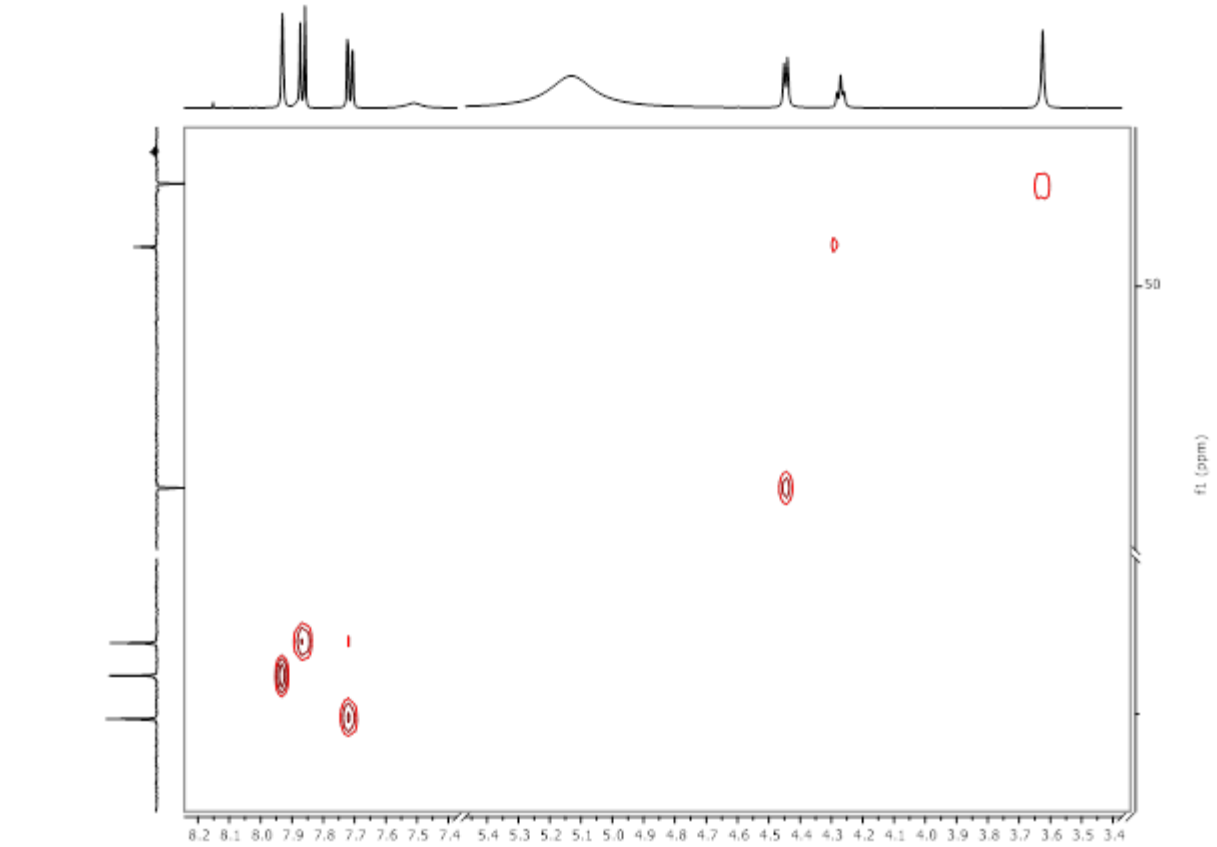

Figure 166: ^{1}H-^{13}C HSQC-NMR of Smoc-Gly-OH **12**.

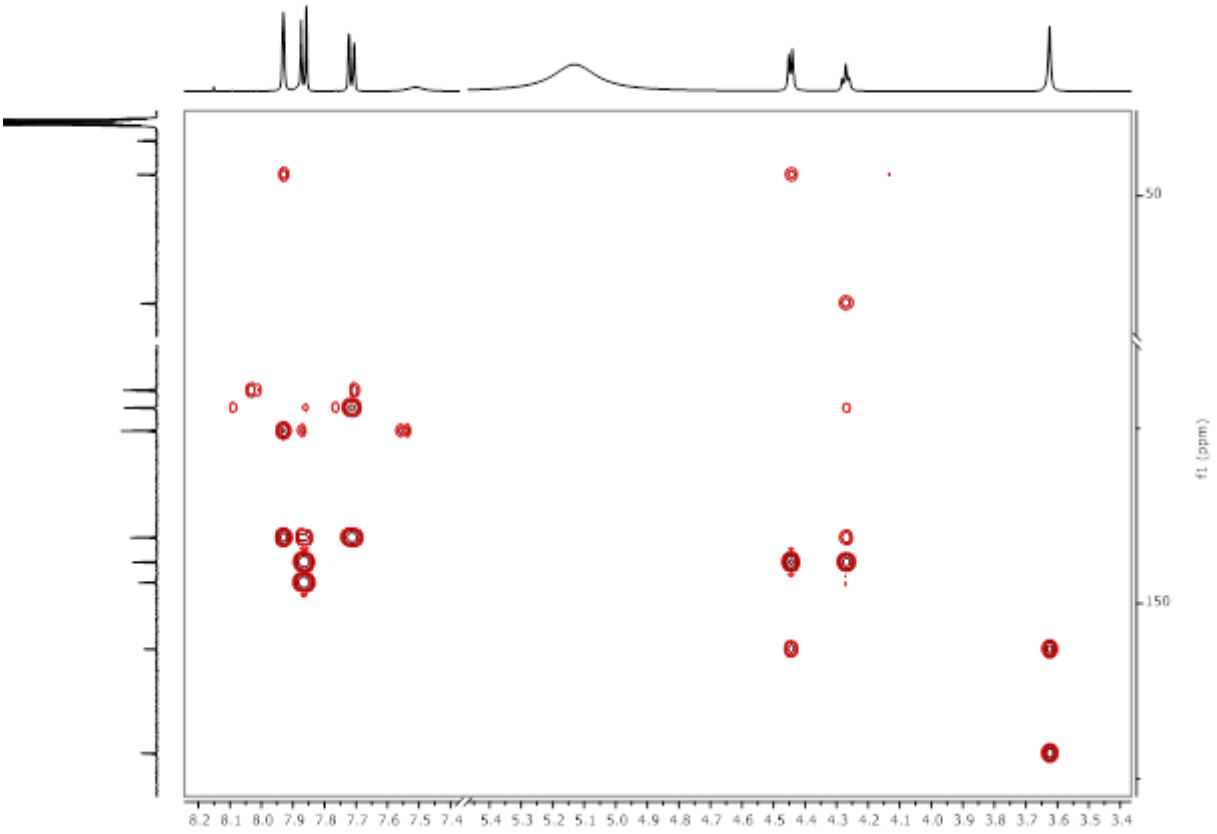

Figure 167: ^{1}H-^{13}C HMBC-NMR of Smoc-Gly-OH **12**.

8.2.11.Analytical data of Smoc-L-His-OH 13

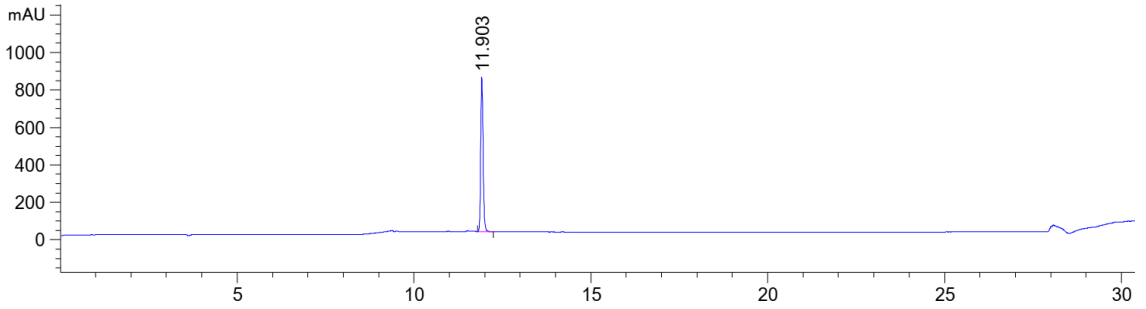

Figure 168: HPLC chromatogram of Smoc-L-His-OH **13** at λ=220 nm (0 to 40% MeCN).

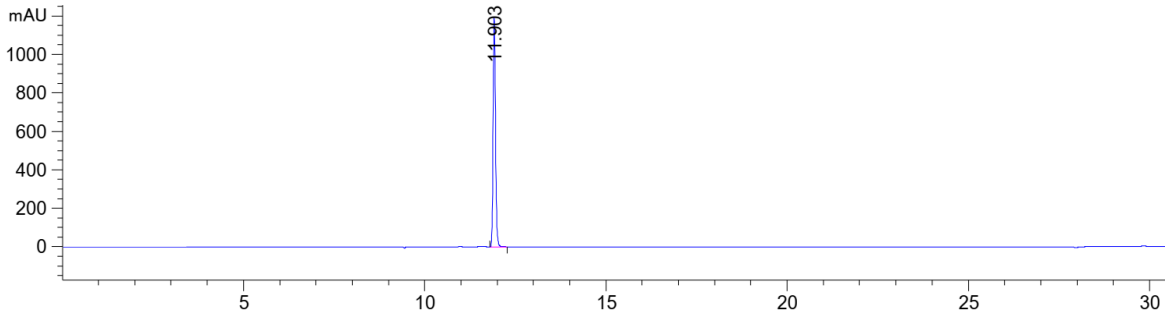

Figure 169: HPLC chromatogram of Smoc-L-His-OH **13** at λ=280 nm (0 to 40% MeCN).

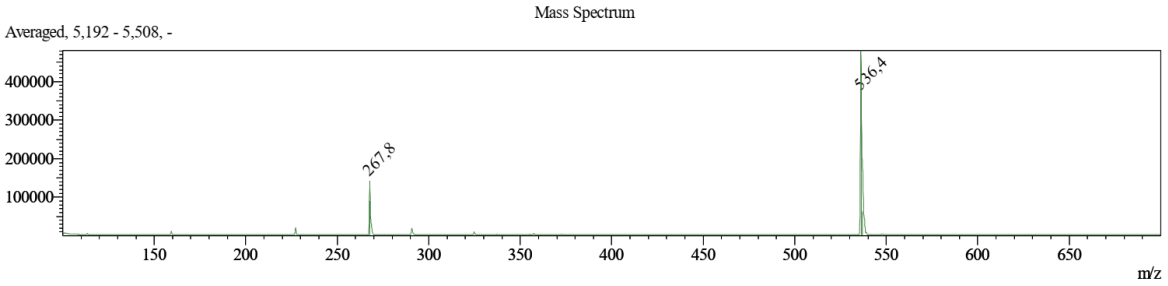

Figure 170: ESI-MS of Smoc-L-His-OH **13** (M measured=534.40 $[M-H]^-$, M calc.=537.51).

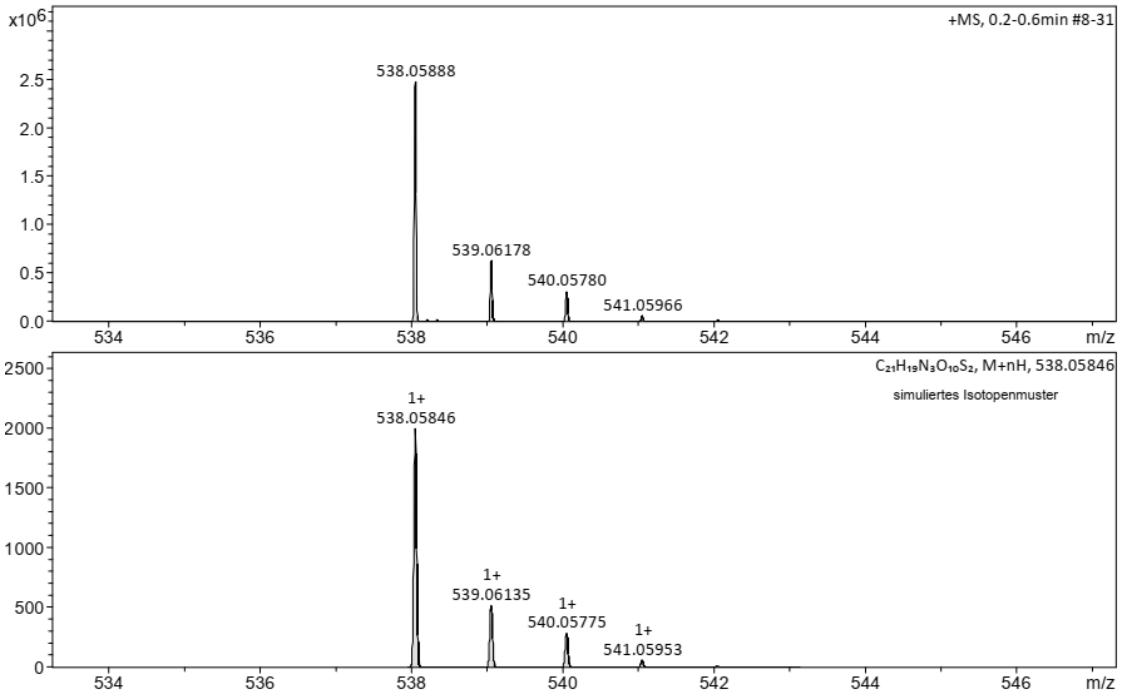

Figure 171: HR-MS of Smoc-L-His-OH **13** (M measured=538.05888 $[M+H]^+$, M calc.=538.05846).

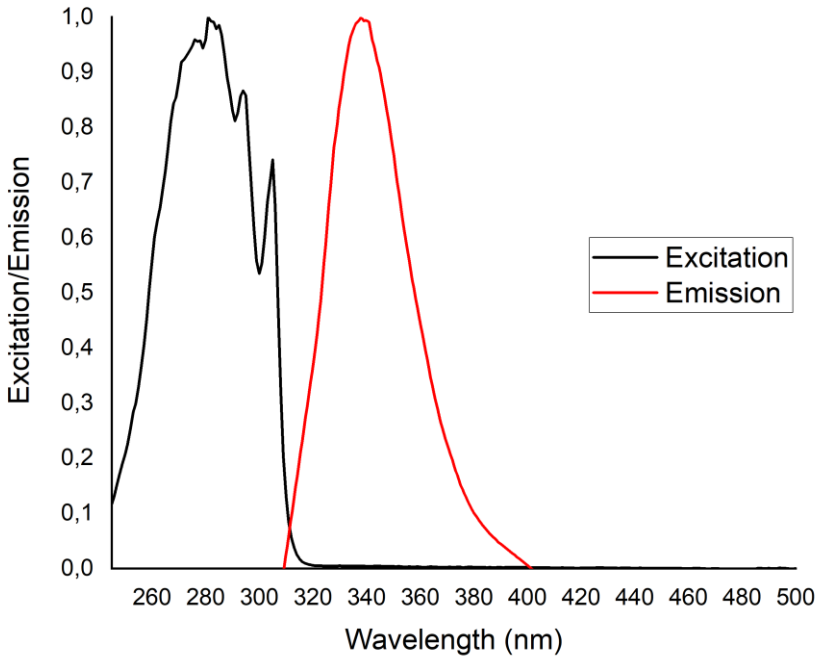

Figure 172: Excitation and emission spectra of Smoc-L-His-OH **13**, excitation and emission have been normalized between 0 and 1 for illustration.

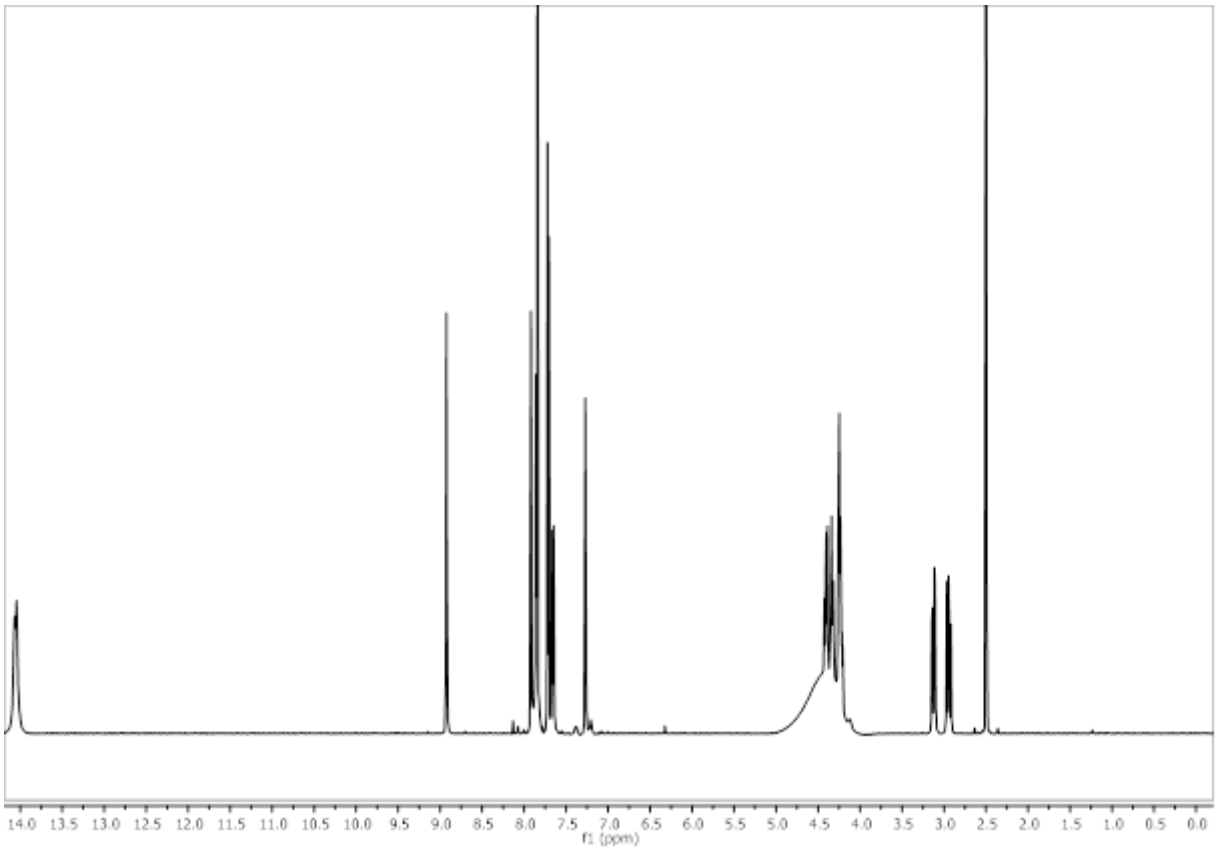

Figure 173: ^{1}H-NMR of Smoc-L-His-OH **13**.

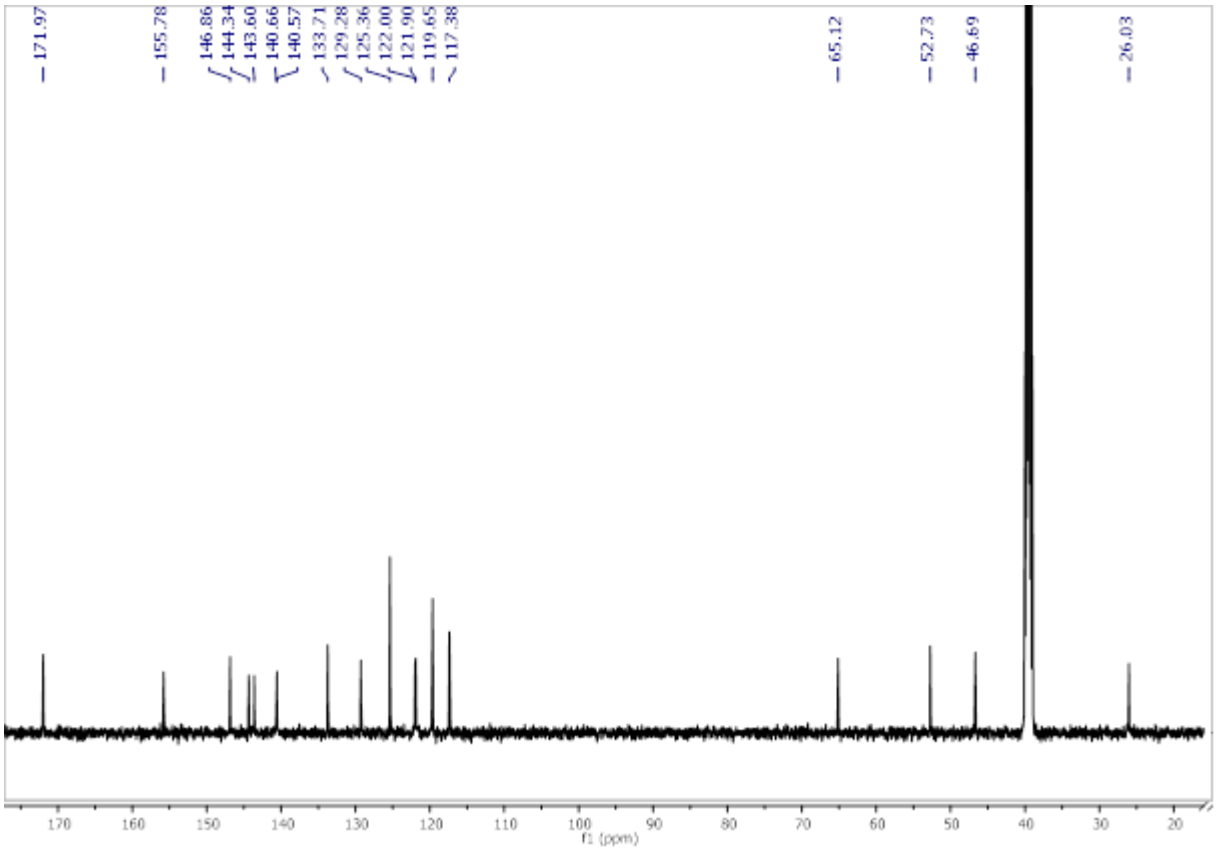

Figure 174: ^{13}C-NMR of Smoc-L-His-OH **13**.

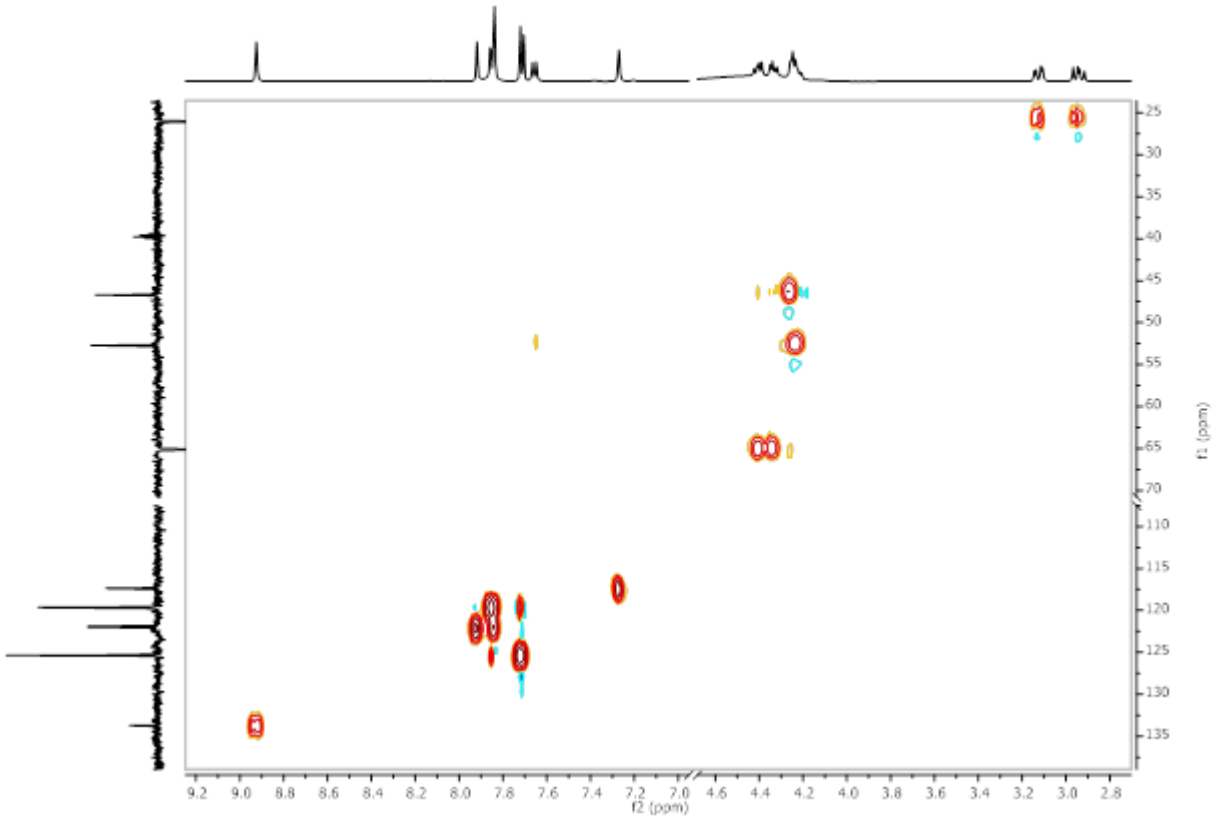

Figure 175: ^{1}H-^{13}C HSQC-NMR of Smoc-L-His-OH **13**.

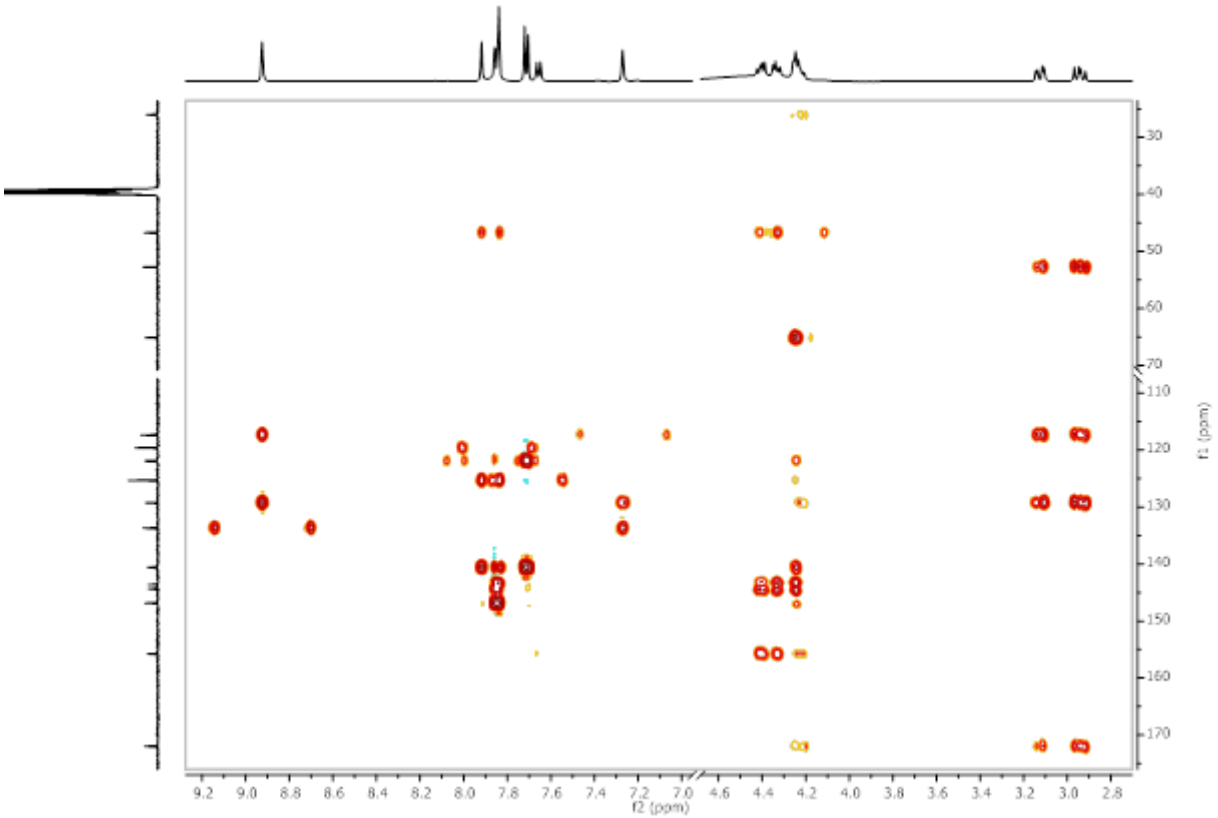

Figure 176: ^{1}H-^{13}C HMBC-NMR of Smoc-L-His-OH **13**.

8.2.12.Analytical data of Smoc-L-His(Trt)-OH 14

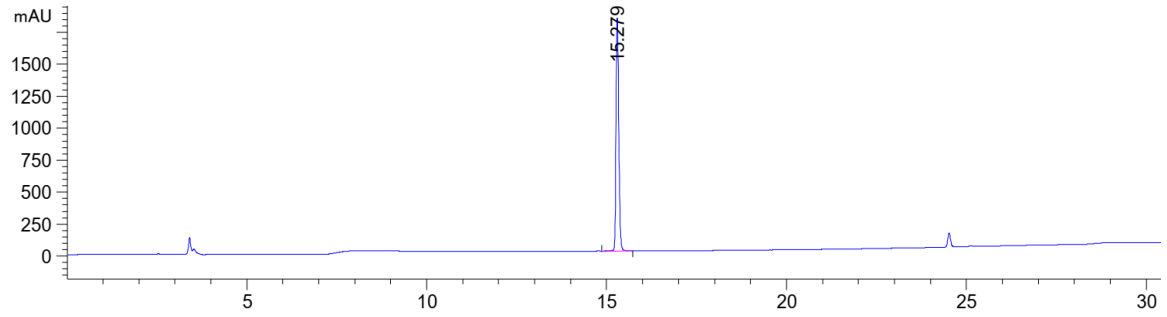

Figure 177: HPLC chromatogram of Smoc-L-His(Trt)-OH **14** at λ=220 nm (10 to 100% MeCN).

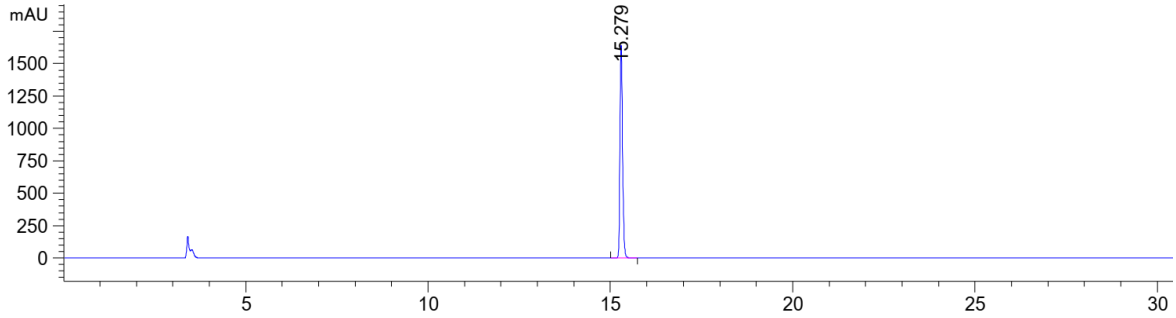

Figure 178: HPLC chromatogram of Smoc-L-His(Trt)-OH **14** at λ=280 nm (10 to 100% MeCN).

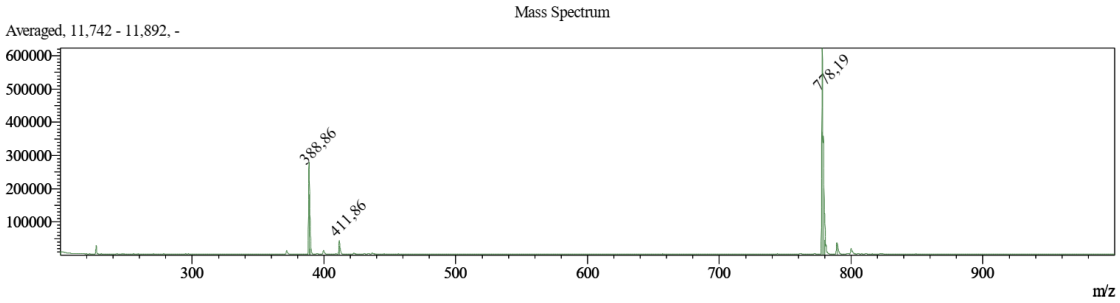

Figure 179: ESI-MS of Smoc-L-His(Trt)-OH **14** (M measured=778.19 $[M-H]^-$, M calc.=779.84).

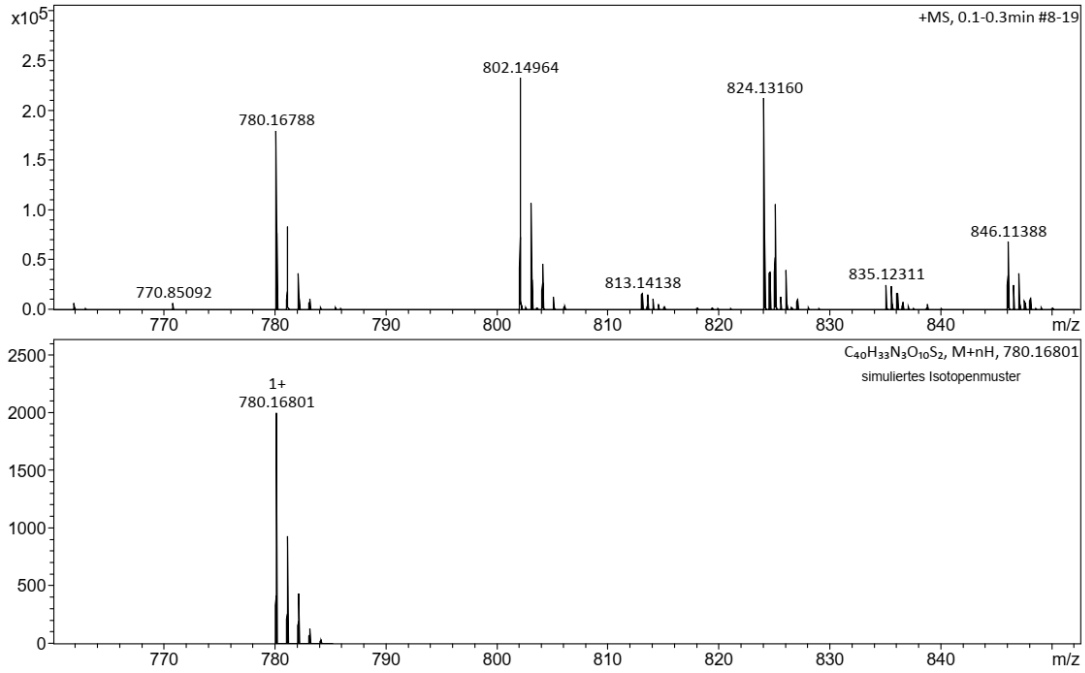

Figure 180: HR-MS of Smoc-L-His(Trt)-OH **14** (M measured=780.16788 $[M+H]^+$, M calc.=780.16801).

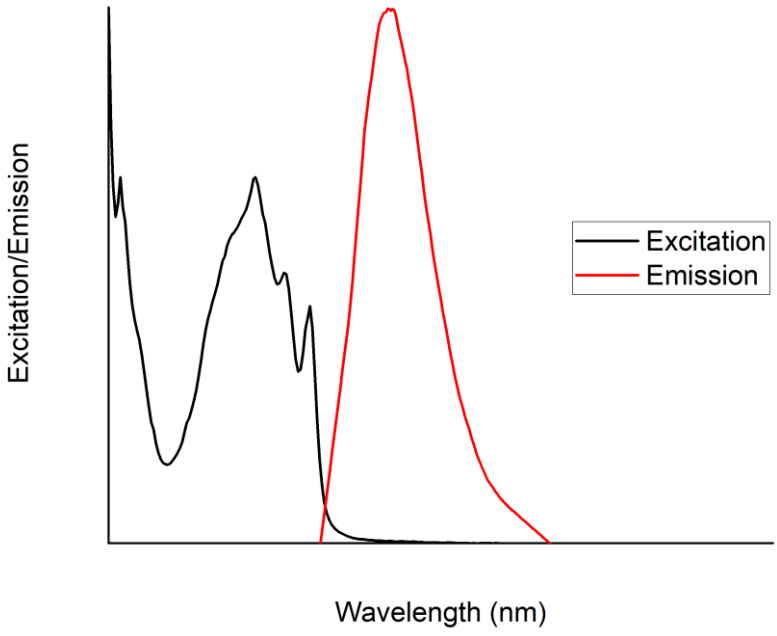

Figure 181: Excitation and emission spectra of Smoc-L-His(Trt)-OH **14**, excitation and emission have been normalized between 0 and 1 for illustration.

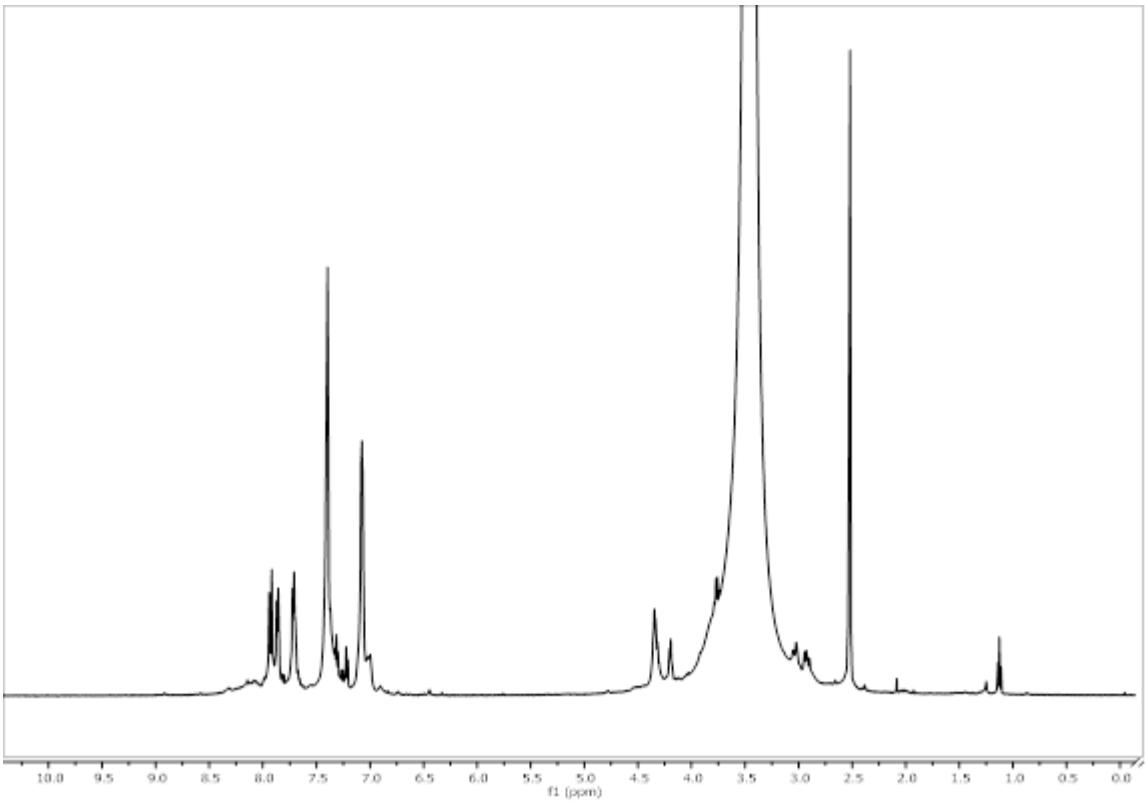

Figure 182: ^{1}H-NMR of Smoc-L-His(Trt)-OH **14**.

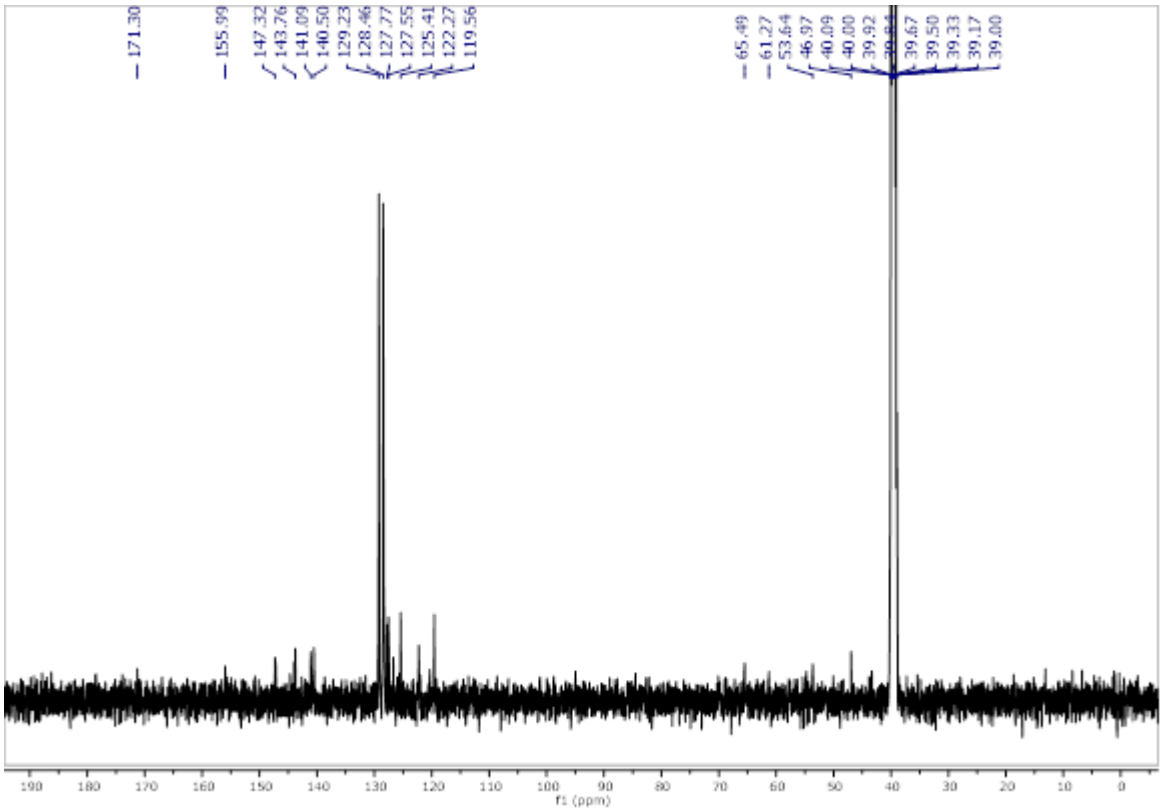

Figure 183: ^{13}C-NMR of Smoc-L-His(Trt)-OH **14**.

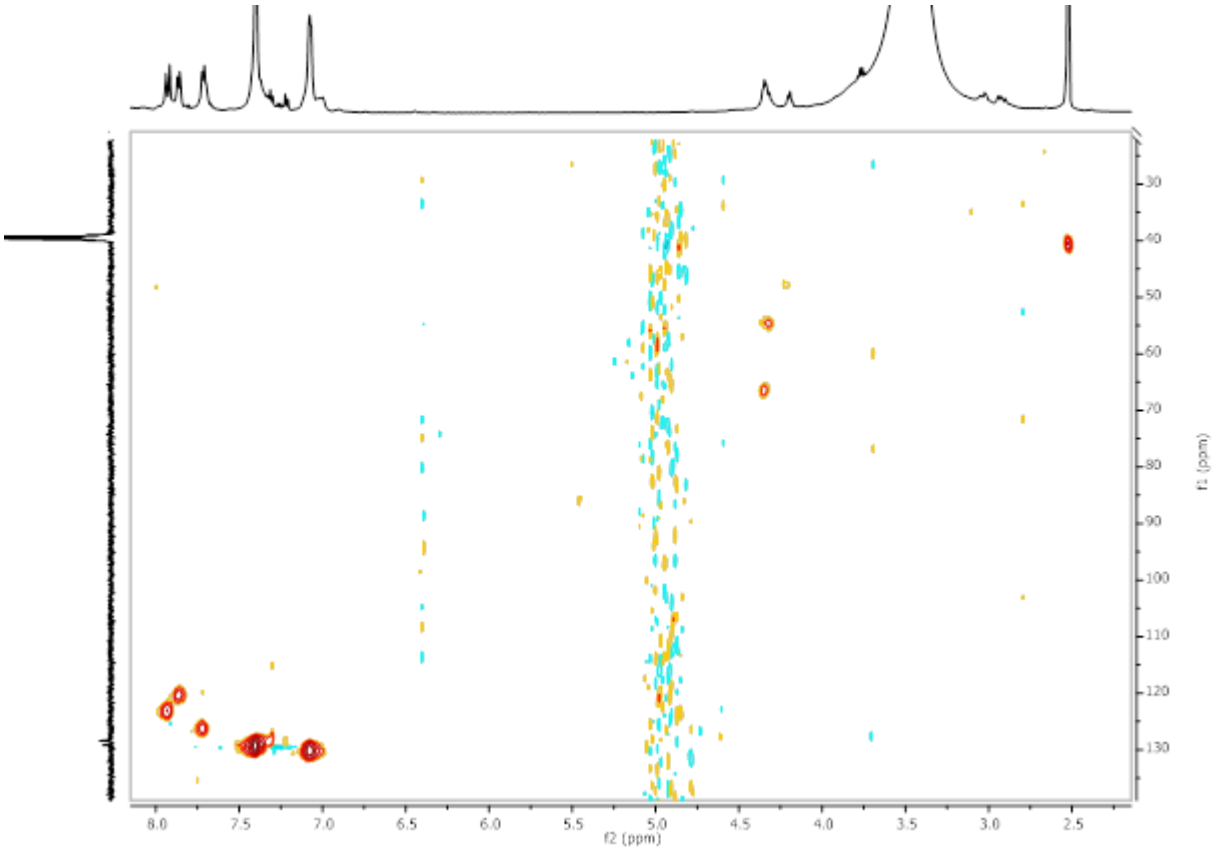

Figure 184: ^{1}H-^{13}C HSQC-NMR of Smoc-L-His(Trt)-OH **14**.

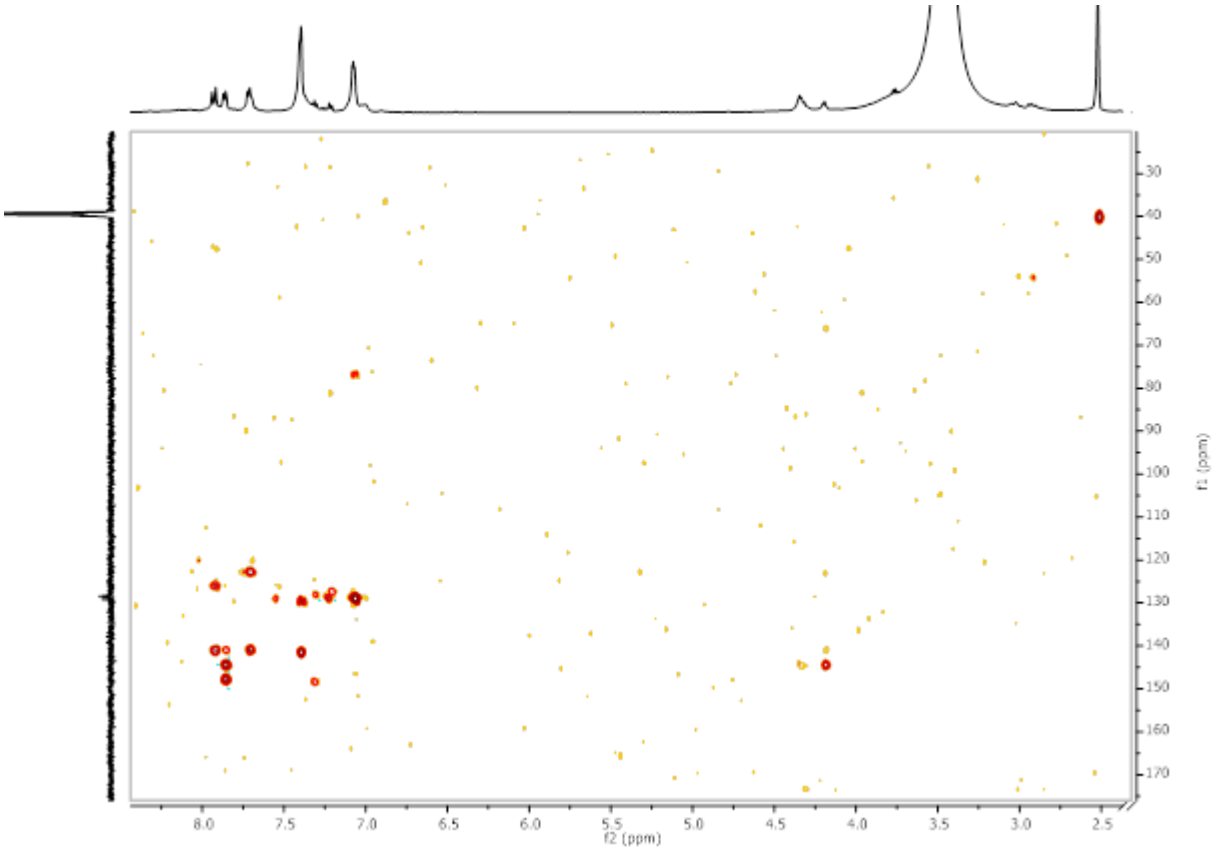

Figure 185: ^{1}H-^{13}C HMBC-NMR of Smoc-L-His(Trt)-OH **14**.

8.2.13.Analytical data of Smoc-L-Ile-OH 15

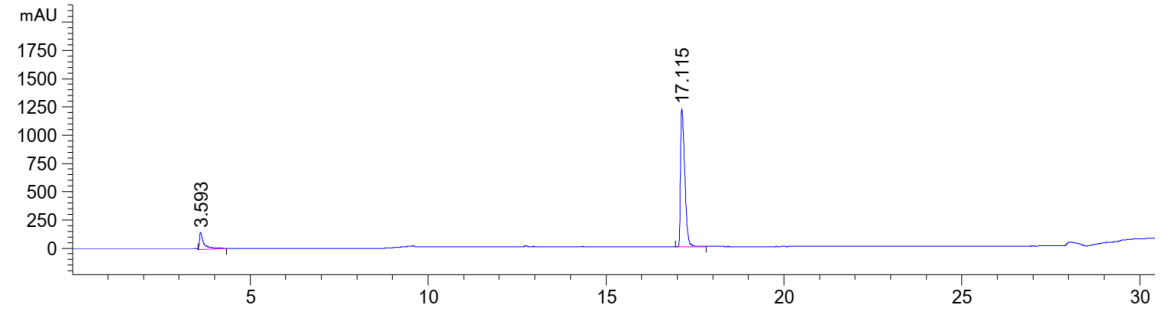

Figure 186: HPLC chromatogram of Smoc-L-Ile-OH **15** at λ=220 nm (0 to 40% MeCN).

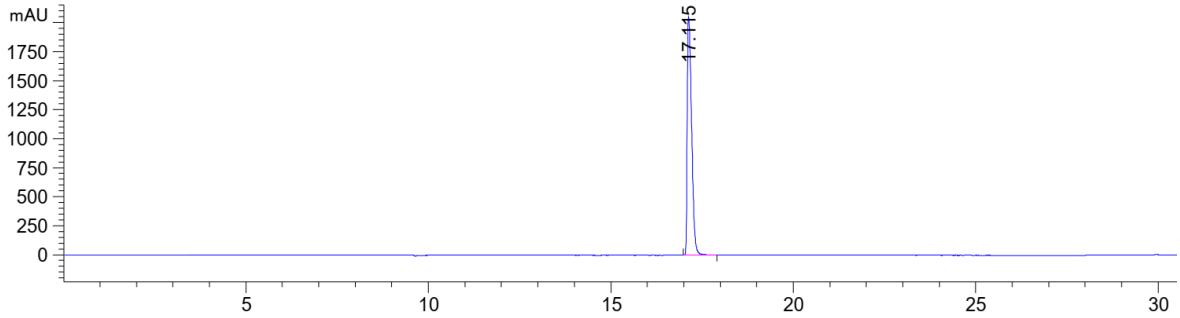

Figure 187: HPLC chromatogram of Smoc-L-Ile-OH **15** at λ=280 nm (0 to 40% MeCN).

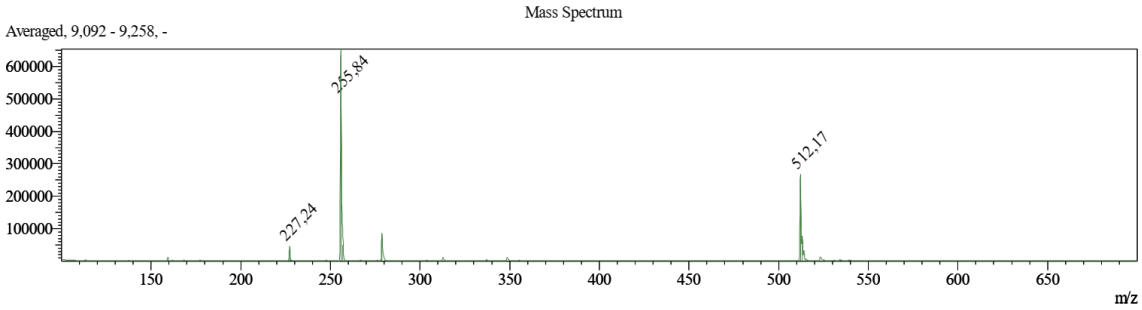

Figure 188: ESI-MS of Smoc-L-Ile-OH **15** (M measured=512.17 $[M-H]^-$, M calc.=513.53).

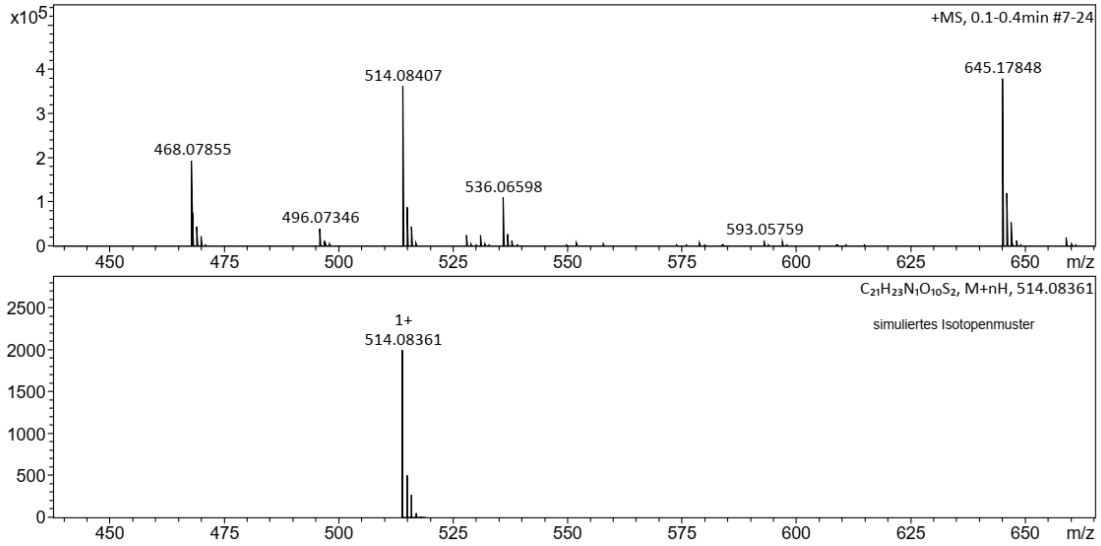

Figure 189: HR-MS of Smoc-L-Ile-OH **15** (M measured=514.08407 $[M+H]^+$, M calc.=514.08361).

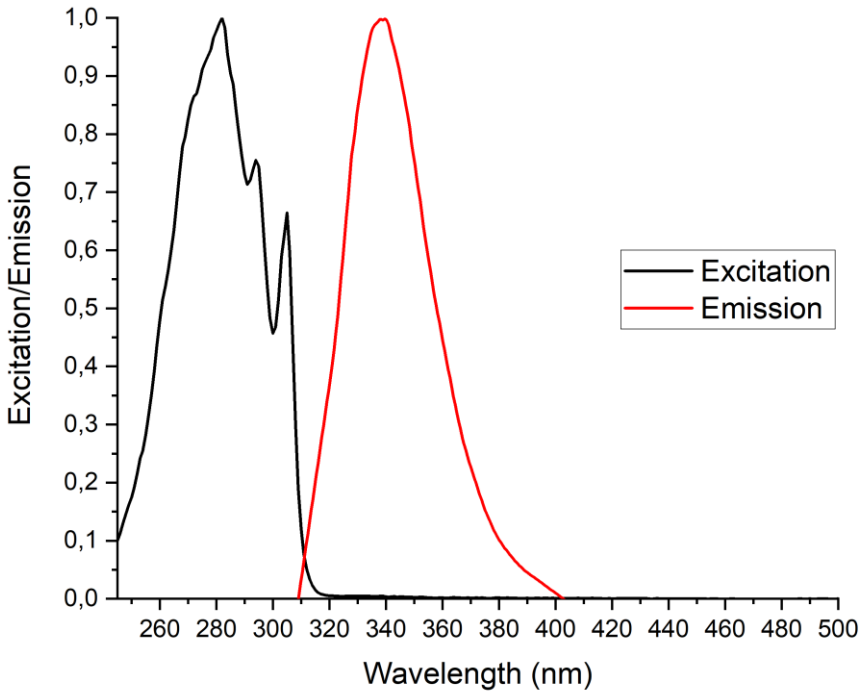

Figure 190: Excitation and emission spectra of Smoc-L-Ile-OH **15**, excitation and emission have been normalized between 0 and 1 for illustration.

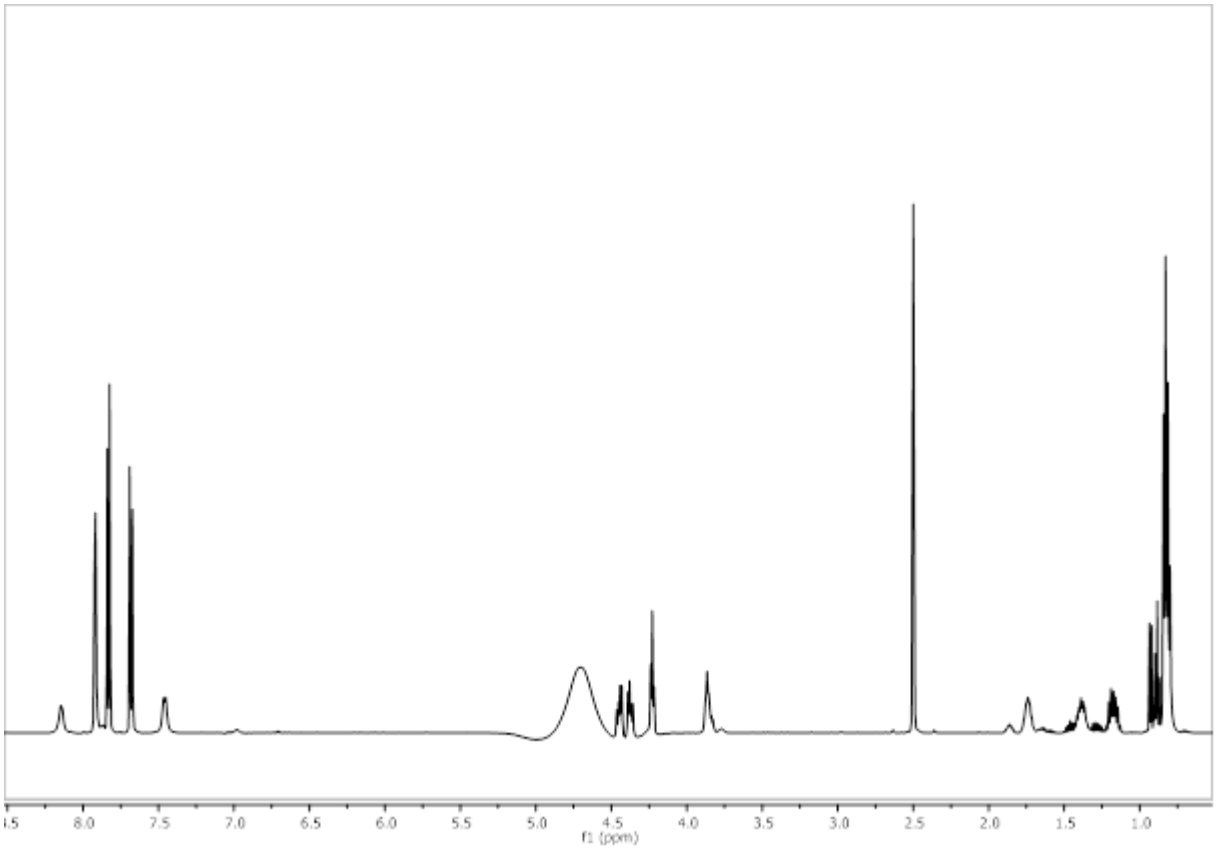

Figure 191: ^{1}H-NMR of Smoc-L-Ile-OH **15**.

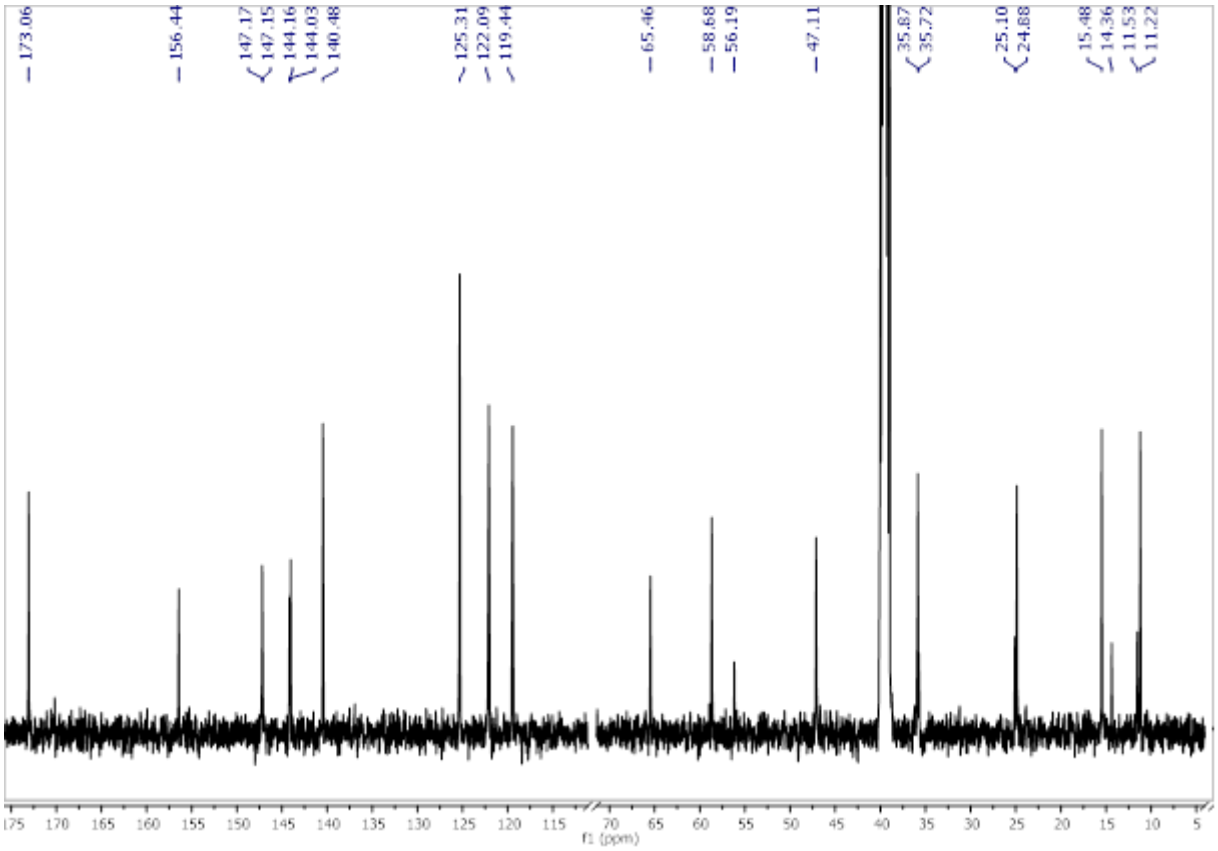

Figure 192: ^{13}C-NMR of Smoc-L-Ile-OH **15**.

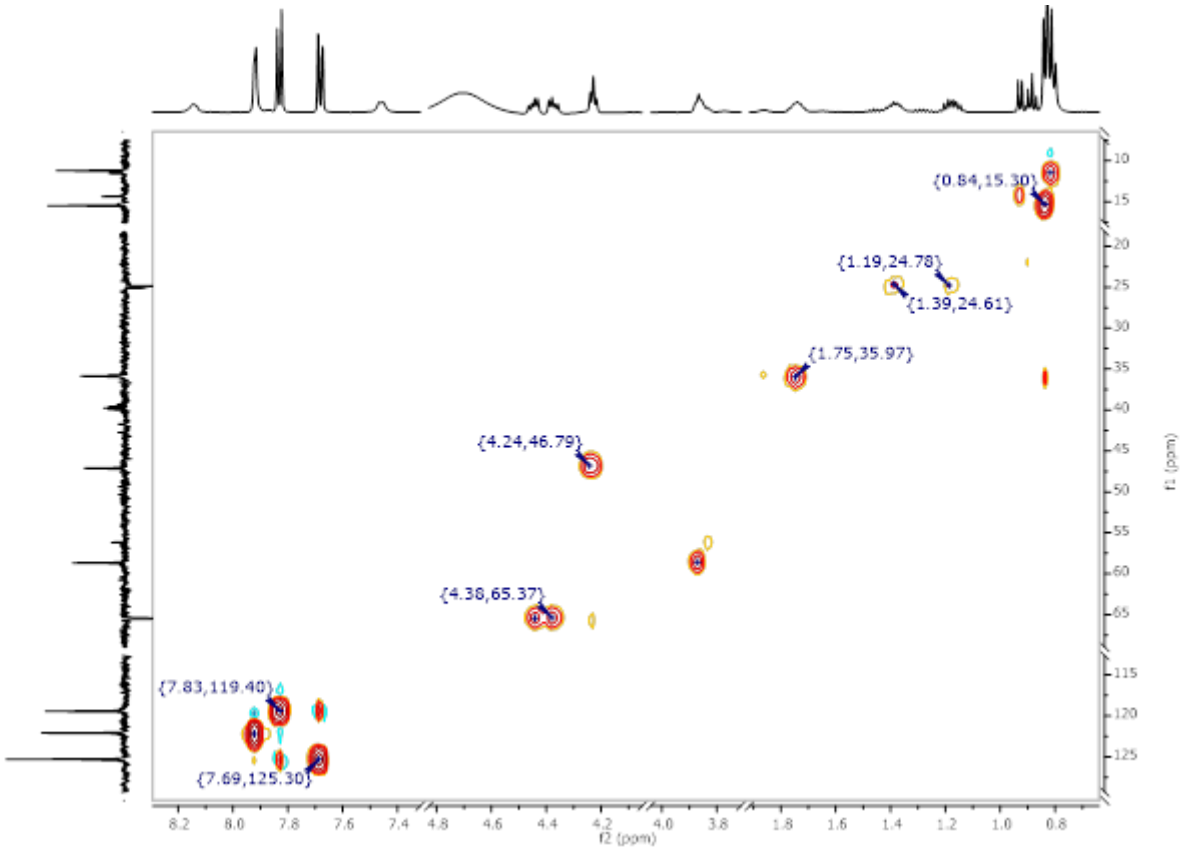

Figure 193: ^{1}H-^{13}C HSQC-NMR of Smoc-L-Ile-OH **15**.

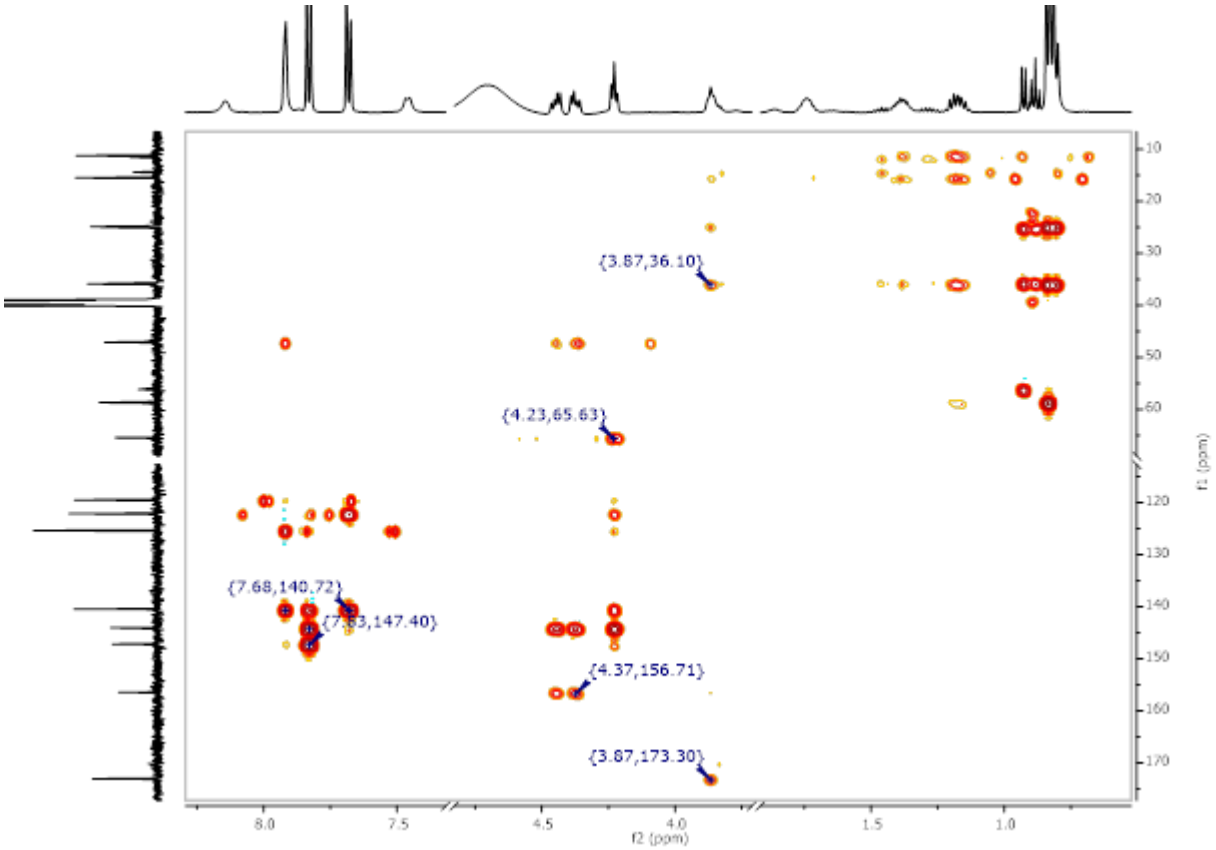

Figure 194: ^{1}H-^{13}C HMBC-NMR of Smoc-L-Ile-OH **15**.

8.2.14.Analytical data of Smoc-L-Leu-OH 16

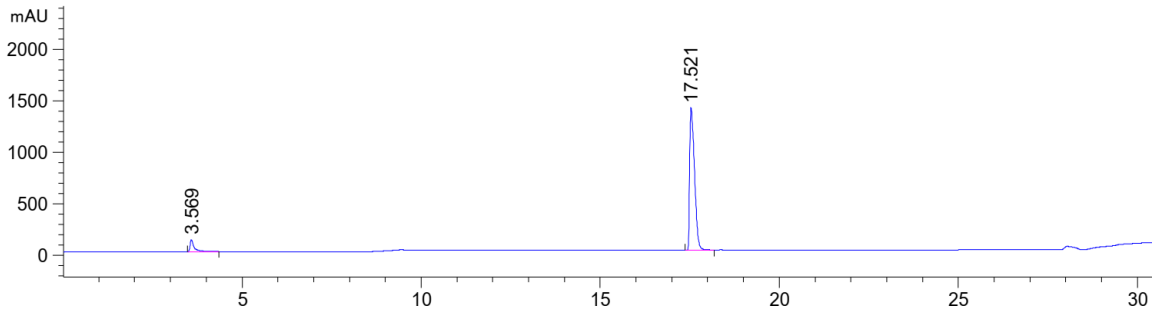

Figure 195: HPLC chromatogram of Smoc-L-Leu-OH **16** at λ=220 nm (0 to 40% MeCN).

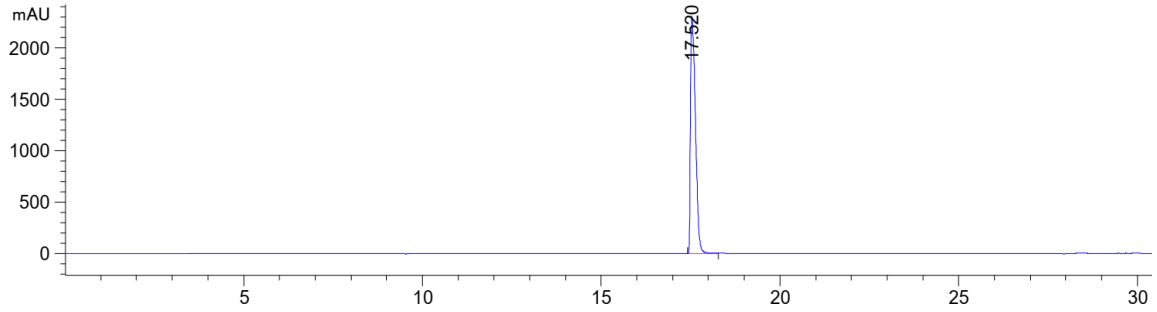

Figure 196: HPLC chromatogram of Smoc-L-Leu-OH **16** at λ=280 nm (0 to 40% MeCN).

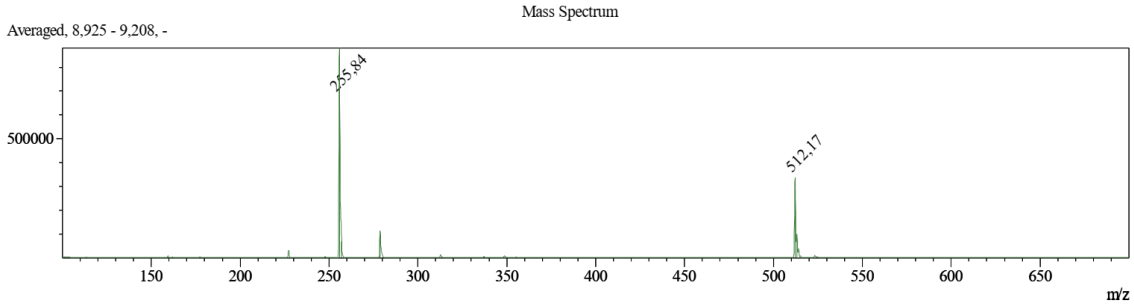

Figure 197: ESI-MS of Smoc-L-Leu-OH **16** (M measured=512.17 $[M-H]^-$, M calc.=513.53).

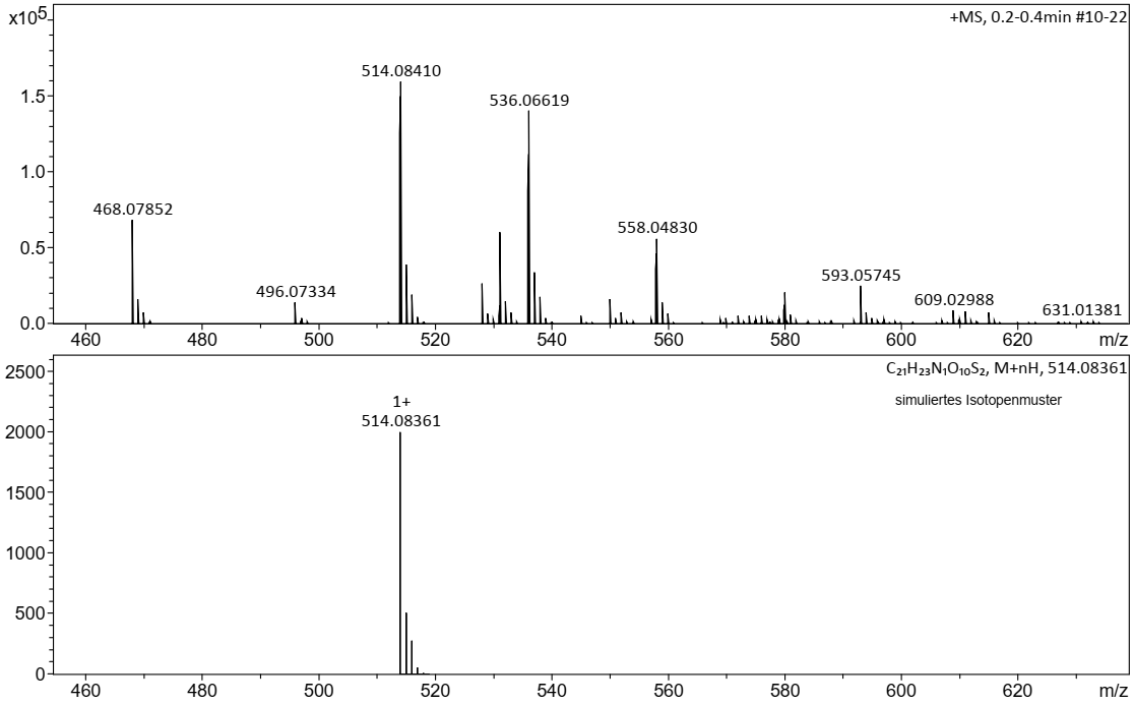

Figure 198: HR-MS of Smoc-L-Leu-OH **16** (M measured=514.08410 $[M+H]^+$, M calc.=514.08361).

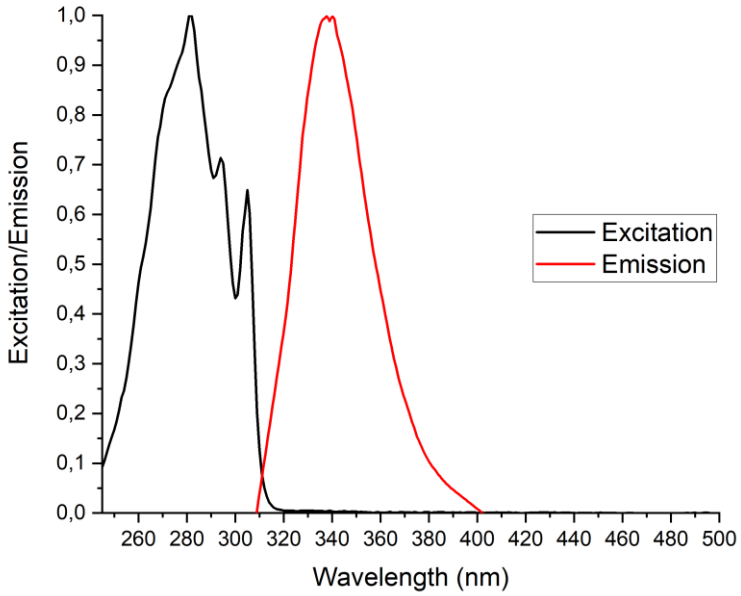

Figure 199: Excitation and emission spectra of Smoc-L-Leu-OH **16**, excitation and emission have been normalized between 0 and 1 for illustration.

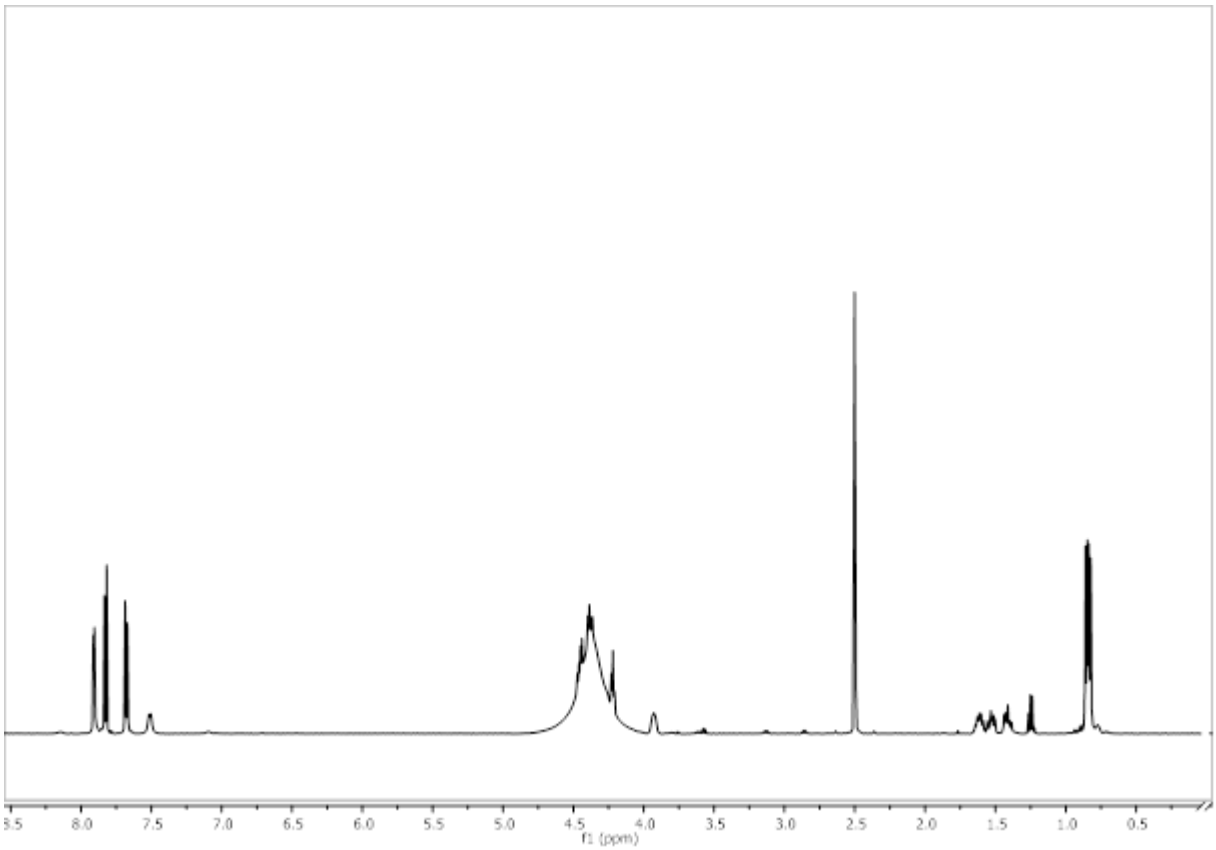

Figure 200: ^{1}H-NMR of Smoc-L-Leu-OH **16**.

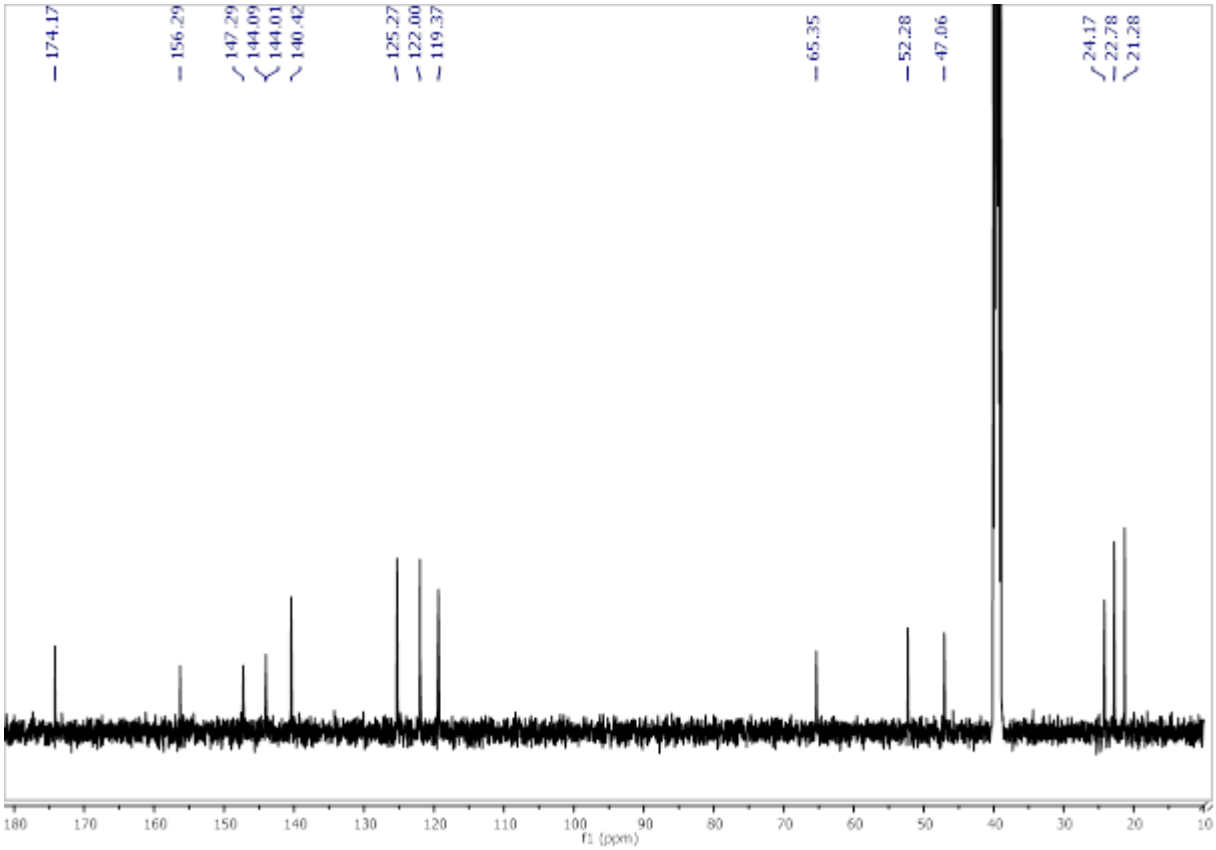

Figure 201: ^{13}C-NMR of Smoc-L-Leu-OH **16**.

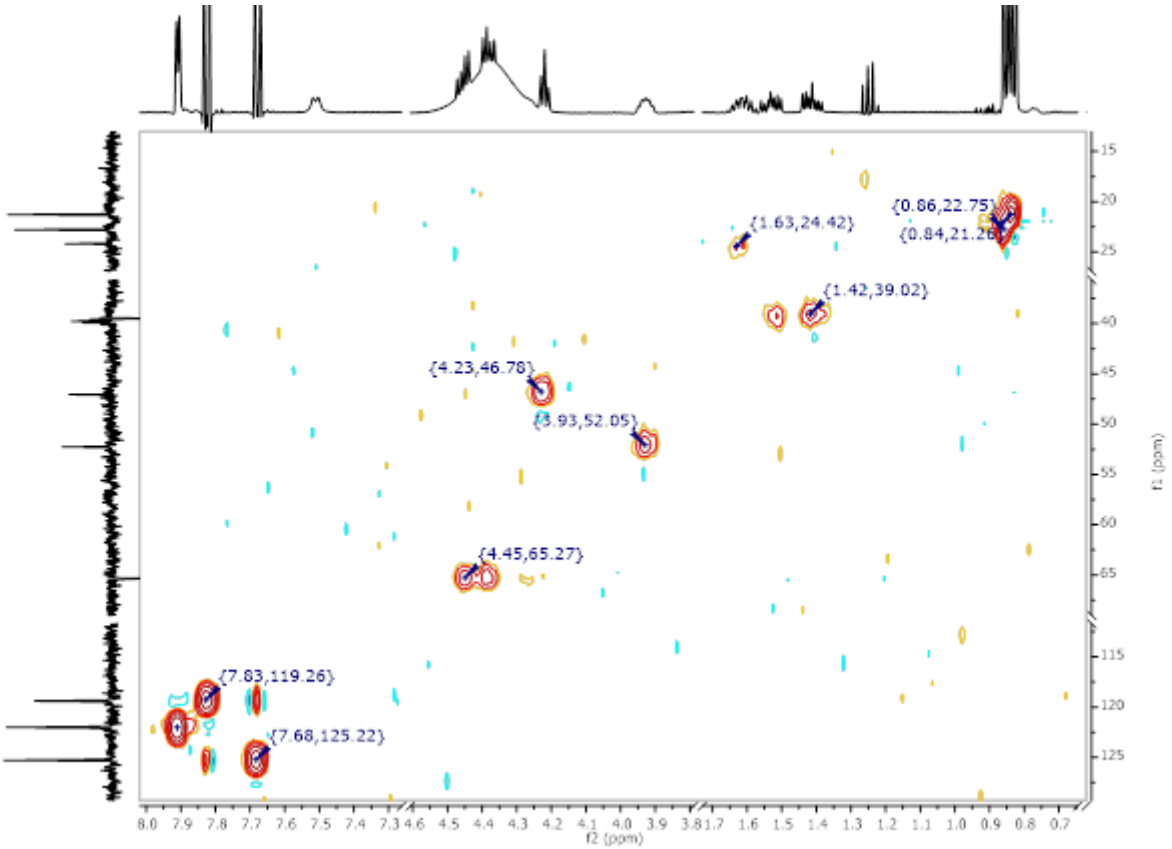

Figure 202: ^{1}H-^{13}C HSQC-NMR of Smoc-L-Leu-OH **16**.

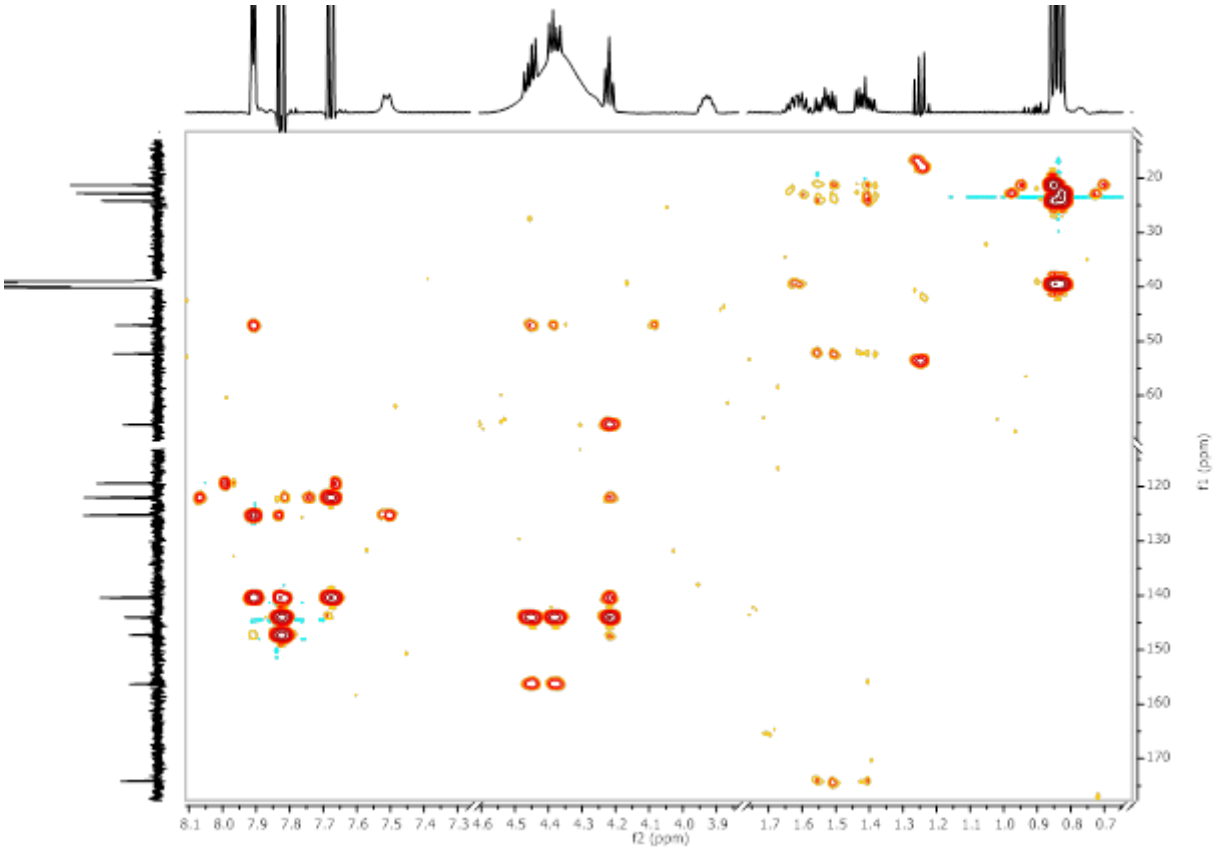

Figure 203: ^{1}H-^{13}C HMBC-NMR of Smoc-L-Leu-OH **16**.

8.2.15.Analytical data of Smoc-D-Leu-OH 17

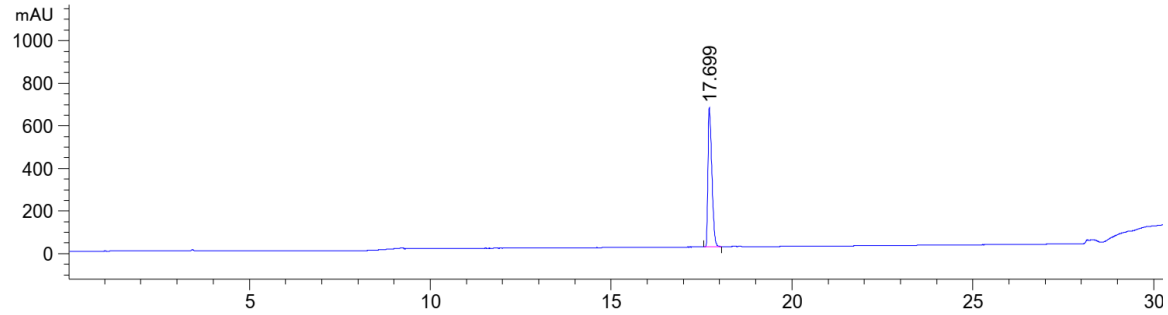

Figure 204: HPLC chromatogram of Smoc-D-Leu-OH **17** at λ=220 nm (0 to 40% MeCN).

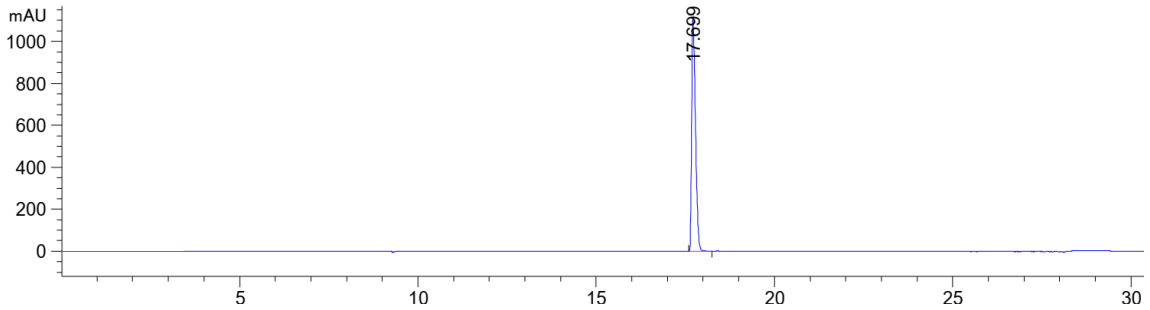

Figure 205: HPLC chromatogram of Smoc-D-Leu-OH **17** at λ=280 nm (0 to 40% MeCN).

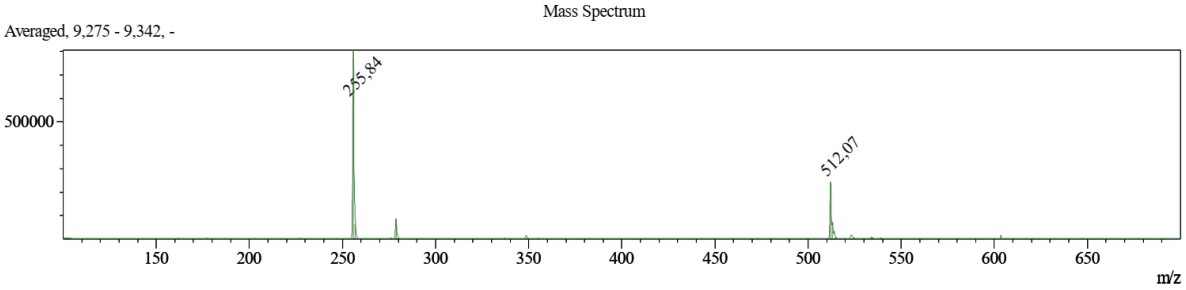

Figure 206: ESI-MS of Smoc-D-Leu-OH **17** (M measured=512.07 $[M-H]^-$, M calc.=513.53).

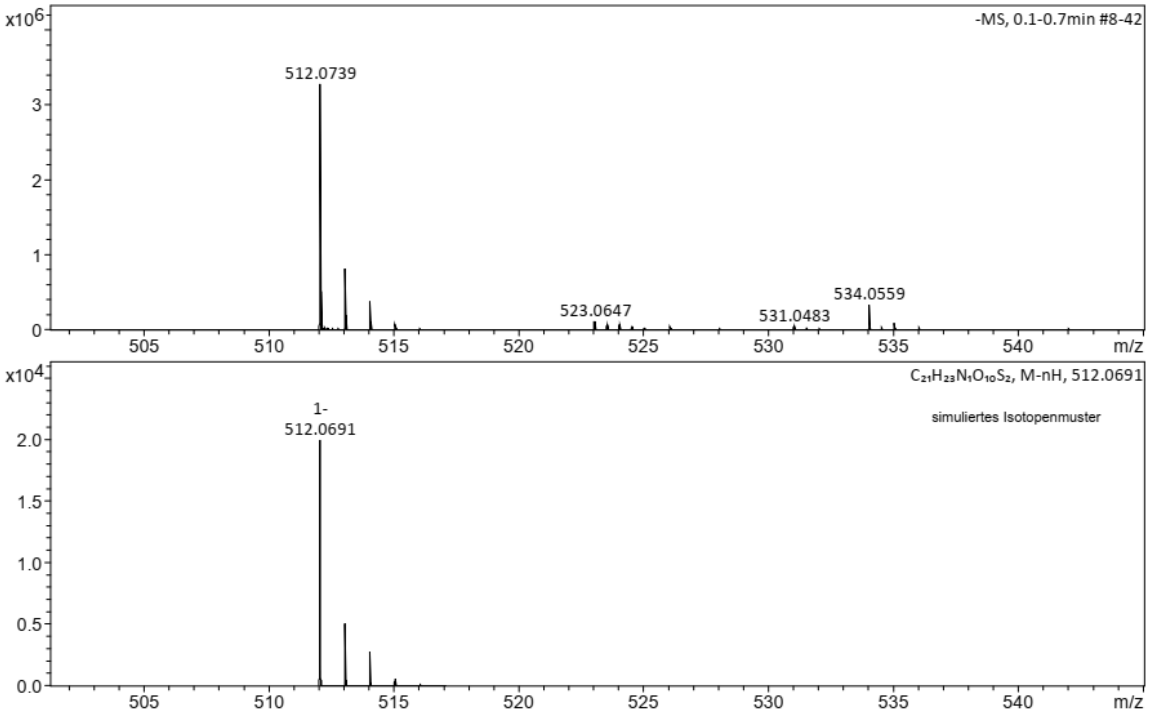

Figure 207: HR-MS of Smoc-D-Leu-OH **17** (M measured=512.0739 $[M+H]^+$, M calc.=512.0691).

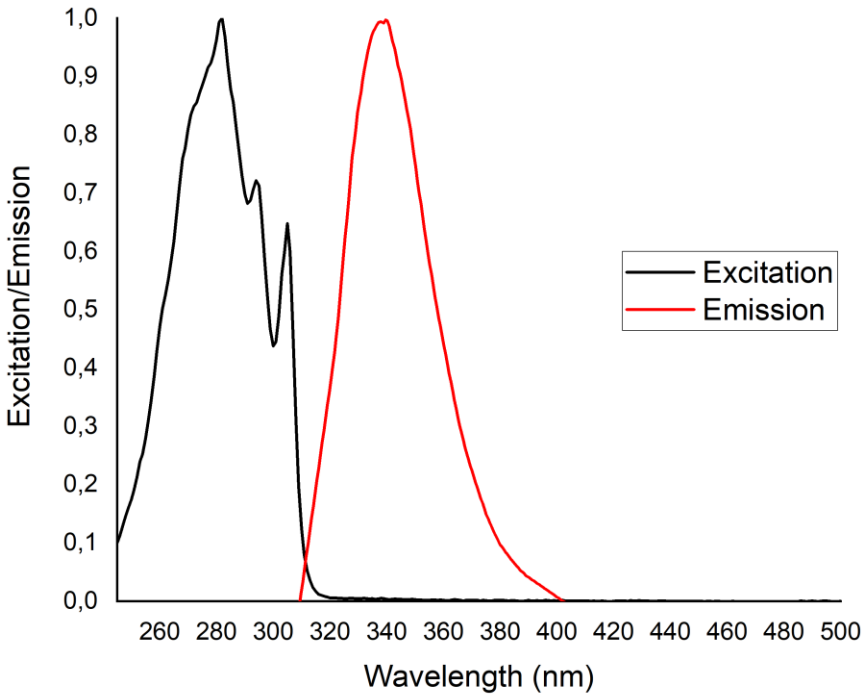

Figure 208: Excitation and emission spectra of Smoc-D-Leu-OH **17**, excitation and emission have been normalized between 0 and 1 for illustration.

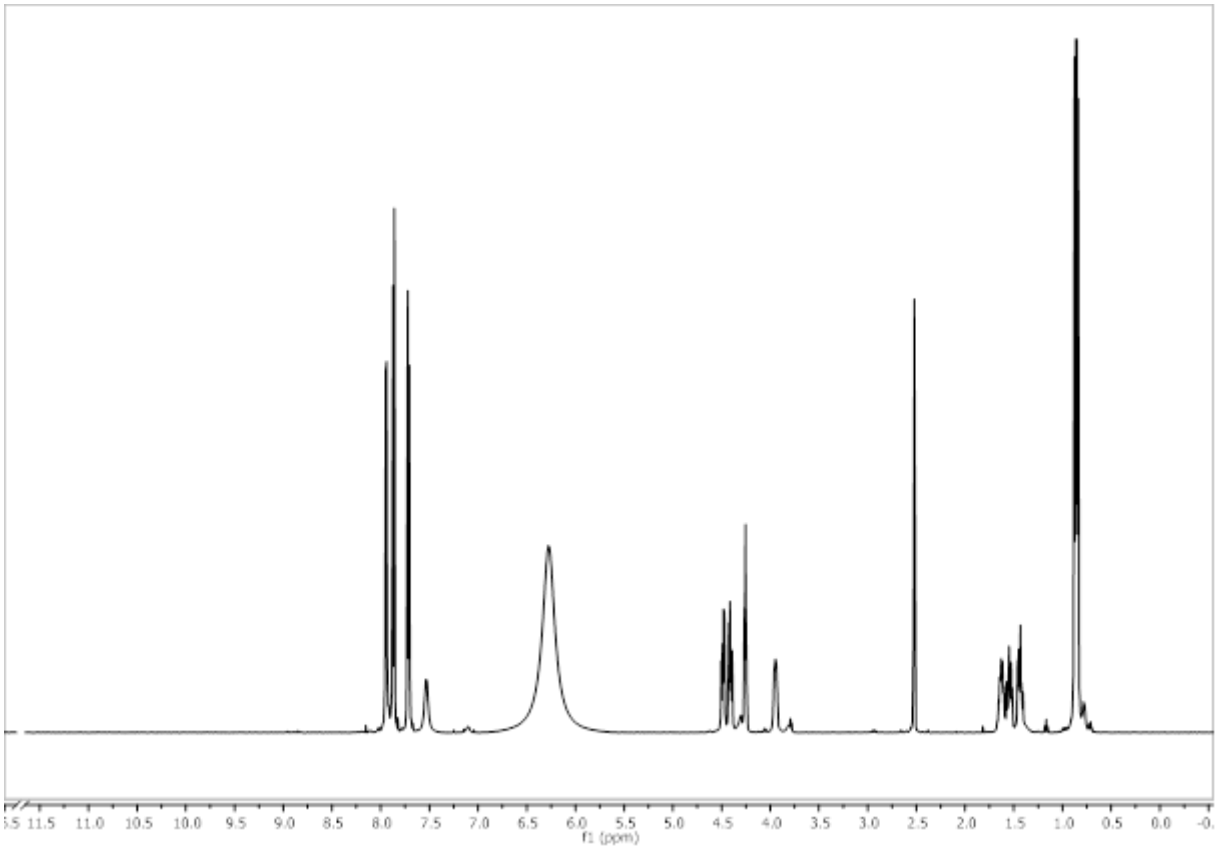

Figure 209: ^{1}H-NMR of Smoc-D-Leu-OH **17**.

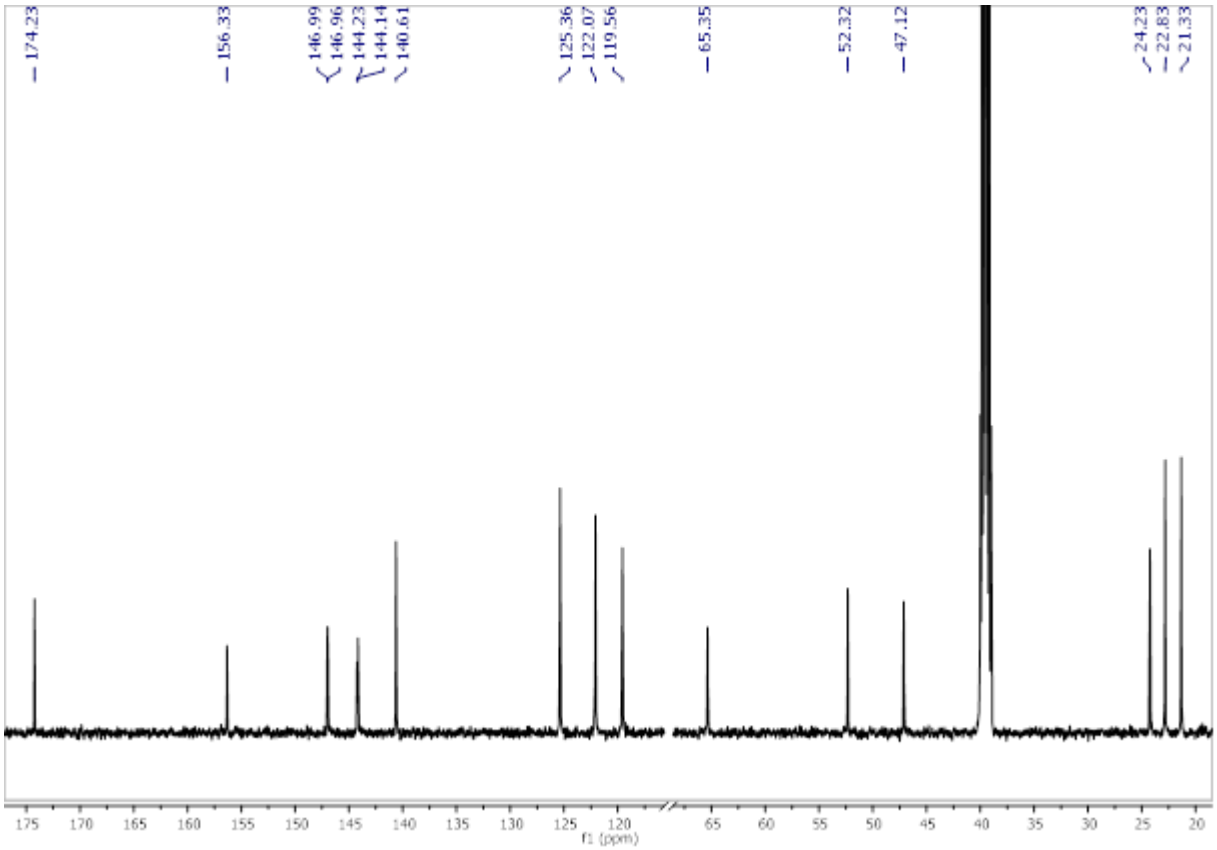

Figure 210: ^{13}C-NMR of Smoc-D-Leu-OH **17**.

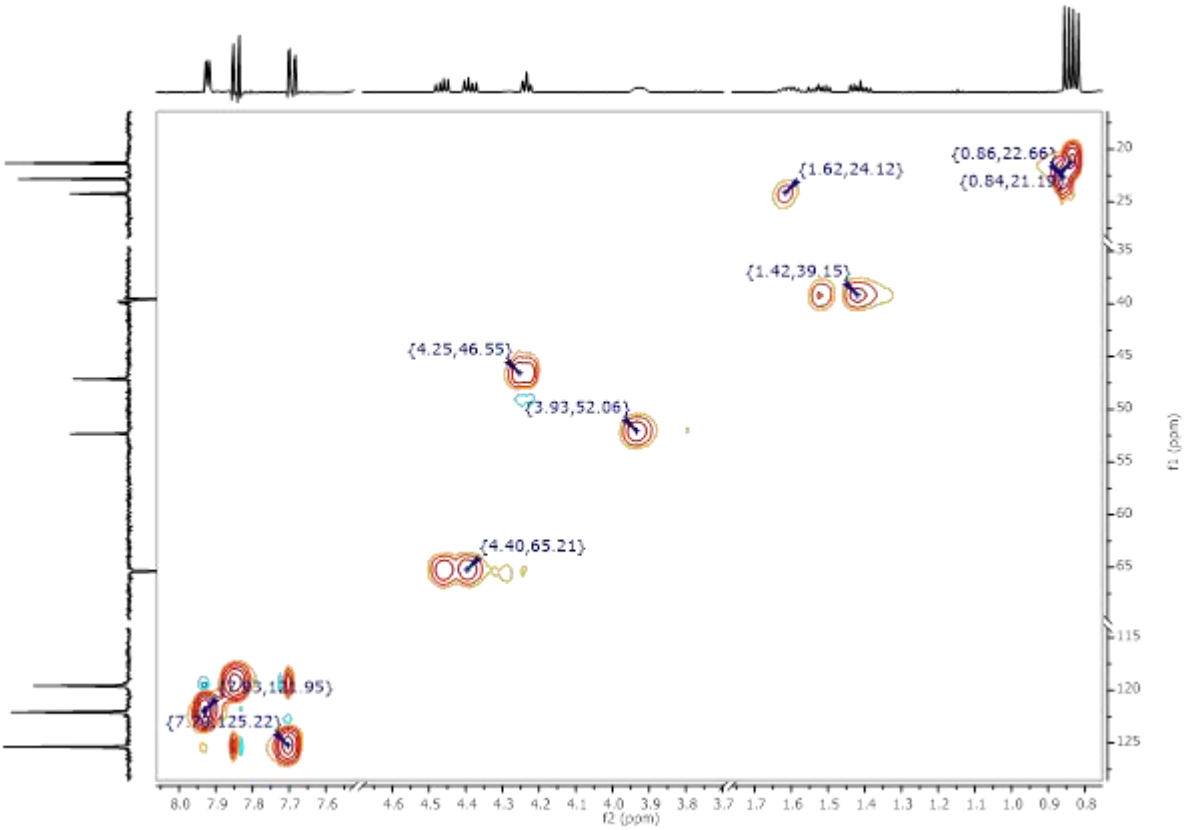

Figure 211: ^{1}H-^{13}C HSQC-NMR of Smoc-D-Leu-OH **17**.

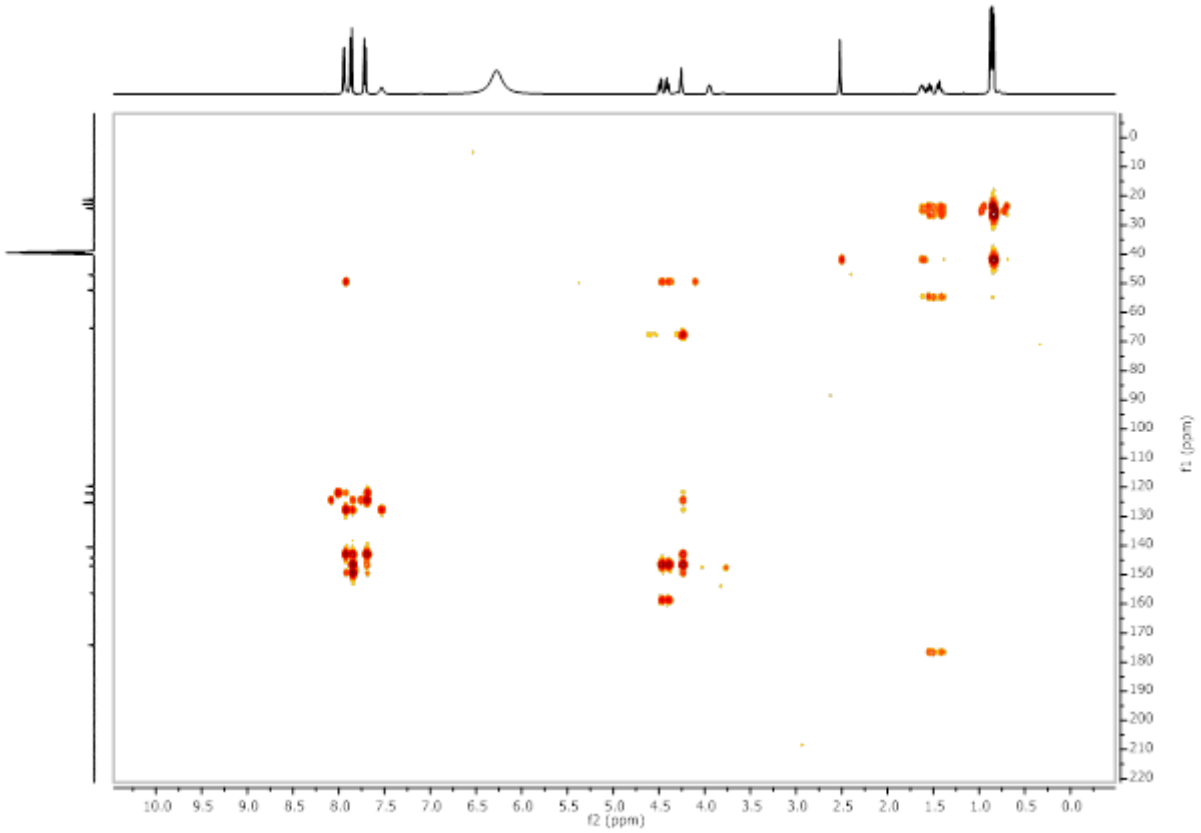

Figure 212: ^{1}H-^{13}C HMBC-NMR of Smoc-D-Leu-OH **17**.

8.2.16.Analytical data of Smoc-L-Lys(Boc)-OH 18

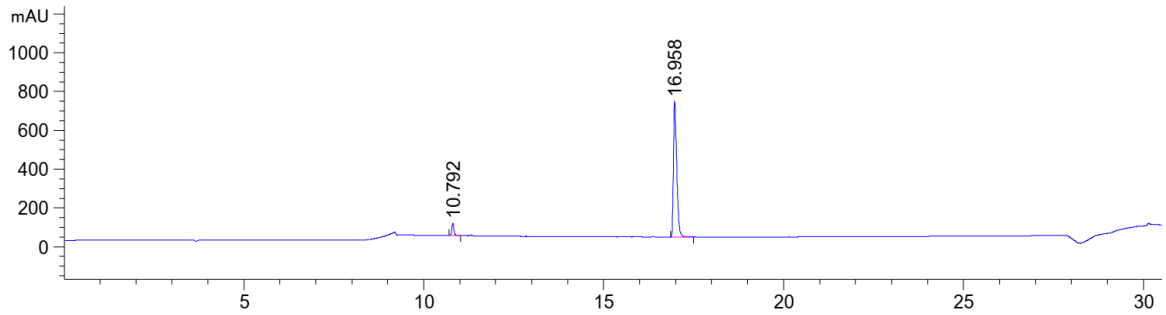

Figure 213: HPLC chromatogram of Smoc-L-Lys(Boc)-OH **18** at λ=220 nm (0 to 60% MeCN).

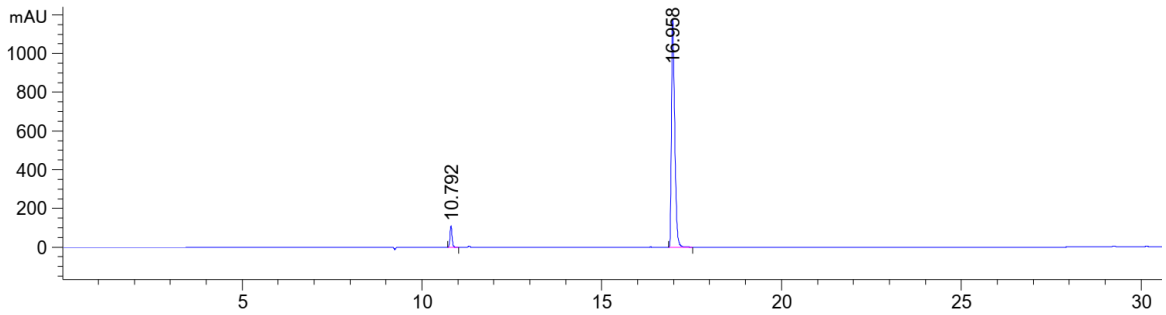

Figure 214: HPLC chromatogram of Smoc-L-Lys(Boc)-OH **18** at λ=280 nm (0 to 60% MeCN).

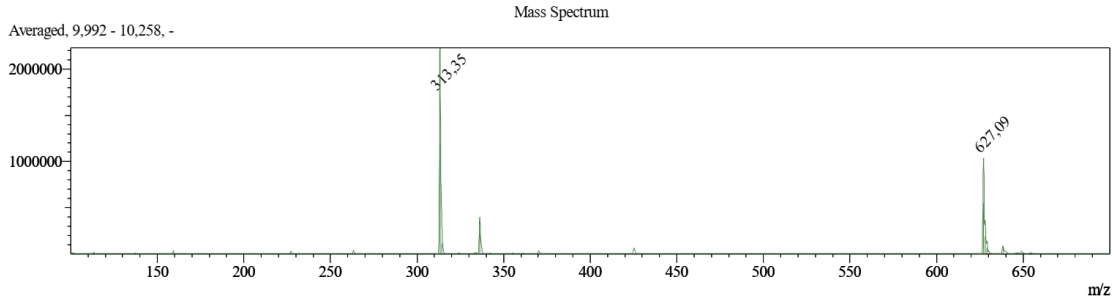

Figure 215: ESI-MS of Smoc-L-Lys(Boc)-OH **18** (M measured=627.09 $[M-H]^-$, M calc.=628.66).

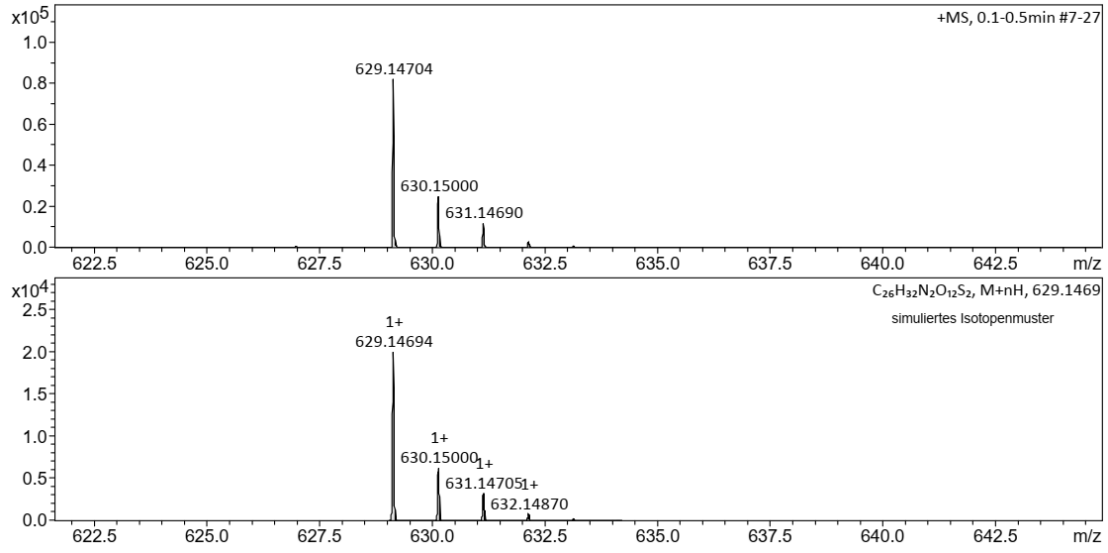

Figure **216:** HR-MS of Smoc-L-Lys(Boc)-OH **18** (M measured= 629.14704 $[M+H]^+$, M calc.=629.14694).

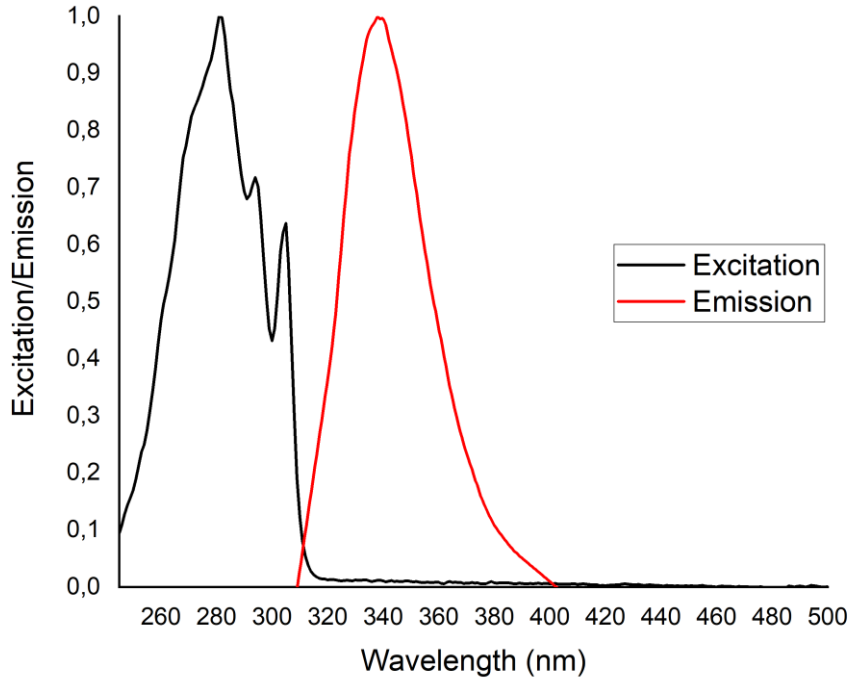

Figure 217: Excitation and emission spectra of Smoc-L-Lys(Boc)-OH **18**, excitation and emission have been normalized between 0 and 1 for illustration.

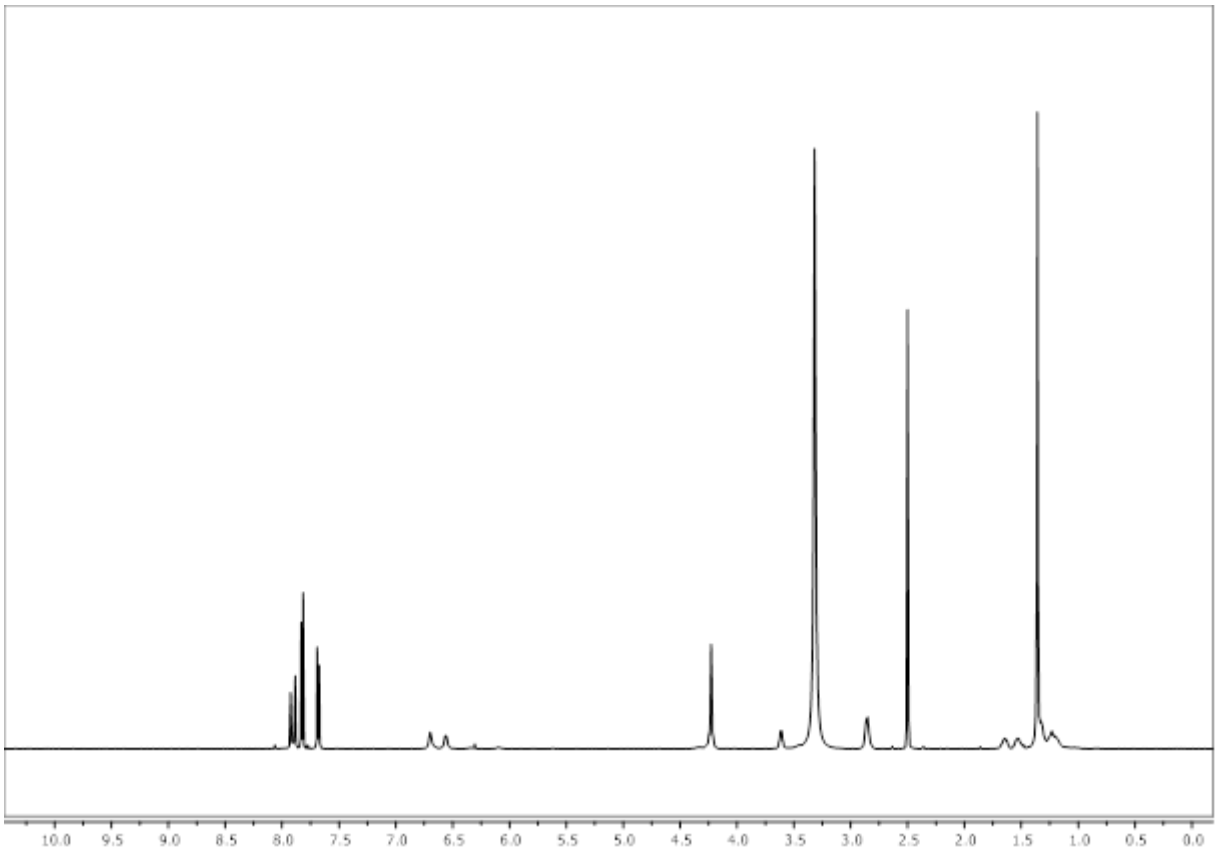

Figure 218: ^{1}H-NMR of Smoc-L-Lys(Boc)-OH **18**.

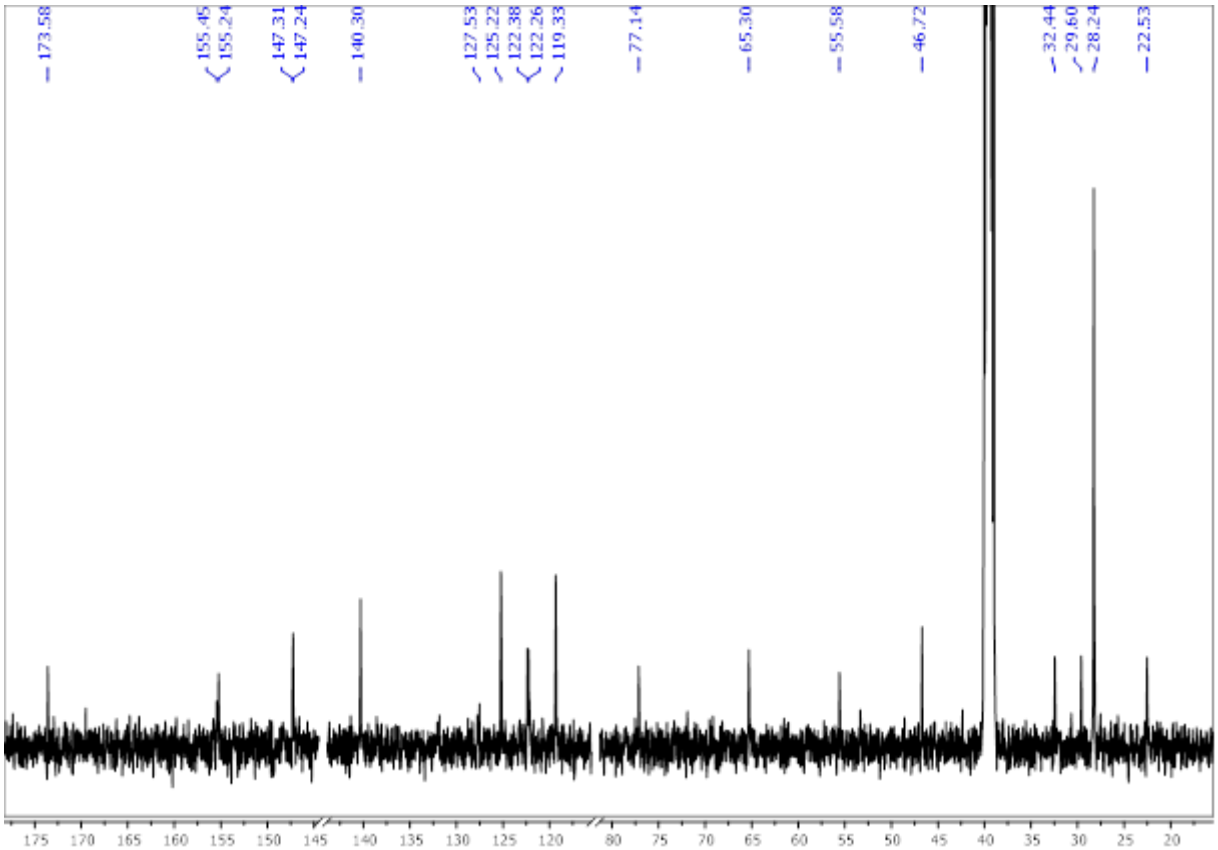

Figure 219: ^{13}C-NMR of Smoc-L-Lys(Boc)-OH **18**.

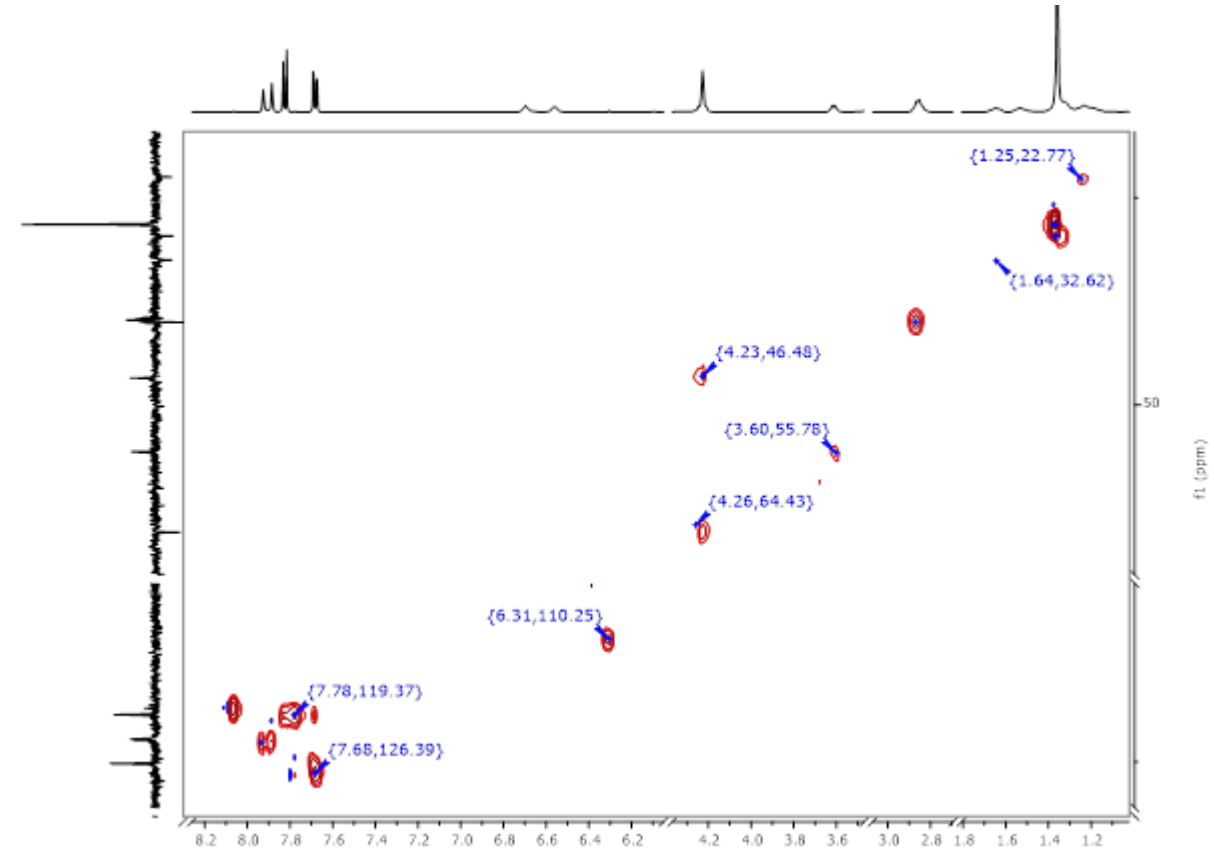

Figure 220: ^{1}H-^{13}C HSQC-NMR of Smoc-L-Lys(Boc)-OH **18**.

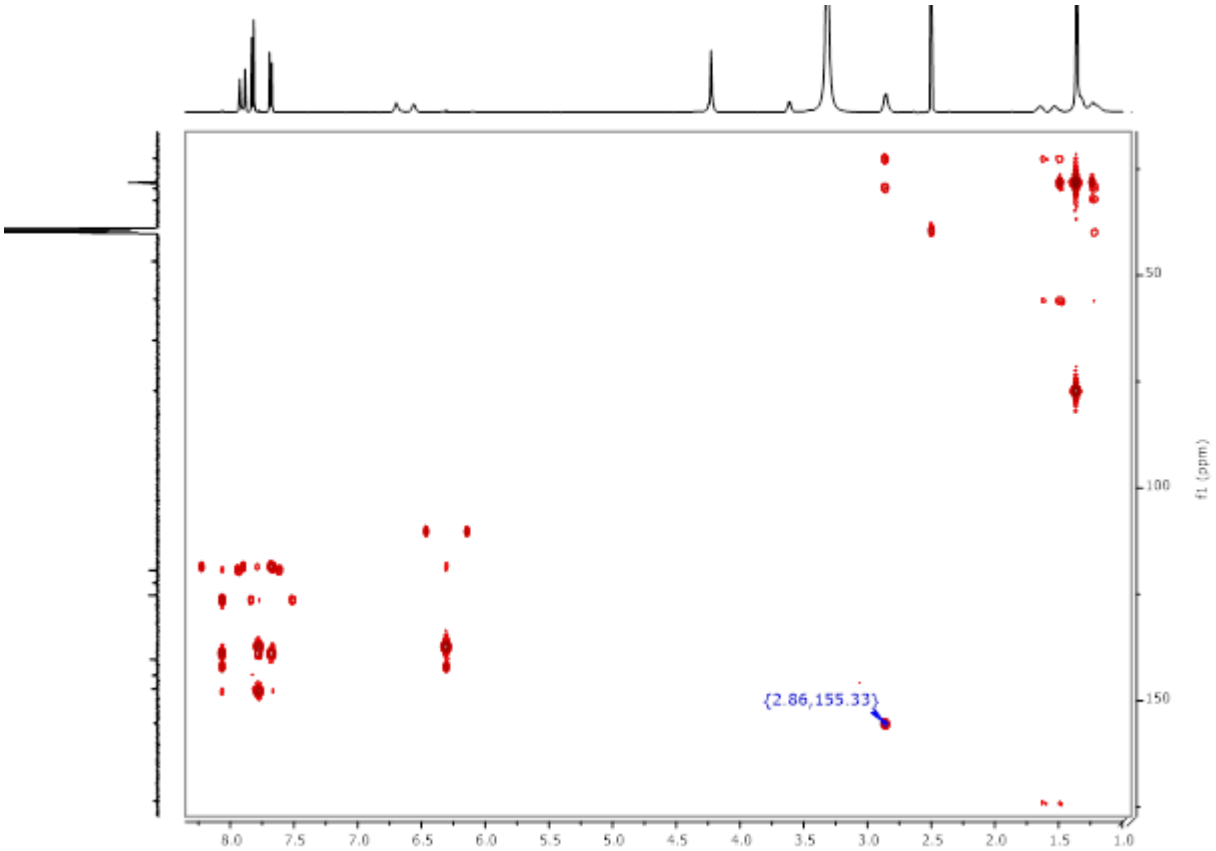

Figure 221: ^{1}H-^{13}C HMBC-NMR of Smoc-L-Lys(Boc)-OH **18**.

8.2.17.Analytical data of Smoc-L-Met-OH 19

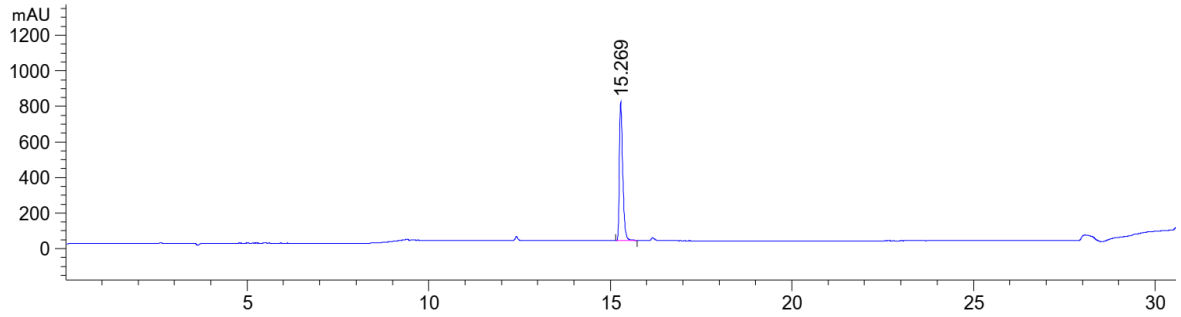

Figure 222: HPLC chromatogram of Smoc-L-Met-OH **19** at λ=220 nm (0 to 40% MeCN).

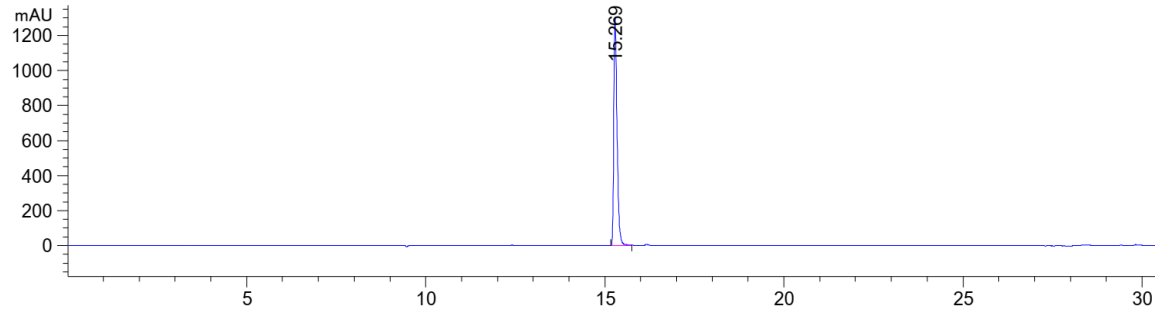

Figure 223: HPLC chromatogram of Smoc-L-Met-OH **19** at λ=280 nm (0 to 40% MeCN).

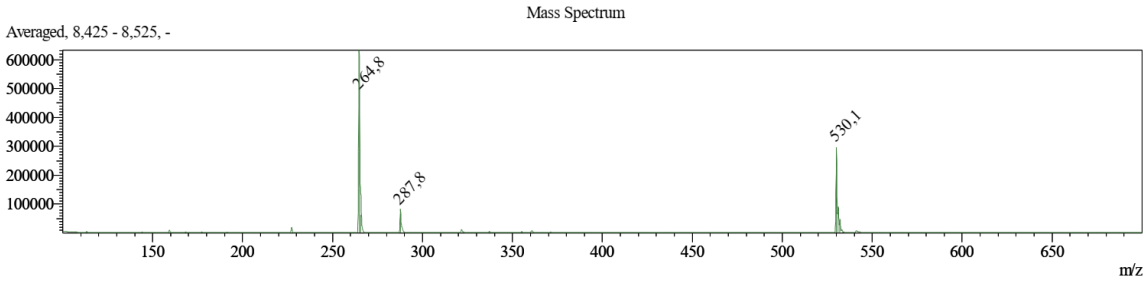

Figure 224: ESI-MS of Smoc-L-Met-OH **19** (M measured=530.10 $[M-H]^-$, M calc.=531.57).

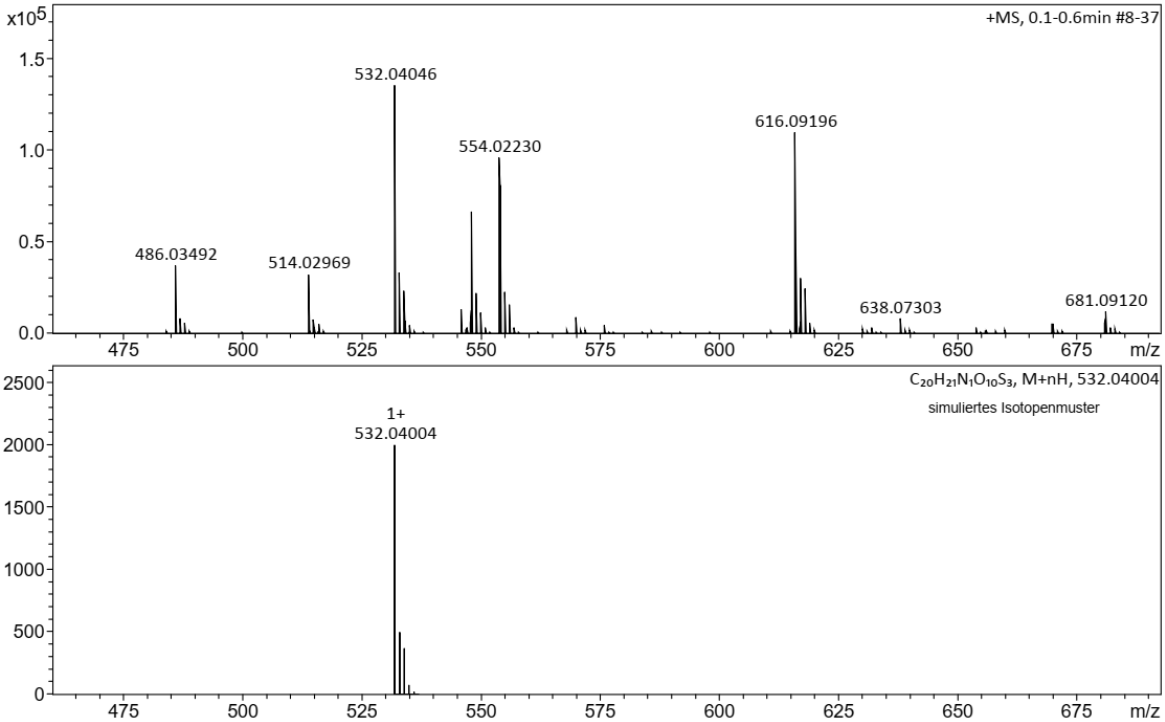

Figure 225: HR-MS of Smoc-L-Met-OH **19** (M measured=532.04046 $[M+H]^+$, M calc.=532.04004).

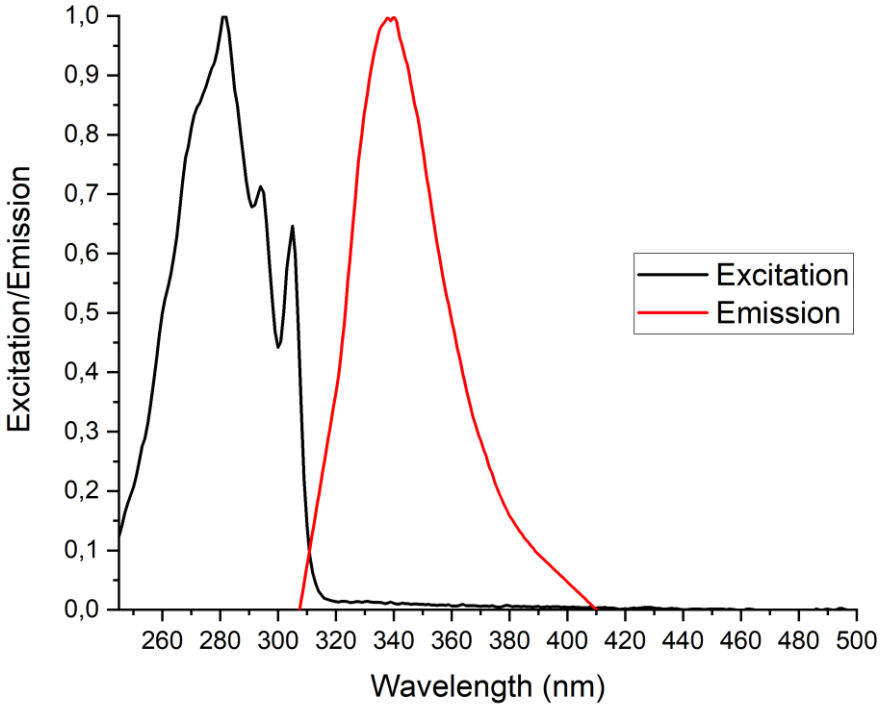

Figure 226: Excitation and emission spectra of Smoc-L-Met-OH **19**, excitation and emission have been normalized between 0 and 1 for illustration.

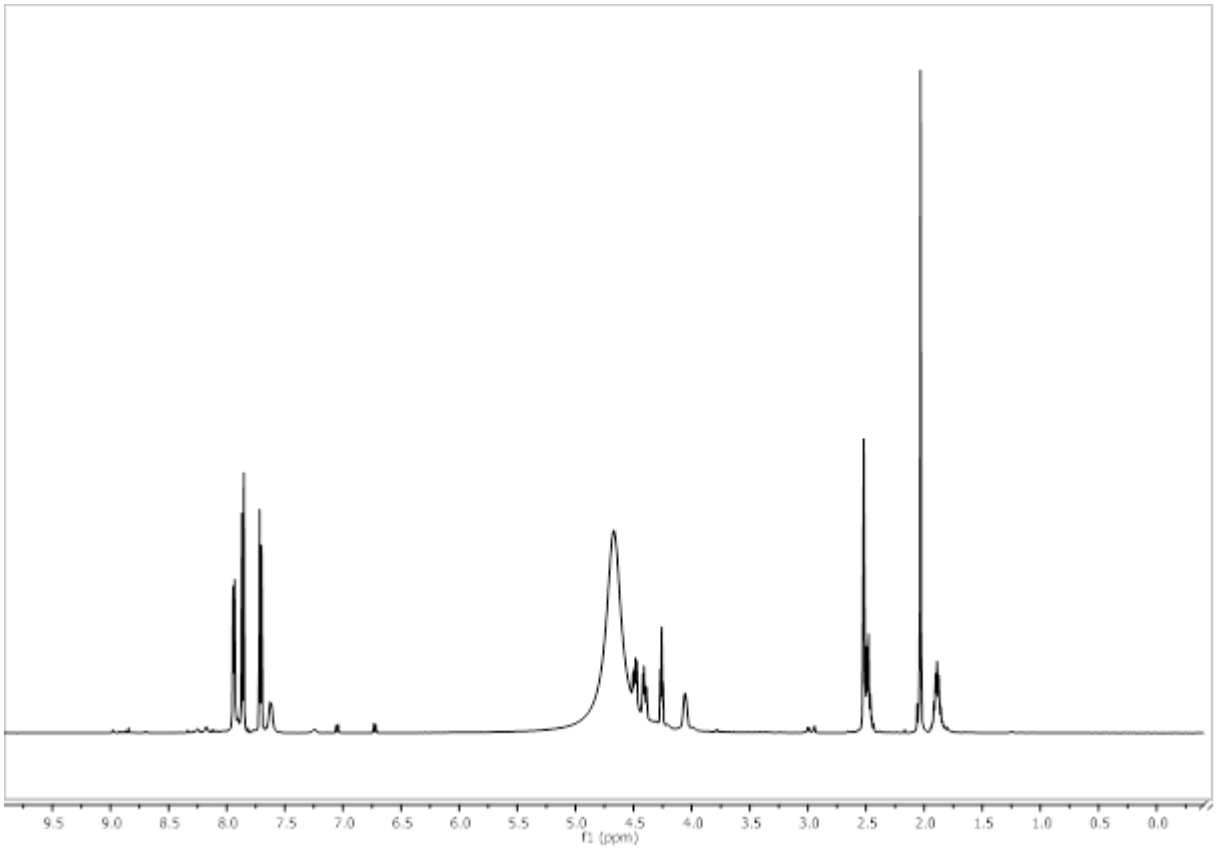

Figure 227: ^{1}H-NMR of Smoc-L-Met-OH **19**.

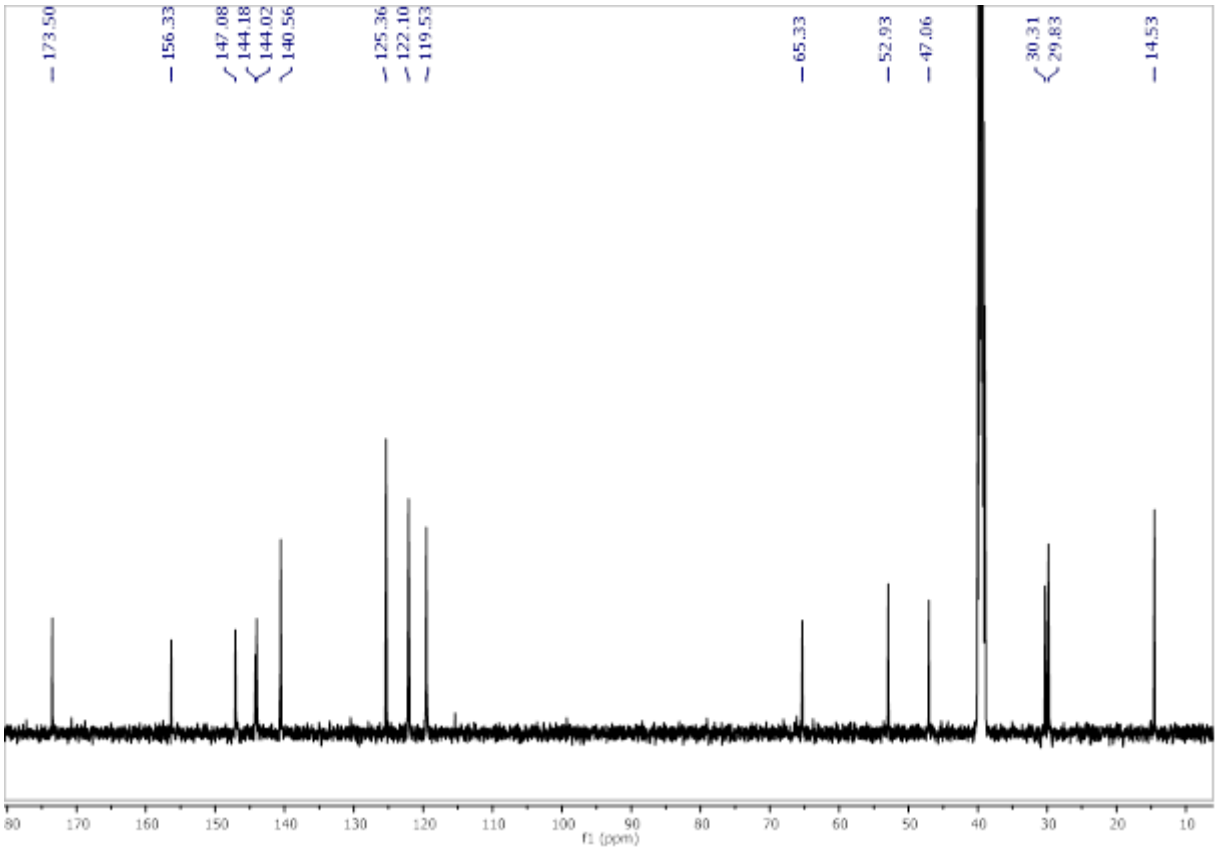

Figure 228: ^{13}C-NMR of Smoc-L-Met-OH **19**.

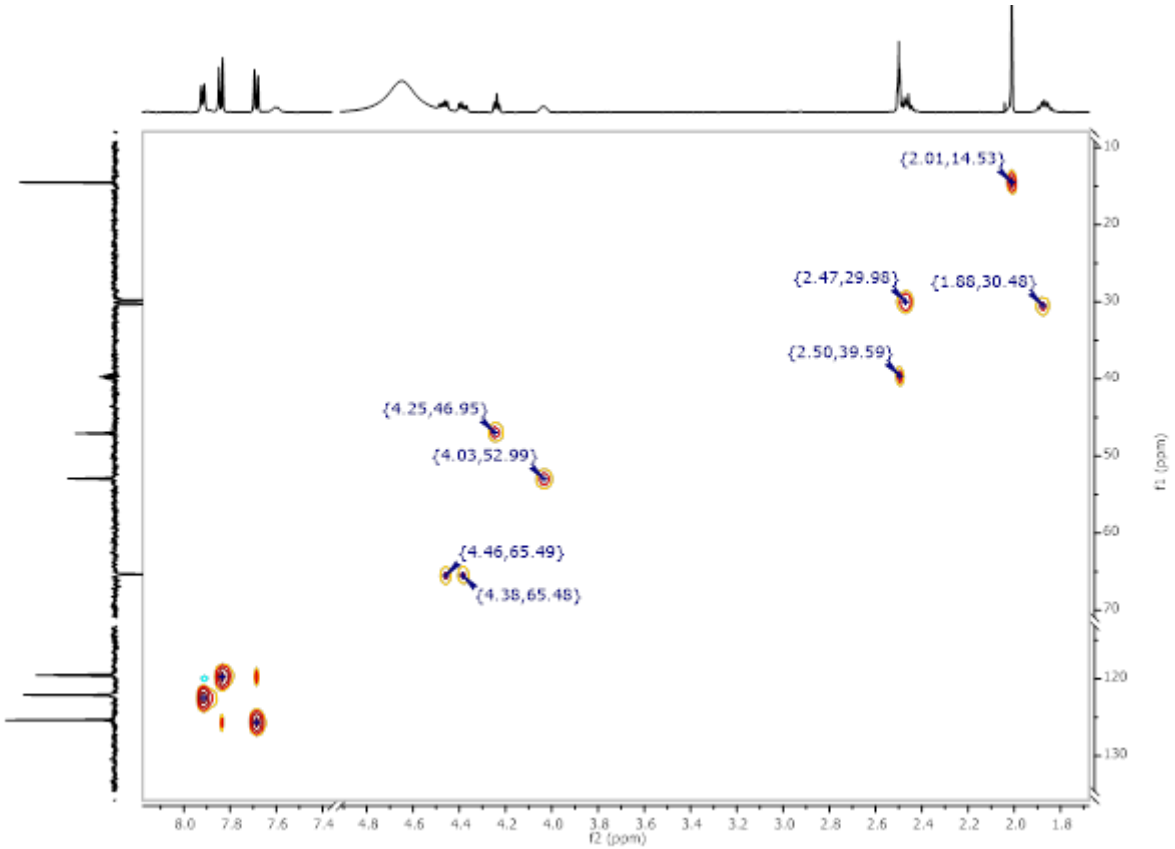

Figure 229: ^{1}H-^{13}C HSQC-NMR of Smoc-L-Met-OH **19**.

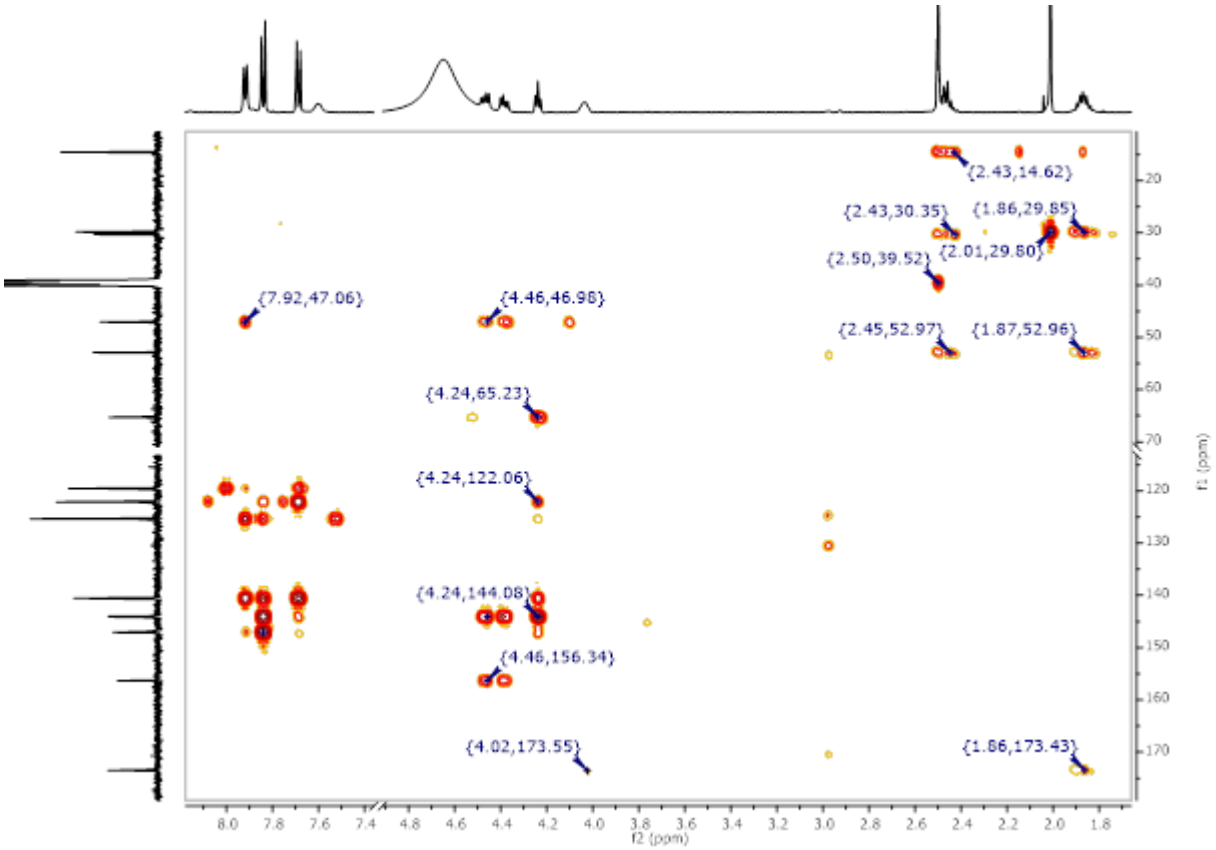

Figure 230: ^{1}H-^{13}C HMBC-NMR of Smoc-L-Met-OH **19**.

8.2.18.Analytical data of Smoc-L-Phe-OH 20

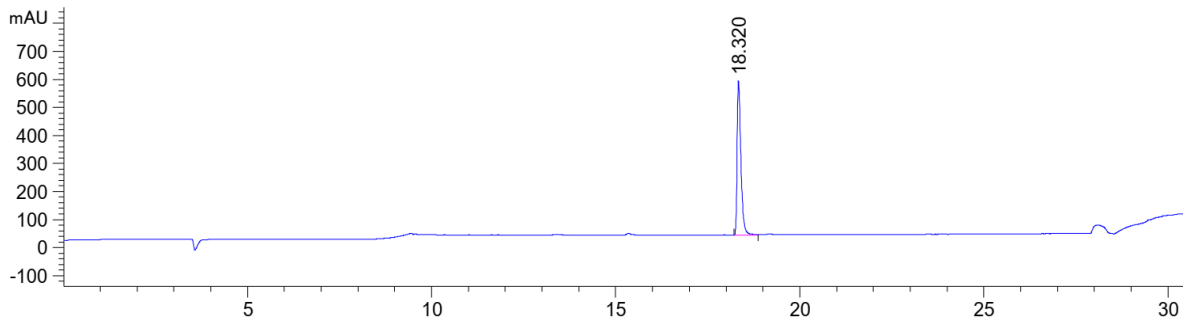

Figure 231: HPLC chromatogram of Smoc-L-Phe-OH **20** at λ=220 nm (0 to 40% MeCN).

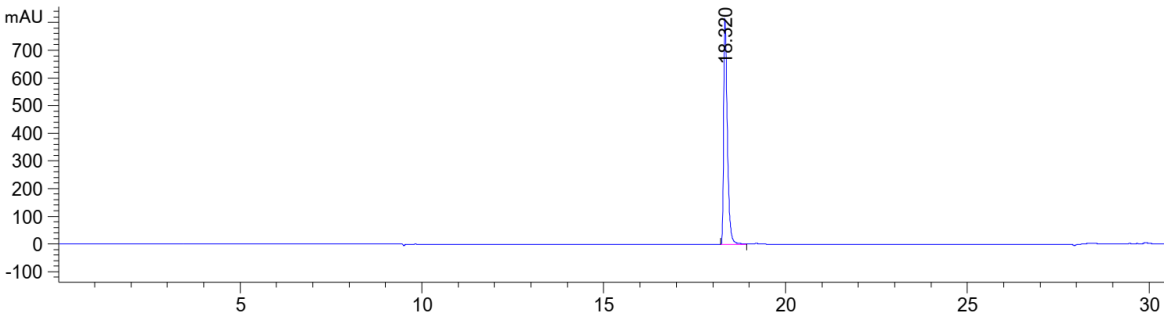

Figure 232: HPLC chromatogram of Smoc-L-Phe-OH **20** at λ=280 nm (0 to 40% MeCN).

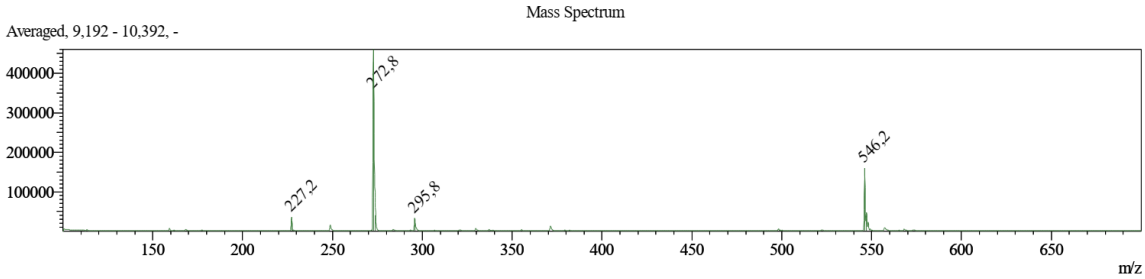

Figure 233: ESI-MS of Smoc-L-Phe-OH **20** (M measured=546.20 $[M-H]^-$, M calc.=547.55).

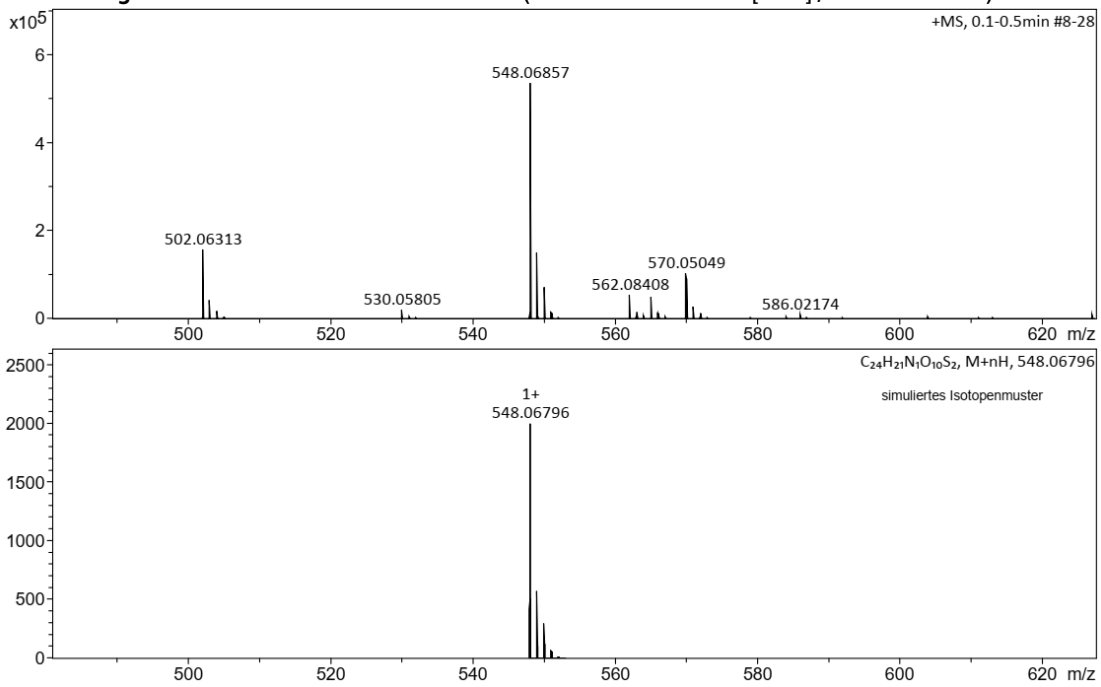

Figure 234: HR-MS of Smoc-L-Phe-OH **20** (M measured=548.06857 $[M+H]^+$, M calc.=548.006796).

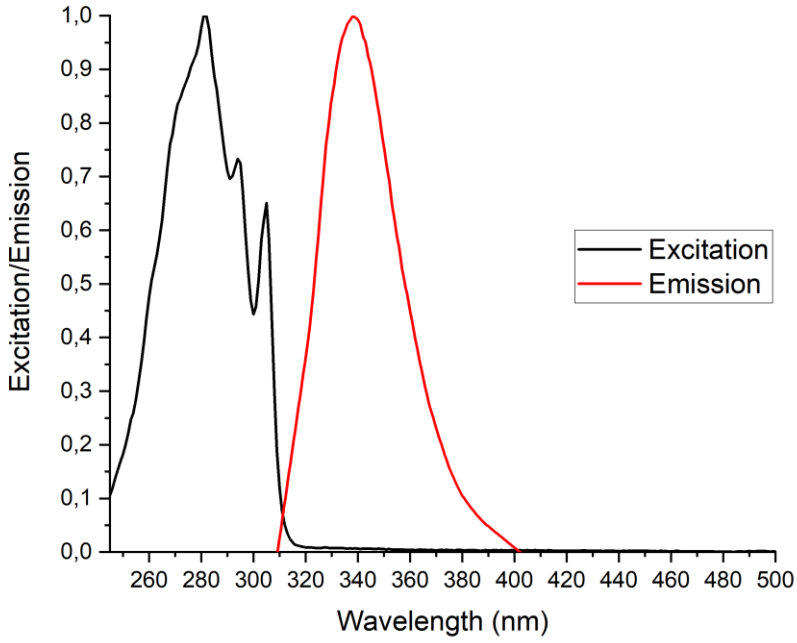

Figure 235: Excitation and emission spectra of Smoc-L-Phe-OH **20**, excitation and emission have been normalized between 0 and 1 for illustration.

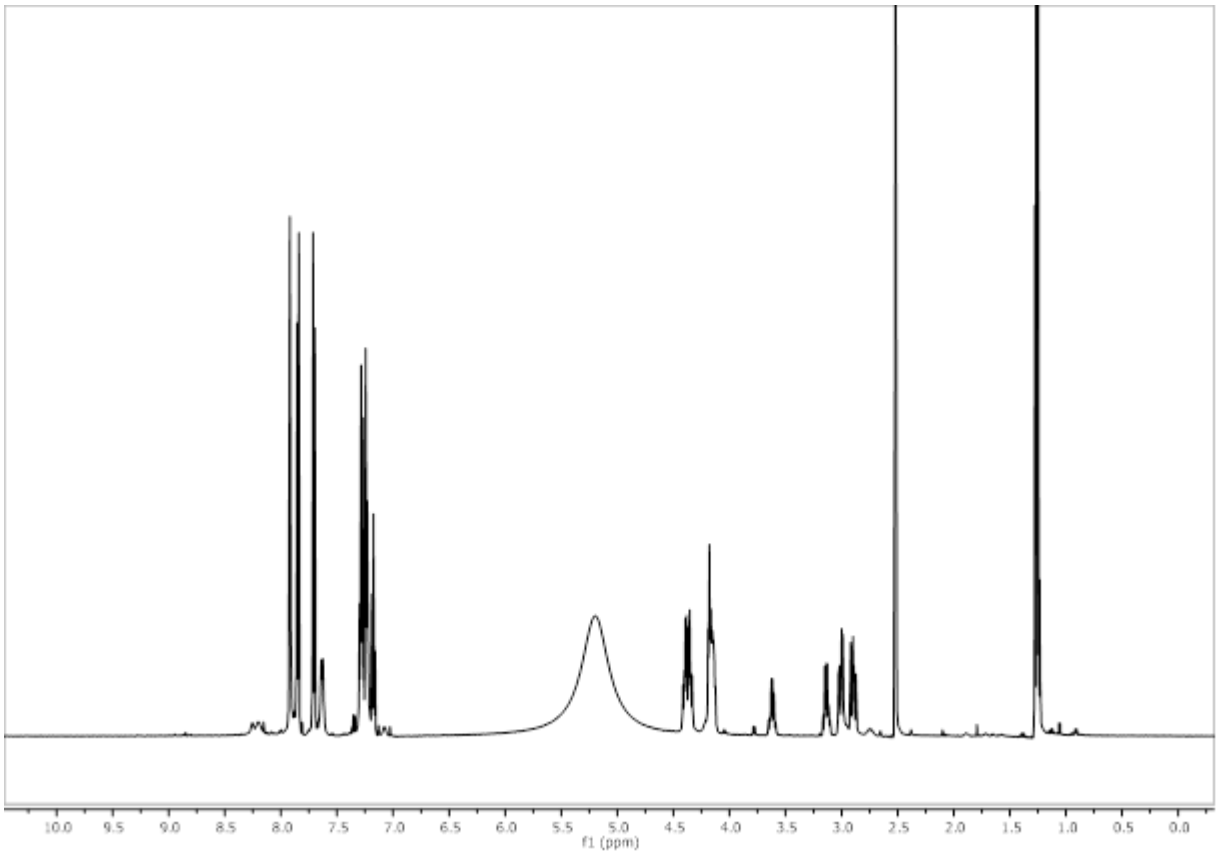

Figure 236: ^{1}H-NMR of Smoc-L-Phe-OH **20**.

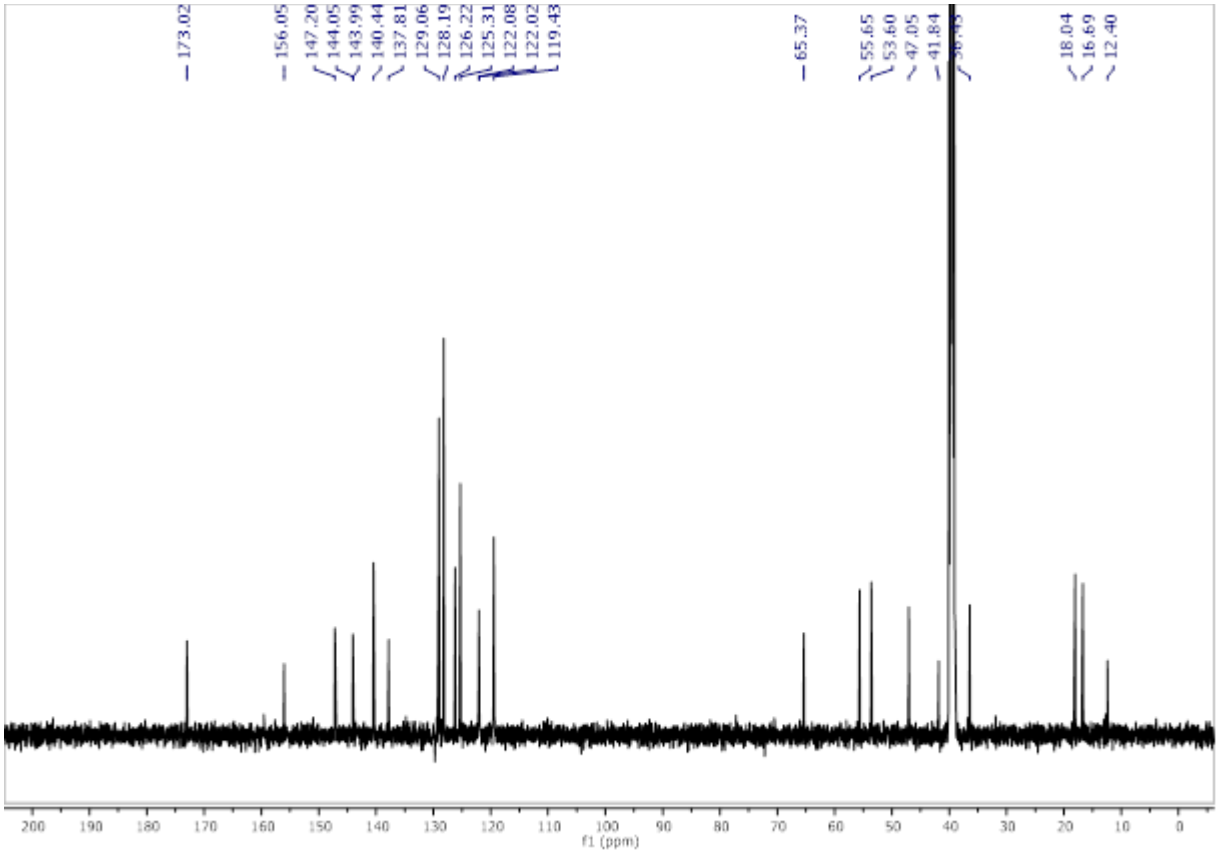

Figure 237: ^{13}C-NMR of Smoc-L-Phe-OH **20**.

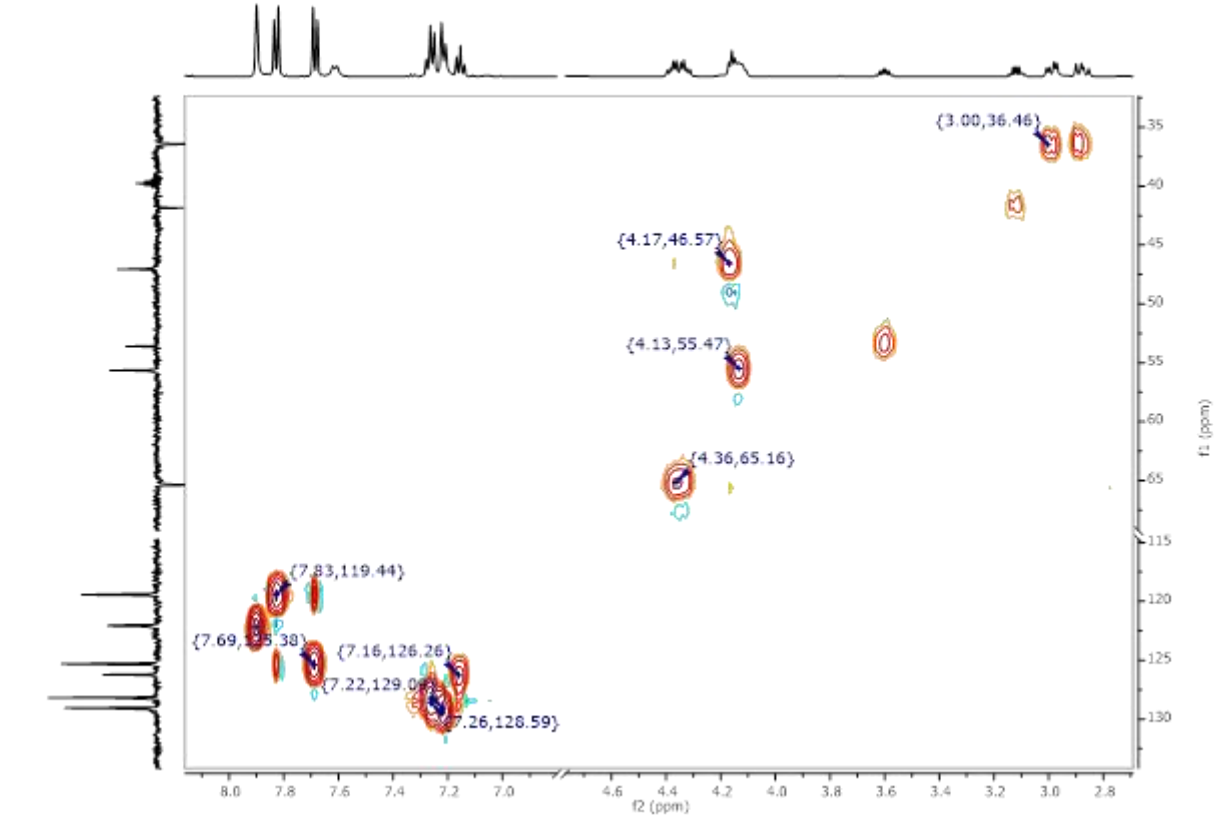

Figure 238: ^{1}H-^{13}C HSQC-NMR of Smoc-L-Phe-OH **20**.

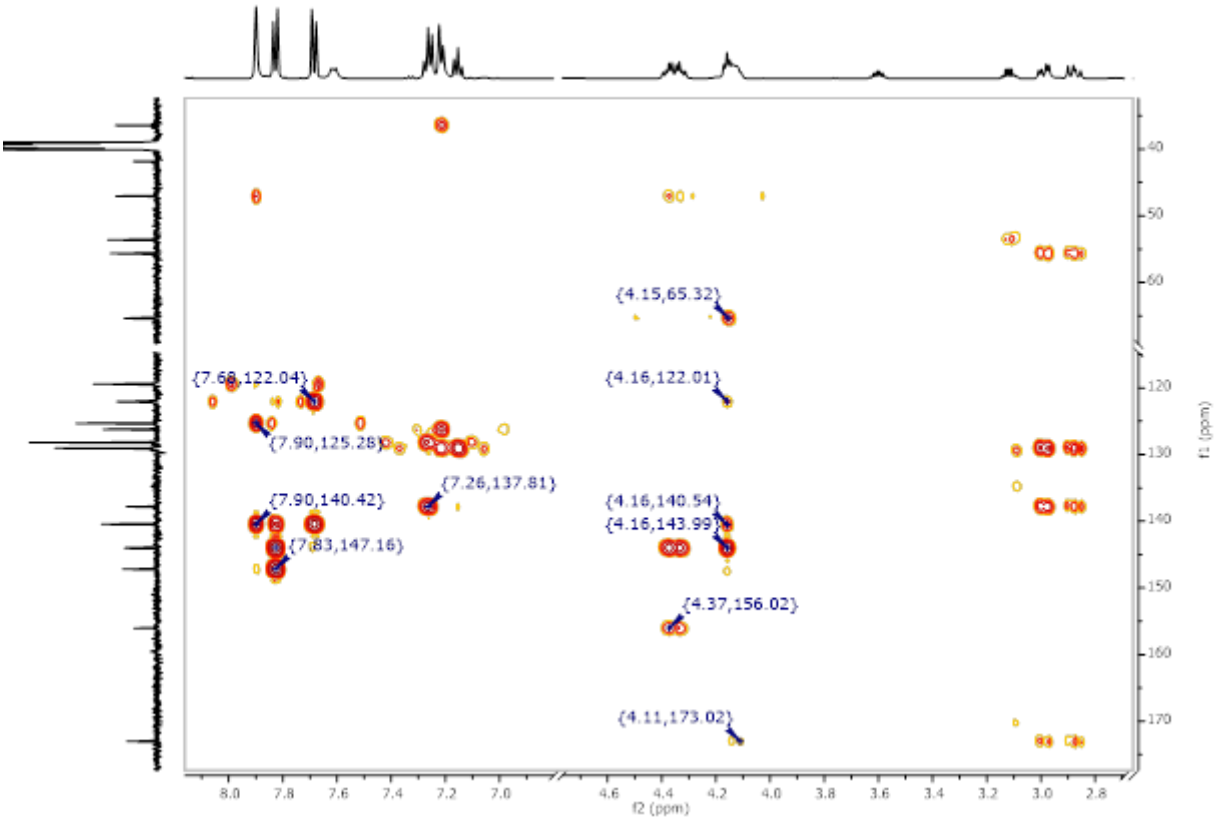

Figure 239: ^{1}H-^{13}C HMBC-NMR of Smoc-L-Phe-OH **20**.

8.2.19.Analytical data of Smoc-L-Pro-OH 21

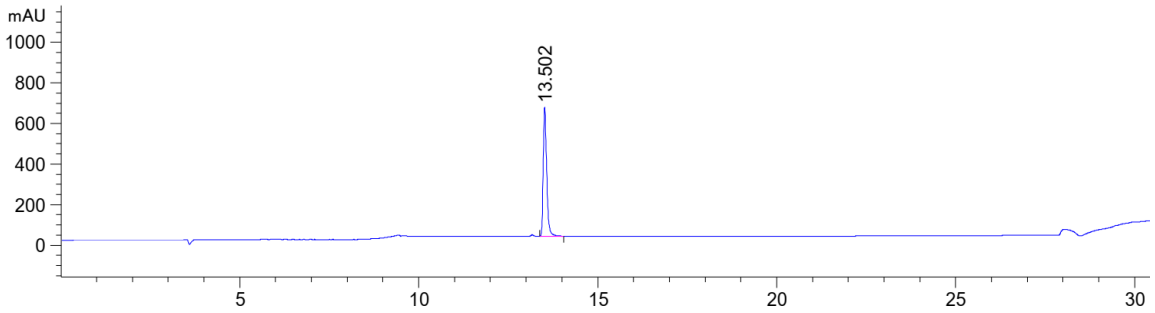

Figure 240: HPLC chromatogram of Smoc-L-Pro-OH **21** at λ=220 nm (0 to 40% MeCN).

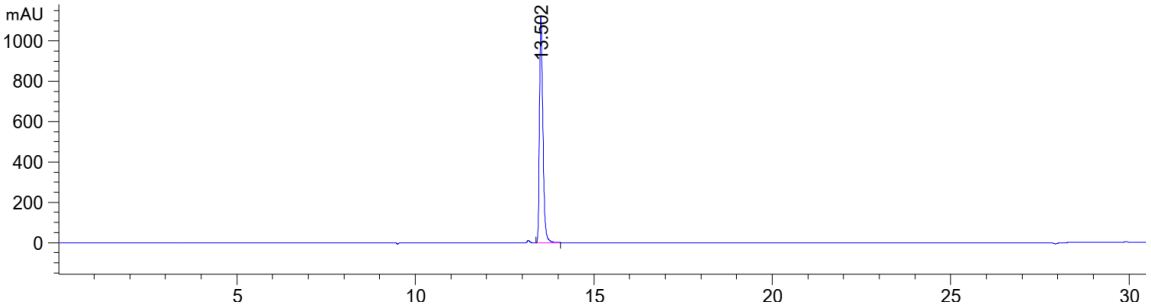

Figure 241: HPLC chromatogram of Smoc-L-Pro-OH **21** at λ=280 nm (0 to 40% MeCN).

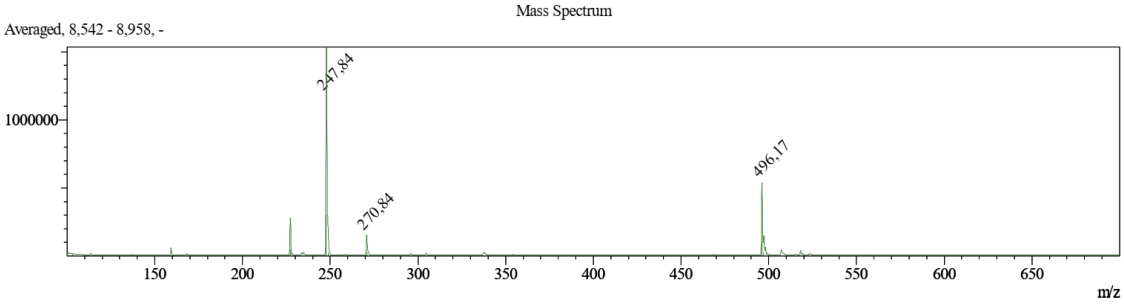

Figure 242: ESI-MS of Smoc-L-Pro-OH **21** (M measured=496.17 $[M-H]^-$, M calc.=497.49).

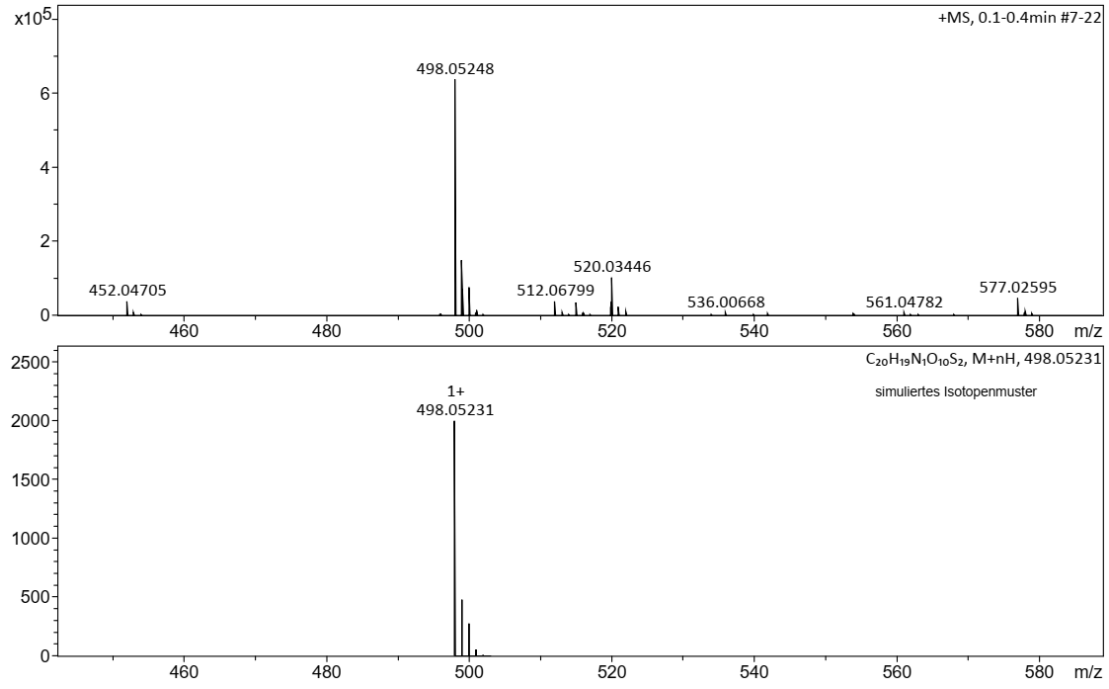

Figure 243: HR-MS of Smoc-L-Pro-OH **21** (M measured=498.05248 $[M+H]^+$, M calc.=498.05231).

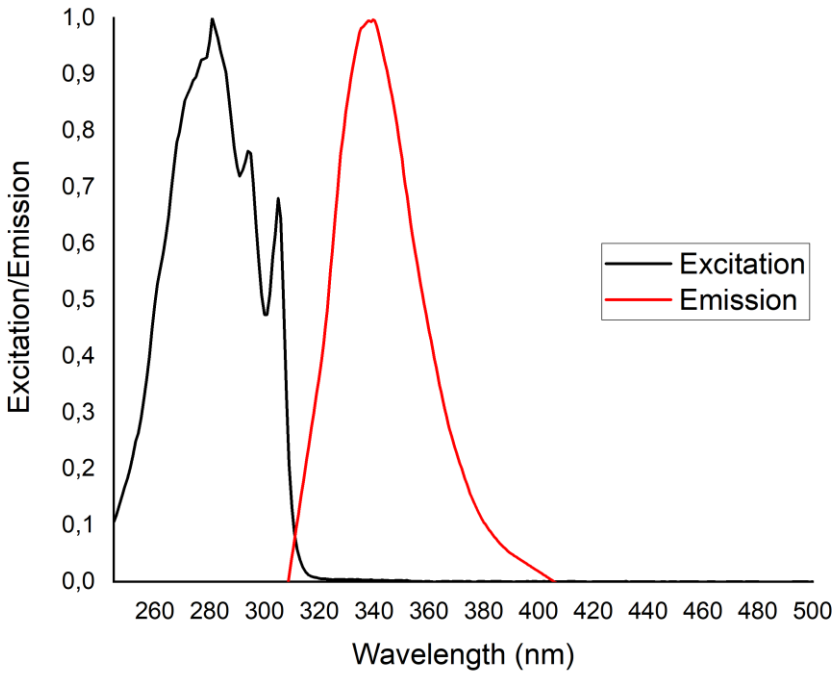

Figure 244: Excitation and emission spectra of Smoc-L-Pro-OH **21**, excitation and emission have been normalized between 0 and 1 for illustration.

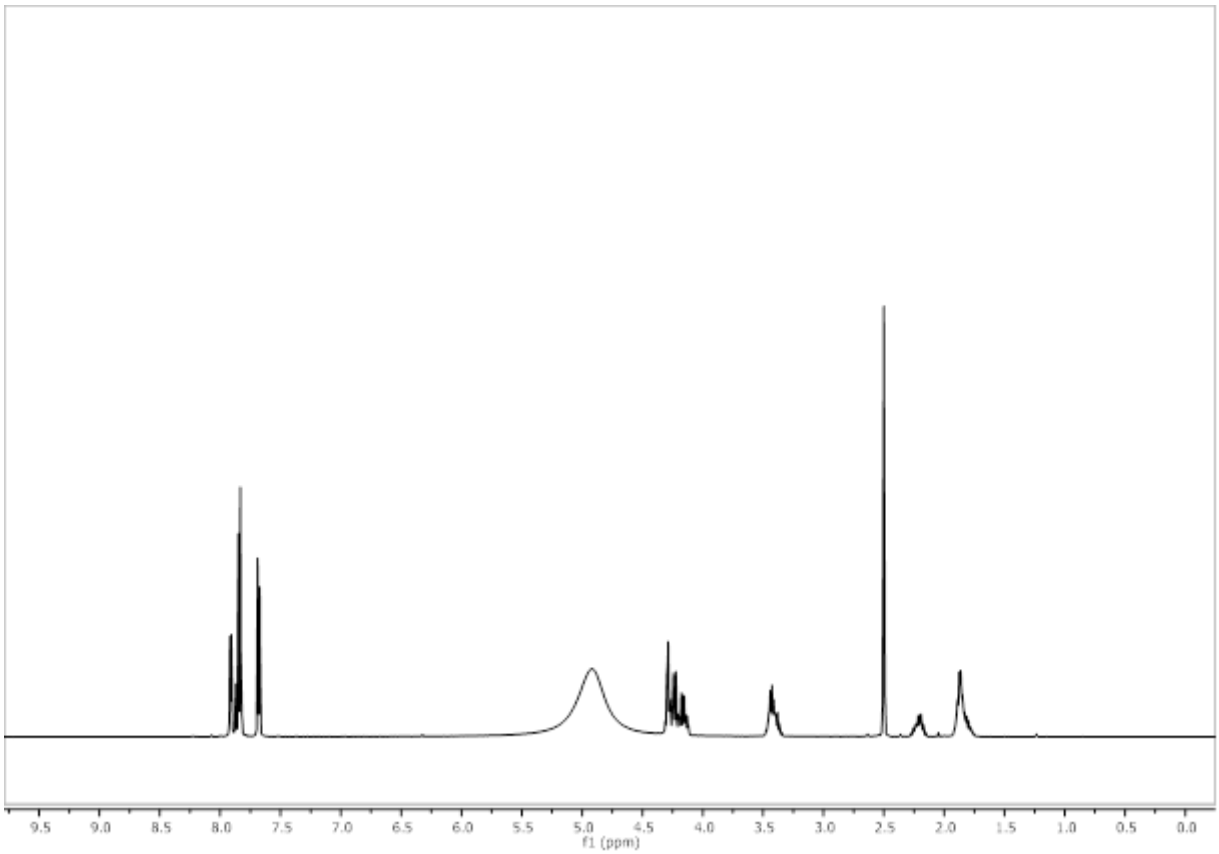

Figure 245: ^{1}H-NMR of Smoc-L-Pro-OH **21**.

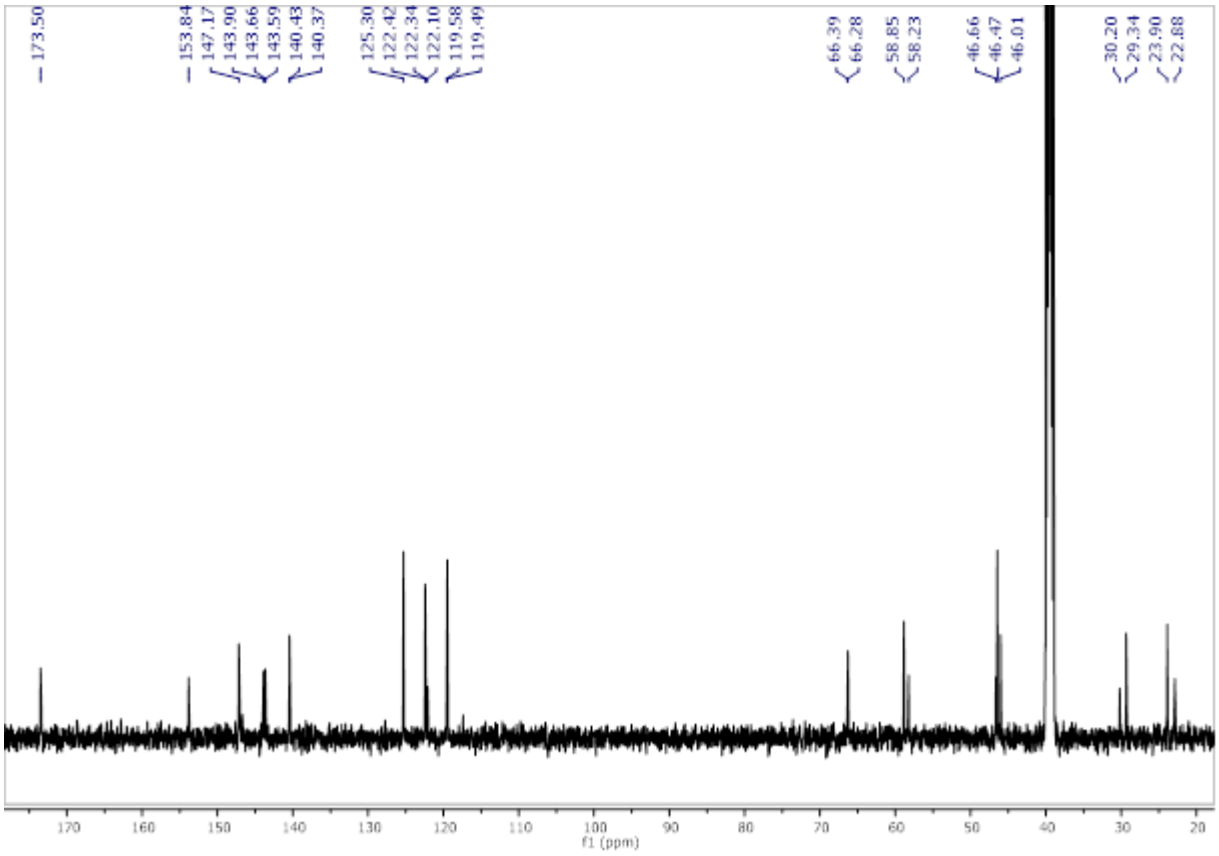

Figure 246: ^{13}C-NMR of Smoc-L-Pro-OH **21**.

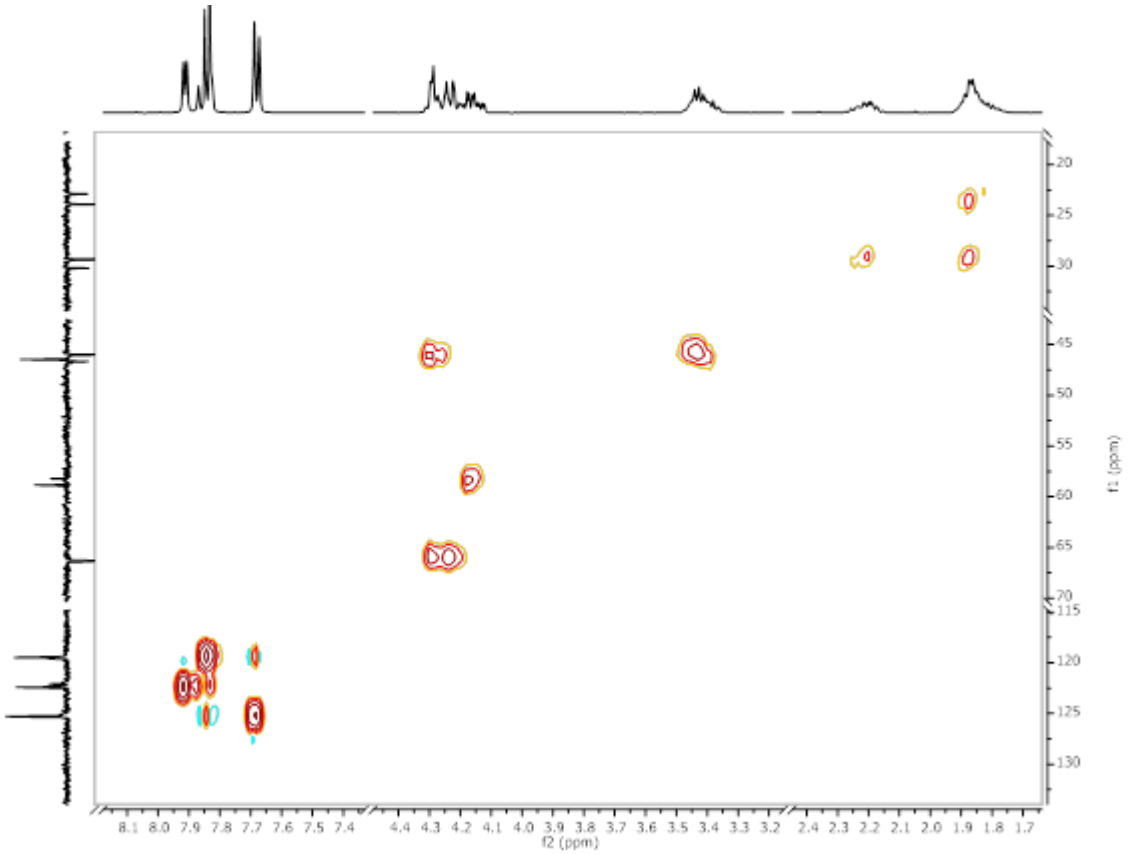

Figure 247: ^{1}H-^{13}C HSQC-NMR of Smoc-L-Pro-OH **21**.

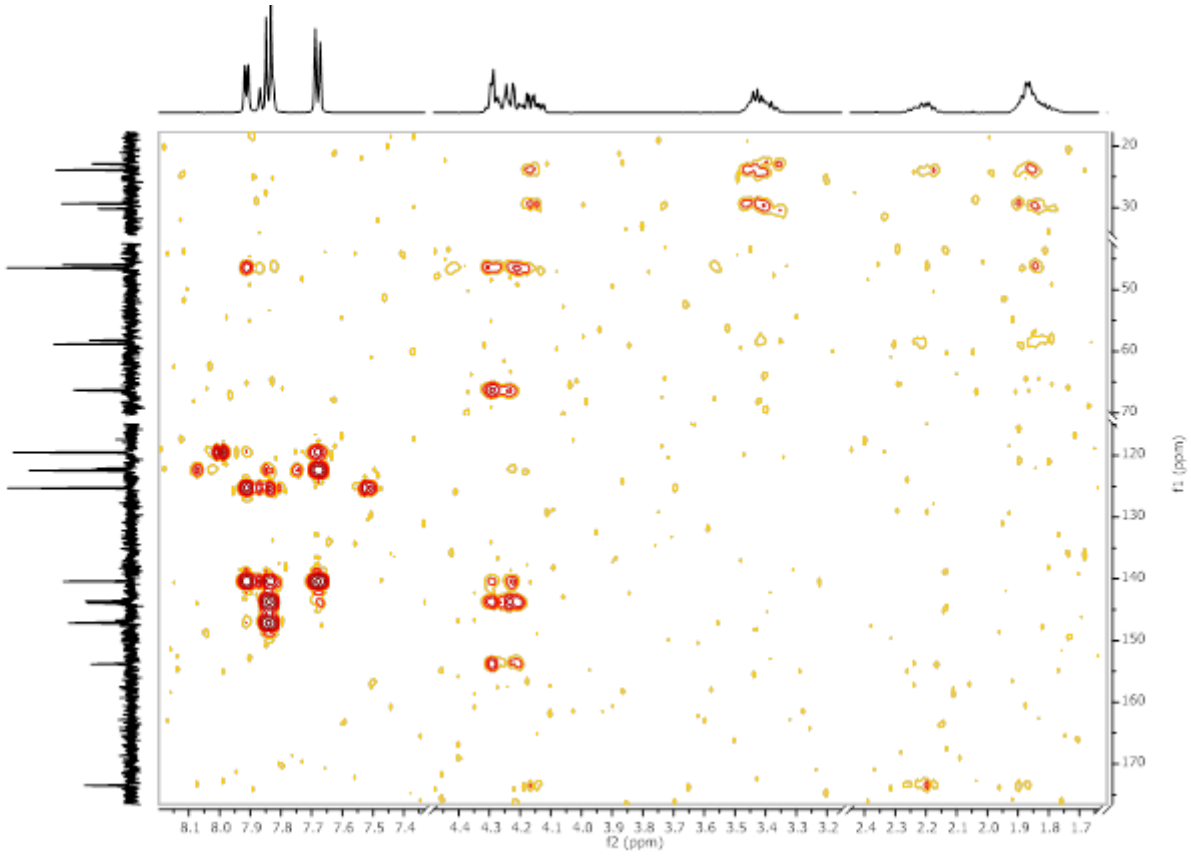

Figure 248: ^{1}H-^{13}C HMBC-NMR of Smoc-L-Pro-OH **21**.

8.2.20.Analytical data of Smoc-L-Ser-OH 22

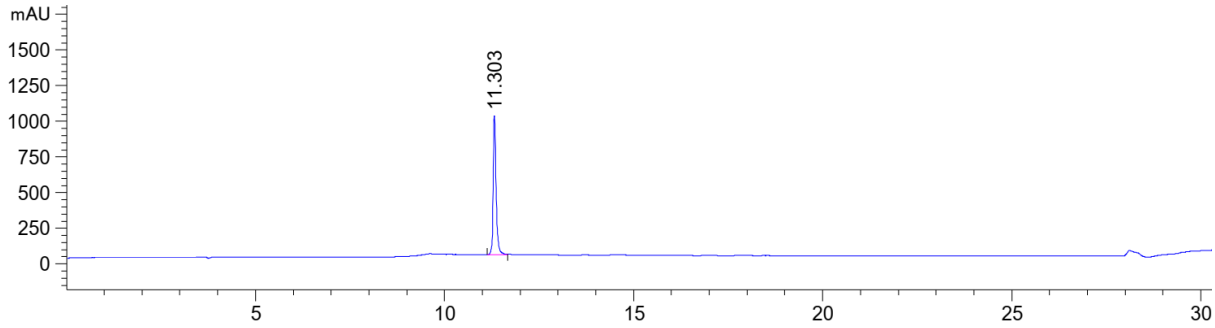

Figure 249: HPLC chromatogram of Smoc-L-Ser-OH **22** at λ=220 nm (0 to 40% MeCN).

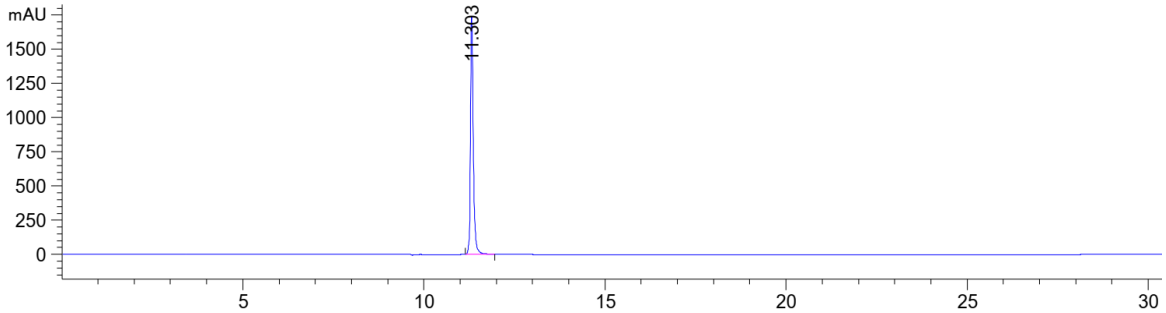

Figure 250: HPLC chromatogram of Smoc-L-Ser-OH **22** at λ=280 nm (0 to 40% MeCN).

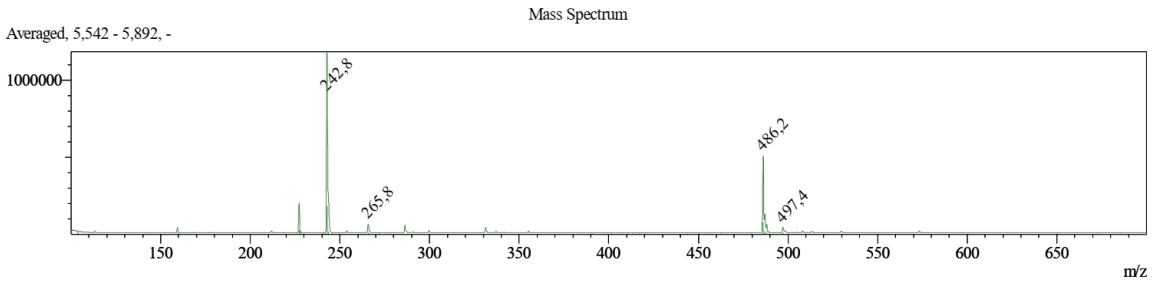

Figure 251: ESI-MS of Smoc-L-Ser-OH **22** (M measured=486.20 $[M-H]^-$, M calc.=487.45).

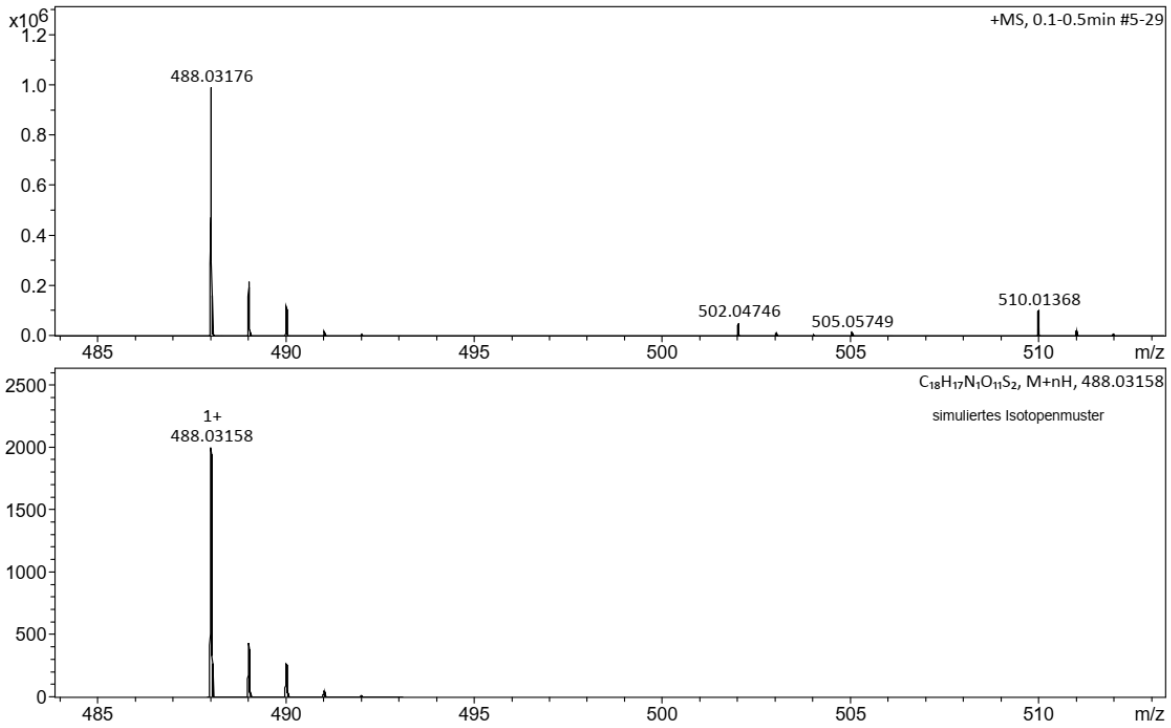

Figure **252:** HR-MS of Smoc-L-Ser-OH **22** (M measured=488.03176 $[M+H]^+$, M calc.=488.03158).

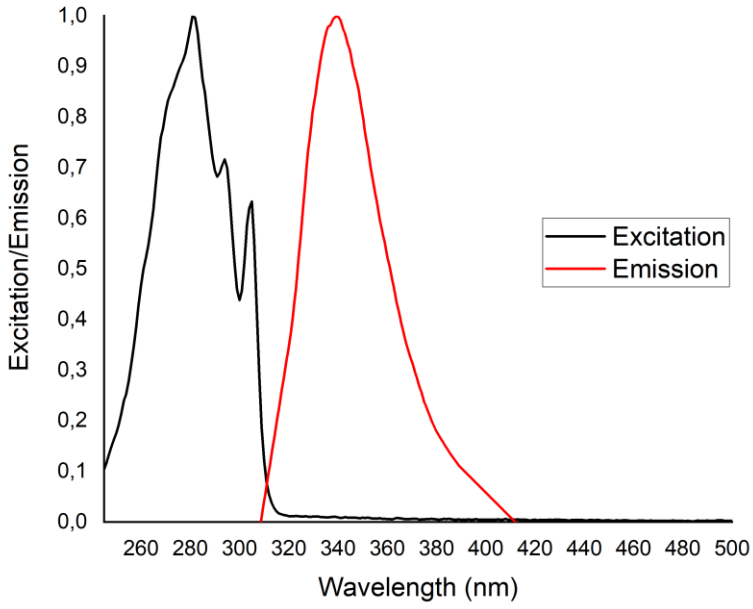

Figure 253: Excitation and emission spectra of Smoc-L-Ser-OH **22**, excitation and emission have been normalized between 0 and 1 for illustration.

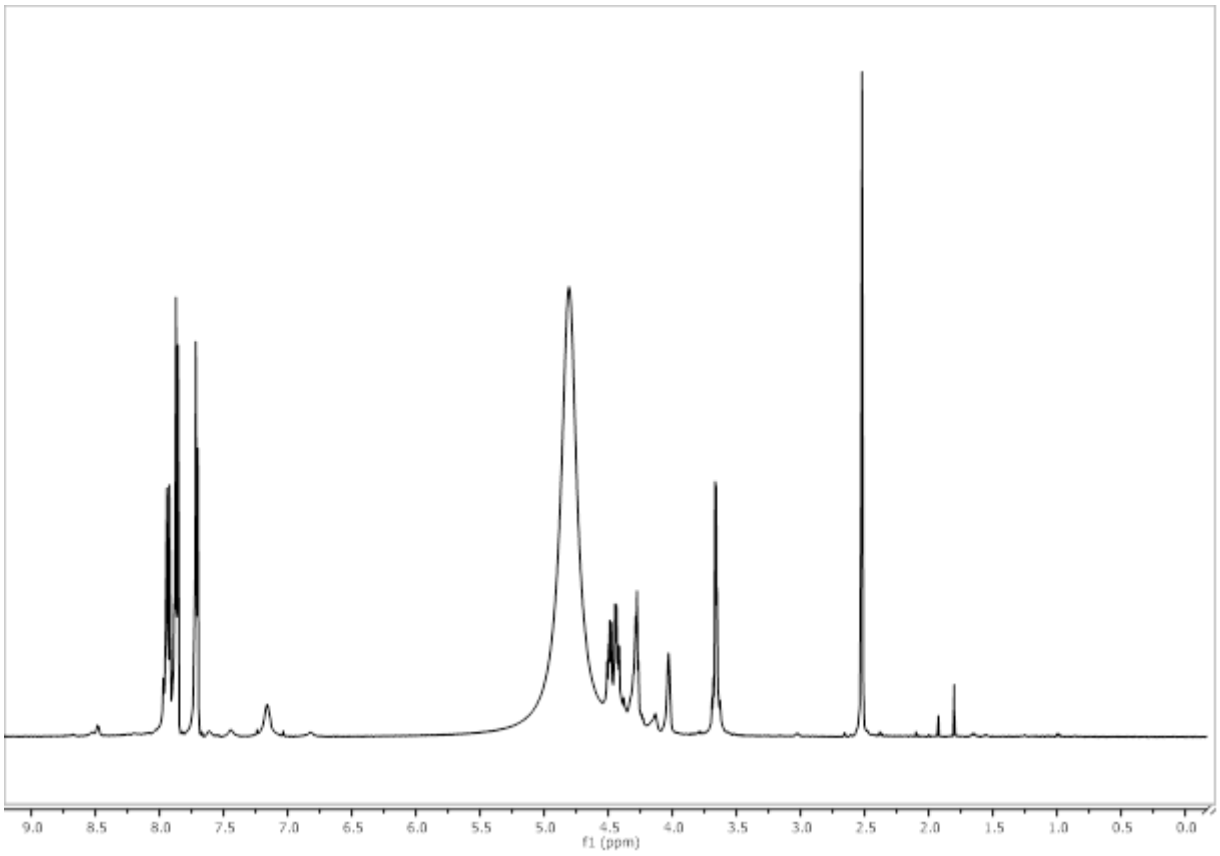

Figure 254: ^{1}H-NMR of Smoc-L-Ser-OH **22**.

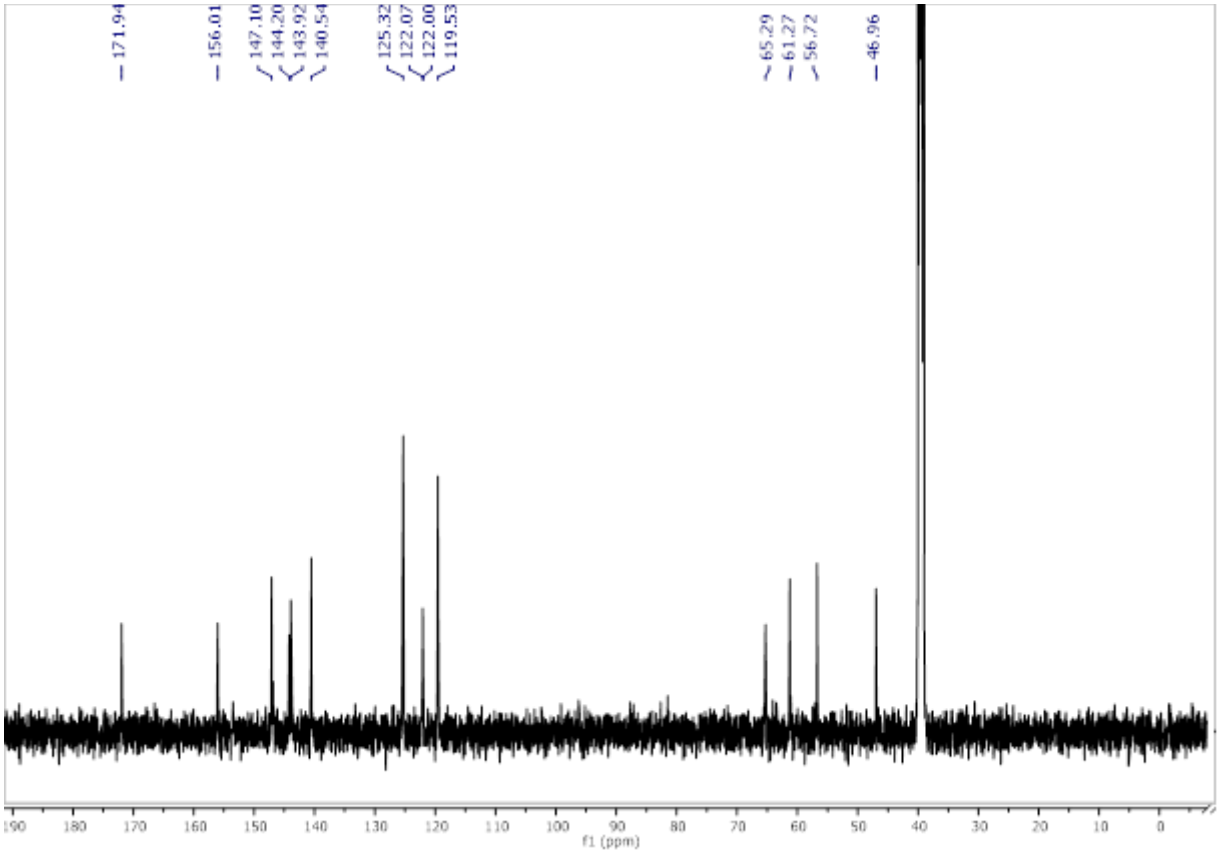

Figure 255: ^{13}C-NMR of Smoc-L-Ser-OH **22**.

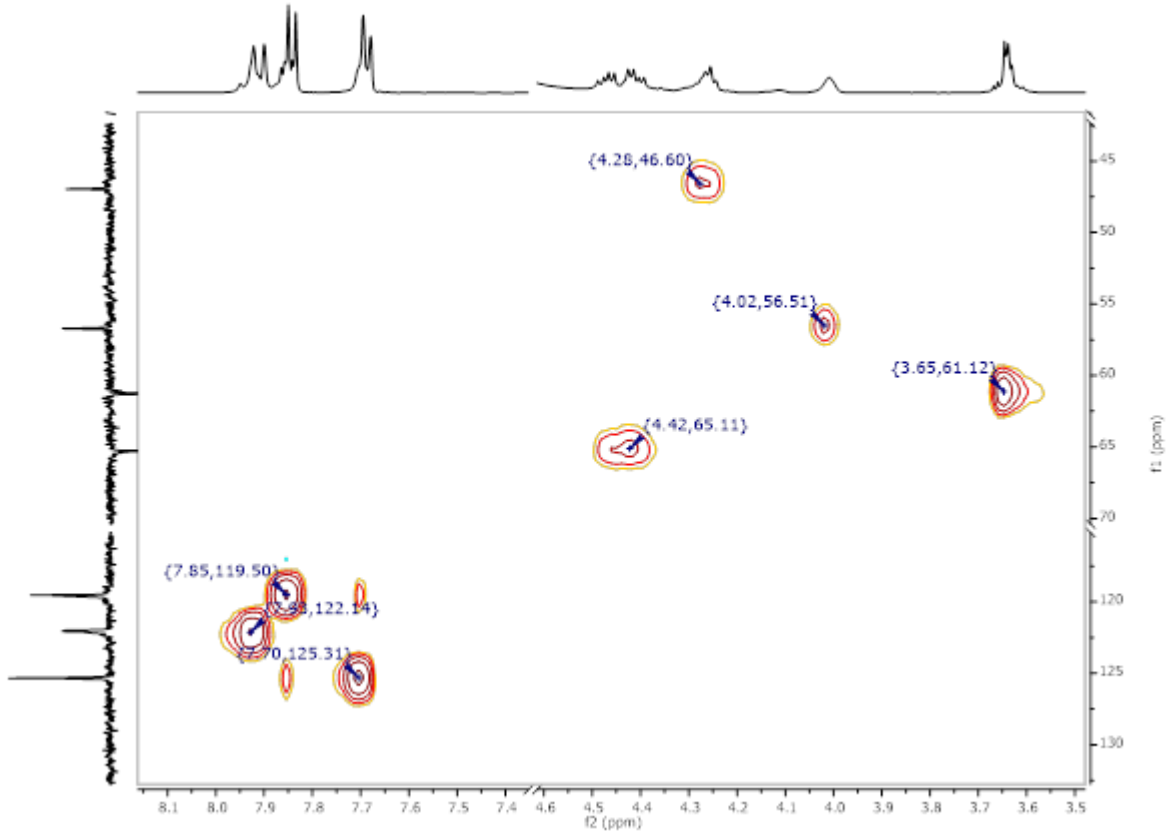

Figure 256: ^{1}H-^{13}C HSQC-NMR of Smoc-L-Ser-OH **22**.

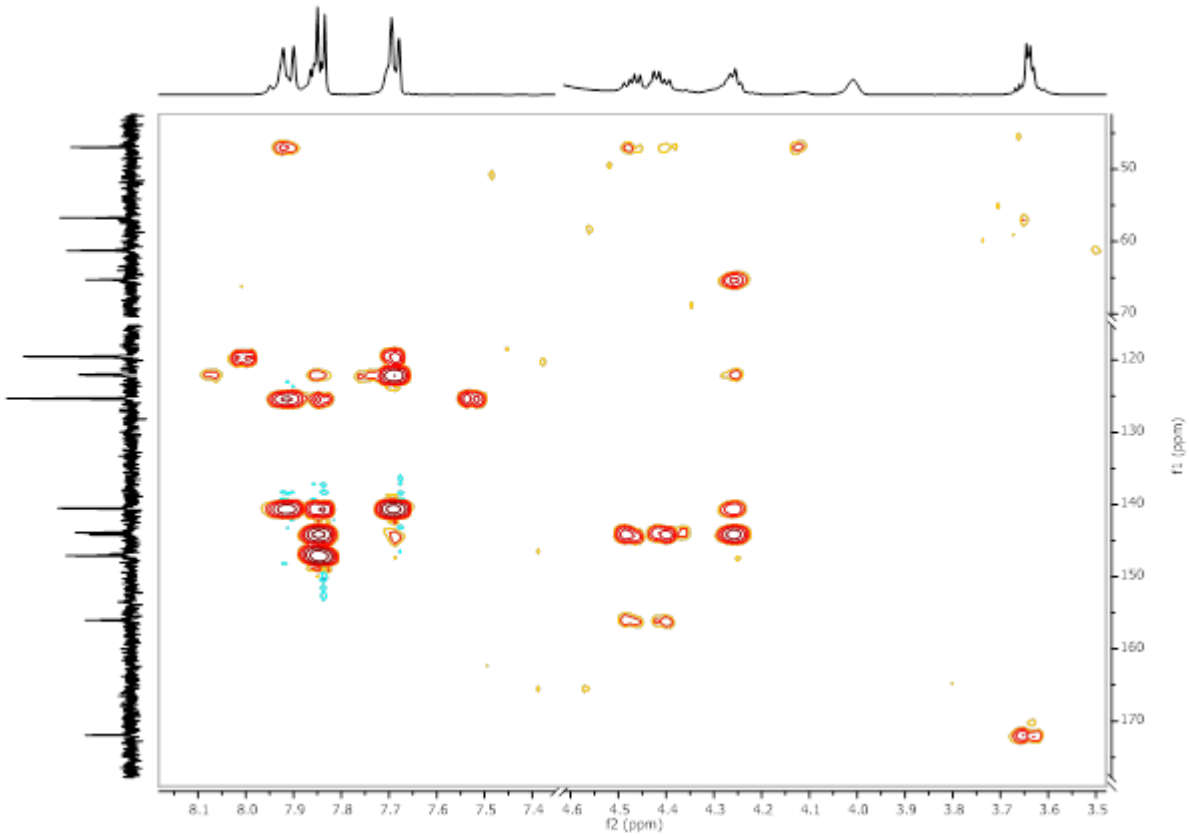

Figure 257: ^{1}H-^{13}C HMBC-NMR of Smoc-L-Ser-OH **22**.

8.2.21.Analytical data of Smoc-L-Ser(tBu)-OH 23

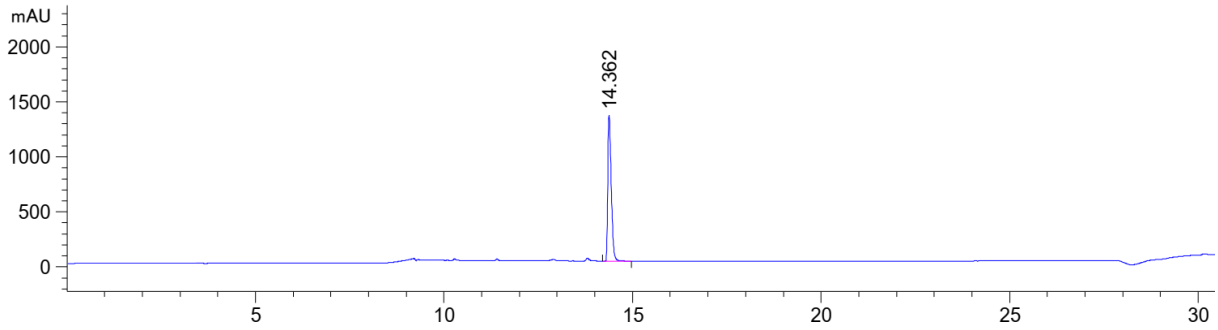

Figure 258: HPLC chromatogram of Smoc-L-Ser(tBu)-OH **23** at λ=220 nm (0 to 60% MeCN).

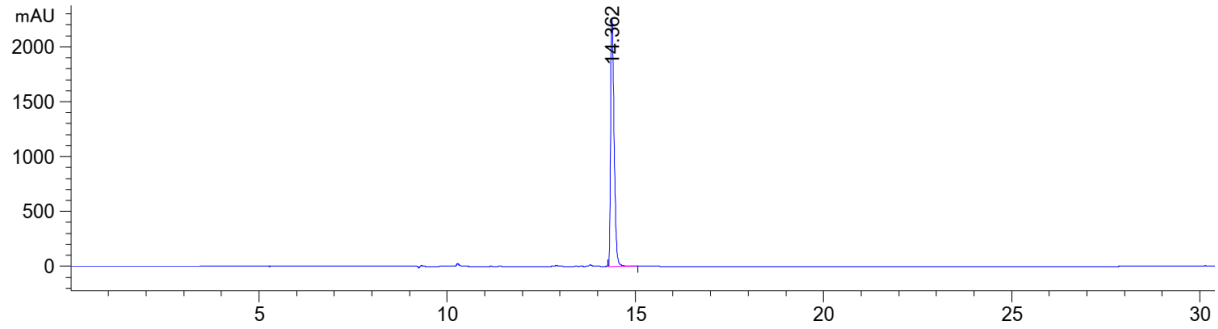

Figure 259: HPLC chromatogram of Smoc-L-Ser(tBu)-OH **23** at λ=280 nm (0 to 60% MeCN).

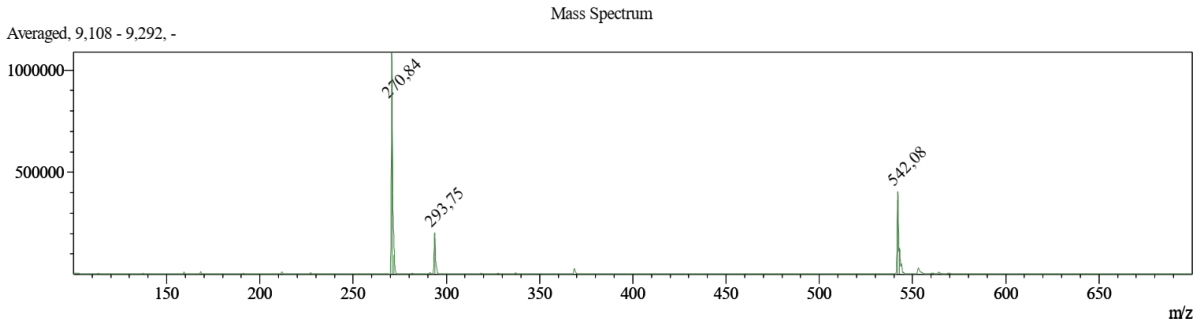

Figure 260: ESI-MS of Smoc-L-Ser(tBu)-OH **23** (M measured=542.08 $[M-H]^-$, M calc.=543.56).

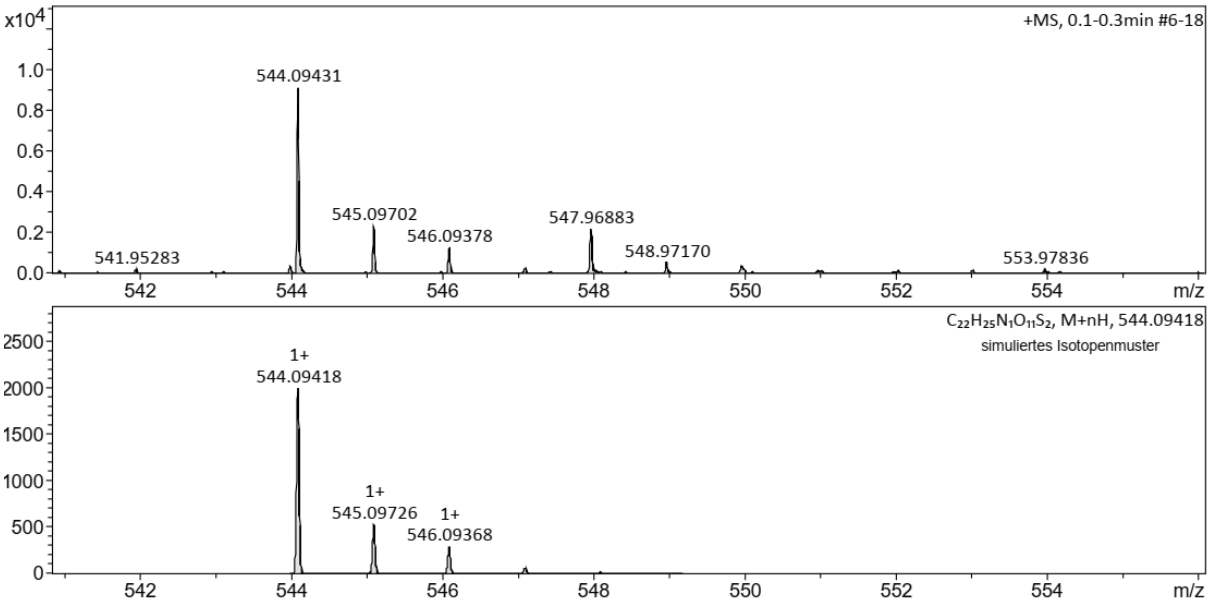

Figure 261: HR-MS of Smoc-L-Ser(tBu)-OH **23** (M measured=544.09431 $[M+H]^+$, M calc.=544.09418).

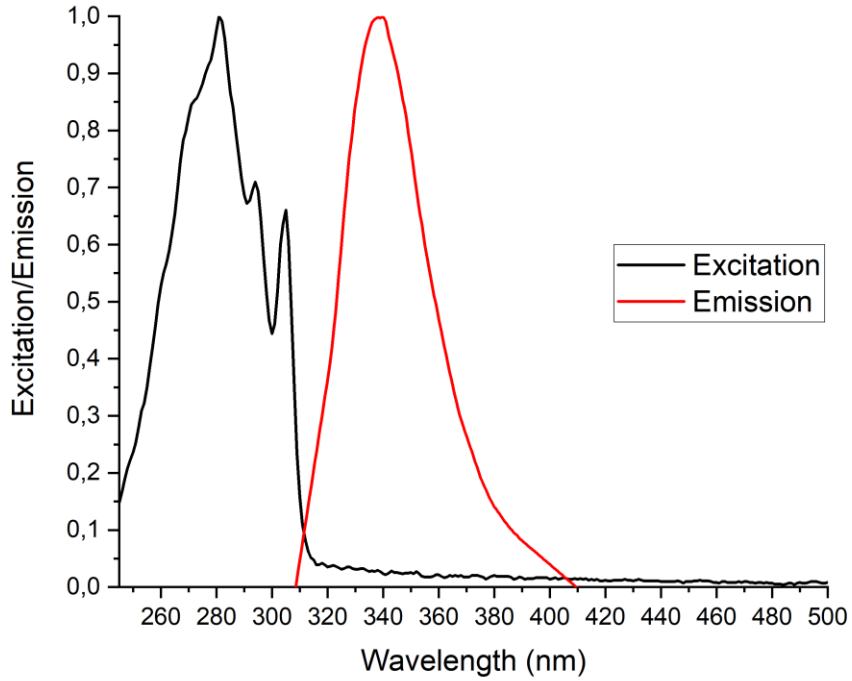

Figure 262: Excitation and emission spectra of Smoc-L-Ser(tBu)-OH **23**, excitation and emission have been normalized between 0 and 1 for illustration.

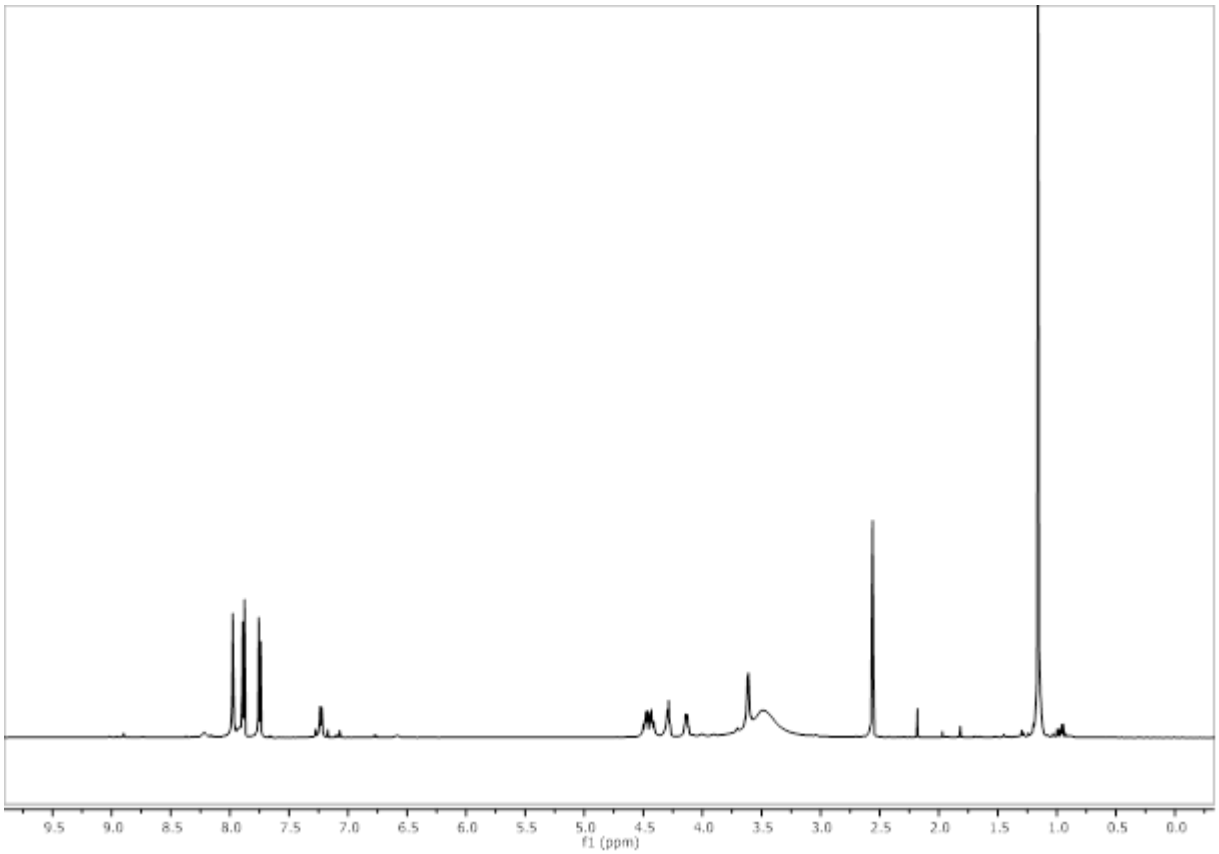

Figure 263: ^{1}H-NMR of Smoc-L-Ser(tBu)-OH **23**.

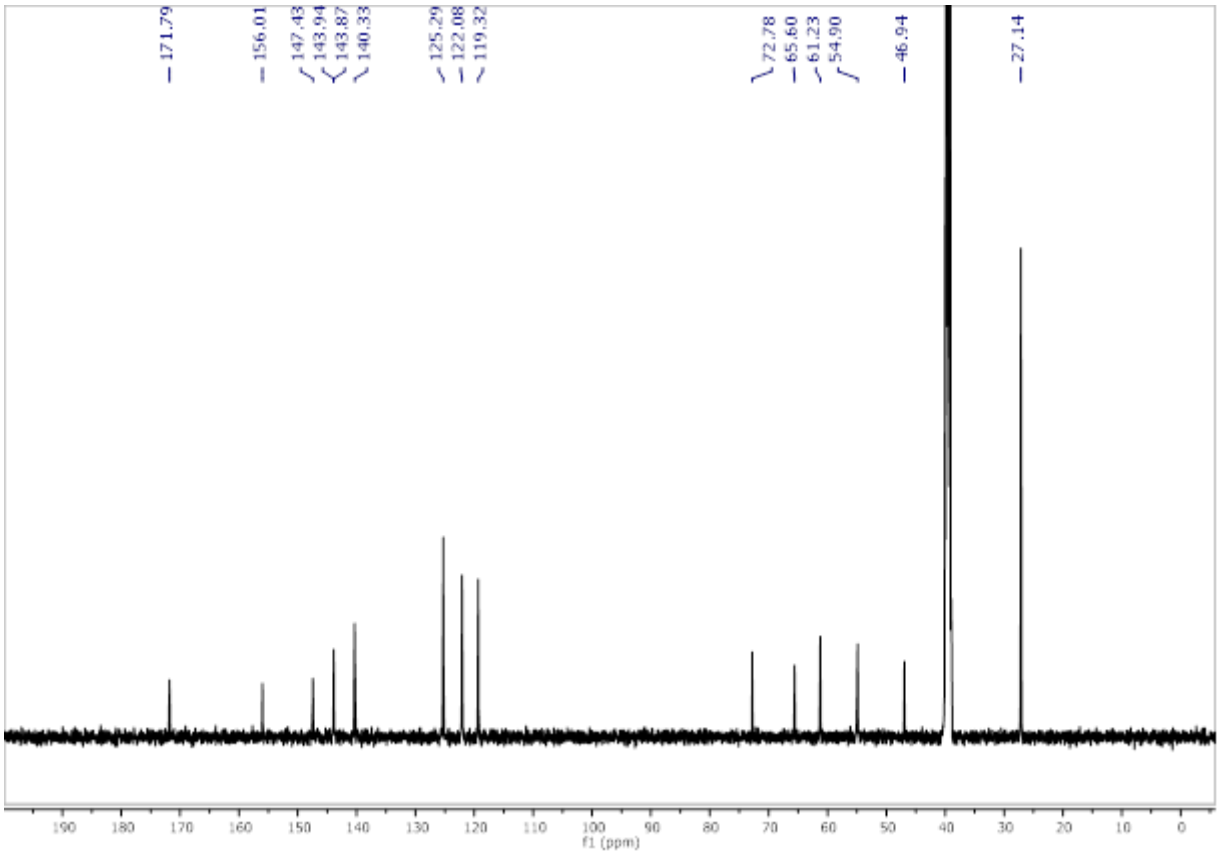

Figure 264: ^{13}C-NMR of Smoc-L-Ser(tBu)-OH **23**.

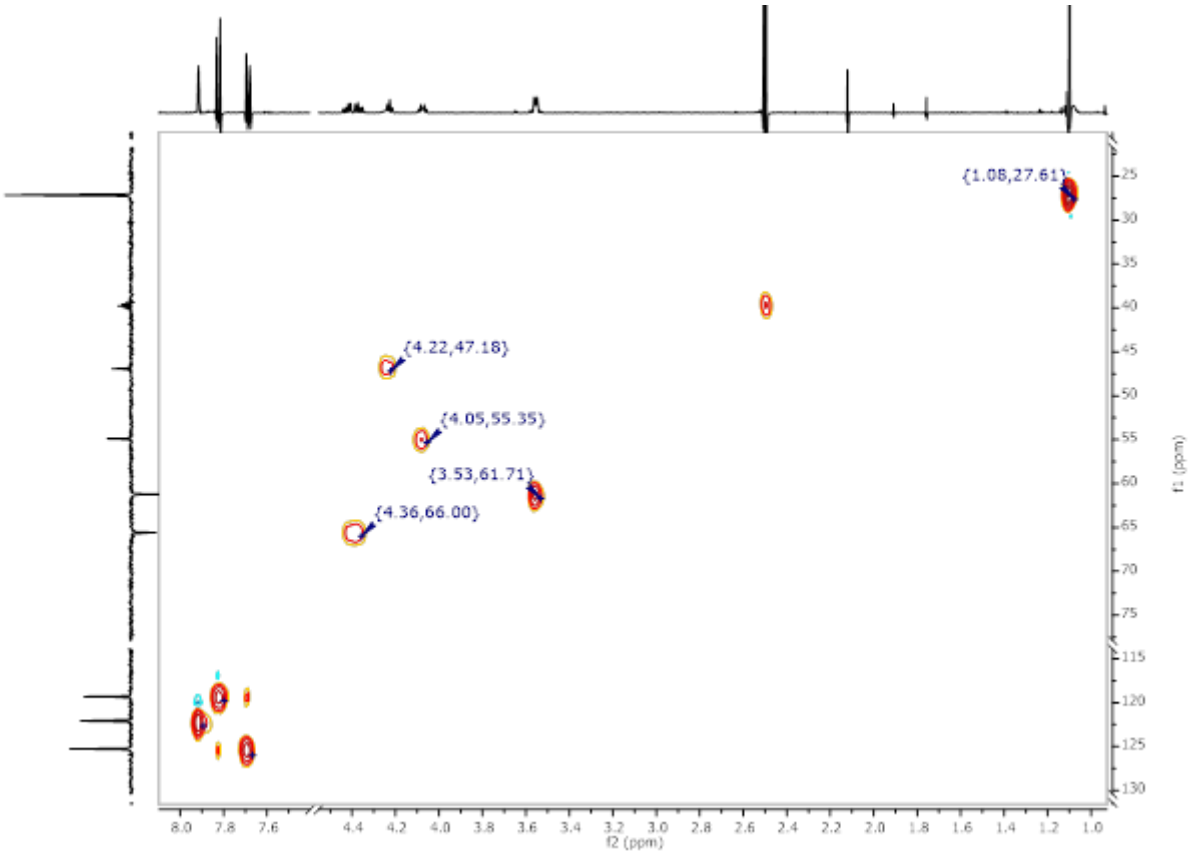

Figure 265: ^{1}H-^{13}C HSQC-NMR of Smoc-L-Ser(tBu)-OH **23**.

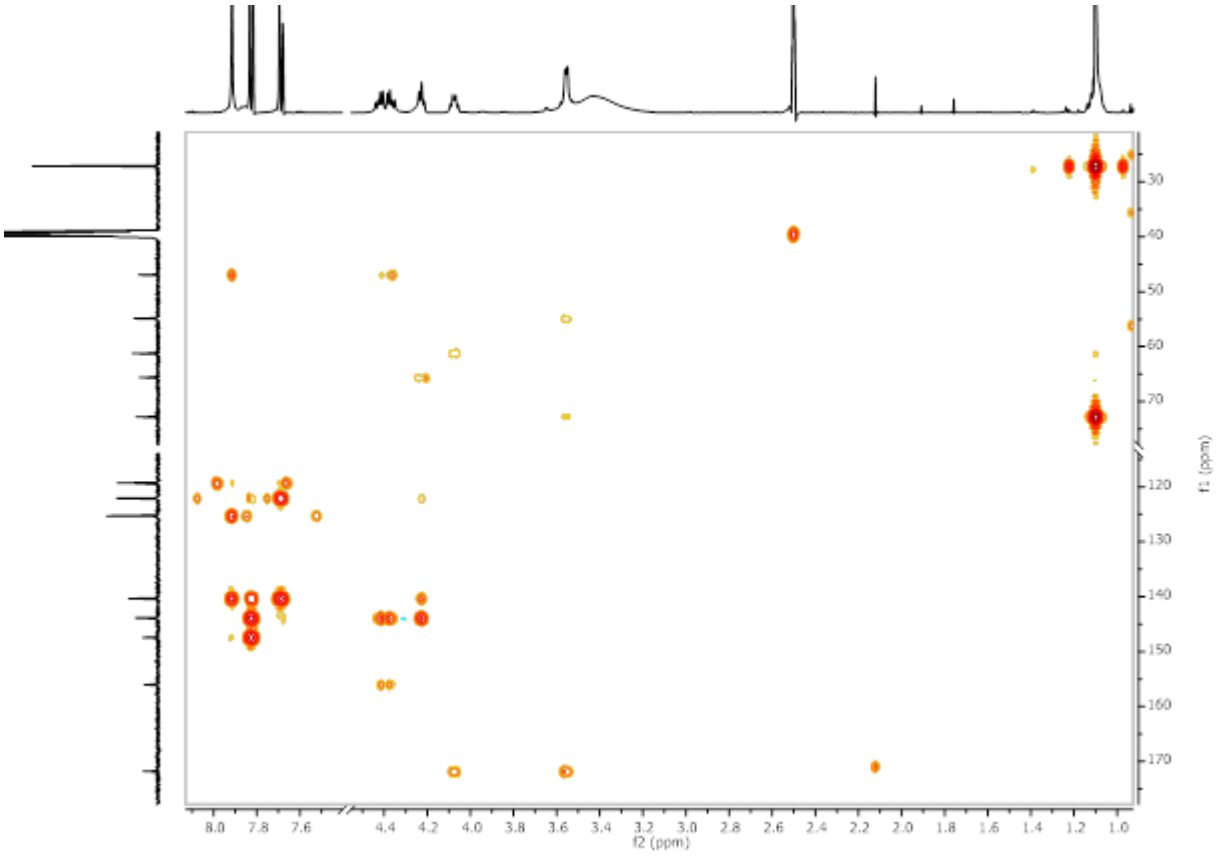

Figure 266: ^{1}H-^{13}C HMBC-NMR of Smoc-L-Ser(tBu)-OH **23**.

8.2.22. Analytical data of Smoc-L-Thr-OH 24

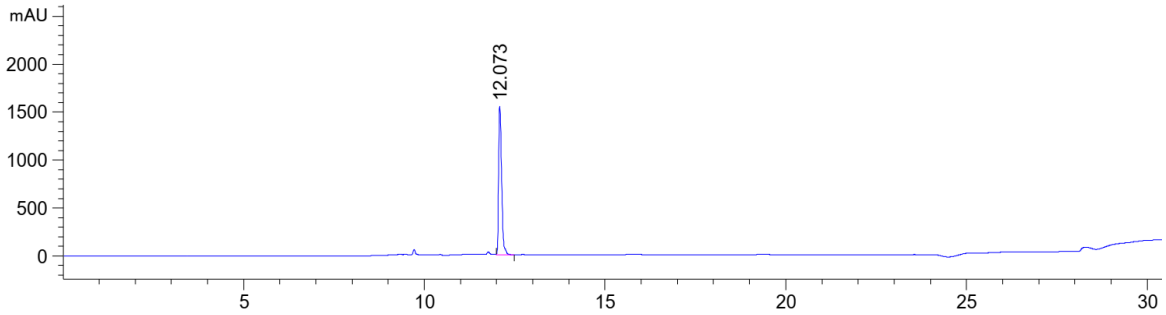

Figure 267: HPLC chromatogram of Smoc-L-Thr-OH **24** at λ=220 nm (0 to 40% MeCN).

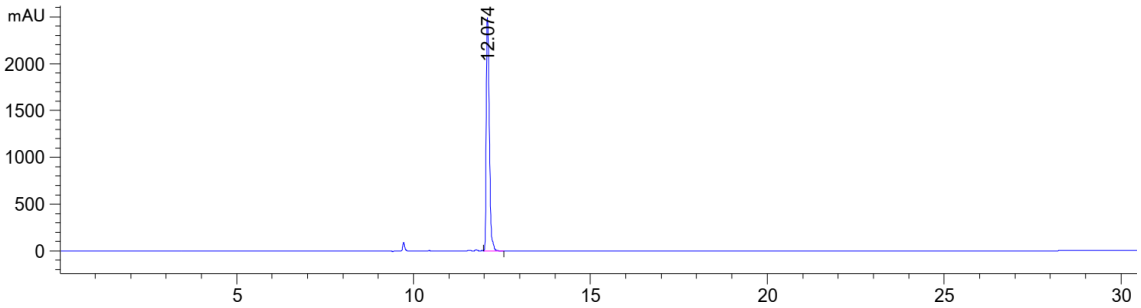

Figure 268: HPLC chromatogram of Smoc-L-Thr-OH **24** at λ=280 nm (0 to 40% MeCN).

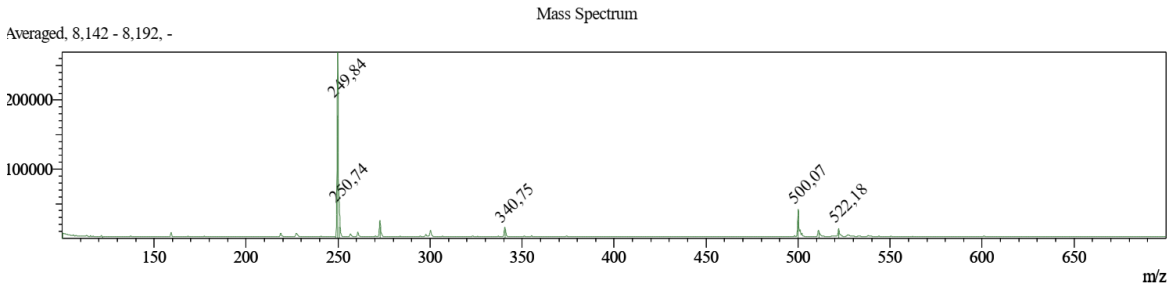

Figure 269: ESI-MS of Smoc-L-Thr-OH **24** (M measured=500.07 $[M-H]^-$, M calc.=501.48).

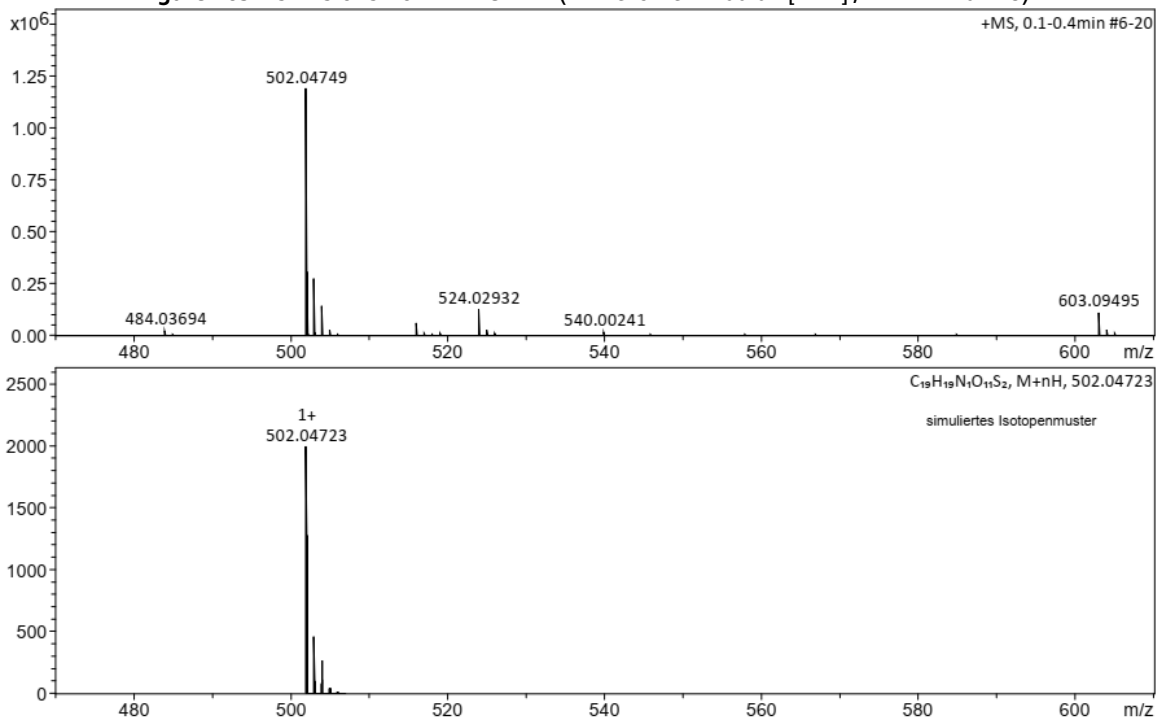

Figure **270:** HR-MS of Smoc-L-Thr-OH **24** (M measured=502.04749 $[M+H]^+$, M calc.=502.04723).

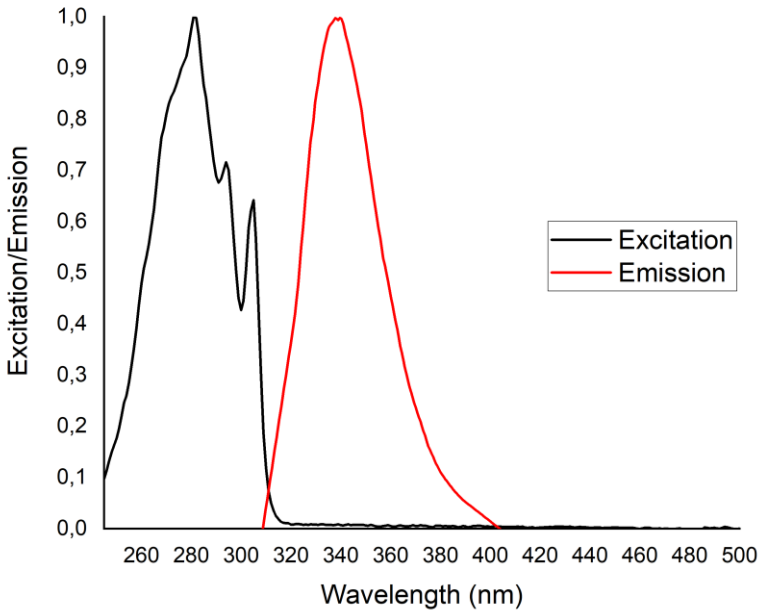

Figure 271: Excitation and emission spectra of Smoc-L-Thr-OH **24**, excitation and emission have been normalized between 0 and 1 for illustration.

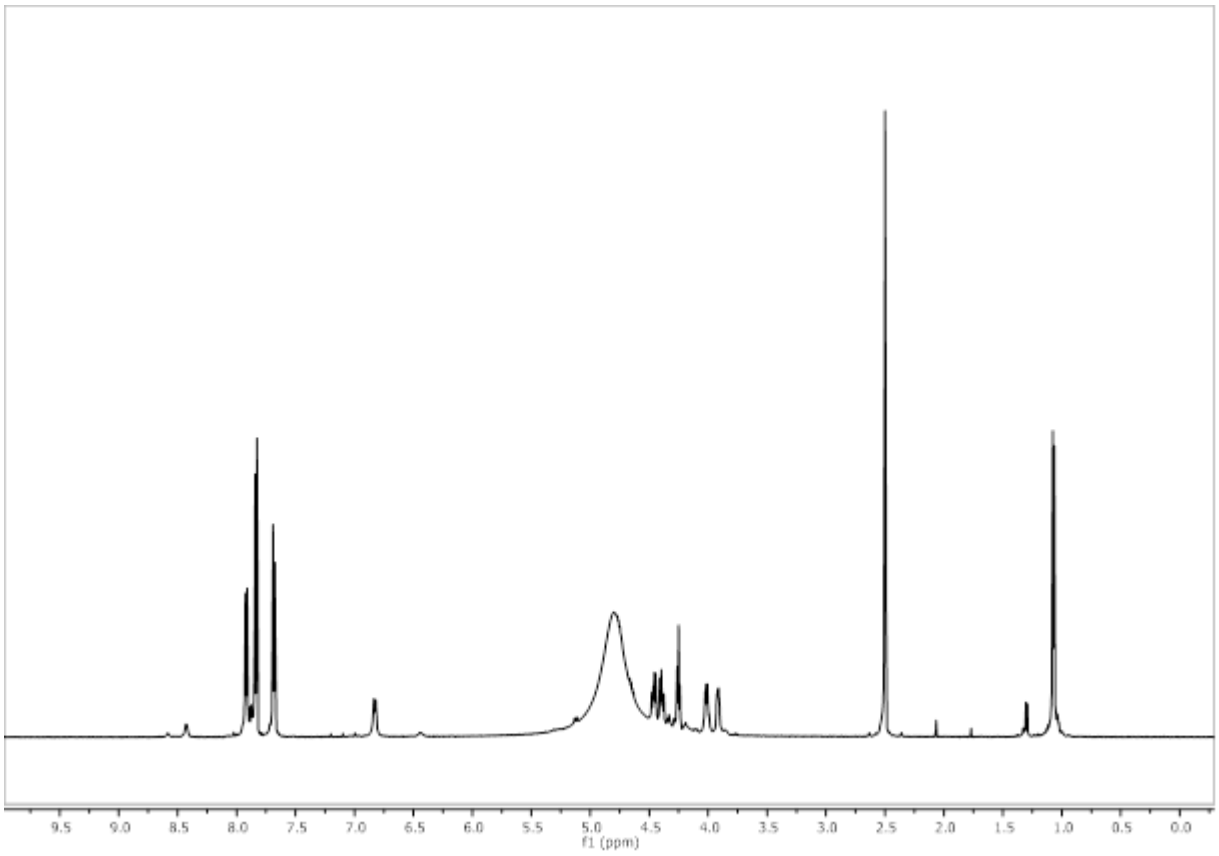

Figure 272: ^{1}H-NMR of Smoc-L-Thr-OH **24**.

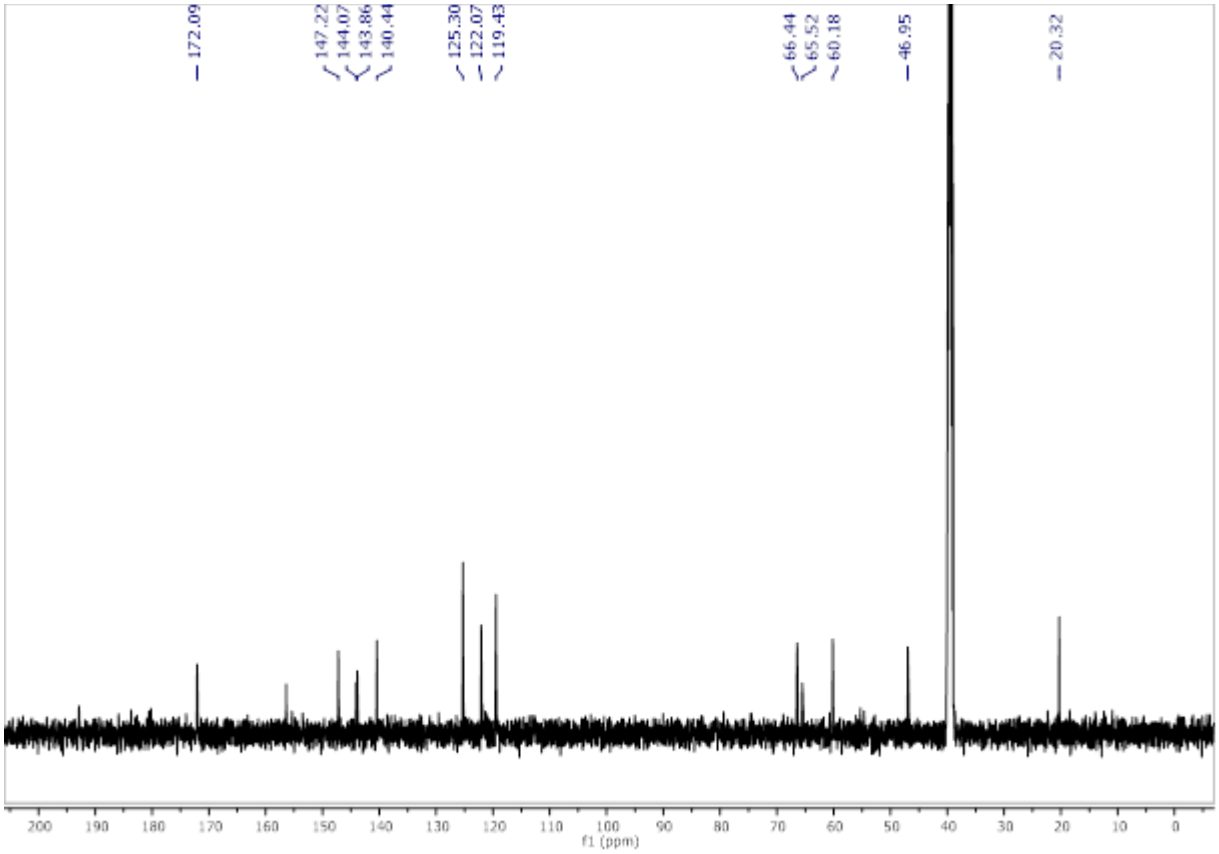

Figure 273: ^{13}C-NMR of Smoc-L-Thr-OH **24**.

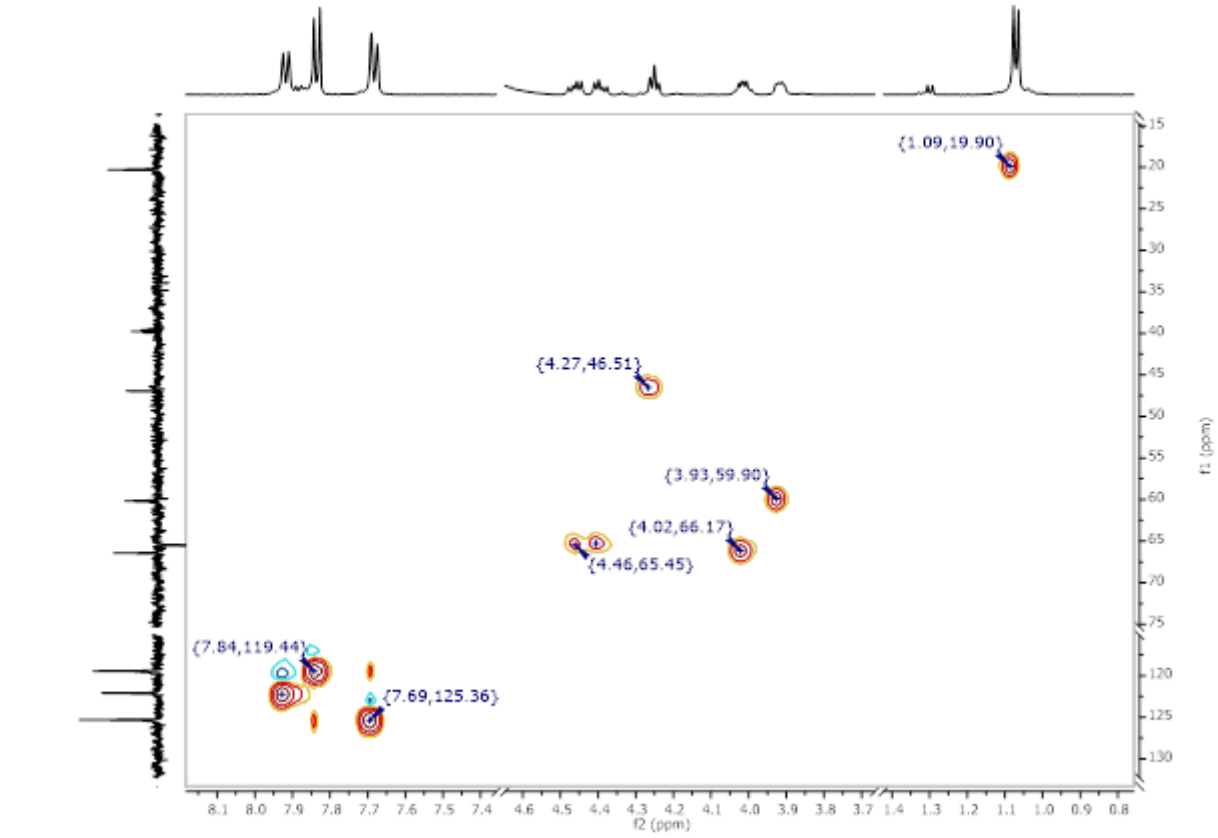

Figure 274: ^{1}H-^{13}C HSQC-NMR of Smoc-L-Thr-OH **24**.

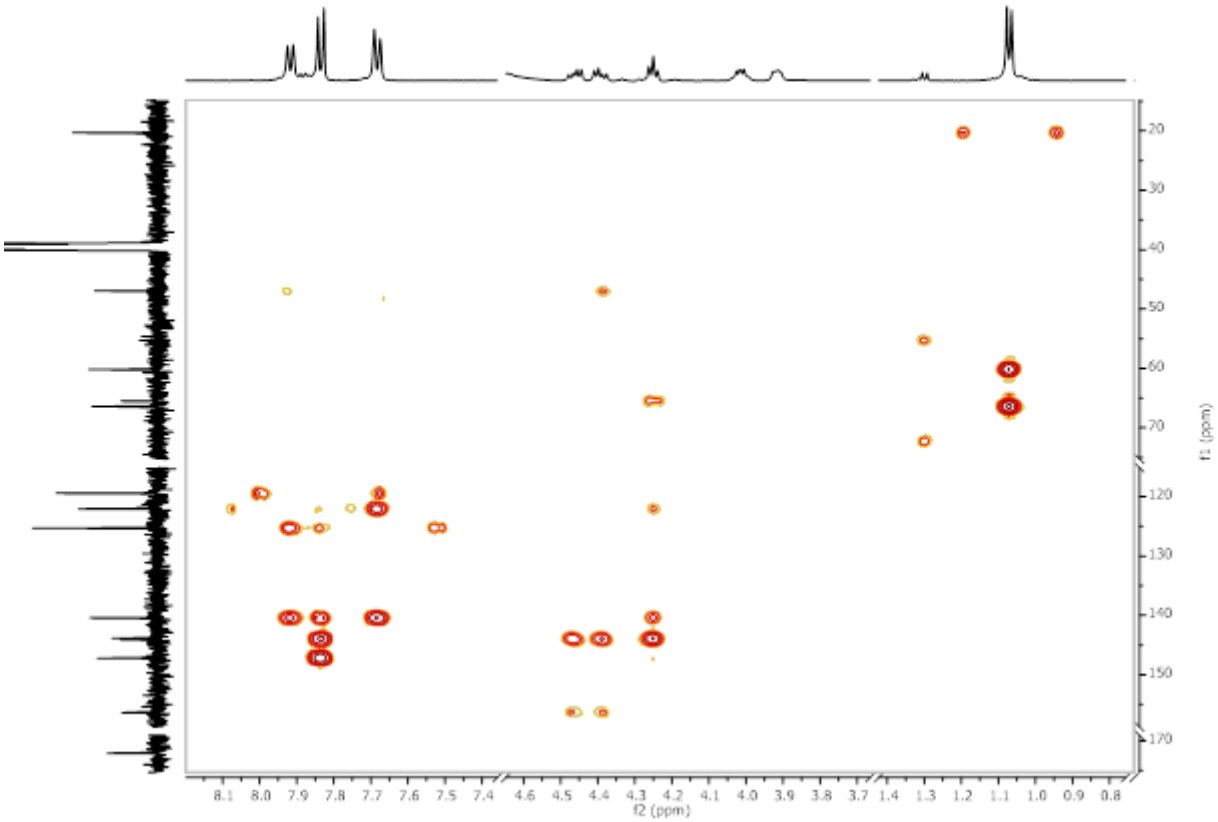

Figure 275: ^{1}H-^{13}C HMBC-NMR of Smoc-L-Thr-OH **24**.

8.2.23.Analytical data of Smoc-L-Thr(tBu)-OH 25

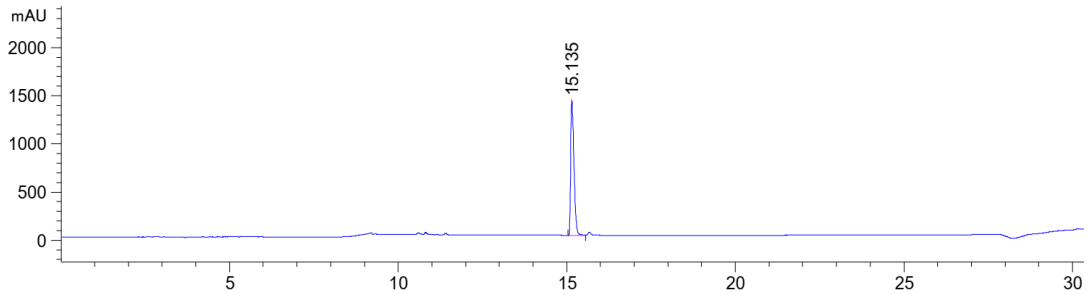

Figure 276: HPLC chromatogram of Smoc-L-Thr(tBu)-OH **25** at λ=220 nm (0 to 60% MeCN).

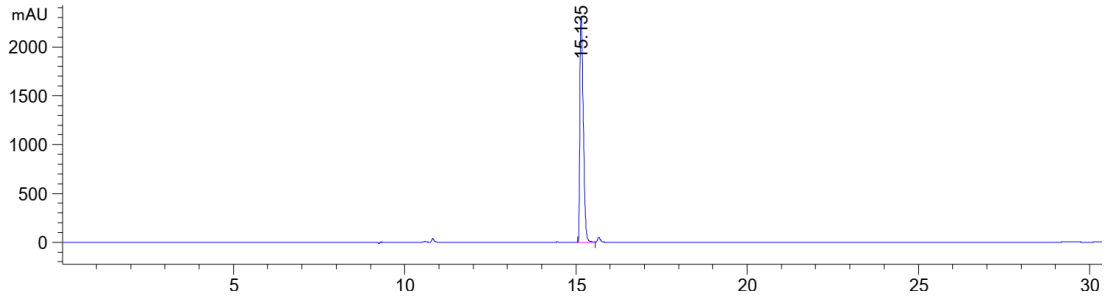

Figure 277: HPLC chromatogram of Smoc-L-Thr(tBu)-OH **25** at λ=280 nm (0 to 60% MeCN).

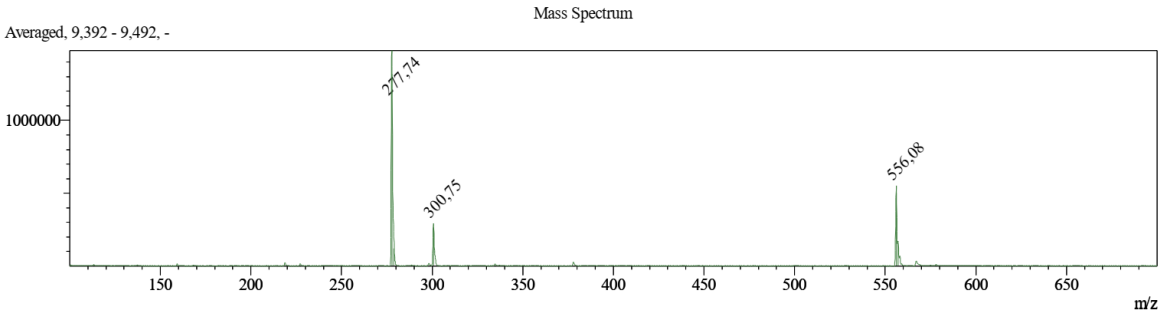

Figure 278: ESI-MS of Smoc-L-Thr(tBu)-OH **25** (M measured=556.08 $[M-H]^-$, M calc.=557.59).

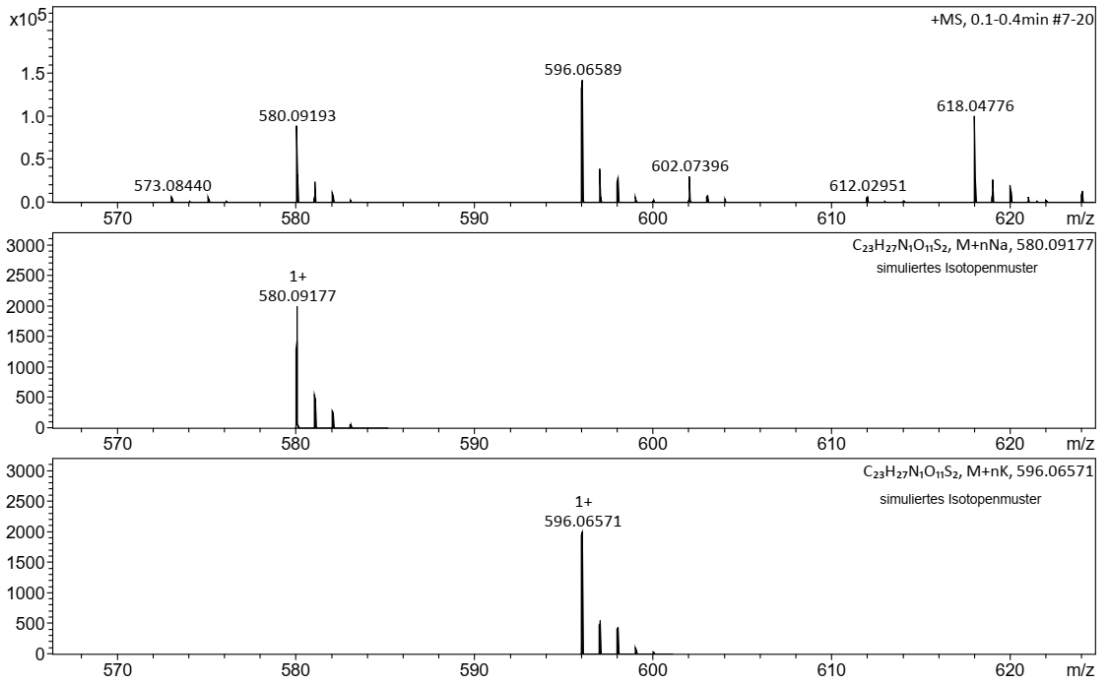

Figure 279: HR-MS of Smoc-L-Thr(tBu)-OH **25** (M measured=580.09193 $[M+Na]^+$, M calc.=580.09177; M measured=596.06589 $[M+K]^+$, M calc.=596.06571).

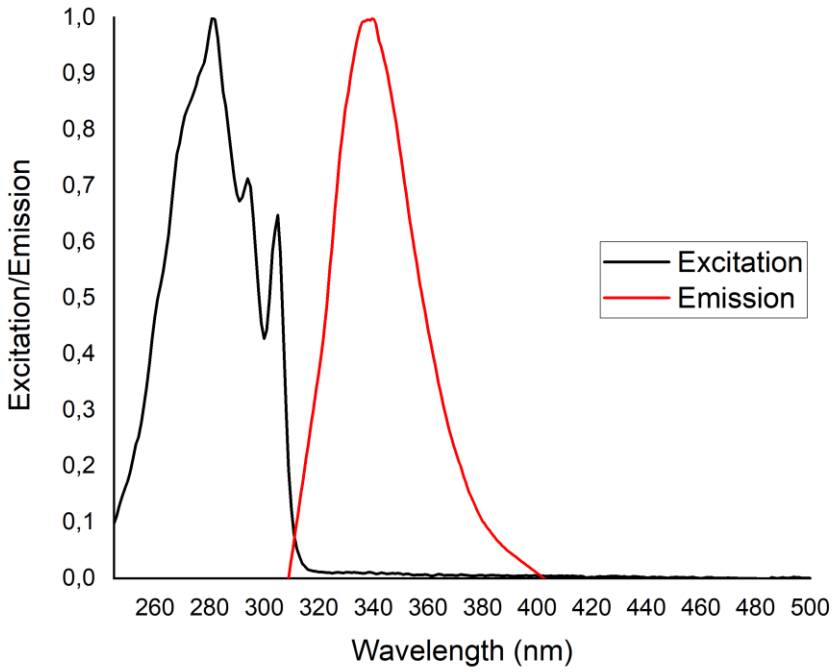

Figure 280: Excitation and emission spectra of Smoc-L-Thr(tBu)-OH **25**, excitation and emission have been normalized between 0 and 1 for illustration.

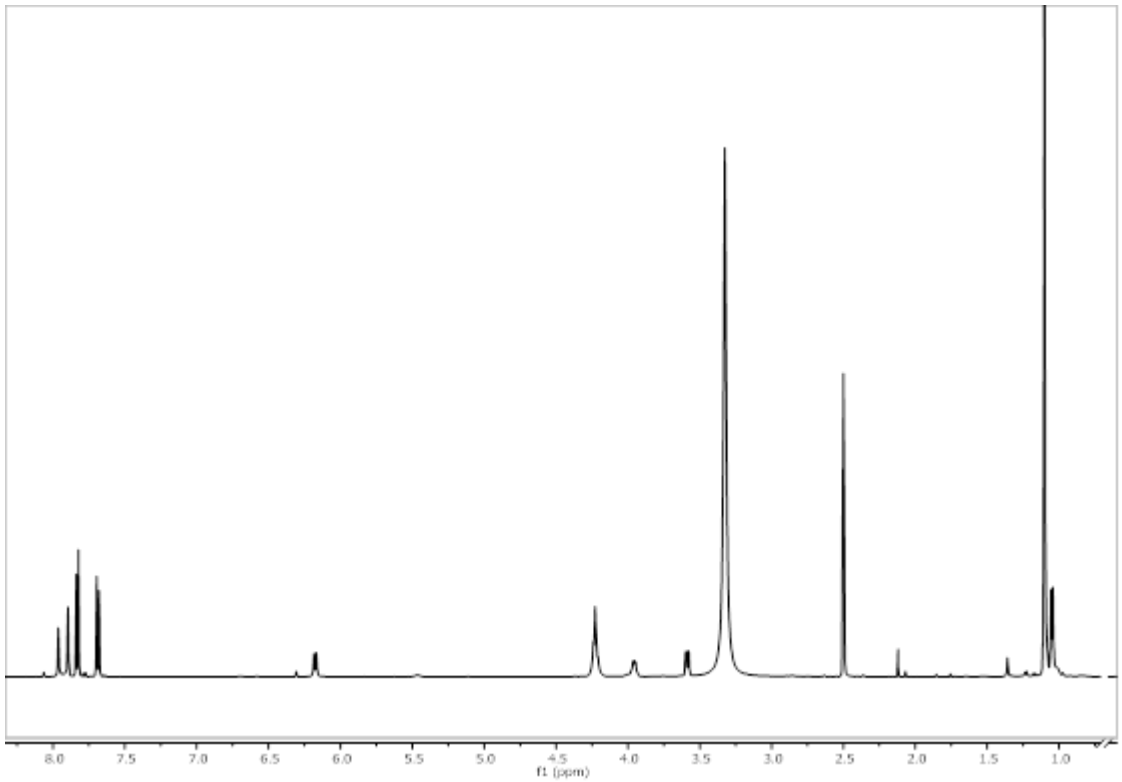

Figure 281: ^{1}H-NMR of Smoc-L-Thr(tBu)-OH **25**.

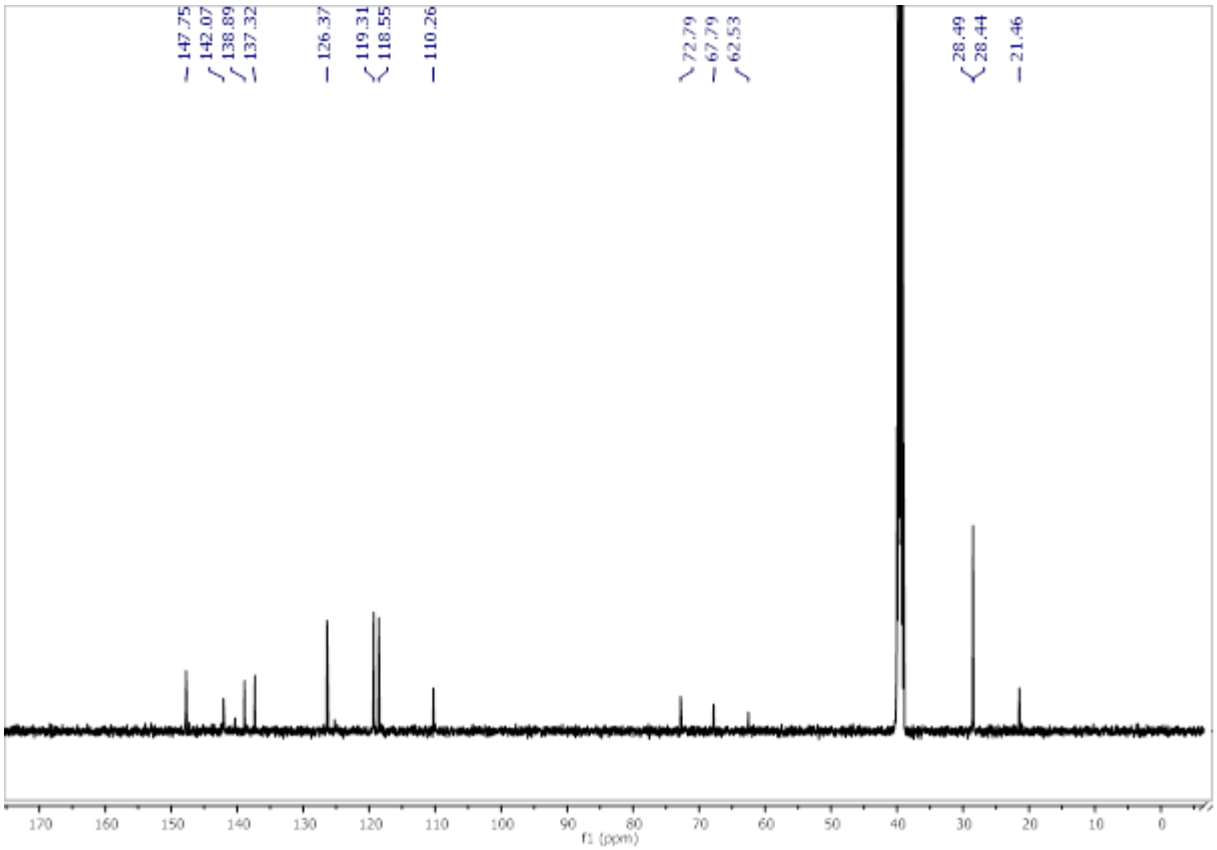

Figure 282: ^{13}C-NMR of Smoc-L-Thr(tBu)-OH **25**.

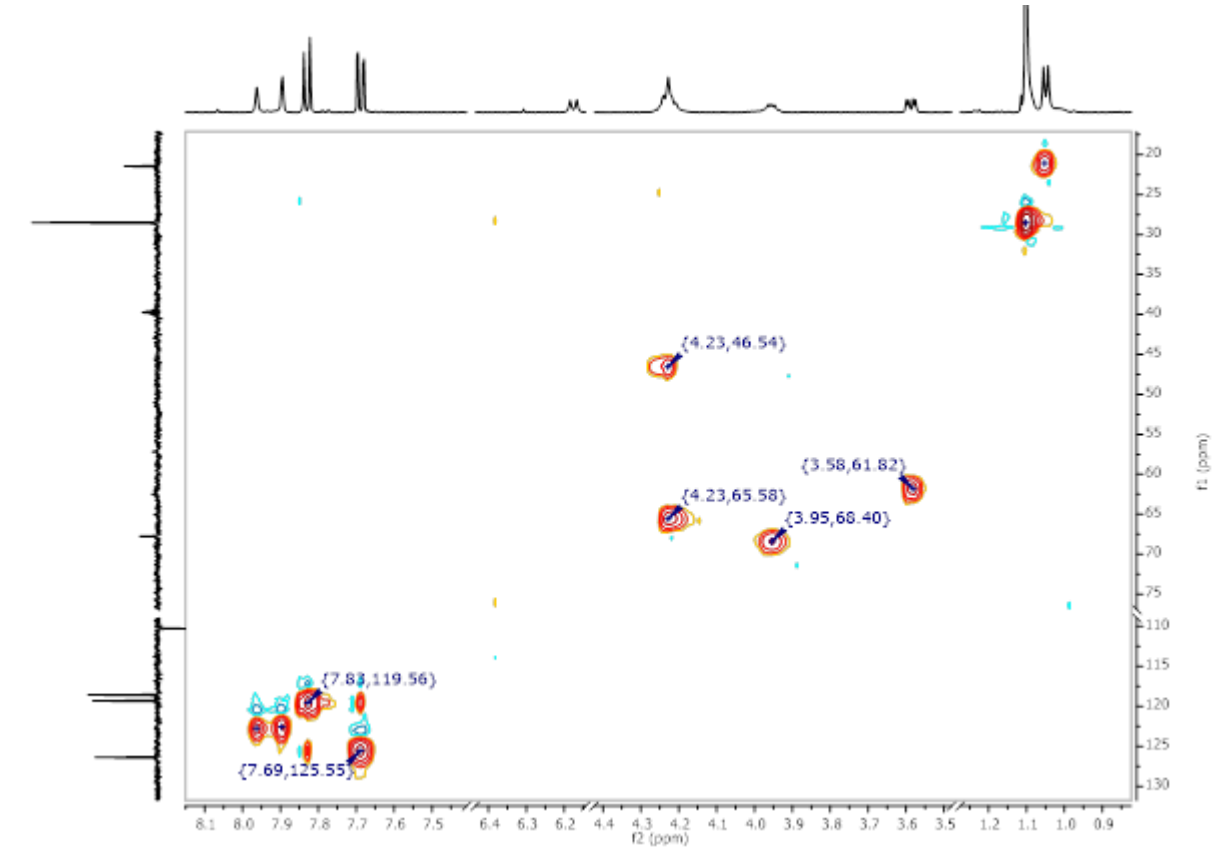

Figure 283: ^{1}H-^{13}C HSQC-NMR of Smoc-L-Thr(tBu)-OH **25**.

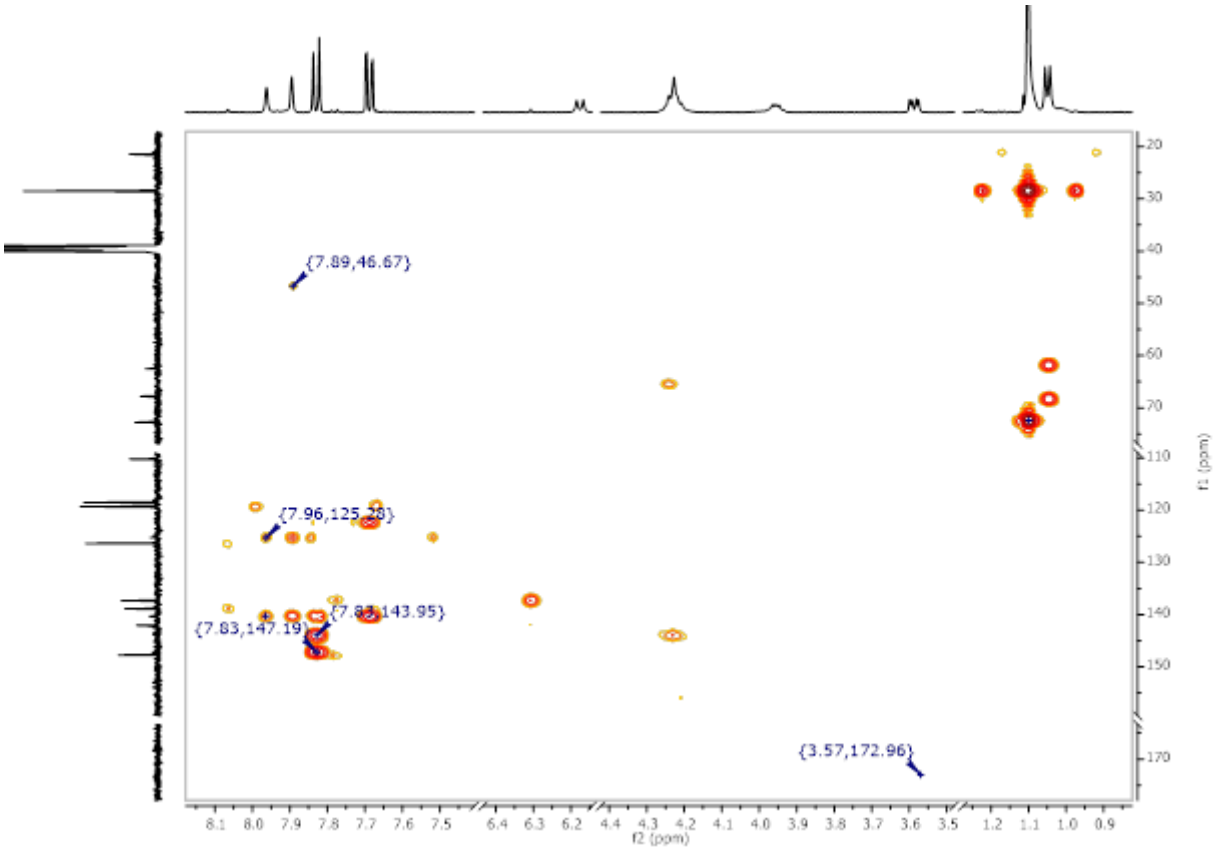

Figure 284: ^{1}H-^{13}C HMBC-NMR of Smoc-L-Thr(tBu)-OH **25**.

8.2.24.Analytical data of Smoc-L-Trp-OH 26

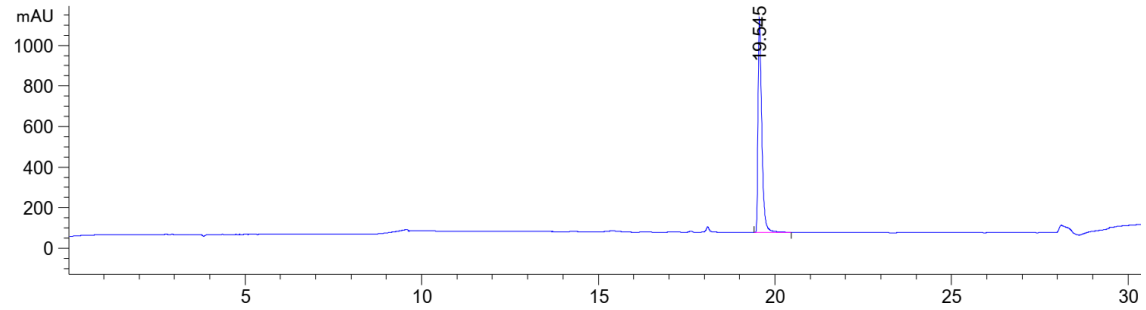

Figure 285: HPLC chromatogram of Smoc-L-Trp-OH **26** at λ=220 nm (0 to 40% MeCN).

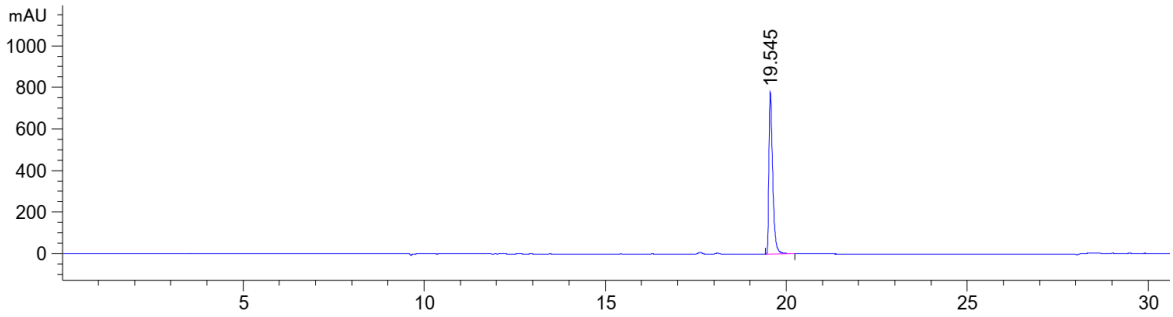

Figure 286: HPLC chromatogram of Smoc-L-Trp-OH **26** at λ=280 nm (0 to 40% MeCN).

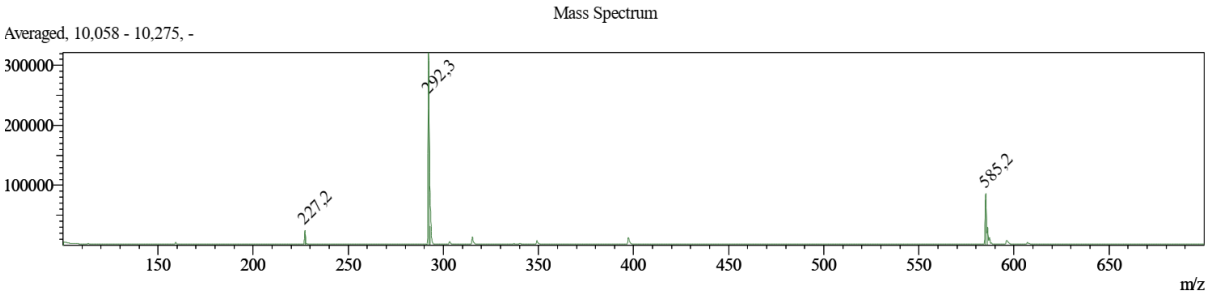

Figure 287: ESI-MS of Smoc-L-Trp-OH **26** (M measured=585.20 $[M-H]^-$, M calc.=586.59).

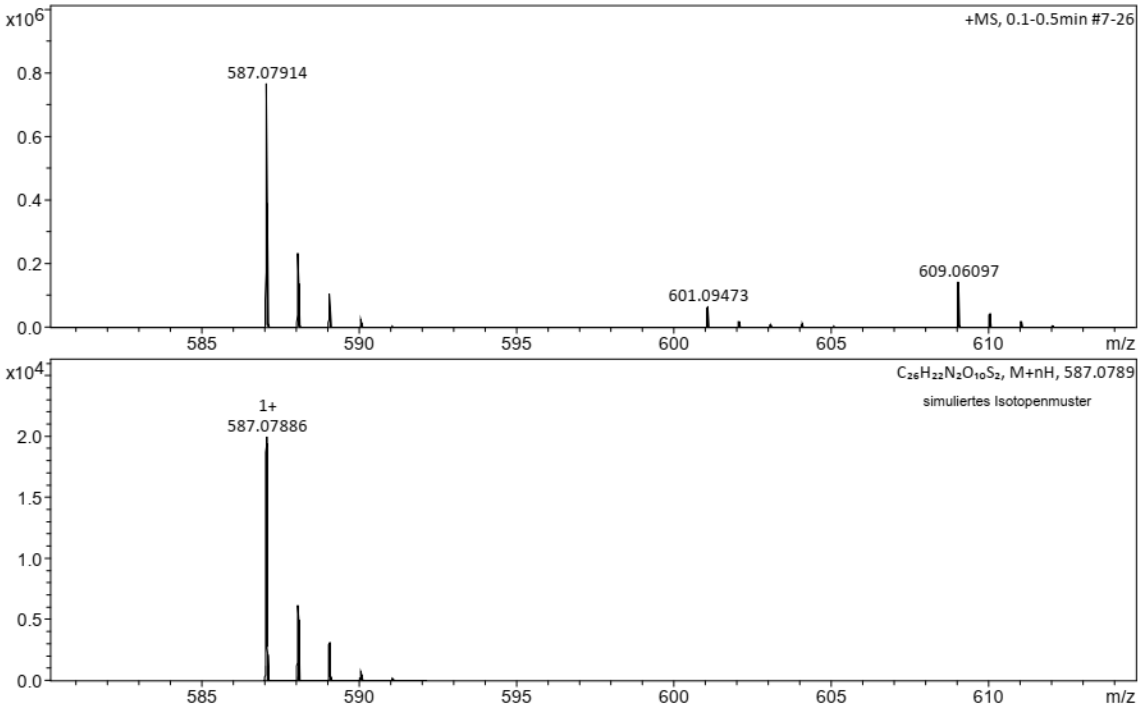

Figure 288: HR-MS of Smoc-L-Trp-OH **26** (M measured=587.07914 $[M+H]^+$, M calc.=587.07886).

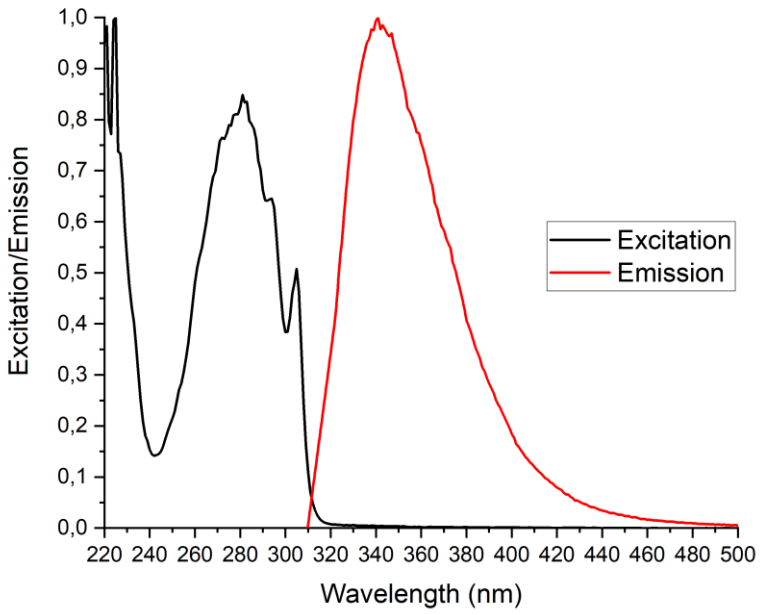

Figure 289: Excitation and emission spectra of Smoc-L-Trp-OH **26**, excitation and emission have been normalized between 0 and 1 for illustration.

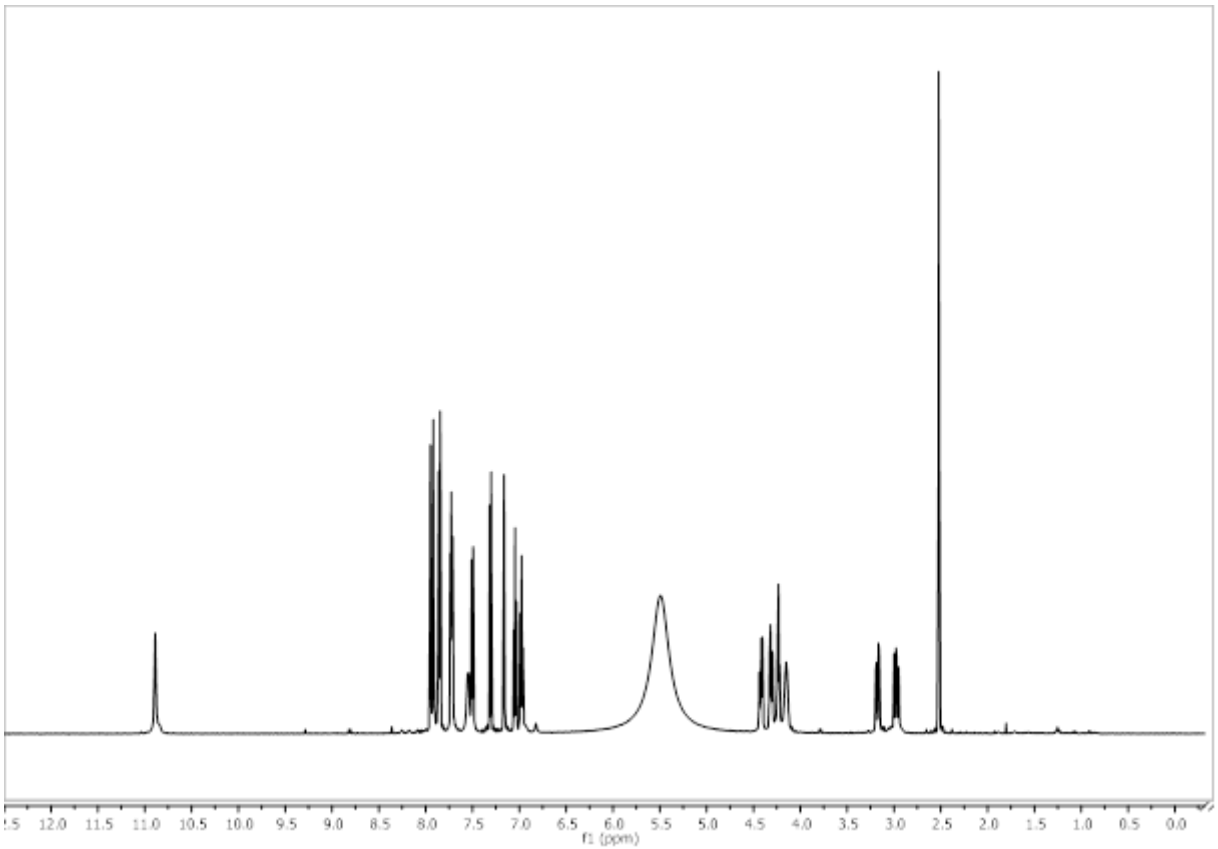

Figure 290: ^{1}H-NMR of Smoc-L-Trp-OH **26**.

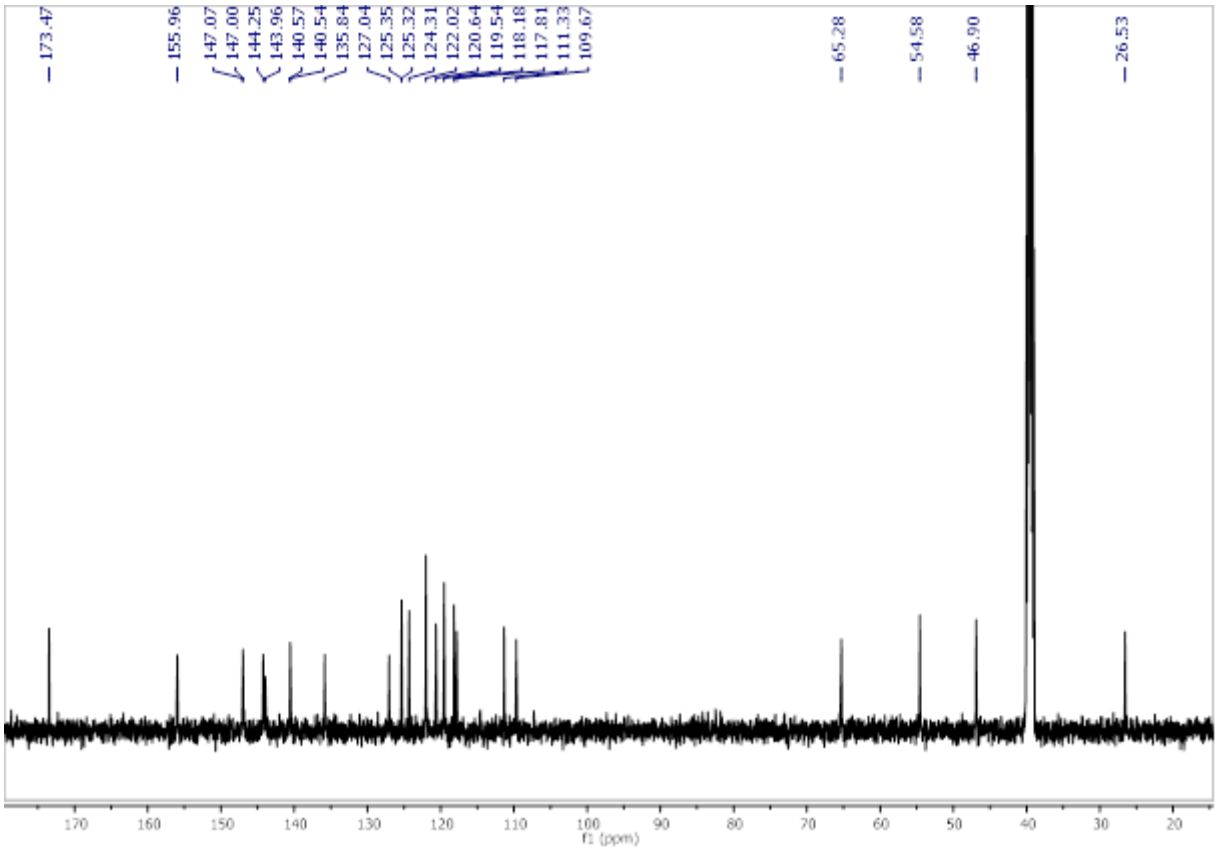

Figure 291: ^{13}C-NMR of Smoc-L-Trp-OH **26**.

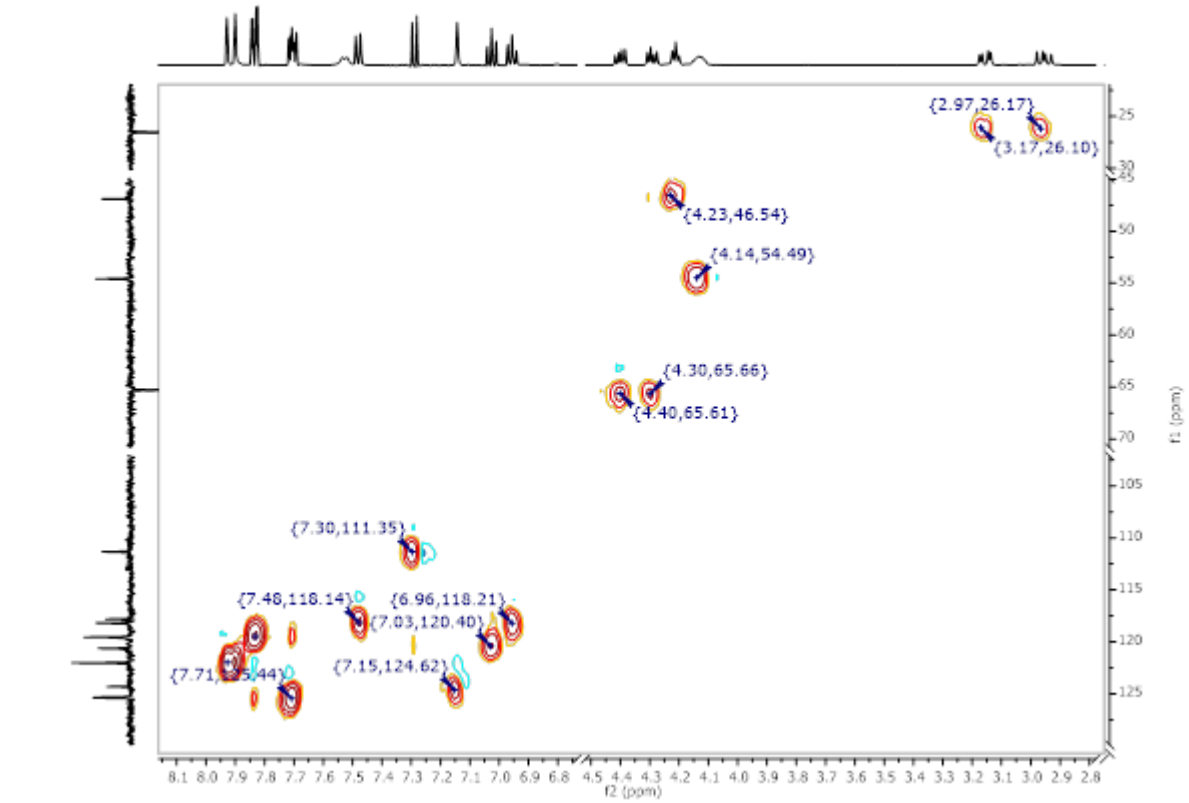

Figure 292: ^{1}H-^{13}C HSQC-NMR of Smoc-L-Trp-OH **26**.

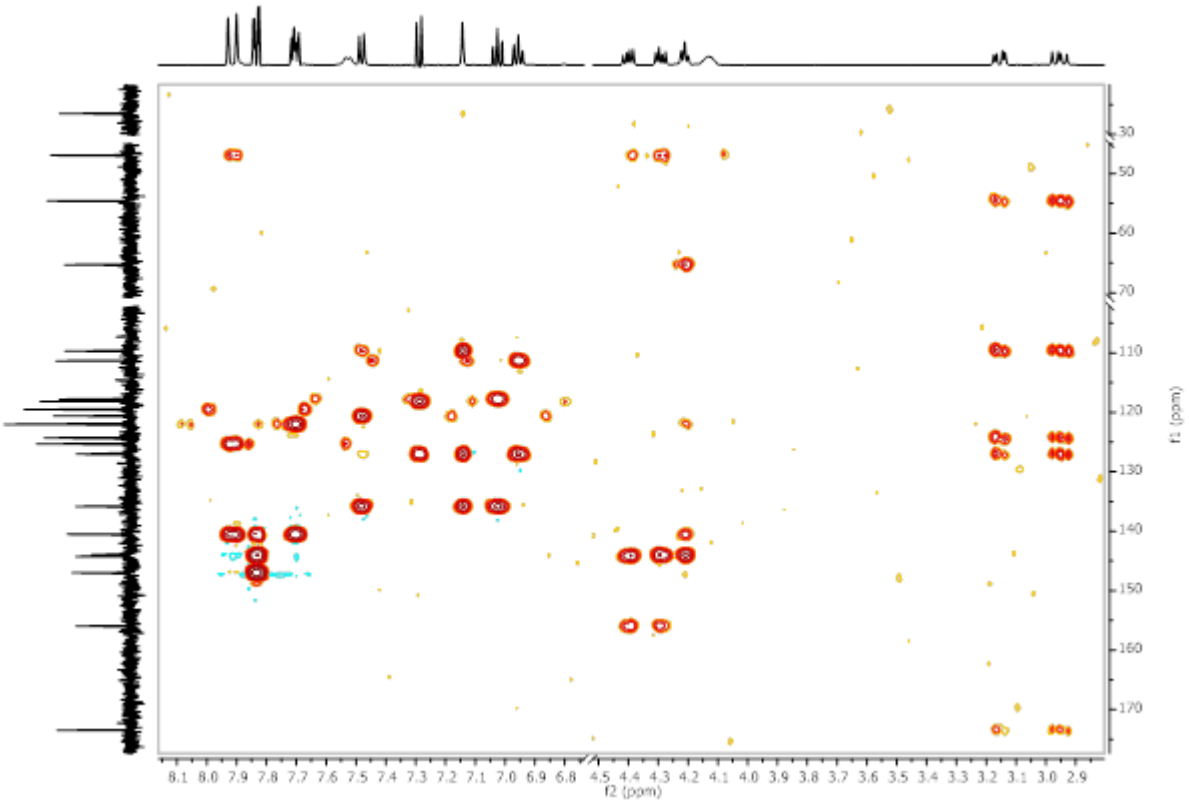

Figure 293: ^{1}H-^{13}C HMBC-NMR of Smoc-L-Trp-OH **26**.

8.2.25.Analytical data of Smoc-L-Trp(Boc)-OH 27

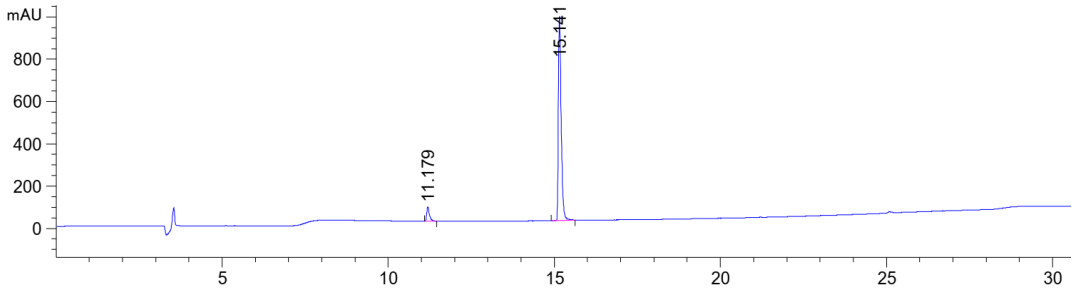

Figure 294: HPLC chromatogram of Smoc-L-Trp(Boc)-OH **27** at λ=220 nm (0 to 100% MeCN).

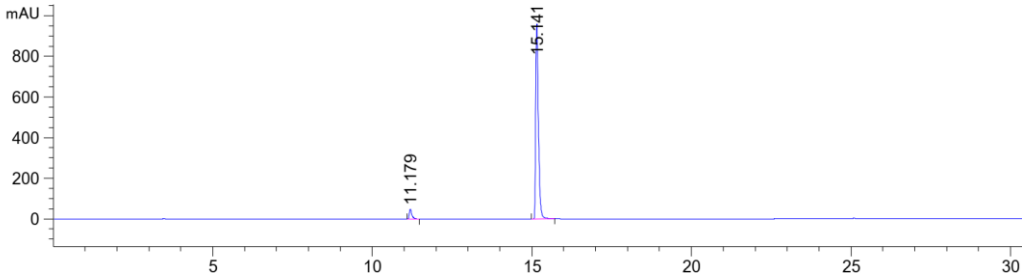

Figure 295: HPLC chromatogram of Smoc-L-Trp(Boc)-OH **27** at λ=280 nm (0to 100% MeCN).

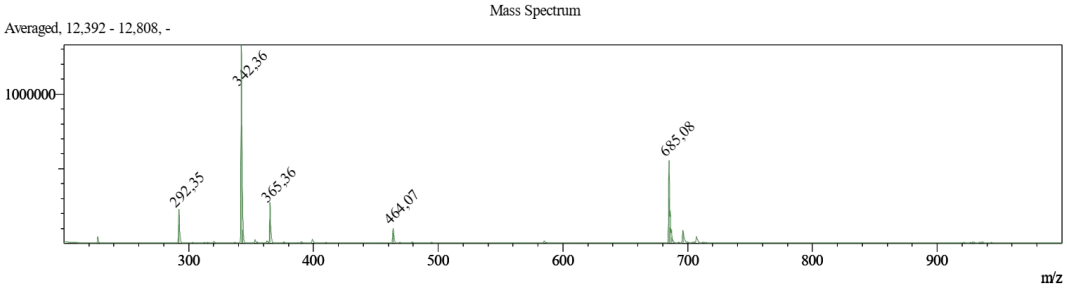

Figure 296: ESI-MS of Smoc-L-Trp(Boc)-OH **27** (M measured=685.08 [M-H]$^-$, M calc.=686.70).

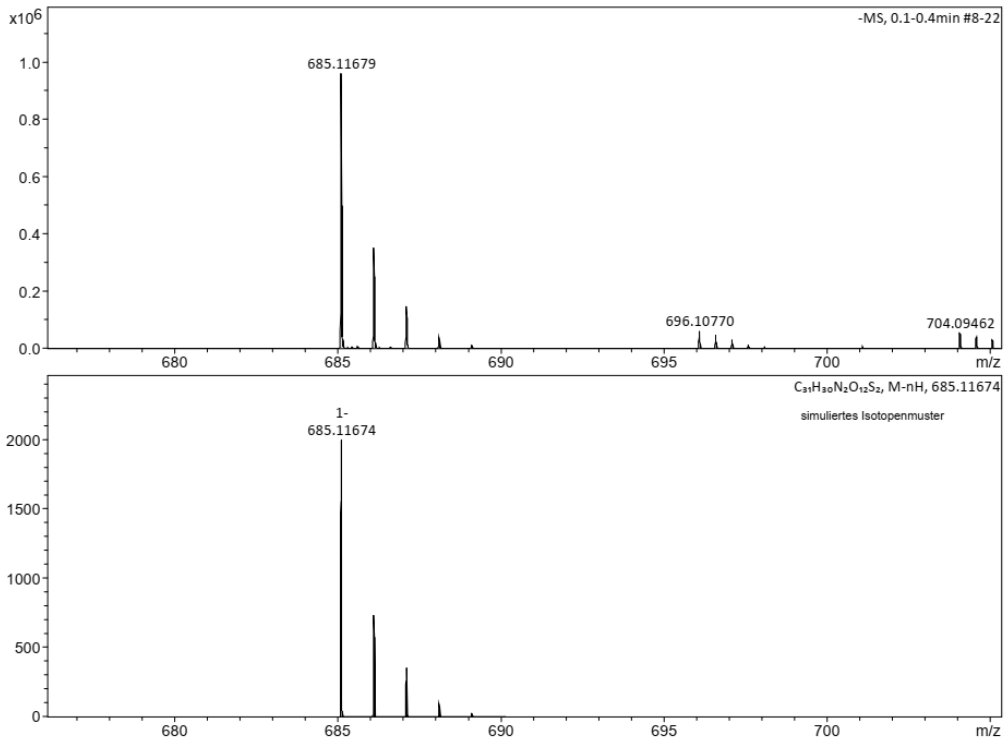

Figure 297: HR-MS of Smoc-L-Trp(Boc)-OH **27** (M measured=685.11679 [M-H]$^-$, M calc.=685.11674).

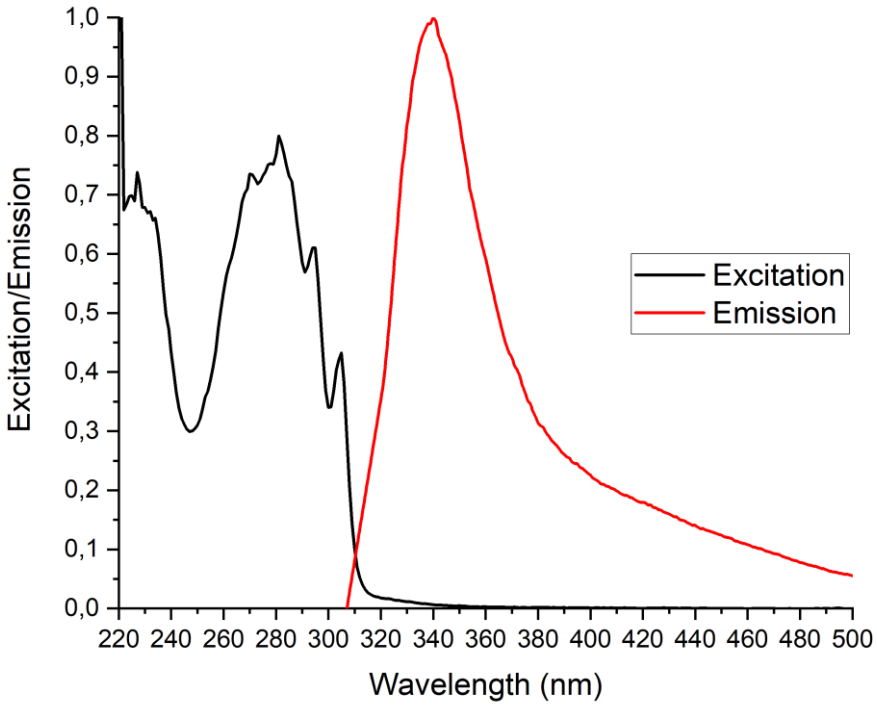

Figure 298: Excitation and emission spectra of Smoc-L-Trp(Boc)-OH **27**, excitation and emission have been normalized between 0 and 1 for illustration.

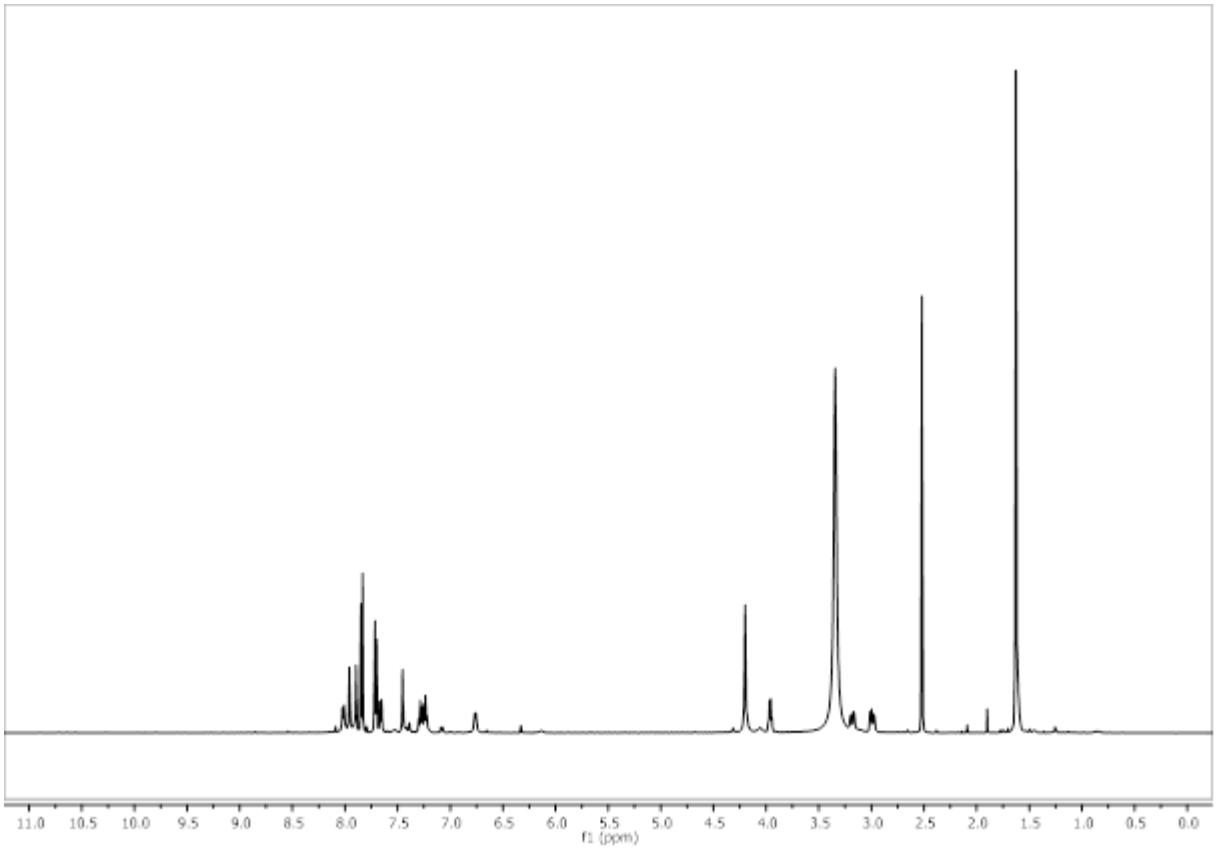

Figure 299: ^{1}H-NMR of Smoc-L-Trp(Boc)-OH **27**.

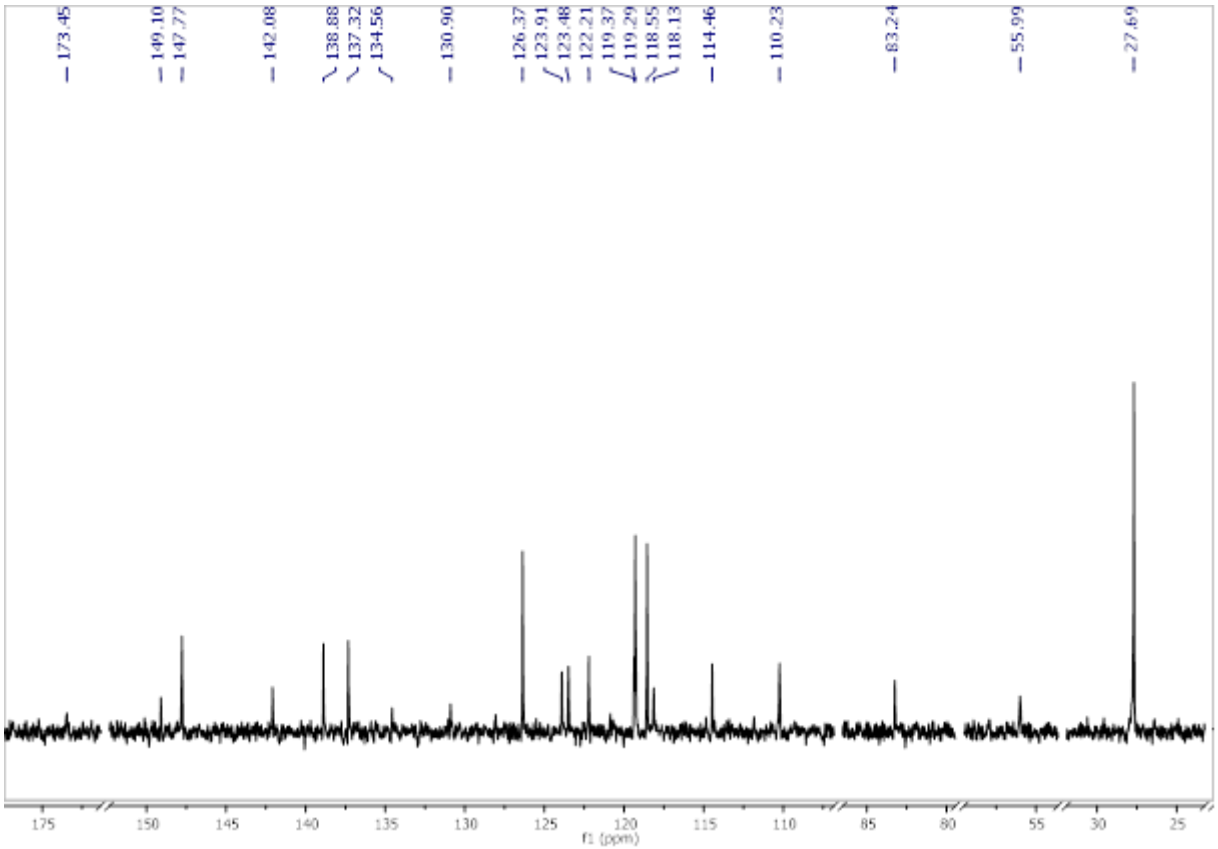

Figure 300: ^{13}C-NMR of Smoc-L-Trp(Boc)-OH **27**.

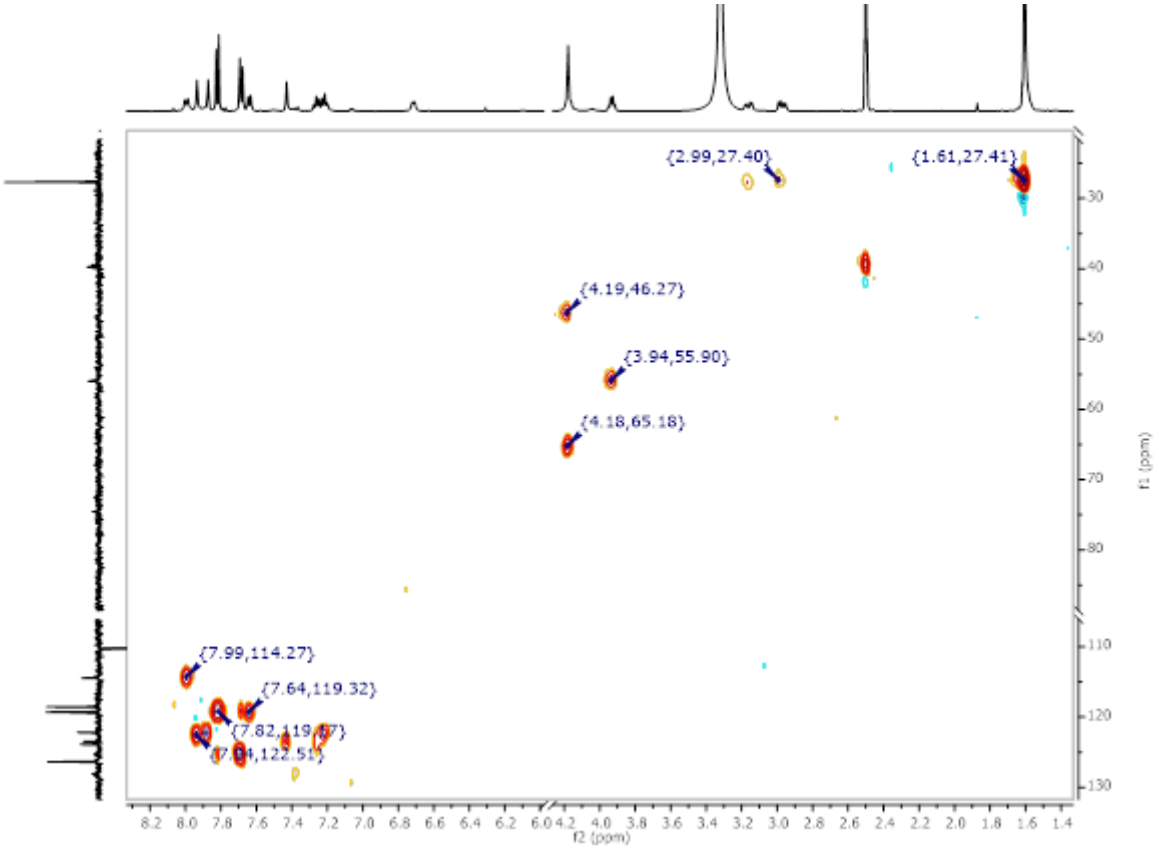

Figure 301: ^{1}H-^{13}C HSQC-NMR of Smoc-L-Trp(Boc)-OH **27**.

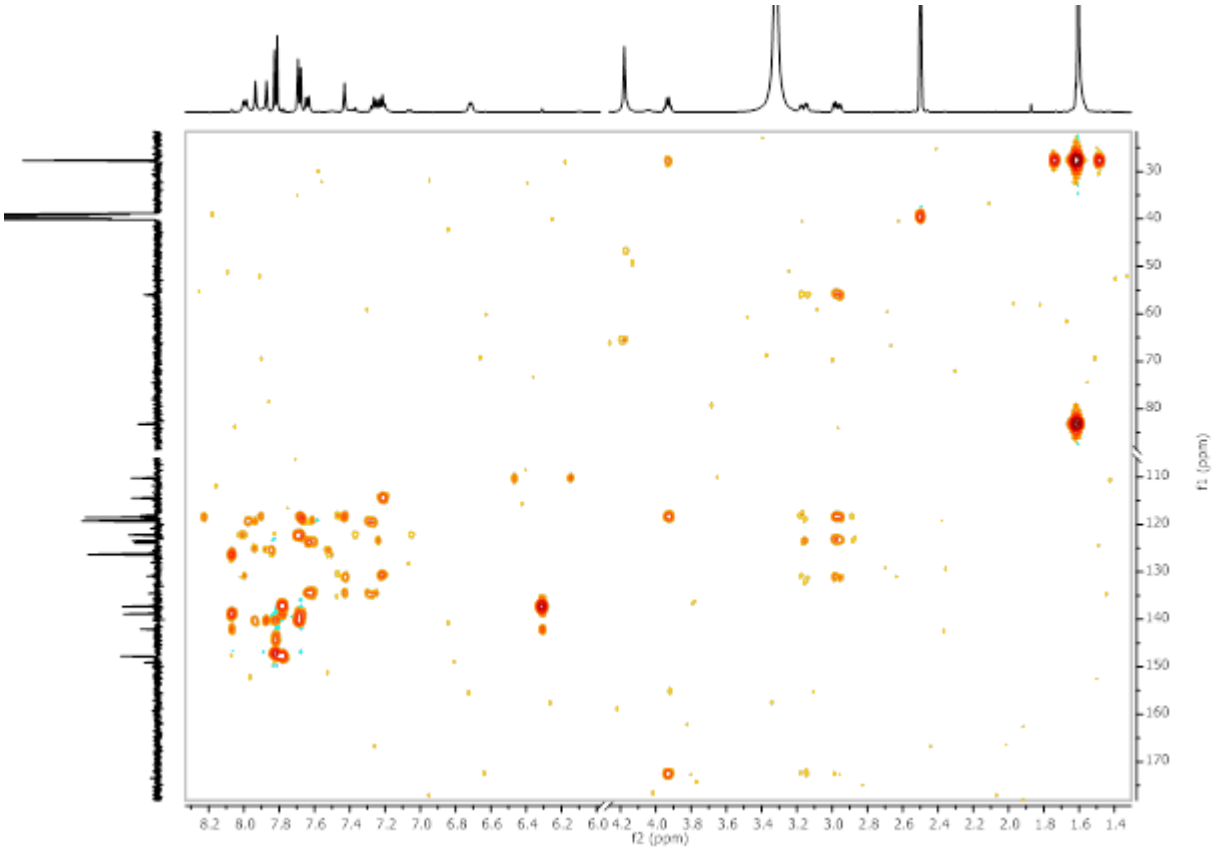

Figure 302: ^{1}H-^{13}C HMBC-NMR of Smoc-L-Trp(Boc)-OH **27**.

8.2.26.Analytical data of Smoc-L-Tyr-OH 28

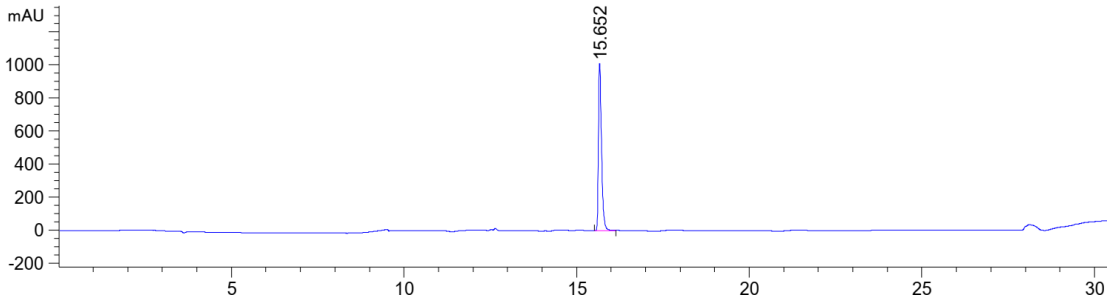

Figure 303: HPLC chromatogram of Smoc-L-Tyr-OH **28** at λ=220 nm (0 to 40% MeCN).

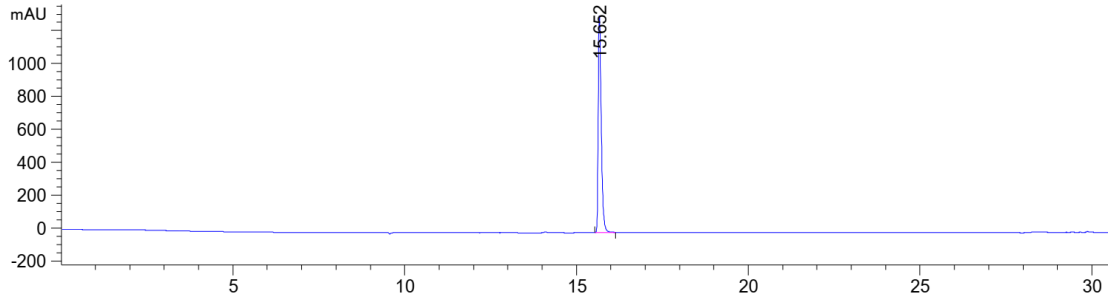

Figure 304: HPLC chromatogram of Smoc-L-Tyr-OH **28** at λ=280 nm (0 to 40% MeCN).

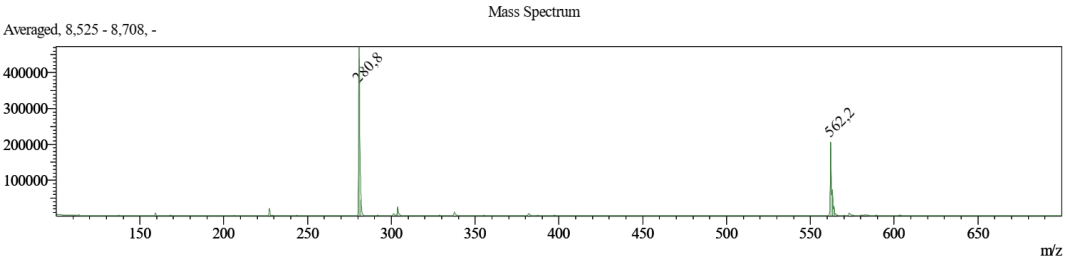

Figure 305: ESI-MS of Smoc-L-Tyr-OH **28** (M measured=562.20 [M-H]$^-$, M calc.=563.55).

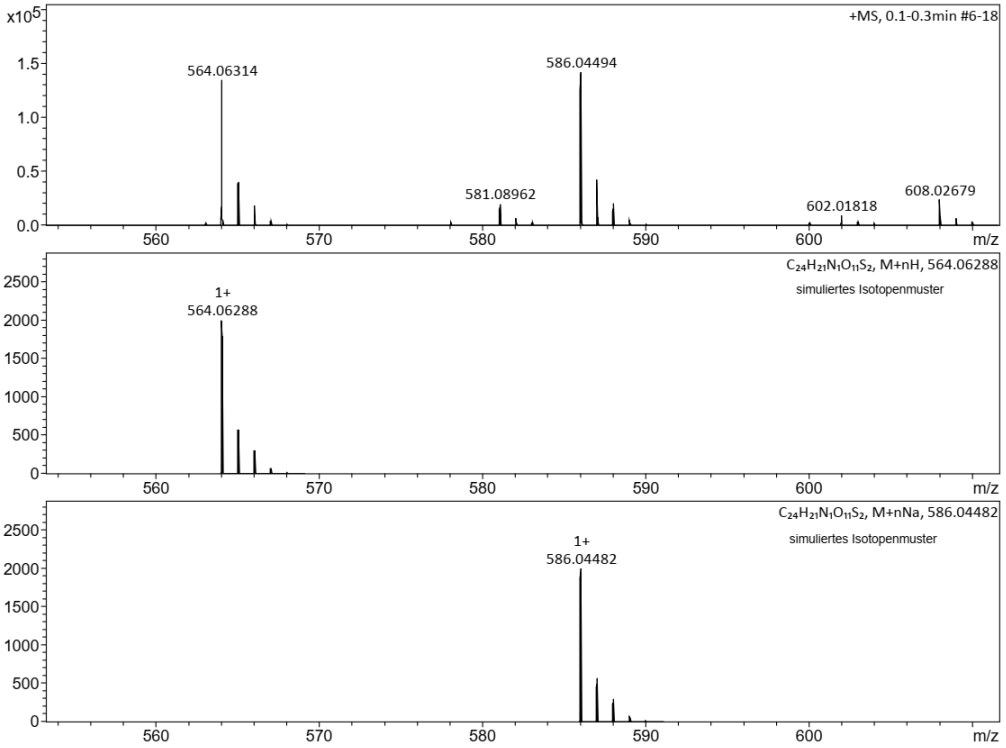

Figure 306: HR-MS of Smoc-L-Tyr-OH **28** (M measured=564.06314 [M+H]$^+$, M calc.=564.06288).

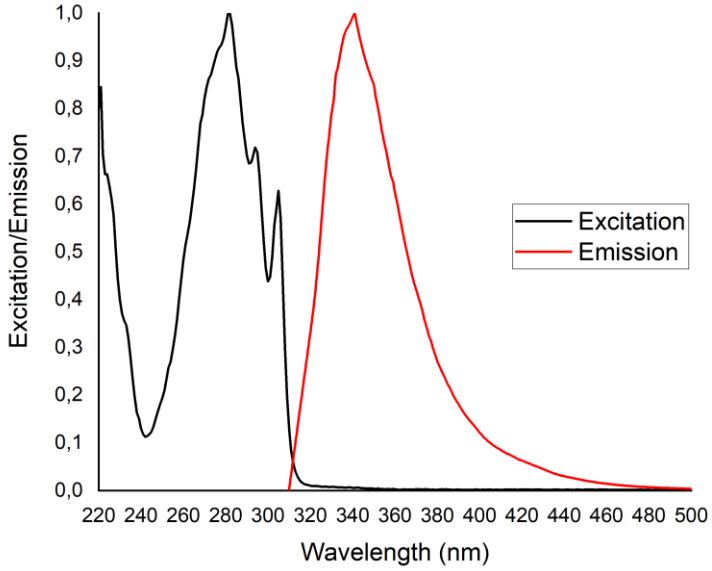

Figure 307: Excitation and emission spectra of Smoc-L-Tyr-OH **28**, excitation and emission have been normalized between 0 and 1 for illustration.

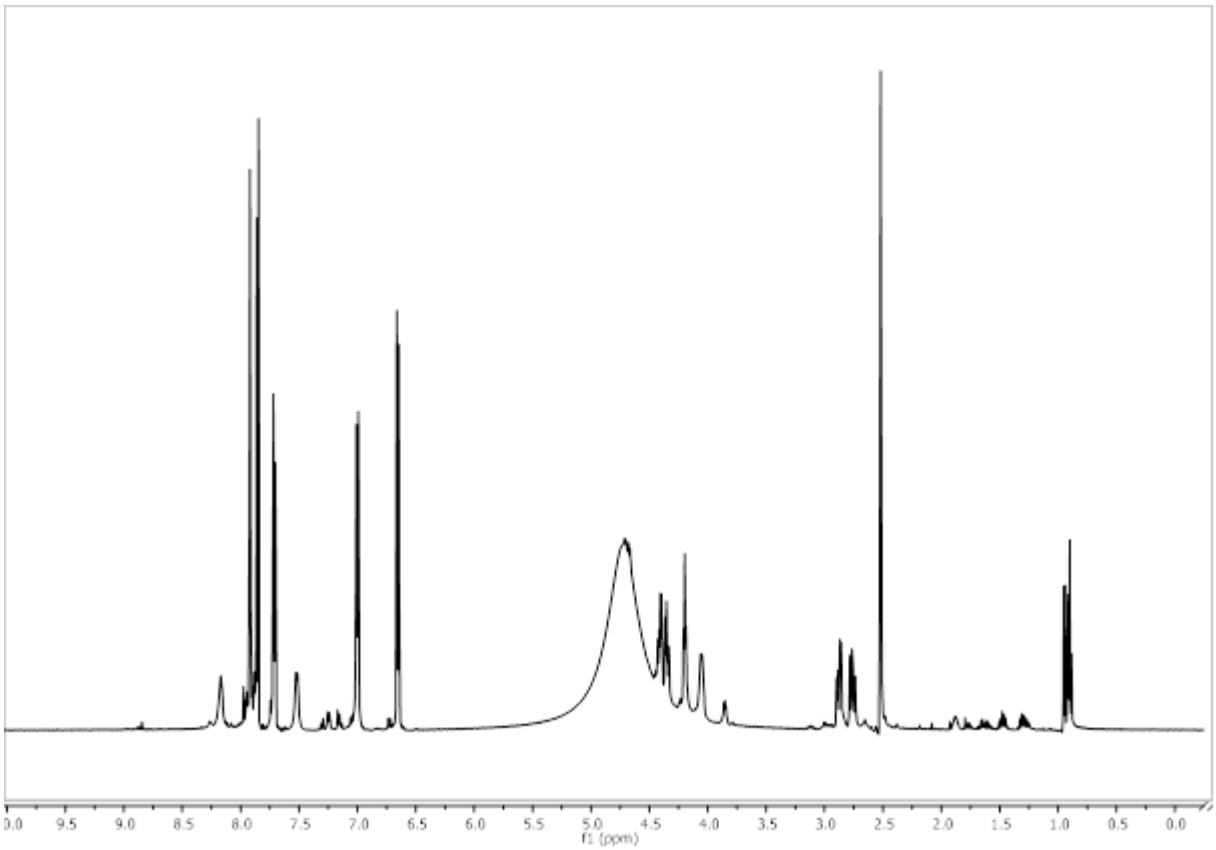

Figure 308: ^{1}H-NMR of Smoc-L-Tyr-OH **28**.

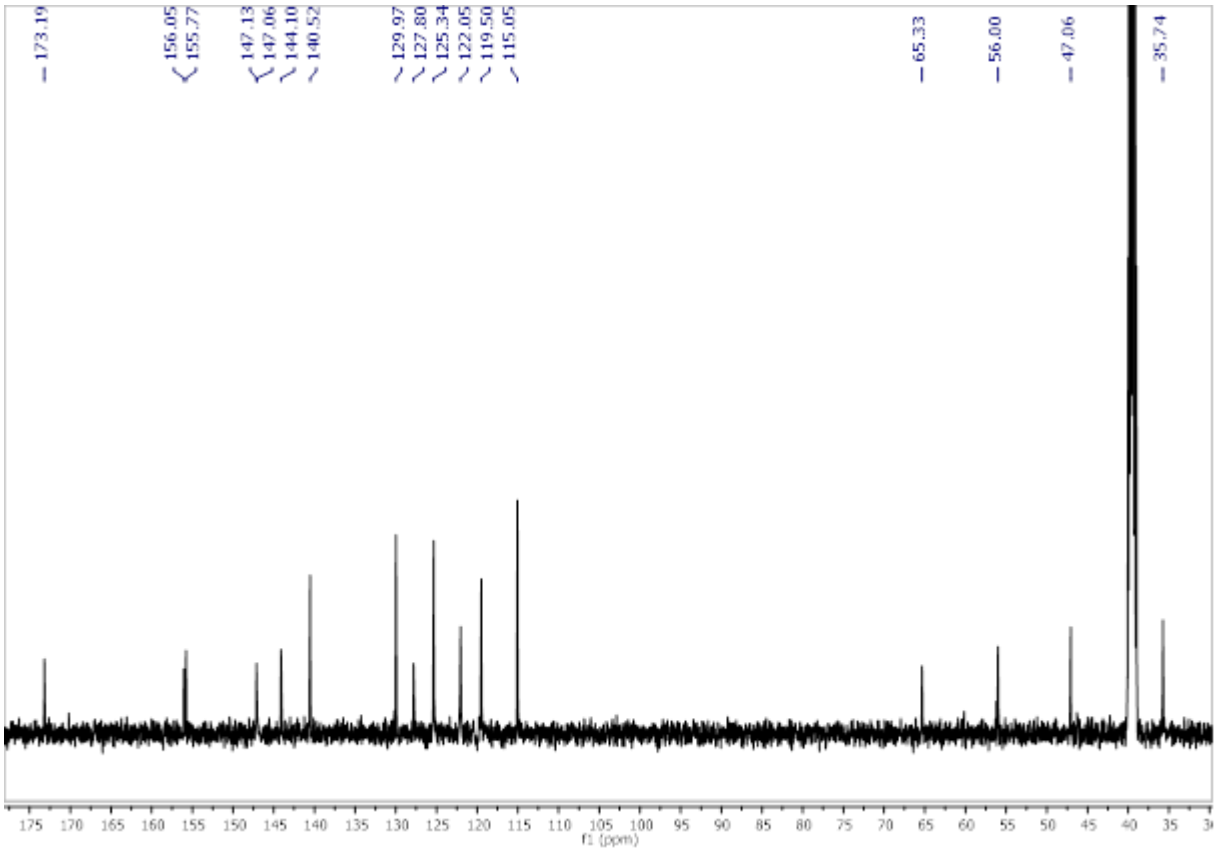

Figure 309: ^{13}C-NMR of Smoc-L-Tyr-OH **28**.

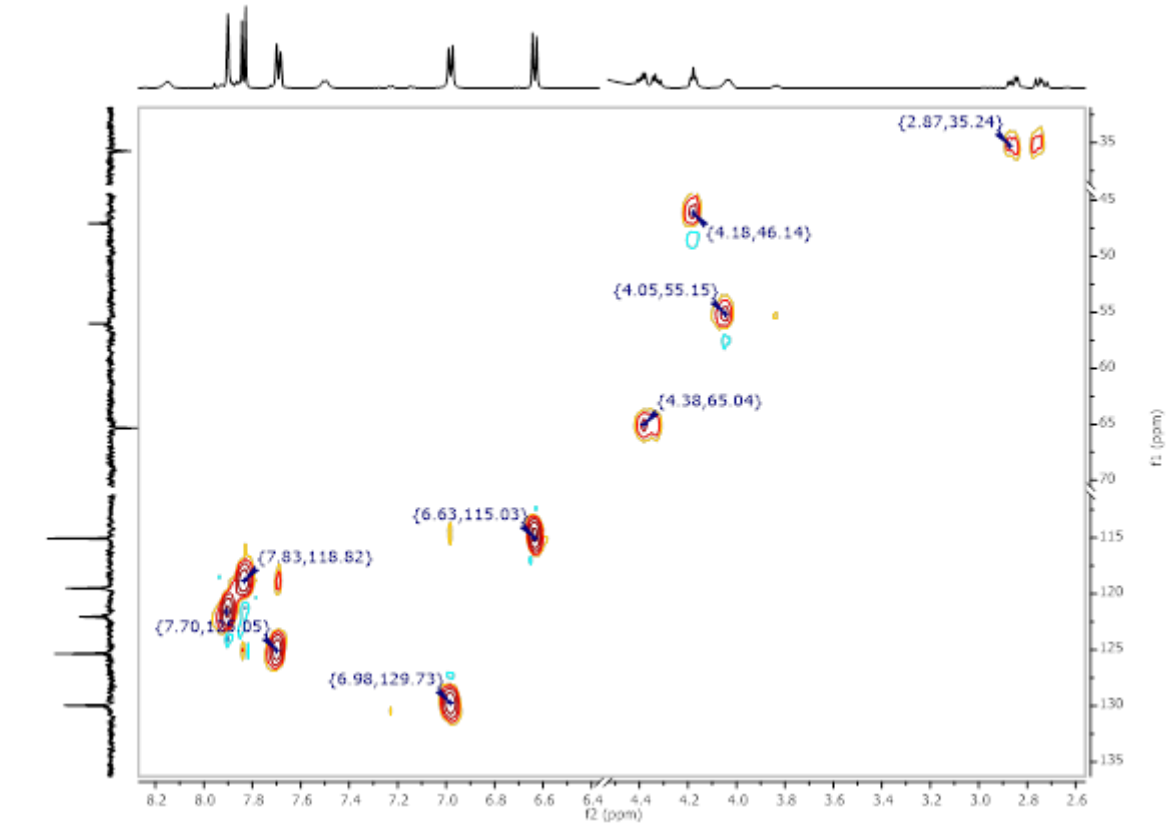

Figure 310: ^{1}H-^{13}C HSQC-NMR of Smoc-L-Tyr-OH **28**.

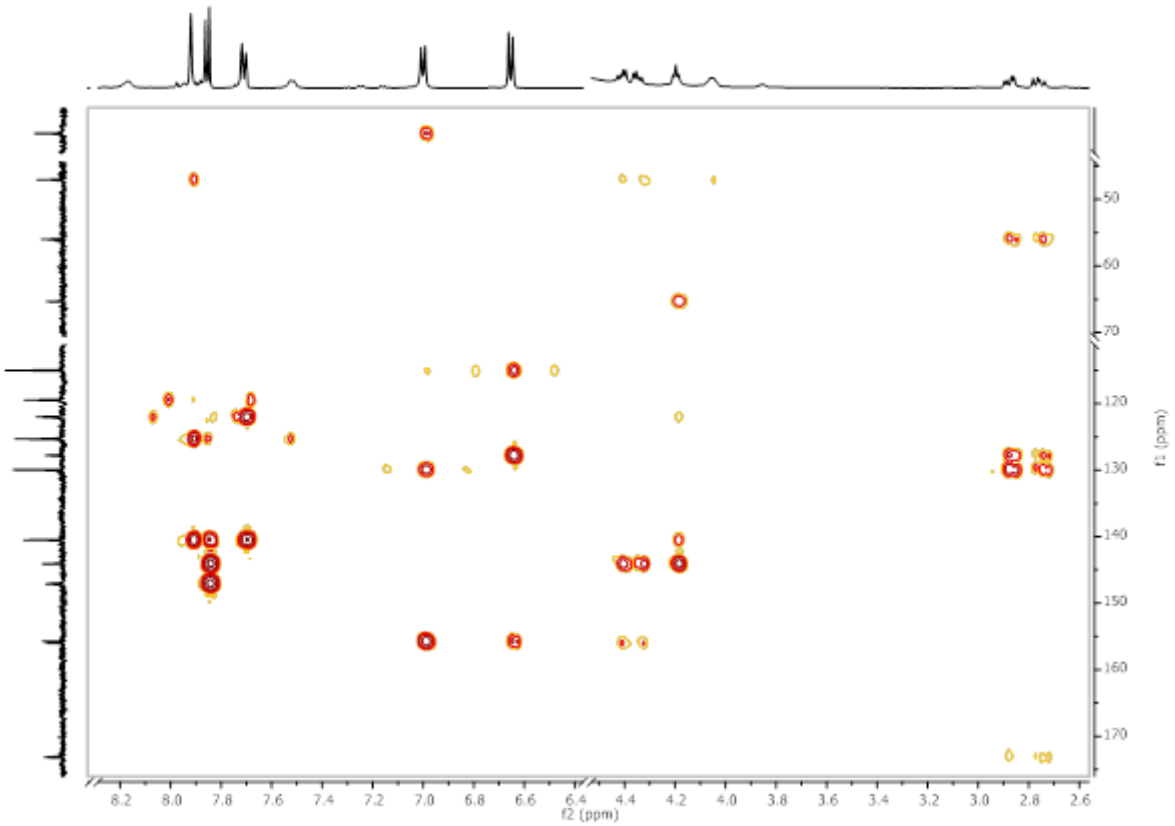

Figure 311: ^{1}H-^{13}C HMBC-NMR of Smoc-L-Tyr-OH **28**.

8.2.27.Analytical data of Smoc-L-Tyr(tBu)-OH 29

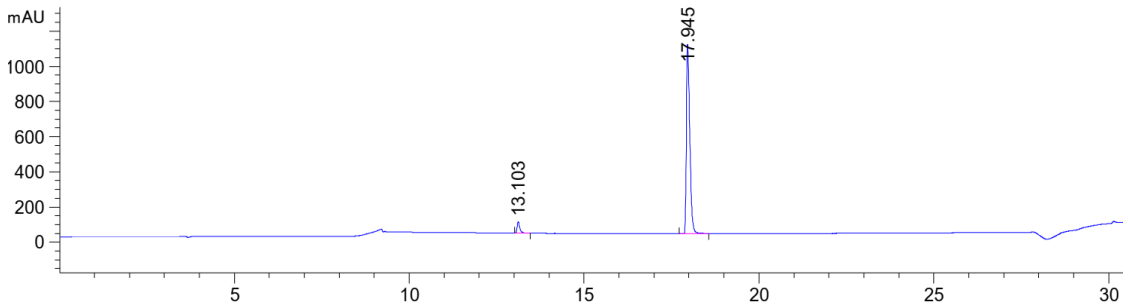

Figure 312: HPLC chromatogram of Smoc-L-Tyr(tBu)-OH **29** at λ=220 nm (0 to 60% MeCN).

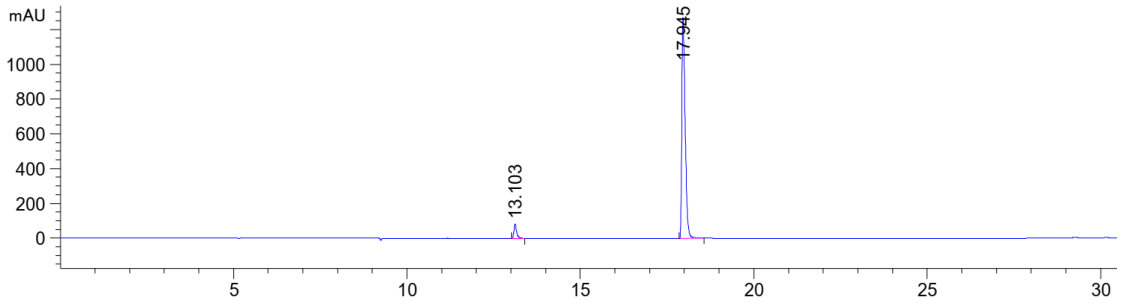

Figure 313: HPLC chromatogram of Smoc-L-Tyr(tBu)-OH **29** at λ=280 nm (0 to 60% MeCN).

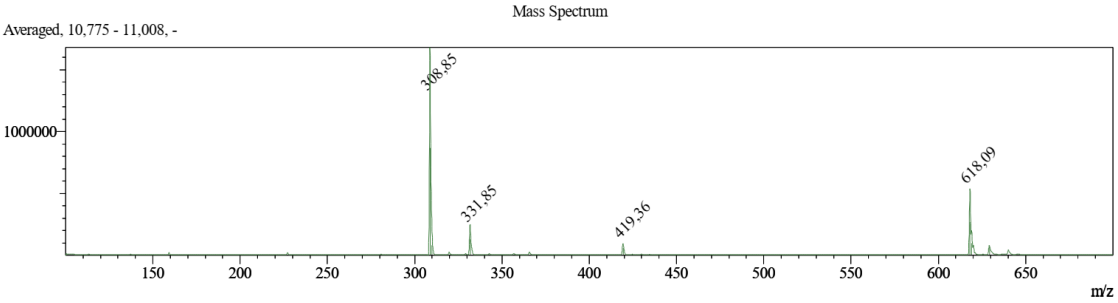

Figure 314: ESI-MS of Smoc-L-Tyr(tBu)-OH **29** (M measured=618.09 $[M-H]^-$, M calc.=619.66).

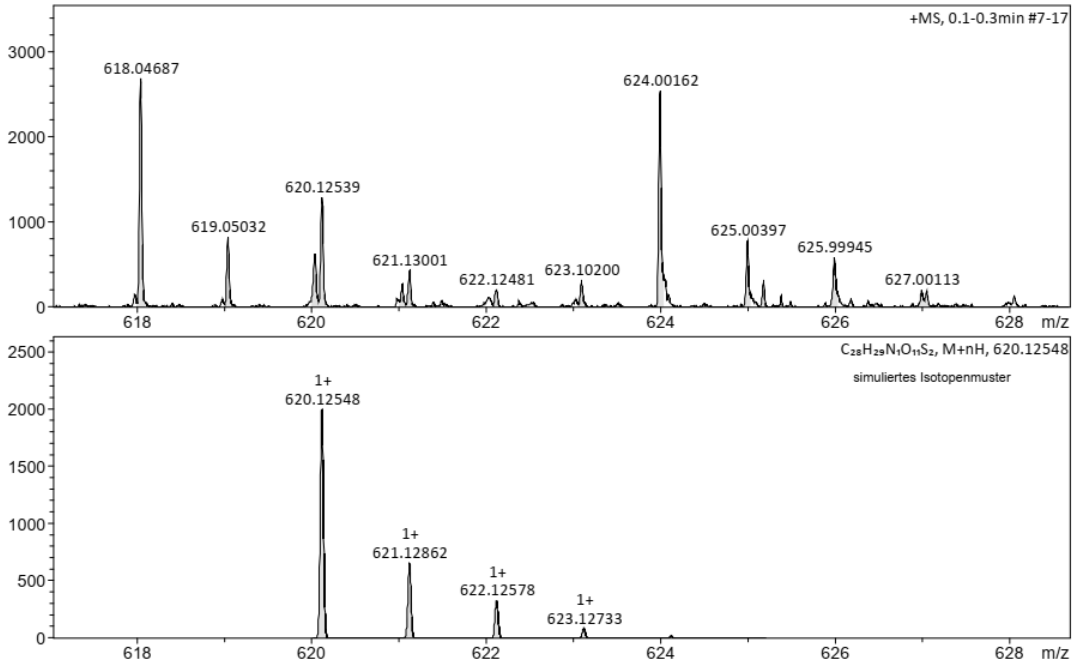

Figure 315: HR-MS of Smoc-L-Tyr(tBu)-OH **29** (M measured=620.12539 $[M+H]^+$, M calc.=620.12548).

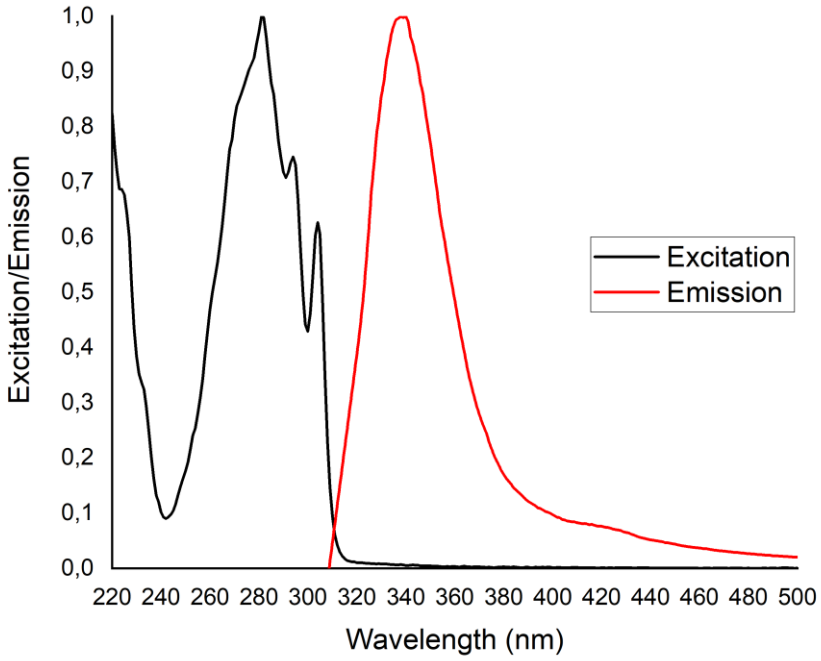

Figure 316: Excitation and emission spectra of Smoc-L-Tyr(tBu)-OH **29**, excitation and emission have been normalized between 0 and 1 for illustration.

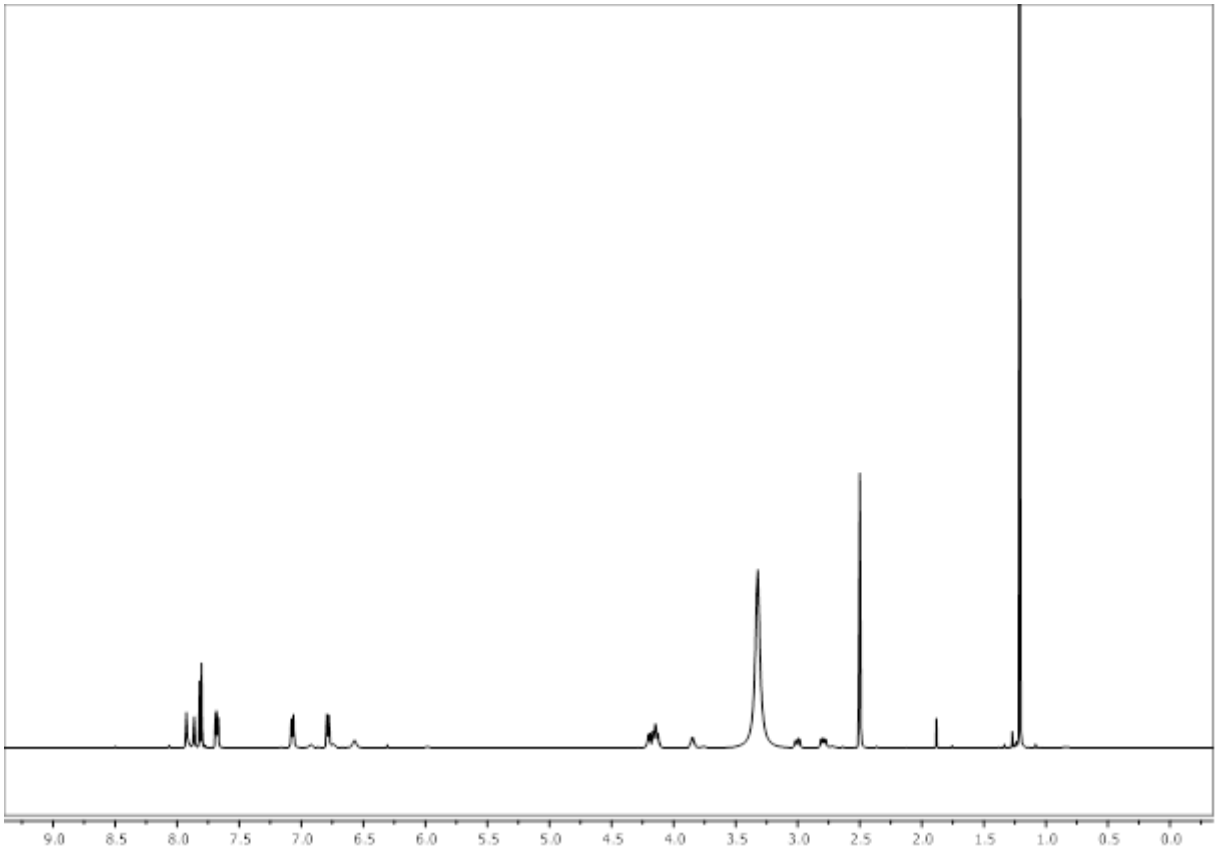

Figure 317: ^{1}H-NMR of Smoc-L-Tyr(tBu)-OH **29**.

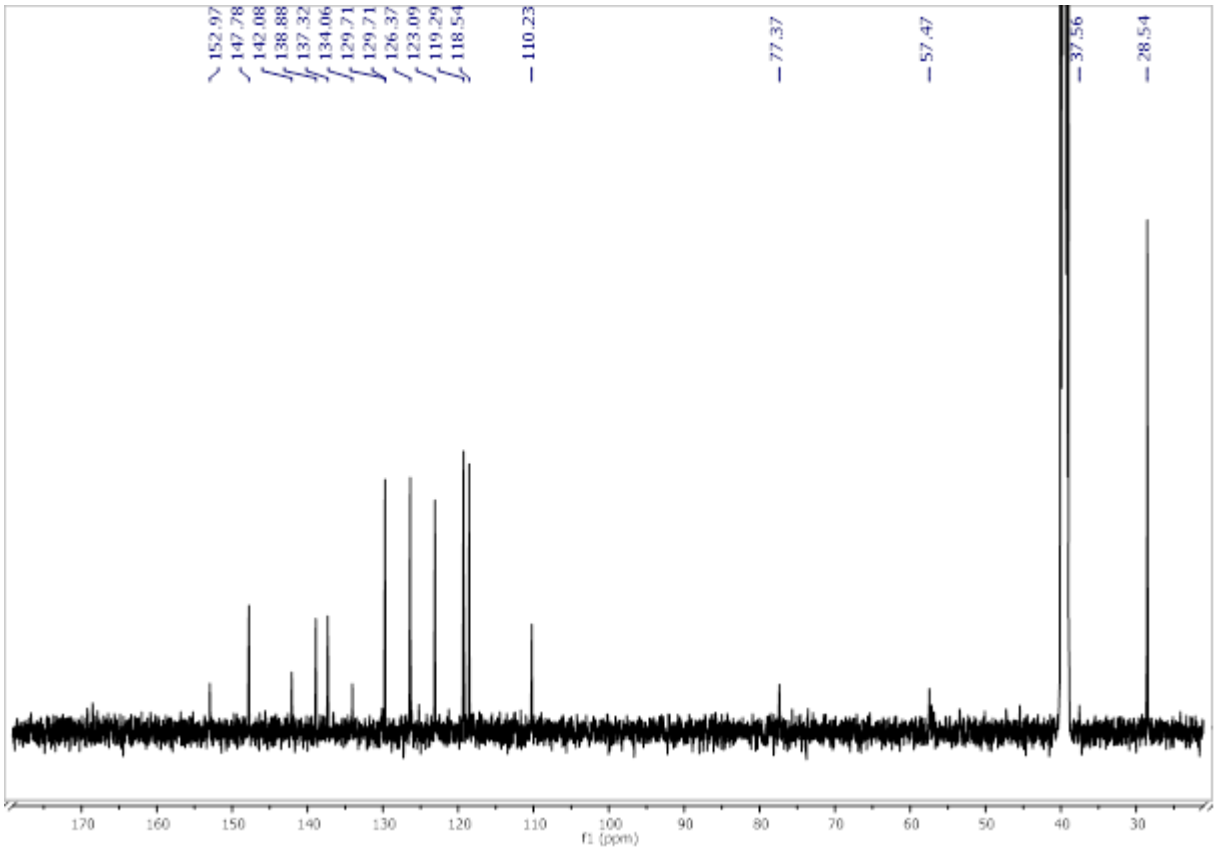

Figure 318: ^{13}C-NMR of Smoc-L-Tyr(tBu)-OH **29**.

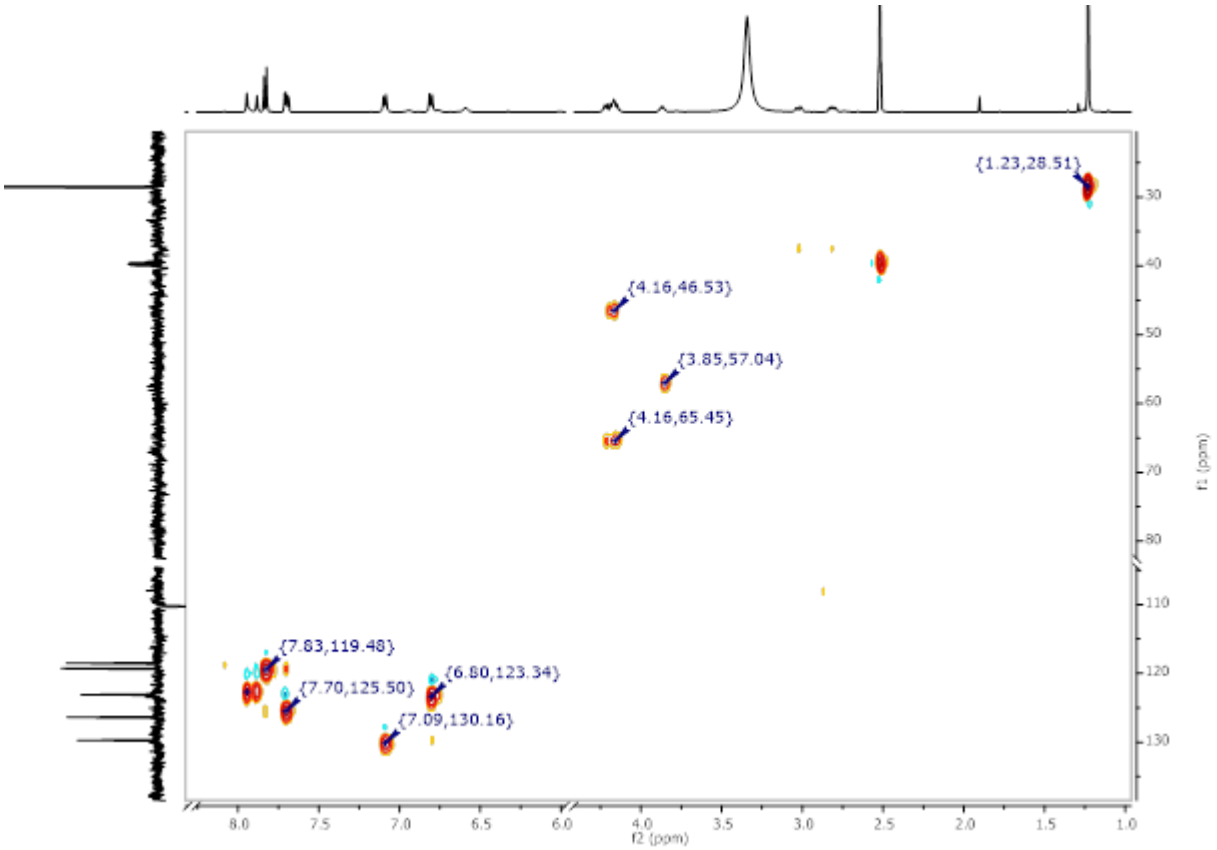

Figure 319: ^{1}H-^{13}C HSQC-NMR of Smoc-L-Tyr(tBu)-OH **29**.

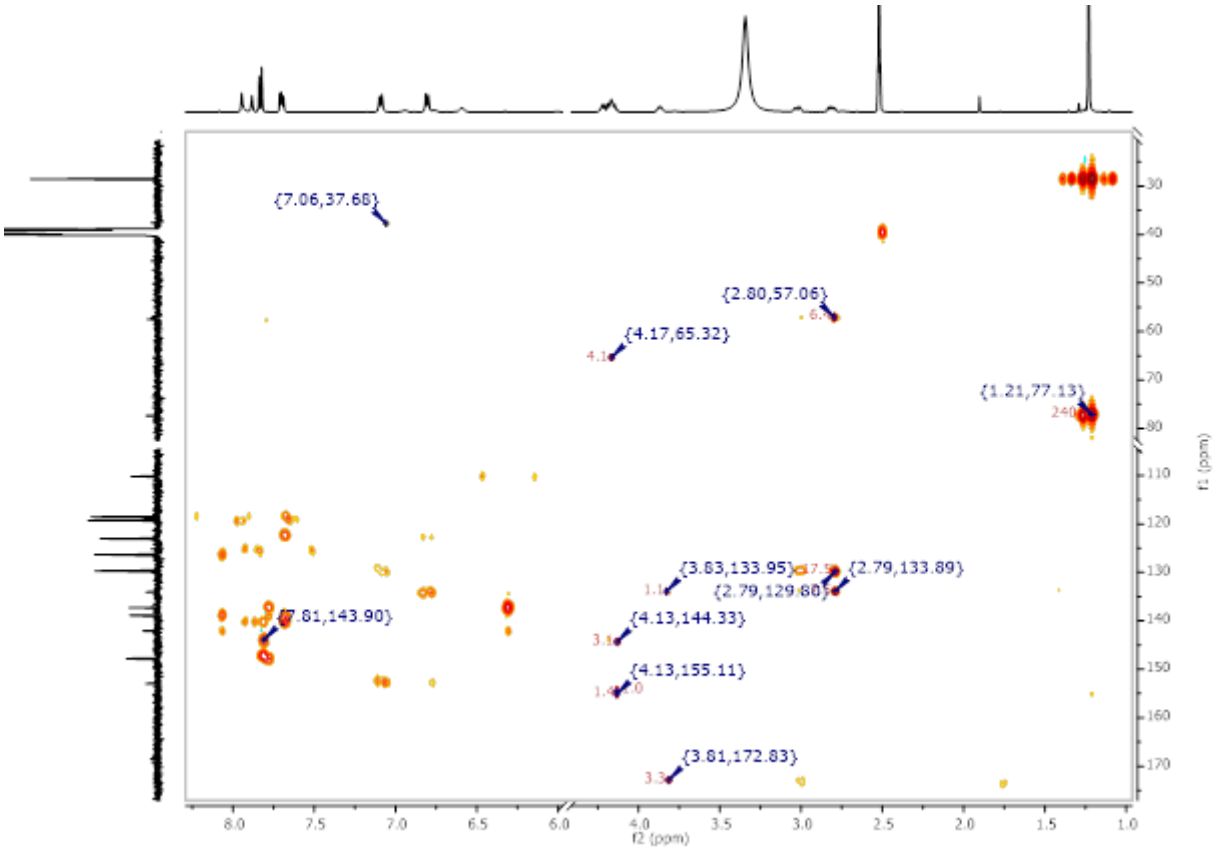

Figure 320: ^{1}H-^{13}C HMBC-NMR of Smoc-L-Tyr(tBu)-OH **29**.

8.2.28.Analytical data of Smoc-L-Val-OH 30

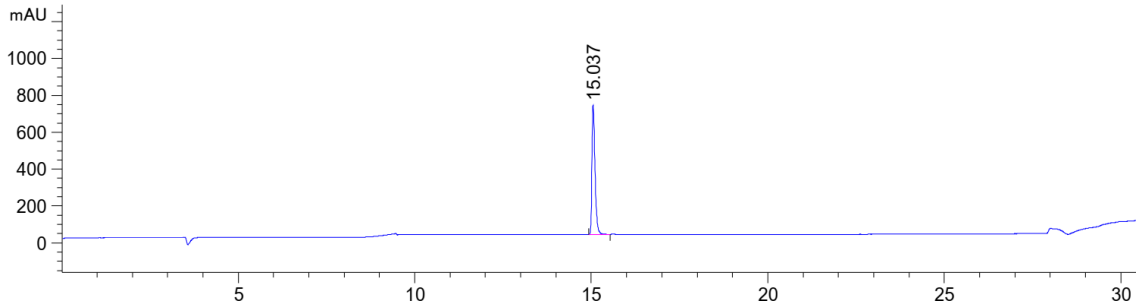

Figure 321: HPLC chromatogram of Smoc-L-Val-OH **30** at λ=220 nm (0 to 40% MeCN).

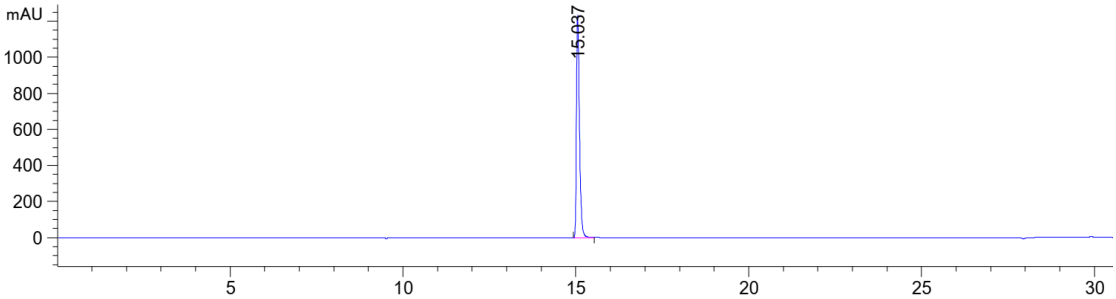

Figure 322: HPLC chromatogram of Smoc-L-Val-OH **30** at λ=280 nm (0 to 40% MeCN).

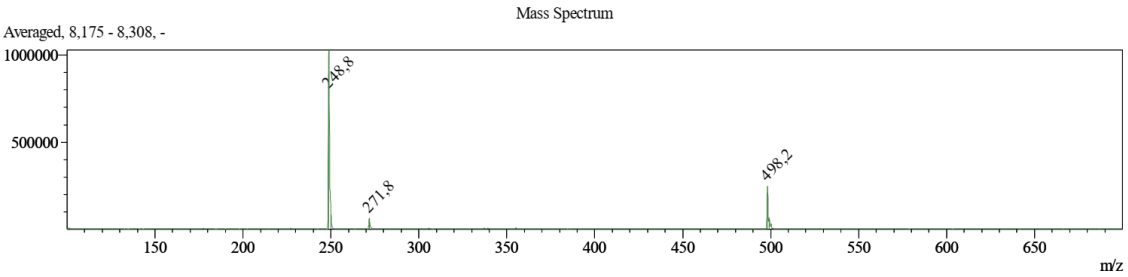

Figure 323: ESI-MS of Smoc-L-Val-OH **30** (M measured=498.20 $[M-H]^-$, M calc.=499.51).

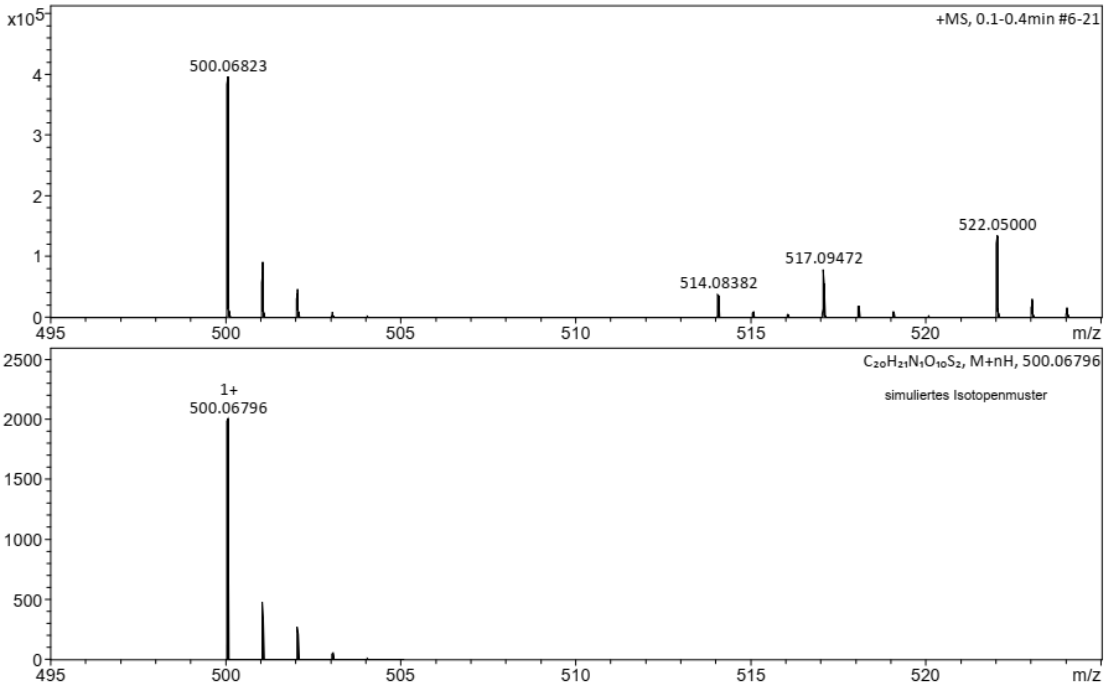

Figure 324: HR-MS of Smoc-L-Val-OH **30** (M measured=500.06823 $[M+H]^+$, M calc.=500.06796).

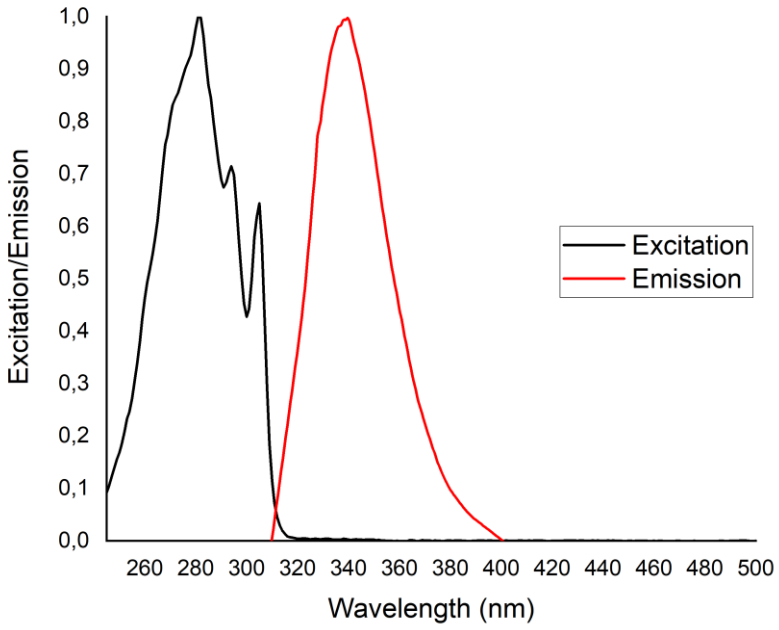

Figure 325: Excitation and emission spectra of Smoc-L-Val-OH **30**, excitation and emission have been normalized between 0 and 1 for illustration.

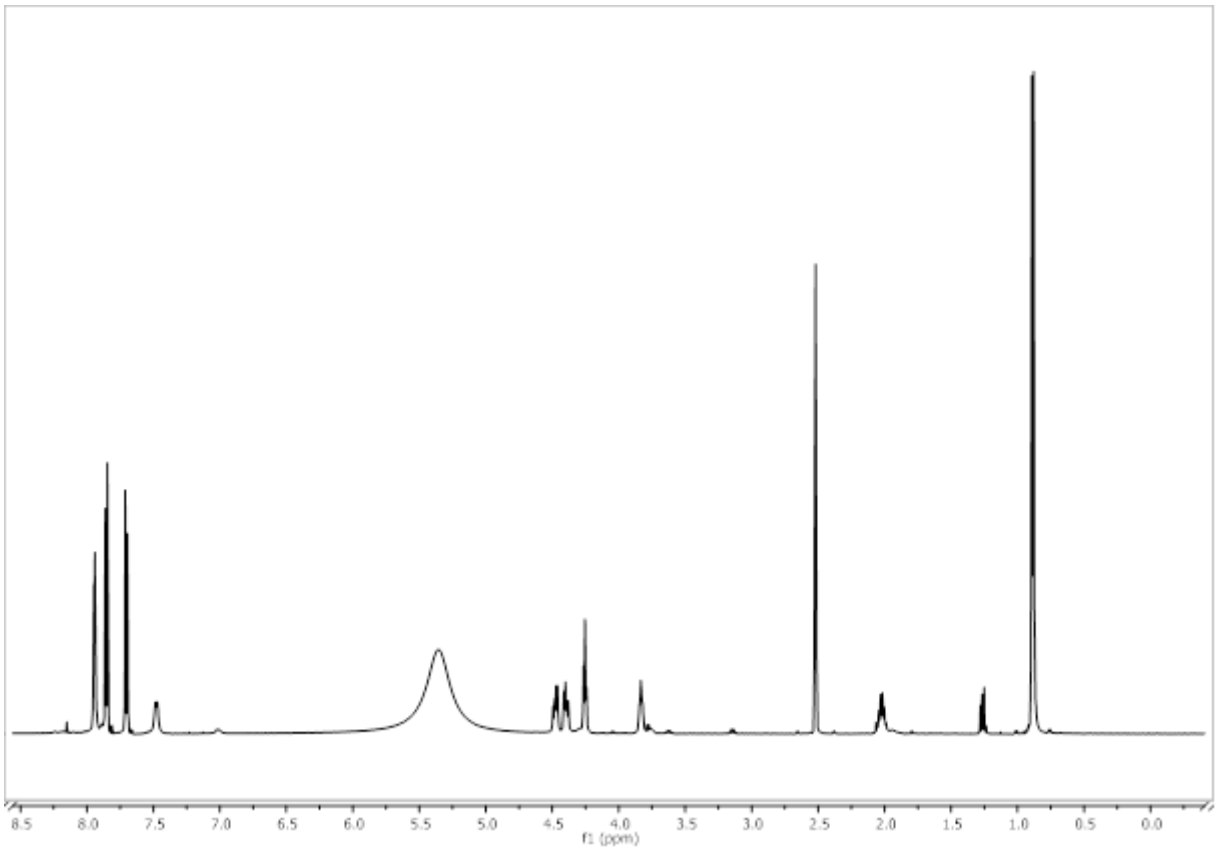

Figure 326: ^{1}H-NMR of Smoc-L-Val-OH **30**.

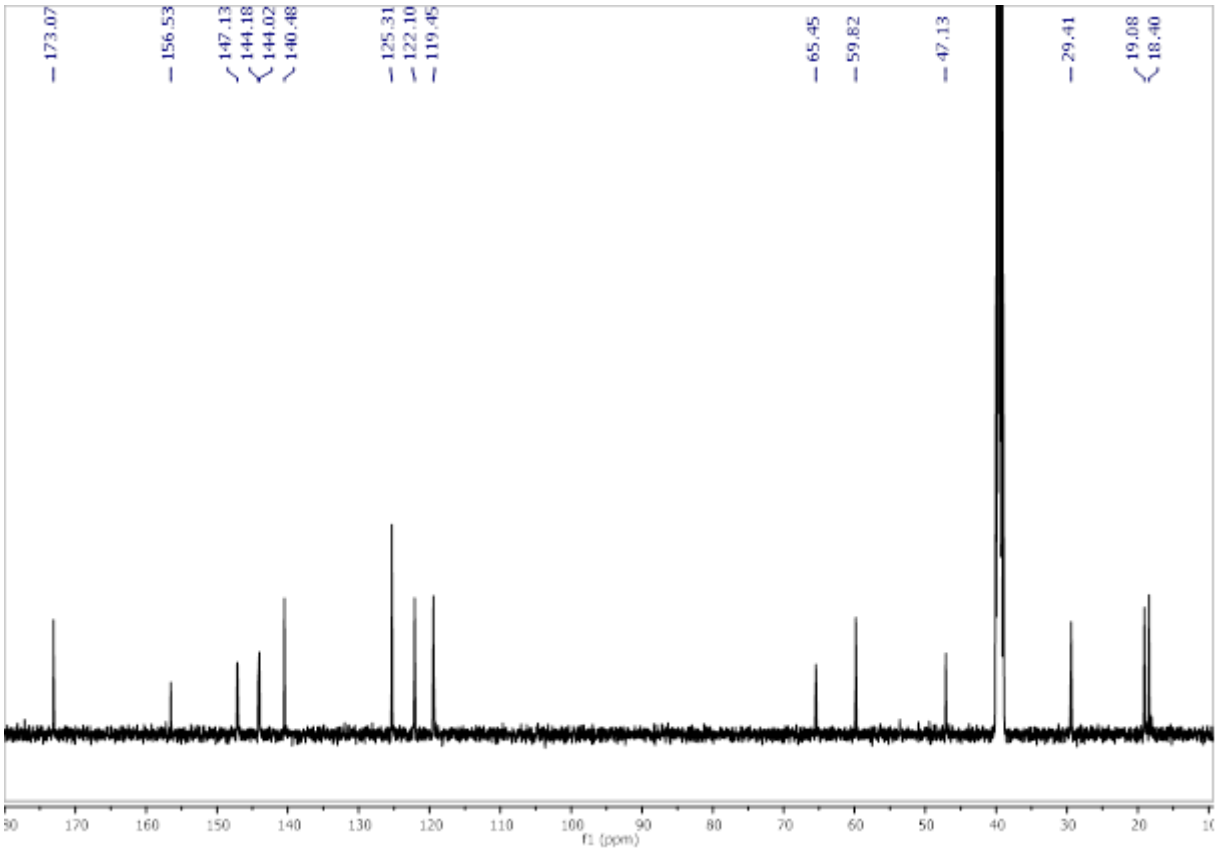

Figure 327: ^{13}C-NMR of Smoc-L-Val-OH **30**.

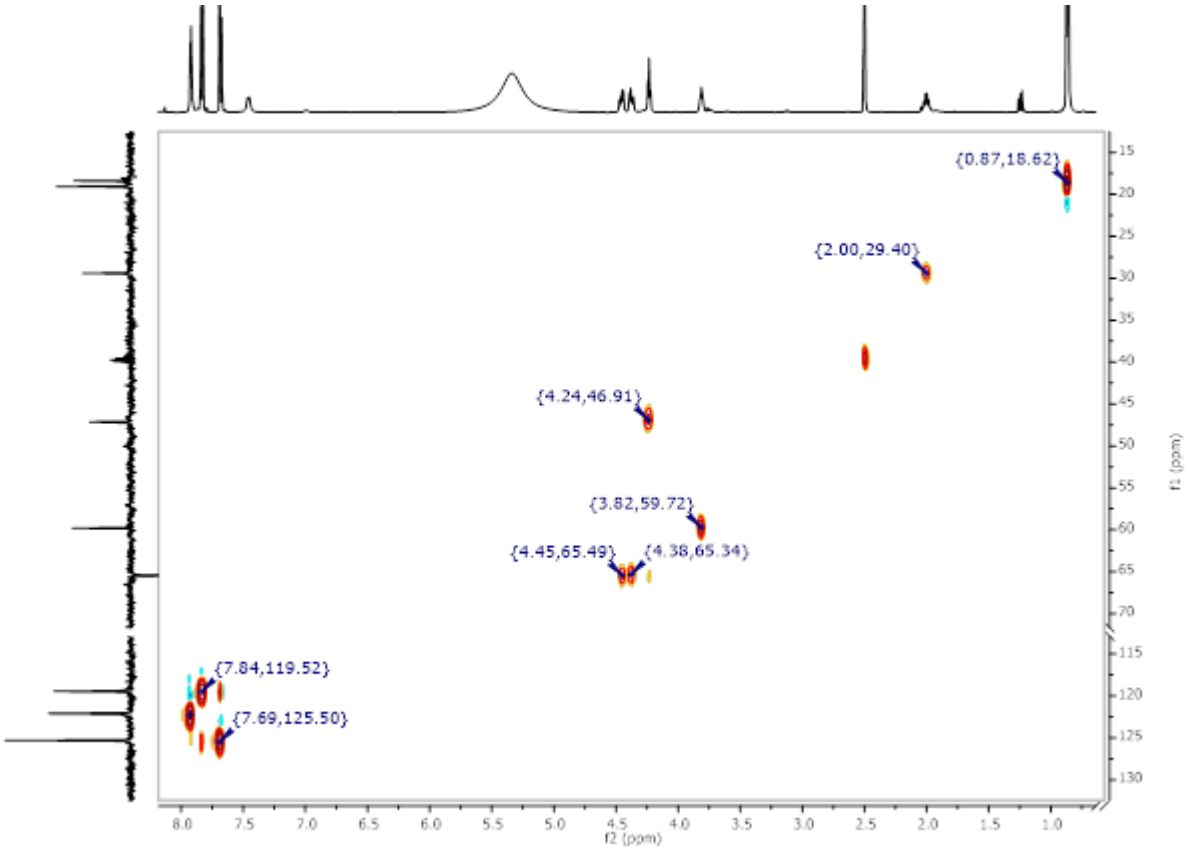

Figure 328: ^{1}H-^{13}C HSQC-NMR of Smoc-L-Val-OH **30**.

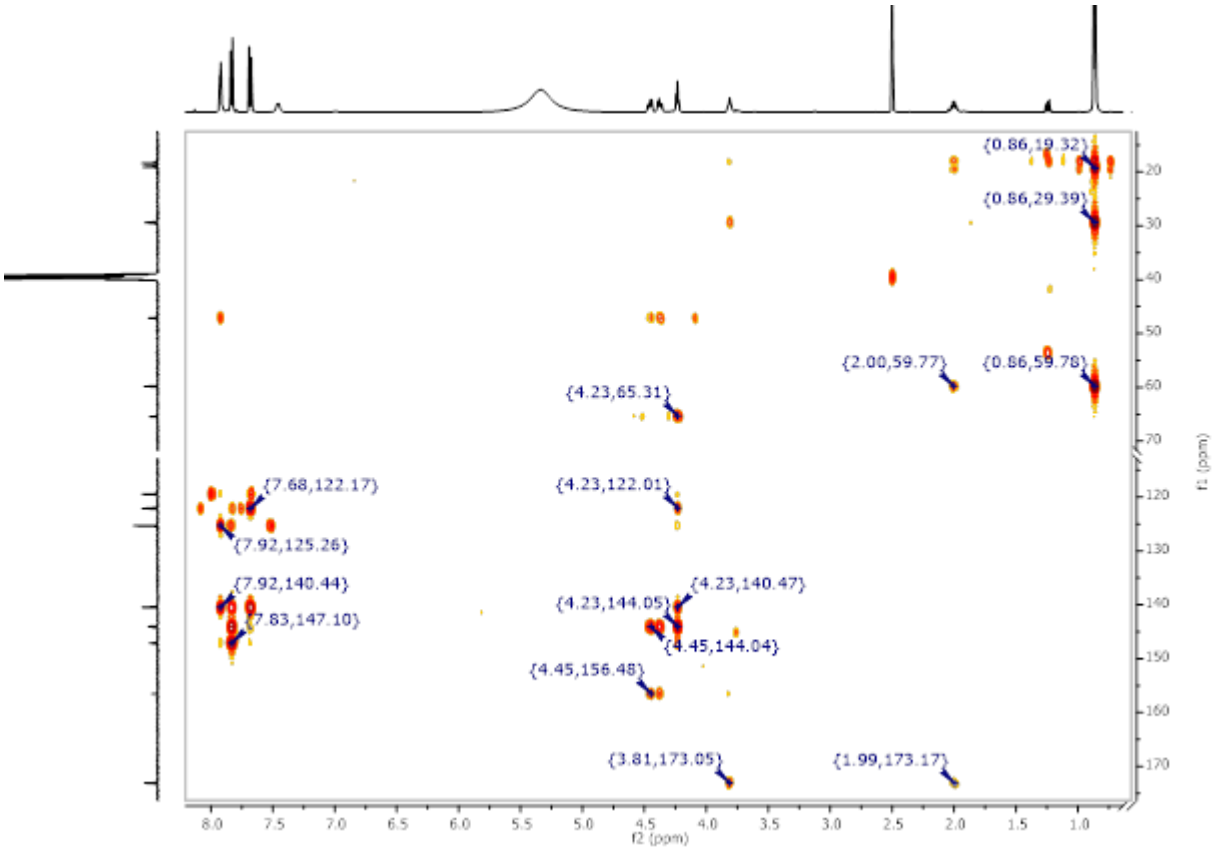

Figure 329: ^{1}H-^{13}C HMBC-NMR of Smoc-L-Val-OH **30**.

8.2.29.Analytical data of Smoc-β-Ala-OH 31

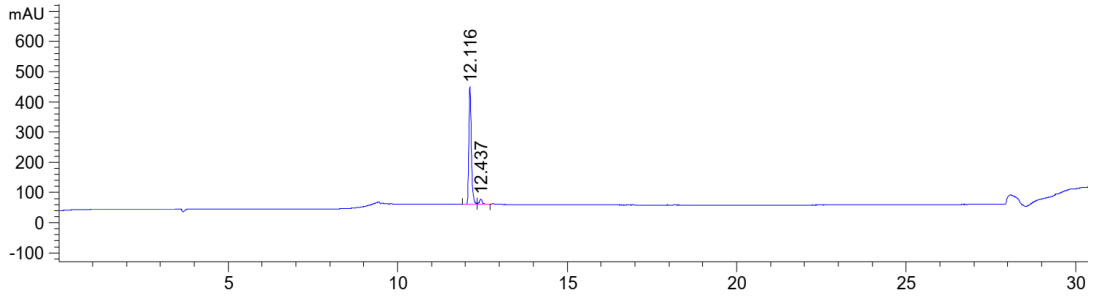

Figure 330: HPLC chromatogram of Smoc-β-Ala-OH **31** at λ=220 nm (0 to 40% MeCN).

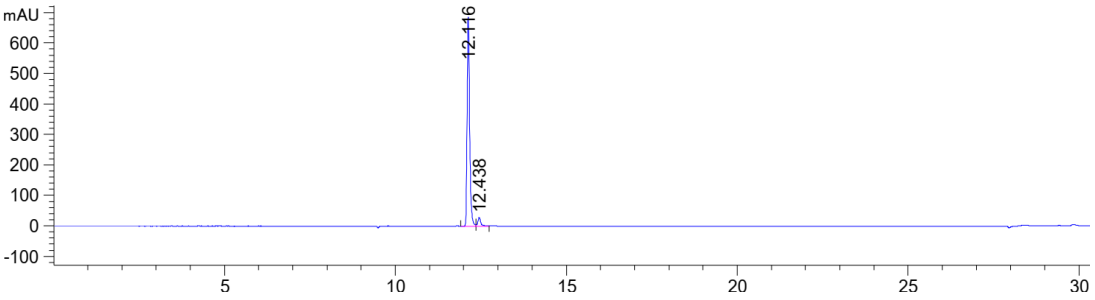

Figure 331: HPLC chromatogram of Smoc-β-Ala-OH **31** at λ=280 nm (0 to 40% MeCN).

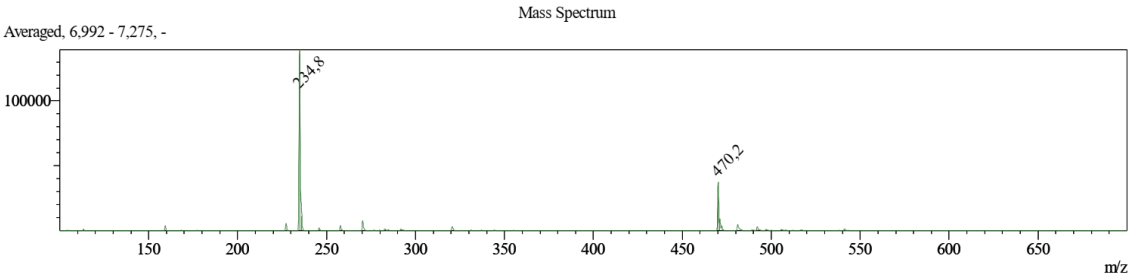

Figure 332: ESI-MS of Smoc-β-Ala-OH **31** (M measured=470.20 [M-H]$^-$, M calc.=471.45).

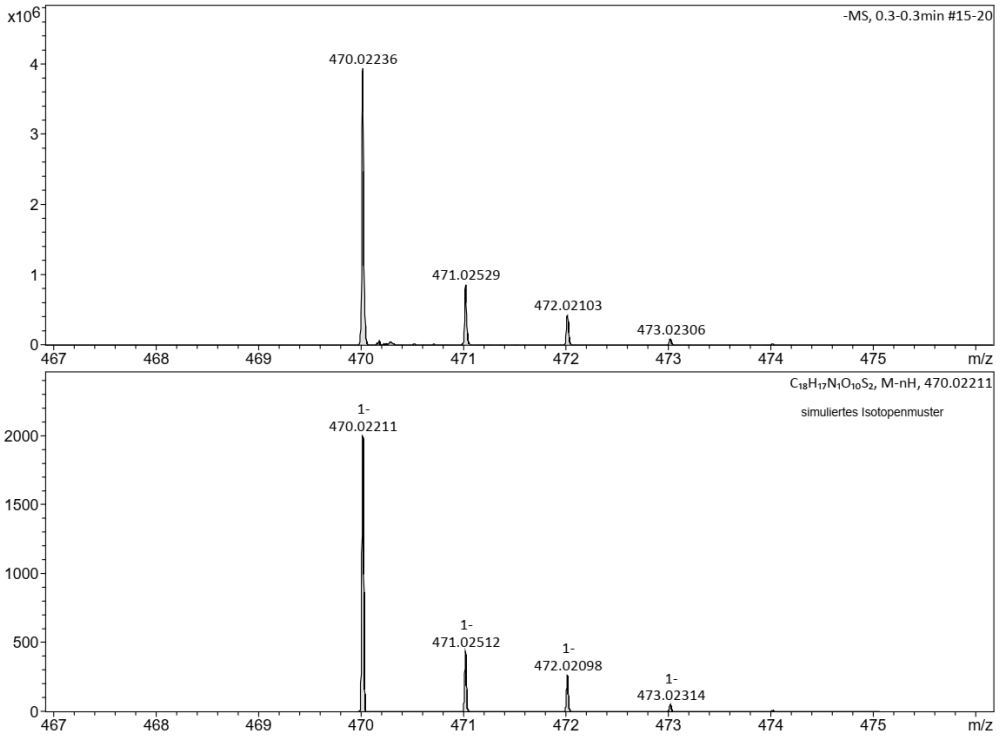

Figure 333: HR-MS of Smoc-β-Ala-OH **31** (M measured=470.02236 [M-H]$^-$, M calc.=470.02211).

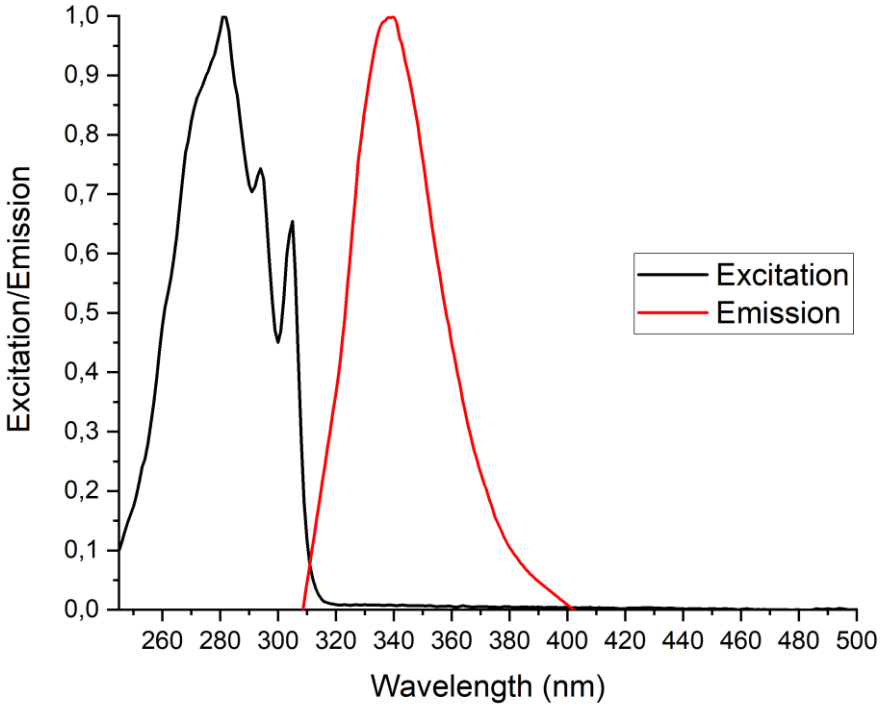

Figure 334: Excitation and emission spectra of Smoc-β-Ala-OH **31**, excitation and emission have been normalized between 0 and 1 for illustration.

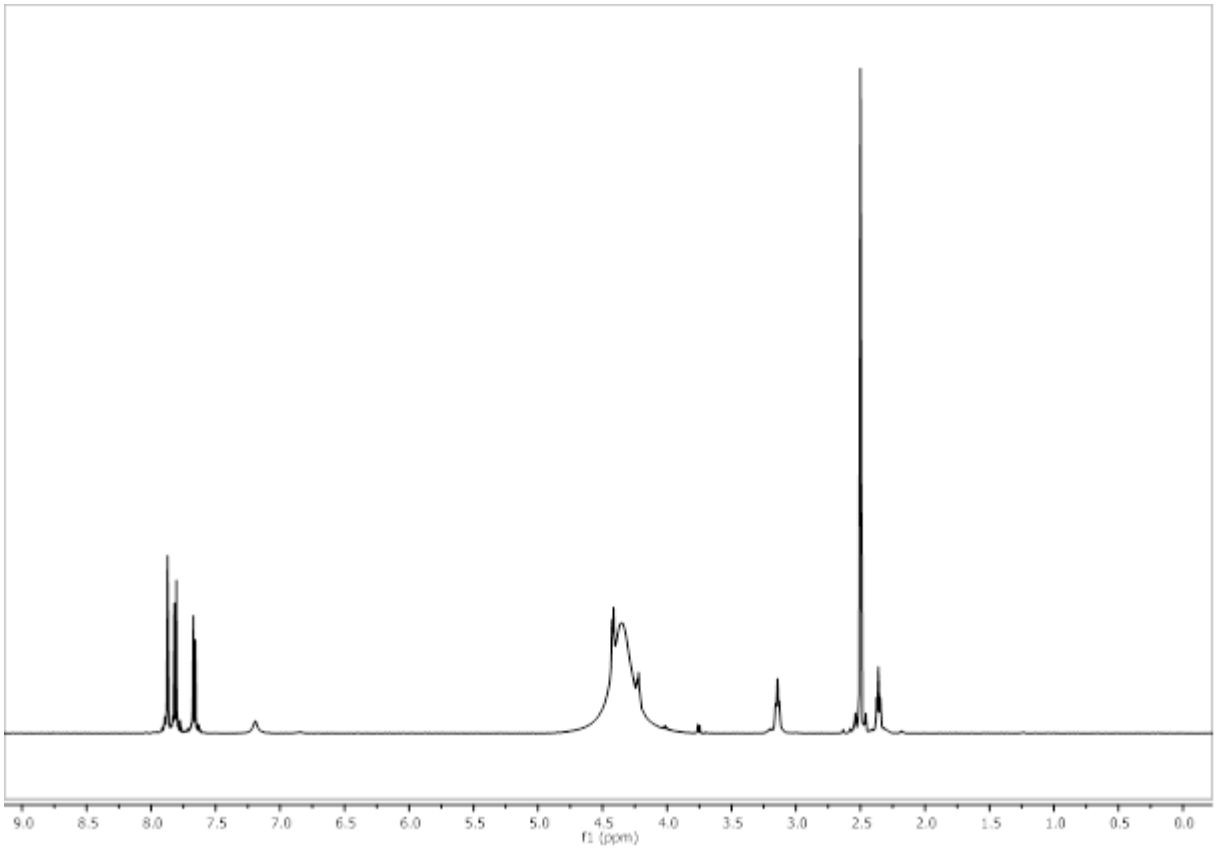

Figure 335: ^{1}H-NMR of Smoc-β-Ala-OH **31**.

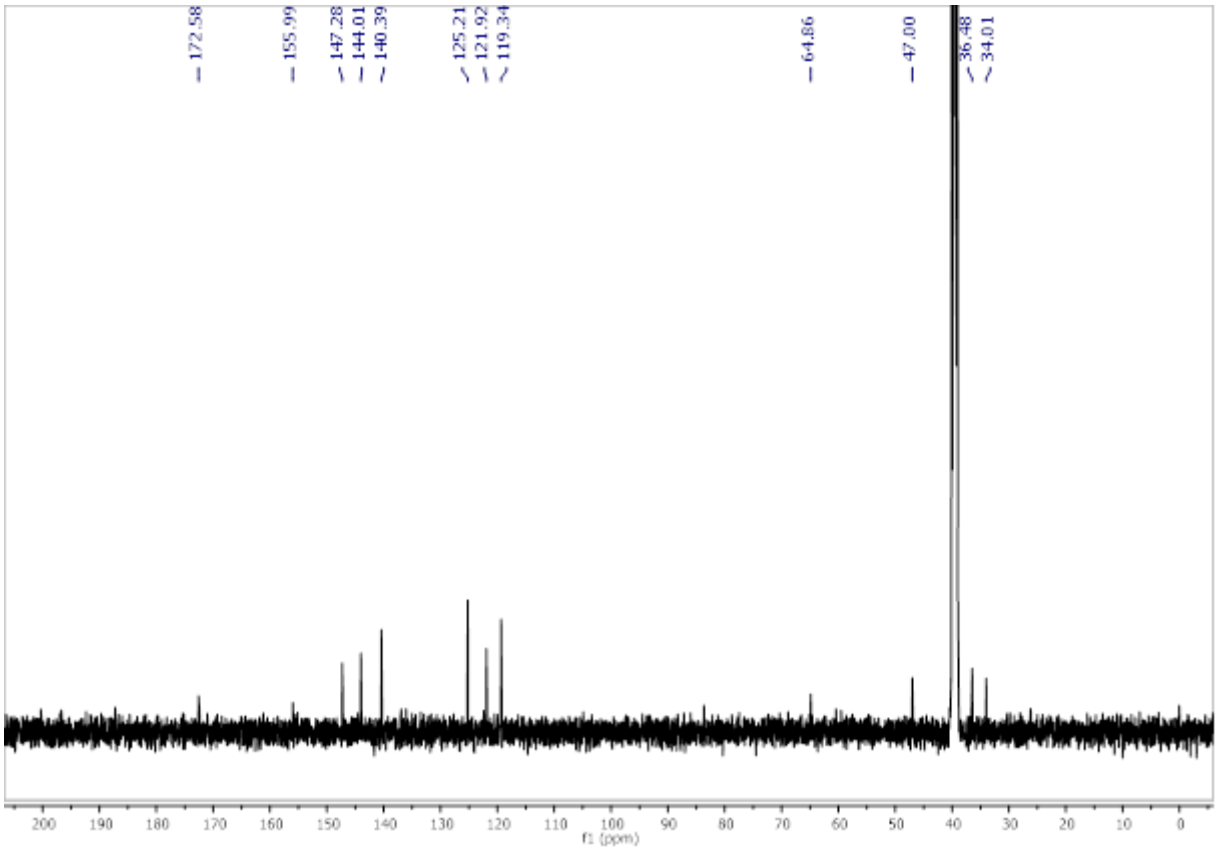

Figure 336: ^{13}C-NMR of Smoc-β-Ala-OH **31**.

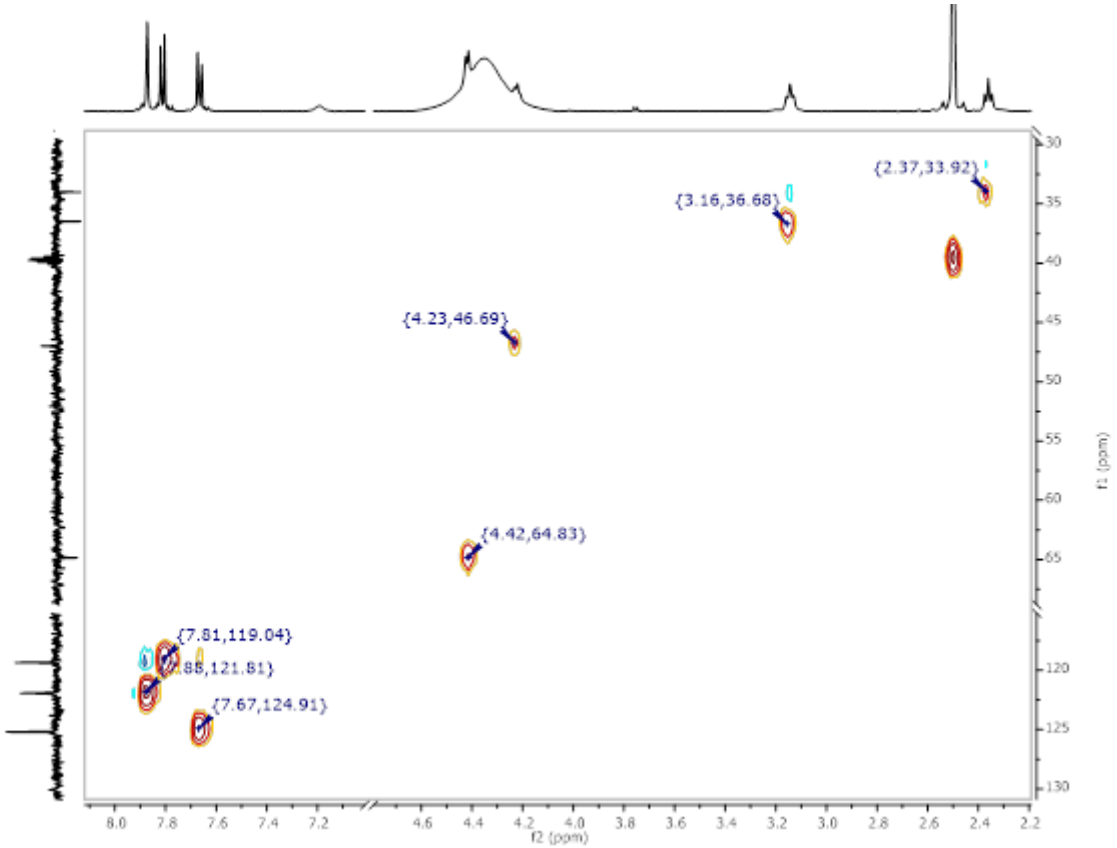

Figure 337: ^{1}H-^{13}C HSQC-NMR of Smoc-β-Ala-OH **31**.

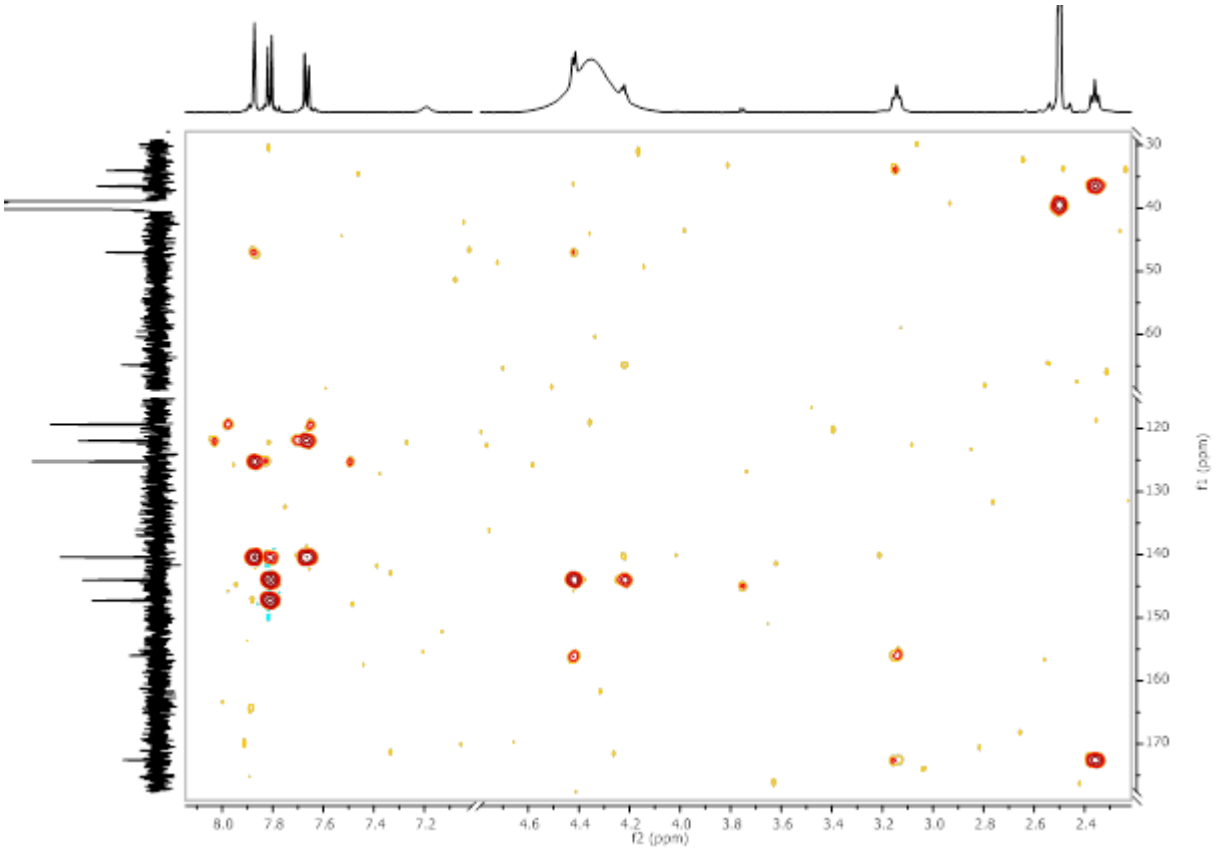

Figure 338: ^{1}H-^{13}C HMBC-NMR of Smoc-β-Ala-OH **31**.

8.2.30.Analytical data of Smoc-Aib-OH 32

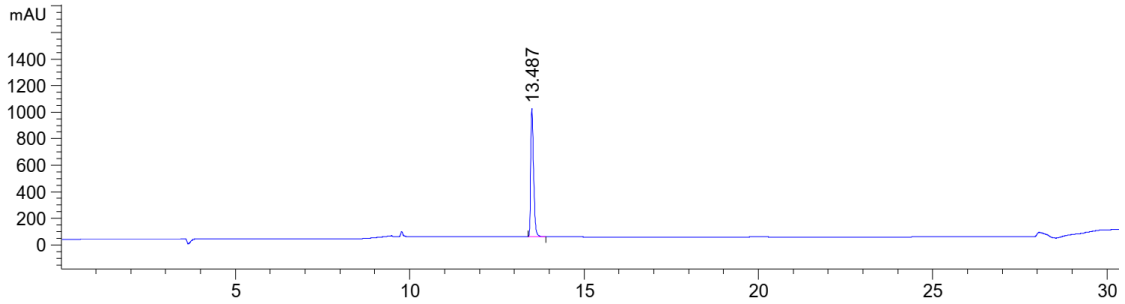

Figure 339: HPLC chromatogram of Smoc-Aib-OH **32** at λ=220 nm (0 to 40% MeCN).

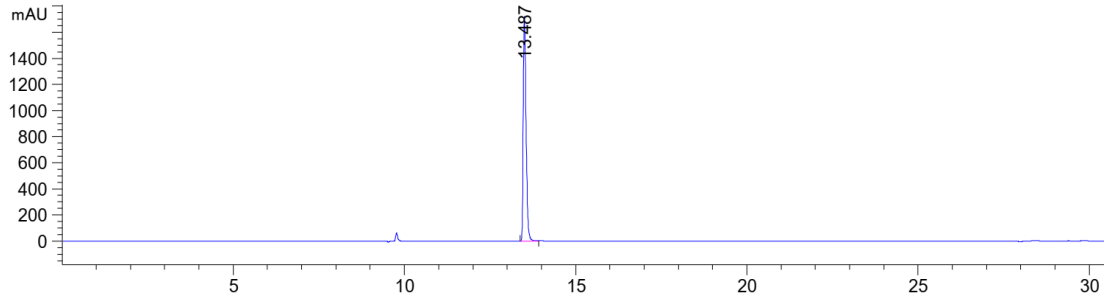

Figure 340: HPLC chromatogram of Smoc-Aib-OH **32** at λ=280 nm (0 to 40% MeCN).

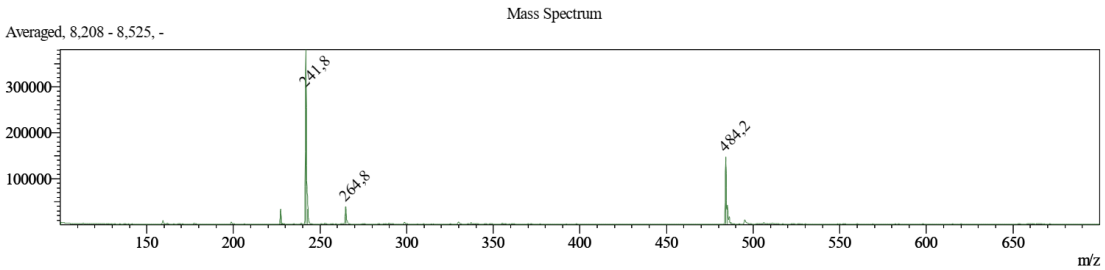

Figure 341: ESI-MS of Smoc-Aib-OH **32** (M measured=484.20 $[M-H]^-$, M calc.=485.48).

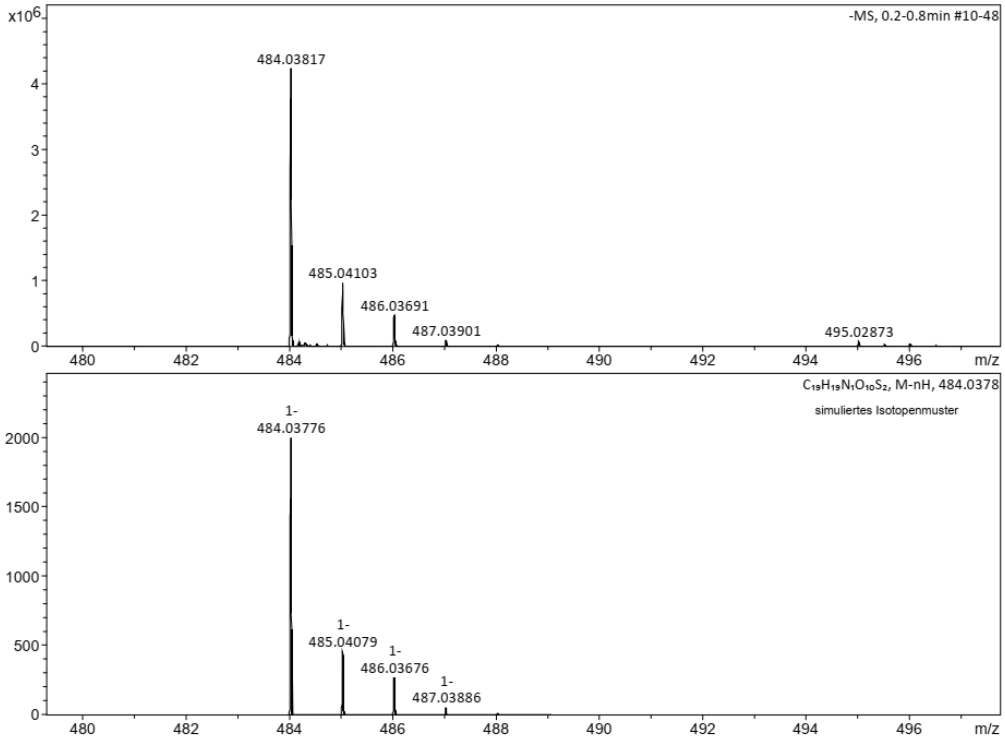

Figure 342: HR-MS of Smoc-Aib-OH **32** (M measured=484.03817 $[M-H]^-$, M calc.=484.03776).

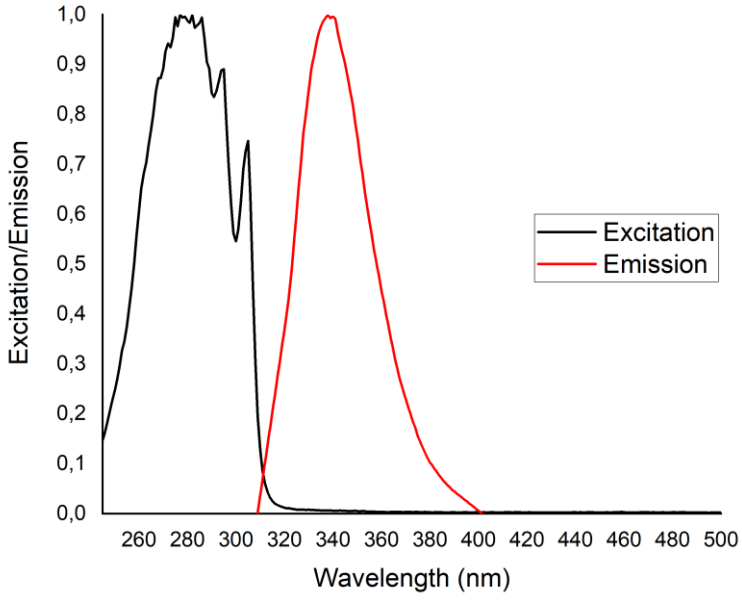

Figure 343: Excitation and emission spectra of Smoc-Aib-OH **32**, excitation and emission have been normalized between 0 and 1 for illustration.

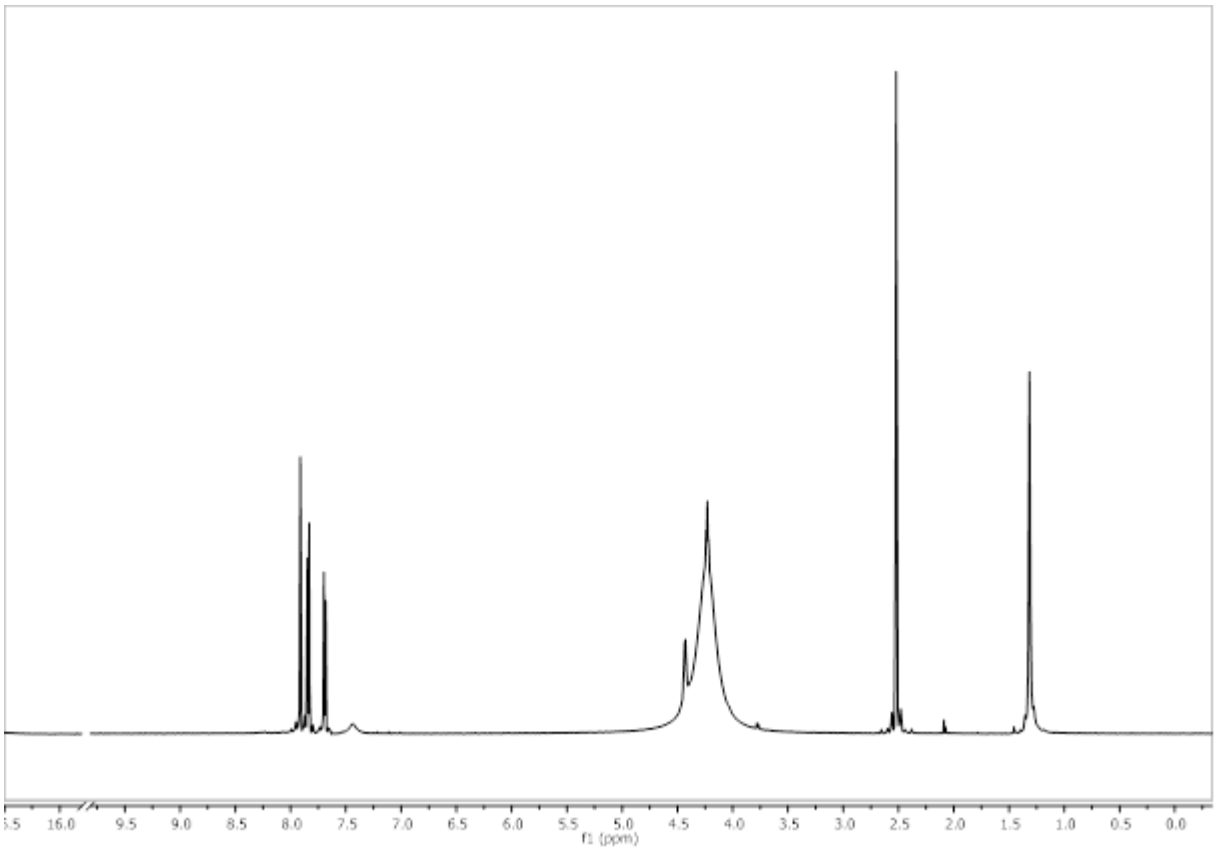

Figure 344: ^{1}H-NMR of Smoc-Aib-OH **32**.

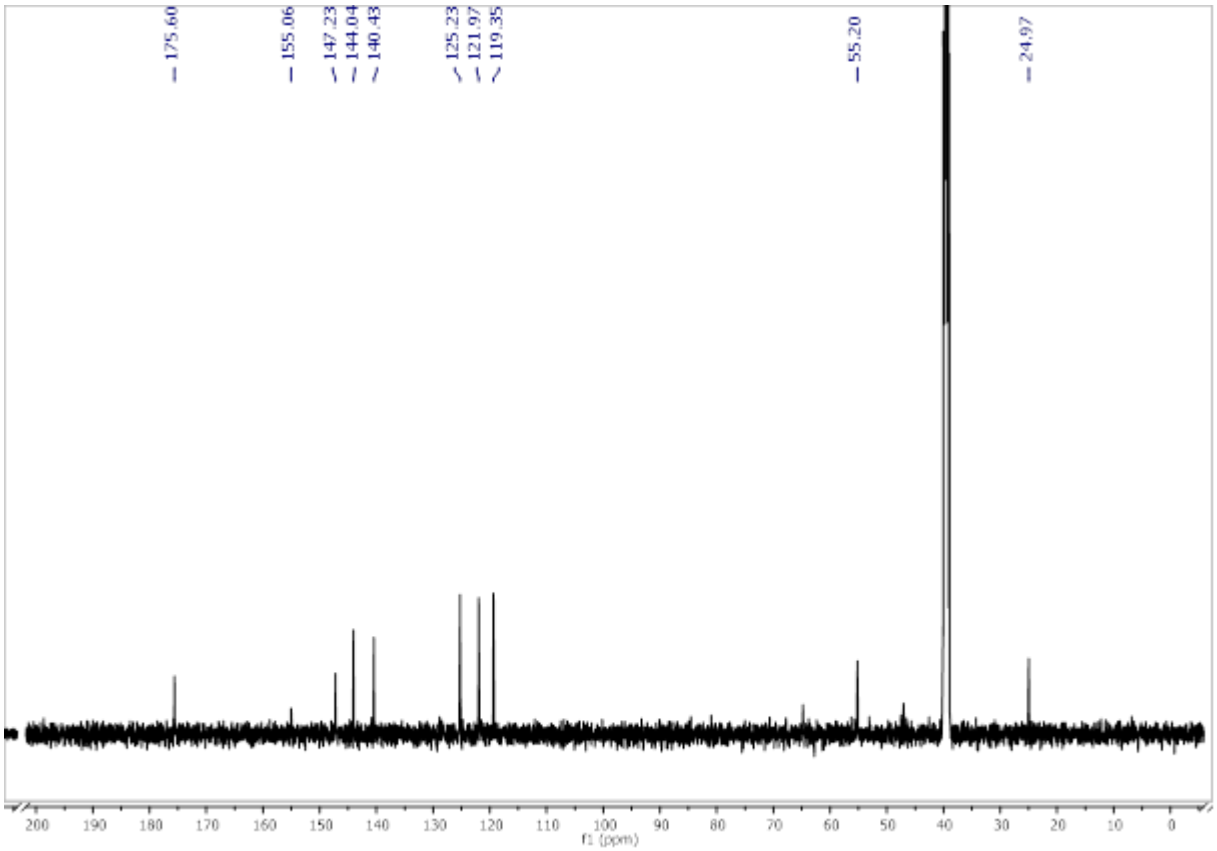

Figure 345: ^{13}C-NMR of Smoc-Aib-OH **32**.

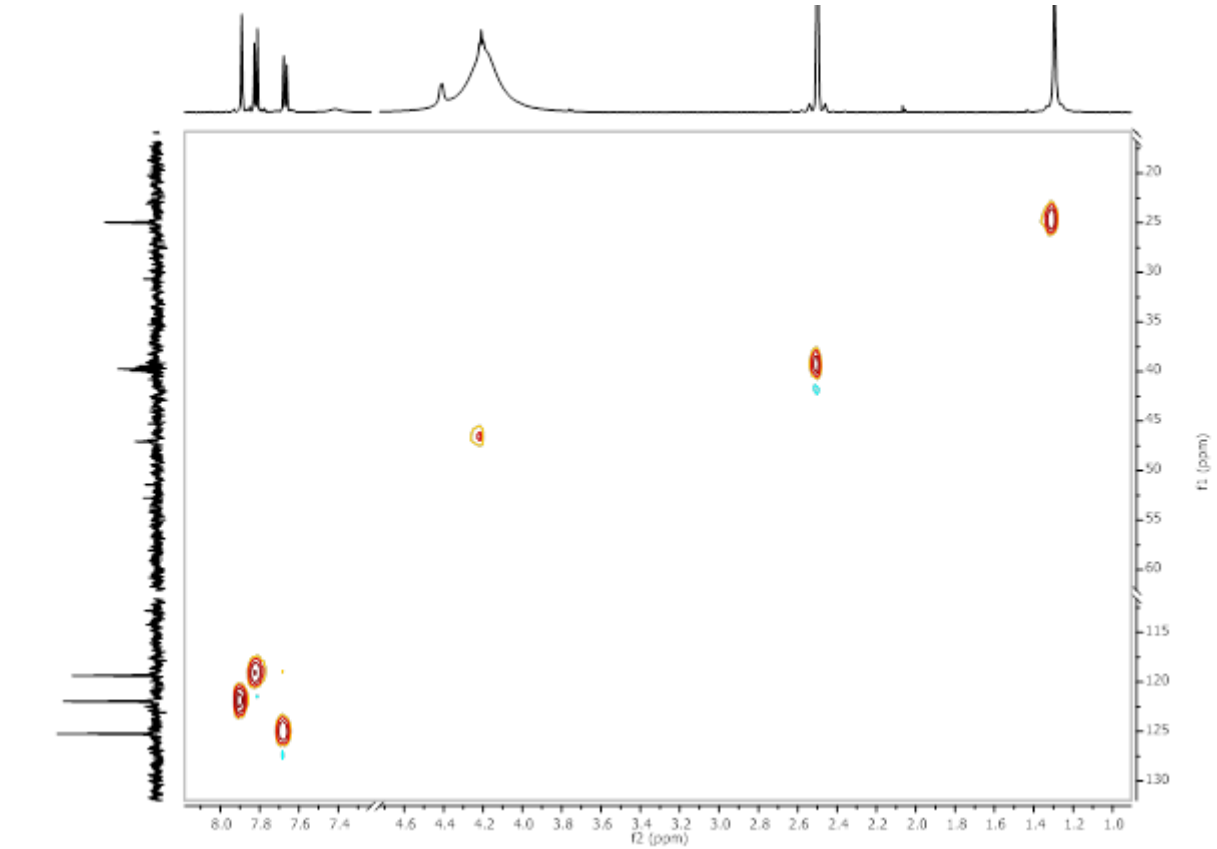

Figure 346: ^{1}H-^{13}C HSQC-NMR of Smoc-Aib-OH **32**.

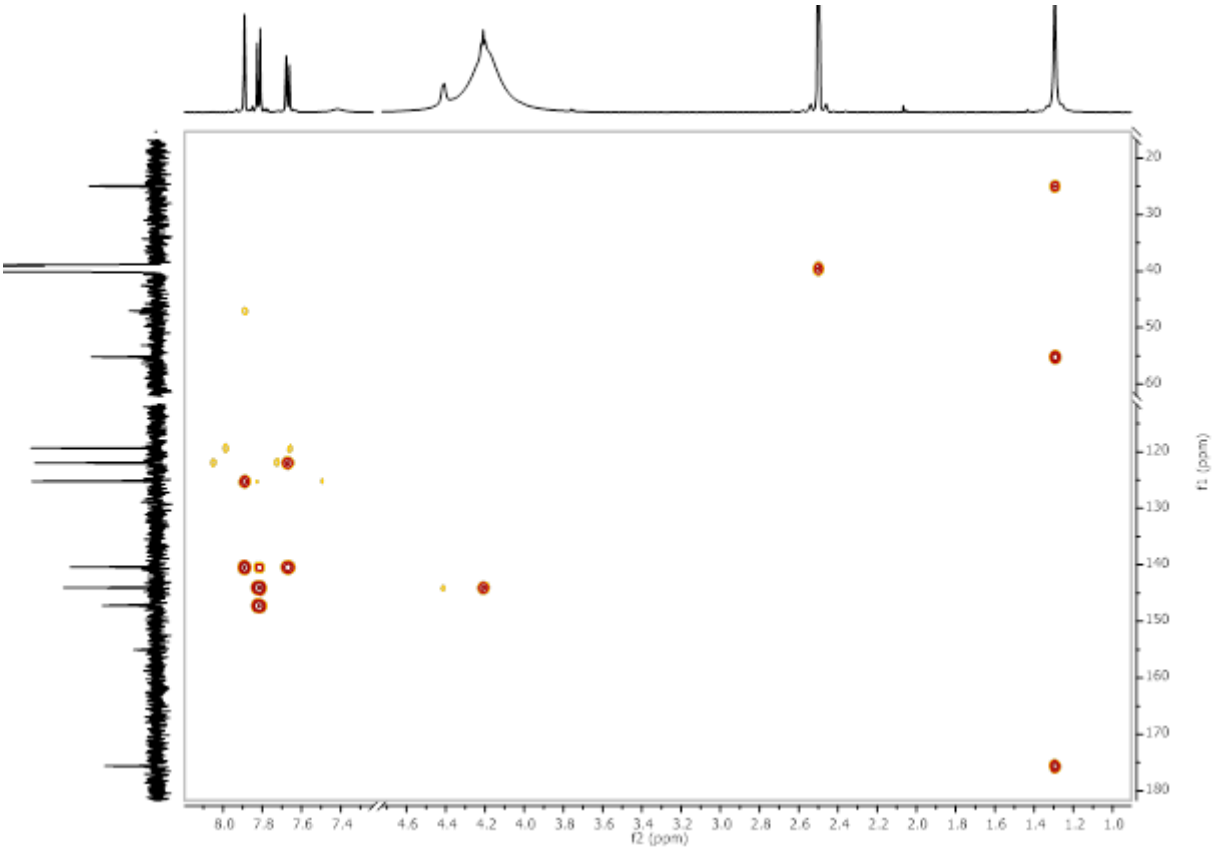

Figure 347: ^{1}H-^{13}C HMBC-NMR of Smoc-Aib-OH **32**.

8.3. Analytical data of deprotection studies

8.3.1. Analytical data of Smoc-Arg-OH 5 deprotection

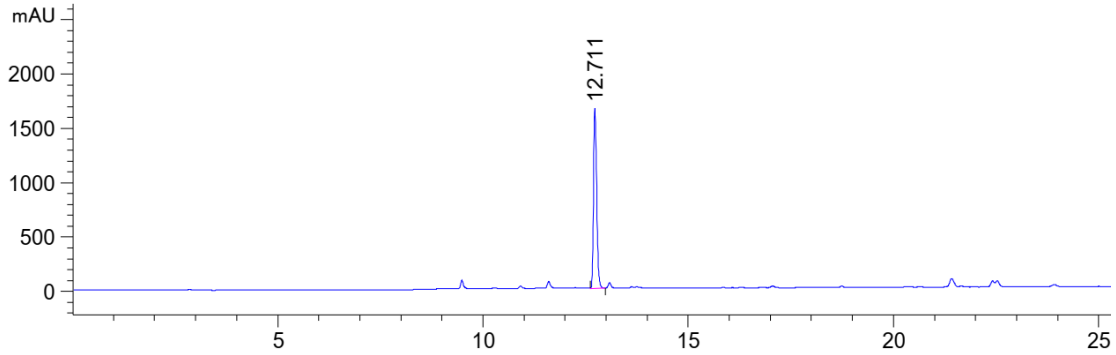

Figure 348: HPLC chromatogram of Smoc-L-Arg-OH **5** Ref for deprotection at λ=220 nm (0 to 40% MeCN).

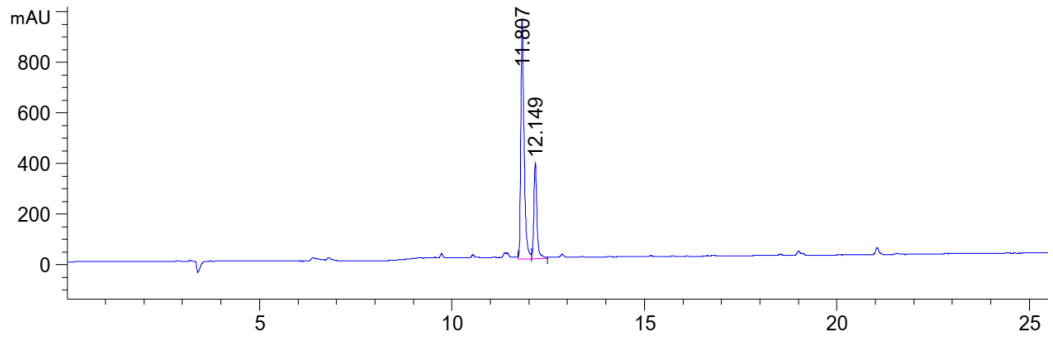

Figure 349: HPLC chromatogram of Smoc-L-Arg-OH **5** deprotection with 20% piperidine in water after 5min at λ=220 nm (0 to 40% MeCN).

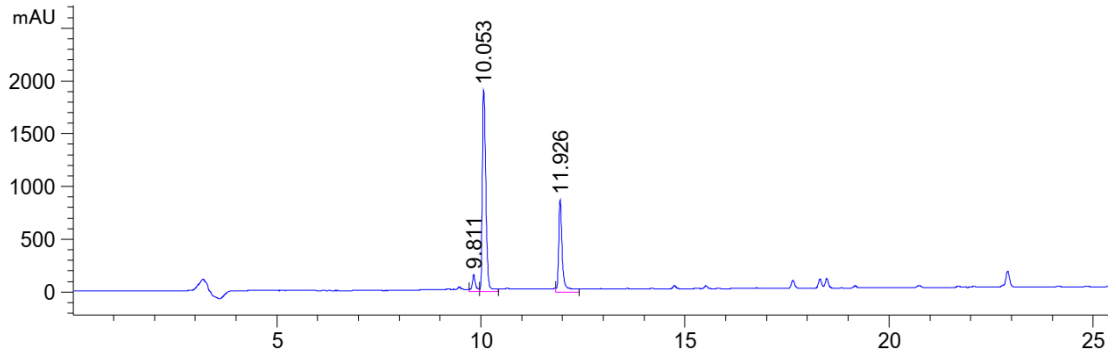

Figure 350: HPLC chromatogram of Smoc-L-Arg-OH **5** deprotection with 10% ethanolamine in water after 5min at λ=220 nm (0 to 40% MeCN).

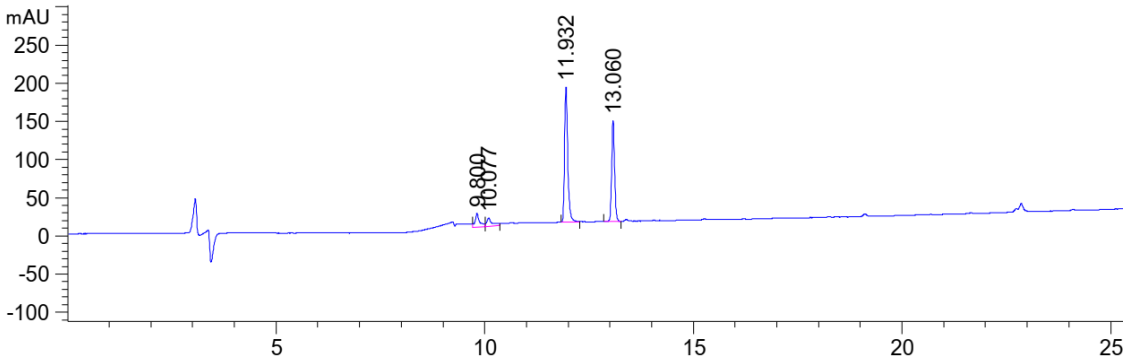

Figure 351: HPLC chromatogram of Smoc-L-Arg-OH **5** deprotection with 10% ethanolamine in Ethanol after 5min at λ=220 nm (0 to 40% MeCN).

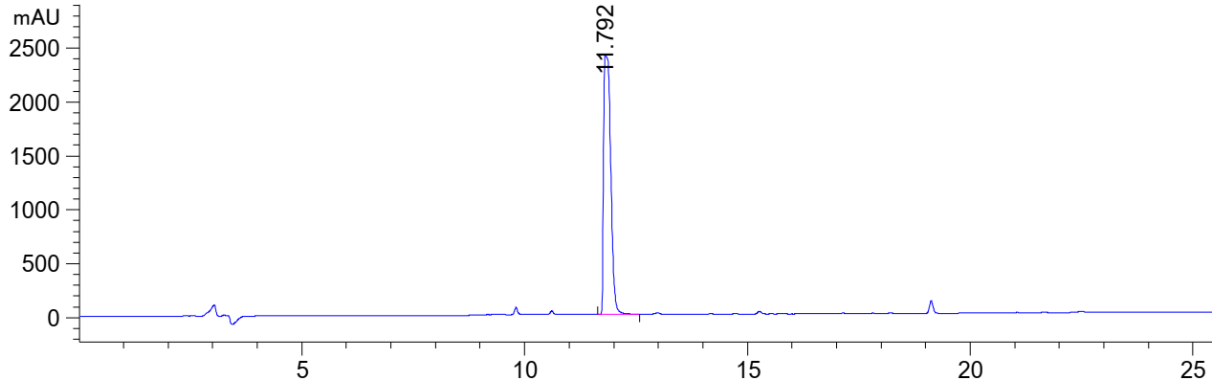

Figure 352: HPLC chromatogram of Smoc-L-Arg-OH **5** deprotection with 1M NaOH in water after 5min at λ=220 nm (0 to 40% MeCN).

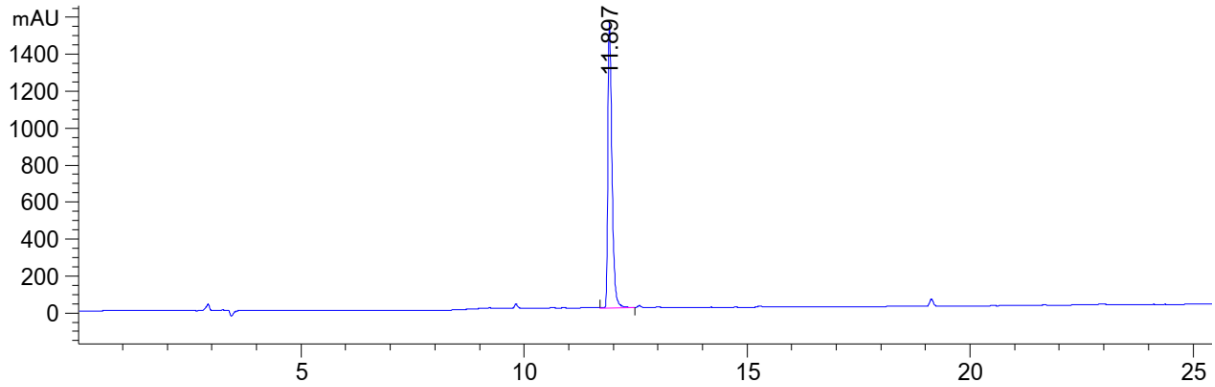

Figure 353: HPLC chromatogram of Smoc-L-Arg-OH **5** deprotection with 1M NaOH in ethanol after 5min at λ=220 nm (0 to 40% MeCN).

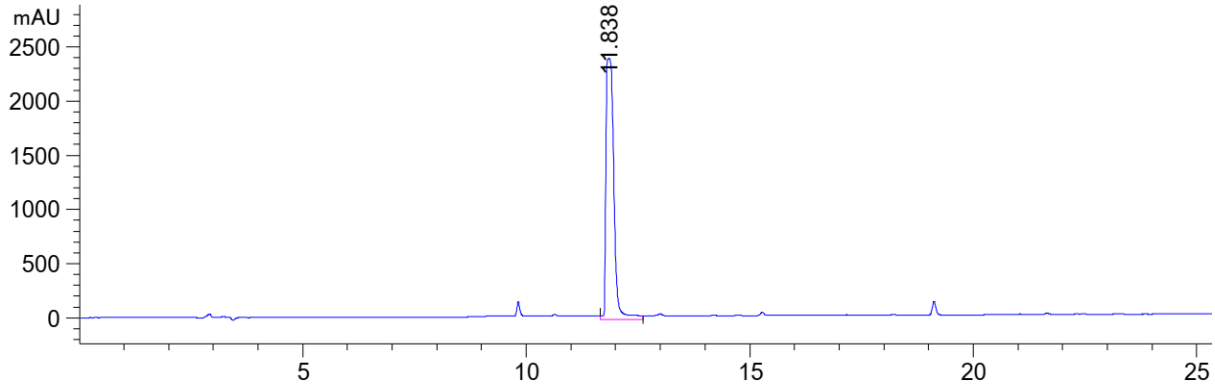

Figure 354: HPLC chromatogram of Smoc-L-Arg-OH **5** deprotection with 0.2M NaOH in water after 5min at λ=220 nm (0 to 40% MeCN).

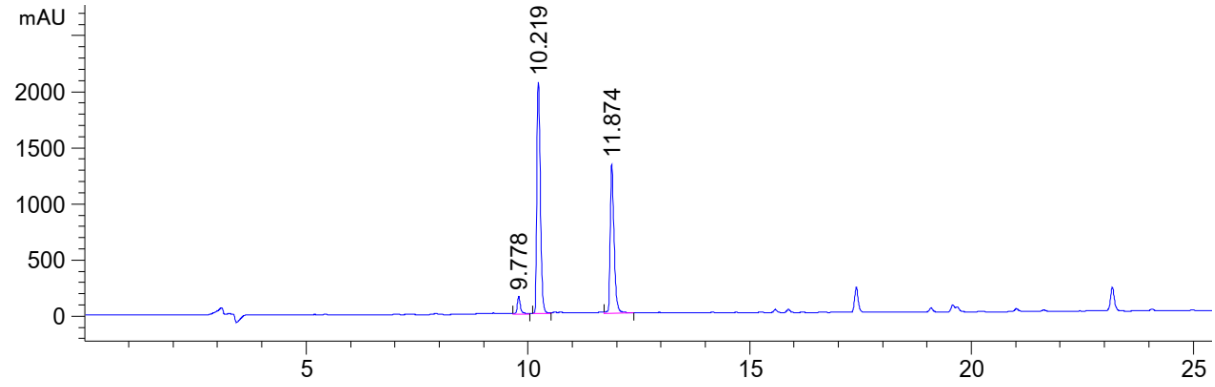

Figure 355: HPLC chromatogram of Smoc-L-Arg-OH **5** deprotection with 5% piperazine in water after 5min at λ=220 nm (0 to 40% MeCN).

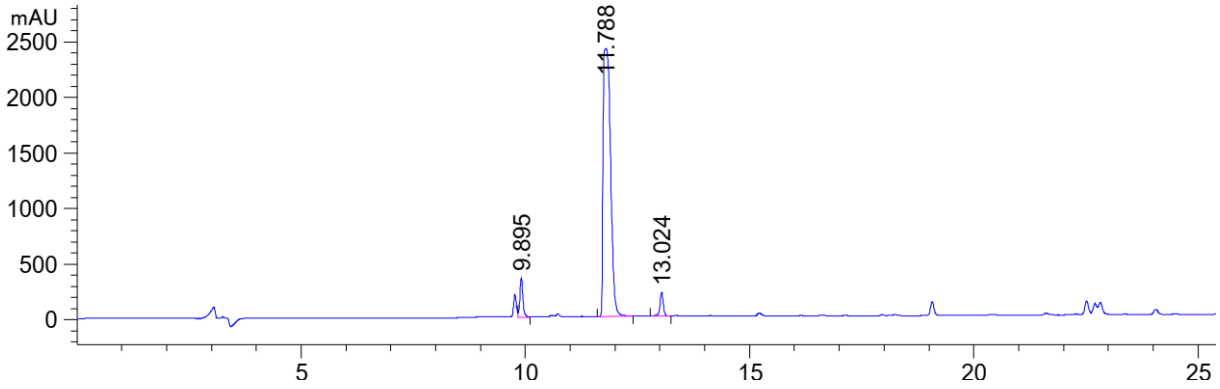

Figure 356: HPLC chromatogram of Smoc-L-Arg-OH **5** deprotection with 10% ammonia in water after 5min at λ=220 nm (0 to 40% MeCN).

8.3.2. Analytical data of Smoc-Leu-OH 16 deprotection

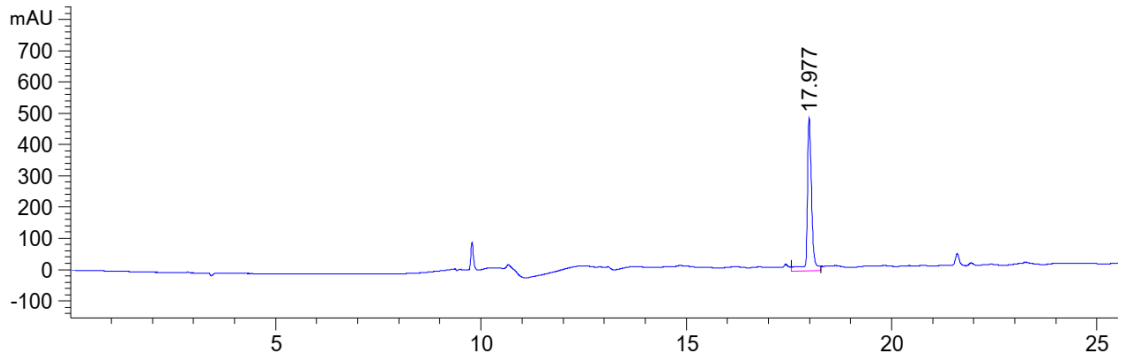

Figure 357: HPLC chromatogram of Smoc-L-Leu-OH **16** Ref for deprotection at λ=220 nm (0 to 40% MeCN).

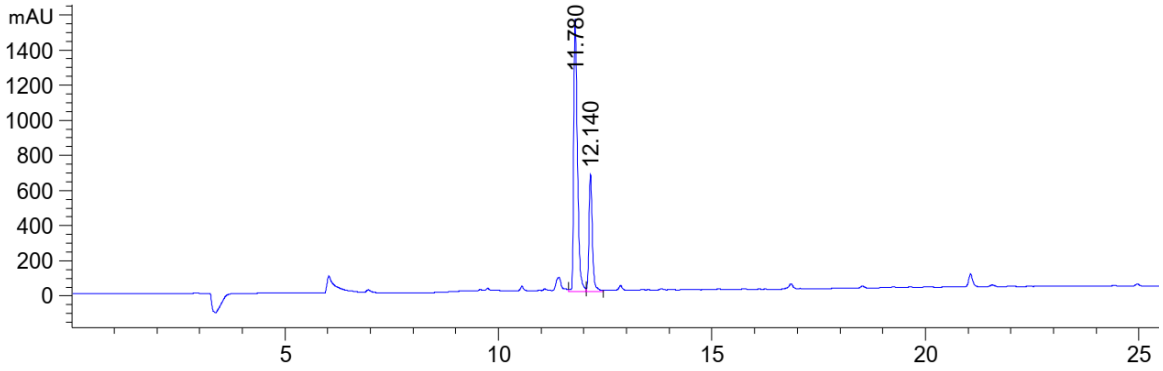

Figure 358: HPLC chromatogram of Smoc-L-Leu-OH **16** deprotection with 20% piperidine in water after 5min at λ=220 nm (0 to 40% MeCN).

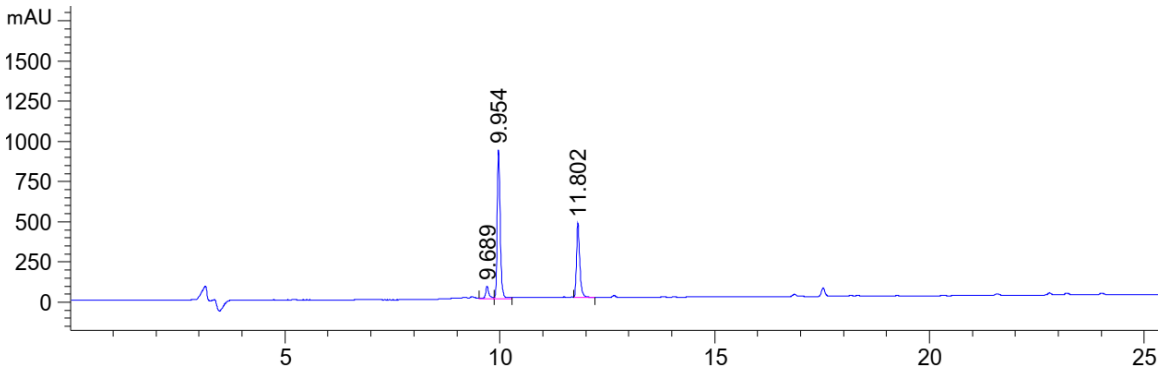

Figure 359: HPLC chromatogram of Smoc-L-Leu-OH **16** deprotection with 10% ethanolamine in water after 5min at λ=220 nm (0 to 40% MeCN).

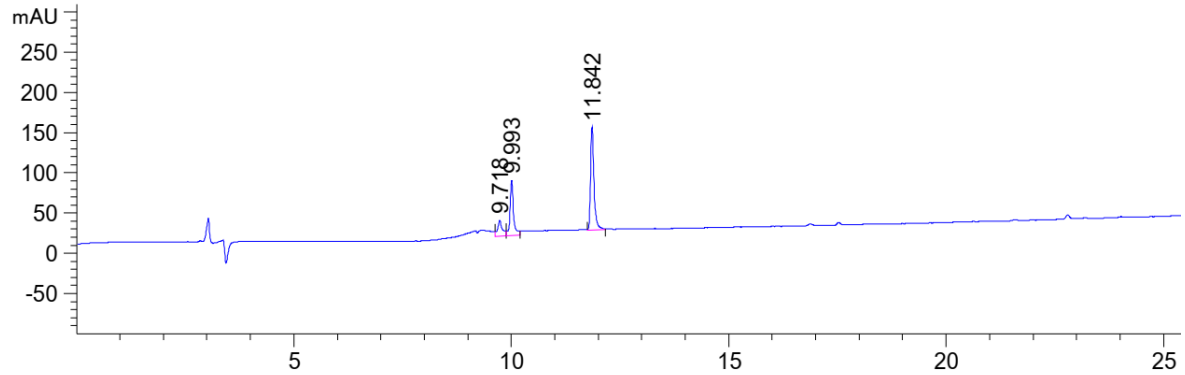

Figure 360: HPLC chromatogram of Smoc-L-Leu-OH **16** deprotection with 10% ethanolamine in Ethanol after 5min at λ=220 nm (0 to 40% MeCN).

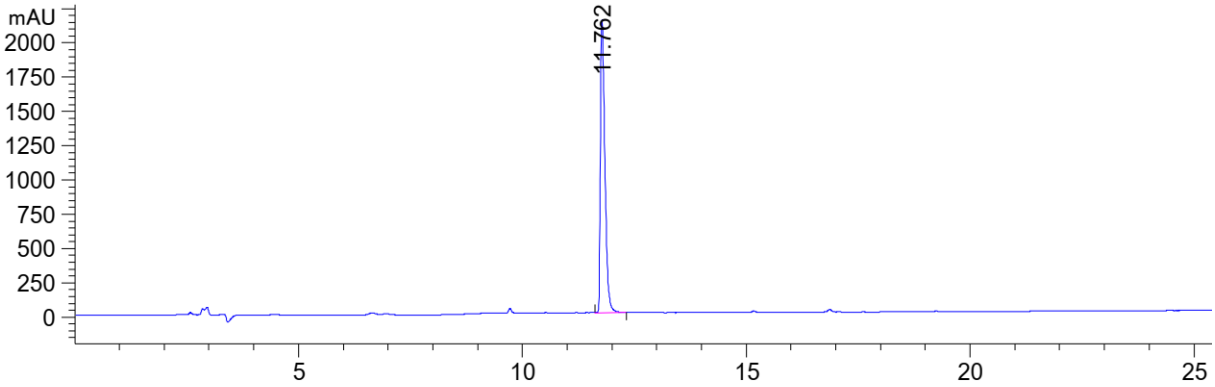

Figure 361: HPLC chromatogram of Smoc-L-Leu-OH **16** deprotection with 1M NaOH in water after 5min at λ=220 nm (0 to 40% MeCN).

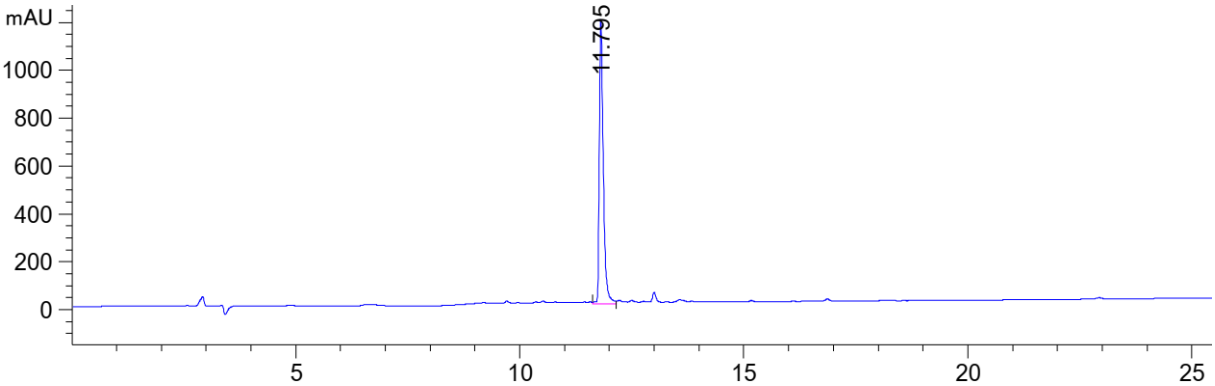

Figure 362: HPLC chromatogram of Smoc-L-Leu-OH **16** deprotection with 1M NaOH in ethanol after 5min at λ=220 nm (0 to 40% MeCN).

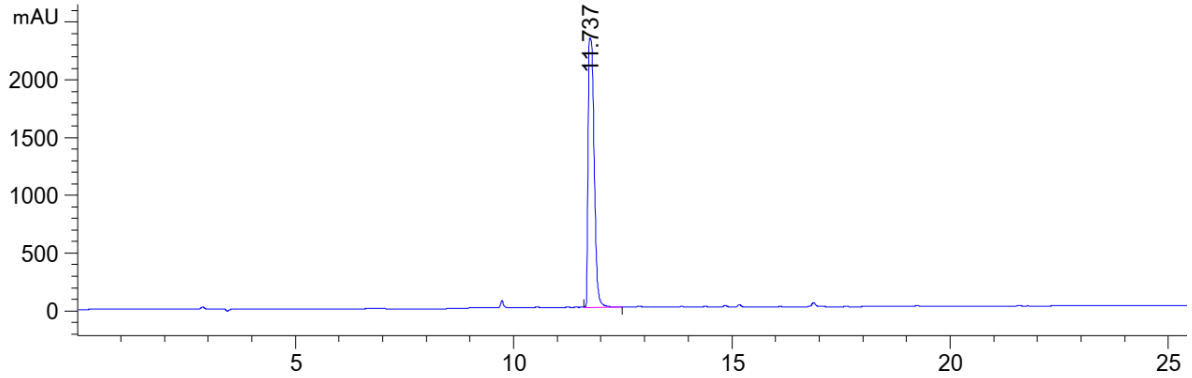

Figure 363: HPLC chromatogram of Smoc-L-Leu-OH **16** deprotection with 0.2M NaOH in water after 5min at λ=220 nm (0 to 40% MeCN).

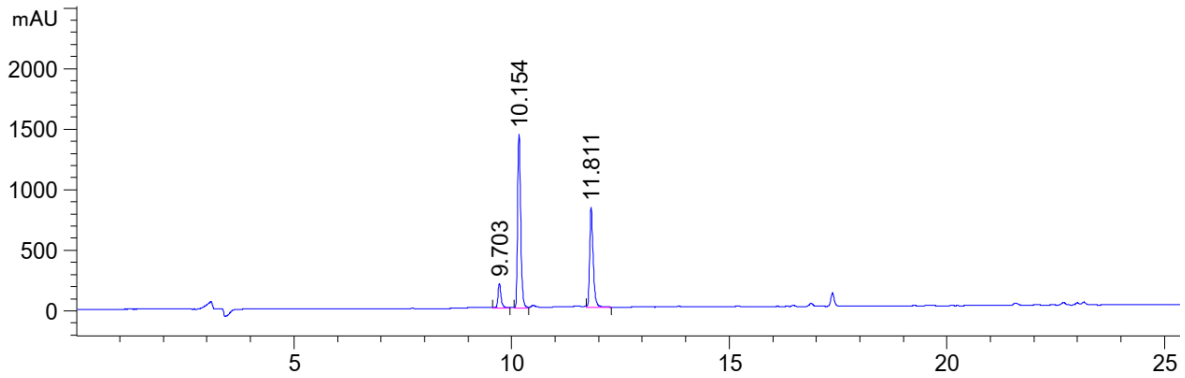

Figure 364: HPLC chromatogram of Smoc-L-Leu-OH **16** deprotection with 5% piperazine in water after 5min at λ=220 nm (0 to 40% MeCN).

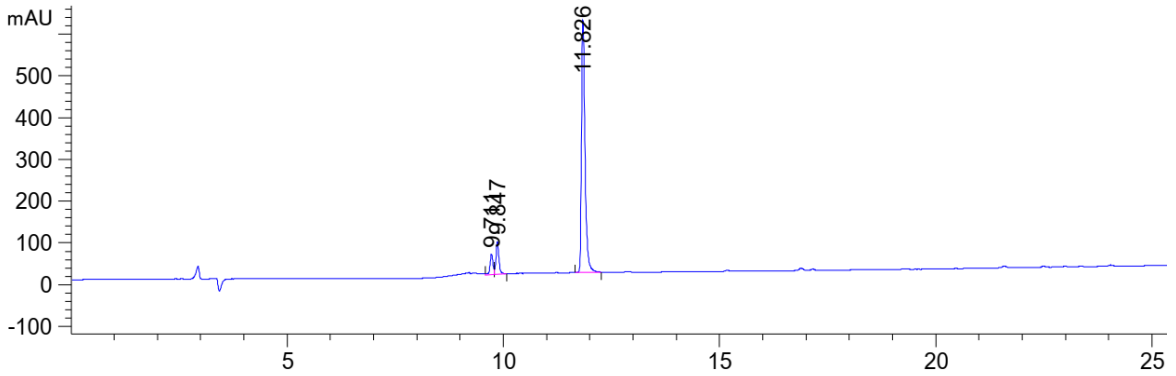

Figure 365: HPLC chromatogram of Smoc-L-Leu-OH **16** deprotection with 10% ammonia in water after 5min at λ=220 nm (0 to 40% MeCN).

8.3.3. Analytical data of Smoc-Tyr-OH 28 deprotection

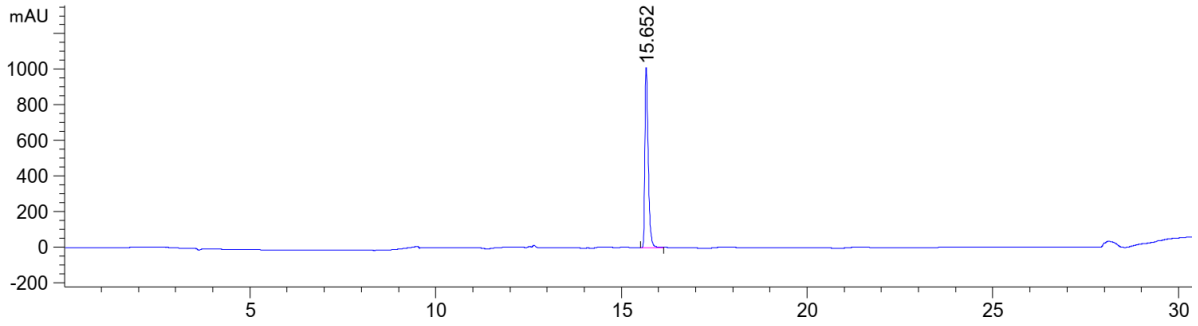

Figure 366: HPLC chromatogram of Smoc-L-Tyr-OH **28** Ref for deprotection at λ=220 nm (0 to 40% MeCN).

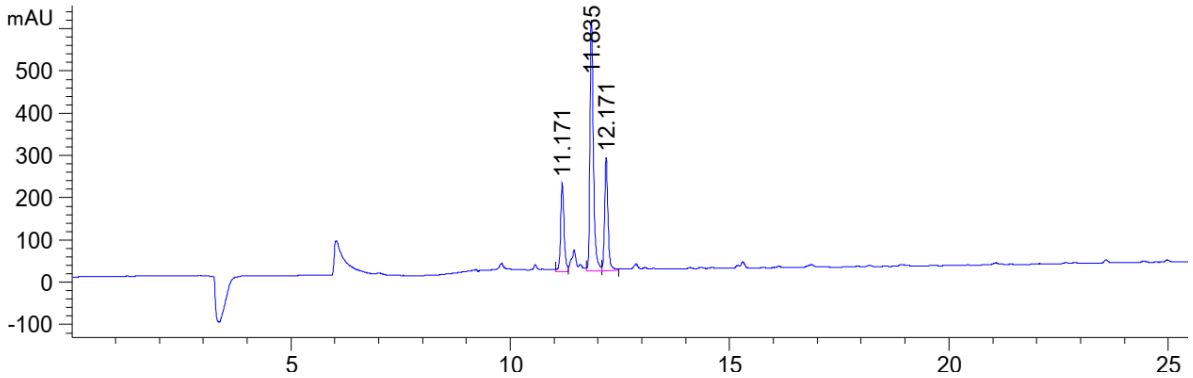

Figure 367: HPLC chromatogram of Smoc-L-Tyr-OH **28** deprotection with 20% piperidine in water after 5min at λ=220 nm (0 to 40% MeCN).

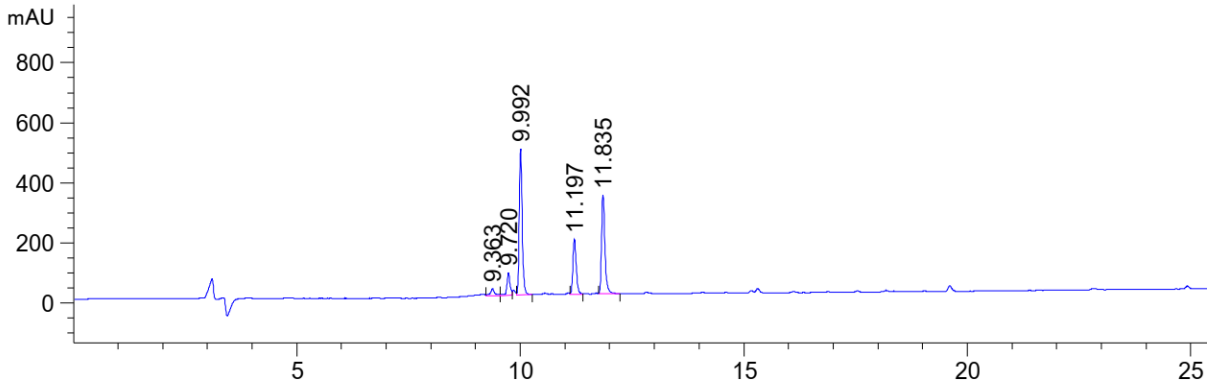

Figure 368: HPLC chromatogram of Smoc-L-Tyr-OH **28** deprotection with 10% ethanolamine in water after 5min at λ=220 nm (0 to 40% MeCN).

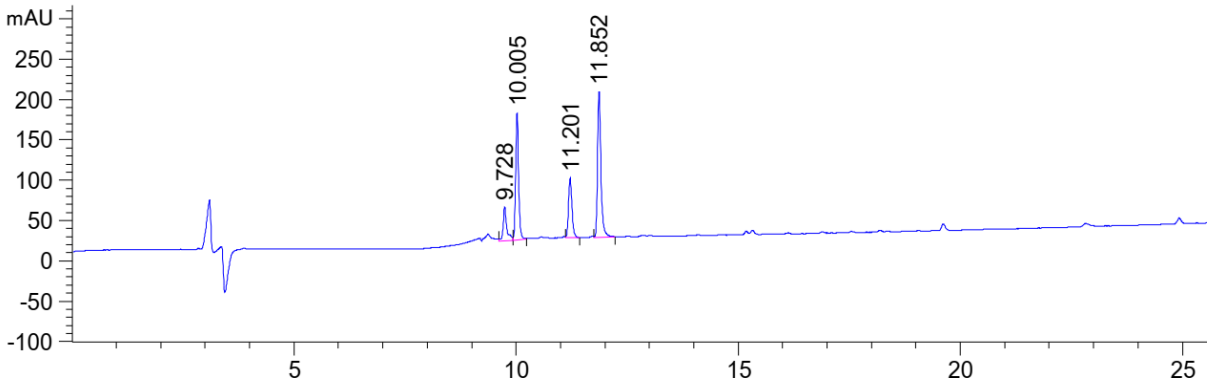

Figure 369: HPLC chromatogram of Smoc-L-Tyr-OH **28** deprotection with 10% ethanolamine in Ethanol after 5min at λ=220 nm (0 to 40% MeCN).

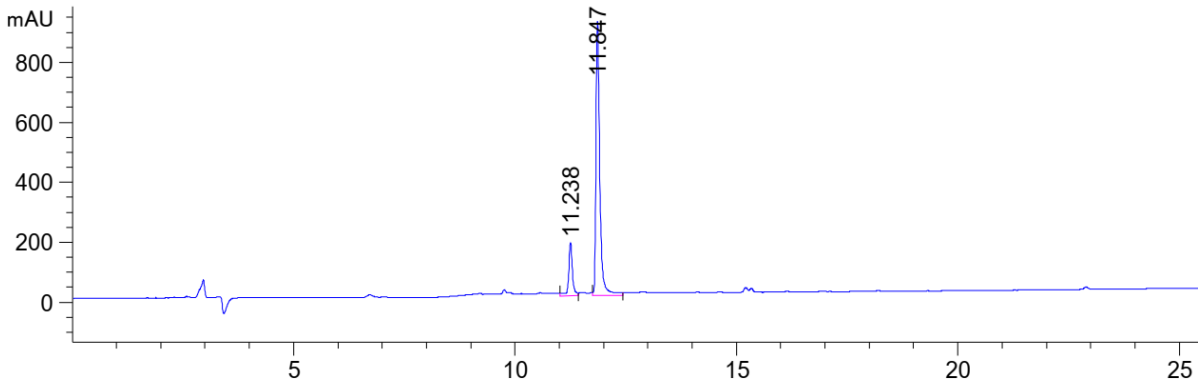

Figure 370: HPLC chromatogram of Smoc-L-Tyr-OH **28** deprotection with 1M NaOH in water after 5min at λ=220 nm (0 to 40% MeCN).

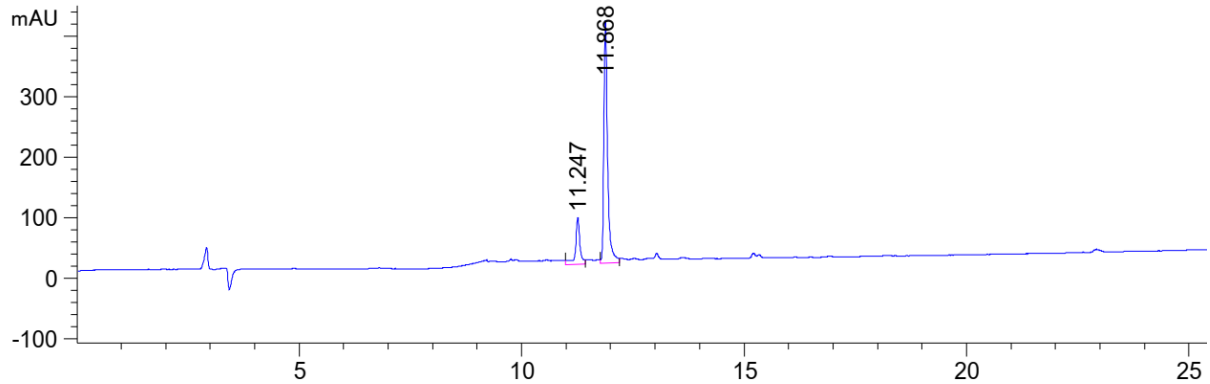

Figure 371: HPLC chromatogram of Smoc-L-Tyr-OH **28** deprotection with 1M NaOH in ethanol after 5min at λ=220 nm (0 to 40% MeCN).

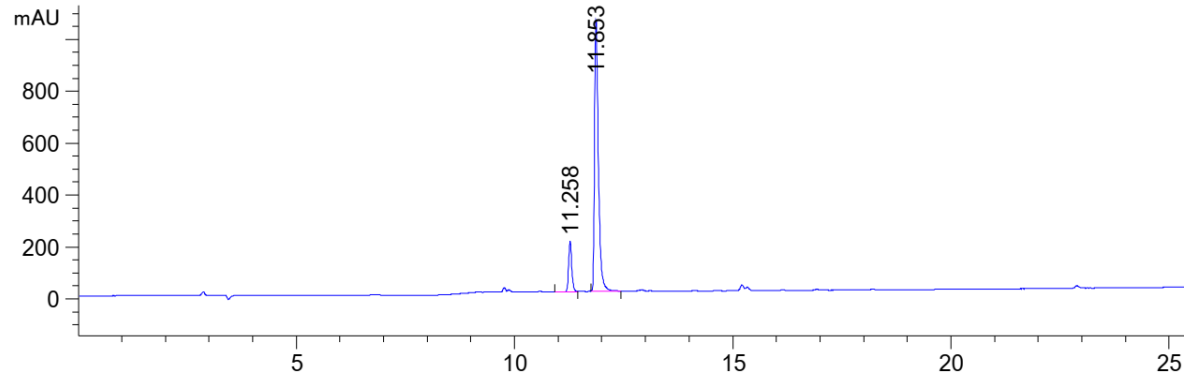

Figure 372: HPLC chromatogram of Smoc-L-Tyr-OH **28** deprotection with 0.2M NaOH in water after 5min at λ=220 nm (0 to 40% MeCN).

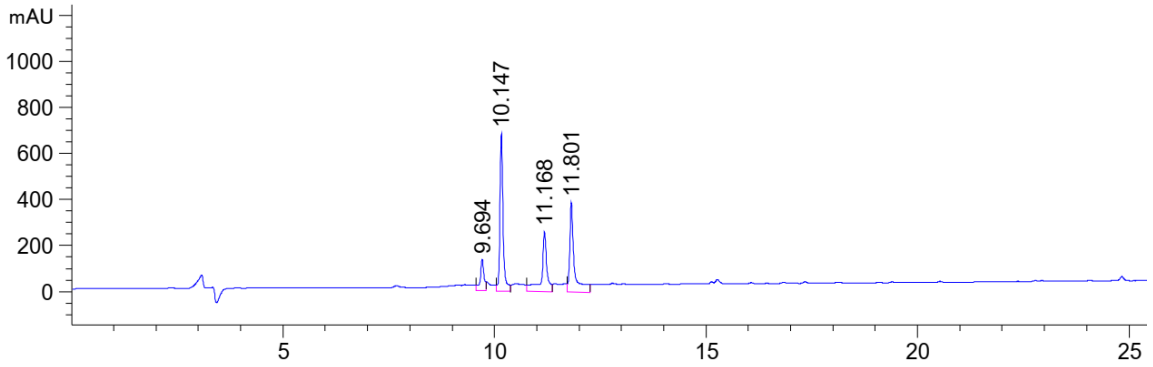

Figure 373: HPLC chromatogram of Smoc-L-Tyr-OH **28** deprotection with 5% piperazine in water after 5min at λ=220 nm (0 to 40% MeCN).

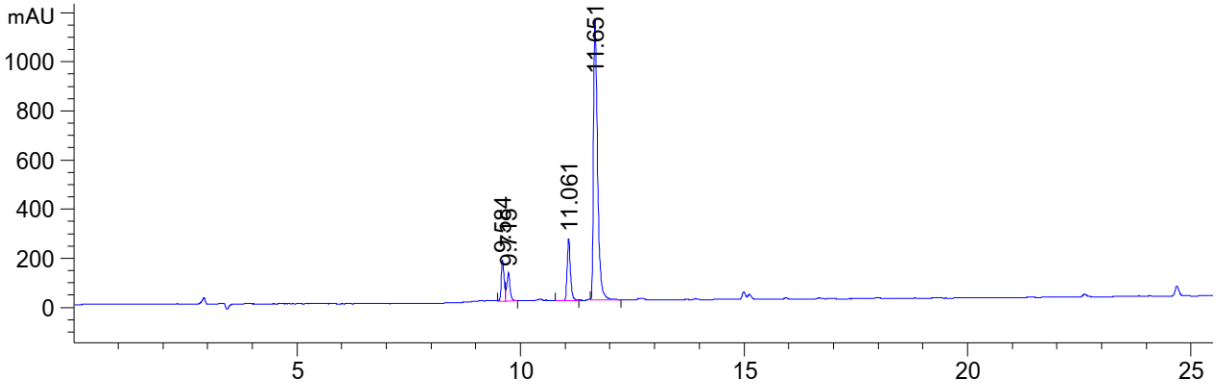

Figure 374: HPLC chromatogram of Smoc-L-Tyr-OH **28** deprotection with 10% ammonia in water after 5min at λ=220 nm (0 to 40% MeCN).

8.4. Analytical data of stability studies of Smoc-protected amino acids

8.4.1. Analytical data of Smoc-Arg-OH 5 stability studies

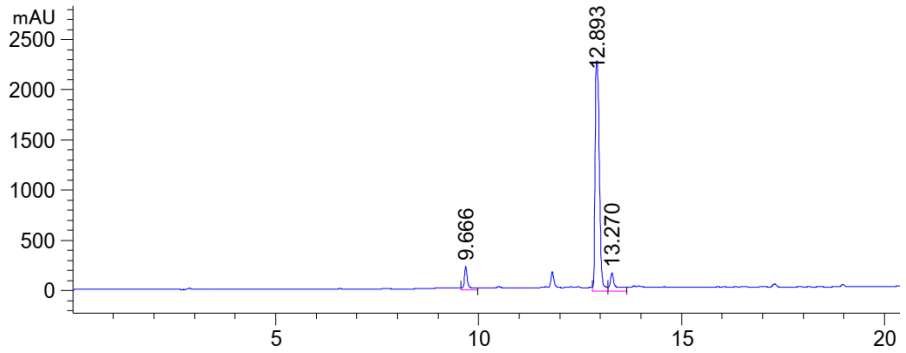

Figure 375: HPLC chromatogram of Smoc-L-Arg-OH **5** under reaction conditions reference at λ=220 nm (0 to 40% MeCN).

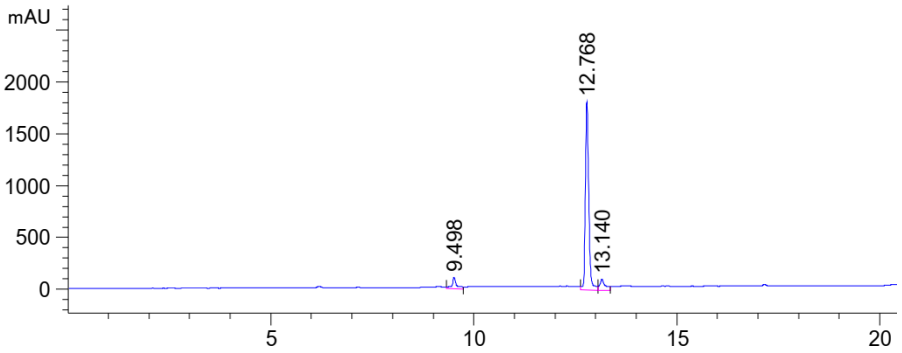

Figure 376: HPLC chromatogram of Smoc-L-Arg-OH **5** under reaction conditions after 7 days at λ=220 nm (0 to 40% MeCN).

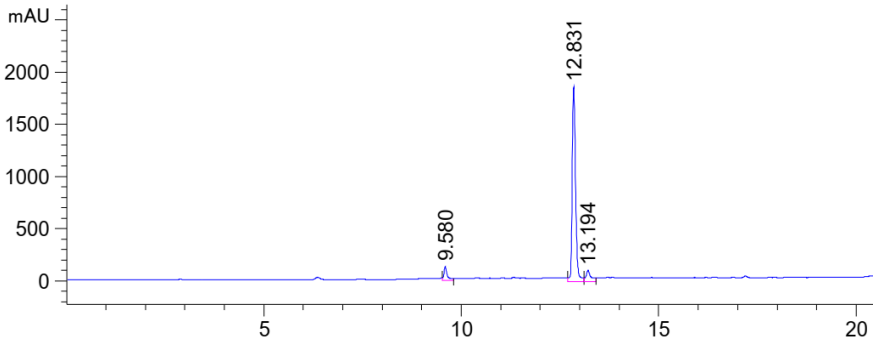

Figure 377: HPLC chromatogram of Smoc-L-Arg-OH **5** under reaction conditions after 14 days at λ=220-nm (0 to 40% MeCN).

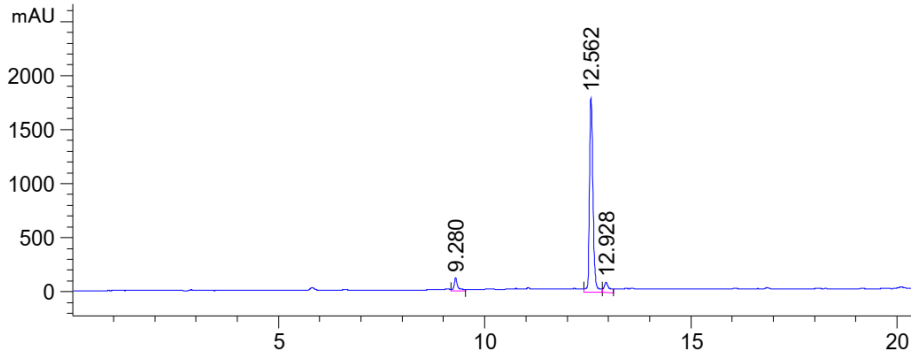

Figure 378: HPLC chromatogram of Smoc-L-Arg-OH **5** under reaction conditions after 21 days at λ=220-nm (0 to 40% MeCN).

8.4.2. Analytical data of Smoc-Ile-OH 15 stability studies

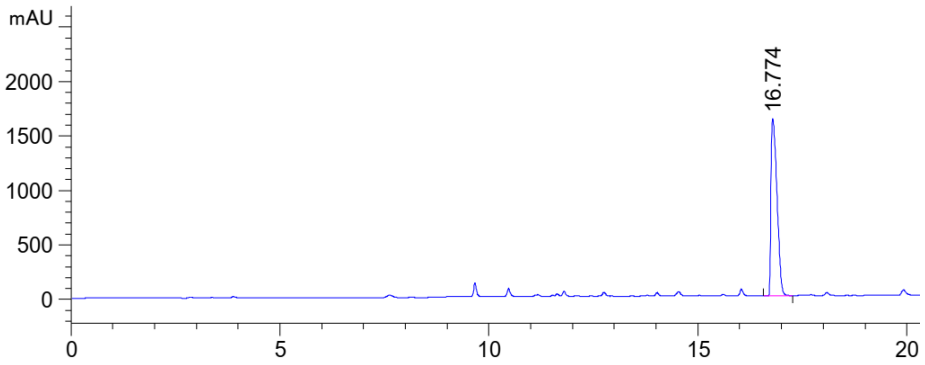

Figure 379: HPLC chromatogram of Smoc-L-Ile-OH **15** under reaction conditions reference at λ=220 nm (0 to 40% MeCN).

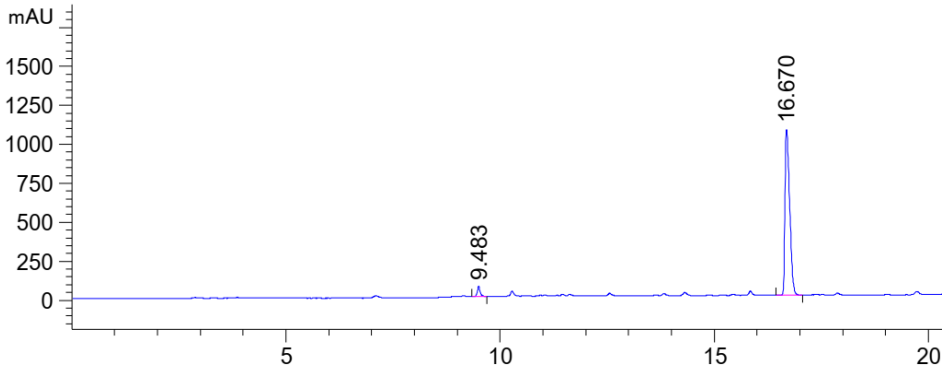

Figure 380: HPLC chromatogram of Smoc-L-Ile-OH **15** under reaction conditions after 7 days at λ=220 nm (0 to 40% MeCN).

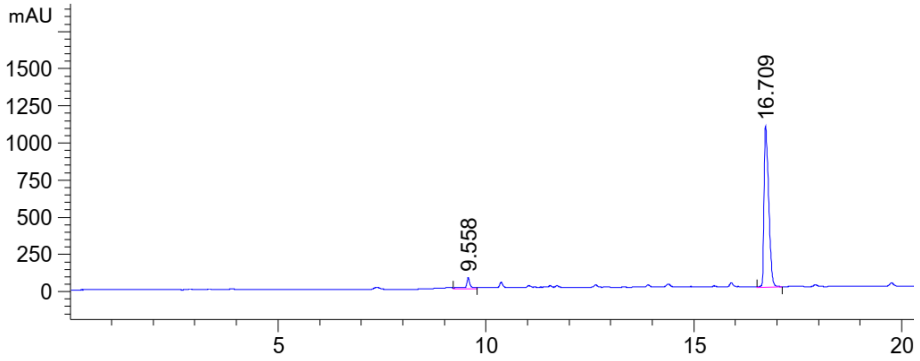

Figure 381: HPLC chromatogram of Smoc-L-Ile-OH **15** under reaction conditions after 14 days at λ=220-nm (0 to 40% MeCN).

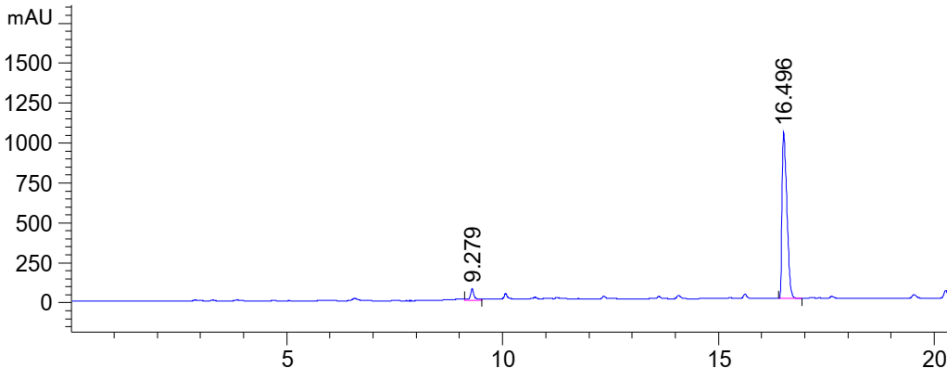

Figure 382: HPLC chromatogram of Smoc-L-Ile-OH **15** under reaction conditions after 21 days at λ=220-nm (0 to 40% MeCN).

8.4.3. Analytical data of Smoc-Phe-OH 20 stability studies

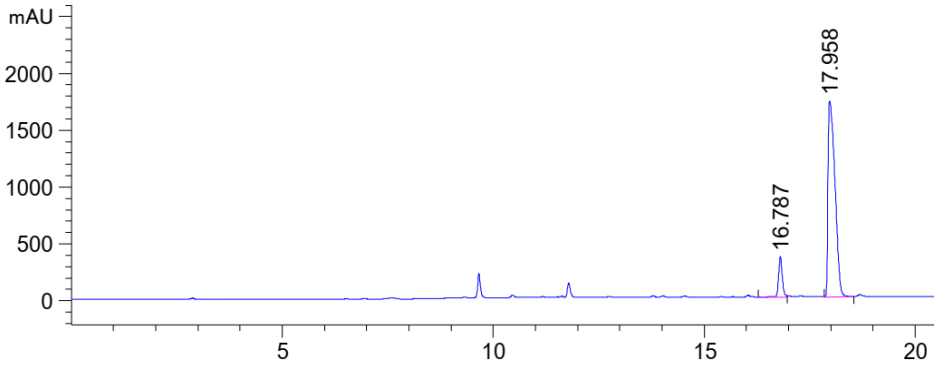

Figure 383: HPLC chromatogram of Smoc-L-Phe-OH **20** under reaction conditions reference at λ=220 nm (0 to 40% MeCN).

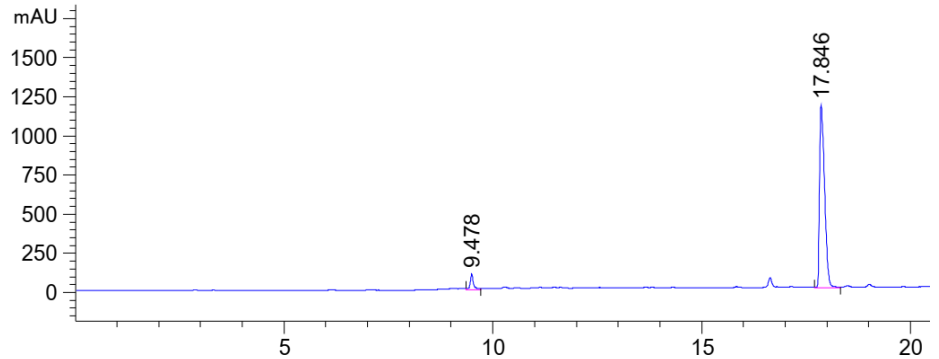

Figure 384: HPLC chromatogram of Smoc-L-Phe-OH **20** under reaction conditions after 7 days at λ=220 nm (0 to 40% MeCN).

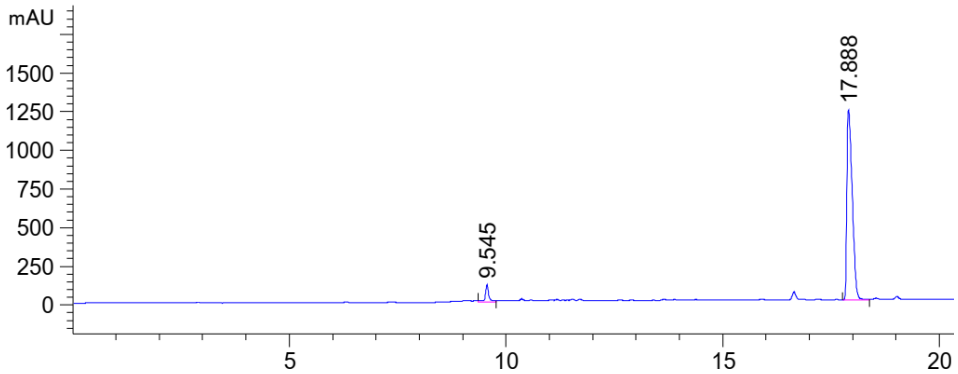

Figure 385: HPLC chromatogram of Smoc-L-Phe-OH **20** under reaction conditions after 14 days at λ=220-nm (0 to 40% MeCN).

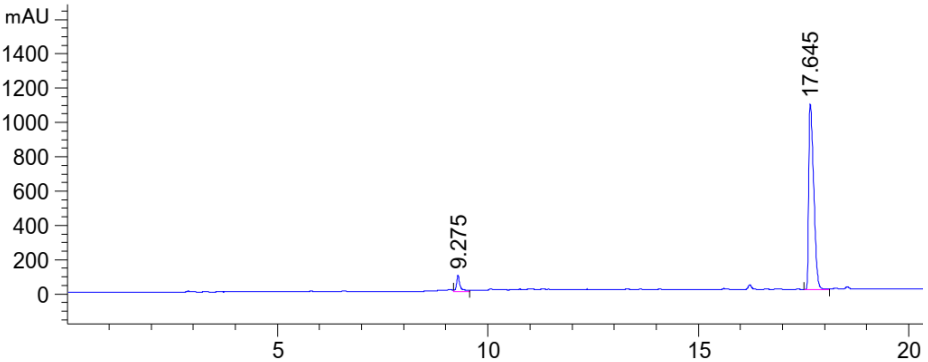

Figure 386: HPLC chromatogram of Smoc-L-Phe-OH **20** under reaction conditions after 21 days at λ=220-nm (0 to 40% MeCN).

8.4.4. Analytical data of Smoc-Pro-OH 21 stability studies

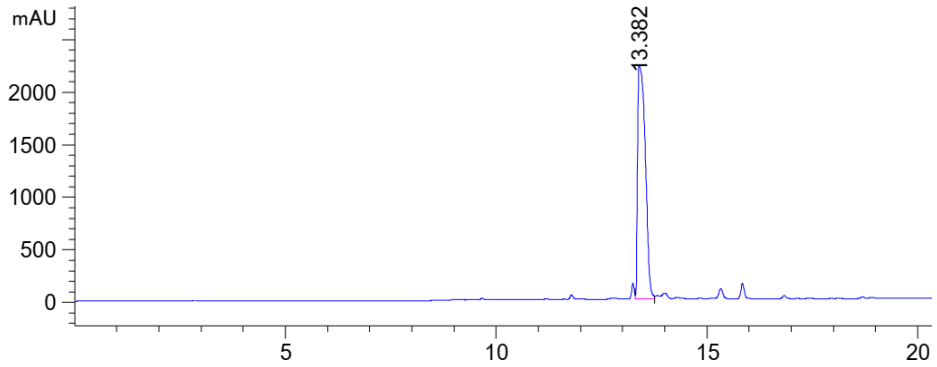

Figure 387: HPLC chromatogram of Smoc-L-Pro-OH **21** under reaction conditions reference at λ=220 nm (0 to 40% MeCN).

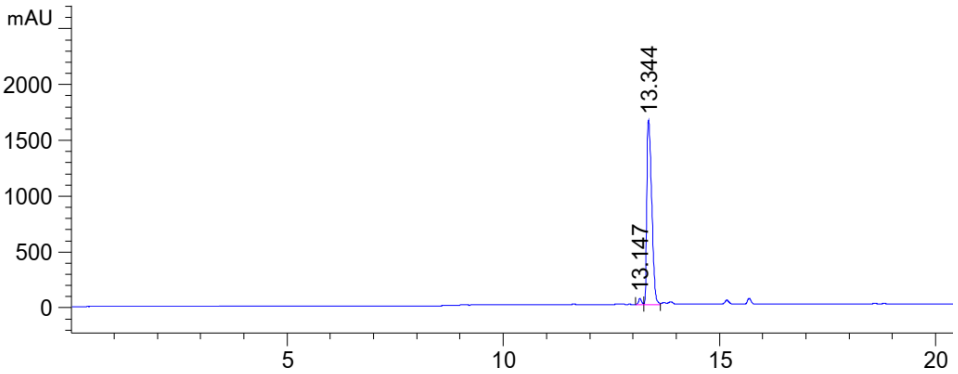

Figure 388: HPLC chromatogram of Smoc-L-Pro-OH **21** under reaction conditions after 7 days at λ=220 nm (0 to 40% MeCN).

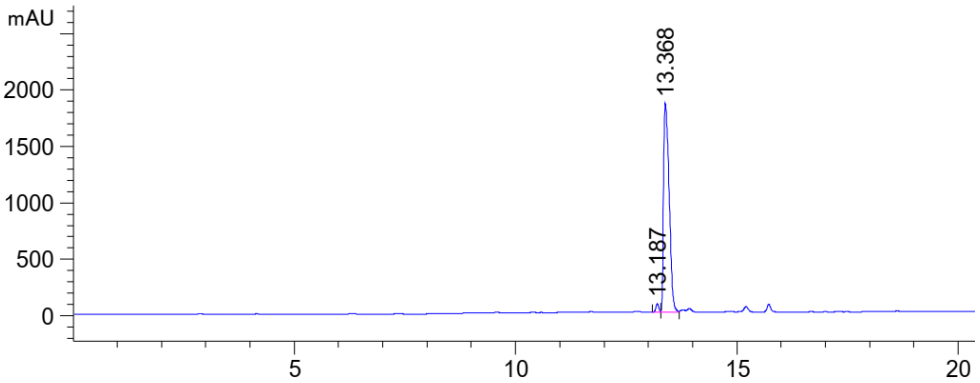

Figure 389: HPLC chromatogram of Smoc-L-Pro-OH **21** under reaction conditions after 14 days at λ=220-nm (0 to 40% MeCN).

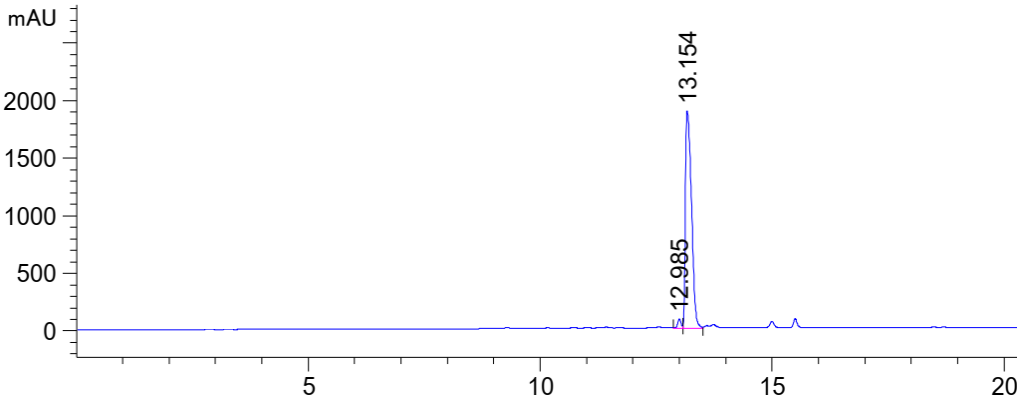

Figure 390: HPLC chromatogram of Smoc-L-Pro-OH **21** under reaction conditions after 21 days at λ=220-nm (0 to 40% MeCN).

8.4.5. Analytical data of Smoc-Ser-OH 22 stability studies

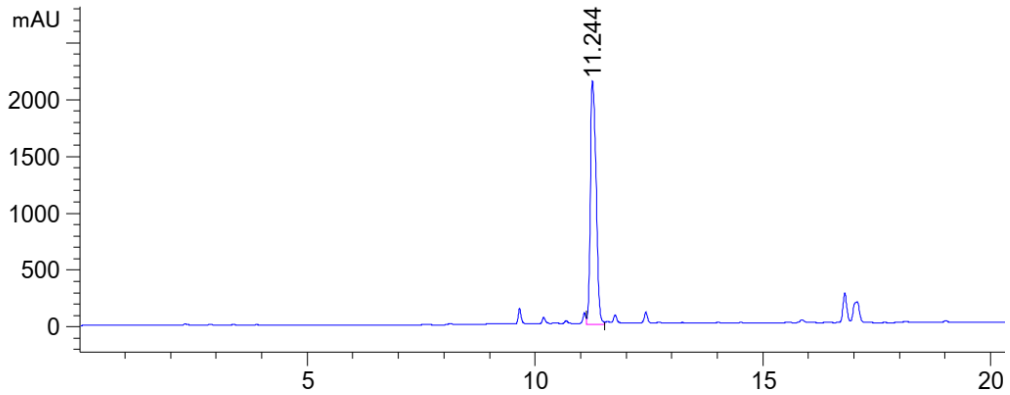

Figure 391: HPLC chromatogram of Smoc-L-Ser-OH **22** under reaction conditions reference at λ=220 nm (0 to 40% MeCN).

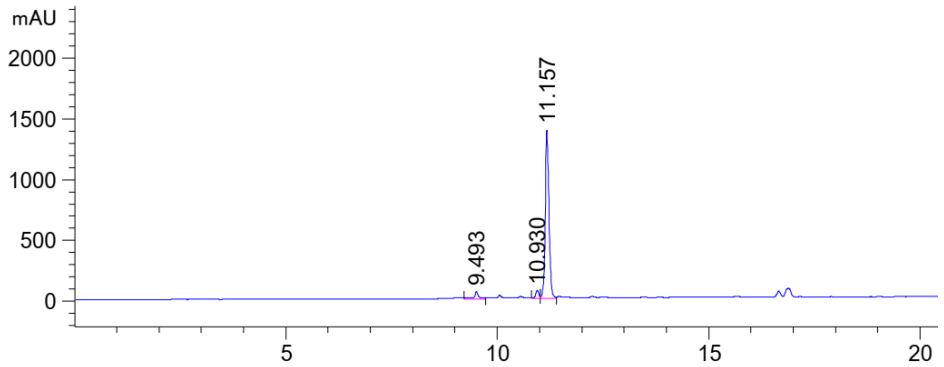

Figure 392: HPLC chromatogram of Smoc-L-Ser-OH **22** under reaction conditions after 7 days at λ=220 nm (0 to 40% MeCN).

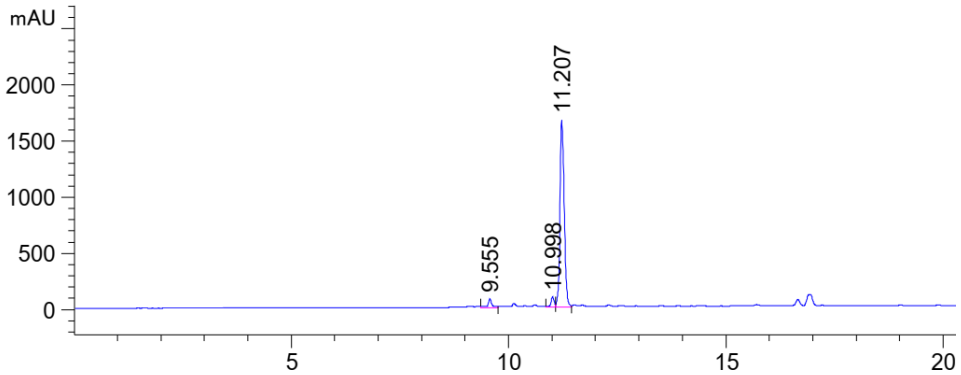

Figure 393: HPLC chromatogram of Smoc-L-Ser-OH **22** under reaction conditions after 14 days at λ=220-nm (0 to 40% MeCN).

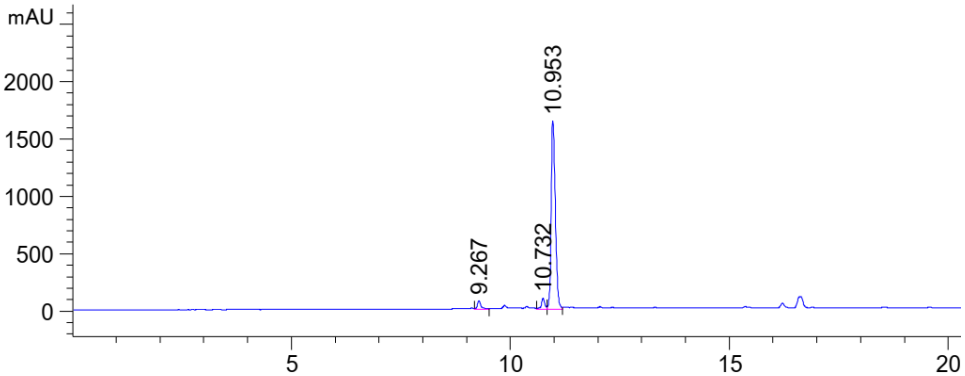

Figure 394: HPLC chromatogram of Smoc-L-Ser-OH **22** under reaction conditions after 21 days at λ=220-nm (0 to 40% MeCN).

8.5. Analytical data of coupling efficiency and solvent influence

8.5.1. Analytical Reference data

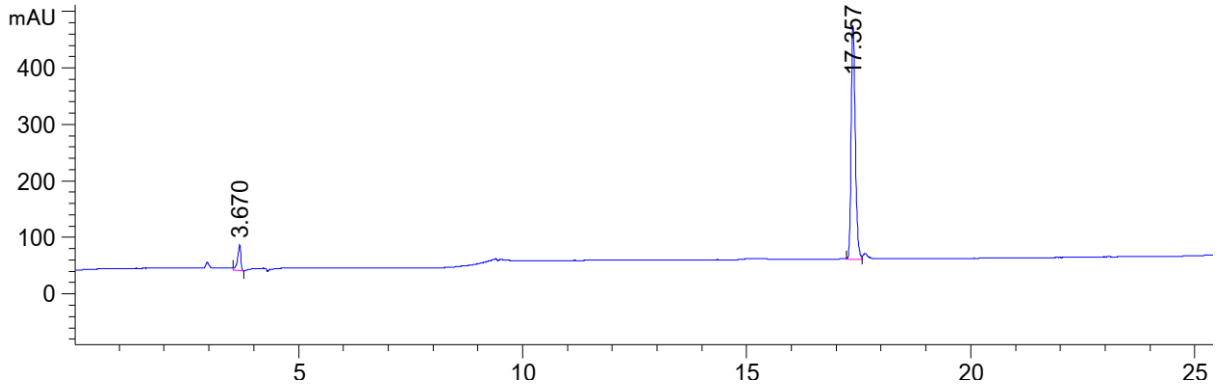

Figure 395: HPLC chromatogram of Smoc-L-Pro-L-Tyr-OMe **36** Reference at λ=220 nm (0 to 40% MeCN).

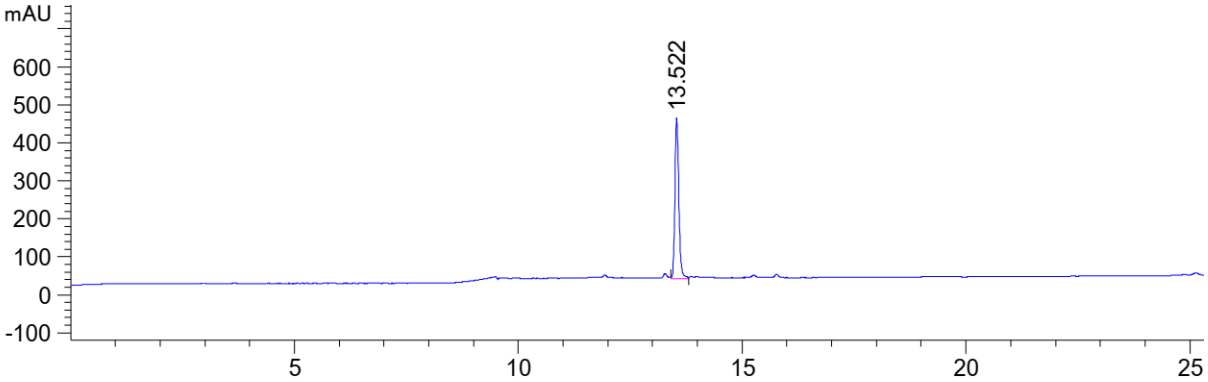

Figure 396: HPLC chromatogram of Smoc-L-Pro-OH **21** Reference at λ=220 nm (0 to 40% MeCN).

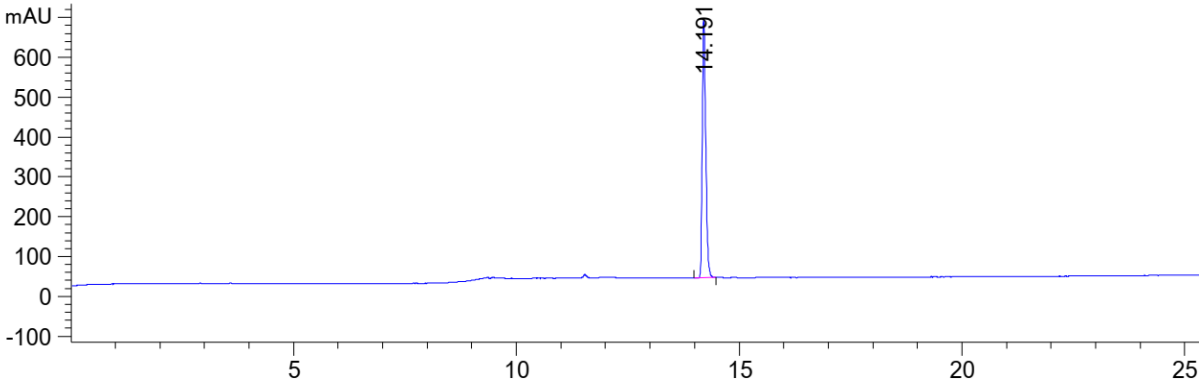

Figure 397: HPLC chromatogram of L-Tyr-OMe **35** Reference at λ=220 nm (0 to 40% MeCN).

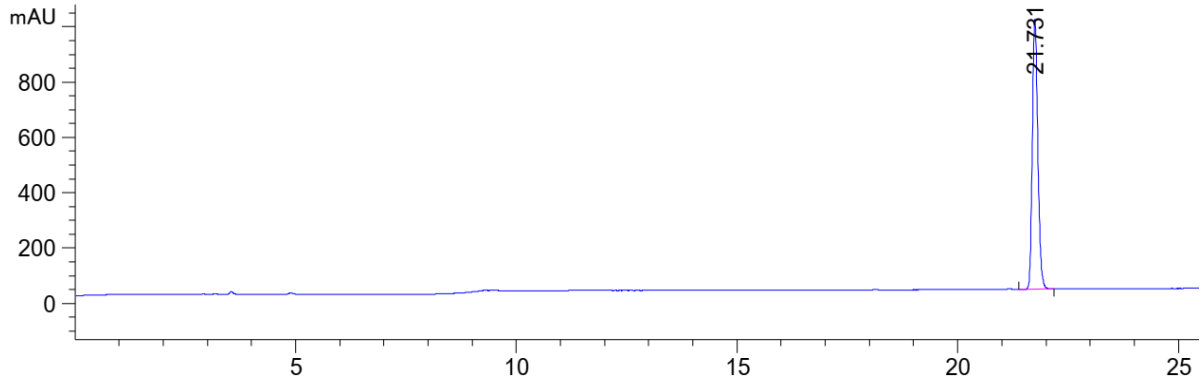

Figure 398: HPLC chromatogram of Oxyma **39** Reference at λ=220 nm (0 to 40% MeCN).

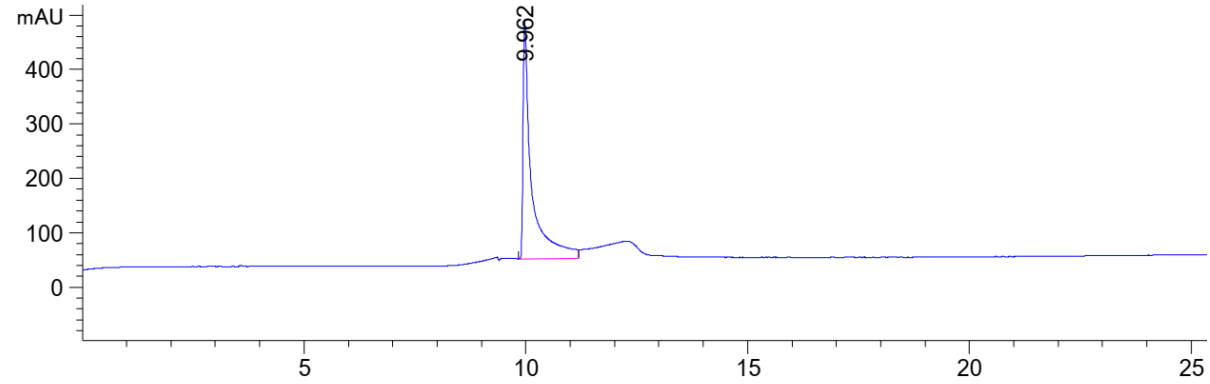

Figure 399: HPLC chromatogram of HOPO **40** Reference at λ=220 nm (0 to 40% MeCN).

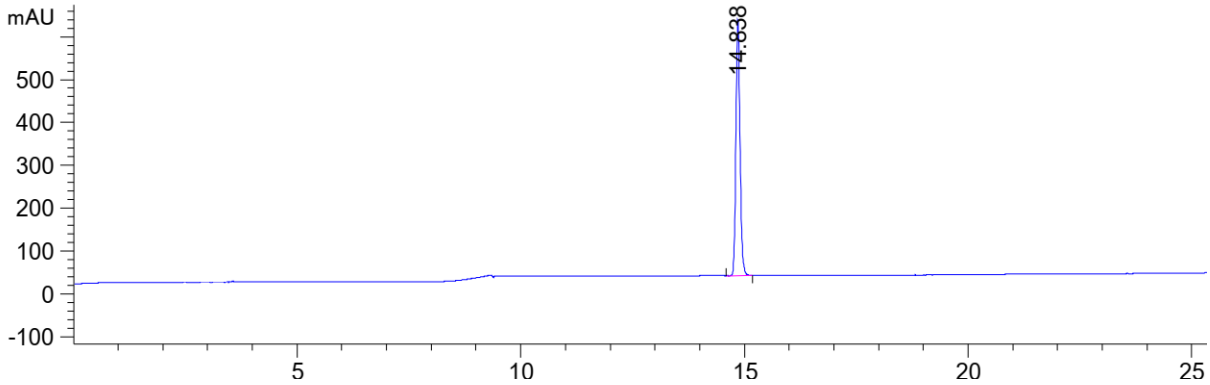

Figure 400: HPLC chromatogram of HONB **41** Reference at λ=220 nm (0 to 40% MeCN).

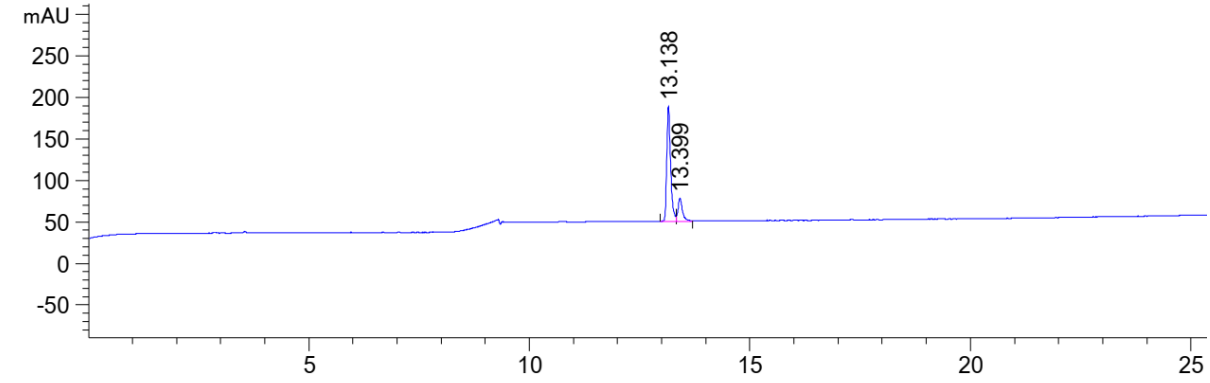

Figure 401: HPLC chromatogram of EEDQ **42** Reference at λ=220 nm (0 to 40% MeCN).

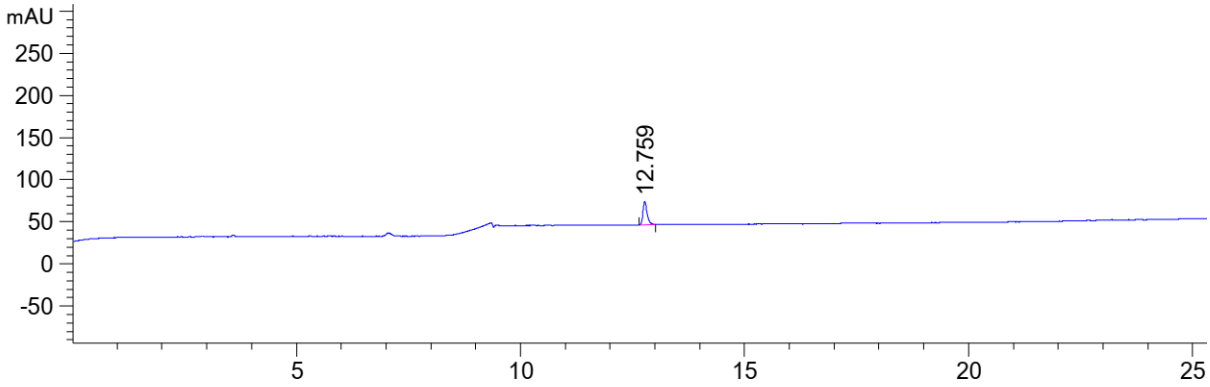

Figure 402: HPLC chromatogram of DMT-MM **43** Reference at λ=220 nm (0 to 40% MeCN).

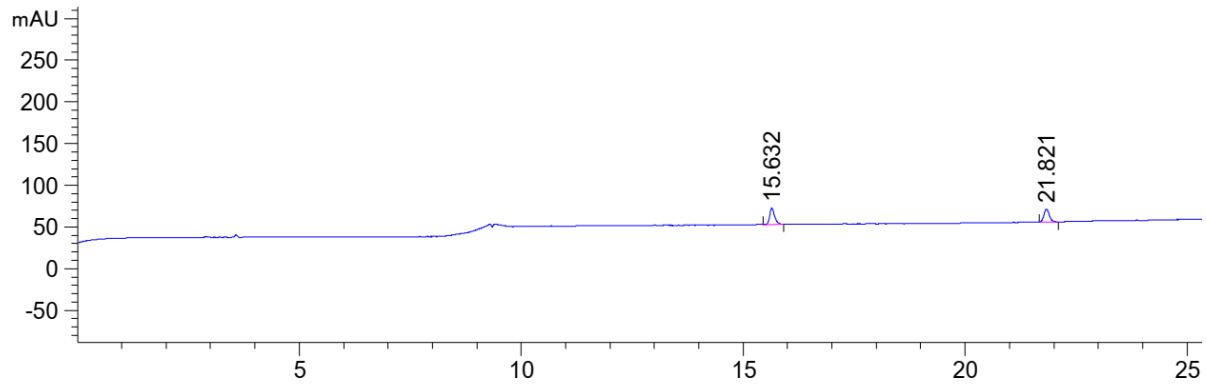

Figure 403: HPLC chromatogram of COMU **44** Reference at λ=220 nm (0 to 40% MeCN).

8.5.2. ESI-MS data of isolated side products

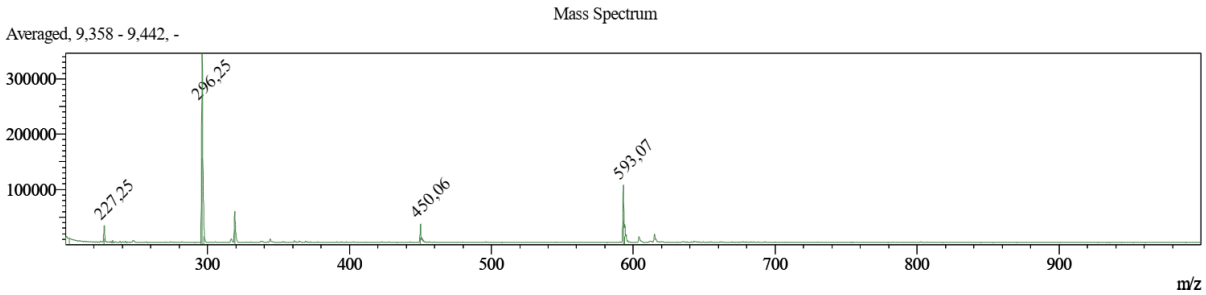

Figure 404: ESI-MS of isolated Smoc-Pro-NHS **45** (M measured=593.07 $[M-H]^-$, M calc.=592.54) at 15.5min.

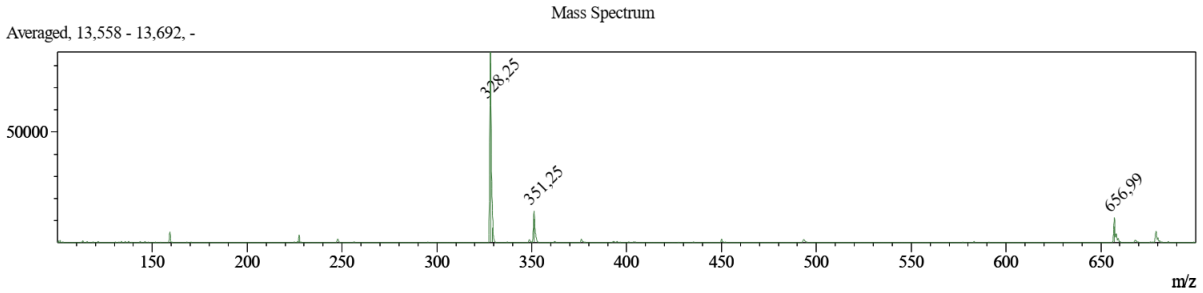

Figure 405: ESI-MS of isolated Smoc-Pro-HONB **46** (M measured=656.99 $[M-H]^-$, M calc.=656.63) at 20.55min.

8.5.3. Analytical data of the synthesis of Smoc-L-Pro-L-Tyr-OMe 36 in water

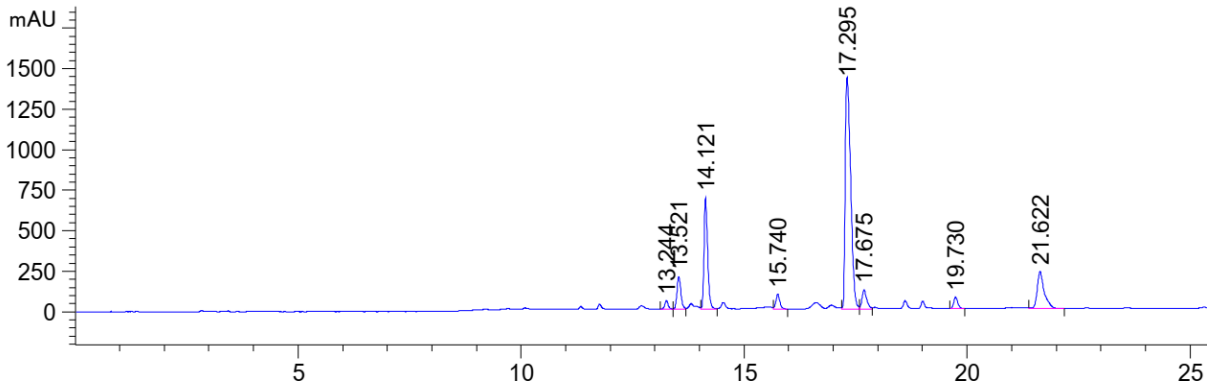

Figure 406: HPLC chromatogram of the synthesis of Smoc-L-Pro-L-Tyr-OMe **36** (17.3min) with EDC-HCl **37**/Oxyma **39** in water after 25min at λ=220 nm (0 to 40% MeCN).

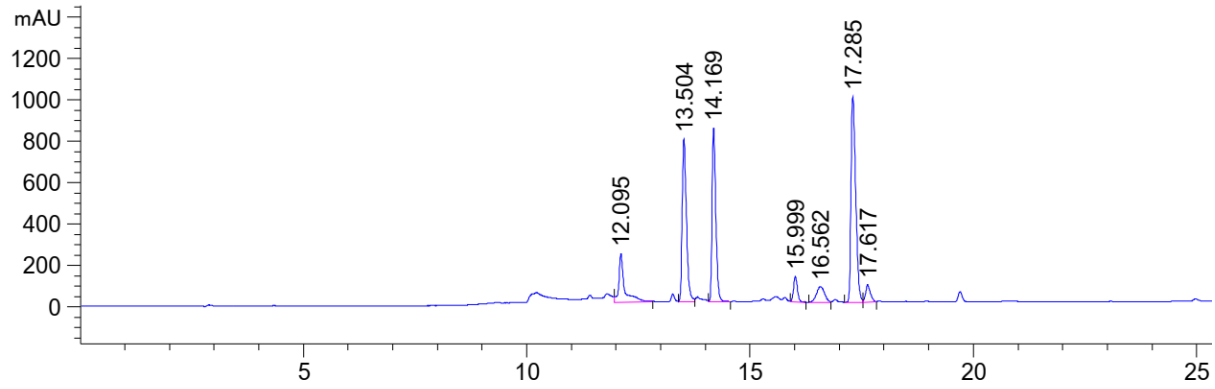

Figure 407: HPLC chromatogram of the synthesis of Smoc-L-Pro-L-Tyr-OMe **36** (17.3min) with EDC-HCl **37**/HOPO **40** in water after 25min at λ=220 nm (0 to 40% MeCN).

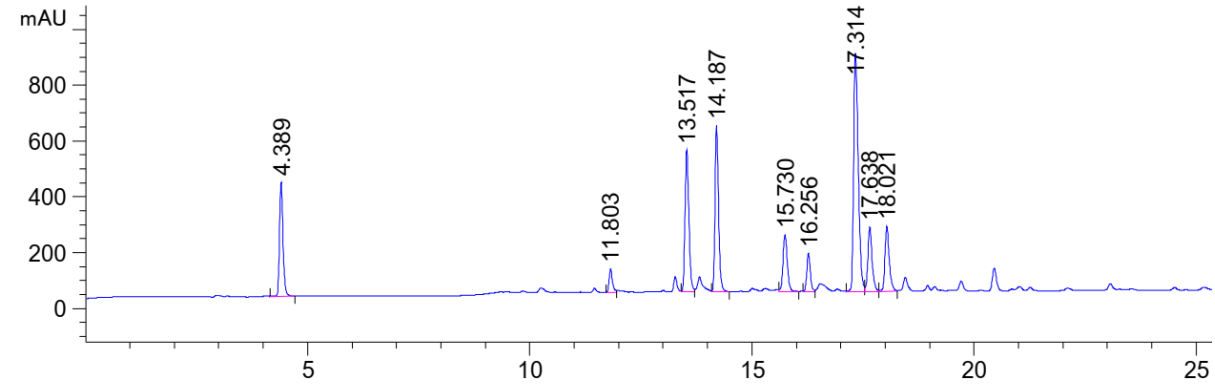

Figure 408: HPLC chromatogram of the synthesis of Smoc-L-Pro-L-Tyr-OMe **36** (17.3min) with EDC-HCl **37**/NHS **38** in water after 25min at λ=220 nm (0 to 40% MeCN).

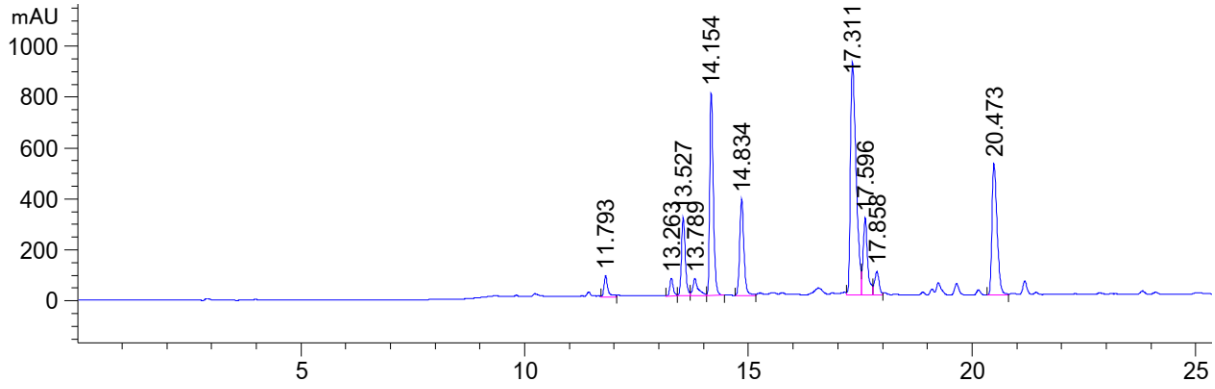

Figure 409: HPLC chromatogram of the synthesis of Smoc-L-Pro-L-Tyr-OMe **36** (17.3min) with EDC-HCl **37**/HONB **41** in water after 25min at λ=220 nm (0 to 40% MeCN).

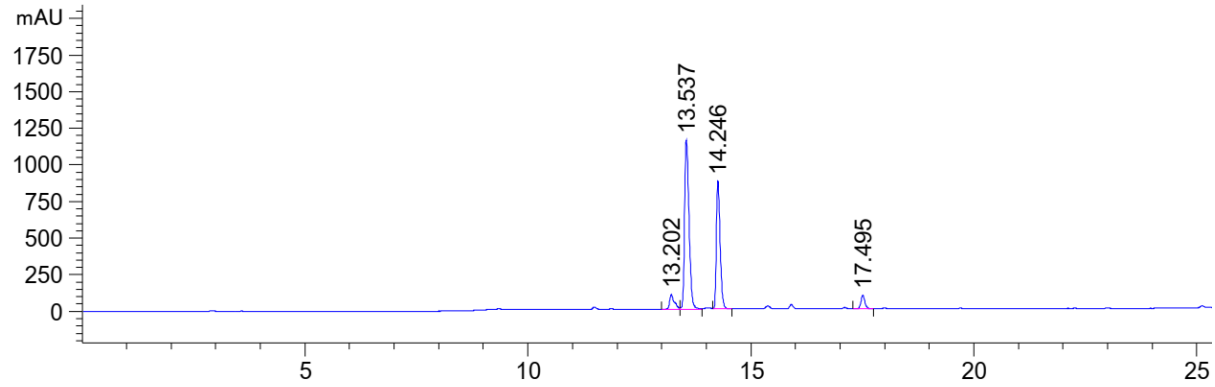

Figure 410: HPLC chromatogram of the synthesis of Smoc-L-Pro-L-Tyr-OMe **36** (17.5min) with EEDQ **42** in water after 25min at λ=220 nm (0 to 40% MeCN).

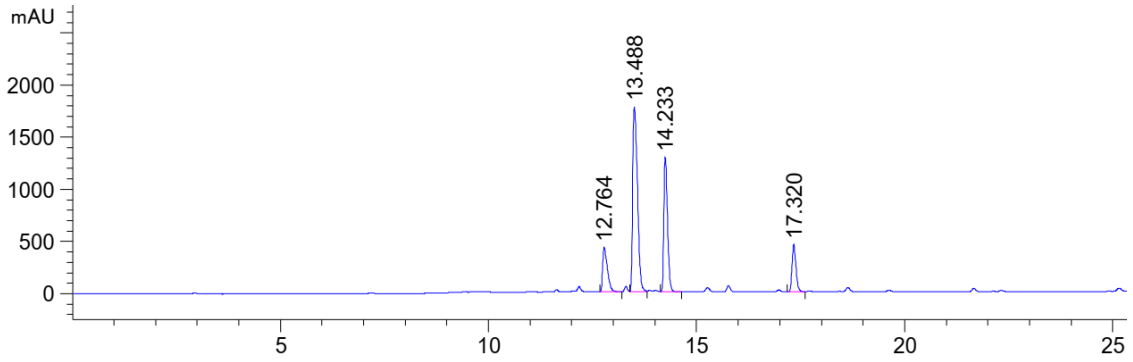

Figure 411: HPLC chromatogram of the synthesis of Smoc-L-Pro-L-Tyr-OMe **36** (17.3min) with DMT-MM **43** in water after 25min at λ=220 nm (0 to 40% MeCN).

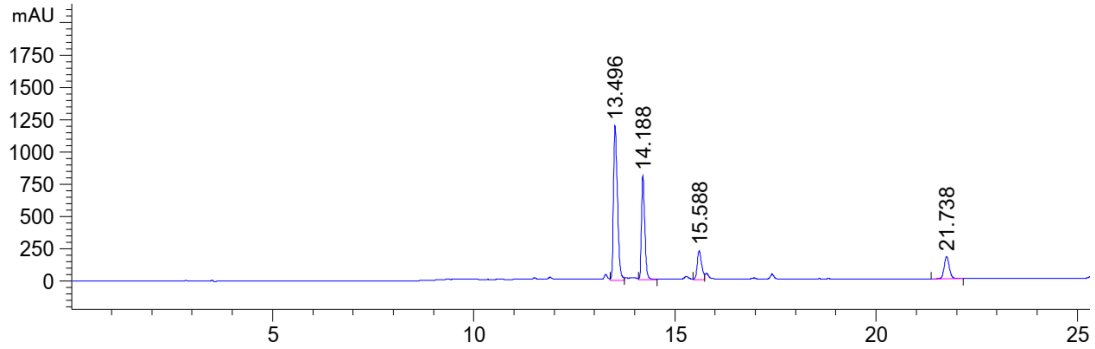

Figure 412: HPLC chromatogram of the synthesis of Smoc-L-Pro-L-Tyr-OMe **36** (17.2min) with COMU **44** in water after 25min at λ=220 nm (0 to 40% MeCN).

8.5.4. Analytical data of the synthesis of Smoc-Pro-Tyr-OMe 36 in 30% aq. MeCN

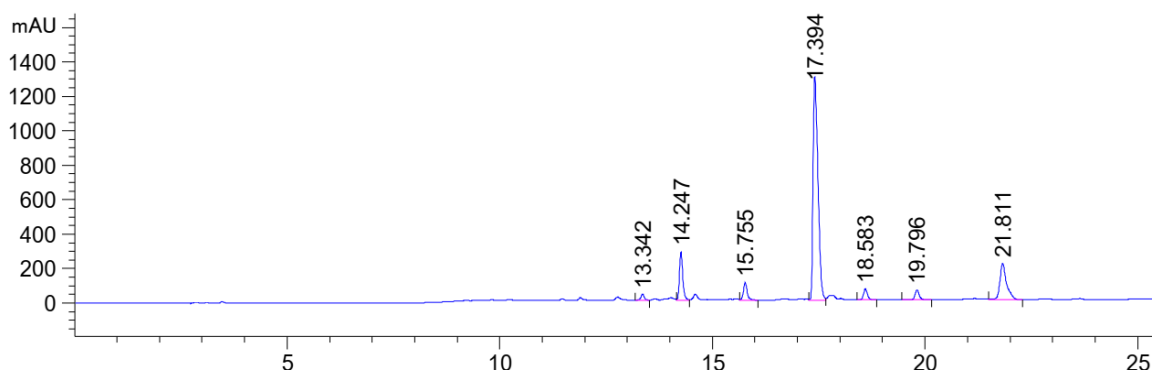

Figure 413: HPLC chromatogram of the synthesis of Smoc-L-Pro-L-Tyr-OMe **36** (17.4min) with EDC-HCl **37**/Oxyma **39** in 30% aq. MeCN after 25min at λ=220 nm (0 to 40% MeCN).

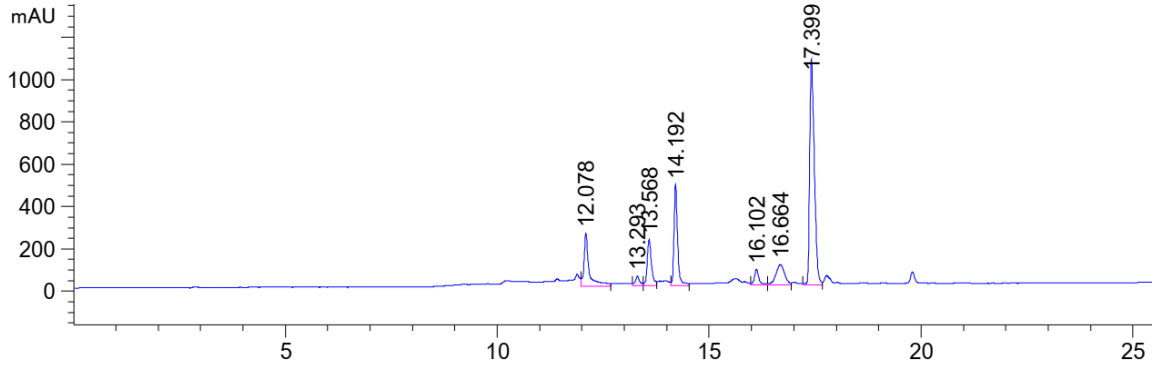

Figure 414: HPLC chromatogram of the synthesis of Smoc-L-Pro-L-Tyr-OMe **36** (17.4min) with EDC-HCl **37**/HOPO **40** in 30% aq. MeCN after 25min at λ=220 nm (0 to 40% MeCN).

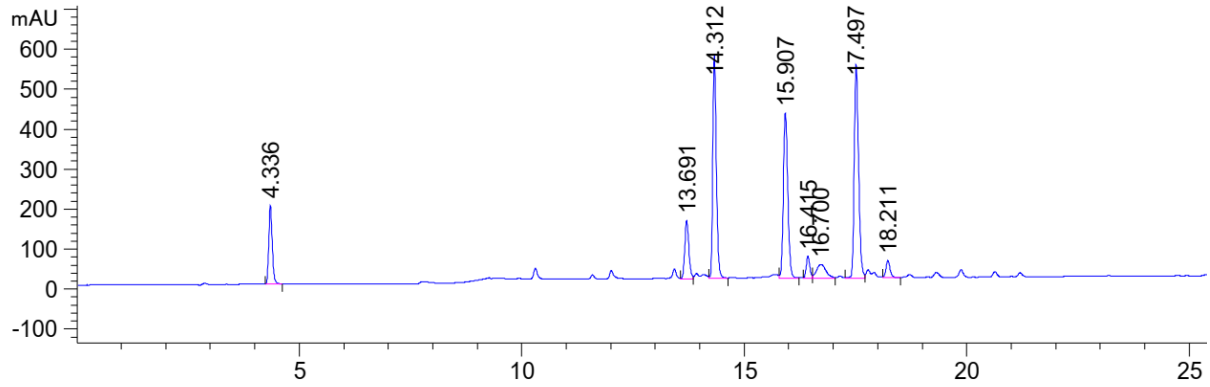

Figure 415: HPLC chromatogram of the synthesis of Smoc-L-Pro-L-Tyr-OMe **36** (17.4min) EDC-HCl **37**/NHS **38** in 30% aq. MeCN after 25min at λ=220 nm (0 to 40% MeCN).

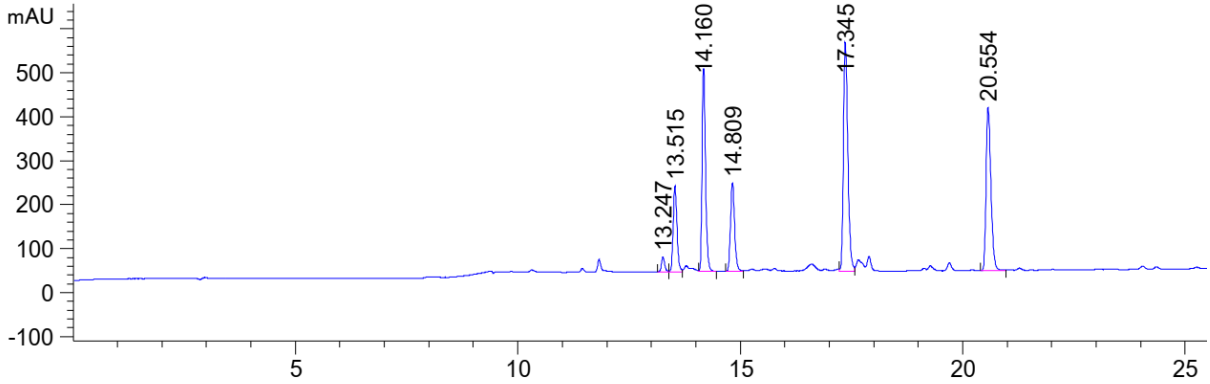

Figure 416: HPLC chromatogram of the synthesis of Smoc-L-Pro-L-Tyr-OMe **36** (17.2min) EDC-HCl **37**/HONB **41** in 30% aq. MeCN after 25min at λ=220 nm (0 to 40% MeCN).

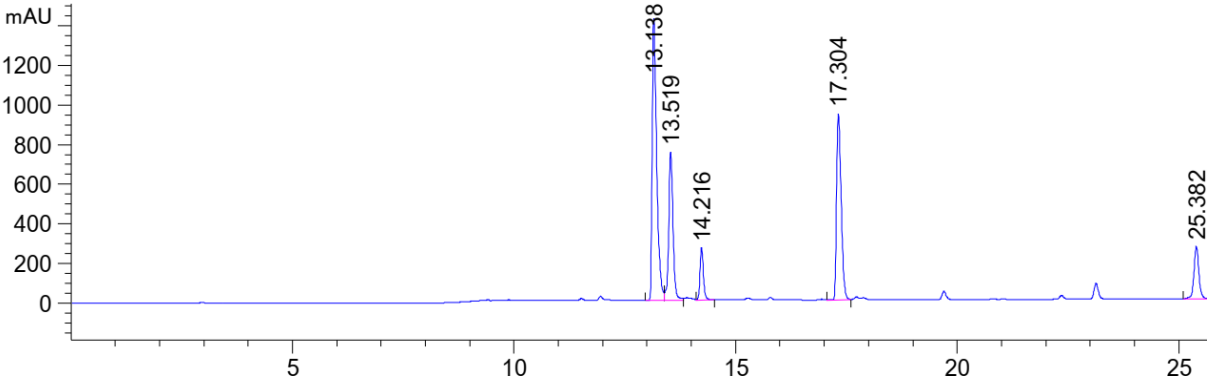

Figure 417: HPLC chromatogram of the synthesis of Smoc-L-Pro-L-Tyr-OMe **36** (17.2min) with EEDQ **42** in 30% aq. MeCN after 25min at λ=220 nm (0 to 40% MeCN).

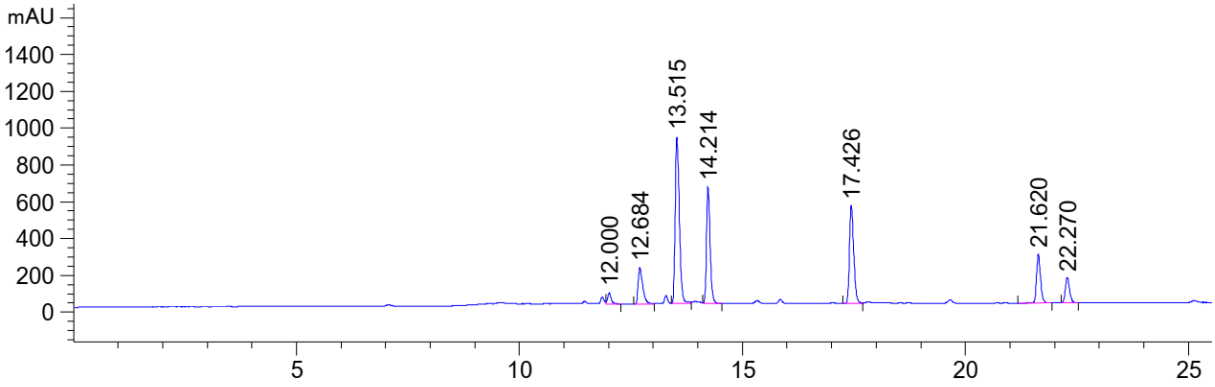

Figure 418: HPLC chromatogram of the synthesis of Smoc-L-Pro-L-Tyr-OMe **36** (17.2min) with DMT-MM **43** in 30% aq. MeCN after 25min at λ=220 nm (0 to 40% MeCN).

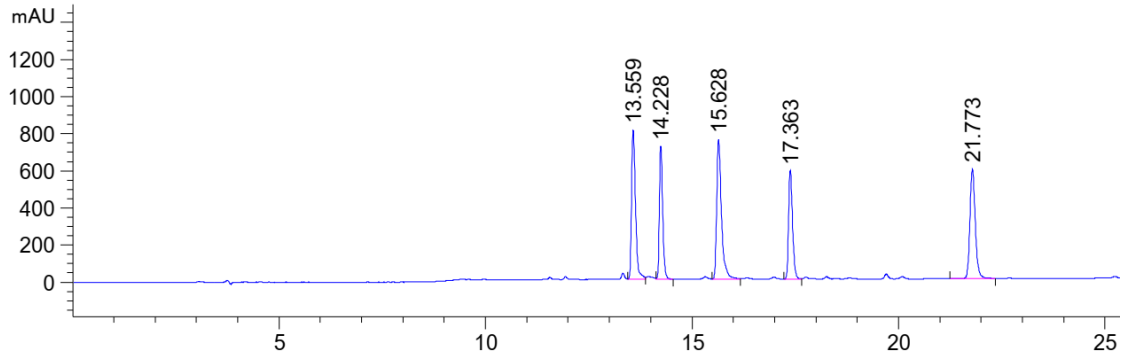

Figure 419: HPLC chromatogram of the synthesis of Smoc-L-Pro-L-Tyr-OMe **36** (17.2min) with COMU **44** in 30% aq. MeCN after 25min at λ=220 nm (0 to 40% MeCN).

8.5.5. Analytical data of the synthesis Smoc-Pro-Tyr-OMe 36 in 30% EtOAc water mixture (biphasic)

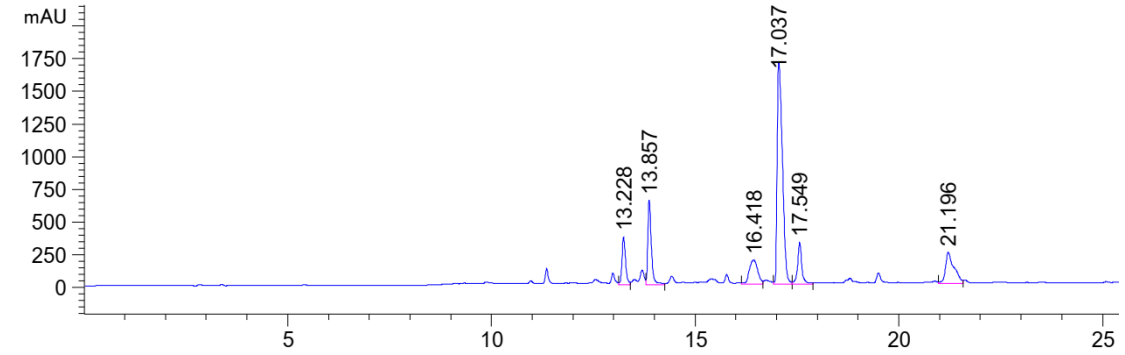

Figure 420: HPLC chromatogram of the synthesis of Smoc-L-Pro-L-Tyr-OMe **36** (17min) with EDC-HCl **37**/Oxyma **39** in 30% EtOAc water mixture (biphasic) after 25min at λ=220 nm (0 to 40% MeCN).

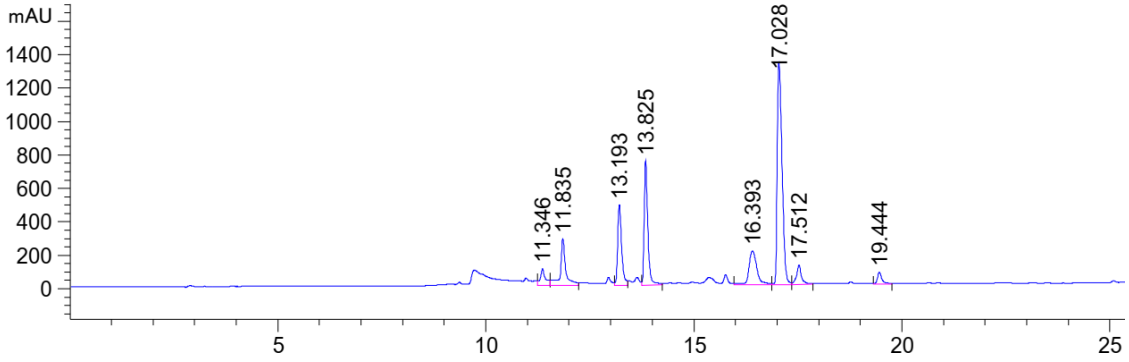

Figure 421: HPLC chromatogram of the synthesis of Smoc-L-Pro-L-Tyr-OMe **36** (17min) with EDC-HCl **37**/HOPO **40** in 30% EtOAc water mixture (biphasic) after 25min at λ=220 nm (0 to 40% MeCN).

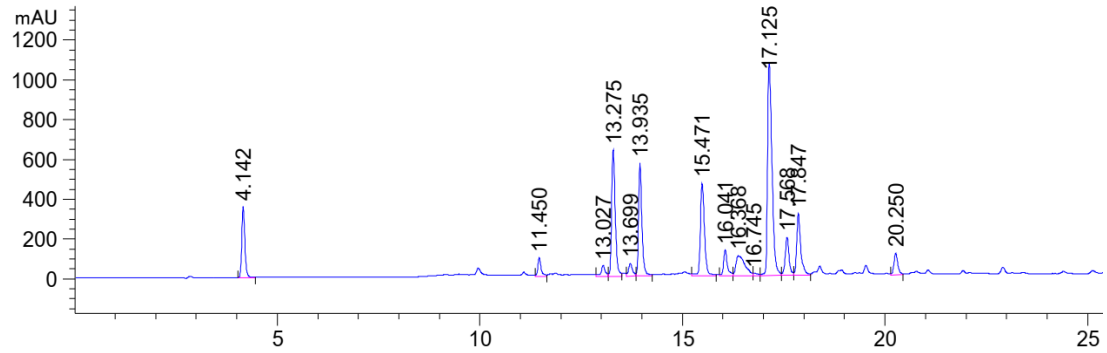

Figure 422: HPLC chromatogram of the synthesis of Smoc-L-Pro-L-Tyr-OMe **36** (17.1min) with EDC-HCl **37**/NHS **38** in 30% EtOAc water mixture (biphasic) after 25min at λ=220 nm (0 to 40% MeCN).

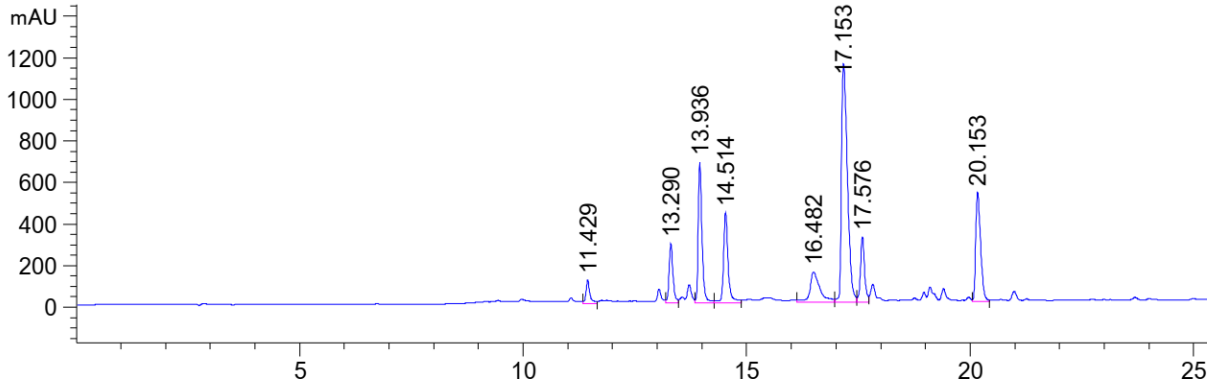

Figure 423: HPLC chromatogram of the synthesis of Smoc-L-Pro-L-Tyr-OMe **36** (17.2min) with EDC-HCl **37**/HONB **41** in 30% EtOAc water mixture (biphasic) after 25min at λ=220 nm (0 to 40% MeCN).

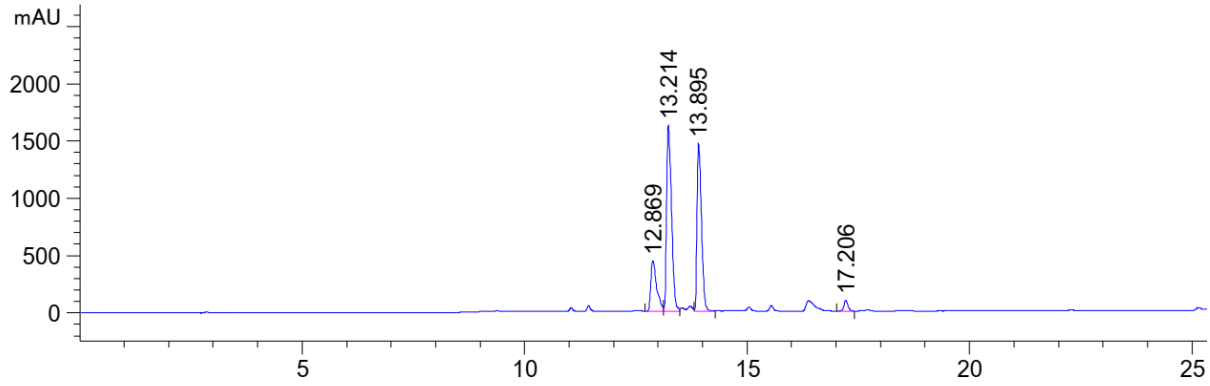

Figure 424: HPLC chromatogram of the synthesis of Smoc-L-Pro-L-Tyr-OMe **36** (17.2min) with EEDQ **42** in 30% EtOAc water mixture (biphasic) after 25min at λ=220 nm (0 to 40% MeCN).

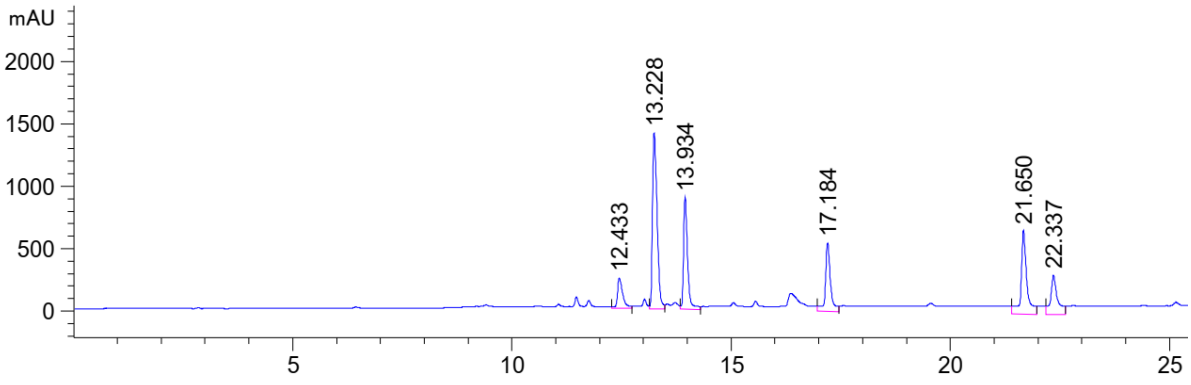

Figure 425: HPLC chromatogram of the synthesis of Smoc-L-Pro-L-Tyr-OMe 36 (17.2min) with DMT-MM **43** in 30% EtOAc water mixture (biphasic) after 25min at λ=220 nm (0 to 40% MeCN).

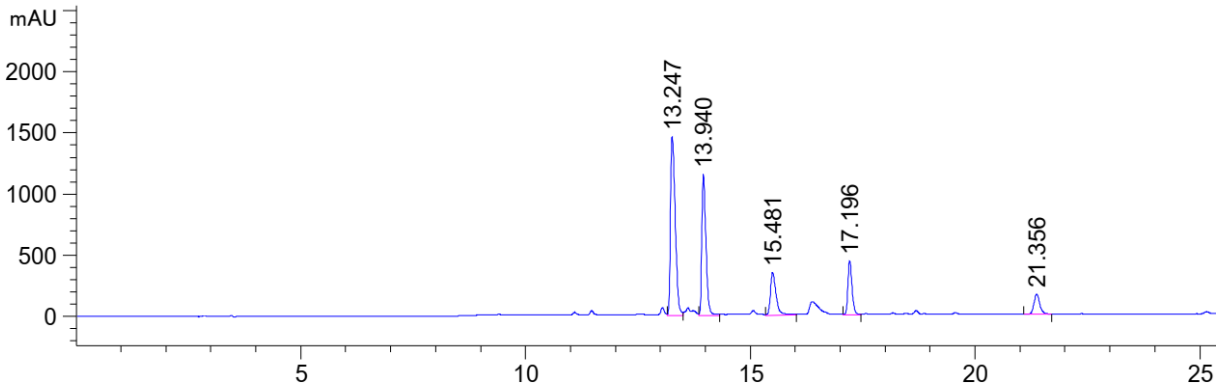

Figure 426: HPLC chromatogram of the synthesis of Smoc-L-Pro-L-Tyr-OMe **36**(17.2min) with COMU **44** in 30% EtOAc water mixture (biphasic) after 25min at λ=220 nm (0 to 40% MeCN).

8.5.6. Analytical data of the synthesis Smoc-Pro-Tyr-OMe 36 in 30% aq. ethanol

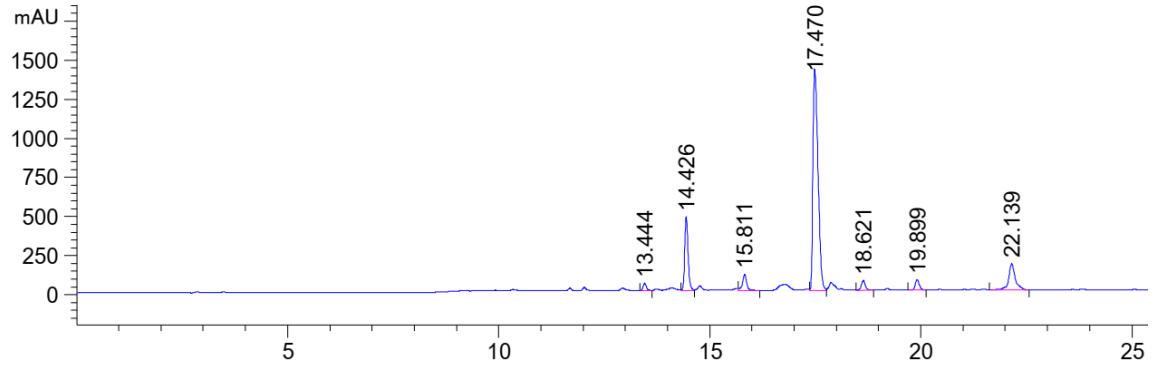

Figure 427: HPLC chromatogram of the synthesis of Smoc-L-Pro-L-Tyr-OMe **36** (17.5min) with EDC-HCl **37**/Oxyma **39** in 30% aq. ethanol after 25min at λ=220 nm (0 to 40% MeCN).

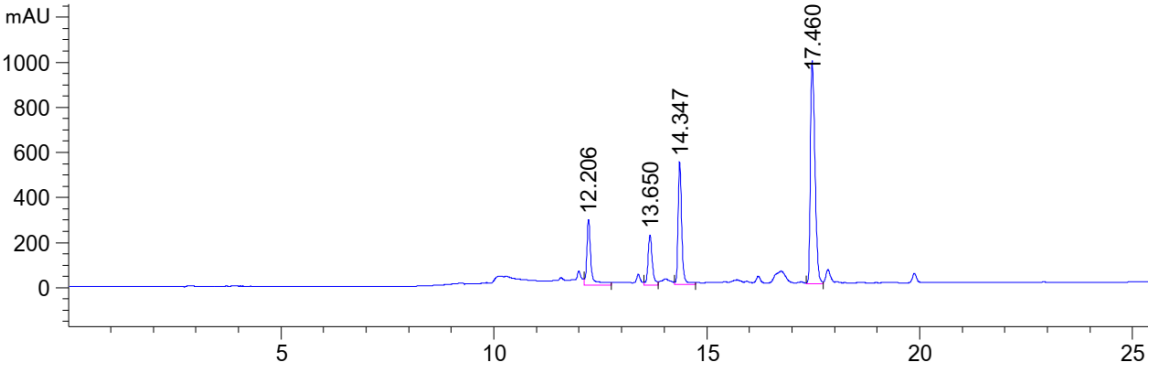

Figure 428: HPLC chromatogram of the synthesis of Smoc-L-Pro-L-Tyr-OMe **36** (17.5min) with EDC-HCl **37**/HOPO **40** in 30% aq. ethanol after 25min at λ=220 nm (0 to 40% MeCN).

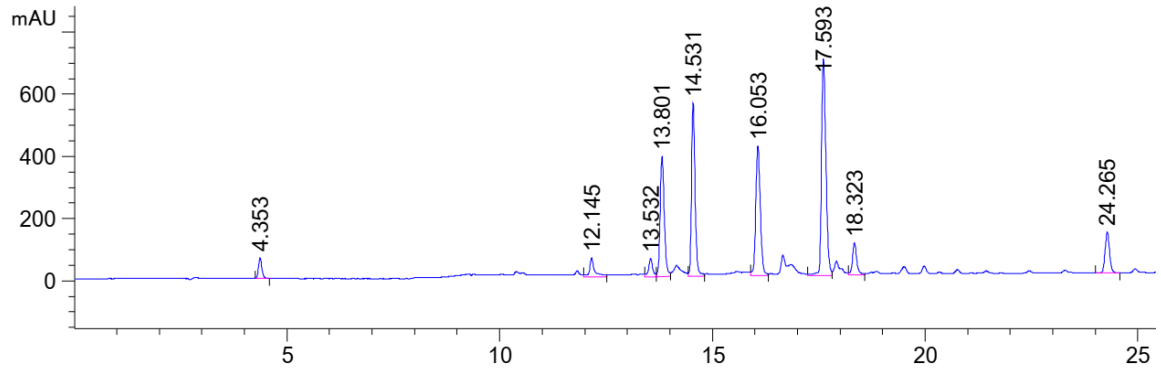

Figure 429: HPLC chromatogram of the synthesis of Smoc-L-Pro-L-Tyr-OMe **36** (17.6min) with EDC-HCl **37**/NHS **38** in 30% aq. ethanol after 25min at λ=220 nm (0 to 40% MeCN).

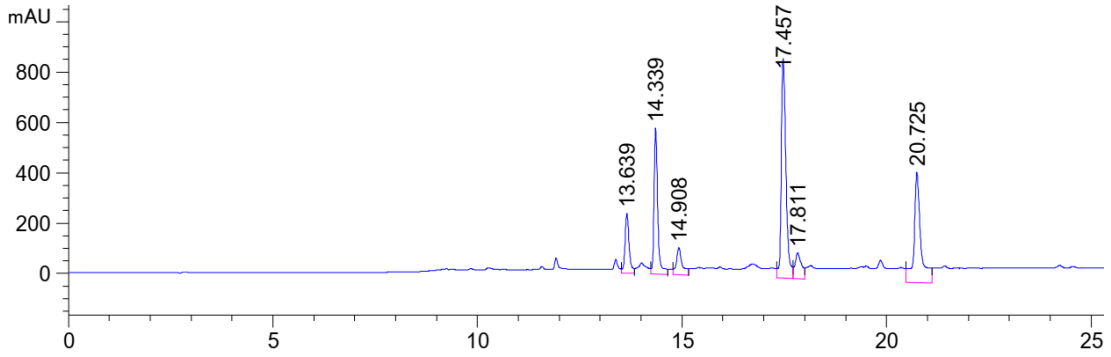

Figure 430: HPLC chromatogram of the synthesis of Smoc-L-Pro-L-Tyr-OMe **36** (17.5min) with EDC-HCl **37**/HONB **41** in 30% aq. ethanol after 25min at λ=220 nm (0 to 40% MeCN).

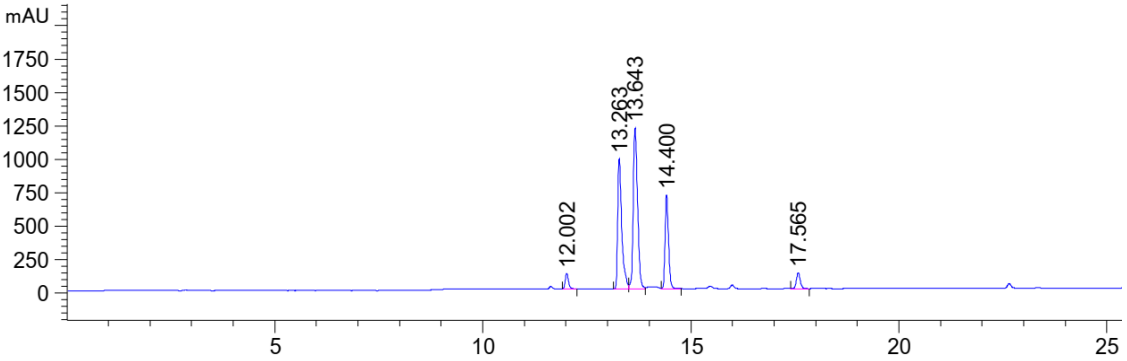

Figure 431: HPLC chromatogram of the synthesis of Smoc-L-Pro-L-Tyr-OMe **36** (17.5min) with EEDQ **42** in 30% aq. ethanol after 25min at λ=220 nm (0 to 40% MeCN).

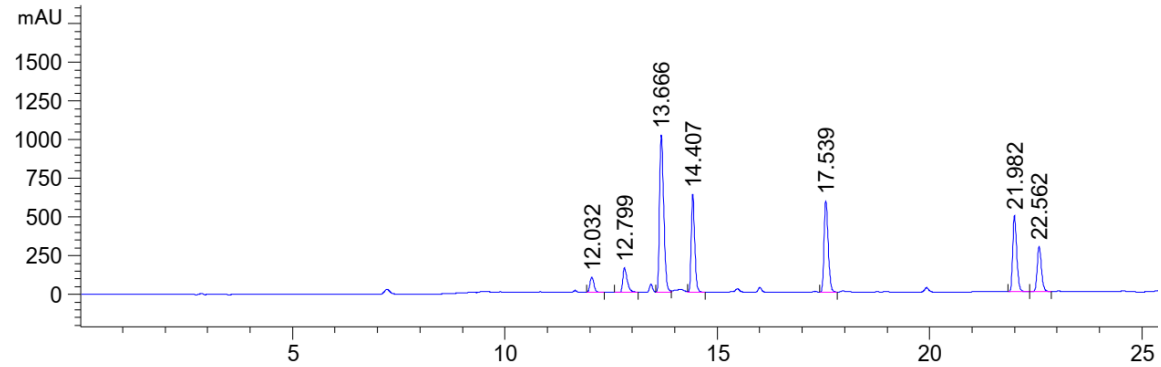

Figure 432: HPLC chromatogram of the synthesis of Smoc-L-Pro-L-Tyr-OMe **36** (17.5min) with DMT-MM **43** in 30% aq. ethanol after 25min at λ=220 nm (0 to 40% MeCN).

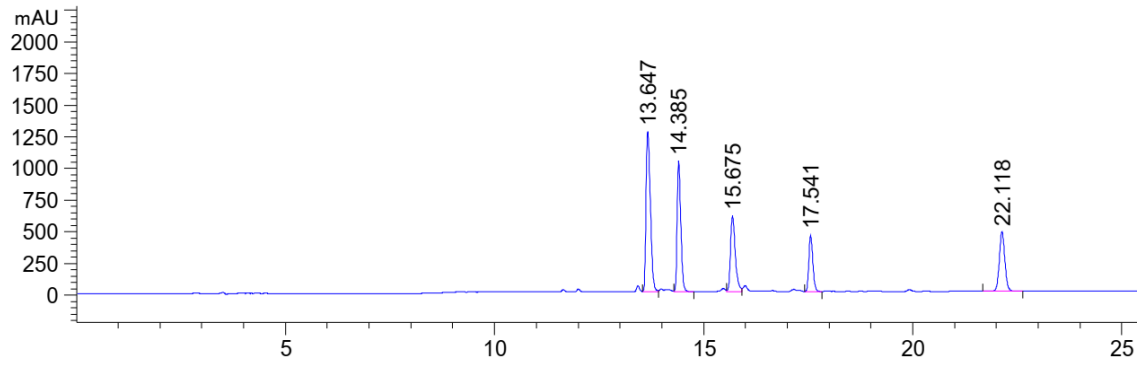

Figure 433: HPLC chromatogram of the synthesis of Smoc-L-Pro-L-Tyr-OMe **36** (17.5min) with COMU **44** in 30% aq. ethanol after 25min at λ=220 nm (0 to 40% MeCN).

8.5.7. Analytical data of the synthesis Smoc-Pro-Tyr-OMe 36 in 30% aq. isopropanol

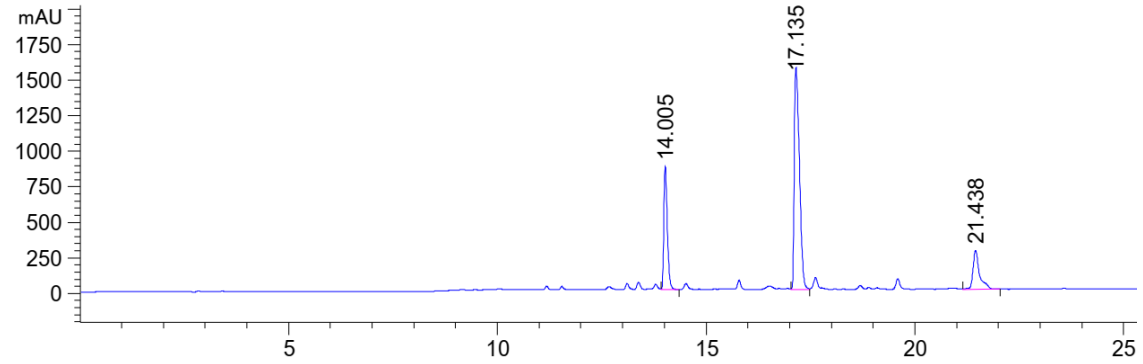

Figure 434: HPLC chromatogram of the synthesis of Smoc-L-Pro-L-Tyr-OMe **36** (17.2min) with EDC-HCl **37**/Oxyma **39** in 30% aq. isopropanol after 25min at λ=220 nm (0 to 40% MeCN).

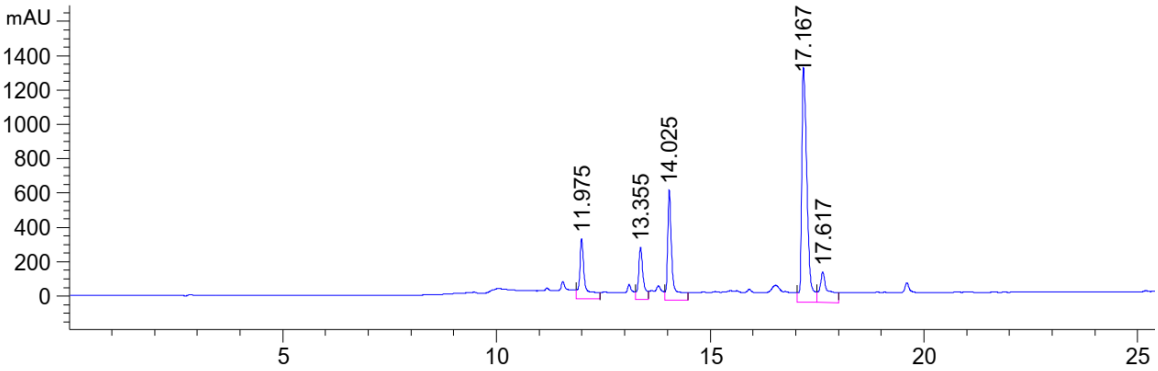

Figure 435: HPLC chromatogram of the synthesis of Smoc-L-Pro-L-Tyr-OMe **36** (17.2min) with EDC-HCl **37**/HOPO **40** in 30% aq. isopropanol after 25min at λ=220 nm (0 to 40% MeCN).

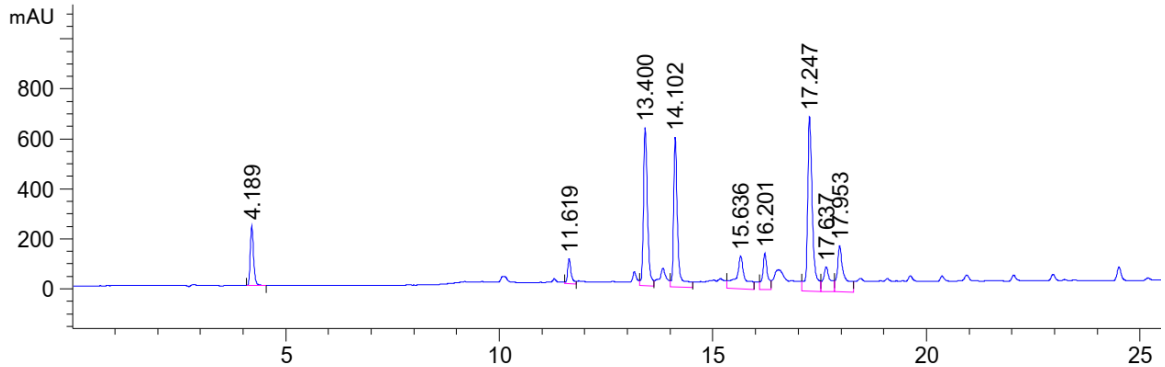

Figure 436: HPLC chromatogram of the synthesis of Smoc-L-Pro-L-Tyr-OMe **36** (17.2min) with EDC-HCl **37**/NHS **38** in 30% aq. isopropanol after 25min at λ=220 nm (0 to 40% MeCN).

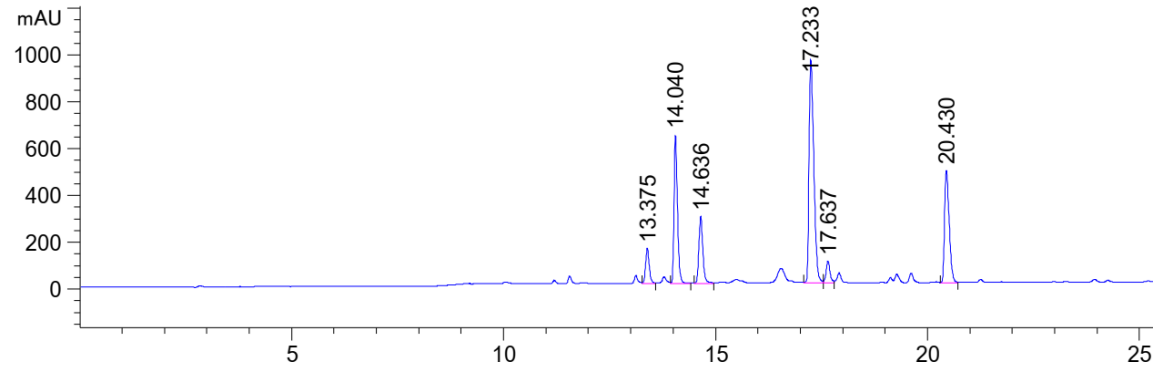

Figure 437: HPLC chromatogram of the synthesis of Smoc-L-Pro-L-Tyr-OMe **36** (17.2min) with EDC-HCl **37**/HONB **41** in 30% aq. isopropanol after 25min at λ=220 nm (0 to 40% MeCN).

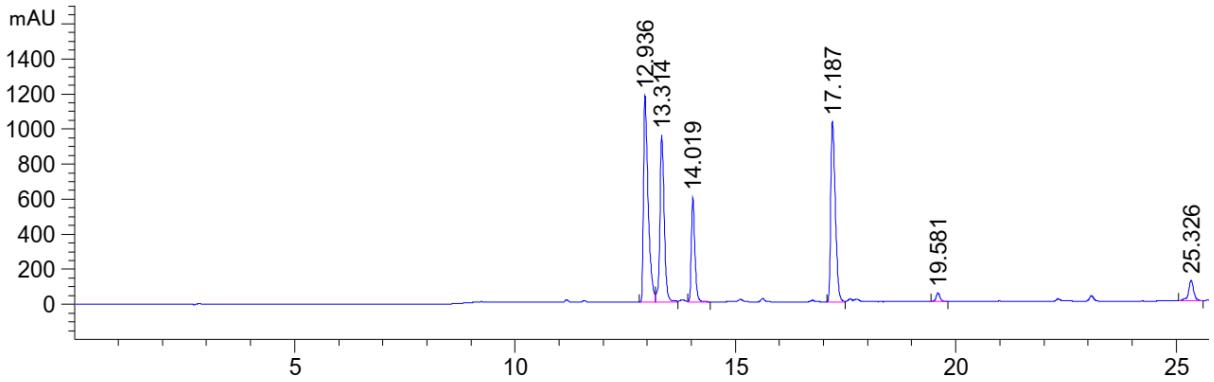

Figure 438: HPLC chromatogram of the synthesis of Smoc-L-Pro-L-Tyr-OMe **36** (17.2min) with EEDQ **42** in 30% aq. isopropanol after 25min at λ=220 nm (0 to 40% MeCN).

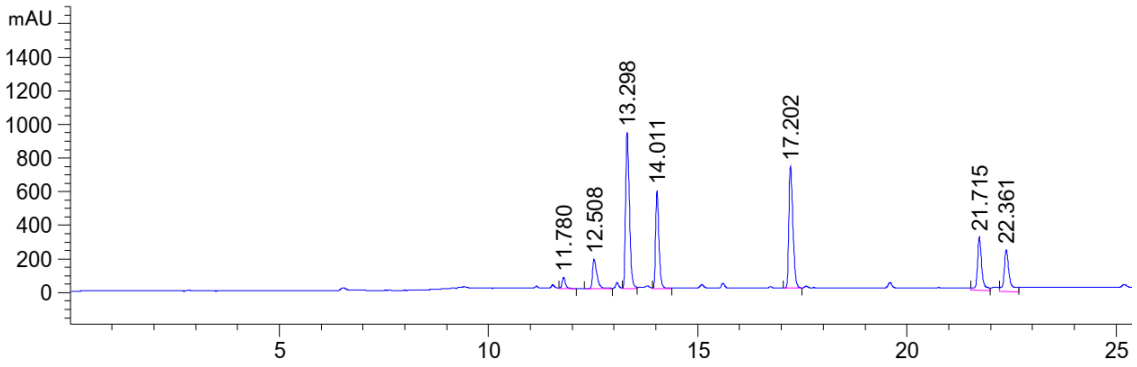

Figure 439: HPLC chromatogram of the synthesis of Smoc-L-Pro-L-Tyr-OMe **36** (17.2min) with DMT-MM **43** in 30% aq. isopropanol after 25min at λ=220 nm (0 to 40% MeCN).

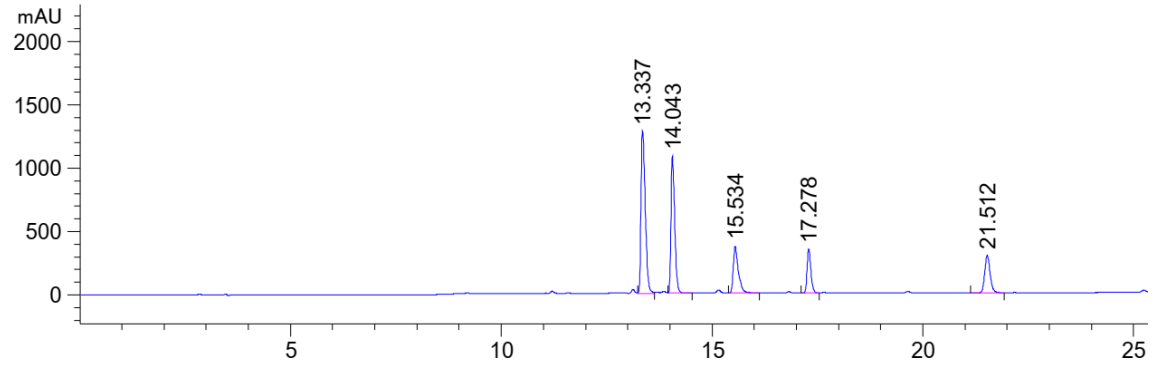

Figure 440: HPLC chromatogram of the synthesis of Smoc-L-Pro-L-Tyr-OMe **36** (17.2min) with COMU **44** in 30% aq. isopropanol after 25min at λ=220 nm (0 to 40% MeCN).

8.5.8. Analytical data of the synthesis Smoc-Pro-Tyr-OMe 36 in 30% MeTHF water mixture (biphasic)

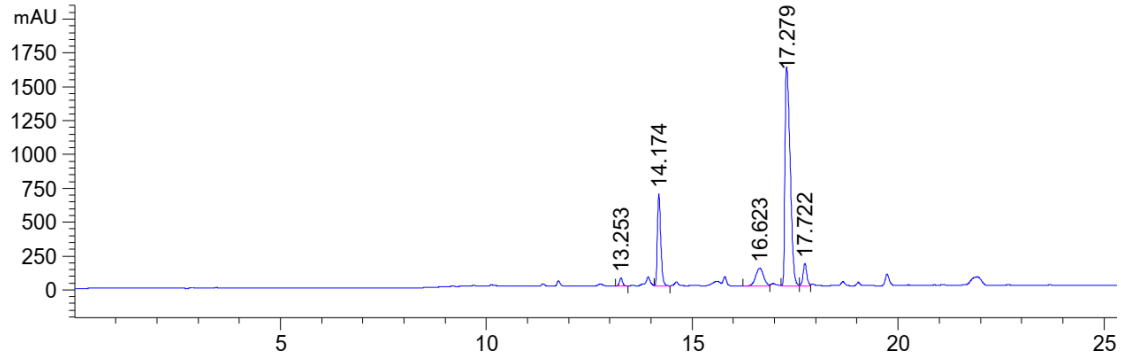

Figure 441: HPLC chromatogram of the synthesis of Smoc-L-Pro-L-Tyr-OMe **36** (17.3min) with EDC-HCl **37**/Oxyma **39** in 30% Me-THF water mixture (biphasic) after 25min at λ=220 nm (0 to 40% MeCN).

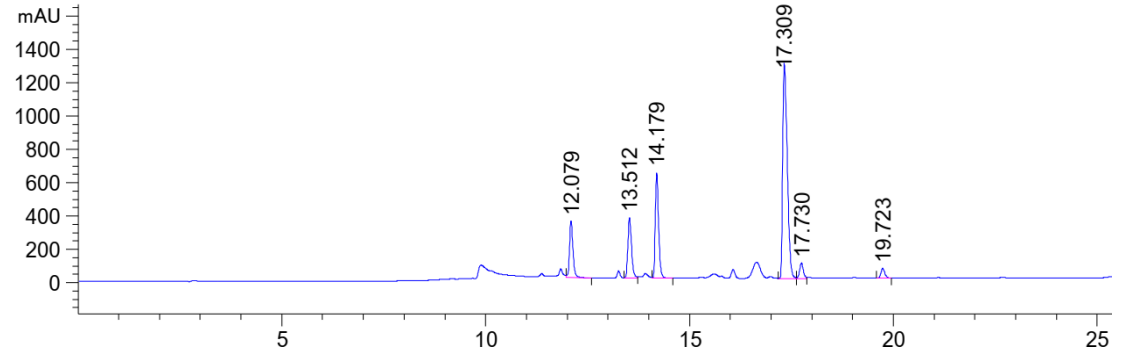

Figure 442: HPLC chromatogram of the synthesis of Smoc-L-Pro-L-Tyr-OMe **36** (17.3min) with EDC-HCl **37**/HOPO **40** in 30% Me-THF water mixture (biphasic) after 25min at λ=220 nm (0 to 40% MeCN).

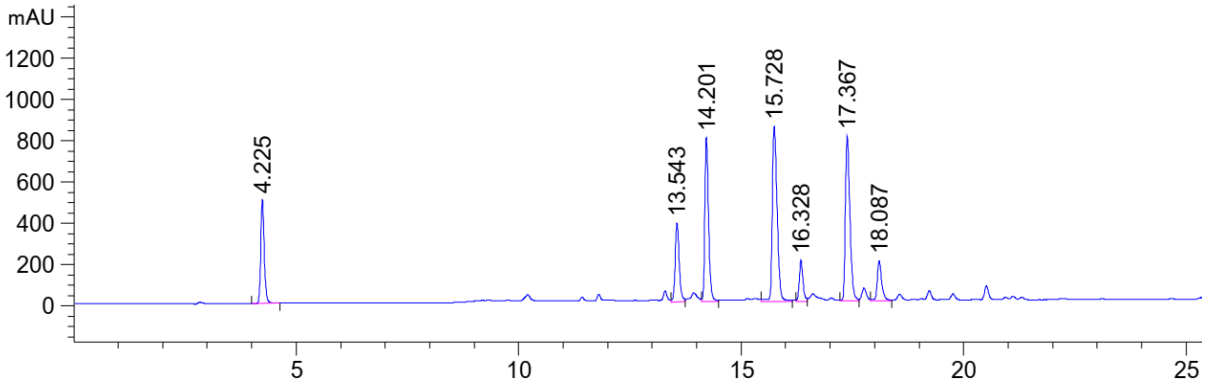

Figure 443: HPLC chromatogram of the synthesis of Smoc-L-Pro-L-Tyr-OMe **36** (17.4min) with EDC-HCl **37**/NHS **38** in 30% Me-THF water mixture (biphasic) after 25min at λ=220 nm (0 to 40% MeCN).

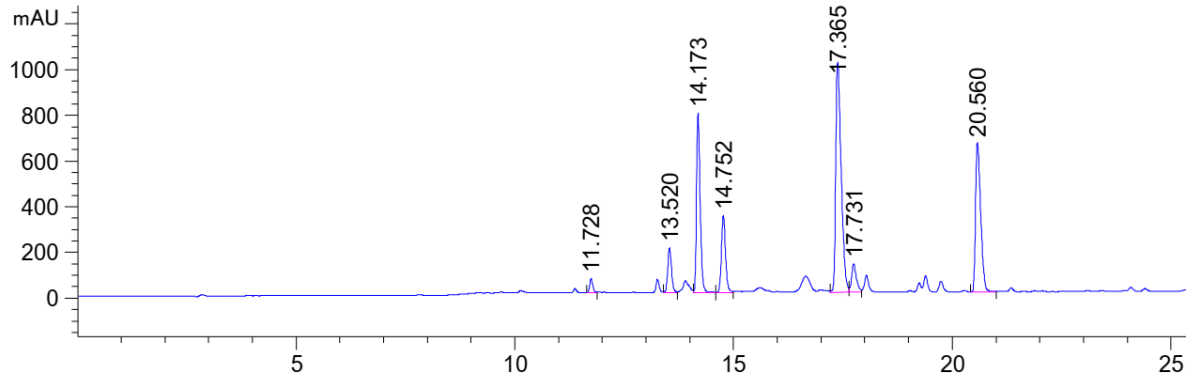

Figure 444: HPLC chromatogram of the synthesis of Smoc-L-Pro-L-Tyr-OMe **36** (17.4min) EDC-HCl **37**/HONB **41** in 30% Me-THF water mixture (biphasic) after 25min at λ=220 nm (0 to 40% MeCN).

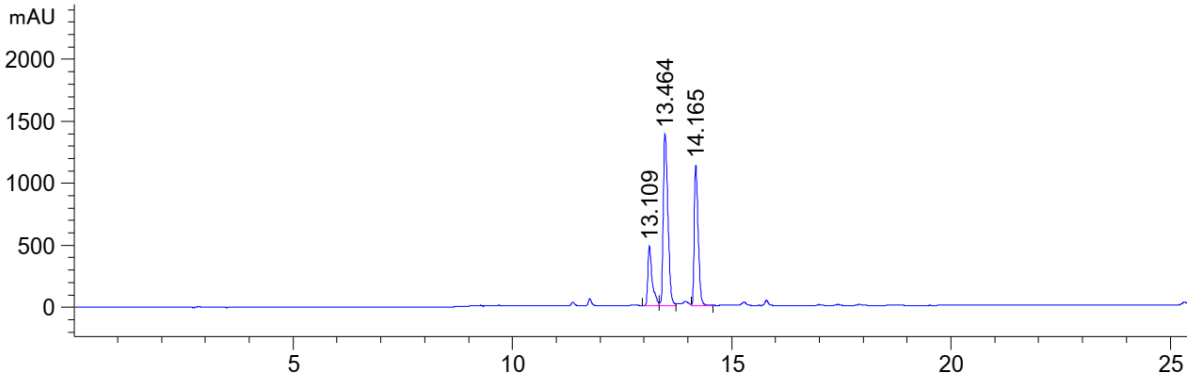

Figure 445: HPLC chromatogram of the synthesis of Smoc-L-Pro-L-Tyr-OMe **36** (17.4min) with EEDQ **42** in 30% Me-THF water mixture (biphasic) after 25min at λ=220 nm (0 to 40% MeCN).

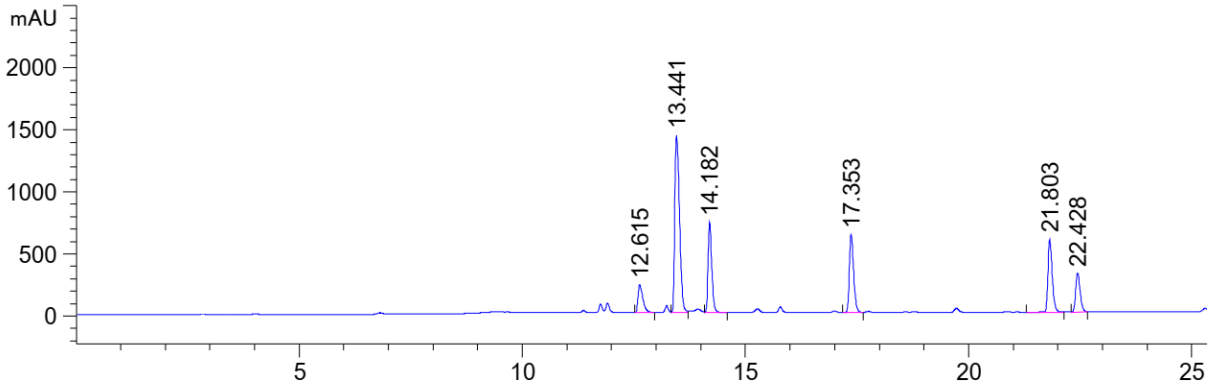

Figure 446: HPLC chromatogram of the synthesis of Smoc-L-Pro-L-Tyr-OMe **36** (17.4min) with DMT-MM **43** in 30% Me-THF water mixture (biphasic) after 25min at λ=220 nm (0 to 40% MeCN).

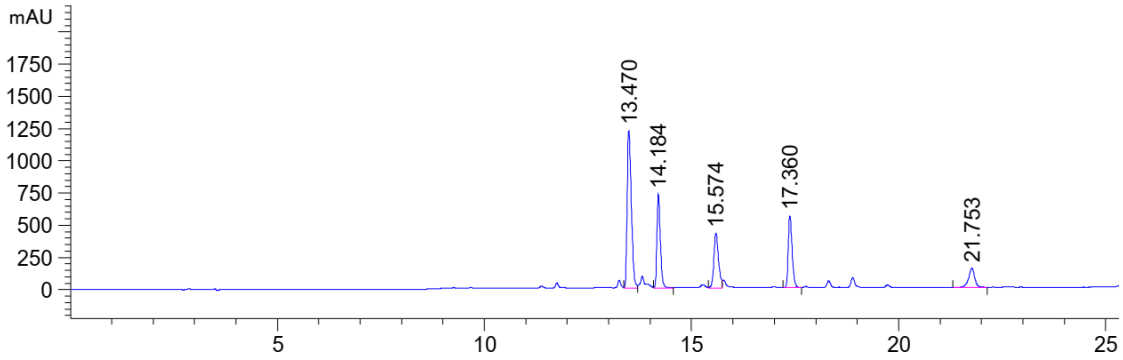

Figure 447: HPLC chromatogram of the synthesis of Smoc-L-Pro-L-Tyr-OMe **36** (17.4min) with COMU **44** in 30% Me-THF water mixture (biphasic) after 25min at λ=220 nm (0 to 40% MeCN).

8.5.9. Analytical data of the synthesis Smoc-Pro-Tyr-OMe 36 in 10% aq. Me-THF

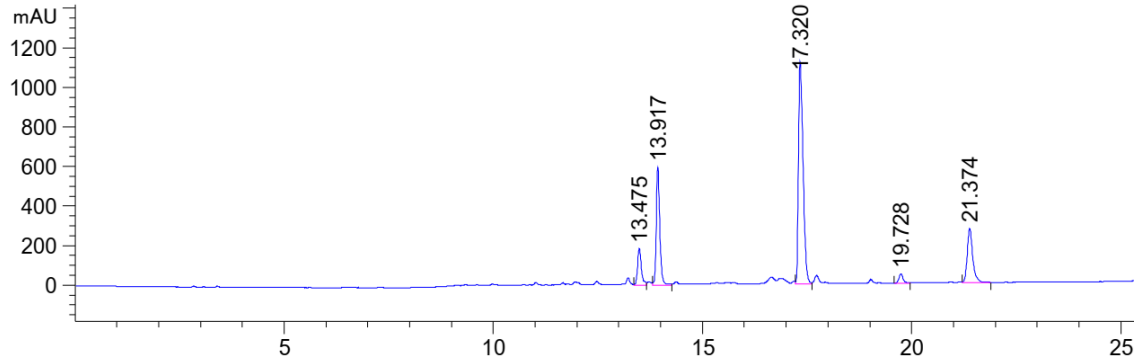

Figure 448: HPLC chromatogram of the synthesis of Smoc-L-Pro-L-Tyr-OMe **36** (17.3min) with EDC-HCl **37**/Oxyma **39** in 10% aq. Me-THF after 25min at λ=220 nm (0 to 40% MeCN).

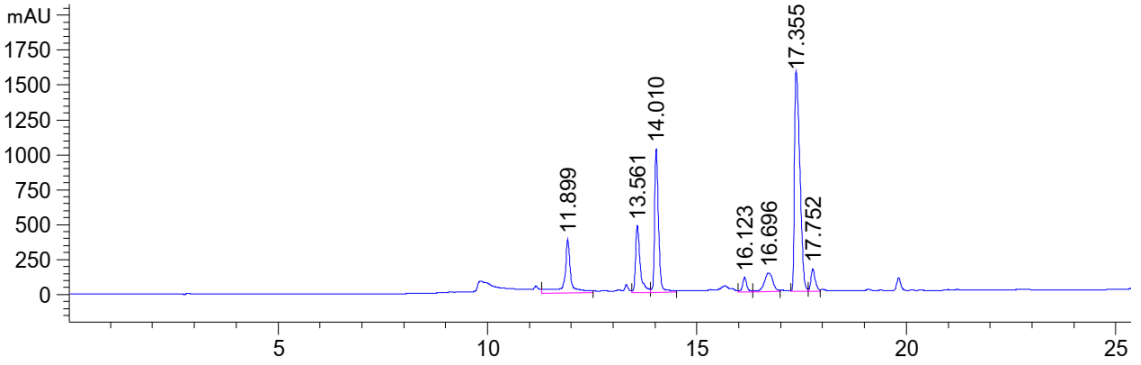

Figure 449: HPLC chromatogram of the synthesis of Smoc-L-Pro-L-Tyr-OMe **36** (17.3min) with EDC-HCl **37**/HOPO **40** in 10% aq. Me-THF after 25min at λ=220 nm (0 to 40% MeCN).

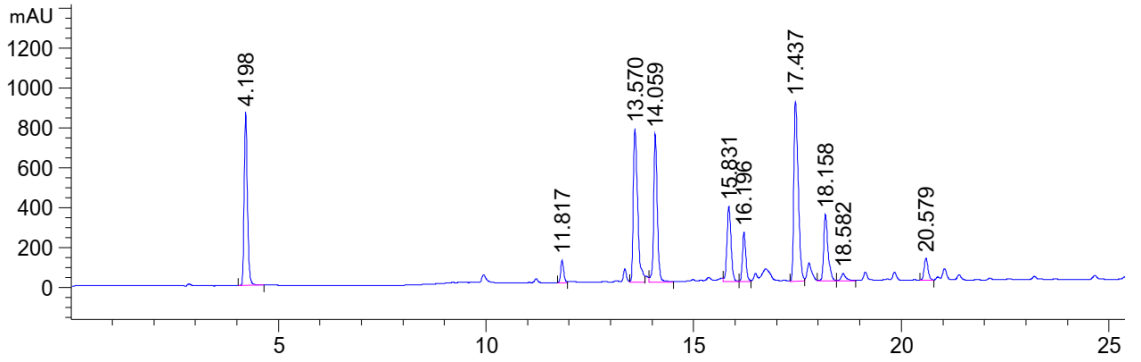

Figure 450: HPLC chromatogram of the synthesis of Smoc-L-Pro-L-Tyr-OMe **36** (17.3min) with EDC-HCl **37**/NHS **38** in 10% aq. Me-THF after 25min at λ=220 nm (0 to 40% MeCN).

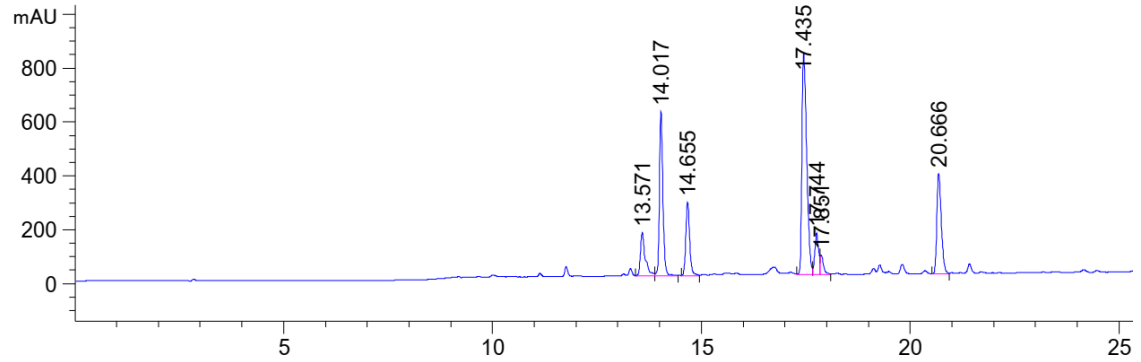

Figure 451: HPLC chromatogram of the synthesis of Smoc-L-Pro-L-Tyr-OMe **36** (17.3min) with EDC-HCl **37**/HONB **41** in 10% aq. Me-THF after 25min at λ=220 nm (0 to 40% MeCN).

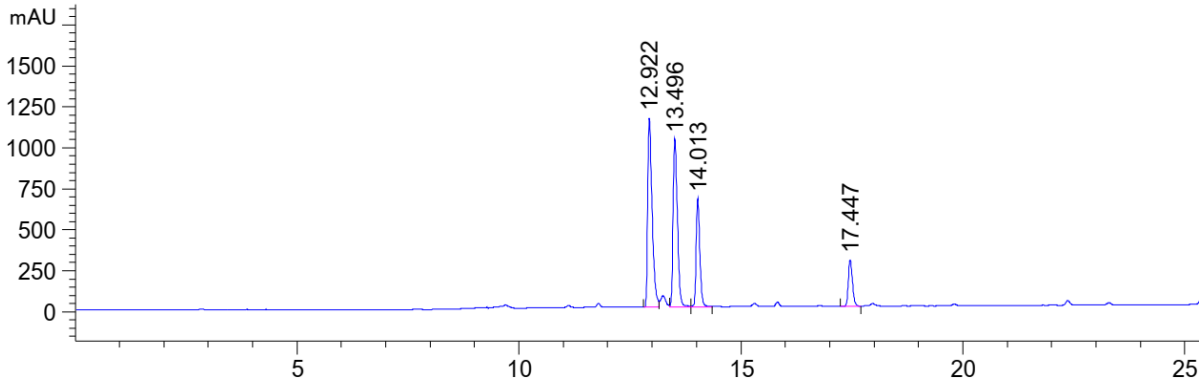

Figure 452: HPLC chromatogram of the synthesis of Smoc-L-Pro-L-Tyr-OMe **36** (17.4min) with EEDQ **42** in 10% aq. Me-THF after 25min at λ=220 nm (0 to 40% MeCN).

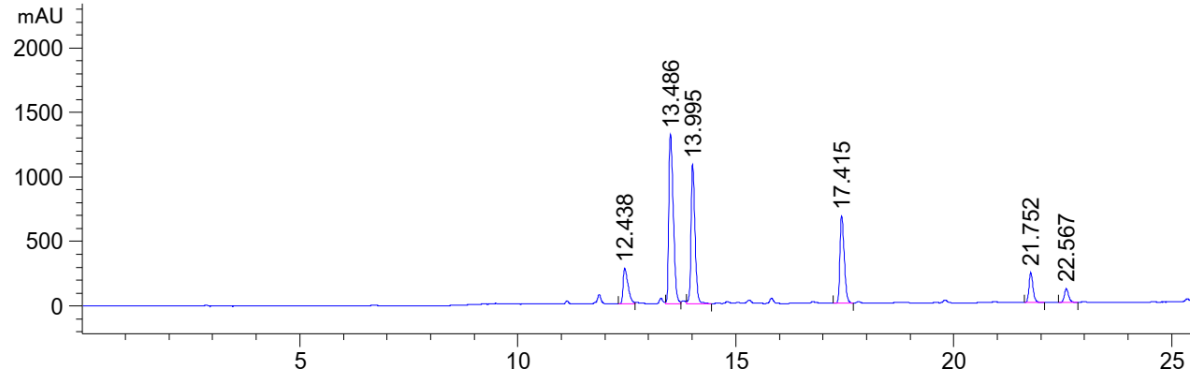

Figure 453: HPLC chromatogram of the synthesis of Smoc-L-Pro-L-Tyr-OMe **36** (17.4min) with DMT-MM **43** in 10% aq. Me-THF after 25min at λ=220 nm (0 to 40% MeCN).

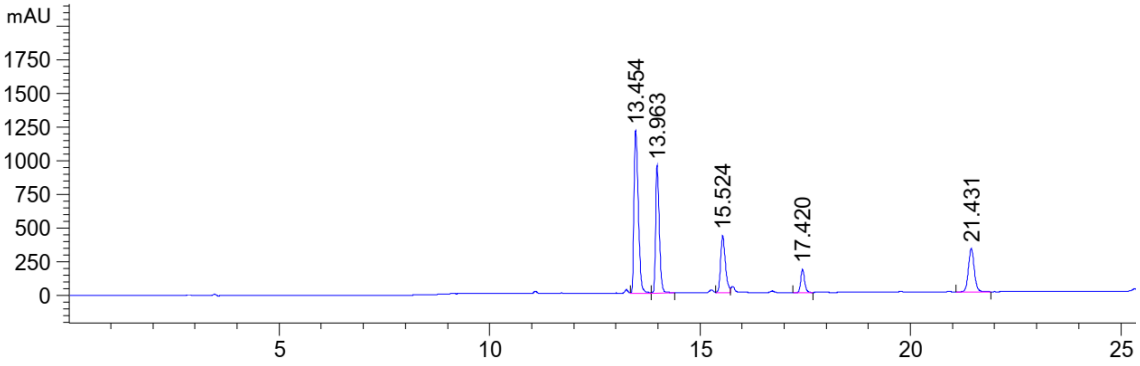

Figure 454: HPLC chromatogram of the synthesis of Smoc-L-Pro-L-Tyr-OMe **36** (17.4min) with COMU **44** in 10% aq. Me-THF after 25min at λ=220 nm (0 to 40% MeCN).

8.6. Analytical data of SPPS coupling efficiency test with Oxyma 39 and HOPO 40

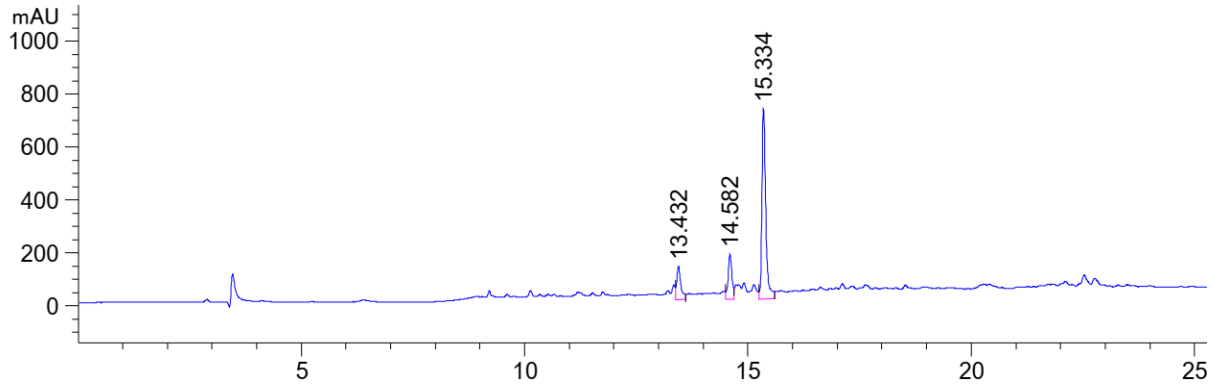

Figure 455: HPLC chromatogram of the synthesis of Smoc-LAGV-NH_2 **47** with EDC-HCl **37** and Oxyma **39** in water at λ=220 nm (0 to 60% MeCN).

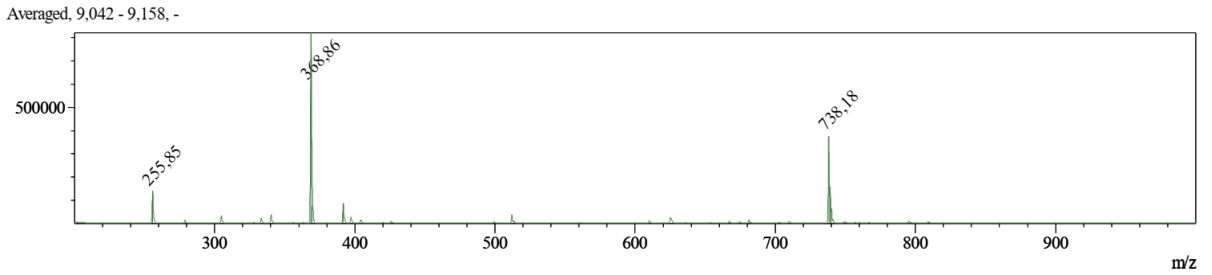

Figure 456: ESI-MS HPLC of the synthesis of Smoc-LAGV-NH2 **47** with EDC-HCl **37** and Oxyma **39** in water (M measured=738.18 $[M-2H]^-$, M calc.=740.80).

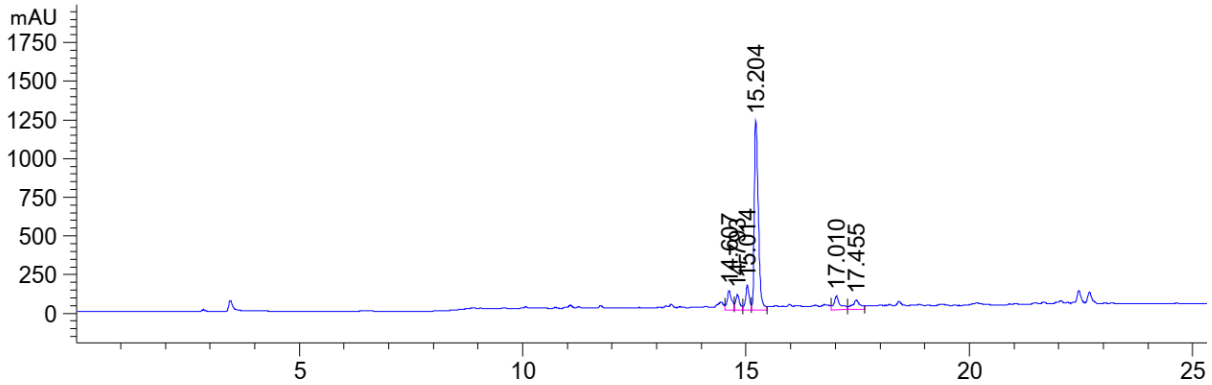

Figure 457: HPLC chromatogram of the synthesis of Smoc-LAGV-NH_2 **47** with EDC-HCl **37** and Oxyma **39** in 30% aq. MeCN at λ=220 nm (0 to 60% MeCN).

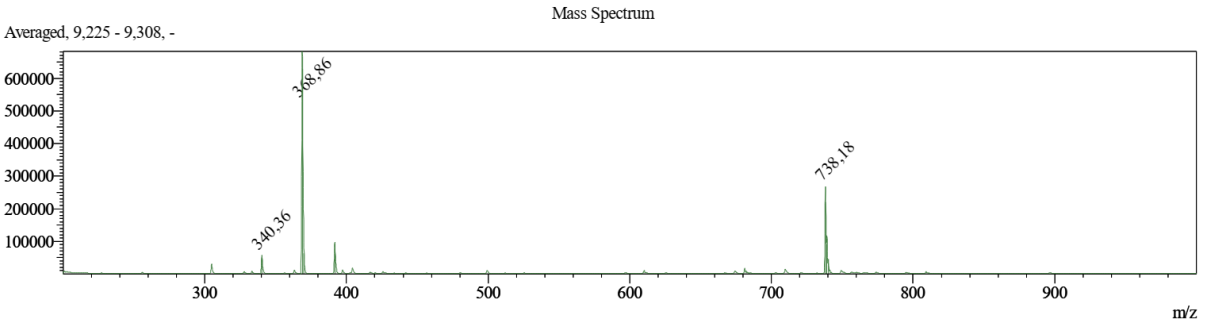

Figure 458: ESI-MS HPLC of the synthesis of Smoc-LAGV-NH_2 **47** with EDC-HCl **37** and Oxyma **39** in 30% aq. MeCN (M measured=738.18 $[M-H]^-$, M calc.=740.80).

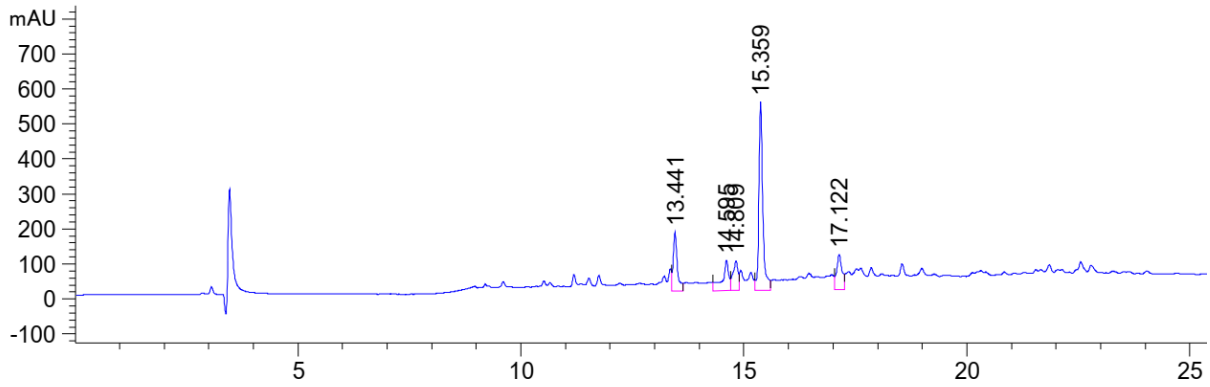

Figure 459: HPLC chromatogram of the synthesis of Smoc-LAGV-NH_2 **47** with EDC-HCl **37** and HOPO **40** in water at λ=220 nm (0 to 60% MeCN).

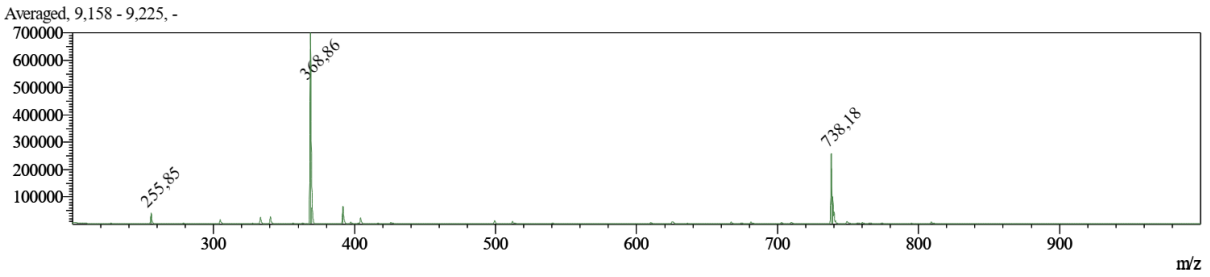

Figure 460: ESI-MS HPLC of the synthesis of Smoc-LAGV-NH_2 **47** with EDC-HCl **37** and HOPO **40** in water (M measured=738.18 $[M-H]^-$, M calc.=740.80).

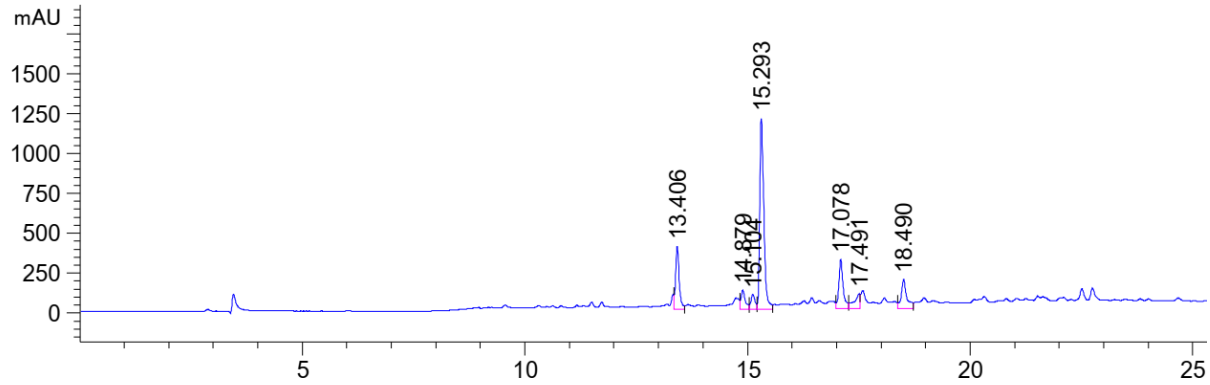

Figure 461: HPLC chromatogram of the synthesis of Smoc-LAGV-NH_2 **47** with EDC-HCl **37** and HOPO **40** in 30% aq. MeCN at λ=220 nm (0 to 60% MeCN).

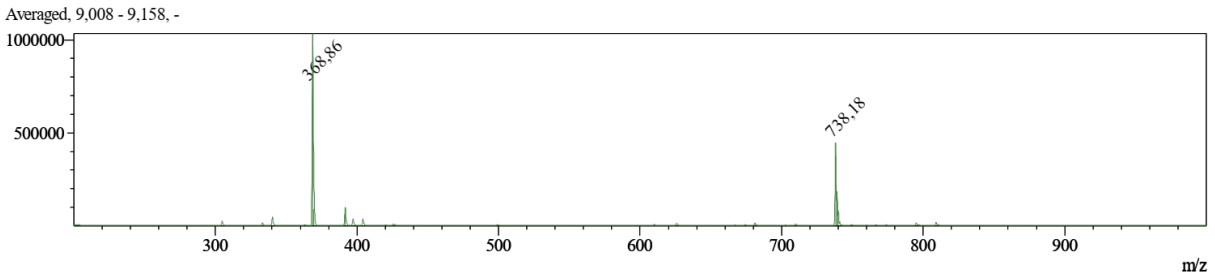

Figure 462: ESI-MS HPLC of the synthesis of Smoc-LAGV-NH_2 **47** with EDC-HCl **37** and HOPO **40** in 30% aq. MeCN (M measured=738.18 $[M-H]^-$, M calc.=740.80).

8.7. Peptides

8.7.1. Analytical data of H-AGELS-NH2 (Pentapeptide-31) 48

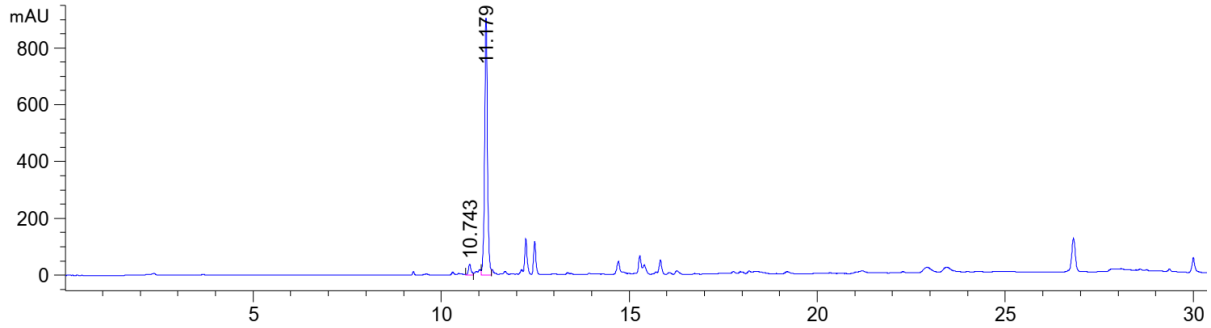

Figure 463: HPLC chromatogram of H-AGELS-NH_2 (Pentapeptide-31) **48** at λ=220 nm (0 to 60% MeCN).

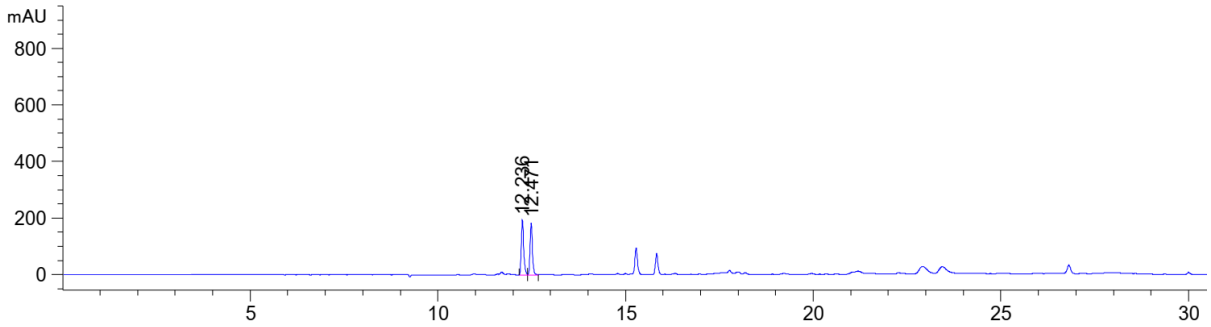

Figure 464: HPLC chromatogram of H-AGELS-NH_2 (Pentapeptide-31) **48** at λ=280 nm (0 to 60% MeCN).

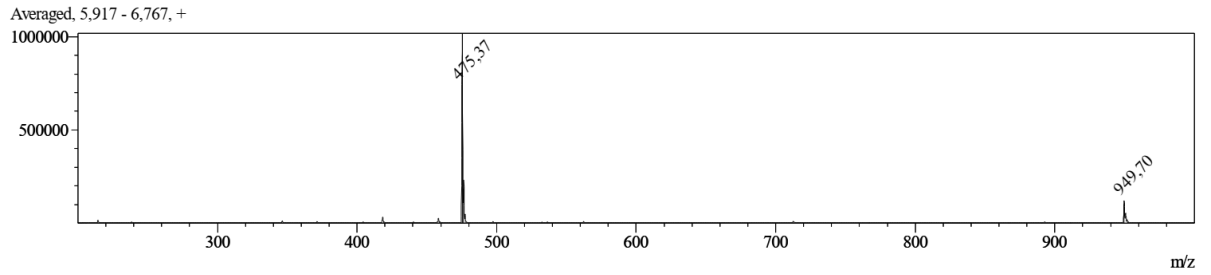

Figure 465: ESI-MS of H-AGELS-NH_2 (Pentapeptide-31) **48** (M measured=475.37 $[M+H]^+$, M calc.=474.52).

8.7.2. Analytical data of H-GPQGPQ-OH (Hexapeptide-9) 49

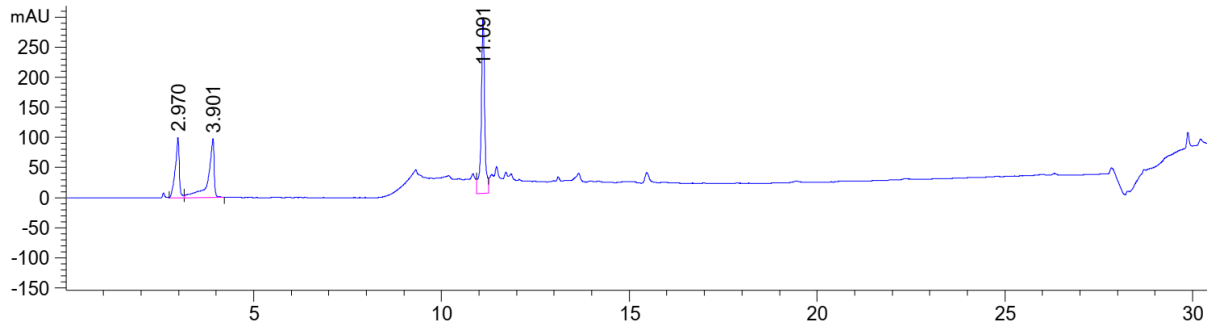

Figure 466: HPLC chromatogram of H-GPQGPQ-OH (Hexapeptide-9) **49** at λ=220 nm (0 to 60% MeCN).

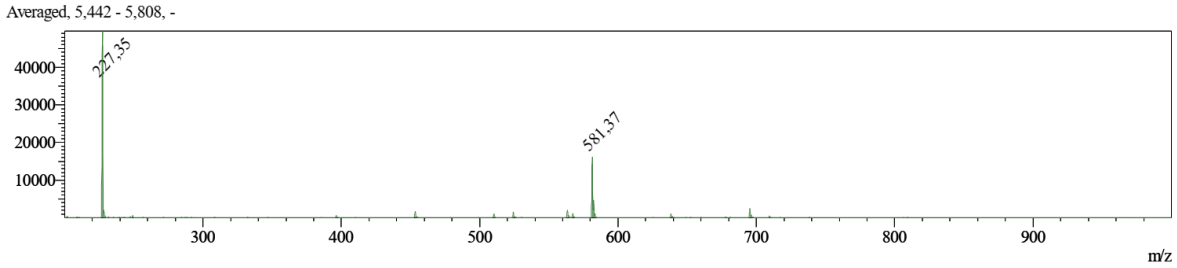

Figure 467: ESI-MS of H-GPQGPQ-OH (Hexapeptide-9) **49** (M measured=581.37 $[M-H]^-$, M calc.=581.37).

8.7.3. Analytical data of H-EEMQRR-NH2 (Hexapeptide 3) 50

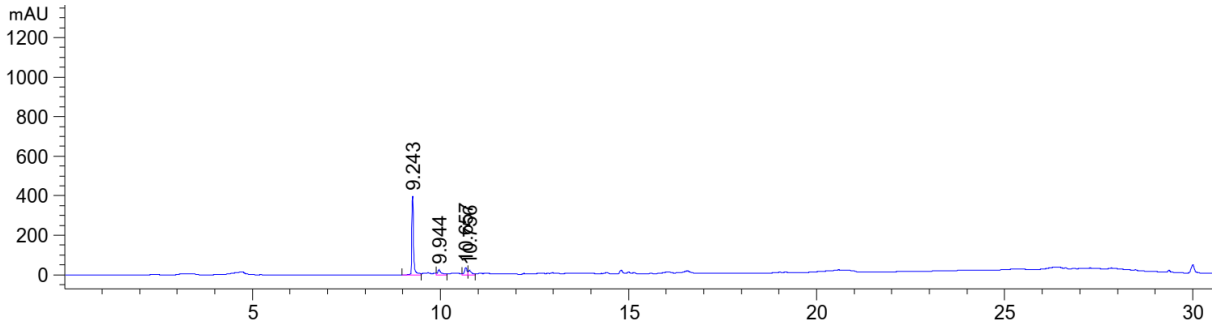

Figure 468: HPLC chromatogram of H-EEMQRR-NH_2 (Hexapeptide 3) **50** at λ=220 nm (0 to 60% MeCN).

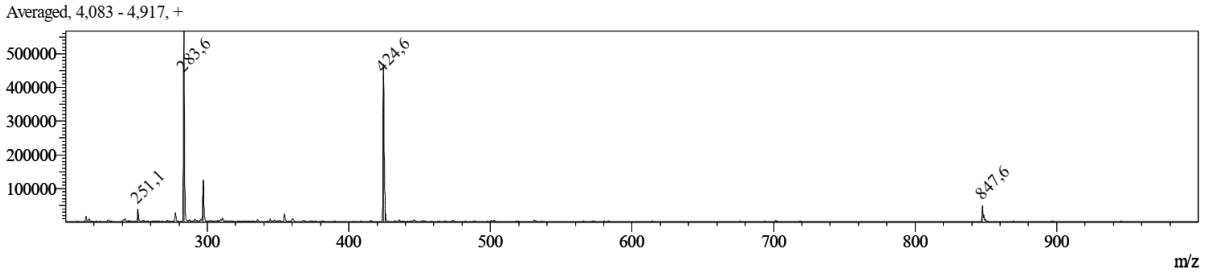

Figure 469: ESI-MS of H-EEMQRR-NH_2 (Hexapeptide 3) **50** (M measured=847.60 $[M+H]^+$, M calc.=846.96).

8.7.4. Analytical data of Ac-EEMQRR-NH2 (Acetyl-Hexapeptide 3) 51

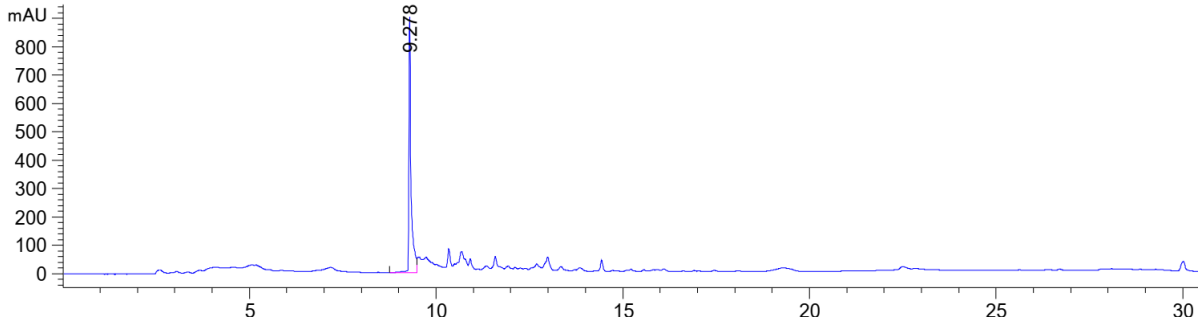

Figure 470: HPLC chromatogram of Ac-EEMQRR-NH_2 **51** at λ=220 nm (0 to 60% MeCN).

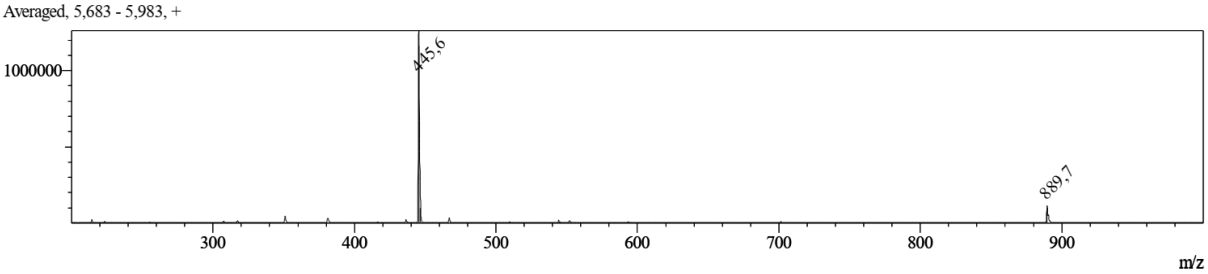

Figure 471: ESI-MS of Ac-EEMQRR-NH_2 **51** (M measured=889.70 $[M+H]^+$, M calc.=889.00).

8.7.5. Analytical data of Synthesis of Leu-Enkephalin amide 52

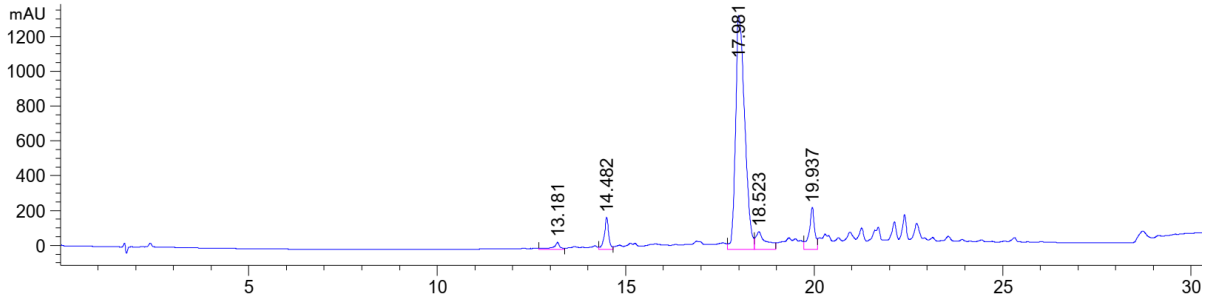

Figure 472: HPLC chromatogram of Synthesis of Leu-Enkephalin amide **52** at λ=220 nm (0 to 60% MeCN).

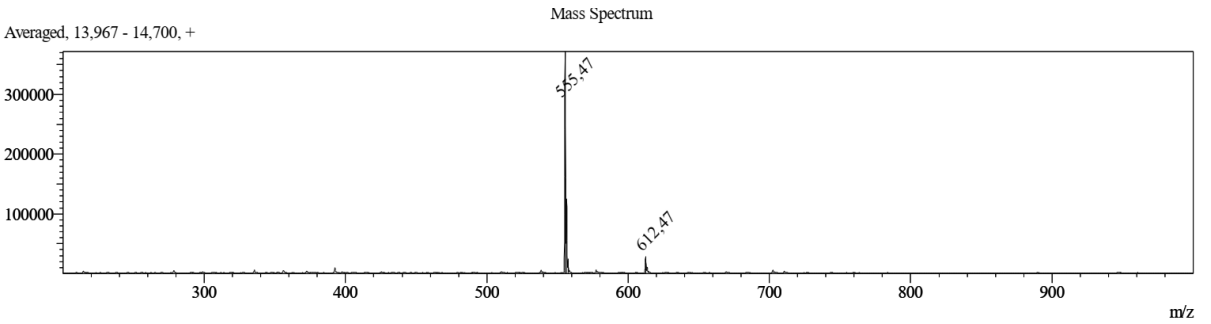

Figure 473: ESI-MS of Synthesis of Leu-Enkephalin amide **52** (M measured=554.65 $[M+H]^+$, M calc.=554.65).

8.7.6. Analytical data of Synthesis of Met-Enkephalin 53

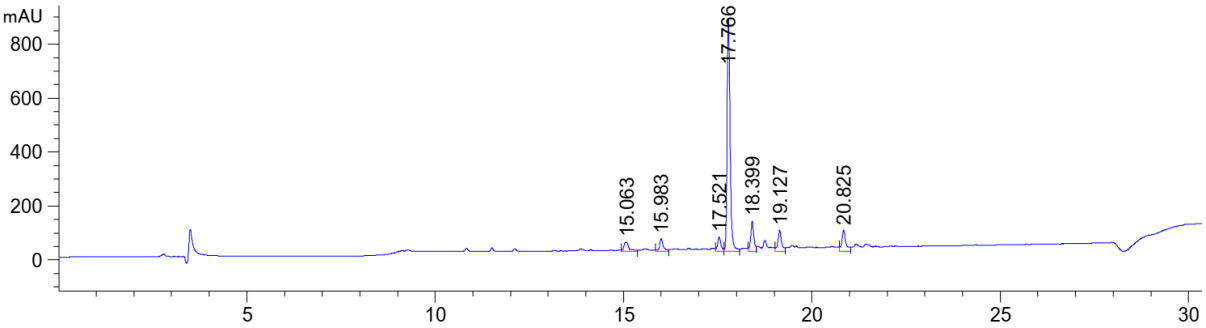

Figure 474: HPLC chromatogram of Synthesis of Met-Enkephalin **53** at λ=220 nm (0 to 60% MeCN).

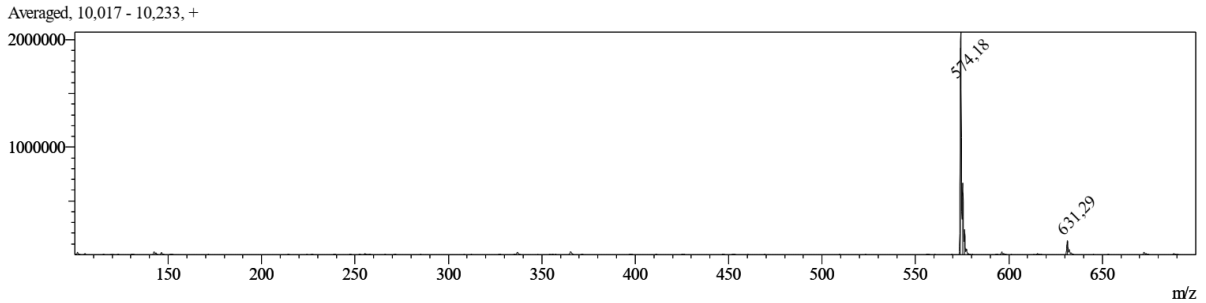

Figure 475: ESI-MS of Synthesis of Met-Enkephalin **53** (M measured=574.18 $[M+H]^+$, M calc.=573.67).

8.7.7. Analytical data of Synthesis of Leu-Enkephalin 54

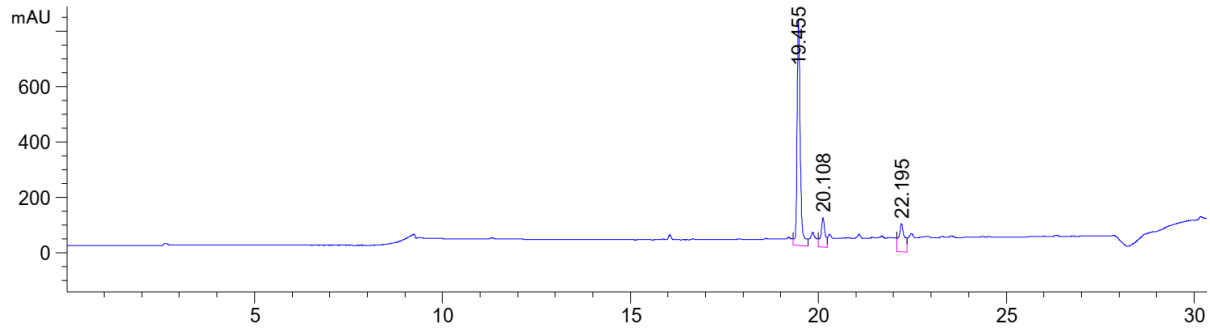

Figure 476: HPLC chromatogram of Synthesis of Leu-Enkephalin **54** at λ=220 nm (0 to 60% MeCN).

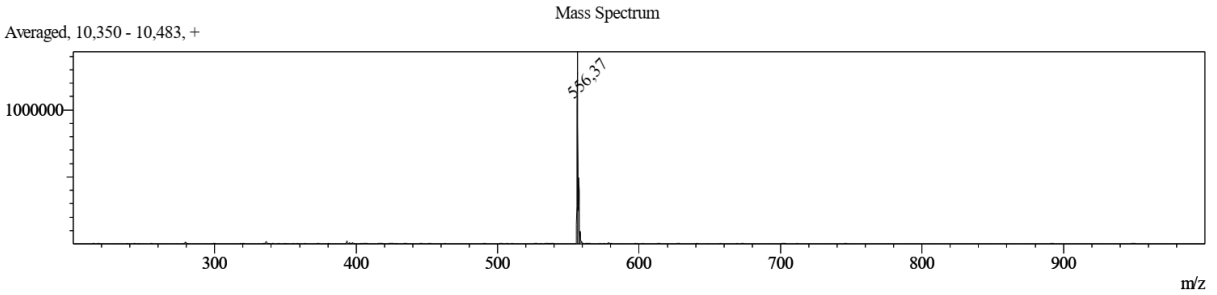

Figure 477: ESI-MS of Synthesis of Leu-Enkephalin **54** (M measured=556.37 $[M+H]^+$, M calc.=555.63).

8.7.8. Analytical data of Synthesis of H-VQAAIDYING-OH 55

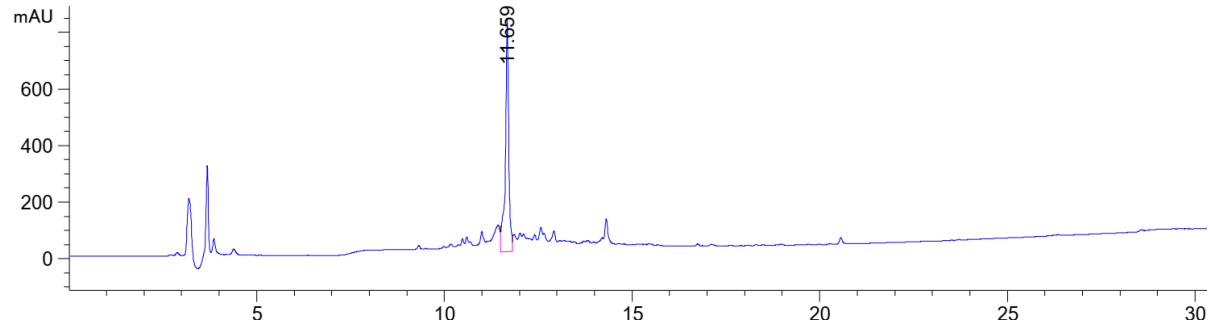

Figure 478: HPLC chromatogram of Synthesis of H-VQAAIDYING-OH **55** at λ=220 nm (10 to 100% MeCN).

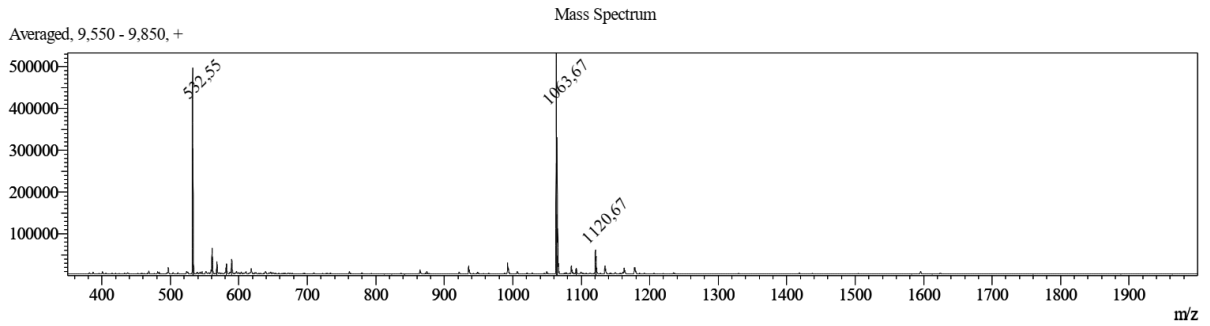

Figure 479: ESI-MS of Synthesis of H-VQAAIDYING-OH **55** (M measured=1063.67 $[M+H]^+$, M calc.=1062.19).

8.7.9. Analytical data of Synthesis of H-VQAAIDYING-NH_2 56

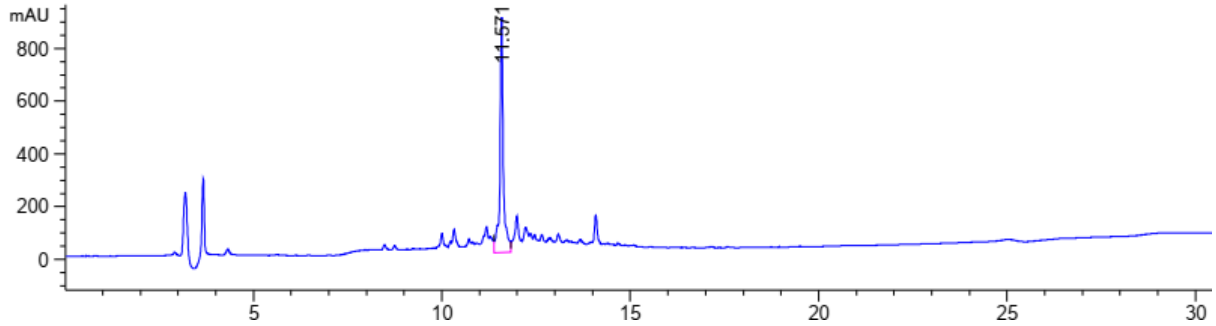

Figure 480: HPLC chromatogram of Synthesis of H-VQAAIDYING-NH_2 **56** at λ=220 nm (10 to 100% MeCN).

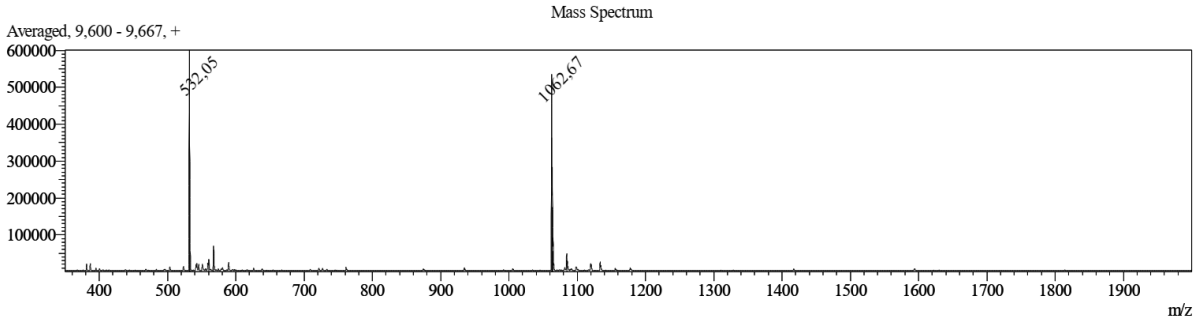

Figure 481: ESI-MS of Synthesis of H-VQAAIDYING-NH_2 **56** (M measured=1062.67 $[M+H]^+$, M calc.=1063.18).

8.7.10.Analytical data of Synthesis of H-GPRP-OH 57

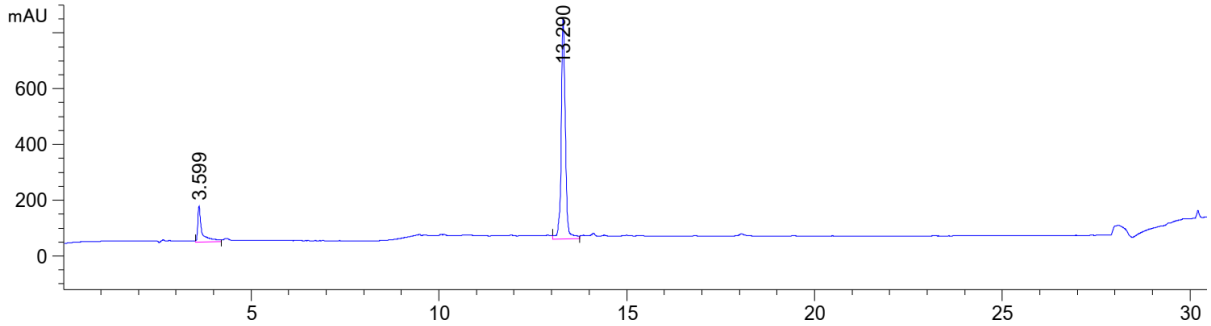

Figure 482: HPLC chromatogram of Synthesis of H-GPRP-OH **57** at λ=220 nm (0 to 40% MeCN).

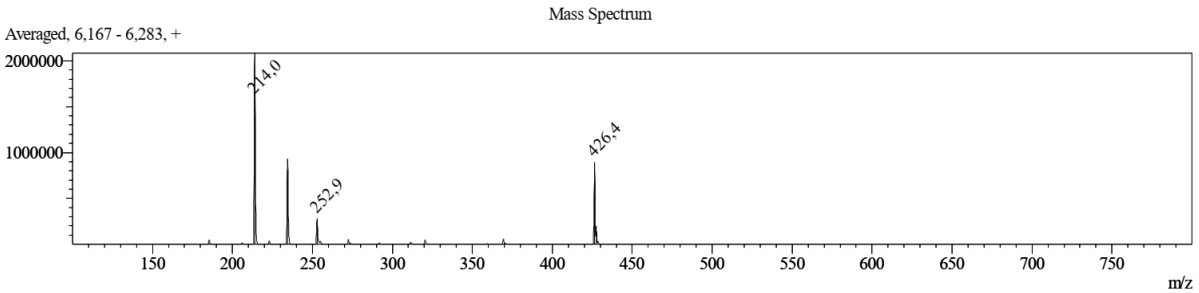

Figure 483: ESI-MS of Synthesis of H-GPRP-OH **57** (M measured=426.40 $[M+H]^+$, M calc.=425.49).

8.7.11.Analytical data of Synthesis of Smoc-VIAA-NH_2 58

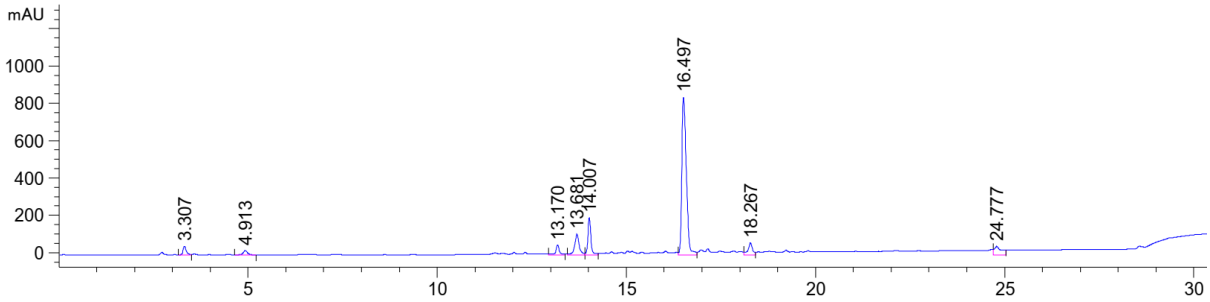

Figure 484: HPLC chromatogram of Synthesis of Smoc-VIAA-NH_2 **58** at λ=220 nm (0 to 40% MeCN).

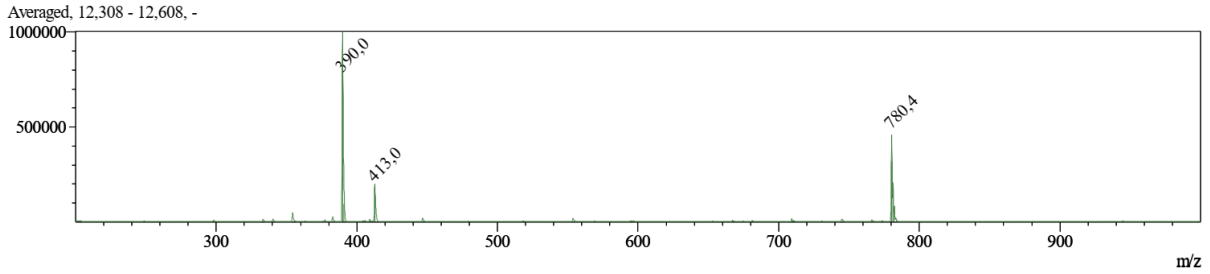

Figure 485: ESI-MS of Synthesis of Smoc-VIAA-NH_2 **58** (M measured=780.40 $[M+H]^+$, M calc.=781.89).

8.7.12.Analytical data of Synthesis of Smoc-DIIW-OH 59

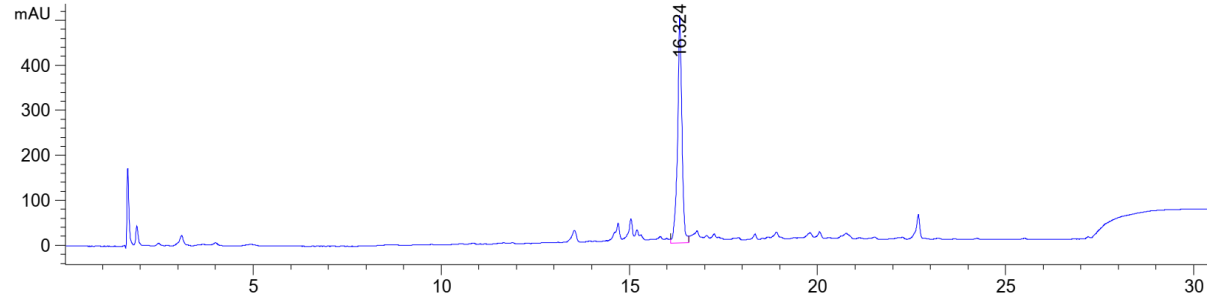

Figure 486: HPLC chromatogram of Synthesis of Smoc-DIIW-OH **59** at λ=220 nm (0 to 40% MeCN).

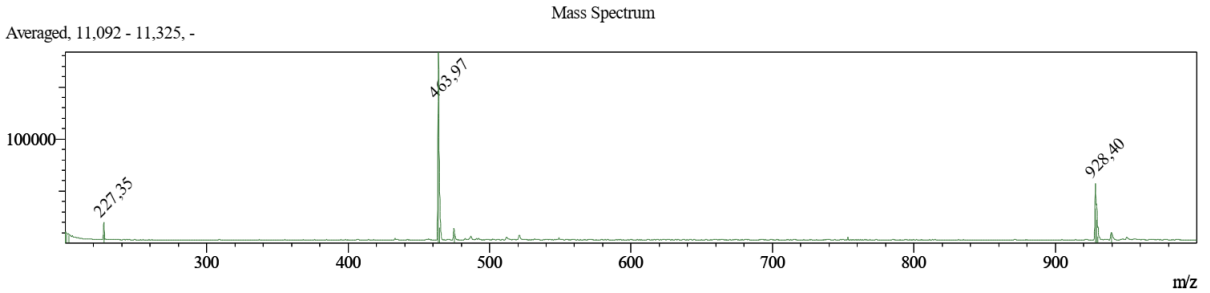

Figure 487: ESI-MS of Synthesis of Smoc-DIIW-OH **59** (M measured=928.40 $[M+H]^+$, M calc.=927.99).

8.7.13. Analytical data of Smoc-E(OtBu)K(Boc)R(Pbf)S(tBu)C(Trt)-OH 60

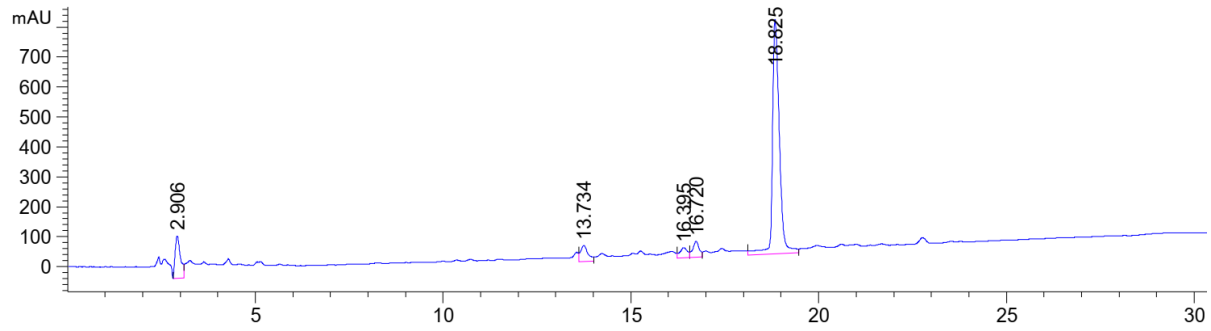

Figure 488: HPLC chromatogram of Smoc-E(OtBu)K(Boc)R(Pbf)S(tBu)C(Trt)-OH **60** at λ=220 nm (50 to 100% MeCN).

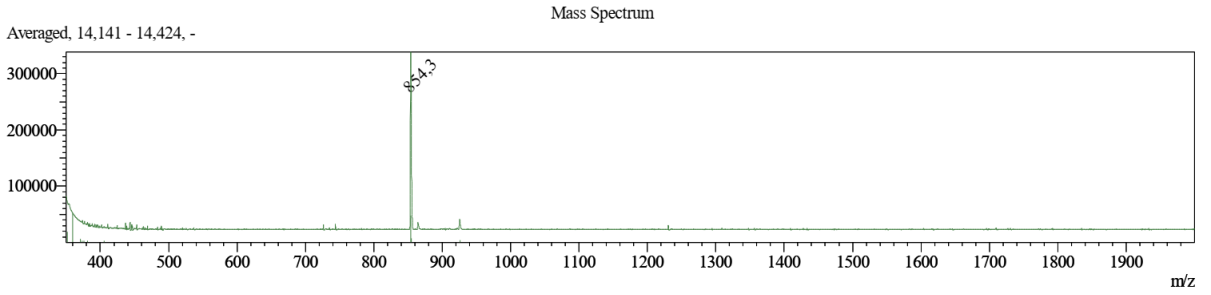

Figure 489: ESI-MS of Smoc-E(OtBu)K(Boc)R(Pbf)S(tBu)C(Trt)-OH **60** (M measured=854.30 $[M-2H]^{2-}$, M calc.= 855.53).

8.7.14.Analytical data of H-CYEIS-NH_2 61

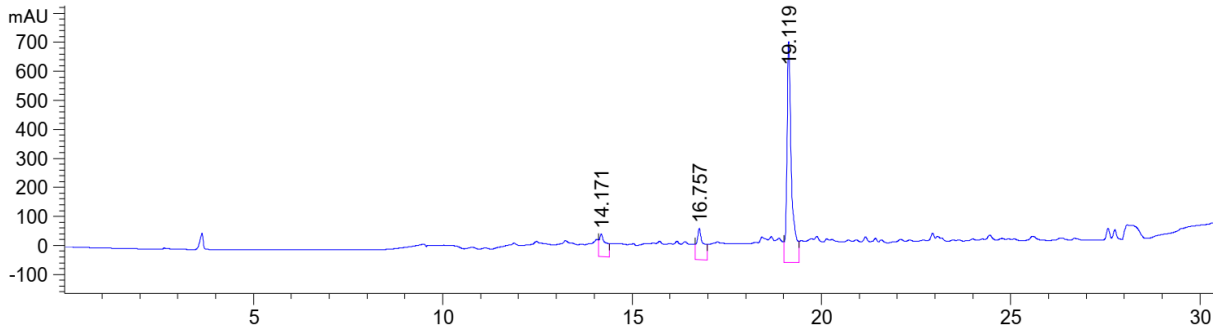

Figure 490: HPLC chromatogram of H-CYEIS-NH_2 **61** at λ=220 nm (0 to 40% MeCN).

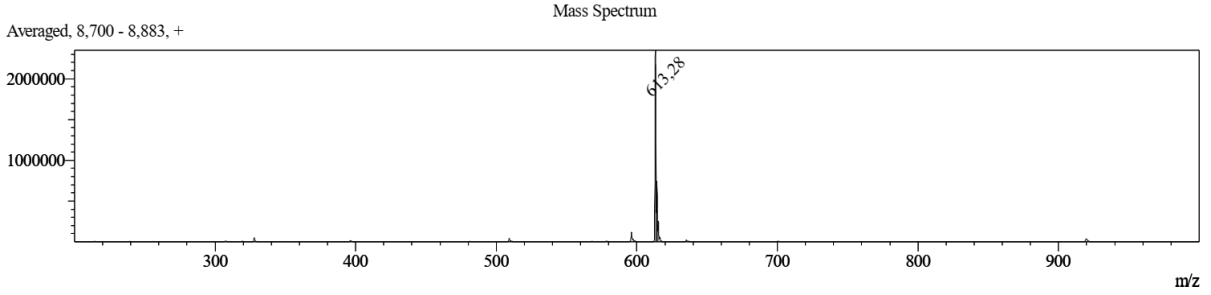

Figure 491: ESI-MS of H-CYEIS-NH_2 **61** (M measured=613.28 $[M+H]^+$, M calc.=612.70).

8.7.15. Analytical data of amino acid racemization of H-CYEIS-NH_2 61 by *C.A.T. GmbH & Co Chromatographie und Analysentechnik KG* (Tübingen, Germany)

C.A.T. GmbH & Co
Chromatographie und
Analysentechnik KG

Analysis number	H-CYEIS-NH2
9999005-1/19	

Method description in accordance to SOP: A.0.3. /rv 161020

If Fmoc and DNP are present protective groups, they need to be cleaved.
The peptide / amino acid derivative is hydrolyzed in 6N DCl in D_2O. (In case of presence of Asn, it will be hydrolyzed to Asp, respectively Gln/Pyr to Glu, and so detected and determined).
If necessary an antioxidant and/or scavenger is added. After completion of hydrolysis excess of reagent is removed and the sample is esterified with deuterochloride in methyl alcohol. In accordance to the column specification homologue alcohols are possible. After evaporation of excess of reagent the residue is acylated using trifluoroacetic anhydrid or pentafluoropropionic anhydride. If histidine is to be determined, the -NH of the imidazol group is derivatized with propyl or butyl chloroformate in a separate step. The residue is dissolved and injected.

Calculation of enantiomeric purity:

$$\% D = \frac{Area_D}{Area_D + Area_L} * 100$$

Change Control:
Minor changes that are not in accordance to the method description are mentioned in the report. Major changes need to be approved.

System Suitability Test:

SST is running before each sequence. Results must meet the acceptance criteria.
For sensitive parameters performance qualification is determined weekly and must meet the acceptance criteria.

Data based on generic validation Revision 010213

Analyte:	:	Free proteinogenic amino acids
Standard deviation	:	≤± 0.1% (at ≤ 1.5% Enantiomer) (For Cys and amino acids linked on to Cys possibly higher)
Limit of detection	:	<<0.1%
Limit of quantitation	:	0.10%
Range	:	0.1 - 5 % Enantiomer

The standard deviation of m-1 contribution that must be considered for some amino acids, is substance and matrix specific. Thus, also the standard deviation of the result for those amino acids could be higher. For amino acids which show complex mass pattern, such as Trp and Nal, standard deviation could be even higher than 0.3%.

We assure that the analysis is performed in accordance to the GMP guidelines and in accordance to ICH guideline Q2(R1)

181112 A_0_3_e.xls

Analysis number	H-CYEIS-NH2
9999005-1/19	

Results: A.0.3. /rv 161020

The listed amino acid(s) were identified via retention time and mass spectra.
The identity of the main component(s) comply.
The following impurity of the optical antipode was found:

Isoleucine	>99.7 % L-Isoleucine
	<0.10 % D-Isoleucine
	<0.10 % L-allo-Isoleucine
	<0.10 % D-allo-Isoleucine
Serine	<0.10 % D-Enantiomer
Cysteine	0.10 % D-Enantiomer
Glutamic acid	<0.10 % D-Enantiomer
Tyrosine	0.25 % D-Enantiomer

Notes:

Method specific deviations or irregularities are not observed.

The method is generically validated. However it may not meet all requirements for the release of drug substances and drug products. It is to prove if substance specific validation is required.

Signal:	MS1Front SIM(182) EI					
RT [min]	**Type**	**Width [min]**	**Area**	**Height**	**Area%**	**Name**
10.829	MM m	0.11	41.4	6.0	0.03	D Ail
11.806	MM m	0.04	5.8	2.0	0.00	D Ile
12.485	MM m	0.09	73.7	10.0	0.05	L Ail
13.046	BB	1.41	141005.4	17553.3	99.91	L Ile

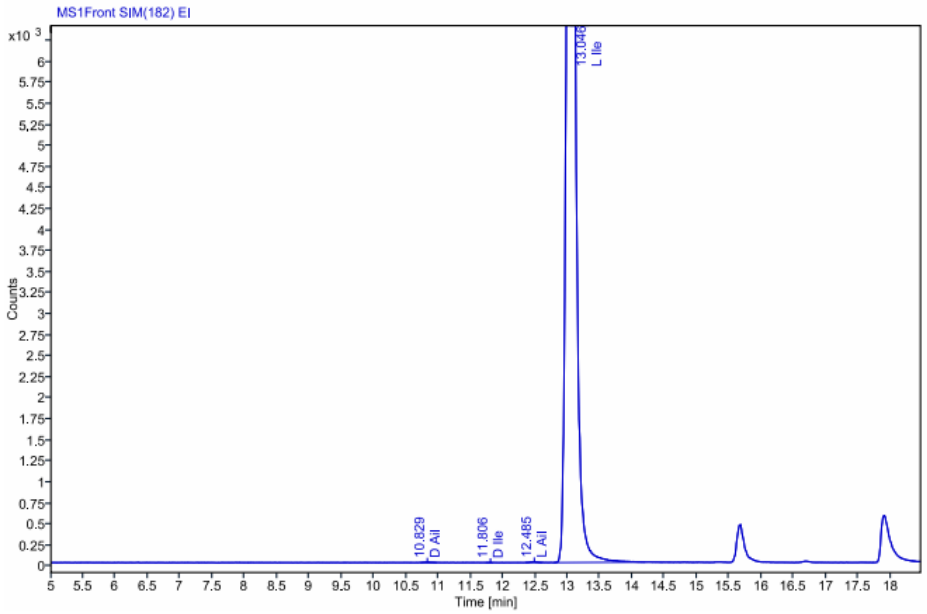

Signal:	MS1Front SIM(138) EI					
RT [min]	**Type**	**Width [min]**	**Area**	**Height**	**Area%**	**Name**
14.533	MM m	0.14	141.8	16.9	0.06	D Ser
15.662	BB	1.36	235395.0	29397.8	99.94	L Ser

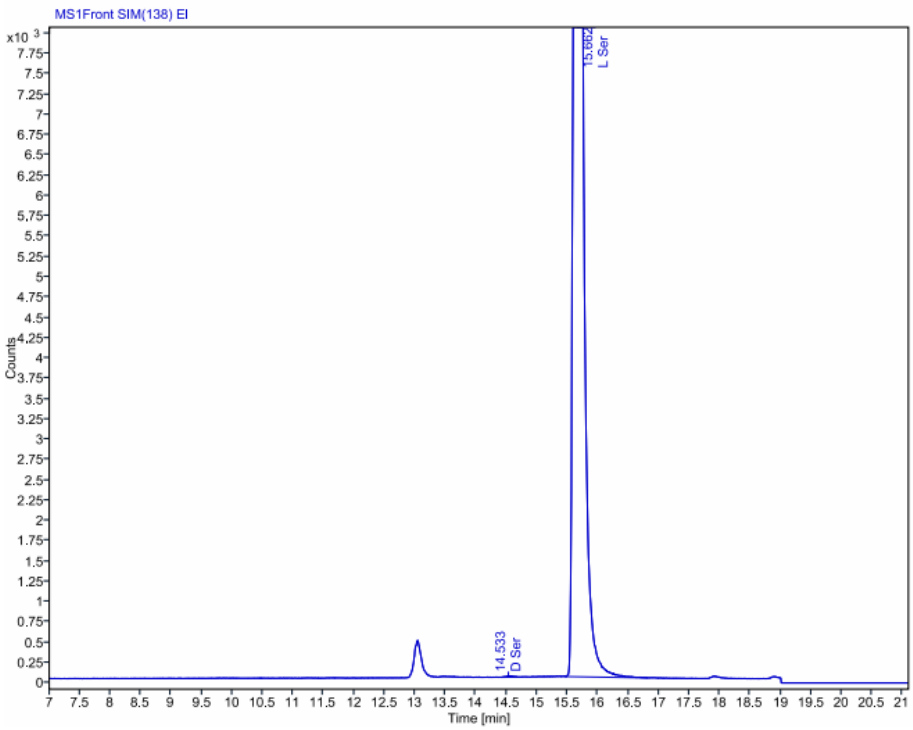

Signal:	MS1Front SIM(268) EI					
RT [min]	**Type**	**Width [min]**	**Area**	**Height**	**Area%**	**Name**
21.549	MM m	0.09	42.3	6.0	0.09	D Cys
22.392	BB	1.37	44609.6	6939.5	99.91	L Cys

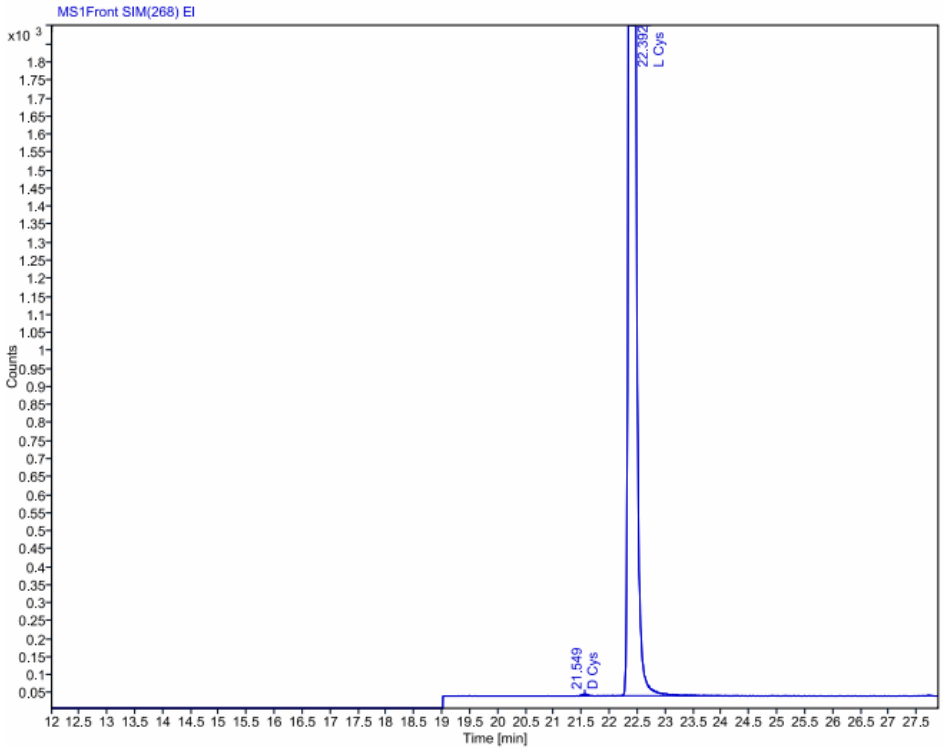

Signal:	MS1Front SIM(226) EI					
RT [min]	**Type**	**Width [min]**	**Area**	**Height**	**Area%**	**Name**
26.570	MM m	0.05	15.6	4.0	0.06	D Glu
27.722	BB	1.11	25187.9	4882.1	99.94	L Glu

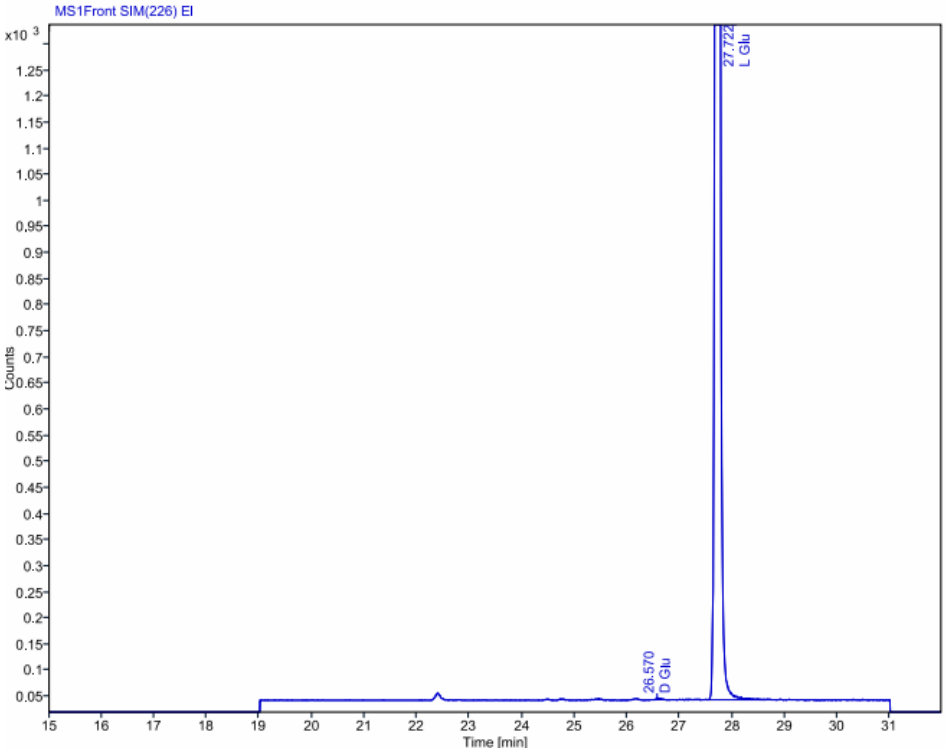

Signal:	MS1Front SIM(288) EI					
RT [min]	Type	Width [min]	Area	Height	Area%	Name
32.116	MM m	0.06	15.2	4.0	0.25	D Tyr
32.538	BB	0.91	5998.4	2044.7	99.75	L Tyr

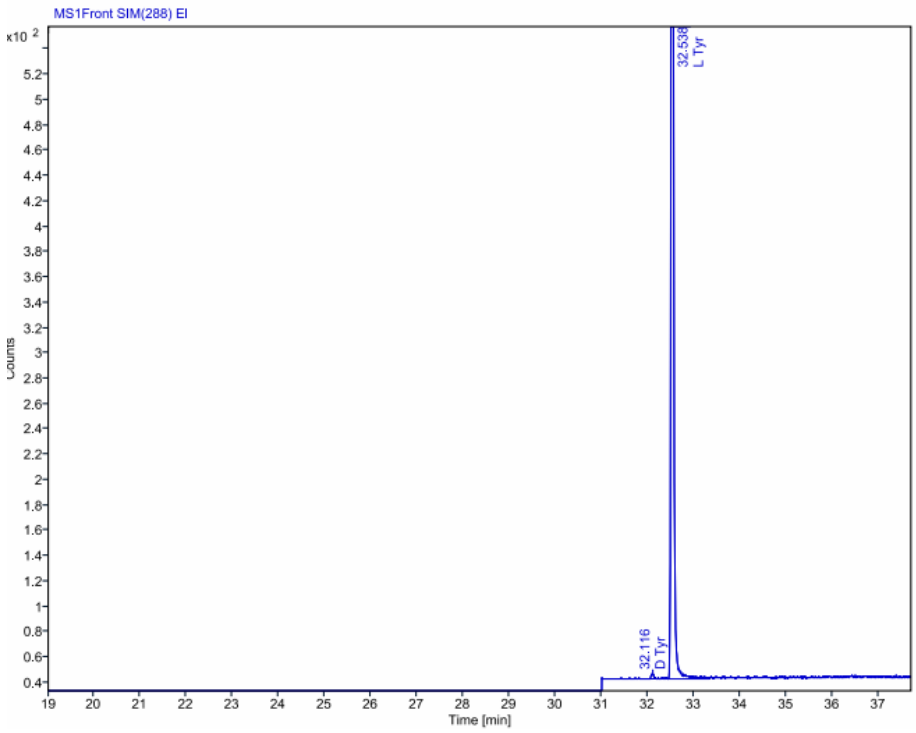

8.7.16.Analytical data of H-ANKPG-NH_2 62

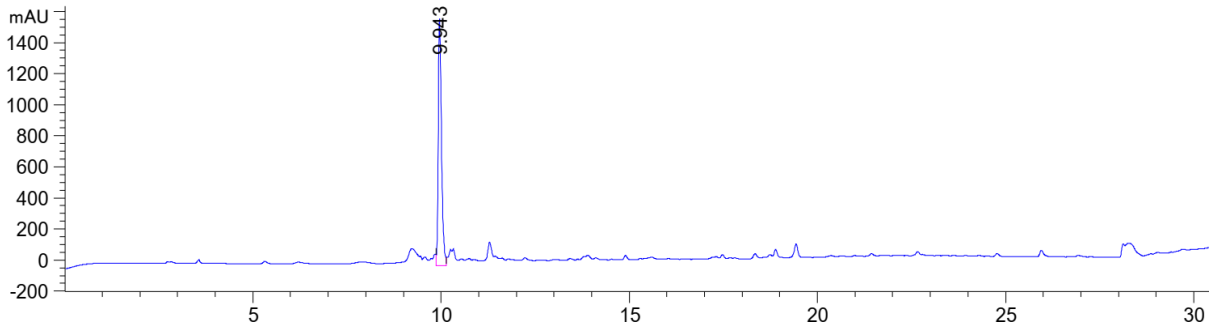

Figure 492: HPLC chromatogram of H-ANKPG-NH_2 **62** at λ=220 nm (0 to 40% MeCN).

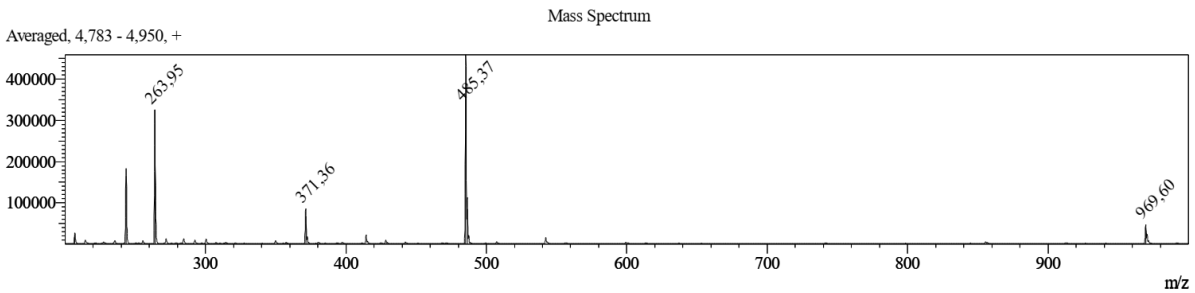

Figure 493: ESI-MS of H-ANKPG-NH_2 **62** (M measured=485.37 $[M+H]^+$, M calc.= 484.56).

8.7.17. Analytical data of amino acid racemization of H-ANKPG-NH_2 62 by *C.A.T. GmbH & Co Chromatographie und Analysentechnik KG* (Tübingen, Germany)

C.A.T. GmbH & Co
Chromatographie und
Analysentechnik KG

Analysis number	H-ANKPG-NH2
9999005-2/19	

Method description in accordance to SOP: **A.0.3.** **/rv 161020**

If Fmoc and DNP are present protective groups, they need to be cleaved.
The peptide / amino acid derivative is hydrolyzed in 6N DCl in D_2O. (In case of presence of Asn, it will be hydrolyzed to Asp, respectively Gln/Pyr to Glu, and so detected and determined).
If necessary an antioxidant and/or scavenger is added. After completion of hydrolysis excess of reagent is removed and the sample is esterified with deuterochloride in methyl alcohol. In accordance to the column specification homologue alcohols are possible. After evaporation of excess of reagent the residue is acylated using trifluoroacetic anhydrid or pentafluoropropionic anhydride. If histidine is to be determined, the -NH of the imidazol group is derivatized with propyl or butyl chloroformate in a separate step. The residue is dissolved and injected.

Calculation of enantiomeric purity:

$$\% D = \frac{Area_D}{Area_D + Area_L} * 100$$

Change Control:
Minor changes that are not in accordance to the method description are mentioned in the report. Major changes need to be approved.

System Suitability Test:

SST is running before each sequence. Results must meet the acceptance criteria.
For sensitive parameters performance qualification is determined weekly and must meet the acceptance criteria.

Data based on generic validation **Revision 010213**

Analyte:	:	Free proteinogenic amino acids
Standard deviation	:	≤± 0.1% (at ≤ 1.5% Enantiomer) (For Cys and amino acids linked on to Cys possibly higher)
Limit of detection	:	<<0.1%
Limit of quantitation	:	0.10%
Range	:	0.1 - 5 % Enantiomer

The standard deviation of m-1 contribution that must be considered for some amino acids, is substance and matrix specific. Thus, also the standard deviation of the result for those amino acids could be higher. For amino acids which show complex mass pattern, such as Trp and Nal, standard deviation could be even higher than 0.3%.

We assure that the analysis is performed in accordance to the GMP guidelines and in accordance to ICH guideline Q2(R1)

181112 A_0_3_e.xls

Analysis number	H-ANKPG-NH2
9999005-2/19	

Results: A.0.3. /rv 161020

The listed amino acid(s) were identified via retention time and mass spectra.
The identity of the main component(s) comply.
The following impurity of the optical antipode was found:

Alanine	0.50 % D-Enantiomer
Proline	0.43 % D-Enantiomer
Aspartic acid	2.04 % D-Enantiomer
Lysine	0.11 % D-Enantiomer

Notes:

Method specific deviations or irregularities are not observed.

The method is generically validated. However it may not meet all requirements for the release of drug substances and drug products. It is to prove if substance specific validation is required.

Signal:	MS1Front SIM(140) EI					
RT [min]	**Type**	**Width [min]**	**Area**	**Height**	**Area%**	**Name**
4.528	MM m	0.12	1254.2	136.5	0.50	D Ala
6.056	BB	1.89	251047.8	23385.5	99.50	L Ala

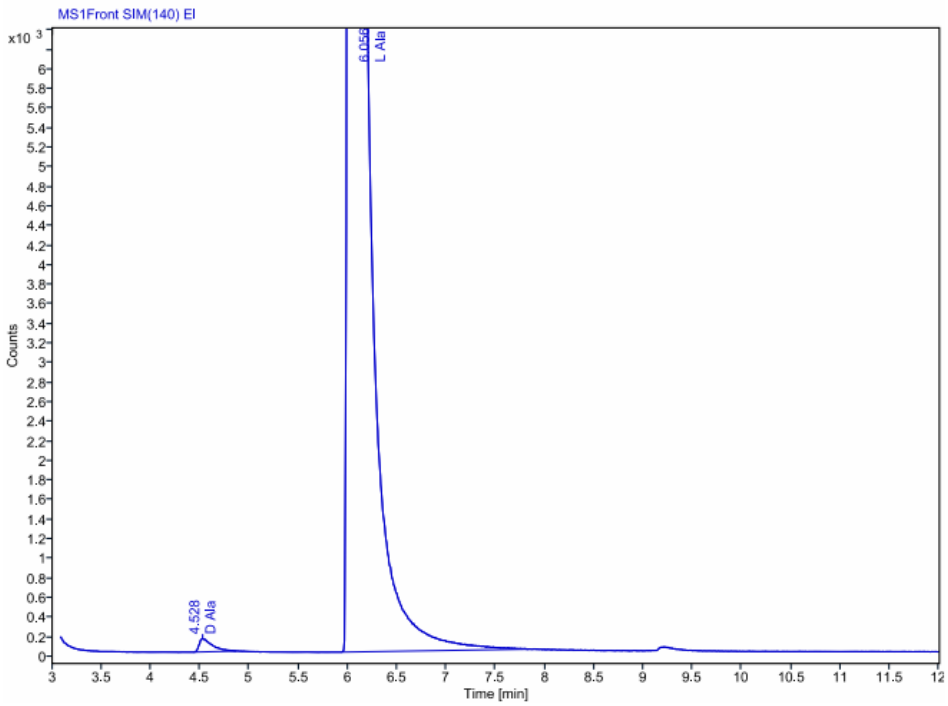

Signal:	MS1Front SIM(166) EI					
RT [min]	**Type**	**Width [min]**	**Area**	**Height**	**Area%**	**Name**
12.127	BV	0.2	1540.6	232.2	0.43	D Pro
12.321	VB	1.8	356320.5	37634.4	99.57	L Pro

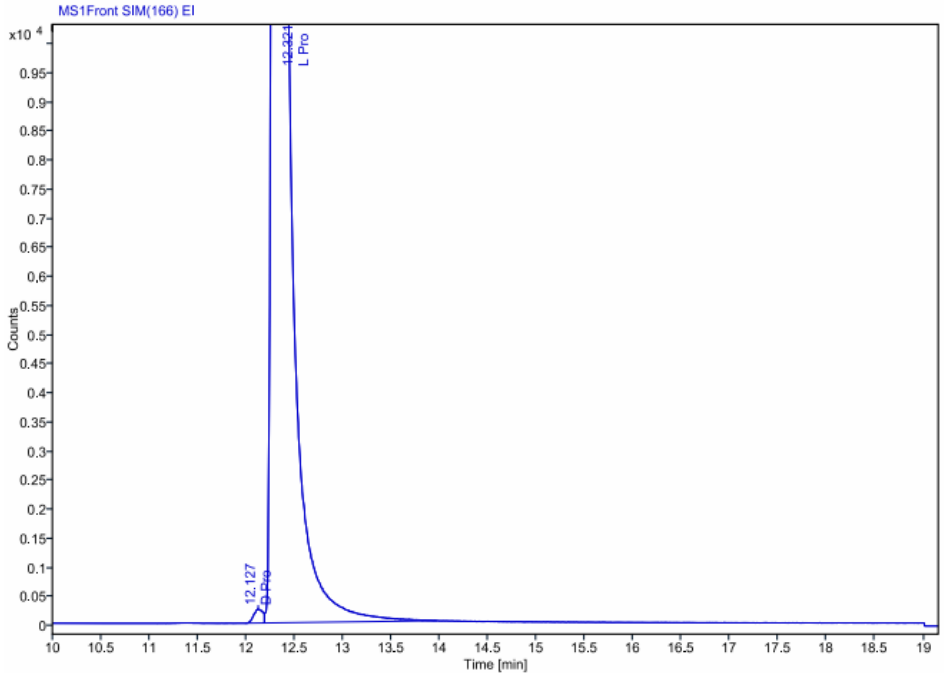

Signal:	MS1Front SIM(214) EI					
RT [min]	**Type**	**Width [min]**	**Area**	**Height**	**Area%**	**Name**
20.435	BV	0.49	2291.2	298.7	2.27	D Asp
20.961	VB	1.40	98466.7	14560.7	97.73	L Asp

M-1 contribution of 0.23% must be subtracted

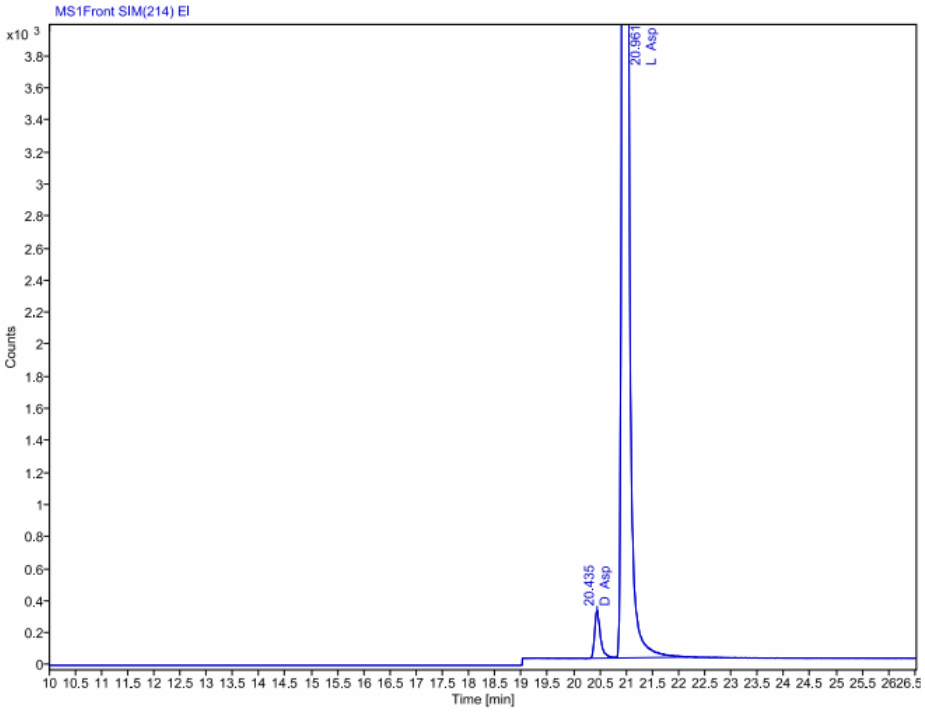

Signal:	MS1Front SIM(180) EI					
RT [min]	**Type**	**Width [min]**	**Area**	**Height**	**Area%**	**Name**
35.095	MM m	0.04	536.0	217.8	0.11	D Lys
35.354	BB	0.72	500473.9	251147.6	99.89	L Lys

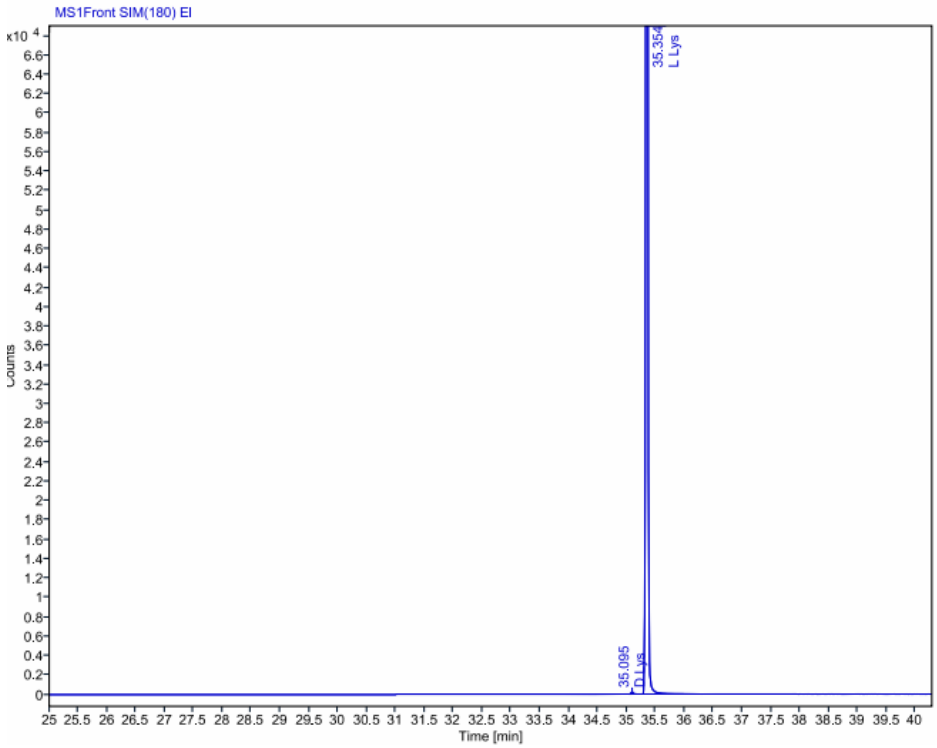

8.7.18. Analytical data of amino acid racemization of Smoc-Asn-OH 7 by *C.A.T. GmbH & Co Chromatographie und Analysentechnik KG* (Tübingen, Germany)

C.A.T. GmbH & Co
Chromatographie und
Analysentechnik KG

Analysis number	Smoc-Asn-OH
9999009-1/19	

Method description in accordance to SOP: A.0.3. /rv 161020

If Fmoc and DNP are present protective groups, they need to be cleaved.
The peptide / amino acid derivative is hydrolyzed in 6N DCl in D_2O. (In case of presence of Asn, it will be hydrolyzed to Asp, respectively Gln/Pyr to Glu, and so detected and determined).
If necessary an antioxidant and/or scavenger is added. After completion of hydrolysis excess of reagent is removed and the sample is esterified with deuterochloride in methyl alcohol. In accordance to the column specification homologue alcohols are possible. After evaporation of excess of reagent the residue is acylated using trifluoroacetic anhydrid or pentafluoropropionic anhydride. If histidine is to be determined, the -NH of the imidazol group is derivatized with propyl or butyl chloroformate in a separate step. The residue is dissolved and injected.

Calculation of enantiomeric purity:

$$\% D = \frac{Area_D}{Area_D + Area_L} * 100$$

Change Control:
Minor changes that are not in accordance to the method description are mentioned in the report. Major changes need to be approved.

System Suitability Test:

SST is running before each sequence. Results must meet the acceptance criteria.
For sensitive parameters performance qualification is determined weekly and must meet the acceptance criteria.

Data based on generic validation Revision 010213

Analyte:	:	Free proteinogenic amino acids
Standard deviation	:	≤± 0.1% (at ≤ 1.5% Enantiomer) (For Cys and amino acids linked on to Cys possibly higher)
Limit of detection	:	<<0.1%
Limit of quantitation	:	0.10%
Range	:	0.1 - 5 % Enantiomer

The standard deviation of m-1 contribution that must be considered for some amino acids, is substance and matrix specific. Thus, also the standard deviation of the result for those amino acids could be higher. For amino acids which show complex mass pattern, such as Trp and Nal, standard deviation could be even higher than 0.3%.
If the LOQ of generic validation cannot be met due to substance-specific infuences, the result will be reported as < <estimated LOQ >.

We assure that the analysis is performed in accordance to the GMP guidelines and in accordance to ICH guideline Q2(R1)

C.A.T. GmbH & Co
Chromatographie und
Analysentechnik KG

Analysis number	Smoc-Asn-OH
9999009-1/19	

Results: A.0.3. /rv 161020

The listed amino acid(s) were identified via retention time and mass spectra.
The identity of the main component(s) comply.
The following impurity of the optical antipode was found:

Aspartic acid	0.30 % D-Enantiomer

Notes:

Method specific deviations or irregularities are not observed.

The method is generically validated. However it may not meet all requirements for the release of drug substances and drug products. It is to prove if substance specific validation is required.

Signal: MS1Other SIM(212) EI

RT [min]	Type	Width [min]	Area	Height	Area%	Name
14.870	MM m	0.06	495.0	124.1	0.30	D_Asp
15.330	MM m	0.07	161845.4	31748.9	99.70	L_Asp

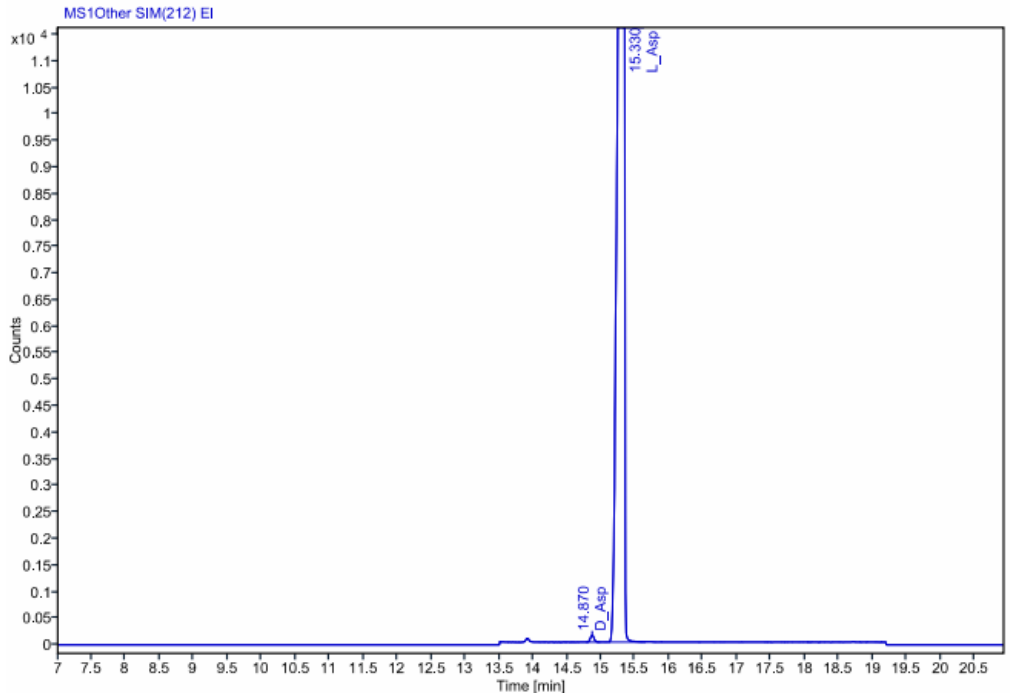

8.7.19.Analytical data of Pal-GHK-OH 63

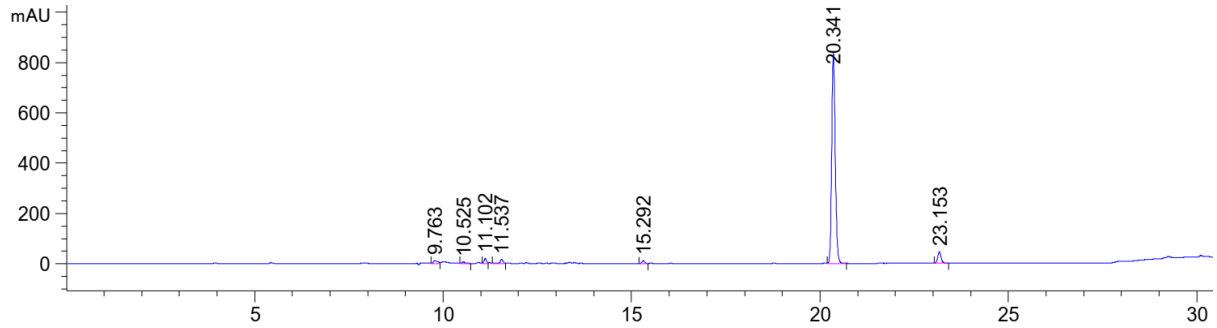

Figure 494: HPLC chromatogram of Pal-GHK-OH **63** at λ=220 nm (10 to 60% MeCN).

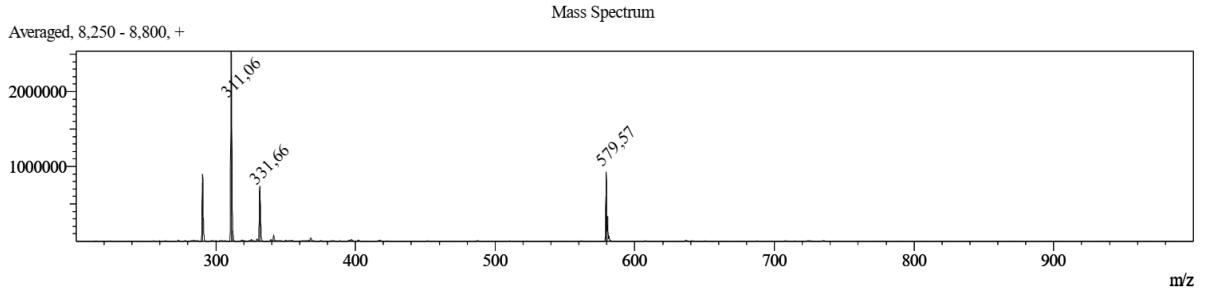

Figure 495: ESI-MS of Pal-GHK-OH **63** (M measured=579.57 $[M+H]^+$, M calc.= 578.80).

8.7.20.Analytical data of Pal-GQPR-OH 64

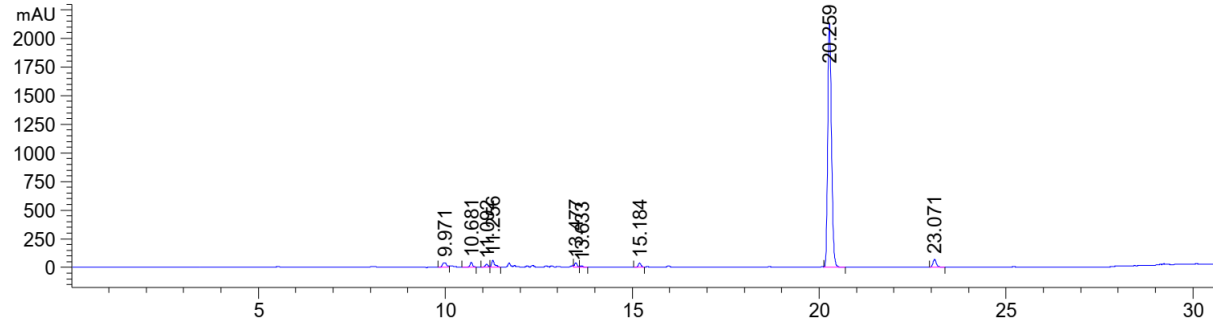

Figure 496: HPLC chromatogram of Pal-GQPR-OH **64** at λ=220 nm (0 to 60% MeCN).

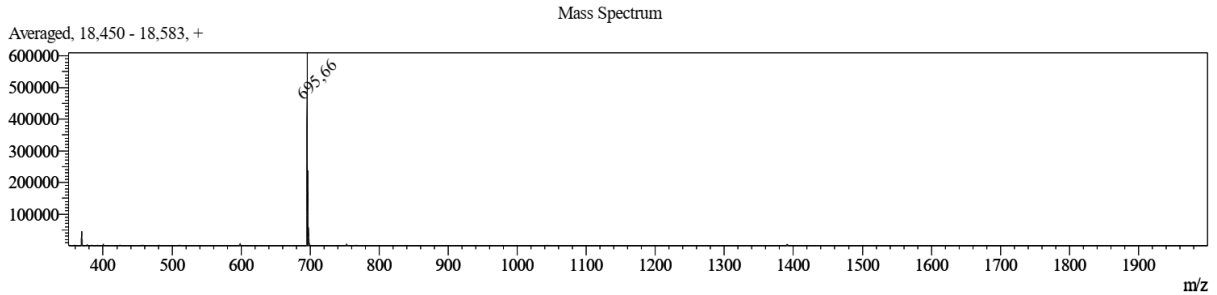

Figure 497: ESI-MS of Pal-GQPR-OH **64** (M measured=695.66 $[M+H]^+$, M calc.=695.66).

8.7.21.Analytical data of H-GPRPA-NH_2 Vialox (Pentapeptide-3) 65

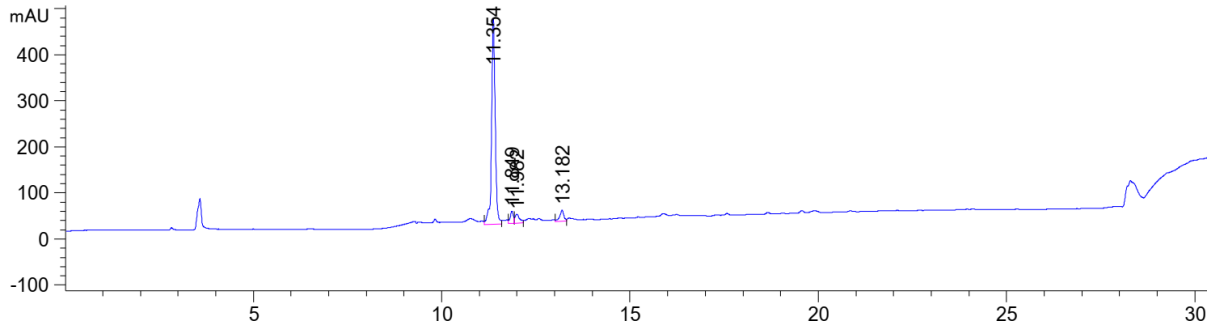

Figure 498: HPLC chromatogram of H-GPRPA-NH_2 **65** at λ=220 nm (0 to 60% MeCN).

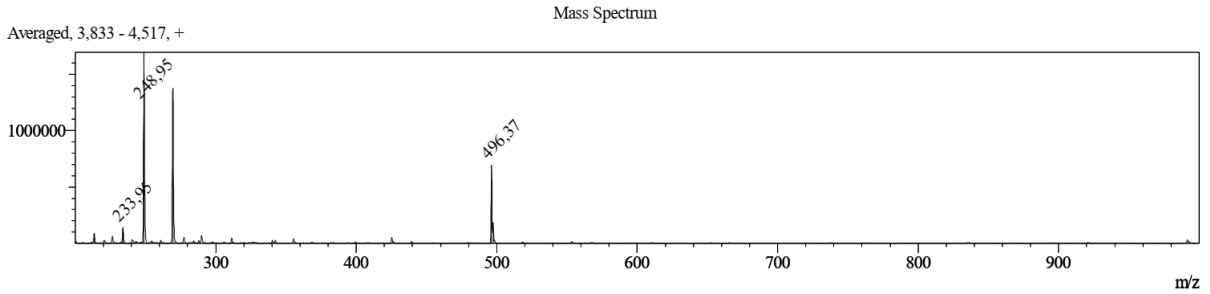

Figure 499: ESI-MS of H-GPRPA-NH_2 **65** (M measured=496.37 $[M+H]^+$, M calc.=495.59).

8.7.22.Analytical data of Oxytocin 66

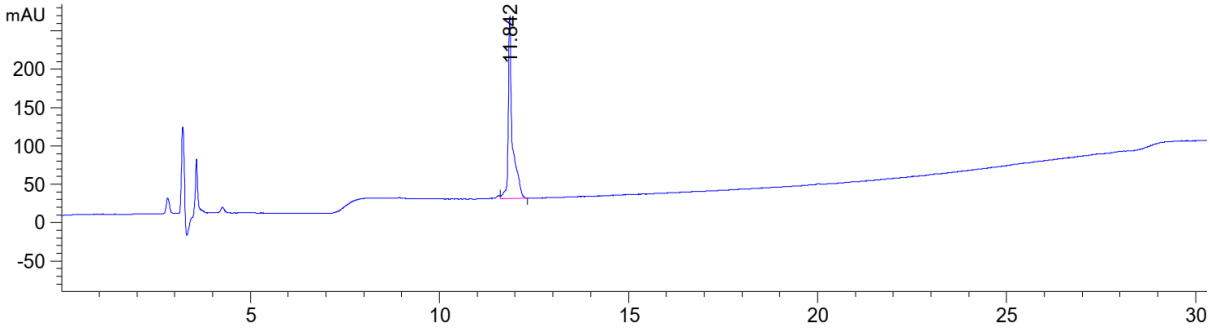

Figure 500: HPLC chromatogram of Oxytocin **66** at λ=220 nm (10 to 100% MeCN).

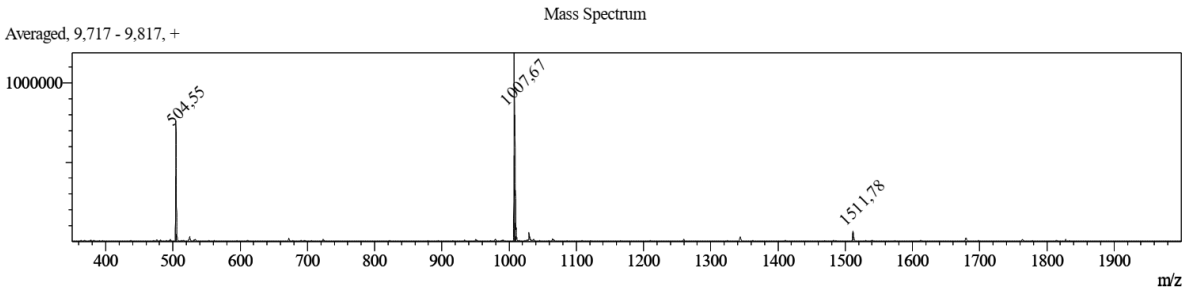

Figure 501: ESI-MS of Oxytocin **66** (M measured=1007.67 $[M+H]^+$, M calc.=1007.19).

8.7.23.Analytical data of Vasopressin 67 (peptide hormone)

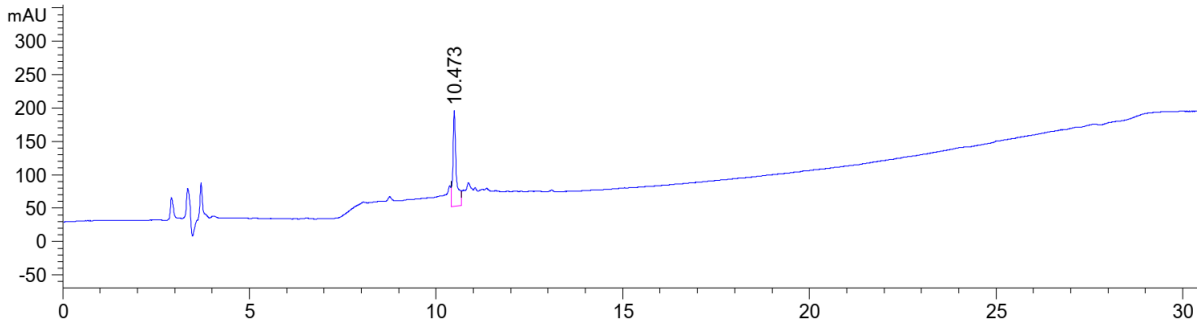

Figure 502: HPLC chromatogram of Vasopressin **67** at λ=220 nm (10 to 100% MeCN).

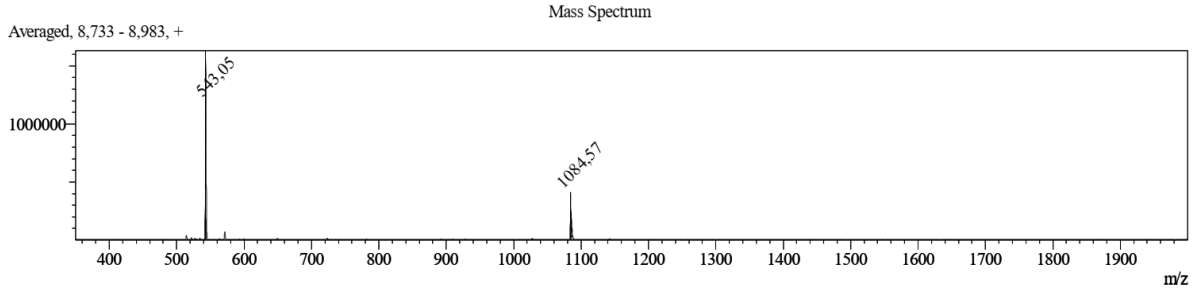

Figure 503: ESI-MS of Vasopressin **67** (M measured=1084.57 $[M+H]^+$, M calc.=1084.57).

8.7.24.Analytical data of heptaarginine 68

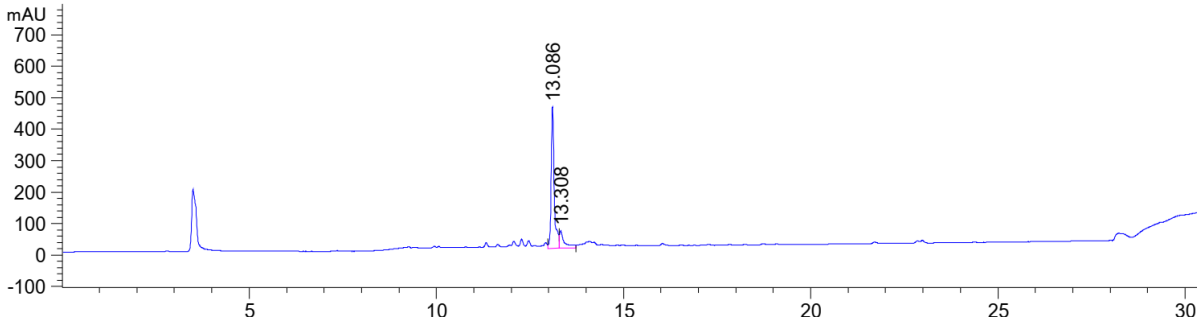

Figure 504: HPLC chromatogram of Smoc-heptaarginine **68** at λ=220 nm (10 to 100% MeCN).

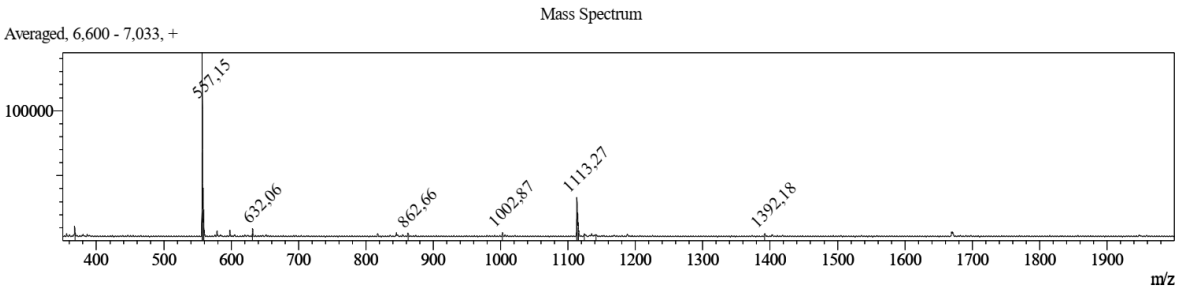

Figure 505: ESI-MS of heptaarginine **68** (M measured=1113.27 $[M+H]^+$, M calc.=1110.35).

8.7.25.Analytical data of H-YDAGFL-OH Leuphasyl 69

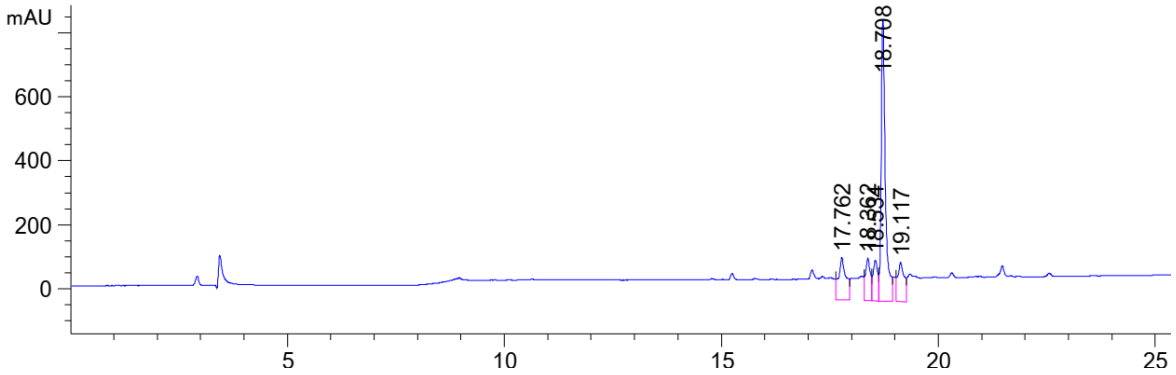

Figure 506: HPLC chromatogram of H-YDAGFL-OH **69** at λ=220 nm (0 to 60% MeCN).

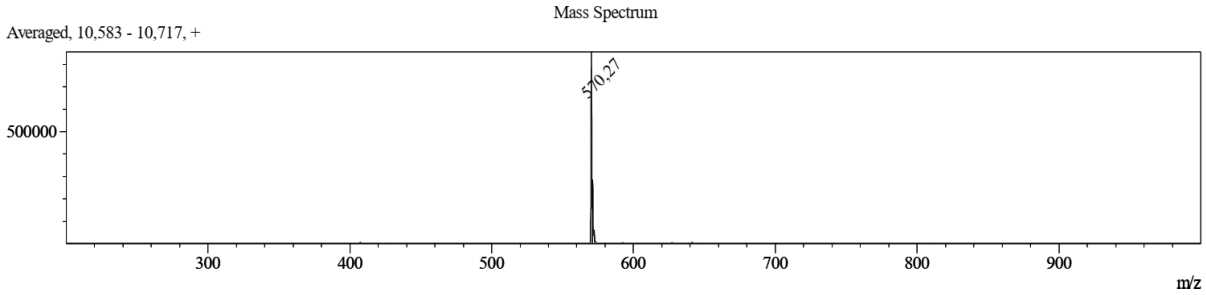

Figure 507: ESI-MS of H-YDAGFL-OH **69** (M measured=570.27 $[M+H]^+$, M calc.=569.66).

8.8. Analytical data of Aspartimide formation

8.8.1. Reference HPLC data of peptides 70-73

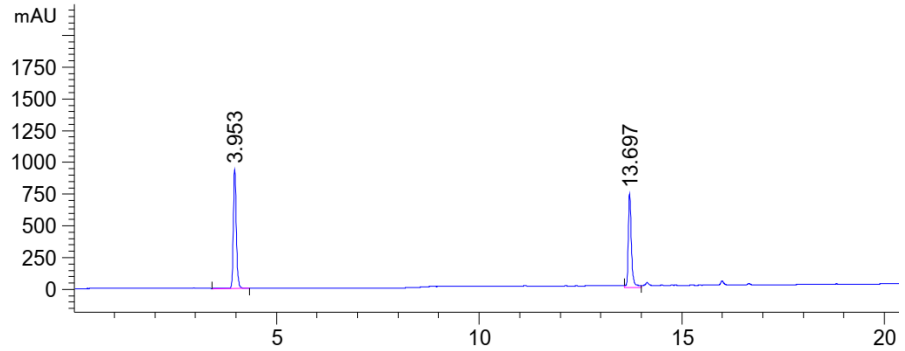

Figure 508: HPLC chromatogram of H-VKDGYI-NH_2 **70** as reference at λ=220 nm (0 to 60% MeCN) with ascorbic acid as standard at ≈3.95 min.

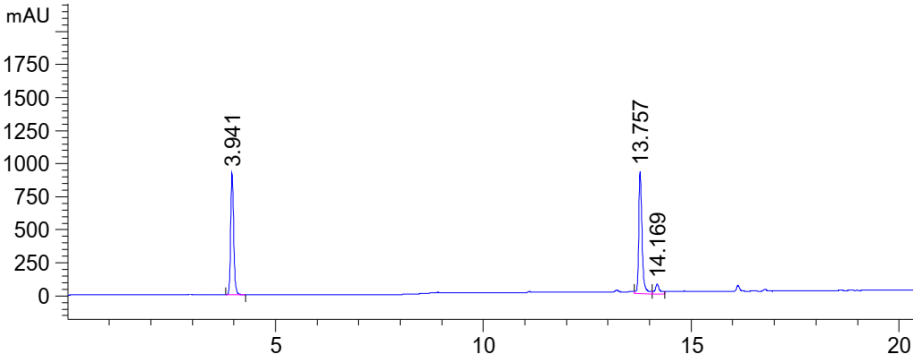

Figure 509: HPLC chromatogram of H-VK(D-D)GYI-NH_2 **71** as reference at λ=220 nm (0 to 60% MeCN) with ascorbic acid as standard at ≈3.95 min.

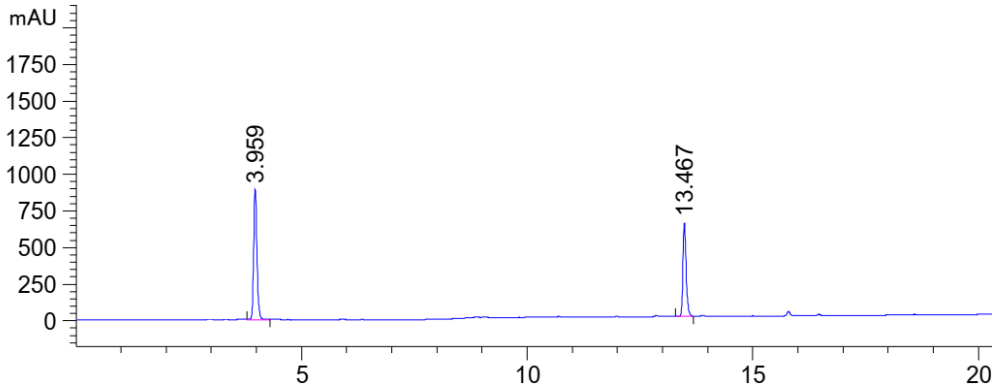

Figure 510: HPLC chromatogram of H-VKNGYI-NH_2 **72** as reference at λ=220 nm (0 to 60% MeCN) with ascorbic acid as standard at ≈3.95 min.

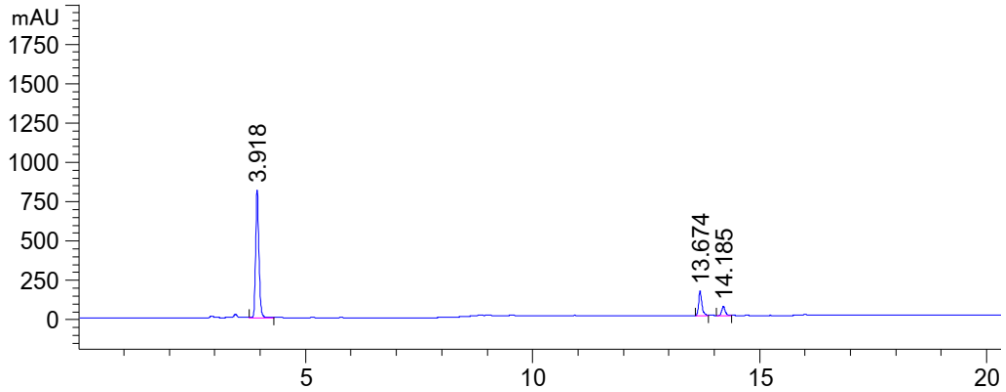

Figure 511: HPLC chromatogram of H-VK(β-D)GYI-NH_2**73** as reference at λ=220 nm (0 to 60% MeCN) with ascorbic acid as standard at ≈3.95 min.

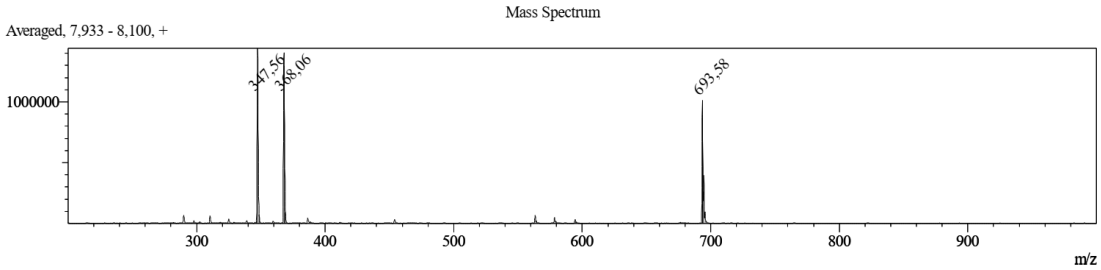

Figure 512: ESI-MS of H-VKDGYI-NH_2 **70** (M measured=693.58 $[M+H]^+$, M calc.=692.82).

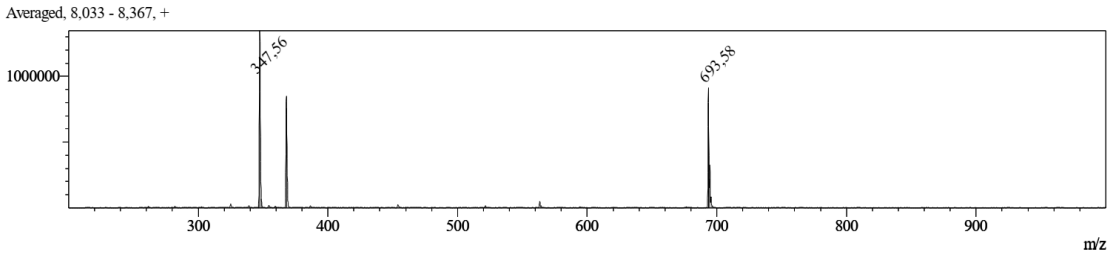

Figure 513: ESI-MS of H-VK(D-D)GYI-NH_2 **71** (M measured=693.58 $[M+H]^+$, M calc.=692.82).

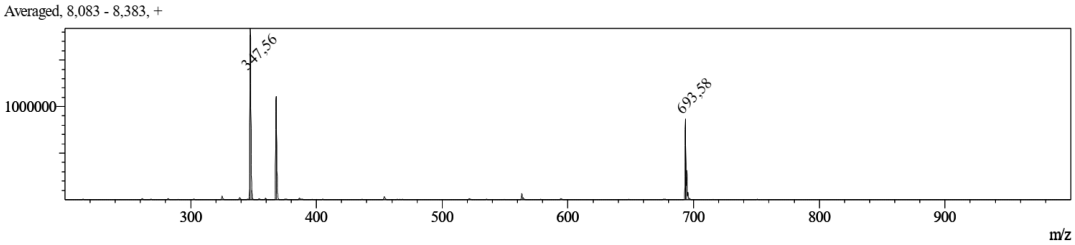

Figure 514: ESI-MS of H-VK(β-D)GYI-NH_2 **73** (M measured=693.58 $[M+H]^+$, M calc.=692.82).

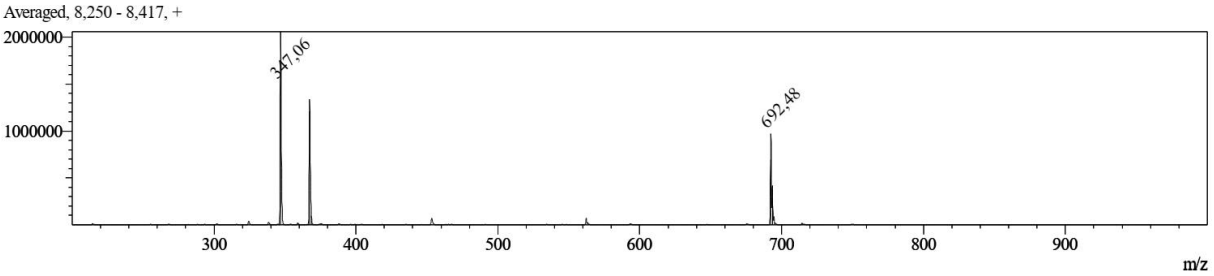

Figure 515: ESI-MS of H-VKNGYI-NH_2 **72** (M measured=692.48 $[M+H]^+$, M calc.=691.83).

8.8.2. HPLC data of H-VKDGYI-OH 70 after 3h incubation with different bases

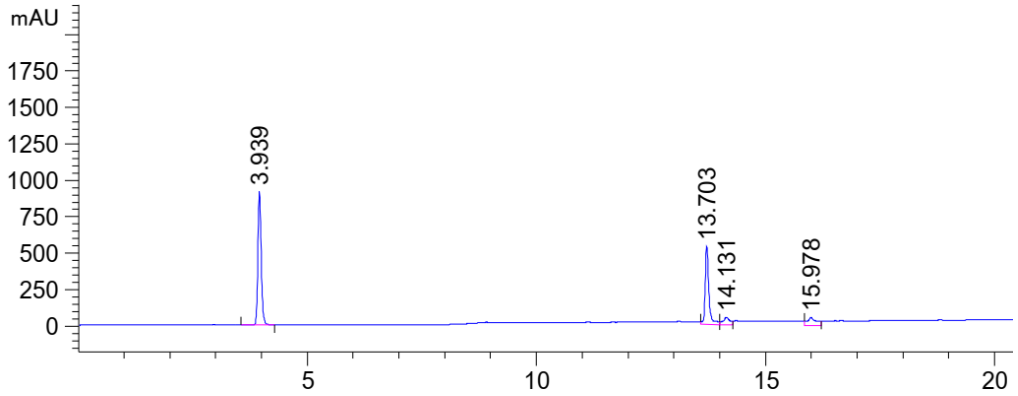

Figure 516: HPLC chromatogram of H-VKDGYI-NH_2 **70** after 3h with 5% piperazine in DMF at λ=220 nm (0 to 60% MeCN) with ascorbic acid as standard at ≈3.95 min.

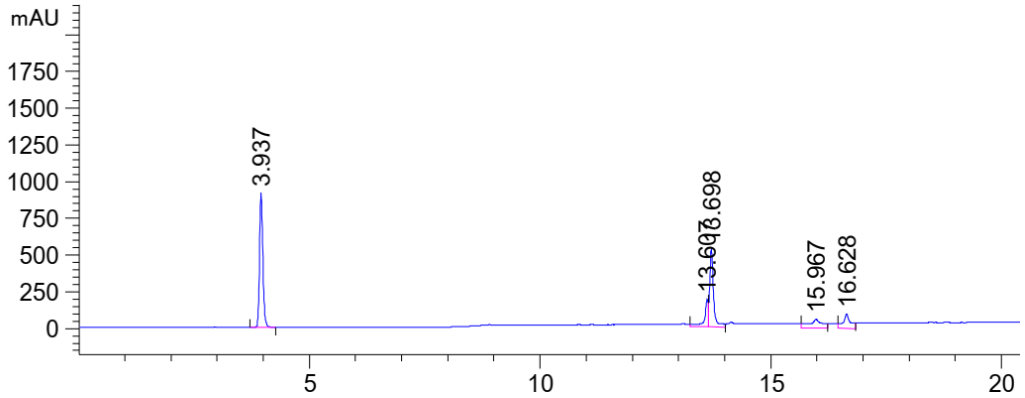

Figure 517: HPLC chromatogram of H-VKDGYI-NH_2 **70** after 3h with 5% piperazine in water at λ=220 nm (0 to 60% MeCN) with ascorbic acid as standard at ≈3.95 min.

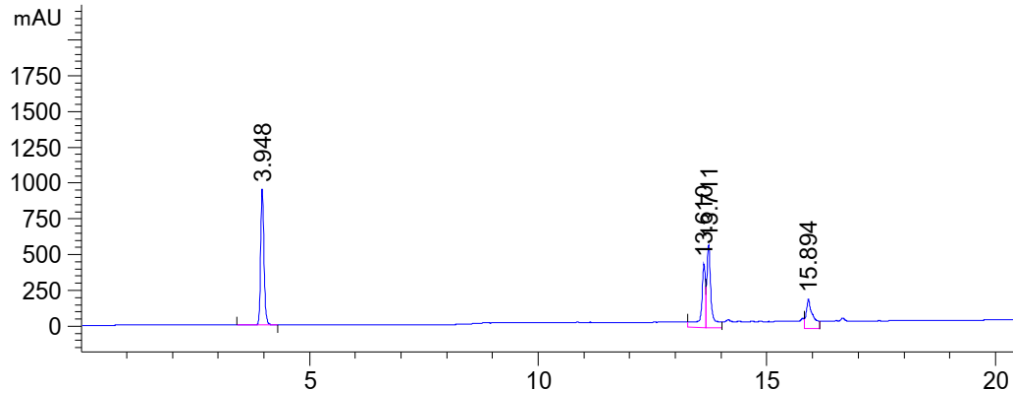

Figure 518: HPLC chromatogram of H-VKDGYI-NH_2 **70** after 3h with 10% ethanolamine in water at λ=220 nm (0 to 60% MeCN) with ascorbic acid as standard at ≈3.95 min.

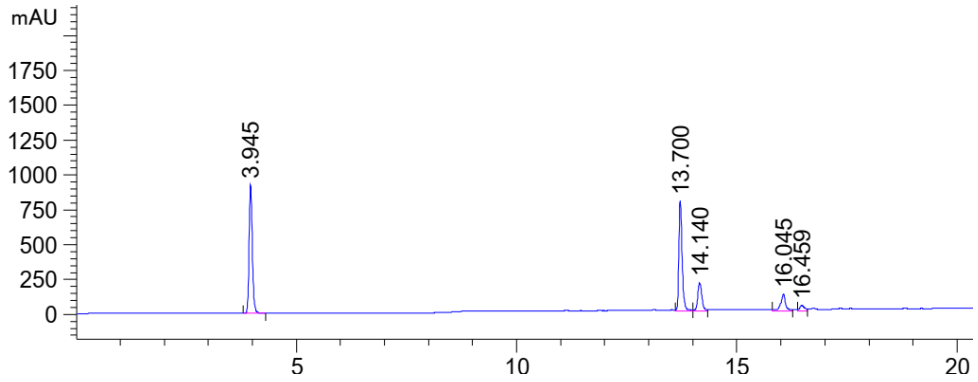

Figure 519: HPLC chromatogram of H-VKDGYI-NH_2 **70** after 3h with 20% piperidine in DMF at λ=220 nm (0 to 60% MeCN) with ascorbic acid as standard at ≈3.95 min.

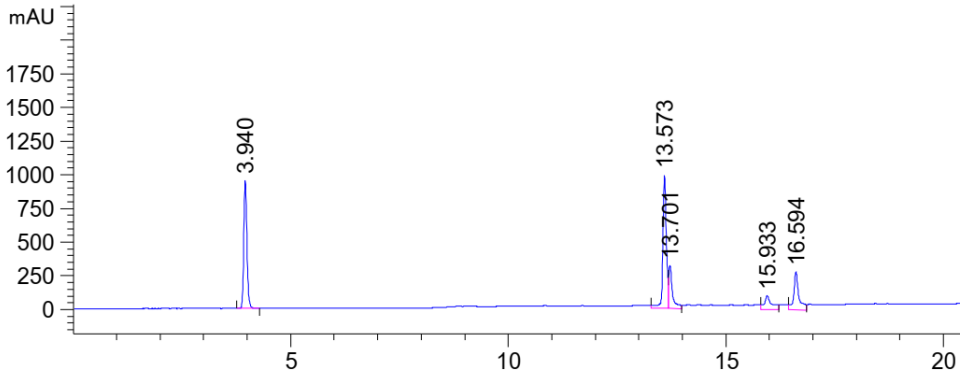

Figure 520: HPLC chromatogram of H-VKDGYI-NH_2 **70** after 3h with 1M NaOH in water at λ=220 nm (0 to 60% MeCN) with ascorbic acid as standard at ≈3.95 min.

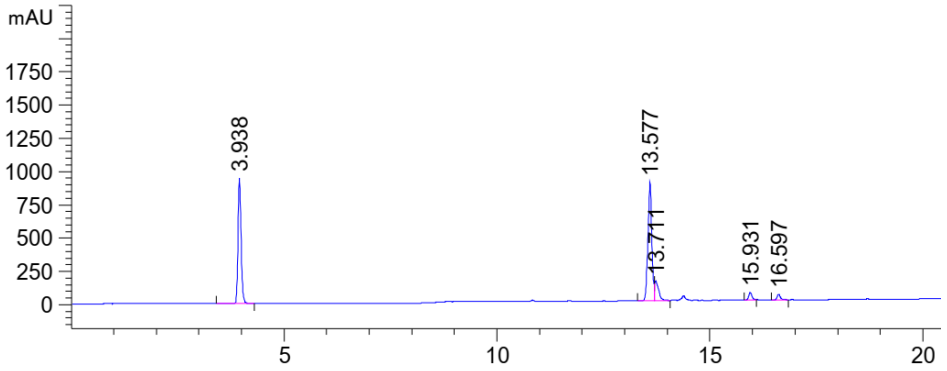

Figure 521: HPLC chromatogram of H-VKDGYI-NH_2 **70** after 3h with 1M NaOH in ethanol at λ=220 nm (0 to 60% MeCN) with ascorbic acid as standard at ≈3.95 min.

8.8.3. HPLC data of H-VKDGYI-OH 70 after 16h incubation with different bases

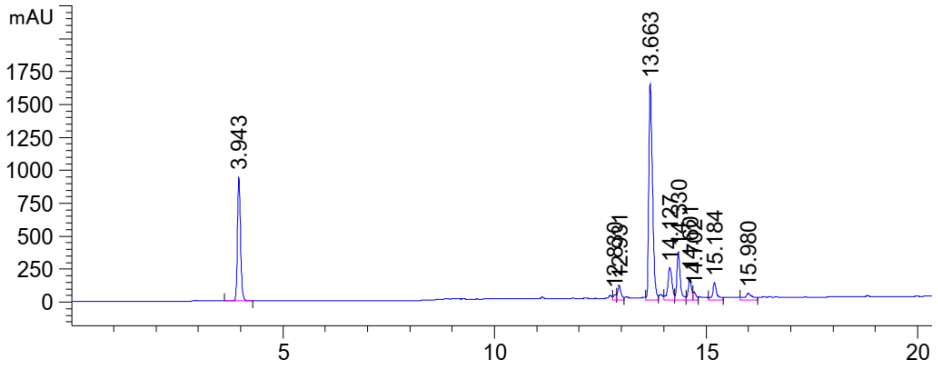

Figure 522: HPLC chromatogram of H-VKDGYI-NH_2 **70** after 16h with 5% piperazine in DMF at λ=220 nm (0 to 60% MeCN) with ascorbic acid as standard at ≈3.95 min.

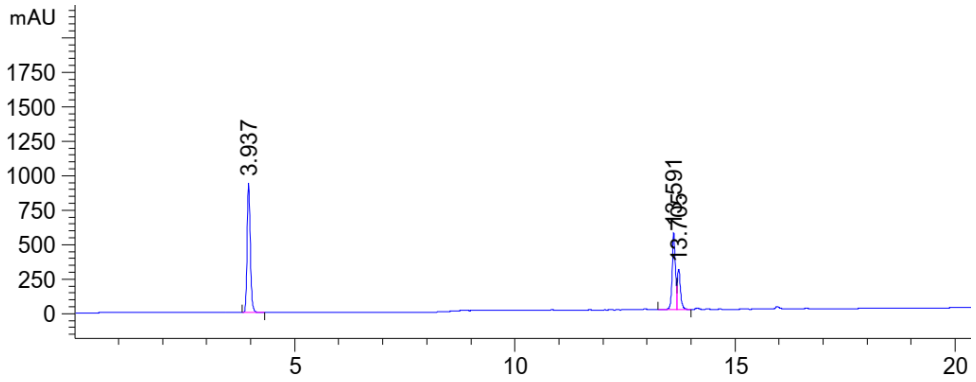

Figure 523: HPLC chromatogram of H-VKDGYI-NH_2 **70** after 16h with 5% piperazine in water at λ=220 nm (0 to 60% MeCN) with ascorbic acid as standard at ≈3.95 min.

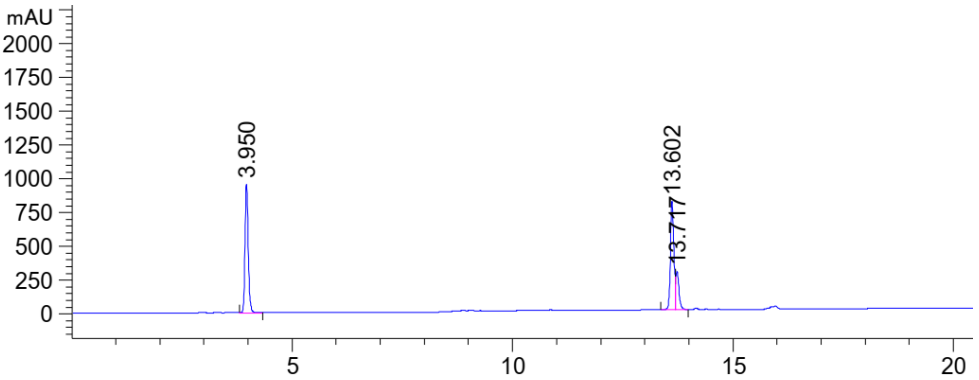

Figure 524: HPLC chromatogram of H-VKDGYI-NH_2 **70** after 16h with 10% ethanolamine in water at λ=220 nm (0 to 60% MeCN) with ascorbic acid as standard at ≈3.95 min.

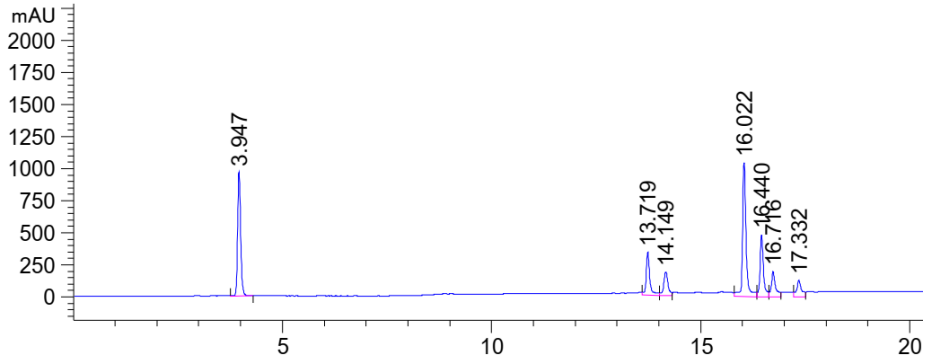

Figure 525: HPLC chromatogram of H-VKDGYI-NH_2 **70** after 16h with 20% piperidine in DMF at λ=220 nm (0 to 60% MeCN) with ascorbic acid as standard at ≈3.95 min.

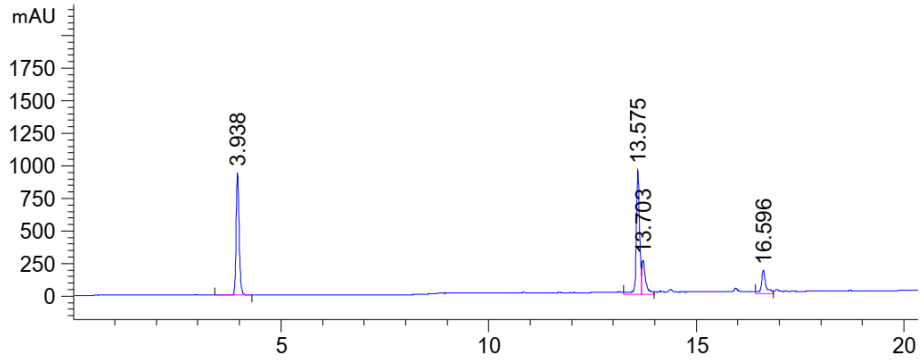

Figure 526: HPLC chromatogram of H-VKDGYI-NH_2 **70** after 16h with 1M NaOH in water at λ=220 nm (0 to 60% MeCN) with ascorbic acid as standard at ≈3.95 min.

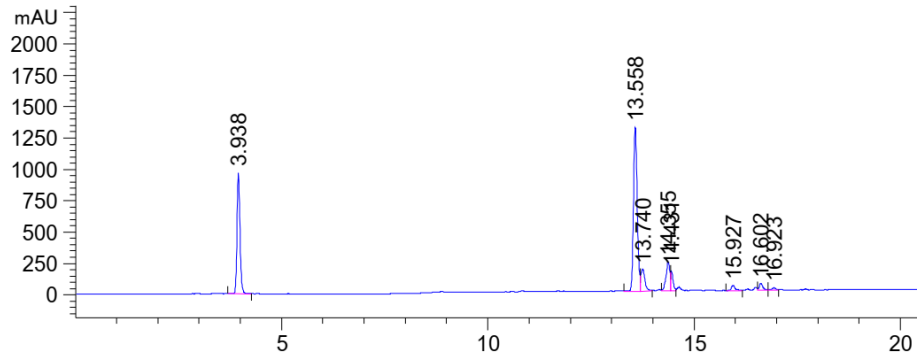

Figure 527: HPLC chromatogram of H-VKDGYI-NH_2 **70** after 16h with 1M NaOH in ethanol at λ=220 nm (0 to 60% MeCN) with ascorbic acid as standard at ≈3.95 min.

8.8.4. HPLC data of H-VK(D-D)GYI-NH_2 71 after 3h incubation with different bases

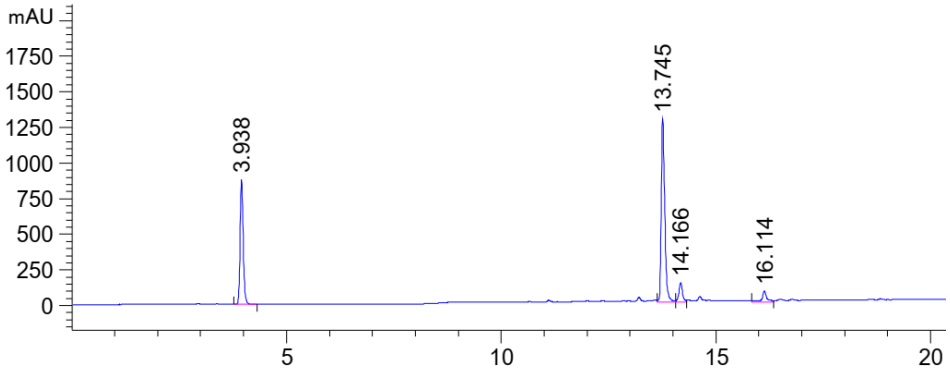

Figure 528: HPLC chromatogram of H-VK(D-D)GYI-NH_2 **71** after 3h with 5% piperazine in DMF at λ=220 nm (0 to 60% MeCN) with ascorbic acid as standard at ≈3.95 min.

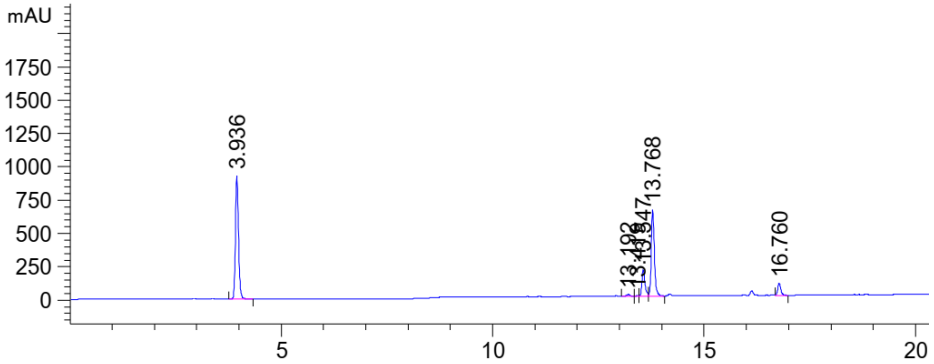

Figure 529: HPLC chromatogram of H-VK(D-D)GYI-NH_2 **71** after 3h with 5% piperazine in water at λ=220 nm (0 to 60% MeCN) with ascorbic acid as standard at ≈3.95 min.

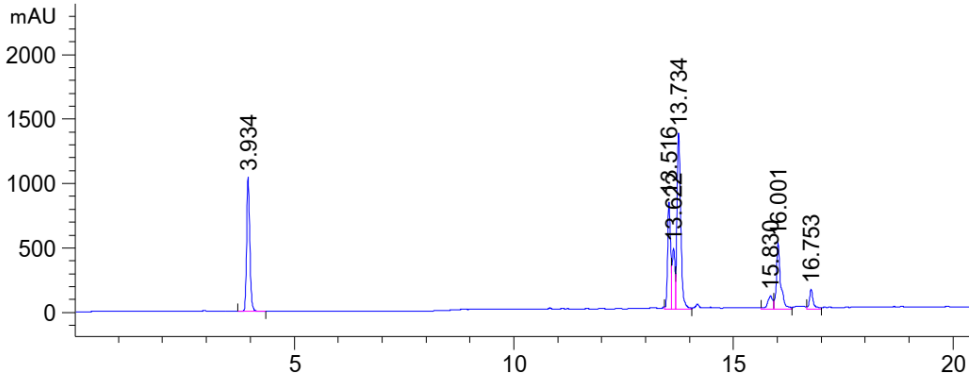

Figure 530: HPLC chromatogram of H-VK(D-D)GYI-NH_2 **71** after 3h with 10% ethanolamine in water at λ=220 nm (0 to 60% MeCN) with ascorbic acid as standard at ≈3.95 min.

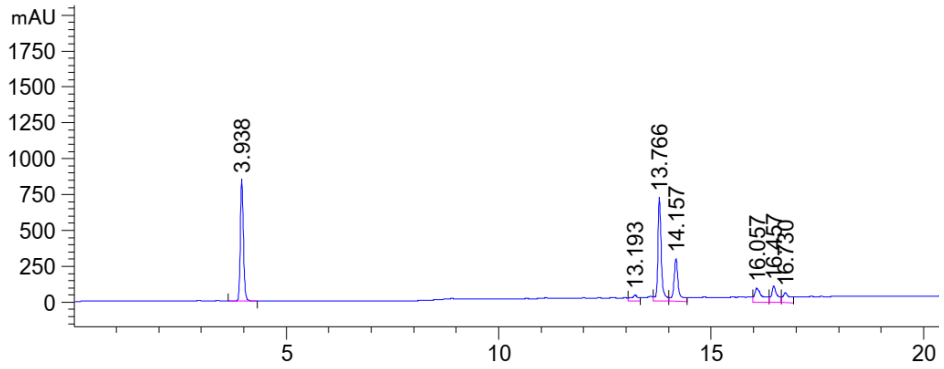

Figure 531: HPLC chromatogram of H H-VK(D-D)GYI-NH_2 **71** after 3h with 20% piperidine in DMF at λ=220 nm (0 to 60% MeCN) with ascorbic acid as standard at ≈3.95 min.

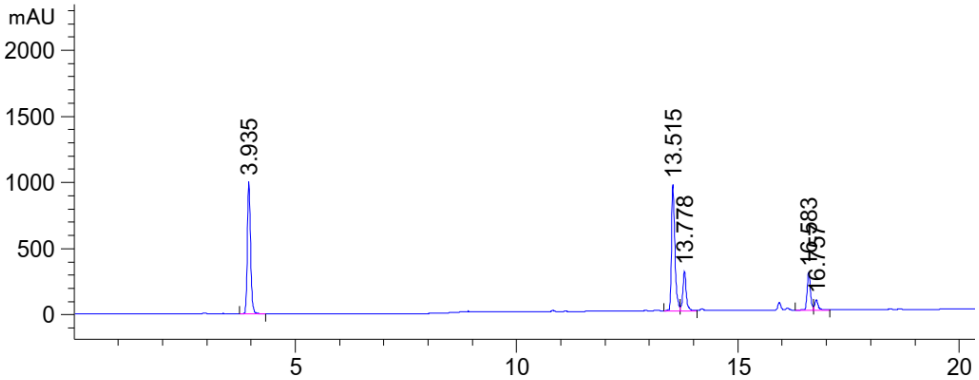

Figure 532: HPLC chromatogram of H-VK(D-D)GYI-NH_2 **71** after 3h with 1M NaOH in water at λ=220 nm (0 to 60% MeCN) with ascorbic acid as standard at ≈3.95 min.

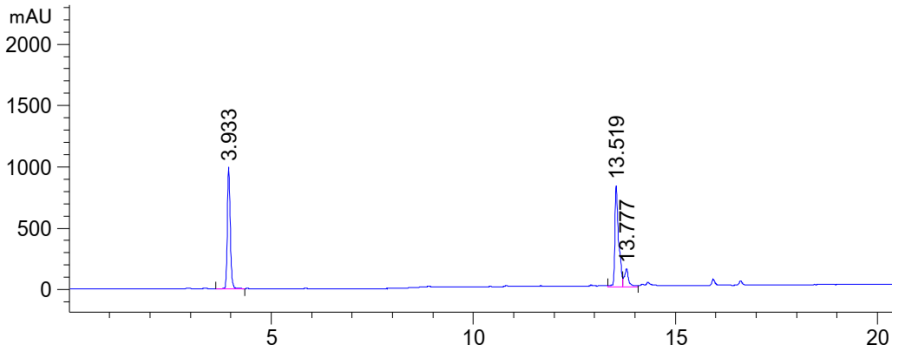

Figure 533: HPLC chromatogram of H-VK(D-D)GYI-NH_2 **71** after 3h with 1M NaOH in ethanol at λ=220 nm (0 to 60% MeCN) with ascorbic acid as standard at ≈3.95 min.

8.8.5. HPLC data of H-VK(D-D)GYI-NH_2 71 after 16h incubation with different bases

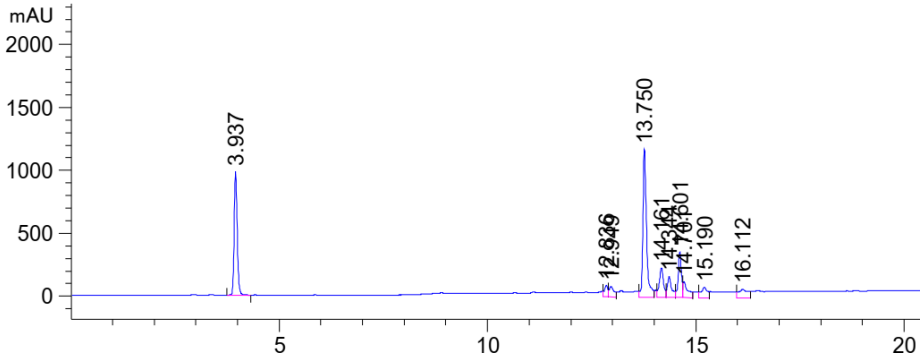

Figure 534: HPLC chromatogram of H-VK(D-D)GYI-NH_2 **71** after 16h with 5% piperazine in DMF at λ=220 nm (0 to 60% MeCN) with ascorbic acid as standard at ≈3.95 min.

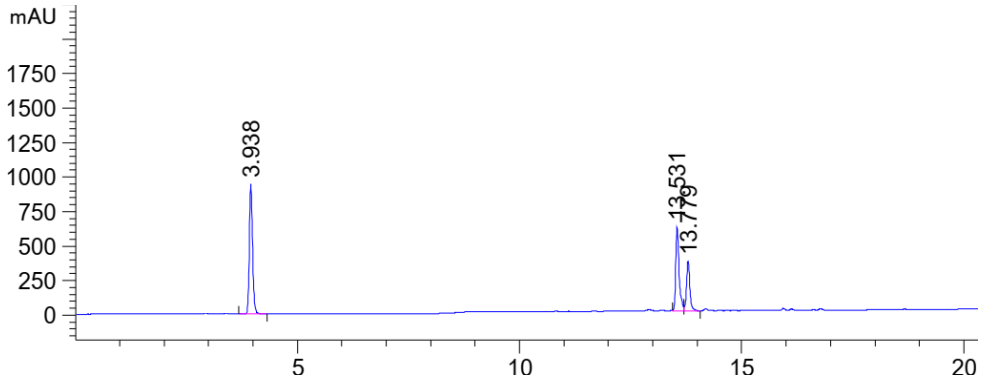

Figure 535: HPLC chromatogram of H-VK(D-D)GYI-NH_2 **71** after 16h with 5% piperazine in water at λ=220 nm (0 to 60% MeCN) with ascorbic acid as standard at ≈3.95 min.

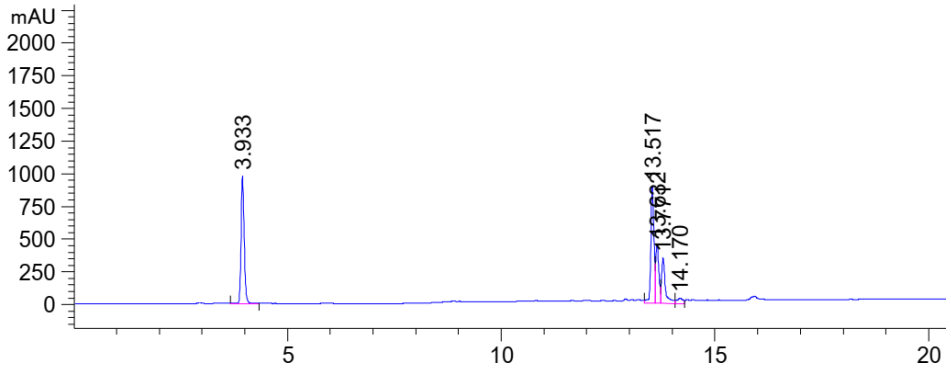

Figure 536: HPLC chromatogram of H-VK(D-D)GYI-NH_2 **71** after 16h with 10% ethanolamine in water at λ=220 nm (0 to 60% MeCN) with ascorbic acid as standard at ≈3.95 min.

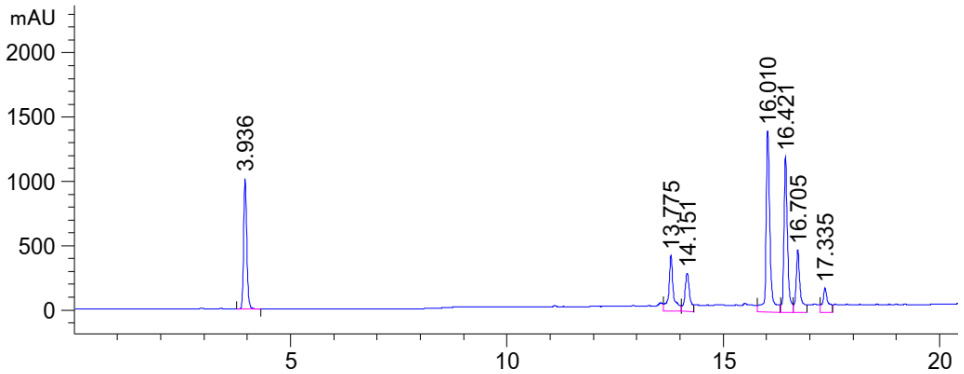

Figure 537: HPLC chromatogram of H-VK(D-D)GYI-NH_2 **71** after 16h with 20% piperidine in DMF at λ=220 nm (0 to 60% MeCN) with ascorbic acid as standard at ≈3.95 min.

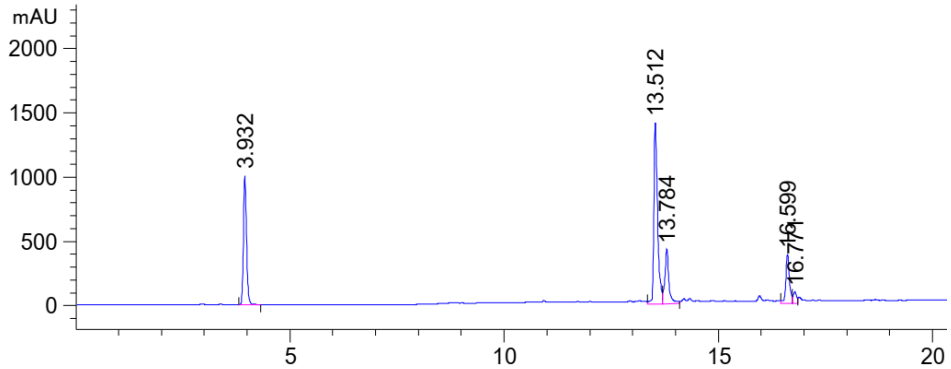

Figure 538: HPLC chromatogram of H-VK(D-D)GYI-NH_2 **71** after 16h with 1M NaOH in water at λ=220 nm (0 to 60% MeCN) with ascorbic acid as standard at ≈3.95 min.

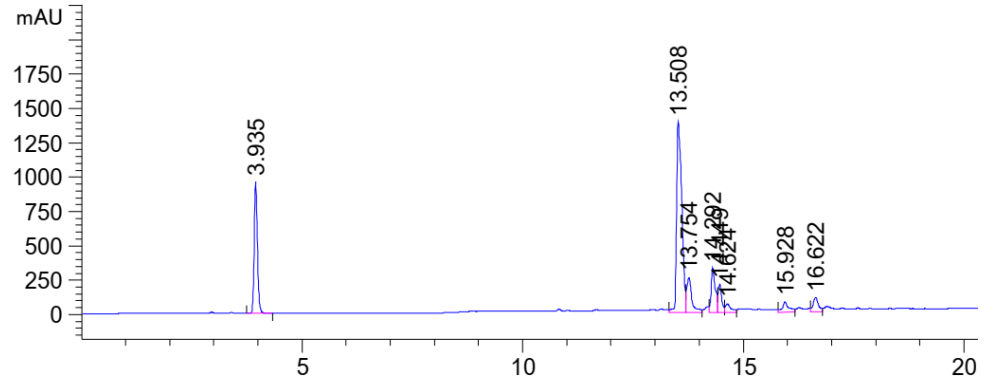

Figure 539: HPLC chromatogram of H-VK(D-D)GYI-NH_2 **71** after 16h with 1M NaOH in ethanol at λ=220 nm (0 to 60% MeCN) with ascorbic acid as standard at ≈3.95 min.

8.8.6. HPLC data of H-VKNGYI-NH_2 72 after 3h incubation with different bases

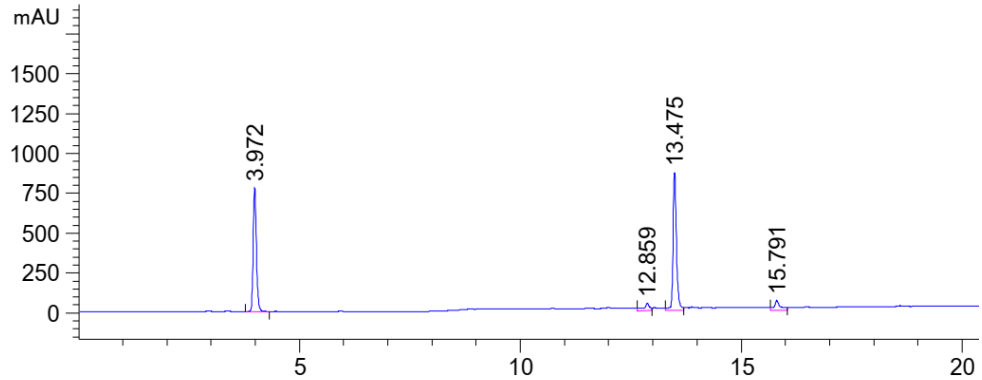

Figure 540: HPLC chromatogram of H-VKNGYI-NH_2 **72** after 3h with 5% piperazine in DMF at λ=220 nm (0 to 60% MeCN) with ascorbic acid as standard at ≈3.95 min.

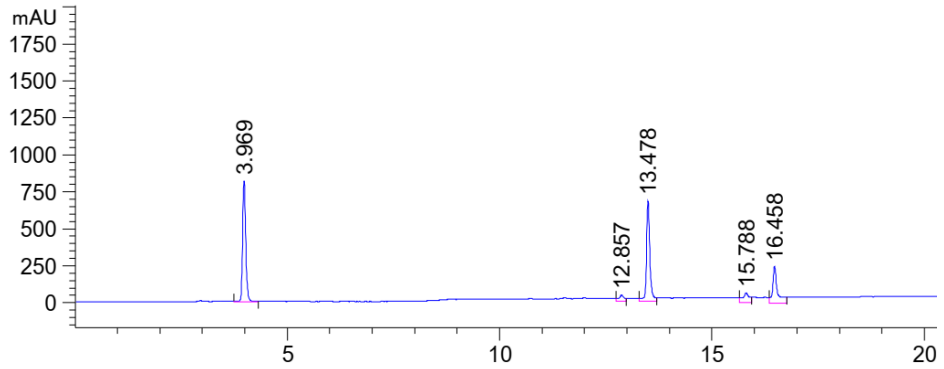

Figure 541: HPLC chromatogram of H-VKNGYI-NH_2 **72** after 3h with 5% piperazine in water at λ=220 nm (0 to 60% MeCN) with ascorbic acid as standard at ≈3.95 min.

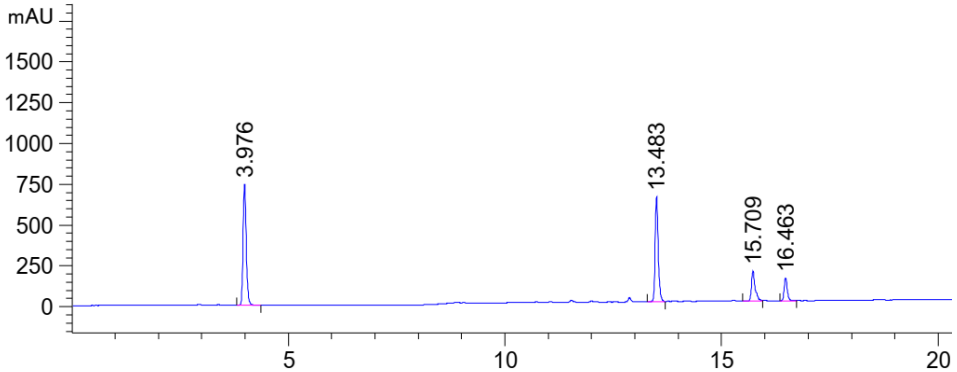

Figure 542: HPLC chromatogram of H-VKNGYI-NH_2 **72** after 3h with 10% ethanolamine in water at λ=220 nm (0 to 60% MeCN) with ascorbic acid as standard at ≈3.95 min.

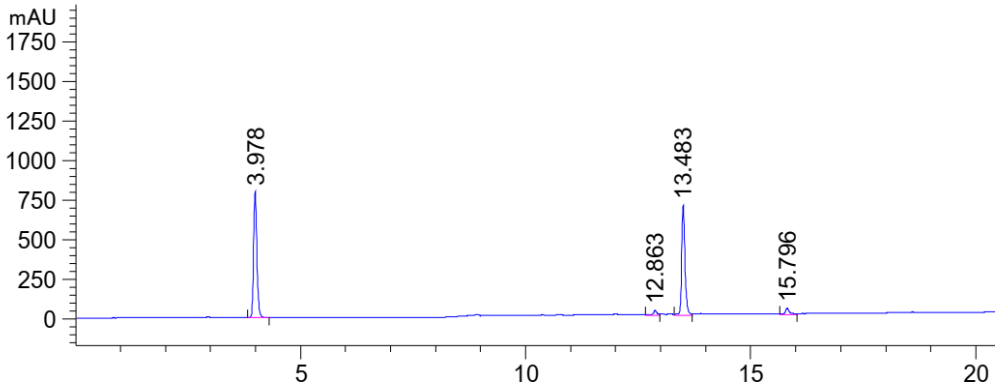

Figure 543: HPLC chromatogram of H H-VKNGYI-NH_2 **72** after 3h with 20% piperidine in DMF at λ=220 nm (0 to 60% MeCN) with ascorbic acid as standard at ≈3.95 min.

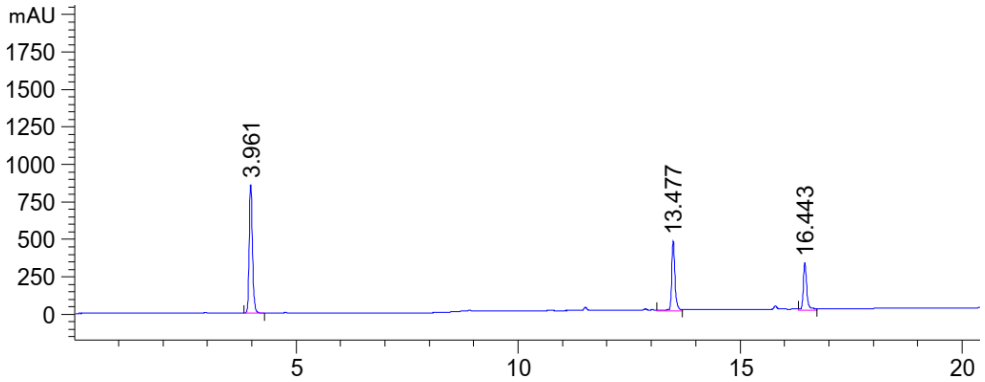

Figure 544: HPLC chromatogram of H-VKNGYI-NH_2 **72** after 3h with 1M NaOH in water at λ=220 nm (0 to 60% MeCN) with ascorbic acid as standard at ≈3.95 min.

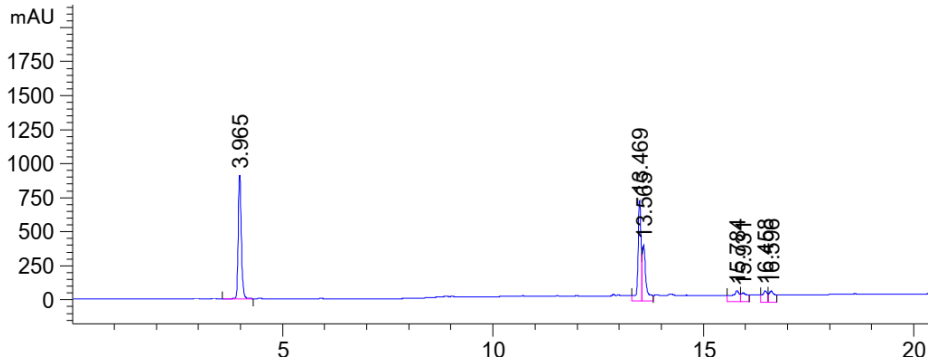

Figure 545: HPLC chromatogram of H-VKNGYI-NH_2 **72** after 3h with 1M NaOH in ethanol at λ=220 nm (0 to 60% MeCN) with ascorbic acid as standard at ≈3.95 min.

8.8.7. HPLC data of H-VKNGYI-NH_2 72 after 16h incubation with different bases

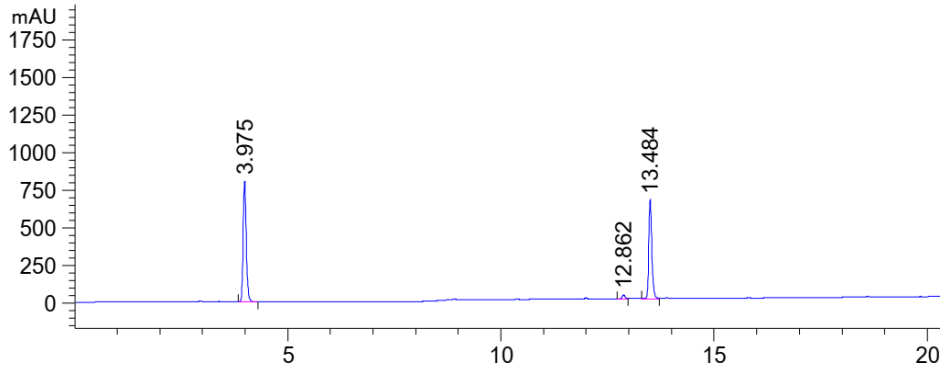

Figure 546: HPLC chromatogram of H-VKNGYI-NH_2 **72** after 16h with 5% piperazine in DMF at λ=220 nm (0 to 60% MeCN) with ascorbic acid as standard at ≈3.95 min.

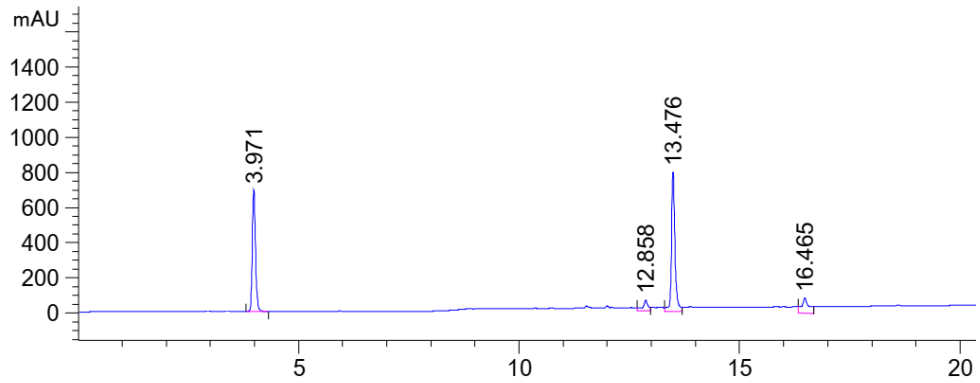

Figure 547: HPLC chromatogram of H-VKNGYI-NH_2 **72** after 16h with 5% piperazine in water at λ=220 nm (0 to 60% MeCN) with ascorbic acid as standard at ≈3.95 min.

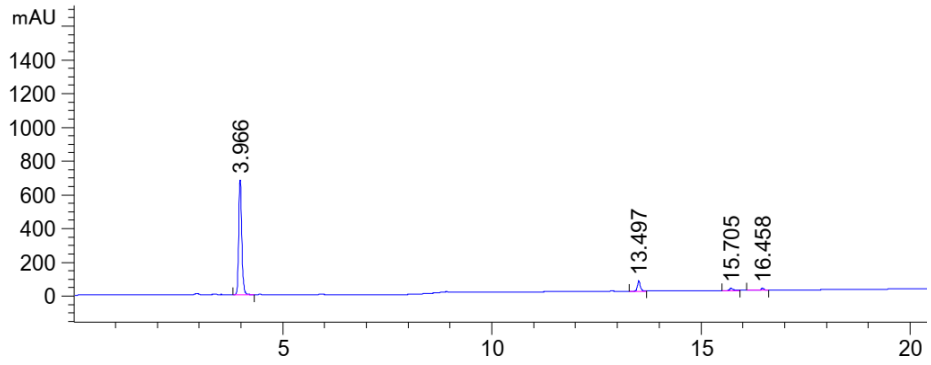

Figure 548: HPLC chromatogram of H-VKNGYI-NH_2 **72** after 16h with 10% ethanolamine in water at λ=220 nm (0 to 60% MeCN) with ascorbic acid as standard at ≈3.95 min.

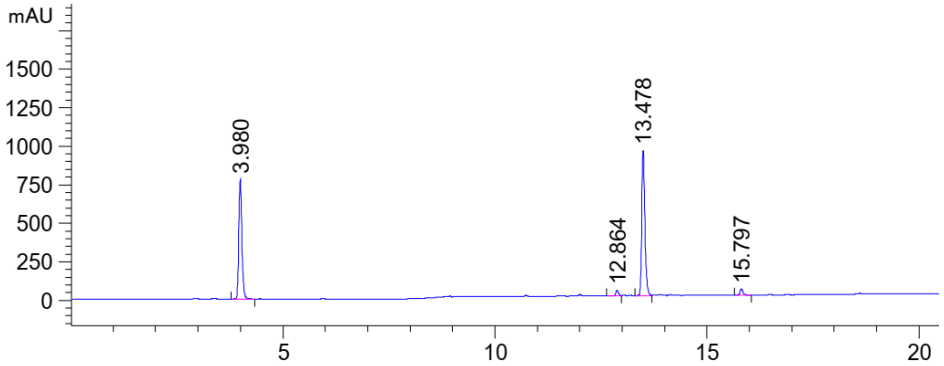

Figure 549: HPLC chromatogram of H-VKNGYI-NH_2 **72** after 16h with 20% piperidine in DMF at λ=220 nm (0 to 60% MeCN) with ascorbic acid as standard at ≈3.95 min.

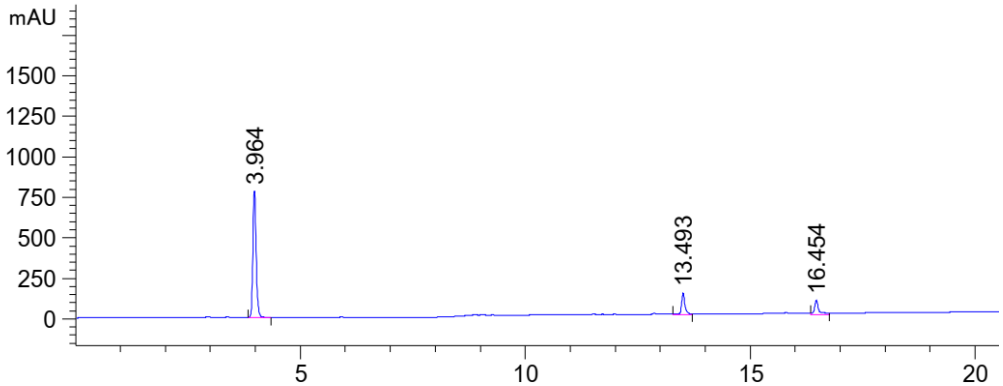

Figure 550: HPLC chromatogram of H-VKNGYI-NH_2 **72** after 16h with 1M NaOH in water at λ=220 nm (0 to 60% MeCN) with ascorbic acid as standard at ≈3.95 min.

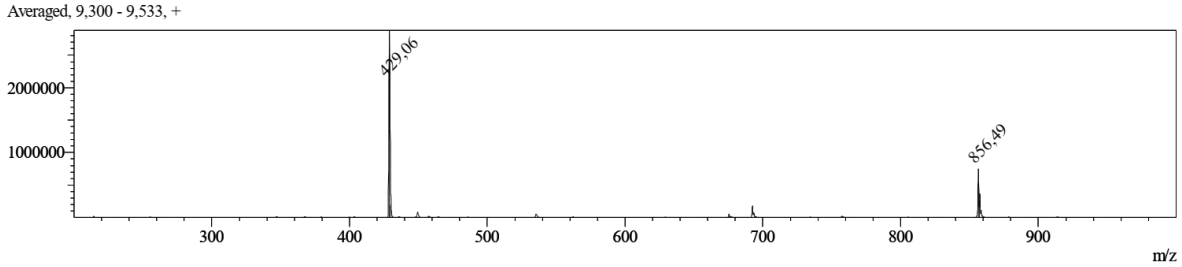

Figure 551: ESI-MS of H-VKNGYI-NH_2 **72** after 16h with 1M NaOH showing unidentified side product at 16.45min.

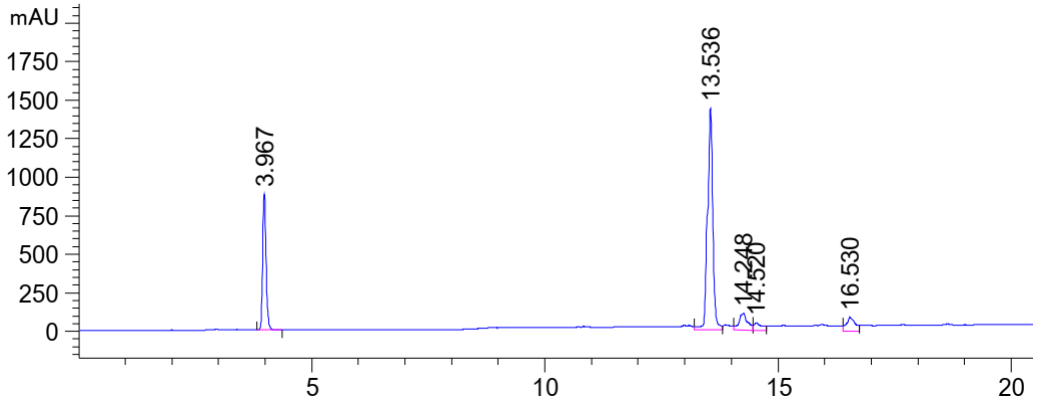

Figure 552: HPLC chromatogram of H-VKNGYI-NH_2 **72** after 16h with 1M NaOH in ethanol at λ=220 nm (0 to 60% MeCN) with ascorbic acid as standard at ≈3.95 min.

8.8.8. Temperature dependent formation of H-VK(β-D)GYI-NH_2 73 in water

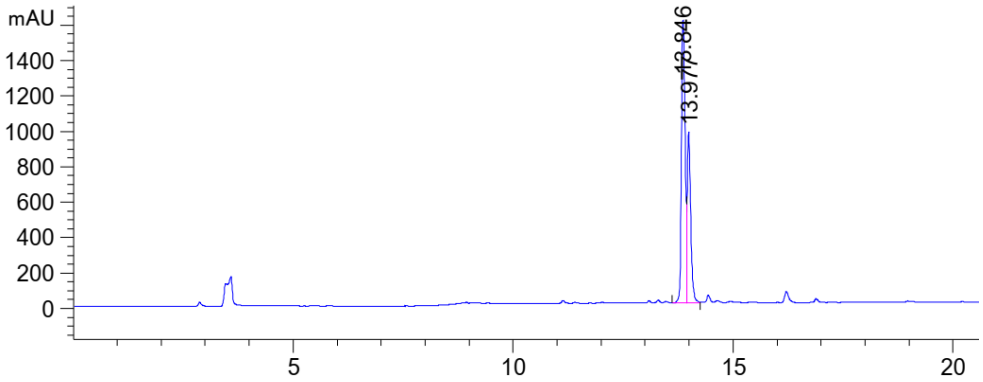

Figure 553: HPLC chromatogram of H-VK(β-D)GYI-NH_2 **73** formation at ambient temperature (26°C) in water at λ=220 nm (0 to 60% MeCN) with ascorbic acid as standard at ≈3.95 min.

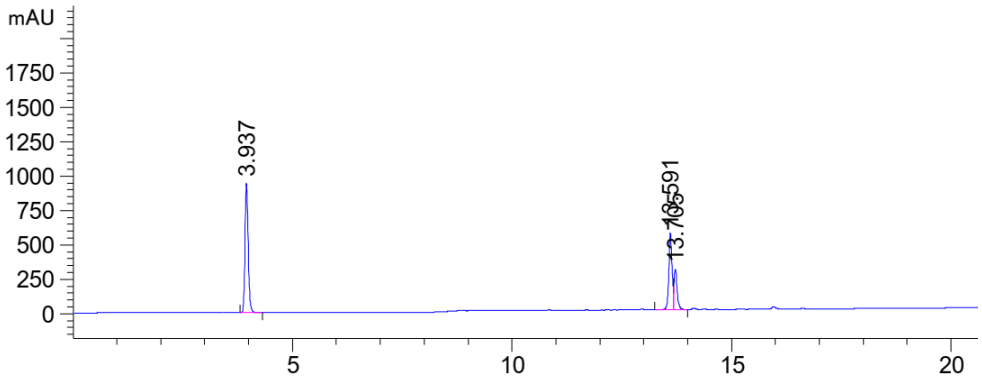

Figure 554: HPLC chromatogram of H-VK(β-D)GYI-NH_2 **73** formation at 40°C in water at λ=220 nm (0 to 60% MeCN) with ascorbic acid as standard at ≈3.95 min.

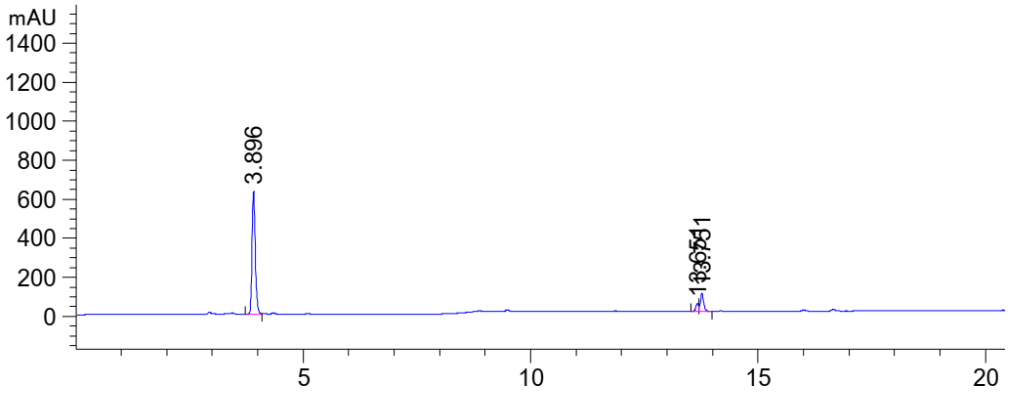

Figure 555: HPLC chromatogram of H-VK(β-D)GYI-NH_2 **73** formation at 4°C in water at λ=220 nm (0 to 60% MeCN) with ascorbic acid as standard at ≈3.95 min.

8.9. HPLC data of the capping experiments

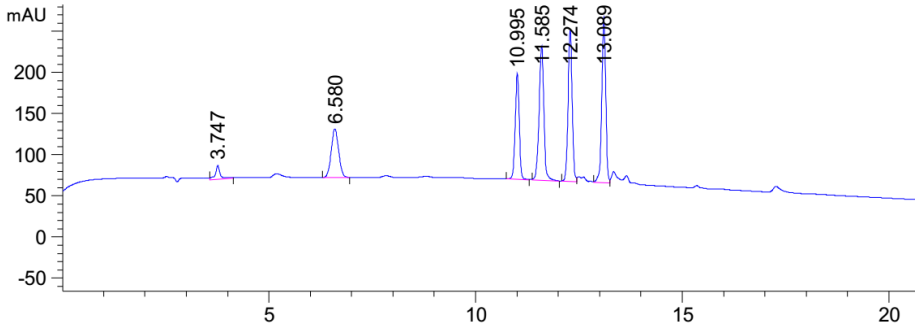

Figure 556: HPLC chromatogram of crude H-GPQGPQ-OH Hexapeptide 9 **49** in water using 0.95 eq. of N_{α}-Smoc amino acid compared to prior coupling in order to maximize by-product formation, capping was performed with sulfoacetic acid **76** at λ=220 nm (0 to 40% MeCN).

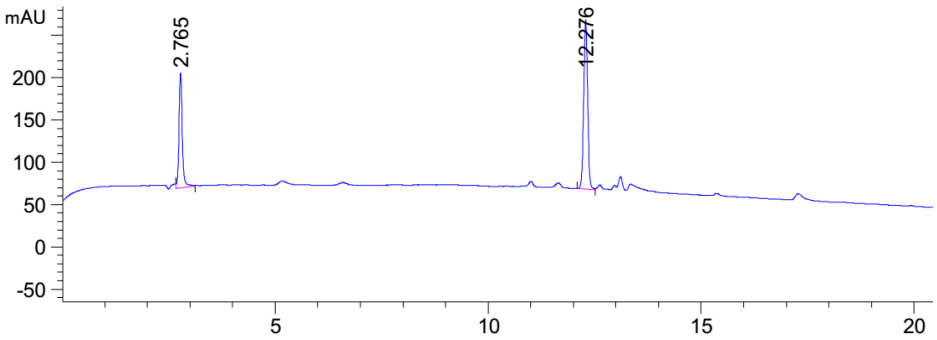

Figure 557: HPLC chromatogram of H-GPQGPQ-OH Hexapeptide 9 **49** after purification with IEC and the removal of all labelled side products at λ=220 nm (0 to 40% MeCN).

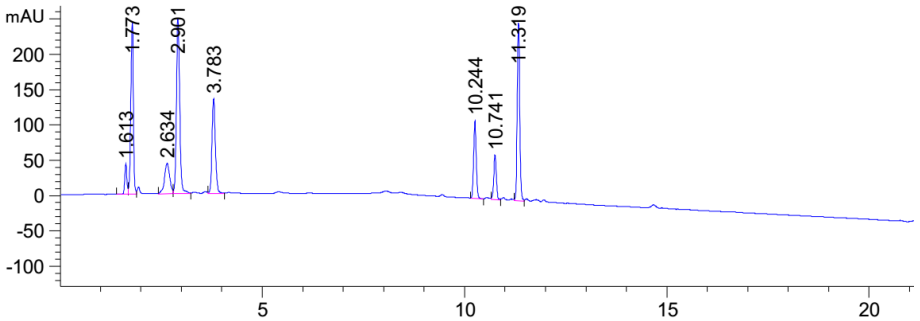

Figure 558: HPLC chromatogram of crude H-YGGFMRRV-NH_2 **77** in DMF using 0.95 eq. of N_{α}-Fmoc amino acid compared to prior coupling in order to maximize by-product formation, capping was performed with 4-sulfobenzoic acid **75** at λ=220 nm (10 to 60% MeCN).

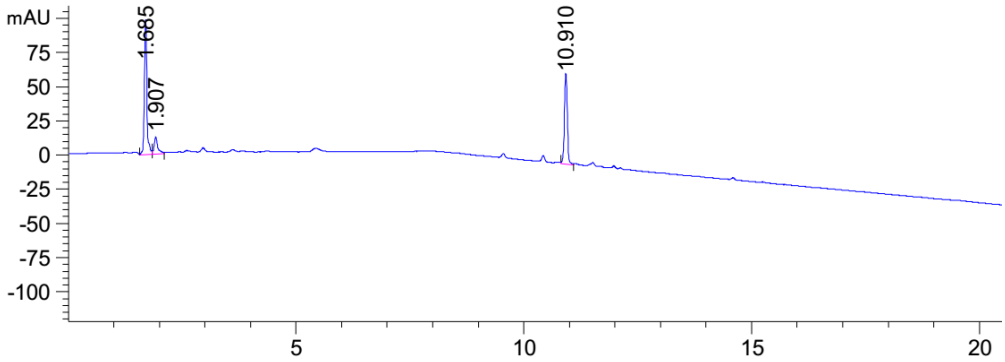

Figure 559: HPLC chromatogram of H-YGGFMRRV-NH2 **77** after purification with IEC and the removal of all labelled side products at λ=220 nm (10 to 60% MeCN).

References

[1] S. Hörner, S. Knauer, C. Uth, M. Jöst, V. Schmidts, H. Frauendorf, C. M. Thiele, O. Avrutina, H. Kolmar, *Angewandte Chemie International Edition* **2016**, *55*, 14842-14846.

[2] A. Loffet, *Journal of Peptide Science* **2002**, *8*, 1-7.

[3] T. Uhlig, T. Kyprianou, F. G. Martinelli, C. A. Oppici, D. Heiligers, D. Hills, X. R. Calvo, P. Verhaert, *EuPA Open Proteomics* **2014**, *4*, 58-69.

[4] J. L. Lau, M. K. Dunn, *Bioorganic & Medicinal Chemistry* **2018**, *26*, 2700-2707.

[5] H. Husein el Hadmed, R. F. Castillo, *Journal of Cosmetic Dermatology* **2016**, *15*, 514-519.

[6] C.-M. Lee, *Journal of Cosmetic Dermatology* **2016**, *15*, 527-539.

[7] P. J. Perez Espitia, N. de Fátima Ferreira Soares, J. S. dos Reis Coimbra, N. J. de Andrade, R. Souza Cruz, E. A. Alves Medeiros, *Comprehensive Reviews in Food Science and Food Safety* **2012**, *11*, 187-204.

[8] V. d. Vigneaud, C. Ressler, C. J. M. Swan, C. W. Roberts, P. G. Katsoyannis, S. Gordon, *Journal of the American Chemical Society* **1953**, *75*, 4879-4880.

[9] T. Curtius, *Journal für Praktische Chemie* **1882**, *26*, 145-208.

[10] E. Fischer, *Berichte der Deutschen Chemischen Gesellschaft* **1904**, *37*, 2486.

[11] E. Fischer, *Berichte der Deutschen Chemischen Gesellschaft* **1907**, 1755.

[12] M. Bergmann, L. Zervas, *Berichte der deutschen chemischen Gesellschaft (A and B Series)* **1932**, *65*, 1192-1201.

[13] G. W. Anderson, A. C. McGregor, *Journal of the American Chemical Society* **1957**, *79*, 6180-6183.

[14] R. B. Merrifield, *Journal of the American Chemical Society* **1963**, *85*, 2149-2154.

[15] R. B. Merrifield, *Recent progress in hormone research* **1967**, *23*, 451-482.

[16] S. Sakakibara, Y. Shimonishi, Y. Kishida, M. Okada, H. Sugihara, *Bulletin of the Chemical Society of Japan* **1967**, *40*, 2164-2167.

[17] B. Merrifield, *Science* **1986**, *232*, 341-347.

[18] I. Clark-Lewis, R. Aebersold, H. Ziltener, J. W. Schrader, L. E. Hood, S. B. Kent, *Science* **1986**, *231*, 134-139.

[19] B. W. Erickson, R. Merrifield, in *The proteins*, Elsevier, **1976**, pp. 255-527.

[20] L. A. Carpino, G. Y. Han, *Journal of the American Chemical Society* **1970**, *92*, 5748-&.

[21] L. A. Carpino, G. Y. Han, *J Org Chem* **1972**, *37*, 3404-&.

[22] M. Bodanszky, S. S. Deshmane, J. Martinez, *J Org Chem* **1979**, *44*, 1622-1625.

[23] E. Atherton, C. J. Logan, R. C. Sheppard, *J. Chem. Soc., Perkin Trans. 1* **1981**, 538-546.

[24] C.-D. Chang, J. Meienhofer, *International Journal of Peptide and Protein Research* **2009**, *11*, 246-249.

[25] L. Cameron, M. Meldal, R. C. Sheppard, *Journal of the Chemical Society-Chemical Communications* **1987**, 270-272.

[26] E. Hlebowicz, A. J. Andersen, L. Andersson, B. A. Moss, *The journal of peptide research : official journal of the American Peptide Society* **2005**, *65*, 90-97.

[27] M. Obkircher, C. Stahelin, F. Dick, *Journal of peptide science : an official publication of the European Peptide Society* **2008**, *14*, 763-766.

[28] M. Tessier, F. Albericio, E. Pedroso, A. Grandas, R. Eritja, E. Giralt, C. Granier, J. Rietschoten, *International Journal of Peptide and Protein Research* **2009**, *22*, 125-128.

[29] G. F. Sigler, W. D. Fuller, N. C. Chaturvedi, M. Goodman, M. Verlander, *Biopolymers* **1983**, *22*, 2157-2162.

[30] E. Bayer, M. Mutter, *Nature* **1972**, *237*, 512-513.

[31] Y. Nishiuchi, T. Inui, H. Nishio, J. Bodi, T. Kimura, F. I. Tsuji, S. Sakakibara, *Proceedings of the National Academy of Sciences of the United States of America* **1998**, *95*, 13549-13554.

[32] R. B. Merrifield, *Journal of the American Chemical Society* **1964**, *86*, 304-305.
[33] R. A. Boissonnas, S. Guttmann, P. A. Jaquenoud, *Helvetica Chimica Acta* **1960**, *43*, 1349-1358.
[34] J. Pless, E. Stürmer, S. Guttman, R. A. Boissonnas, *Helvetica Chimica Acta* **1962**, *45*, 394-396.
[35] E. D. Nicolaides, H. A. D. Wald, *The Journal of Organic Chemistry* **1961**, *26*, 3872-3876.
[36] W. S. Hancock, D. J. Prescott, P. R. Vagelos, G. R. Marshall, *The Journal of Organic Chemistry* **1973**, *38*, 774-781.
[37] T. F. Gabriel, J. Michalewsky, J. Meienhofer, *J Chromatogr* **1976**, *129*, 287-293.
[38] I. Molnár, C. Horváth, *Journal of Chromatography A* **1977**, *142*, 623-640.
[39] C. T. Mant, Y. Chen, Z. Yan, T. V. Popa, J. M. Kovacs, J. B. Mills, B. P. Tripet, R. S. Hodges, *Methods in molecular biology (Clifton, N.J.)* **2007**, *386*, 3-55.
[40] C.-. Bruce Merrifield lecture from Nobel Lectures, Editor-in-Charge Tore Frängsmyr, Editor Bo G. Malmström, World Scientific Publishing Co., Singapore, 1992
[41] G. F. Domagk, *Deutsche medizinische Wochenschrift (1946)* **1984**, *109*, 1901-1902.
[42] P. E. Dawson, T. W. Muir, I. Clark-Lewis, S. B. Kent, *Science* **1994**, *266*, 776-779.
[43] R. Nyfeler, *Methods in molecular biology (Clifton, N.J.)* **1994**, *35*, 303-316.
[44] M. Rinnova, M. Lebl, M. Soucek, *Letters in Peptide Science* **1999**, *6*, 15-22.
[45] M. Narita, *Bulletin of the Chemical Society of Japan* **1978**, *51*, 1477-1480.
[46] H. Benz, *Synthesis-Stuttgart* **1994**, *1994*, 337-358.
[47] A. C. Conibear, E. E. Watson, R. J. Payne, C. F. W. Becker, *Chem Soc Rev* **2018**, *47*, 9046-9068.
[48] L. Raibaut, N. Ollivier, O. Melnyk, *Chem Soc Rev* **2012**, *41*, 7001-7015.
[49] T. Wieland, E. Bokelmann, L. Bauer, H. U. Lang, H. Lau, *Justus Liebigs Annalen der Chemie* **1953**, *583*, 129-149.
[50] J. C. Monbaliu, A. R. Katritzky, *Chem Commun (Camb)* **2012**, *48*, 11601-11622.
[51] F. Bordusa, C. Dahl, H.-D. Jakubke, K. Burger, B. Koksch, *Tetrahedron: Asymmetry* **1999**, *10*, 307-313.
[52] T. Nuijens, A. H. M. Schepers, C. Cusan, J. A. W. Kruijtzer, D. T. S. Rijkers, R. M. J. Liskamp, P. J. L. M. Quaedflieg, *Advanced Synthesis & Catalysis* **2013**, *355*, 287-293.
[53] T. Nuijens, A. Toplak, P. J. L. M. Quaedflieg, J. Drenth, B. Wu, D. B. Janssen, *Advanced Synthesis & Catalysis* **2016**, *358*, 4041-4048.
[54] R. Behrendt, P. White, J. Offer, *Journal of Peptide Science* **2016**, *22*, 4-27.
[55] G. Barany, R. B. Merrifield, *Analytical biochemistry* **1979**, *95*, 160-170.
[56] C. G. Fields, G. B. Fields, R. L. Noble, T. A. Cross, *Int J Pept Protein Res* **1989**, *33*, 298-303.
[57] W. C. W. P. D. Chan, P. White, *Fmoc solid phase peptide synthesis: a practical approach, Vol. 222*, OUP Oxford, **1999**.
[58] G. B. Fields, R. L. Noble, *Int J Pept Protein Res* **1990**, *35*, 161-214.
[59] R. H. Angeletti, L. F. Bonewald, G. B. Fields, *Methods in enzymology* **1997**, *289*, 697-717.
[60] P. G. M. Wuts, *Chem. Listy* **2015**, *109*, 241.
[61] R. A. Gibbs, *American Journal of Pharmaceutical Education* **2000**, *64*, 108.
[62] G. Barany, F. Albericio, *Journal of the American Chemical Society* **1985**, *107*, 4936-4942.
[63] F. Albericio, *Biopolymers* **2000**, *55*, 123-139.
[64] A. Isidro-Llobet, M. Alvarez, F. Albericio, *Chem Rev* **2009**, *109*, 2455-2504.
[65] R. Schwyzer, C. H. Li, *Nature* **1958**, *182*, 1669-1670.
[66] H. Yajima, M. Takeyama, J. Kanaki, K. Mitani, *Journal of the Chemical Society, Chemical Communications* **1978**, 482-483.
[67] R. H. Sifferd, V. du Vigneaud, *Journal of Biological Chemistry* **1935**, *108*, 753-761.

[68] Y. Shimonishi, S. Sakakibara, S. Akabori, *Bulletin of the Chemical Society of Japan* **1962**, *35*, 1966-1970.
[69] M. Verlander, *Organic Process Research & Development* **2001**, *5*, 667-668.
[70] S. Mojsov, A. R. Mitchell, R. B. Merrifield, *The Journal of Organic Chemistry* **1980**, *45*, 555-560.
[71] H. Hibino, Y. Nishiuchi, *Org Lett* **2012**, *14*, 1926-1929.
[72] D. F. Veber, J. D. Milkowski, S. L. Varga, R. G. Denkewalter, R. Hirschmann, *J Am Chem Soc* **1972**, *94*, 5456-5461.
[73] T. Brown, J. H. Jones, *J. Chem. Soc., Chem. Commun.* **1981**, 648-649.
[74] T. Brown, J. H. Jones, J. D. Richards, *J. Chem. Soc., Perkin Trans. 1* **1982**, 1553-1561.
[75] F. Chillemi, R. B. Merrifield, *Biochemistry* **1969**, *8*, 4344-4346.
[76] B. W. Erickson, R. B. Merrifield, *Journal of the American Chemical Society* **1973**, *95*, 3757-3763.
[77] D. Yamashiro, C. H. Li, *J Org Chem* **1973**, *38*, 2594-2597.
[78] G. Mezo, N. Mihala, G. Koczan, F. Hudecz, *Tetrahedron* **1998**, *54*, 6757-6766.
[79] M. Fujino, M. Wakimasu, C. Kitada, *Journal of the Chemical Society-Chemical Communications* **1982**, 445-446.
[80] R. Ramage, J. Green, A. J. Blake, *Tetrahedron* **1991**, *47*, 6353-6370.
[81] L. A. Carpino, H. Shroff, S. A. Triolo, E. M. E. Mansour, H. Wenschuh, F. Albericio, *Tetrahedron Letters* **1993**, *34*, 7829-7832.
[82] R. Roeske, *The Journal of Organic Chemistry* **1963**, *28*, 1251-1253.
[83] G. W. Anderson, F. M. Callahan, *Journal of the American Chemical Society* **1960**, *82*, 3359-3363.
[84] A. Loffet, H. X. Zhang, *Int J Pept Protein Res* **1993**, *42*, 346-351.
[85] C. Yue, J. Thierry, P. Potier, *Tetrahedron Letters* **1993**, *34*, 323-326.
[86] M. Bodanszky, M. A. Bednarek, A. Bodanszky, *Int J Pept Protein Res* **1982**, *20*, 387-395.
[87] K. Barlos, P. Mamos, D. Papaioannou, S. Patrianakou, C. Sanida, W. Schäfer, *Liebigs Annalen der Chemie* **1987**, *1987*, 1025-1030.
[88] R. L. Johnson, R. B. Miller, *Int J Pept Protein Res* **1984**, *23*, 581-590.
[89] B. Sax, F. Dick, R. Tanner, J. Gosteli, *Peptide research* **1992**, *5*, 245-246.
[90] M. C. Munson, C. Garciaecheverria, F. Albericio, G. Barany, *J Org Chem* **1992**, *57*, 3013-3018.
[91] G. M. Dubowchik, S. Radia, *Tetrahedron Letters* **1997**, *38*, 5257-5260.
[92] R. Eritja, J. P. Ziehler-Martin, P. A. Walker, T. D. Lee, K. Legesse, F. Albericio, B. E. Kaplan, *Tetrahedron* **1987**, *43*, 2675-2680.
[93] R. Schwyzer, W. Rittel, *Helvetica Chimica Acta* **1961**, *44*, 159-169.
[94] R. Colombo, F. Colombo, J. H. Jones, *J. Chem. Soc., Chem. Commun.* **1984**, 292-293.
[95] J. G. Adamson, M. A. Blaskovich, H. Groenevelt, G. A. Lajoie, *J Org Chem* **1991**, *56*, 3447-3449.
[96] K. Barlos, D. Gatos, S. Koutsogianni, W. Schäfer, G. Stavropoulos, Y. Wenging, *Tetrahedron Letters* **1991**, *32*, 471-474.
[97] M. Lalonde, T. H. Chan, *Synthesis* **1985**, *1985*, 817-845.
[98] P. M. Fischer, *Tetrahedron Letters* **1992**, *33*, 7605-7608.
[99] H. Choi, J. V. Aldrich, *International Journal of Peptide and Protein Research* **1993**, *42*, 58-63.
[100] B. Yan, A. W. Czarnik, *Optimization of solid-phase combinatorial synthesis*, CRC Press, **2001**.
[101] D. Hudson, *J Comb Chem* **1999**, *1*, 333-360.
[102] S. L. Regen, *Journal of the American Chemical Society* **1977**, *99*, 3838-3840.
[103] S. L. Regen, L. Dulak, *Journal of the American Chemical Society* **1977**, *99*, 623-625.

[104] S. L. Regen, J. J. Besse, J. Mclick, *Journal of the American Chemical Society* **1979**, *101*, 116-120.
[105] A. W. Czarnik, *Biotechnol Bioeng* **1998**, *61*, 77-79.
[106] M. Meldal, in *Methods in enzymology, Vol. 289*, Academic Press, **1997**, pp. 83-104.
[107] P. H. Toy, Y. Lam, *Solid-phase organic synthesis: concepts, strategies, and applications*, John Wiley & Sons, **2012**.
[108] A. R. Vaino, K. D. Janda, *J Comb Chem* **2000**, *2*, 579-596.
[109] W. B. Li, X. Y. Xiao, A. W. Czarnik, *Journal of Combinatorial Chemistry* **1999**, *1*, 127-129.
[110] E. Bayer, M. Dengler, B. Hemmasi, *International Journal of Peptide and Protein Research* **2009**, *25*, 178-186.
[111] F. I. Auzanneau, M. Meldal, K. Bock, *Journal of peptide science : an official publication of the European Peptide Society* **1995**, *1*, 31-44.
[112] M. Renil, V. N. R. Pillai, *J Appl Polym Sci* **1996**, *61*, 1585-1594.
[113] M. Kempe, G. Barany, *Journal of the American Chemical Society* **1996**, *118*, 7083-7093.
[114] F. Oesterhelt, M. Rief, H. E. Gaub, *New J Phys* **1999**, *1*, 6-6.
[115] J. Rademann, M. Grotli, M. Meldal, K. Bock, *Journal of the American Chemical Society* **1999**, *121*, 5459-5466.
[116] F. Garcia-Martin, M. Quintanar-Audelo, Y. Garcia-Ramos, L. J. Cruz, C. Gravel, R. Furic, S. Cote, J. Tulla-Puche, F. Albericio, *J Comb Chem* **2006**, *8*, 213-220.
[117] S. Frutos, J. Tulla-Puche, F. Albericio, E. Giralt, *Int J Pept Res Ther* **2007**, *13*, 221-227.
[118] F. Garcia-Martin, P. White, R. Steinauer, S. Cote, J. Tulla-Puche, F. Albericio, *Biopolymers* **2006**, *84*, 566-575.
[119] H. Rink, *Tetrahedron Letters* **1987**, *28*, 3787-3790.
[120] A. E. Florsheimer, B. in Peptides 1990 Proceedings of the 21st European Peptide Symposium; Girault, E.; Andreu, D. Eds.; ESCOM; Leiden, 1990; pp. 131-133.
[121] K. Barlos, D. Gatos, J. Kallitsis, G. Papaphotiu, P. Sotiriu, Y. Wenqing, W. Schäfer, *Tetrahedron Letters* **1989**, *30*, 3943-3946.
[122] M. Mergler, R. Nyfeler, R. Tanner, J. Gosteli, P. Grogg, *Tetrahedron Letters* **1988**, *29*, 4009-4012.
[123] G. R. Matsueda, J. M. Stewart, *Peptides* **1981**, *2*, 45-50.
[124] J. H. Kirchhoff, S. Brase, D. Enders, *J Comb Chem* **2001**, *3*, 71-77.
[125] B. J. Backes, J. A. Ellman, *The Journal of Organic Chemistry* **1999**, *64*, 2322-2330.
[126] R. C. Sheppard, B. J. Williams, *Int J Pept Protein Res* **1982**, *20*, 451-454.
[127] K. J. Jensen, J. Alsina, M. F. Songster, J. Vágner, F. Albericio, G. Barany, *Journal of the American Chemical Society* **1998**, *120*, 5441-5452.
[128] B. S. Jursic, Z. Zdravkovski, *Synthetic Commun* **1993**, *23*, 2761-2770.
[129] J. C. Sheehan, G. P. Hess, *Journal of the American Chemical Society* **1955**, *77*, 1067-1068.
[130] M. Goodman, W. J. McGahren, *Tetrahedron* **1967**, *23*, 2031-2050.
[131] Y. M. Angell, J. Alsina, F. Albericio, G. Barany, *The journal of peptide research : official journal of the American Peptide Society* **2002**, *60*, 292-299.
[132] Y. Han, F. Albericio, G. Barany, *J Org Chem* **1997**, *62*, 4307-4312.
[133] N. Robertson, L. Jiang, R. Ramage, *Tetrahedron* **1999**, *55*, 2713-2720.
[134] D. S. Kemp, in *Major Methods of Peptide Bond Formation, Vol. 1* (Eds.: E. Gross, J. Meienhofer), Academic Press, **1979**, pp. 315-383.
[135] W. König, R. Geiger, *Chemische Berichte* **1970**, *103*, 788-798.
[136] W. König, R. Geiger, *Chemische Berichte* **1970**, *103*, 2024-2033.
[137] F. Kurzer, K. Douraghi-Zadeh, *Chem Rev* **1967**, *67*, 107-152.
[138] L. A. Carpino, *Journal of the American Chemical Society* **1993**, *115*, 4397-4398.
[139] L. A. Carpino, A. El-Faham, *Tetrahedron* **1999**, *55*, 6813-6830.

[140] R. Subiros-Funosas, R. Prohens, R. Barbas, A. El-Faham, F. Albericio, *Chemistry* **2009**, *15*, 9394-9403.
[141] J. Sheehan, P. Cruickshank, G. Boshart, *The Journal of Organic Chemistry* **1961**, *26*, 2525-2528.
[142] J. C. Sheehan, J. J. Hlavka, *J Org Chem* **1956**, *21*, 439-441.
[143] V. Dourtoglou, J.-C. Ziegler, B. Gross, *Tetrahedron Letters* **1978**, *19*, 1269-1272.
[144] J. Coste, D. Le-Nguyen, B. Castro, *Tetrahedron Letters* **1990**, *31*, 205-208.
[145] O. Marder, Y. Shvo, F. Albericio, *Chim. Oggi-Chem. Today* **2002**, *20*, 37-41.
[146] G. Sabatino, B. Mulinacci, M. C. Alcaro, M. Chelli, P. Rovero, A. M. Papini, *Letters in Peptide Science* **2002**, *9*, 119-123.
[147] L. A. Carpino, H. Imazumi, A. El-Faham, F. J. Ferrer, C. Zhang, Y. Lee, B. M. Foxman, P. Henklein, C. Hanay, C. Mugge, H. Wenschuh, J. Klose, M. Beyermann, M. Bienert, *Angewandte Chemie (International ed. in English)* **2002**, *41*, 441-445.
[148] F. Albericio, J. M. Bofill, A. El-Faham, S. A. Kates, *The Journal of Organic Chemistry* **1998**, *63*, 9678-9683.
[149] S. C. Story, J. V. Aldrich, *Int J Pept Protein Res* **1994**, *43*, 292-296.
[150] L. A. Carpino, A. El-Faham, *Journal of the American Chemical Society* **1995**, *117*, 5401-5402.
[151] A. El-Faham, R. Subiros Funosas, R. Prohens, F. Albericio, *Chemistry* **2009**, *15*, 9404-9416.
[152] Y. E. Jad, S. N. Khattab, B. G. de la Torre, T. Govender, H. G. Kruger, A. El-Faham, F. Albericio, *Molecules* **2014**, *19*, 18953-18965.
[153] R. B. Merrifield, *Science* **1965**, *150*, 178-185.
[154] R. B. Merrifield, J. M. Stewart, N. Jernberg, *Anal Chem* **1966**, *38*, 1905-1914.
[155] S. L. Pedersen, K. J. Jensen, *Methods in molecular biology (Clifton, N.J.)* **2013**, *1047*, 215-224.
[156] T. J. Lukas, M. B. Prystowsky, B. W. Erickson, *Proceedings of the National Academy of Sciences of the United States of America* **1981**, *78*, 2791-2795.
[157] V. Krchnak, J. Vagner, M. Flegel, D. Mach, *Tetrahedron Letters* **1987**, *28*, 4469-4472.
[158] C. P. Gordon, *Org Biomol Chem* **2018**, *16*, 180-196.
[159] I. M. Mandity, B. Olasz, S. B. Otvos, F. Fulop, *ChemSusChem* **2014**, *7*, 3172-3176.
[160] A. Szloszar, F. Fulop, I. M. Mandity, *Chemistryselect* **2017**, *2*, 6036-6039.
[161] R. J. Giguere, T. L. Bray, S. M. Duncan, G. Majetich, *Tetrahedron Letters* **1986**, *27*, 4945-4948.
[162] C. O. Kappe, *Angewandte Chemie* **2004**, *116*, 6408-6443.
[163] S. T. Chen, S. H. Chiou, K. T. Wang, *J Chin Chem Soc-Taip* **1991**, *38*, 85-91.
[164] S. A. Palasek, Z. J. Cox, J. M. Collins, *Journal of peptide science : an official publication of the European Peptide Society* **2007**, *13*, 143-148.
[165] J. M. Collins, N. E. Leadbeater, *Org Biomol Chem* **2007**, *5*, 1141-1150.
[166] B. Bacsa, K. Horvati, S. Bosze, F. Andreae, C. O. Kappe, *J Org Chem* **2008**, *73*, 7532-7542.
[167] D. Obermayer, B. Gutmann, C. O. Kappe, *Angewandte Chemie (International ed. in English)* **2009**, *48*, 8321-8324.
[168] S. L. Pedersen, A. P. Tofteng, L. Malik, K. J. Jensen, *Chem Soc Rev* **2012**, *41*, 1826-1844.
[169] J. H. Jones, W. I. Ramage, *Journal of the Chemical Society, Chemical Communications* **1978**, 472-473.
[170] J. H. Jones, W. I. Ramage, M. J. Witty, *Int J Pept Protein Res* **1980**, *15*, 301-303.
[171] H. Hibino, Y. Nishiuchi, *Tetrahedron Letters* **2011**, *52*, 4947-4949.
[172] H. Hibino, Y. Miki, Y. Nishiuchi, *Journal of Peptide Science* **2012**, *18*, 763-769.

[173] M. A. Mitchell, T. A. Runge, W. R. Mathews, A. K. Ichhpurani, N. K. Harn, P. J. Dobrowolski, F. M. Eckenrode, *International Journal of Peptide and Protein Research* **2009**, *36*, 350-355.
[174] J. M. Collins, K. A. Porter, S. K. Singh, G. S. Vanier, *Organic Letters* **2014**, *16*, 940-943.
[175] H.-J. Musiol, F. Siedler, D. Quarzago, L. Moroder, *Biopolymers* **1994**, *34*, 1553-1562.
[176] H. Hibino, Y. Miki, Y. Nishiuchi, *Journal of Peptide Science* **2014**, *20*, 30-35.
[177] R. Subirós-Funosas, A. El-Faham, F. Albericio, *Tetrahedron* **2011**, *67*, 8595-8606.
[178] R. Behrendt, S. Huber, P. White, *Journal of Peptide Science* **2016**, *22*, 92-97.
[179] M. Mergler, F. Dick, B. Sax, C. Stähelin, T. Vorherr, *Journal of Peptide Science* **2003**, *9*, 518-526.
[180] M. Mergler, F. Dick, B. Sax, P. Weiler, T. Vorherr, *Journal of Peptide Science* **2003**, *9*, 36-46.
[181] M. Mergler, F. Dick, *Journal of Peptide Science* **2005**, *11*, 650-657.
[182] J. D. Wade, M. N. Mathieu, M. Macris, G. W. Tregear, *Letters in Peptide Science* **2000**, *7*, 107-112.
[183] E. Nicolás, E. Pedroso, E. Girald, *Tetrahedron Letters* **1989**, *30*, 497-500.
[184] A. K. Tickler, C. J. Barrow, J. D. Wade, *Journal of Peptide Science* **2001**, *7*, 488-494.
[185] J. Orpiszewski, N. Schormann, B. Kluve-Beckerman, J. J. Liepnieks, M. D. Benson, *FASEB journal : official publication of the Federation of American Societies for Experimental Biology* **2000**, *14*, 1255-1263.
[186] D. W. Aswad, M. V. Paranandi, B. T. Schurter, *Journal of Pharmaceutical and Biomedical Analysis* **2000**, *21*, 1129-1136.
[187] K. Chandra, T. K. Roy, D. E. Shalev, A. Loyter, C. Gilon, R. B. Gerber, A. Friedler, *Angewandte Chemie International Edition* **2014**, *53*, 9450-9455.
[188] T. Michels, R. Dölling, U. Haberkorn, W. Mier, *Organic Letters* **2012**, *14*, 5218-5221.
[189] M. Bodanszky, J. Z. Kwei, *International Journal of Peptide and Protein Research* **2009**, *12*, 69-74.
[190] R. Subirós-Funosas, A. El-Faham, F. Albericio, *Peptide Science* **2012**, *98*, 89-97.
[191] M. Quibell, D. Owen, L. C. Packman, T. Johnson, *Journal of the Chemical Society, Chemical Communications* **1994**, 2343-2344.
[192] L. C. Packman, *Tetrahedron Letters* **1995**, *36*, 7523-7526.
[193] J. Offer, M. Quibell, T. Johnson, *Journal of the Chemical Society, Perkin Transactions 1* **1996**, 175-182.
[194] T. Johnson, M. Quibell, D. Owen, R. C. Sheppard, *Journal of the Chemical Society, Chemical Communications* **1993**, 369-372.
[195] V. Cardona, I. Eberle, S. Barthélémy, J. Beythien, B. Doerner, P. Schneeberger, J. Keyte, P. D. White, *Int J Pept Res Ther* **2008**, *14*, 285-292.
[196] J. Sélambarom, J. Smadja, O. Thomas, I. Parrot, J. Martinez, A. A. Pavia, *Int J Pept Res Ther* **2005**, *11*, 267-270.
[197] T. Haack, M. Mutter, *Tetrahedron Letters* **1992**, *33*, 1589-1592.
[198] T. Wöhr, M. Mutter, *Tetrahedron Letters* **1995**, *36*, 3847-3848.
[199] T. Wöhr, F. Wahl, A. Nefzi, B. Rohwedder, T. Sato, X. Sun, M. Mutter, *Journal of the American Chemical Society* **1996**, *118*, 9218-9227.
[200] M. Paradís-Bas, J. Tulla-Puche, F. Albericio, *Chemical Society Reviews* **2016**, *45*, 631-654.
[201] J. M. Conlon, *Nat Protoc* **2007**, *2*, 191-197.
[202] A. J. Alpert, P. C. Andrews, *J Chromatogr* **1988**, *443*, 85-96.
[203] W. A. Schroeder, B. Robberson, *Anal Chem* **1965**, *37*, 1583-1585.
[204] J. Krenkova, A. Gargano, N. A. Lacher, J. M. Schneiderheinze, F. Svec, *Journal of Chromatography A* **2009**, *1216*, 6824-6830.
[205] S.-I. Ishii, *The Journal of Biochemistry* **1956**, *43*, 531-537.
[206] R. B. Merrifield, A. E. Bach, *The Journal of Organic Chemistry* **1978**, *43*, 4808-4816.

[207] S. Fexby, L. Bulow, *Trends Biotechnol* **2004**, *22*, 511-516.
[208] P. M. Cummins, K. D. Rochfort, B. F. O'Connor, *Methods in molecular biology (Clifton, N.J.)* **2017**, *1485*, 209-223.
[209] W. Kopaciewicz, M. A. Rounds, J. Fausnaugh, F. E. Regnier, *Journal of Chromatography A* **1983**, *266*, 3-21.
[210] Y. C. Lee, *Analytical biochemistry* **1990**, *189*, 151-162.
[211] S. A. Camperi, M. C. Martínez-Ceron, S. L. Giudicessi, M. M. Marani, F. Albericio, O. Cascone, in *Protein Downstream Processing: Design, Development and Application of High and Low-Resolution Methods* (Ed.: N. E. Labrou), Humana Press, Totowa, NJ, **2014**, pp. 277-302.
[212] N. G. Hentz, V. Vukasinovic, S. Daunert, *Anal Chem* **1996**, *68*, 1550-1555.
[213] X. Zhao, G. Li, S. Liang, *J Anal Methods Chem* **2013**, *2013*, 581093.
[214] Y. E. Jad, G. A. Acosta, S. N. Khattab, B. G. de la Torre, T. Govender, H. G. Kruger, A. El-Faham, F. Albericio, *Amino acids* **2016**, *48*, 419-426.
[215] Y. E. Jad, G. A. Acosta, T. Govender, H. G. Kruger, A. El-Faham, B. G. de la Torre, F. Albericio, *ACS Sustainable Chemistry & Engineering* **2016**, *4*, 6809-6814.
[216] M. Cortes-Clerget, J. Y. Berthon, I. Krolikiewicz-Renimel, L. Chaisemartin, B. H. Lipshutz, *Green Chemistry* **2017**, *19*, 4263-4267.
[217] Y. E. Jad, T. Govender, H. G. Kruger, A. El-Faham, B. G. de la Torre, F. Albericio, *Organic Process Research & Development* **2017**, *21*, 365-369.
[218] A. Kumar, Y. E. Jad, A. El-Faham, B. G. de la Torre, F. Albericio, *Tetrahedron Letters* **2017**, *58*, 2986-2988.
[219] S. B. Lawrenson, R. Arav, M. North, *Green Chemistry* **2017**, *19*, 1685-1691.
[220] M. Cortes-Clerget, J.-Y. Berthon, I. Krolikiewicz-Renimel, L. Chaisemartin, B. H. Lipshutz, *Green Chemistry* **2017**, *19*, 4263-4267.
[221] N. Fattahi, M. Ayubi, A. Ramazani, *Tetrahedron* **2018**, *74*, 4351-4356.
[222] M. T. Sabatini, L. T. Boulton, H. F. Sneddon, T. D. Sheppard, *Nature Catalysis* **2019**, *2*, 10-17.
[223] M. Cortes-Clerget, N. R. Lee, B. H. Lipshutz, *Nat Protoc* **2019**, *14*, 1108-1129.
[224] A. Přibylka, V. Krchňák, E. Schütznerová, *Green Chemistry* **2019**, *21*, 775-779.
[225] O. Ludemann-Hombourger, *Speciality Chemicals Magazine* **2013**, 30-33.
[226] C. Capello, U. Fischer, K. Hungerbühler, *Green Chemistry* **2007**, *9*, 927-934.
[227] F. P. Byrne, S. Jin, G. Paggiola, T. H. M. Petchey, J. H. Clark, T. J. Farmer, A. J. Hunt, C. Robert McElroy, J. Sherwood, *Sustainable Chemical Processes* **2016**, *4*, 7.
[228] R. K. Henderson, C. Jiménez-González, D. J. C. Constable, S. R. Alston, G. G. A. Inglis, G. Fisher, J. Sherwood, S. P. Binks, A. D. Curzons, *Green Chemistry* **2011**, *13*, 854-862.
[229] D. Prat, O. Pardigon, H.-W. Flemming, S. Letestu, V. Ducandas, P. Isnard, E. Guntrum, T. Senac, S. Ruisseau, P. Cruciani, P. Hosek, *Organic Process Research & Development* **2013**, *17*, 1517-1525.
[230] K. Alfonsi, J. Colberg, P. J. Dunn, T. Fevig, S. Jennings, T. A. Johnson, H. P. Kleine, C. Knight, M. A. Nagy, D. A. Perry, M. Stefaniak, *Green Chemistry* **2008**, *10*, 31-36.
[231] A. Isidro-Llobet, M. N. Kenworthy, S. Mukherjee, M. E. Kopach, K. Wegner, F. Gallou, A. G. Smith, F. Roschangar, *The Journal of Organic Chemistry* **2019**, *84*, 4615-4628.
[232] D. S. MacMillan, J. Murray, H. F. Sneddon, C. Jamieson, A. J. B. Watson, *Green Chemistry* **2013**, *15*, 596-600.
[233] Y. E. Jad, G. A. Acosta, S. N. Khattab, B. G. de la Torre, T. Govender, H. G. Kruger, A. El-Faham, F. Albericio, *Organic & Biomolecular Chemistry* **2015**, *13*, 2393-2398.
[234] M. S. El-Eskandarany, in *Mechanical Alloying (Second Edition)* (Ed.: M. S. El-Eskandarany), William Andrew Publishing, Oxford, **2015**, pp. 13-47.
[235] V. Declerck, P. Nun, J. Martinez, F. Lamaty, *Angewandte Chemie International Edition* **2009**, *48*, 9318-9321.

[236] J. Bonnamour, T.-X. Métro, J. Martinez, F. Lamaty, *Green Chemistry* **2013**, *15*, 1116-1120.
[237] C. Duangkamol, S. Jaita, S. Wangngae, W. Phakhodee, M. Pattarawarapan, *RSC Advances* **2015**, *5*, 52624-52628.
[238] L. Konnert, A. Gauliard, F. Lamaty, J. Martinez, E. Colacino, *ACS Sustainable Chemistry & Engineering* **2013**, *1*, 1186-1191.
[239] K. Hojo, M. Maeda, K. Kawasaki, *J Peptide Sci* **2001**, *7*.
[240] K. Hojo, M. Maeda, Y. Takahara, S. Yamamoto, K. Kawasaki, *Tetrahedron Letters* **2003**, *44*, 2849-2851.
[241] K. Hojo, M. Maeda, T. J. Smith, E. Kita, F. Yamaguchi, S. Yamamoto, K. Kawasaki, *Chemical & Pharmaceutical Bulletin* **2004**, *52*, 422-427.
[242] K. Hojo, M. Maeda, K. Kawasaki, *Tetrahedron Letters* **2004**, *45*, 9293-9295.
[243] K. Hojo, A. Hara, H. Kitai, M. Onishi, H. Ichikawa, Y. Fukumori, K. Kawasaki, *Chem Cent J* **2011**, *5*, 49.
[244] K. Hojo, H. Ichikawa, M. Maeda, S. Kida, Y. Fukumori, K. Kawasaki, *Journal of Peptide Science* **2007**, *13*, 493-497.
[245] K. Hojo, H. Ichikawa, A. Hara, M. Onishi, K. Kawasaki, Y. Fukumori, *Protein and Peptide Letters* **2012**, *19*, 1231-1236.
[246] K. Hojo, N. Shinozaki, A. Hara, M. Onishi, Y. Fukumori, H. Ichikawa, *Protein and Peptide Letters* **2013**, *20*, 1122-1128.
[247] K. Hojo, N. Shinozaki, K. Hidaka, Y. Tsuda, Y. Fukumori, H. Ichikawa, J. D. Wade, *Amino acids* **2014**, *46*, 2347-2354.
[248] K. Hojo, O. n. i. s. h. i. Mare, H. Ichikawa, Y. Fukumori, K. Kawasaki, *J Peptide Sci* **2011**, *17*.
[249] K. Hojo, N. Shinozaki, Y. Nozawa, Y. Fukumori, H. Ichikawa, *Applied Sciences* **2013**, *3*, 614-623.
[250] A. S. Galanis, F. Albericio, M. Grotli, *Org Lett* **2009**, *11*, 4488-4491.
[251] J. M. Collins, Google Patents, **2012**.
[252] G. B. Fields, *Methods in molecular biology (Clifton, N.J.)* **1994**, *35*, 17-27.
[253] A. Ramazani, F. Zeinali Nasrabadi, A. Rezaei, M. Rouhani, H. Ahankar, P. Azimzadeh, S. Woo Joo, K. Slepokura, T. Lis, *Synthesis of N-acylurea derivatives from carboxylic acids and N,N'-dialkyl carbodiimides in water, Vol. 127*, **2015**.
[254] R. Röder, P. Henklein, H. Weißhoff, C. Mügge, M. Pätzel, U. Schubert, L. A. Carpino, P. Henklein, *Journal of Peptide Science* **2010**, *16*, 65-70.
[255] D. Samson, D. Rentsch, M. Minuth, T. Meier, G. Loidl, *Journal of Peptide Science* **2019**, *25*, e3193.
[256] J. P. Tam, M. W. Riemen, R. B. Merrifield, *Peptide research* **1988**, *1*, 6-18.
[257] L. A. Carpino, *Accounts of Chemical Research* **1987**, *20*, 401-407.
[258] C. S. Nielsen, P. H. Hansen, A. Lihme, P. M. H. Heegaard, *Journal of Biochemical and Biophysical Methods* **1989**, *20*, 69-80.
[259] V. K. Sarin, S. B. H. Kent, J. P. Tam, R. B. Merrifield, *Analytical Biochemistry* **1981**, *117*, 147-157.
[260] R. S. Hodges, R. B. Merrifield, *Analytical Biochemistry* **1975**, *65*, 241-272.
[261] A. M. Felix, M. H. Jimenez, *Analytical Biochemistry* **1973**, *52*, 377-381.
[262] Brunfeld.K, Villemoe.P, Christen.T, *Febs Letters* **1972**, *22*, 238-&.
[263] R. Bollhagen, M. Schmiedberger, K. Barlos, E. Grell, *Journal of the Chemical Society, Chemical Communications* **1994**, 2559-2560.
[264] P. Palladino, D. A. Stetsenko, *Organic Letters* **2012**, *14*, 6346-6349.

Abbreviations

2-Cl-Z 2-chlorobenzyloxycarbonyl
2-CTC 2-chlorotrityl chloride
2-MeTHF 2-methyl tetrahydrofuran
2-PhiPr 2-phenylisopropyl
aa amino acids
Acm acetamidomethyl
AiB 2-aminoisobutyric acid
Al allyl
Alloc allyloxycarbonyl
Arg arginine
Asn asparagine
Asp aspartic acid
ASPPS aqueous solid-phase peptide synthesis
BAL backbone amide linker
Boc *tert*-butyloxycarbonyl
Bom Benzyloxymethyl
Bum *tert*-butoxymethyl
Bzl benzyl
CBz carboxybenzoxy
CMR carcinogenic, mutagenic, or toxic for reproduction
COMBU 4 ((1,3-dimethyl-2,4,6-trioxotetrahydro-pyrimidin-5(6H)ylidene-aminooxy)(dimethylamino)methylene) morpholin-4-ium hexafluorophosphate
COMU (1-cyano-2-ethoxy-2-oxoethylidenaminooxy)dimethylamino-morpholino-carbenium hexafluorophosphate
COSS cube-octameric silsesquioxanes
Cys cysteine
DCC *N,N*'-dicyclohexylcarbodiimide, *N,N*'-dicyclohexylcarbodiimide
DCM dichloromethane
DIC *N,N*'-diisopropylcarbodiimide
DIPEA *N,N*-diisopropylethylamine
DMF *N,N*-dimethylformamide
DNP dinitrophenyl
DVB divinylbenzene
EDC 1-ethyl-3-(3-dimethylaminopropyl)carbodiimid
EDC-HCl 1-ethyl-3-(3-dimethylaminopropyl)carbodiimide hydrochloride
EEDQ *N*-ethoxycarbonyl-2-ethoxy-1,2-dihydroquinoline
Esc ethanesulfonylethoxycarbonyl
Fmoc 9-fluorenylmethoxycarbonyl
Fmoc-Cl 9-fluorenylmethoxycarbonyl chloride
Fmoc-NHS 9-fluorenylmethyl *N*-succinimidyl carbonate
For formyl
Gln glutamine
Glu glutamic acid
GVL γ-valerolactone

HATU 1-[bis(dimethylamino)methylene]-1H-1,2,3-triazolo[4,5-b]pyridinium-3-oxid hexafluorophosphate
HBr hydrogen bromide
HBTU 2-(1H-benzotriazol-1-yl)-1,1,3,3-tetramethyluronium hexafluorophosphate
HCl hydrogen chloride
HCTU O-(1H-6-chlorobenzotriazole-1-yl)-1,1,3,3-tetramethyluronium hexafluorophosphate
HF hydrogen fluoride
His histidine
Hmb 2-hydroxyl-4-methoxybenzyl
HMBA 4-hydroxymethylbenzoic acid
HMPB 4-(4-hydroxymethyl-3-methoxyphenoxy)-butyric acid
HOAt 1-hydroxy-7-azabenzotriazole
HOBt 1-hydroxy-1H-benzotriazole
Hoc cyclohexyloxycarbonyl
HONB *N*-hydoxybicyclo[2.2.1]hept-5-ene-2,3-dicarboximide
HOPO 1-hydroxy-2-pyridone
HPLC high performance liquid chromatography
IE column ion-exchange column
IEC ion-exchange chromatography
Lys lysine
MBHA 4-methylbenzhydrylamine
MBom 4-methoxybenzyloxymethyl
MCC multicolumn chromatography
MeOBzl 4 methoxybenzyl
Me-THF 2-Methyltetrahydrofuran
MMT monomethoxytrityl
Mtr 4-methoxy-2,3,6-trimethyl-benzenesulphonyl
Mts mesitylen-2-sulfonyl
Mtt 4-methyltrityl
NFM *N*-formylmorpholine
NHS *N*-hydroxysuccinimide
NMP *N*-methylpyrrolidon*e*
Nsmoc 1,1-dioxonaptho[1,2-b]thiophene-2-methyloxy-carbonyl
Oxyma ethyl-2-cyano-2-(hydroxyimino)acetate
PA polyamide
Pbf 2,2,4,6,7-pentamethyl-dihydro-benzofuran-5-sulfony
PC propylene carbonate
PEG polyethylene glycol
Pmc 2,2,5,7,8-pentamethyl-chroman-6-sulfonyl
Pms 2 [phenyl(methyl)sulfonio]ethyloxycarbonyl
PS polystyrenes
PyBOP benzotriazole-1-yl-oxy-tris-pyrrolidino-phosphonium hexafluorophosphat
RP-HPLC reversed phase high-performance liquid chromatography
RT room temperature
SASRIN super acid-sensitive resin
Ser serine
Smoc 2,7-disulfo-9-fluorenylmethoxycarbonyl chloride

SPFC solid phase fragment condensation
SPPS solid-phase peptide synthesis
Sps 2-(4-sulfophenylsulfonyl)ethoxy-carbonyl
StBu *tert*-butylsulfenyl
Tbdms *tert*-butyldimethylsilyl
*t*Bu *tert*-butyl
TFA trifluoroacetic acid
TFFH tetramethylfluoroformamidinium hexafluorophosphate
TFMSA trifluoromethanesulfonic acid
Thr threonine
Tmob 2,4,6-trimethoxybenzyl
TOMBU *N*-((1,3-dimethyl-2,4,6-trioxotetra-hydropyrimidin-5(6H)-ylideneaminooxy)(dimethylamino)methylene)-*N*-methylmethanaminiumhexa-fluoro-phosphate
TOS toluolsulfonyl
Trp tryptophan
Trt trityl
Tyr tyrosine
Xan 9-xanthenyl

Acknowledgment

Ich möchte mich bei allen Personen, die diese Arbeit ermöglicht haben und mich in diesem Zeitraum unterstützt haben aufrichtig bedanken:

Meinem Doktorvater **Prof. Dr. Harald Kolmar** möchte ich danken für die Freiheit, die du mir während meiner Arbeit gelassen hast, sowie die entgegengebrachte Unterstützung bei diversen Projekten…auch wenn wir nicht immer einer Meinung waren. Vielen Dank auch für die vielen anregenden wissenschaftlichen Gespräche, leider konnten (bisher) nicht alle Ideen verwirklicht werden.

Dr. Olga Avrutina, danke ich für die uneingeschränkte Unterstützung und dass du immer Zeit für mich hattest.

Dr. Christina Uth und **Dr. Niklas Koch** möchte ich für die Unterstützung meiner Arbeit sowie die Zusammenarbeit bei Sulfotools danken, ohne euch wäre vieles nicht möglich gewesen.

Prof. Dr. R. Meusinger für die Kooperation bei den umfangreichen NMR Auswertungen.

Bastian, Hendrik, Katharina und Simon, meine ehemaligen Masteranden die mich bei meinen Projekten unterstützt haben. Insbesondere möchte ich mich bei meinem ehemaligen Diplomanden Tobias bedanken, der in der Anfangsphase des ASPPS Projektes durch seinen Arbeitseinsatz viele Ideen mit mir verwirklicht hat.

Allen Mitgliedern und ehemaligen Mitgliedern des **AK Kolmar**, für die vielen gemeinsamen Projekte und die entspannte Arbeitsatmosphäre während meiner Dissertation.

Einen besonderen Dank möchte ich meiner **Familie** aussprechen. Ihr habt mich immer unterstützt und mir die notwendigen Freiheiten für meine Arbeit gelassen.

Darmstadt,

Erklärung

Ich erkläre hiermit, dass ich meine Dissertation selbstständig und nur mit den angegebenen Hilfsmitteln angefertigt und noch keinen Promotionsversuch unternommen zu haben.

Dipl.-Ing. Sascha Knauer

Darmstadt,

Erklärung der Übereinstimmung

Ich erkläre hiermit, dass die elektronische Version der Doktorarbeit mit der schriftlichen Version übereinstimmt. Die elektronische Version liegt dem Prüfungssekretariat vor.

Dipl.-Ing. Sascha Knauer